Proceedings of the 35th INGEGRAF
International Technical Conference

DESIGN FOR ONE HEALTH

September, 2026:
Bilbao



Coordinators:
Irantzu Alvarez Gonzalez
Xabier Amezua Lasuen
Maider Iturrondobeitia Ellacuria
Rikardo Minguez Gabiña
Eva Rodriguez Hortelano
Idoia San Sebastian Ibirriaga
José Sebastián Velázquez Blázquez

EHU

CIP. Biblioteca Universitaria

INGEGRAF. International Technical Conference (35º. 2026. Bilbao)

Proceedings of the 35th INGEGRAF International Technical Conference [Recurso electrónico]: Design for One Health /Irantzu Alvarez González… [et al.] (coords.). – Datos. – [Leioa]: Servicio Editorial de la Universidad del País Vasco = Euskal Herriko Unibertsitateko Argitalpen Zerbitzua, [2026]. – 1 recurso en línea : PDF (557 p.)

Modo de acceso: World Wide Web

ISBN. 978-84-1319-818-7

1. Ingeniería – Congresos. 2. Informática gráfica – Congresos. 3. Diseño asistido por ordenador – Congresos. I. Álvarez González, Irantzu, coord.

(0.034)62:744(063)

© Servicio de Publicaciones de la Universidad del País Vasco
Euskal Herriko Unibertsitateko Argitalpen Zerbitzua

Argitalpen Zerbitzua • Servicio Editorial
editorial@ehu.eus - 94 601 2227
www.ehu.eus/argitalpenak
Edificio Biblioteca, 1.ª planta
B.º Sarriena s/n. Campus de Bizkaia

ISBN: 978-84-1319-818-7

ORGANISING COMMITTEE:

Chair: Rikardo MINGUEZ GABIÑA (Euskal Herriko Unibertsitatea)

Members:

- Xabier AMEZUA LASUEN (Euskal Herriko Unibertsitatea)
- Eva RODRIGUEZ HORTELANO (Euskal Herriko Unibertsitatea)
- Maider ITURRONDOBEITIA ELLACURIA (Euskal Herriko Unibertsitatea)
- Erlantz LIZUNDIA FERNANDEZ (Euskal Herriko Unibertsitatea)
- Irantzu ALVAREZ GONZALEZ (Euskal Herriko Unibertsitatea)
- Alberto LOPEZ ARRAIZA (Euskal Herriko Unibertsitatea)
- Idoia SAN SEBASTIAN IBIRRIAGA (Euskal Herriko Unibertsitatea)
- Pello JIMBERT LACHA (Euskal Herriko Unibertsitatea)
- Harkaitz EGUIRAUN MARTINEZ (Euskal Herriko Unibertsitatea)
- Egoitz SIERRA URIA (Euskal Herriko Unibertsitatea)
- Jokin GOROZIKA BIDAURRATZAGA (Euskal Herriko Unibertsitatea)
- Nestor GOIKOETXEA LARRAKOETXEA (Euskal Herriko Unibertsitatea)
- Lander BARRENETXEA APRAIZ (Euskal Herriko Unibertsitatea)
- Gaizka ERKIZIA ESCOLANO (Euskal Herriko Unibertsitatea)
- Olatz ETXANIZ MENDIGUREN (Euskal Herriko Unibertsitatea)
- Iraitz DUARTE FERNANDEZ (Euskal Herriko Unibertsitatea)

SCIENTIFIC COMMITTEE:

Chair: José Sebastián VELÁZQUEZ BLÁZQUEZ (Universidad Politécnica de Cartagena)

Members:

INGEGRAF: Asociación Española de Ingeniería Gráfica

Cristina MARTÍN DOÑATE (Universidad de Jaén) – President of INGEGRAF
Rikardo MINGUEZ GABIÑA (Euskal Herriko Unibertsitatea)
Maria Belén PRENDES GERO (Universidad de Oviedo)
Elidia Beatriz BLÁZQUEZ PARRA (Universidad de Málaga)
Jorge Manuel MERCADO COLMENERO (Universidad de Jaén)
Xabier AMEZUA LASUEN (Euskal Herriko Unibertsitatea)
Valen GÓMEZ JAUREGUI (Universidad de Cantabria)
Manuel ALCALÁ VILAVELLA (Universitat de Girona)
Mercedes VALIENTE LÓPEZ (Universidad Politécnica de Madrid)
Marta MENÉNDEZ FERNÁNDEZ (Universidad de León)
Maria Luisa MARTÍNEZ MUNUETA (Universidad Politécnica de Madrid)
Larisa DUNAI DUNAI (Universitat Politècnica de València)
Lucía DÍAZ VILARIÑO (Universidade de Vigo)
Francisco Javier ESPINACH ORÚS (Universitat de Girona)
Carmelo PINA GADEA (Universidad de Zaragoza)
Cristina MANCHADO DEL VAL(Universidad de Cantabria)
Paula TRIVIÑO TARRADAS (Universidad de Córdoba)

Pedro LASTRA GONZÁLEZ (Universidad de Cantabria)
Diego José GUERRERO MIGUEL (Universidá d'Uviéu)
Miguel SUFFO PINO (Universidad de Cádiz)
Francisco CAVAS MARTÍNEZ (Universidad Politécnica de Cartagena)
Borja ARROYO MARTÍNEZ (Universidad de Cantabria)
Raquel PLUMED FERRER (Universitat Jaume I)
Joan Antoni LÓPEZ MARTÍNEZ (Universitat Politècnica de Catalunya)
María MONCHO SANTOJA (Universitat Politècnica de València)
Maider ITURRONDOBEITIA ELLACURIA (Euskal Herriko Unibertsitatea)
Egoitz SIERRA URIA (Euskal Herriko Unibertsitatea)
Irantzu ALVAREZ GONZALEZ (Euskal Herriko Unibertsitatea)
Alberto LOPEZ ARRAIZA (Euskal Herriko Unibertsitatea)
Harkaitz EGUIRAUN MARTÍNEZ (Euskal Herriko Unibertsitatea)
Erlantz LIZUNDIA FERNÁNDEZ (Euskal Herriko Unibertsitatea)
Pedro José JIMBERT LACHA (Euskal Herriko Unibertsitatea)
Lander BARRENETXEA APRAIZ (Euskal Herriko Unibertsitatea)

ADM: Associazione nazionale Disegno e Metodi dell'ingegneria industriale

Caterina RIZZI (Università degli Studi di Bergamo, Italy) – President of ADM
Paolo DI STEFANO (Università degli Studi dell'Aquila, Italy)
Salvatore GERBINO (Università degli Studi della Campania Luigi Vanvitelli, Italy)
Michele GERMANI (Università Politecnica delle Marche, Italy)
Lapo GOVERNI (Università degli Studi di Firenze, Italy)
Tommaso INGRASSIA (Università degli Studi di Palermo, Italy)
Antonio LANZOTTI (Università degli Studi di Napoli Federico II, Italy)
Massimo MARTORELLI (Università degli Studi di Napoli Federico II, Italy)
Maurizio MUZZUPAPPA (Università della Calabria, Italy)
Armando RAZIONALE (Università degli Studi di Pisa, Italy)
Enrico VEZZETTI (Politecnico di Torino, Italy)
Valerio VILLA (Università degli Studi di Brescia, Italy)

S.mart: Systems, Manufacturing, Academics, Resources, Technologies

Matthieu BRICOGNE (Université de Technologie de Compiègne, France)
Marco MONTEMURRO (Arts et Métiers, Bordeaux, France)
Manuel PAREDES (INSA Toulouse, France)
Jean Philippe PERNOT (Arts et Métiers, Aix-en-Provence, France)
Sébastien REMY (Université de Lorraine, France)

Contents

Foreword / Prólogo / Hitzaurrea
Organising Committee of the 35th INGEGRAF International Technical Conference . 12

Geometric fitting of column cross-sections from noisy point clouds usin constrained minimization
Patricia González-Cabaleiro, Lucía Díaz-Vilariño, Antonio Fernández 15

Multiplayer Virtual Reality for Collaborative Product Evaluation in Industrial Design: Comparing Group and Individual Assessments
Almudena Palacios-Ibáñez, Carlos García-García, Laura Ruiz-Pastor, Francisco Felip-Miralles, Julia Galán 23

Advanced structural design and WAAM additive manufacturing as a strategy for sustainability in metallic components
Ainara Cervera, Virginia Uralde, Fernando Veiga 31

AI-Assisted CAM for DED-Arc: Intelligent Toolpath Planning and Process Optimization
Juan Sustacha, Fernando Veiga, Virginia Uralde, Alvaro Rodríguez. 38

Animal-centered design of monitoring system enclosures in livestock environments under a One Health framework
Ian Frega Molina, Enrique Samperio, Elena Heras-Romanos, Iván Lidón, Rubén Rebollar, Ignacio Gil-Pérez 46

BIM-Integrated Energy Simulation of Radiative Cooling Envelopes in Office Buildings
Laura Carlosena, Xabier Sandúa, Alicia Elena Torres-García, Amaia Pérez, Sara Marcelino, Miguel Beruete 54

Sustainable 3D printing of biomass-based biosensors with tunable electrical and biological properties
Jesús M. Rodríguez-Rego, Laura Mendoza-Cerezo, Alfonso C. Marcos-Romero, Paulo S. Duque-de Brito, Eva M. Hernández-Preciado. 61

Horizontal extrusion bioprinting for tubular structure fabrication: design a nd preliminary feasibility assessment of a rotating-axis system
Jesús M. Rodríguez-Rego, Laura Mendoza-Cerezo, Alfonso C. Marcos-Romero, Juan P. Carrasco-Amador, David Picado-Tejero 69

Redesign of an Electric Scooter through the Application of TPMS Structures
Ramón Miralbes-Buil, David Ranz-Angulo, Clara Luna Martín-Compaired, José Antonio Gómez-García 76

Parametric 3D Modeling and Digital Twin Development for Modular Sofa Design
María Matías, José Manuel Auría, Raquel Acero, Carmelo Pina 83

Pressure Measuring Device for Shoulder Loads during Holy Week Processions
David Sánchez-Murcia, José Macías-García, Óscar D. de-Cózar-Macías, Francisca J. Castillo-Rueda, Laia Miravet-Garret 90

A Blended Learning Approach to Teaching Graphical Expression in Engineering
José S. Velázquez, Francisco L. Sáez, José González-Cabrero, Lucas Díaz-Moreno, Carmelo Gómez, Francisco Cavas 96

Graph-based Structural Characterization of Urban bus Transport Networks Using a Cycle Interaction Approach
Marina Díaz-Jiménez, Yoann Pigné, Patricia Ruiz, Pablo Pavón-Domínguez 104

Reverse Engineering Applied to "Design for one Health": A Teaching Case Study Using Simplified Ribbed Shafts
Rocío Rodríguez, Pablo Rodríguez, Rubén Rodríguez, Pedro Hernández, Manuel Rodríguez 112

Integration of BIM methodology and eco-design for a sustainable olive oil mill design using Autodesk environment and CYPE tools
Miguel Alonso Cueto-García, Lázuli Fernández-Lobato, Fernando Gómez-Hermosa, Antonio Jesús Rodríguez-Pérez 120

Designing a visual information system for monitoring urban cleaning and waste collection services
Elena Heras-Romanos, Ian Frega, Enrique Samperio, Ignacio Gil-Pérez, Iván Lidón, Rubén Rebollar 127

Ecodesign using marine seafloor waste from the Cantabrian Coast
Carlota Alfaro-Ortega, Amaia Garrrido, Julen Ibarretxe, Maider Iturrondobeitia . . . 135

An Interoperable Workflow for LiDAR-Based 3D Mesh Generation and Spatial Data Integration in Engineering Design
M.T. Yubero, E. Bonet, Lluís Sanmiquel 142

AI-Driven Tools Across the Product Design Lifecycle. A Systematic Review and Comparative Analysis for Industrial Design Engineering
Flors García-Malet, Fernando Fernández-Lapuente, Óscar Paseta-Martínez, David Ranz-Angulo 150

From drawn geometry to simulated geometry: a geometric abstraction model in the bim-bem workflow for energy simulation
Ruth Fernández García, Rafael Rodríguez Galindo Díez, Diego José Guerrero Miguel, María Belén Prendes Gero, Marta Menéndez Fernández 158

Development of an interactive book for active learning in Engineering Graphics education
Sandra Munera, Nereida Tarazona, Francisco Albert, Nuria Aleixos, Alejandro Rodríguez-Ortega 165

From conceptual exploration to functional coherence: integrating AI and technical disciplines in industrial design
Victoria Artés, Mar Melgarejo-Torralba, Eva M. Sánchez-García, Alfonso Ramallo-González, Juan Manuel Salmerón Núñez, Dolores Parras-Burgos. 172

Design and Development of a Musculoskeletal and Cardiovascular Rehabilitation Device for Hospital Environments
I. Sola-Arean, D. Ranz 179

Sustainability and structural assessment of urban bicycle frames manufactured using different material systems
Mauricio López-Gutiérrez, David Ranz-Angulo, Carmelo Pina-Gadea, José Antonio Gómez-García 186

Challenge-Based Learning for Higher Education Transformation in Industry 5.0: A UPM-EELISA Ecosystem Perspective
Luisa M-Muneta, Ruth Carrasco-Gallego, Javier Gómez-Fernández, Alejandro Badolato. 194

Development of Foam Filling Strategies in Gyroid TPMS Structures for Enhanced Energy Absorption in Personal Protective Systems
César Aguilar Gázquez, Clara-Luna Martin-Compaired, David Ranz Angulo, Ramón Miralbes 202

Accessible Light: How to Design for People with Autism Spectrum Disorder
Giusi Castaldo, Elidia Beatriz Blázquez Parra, M. Carmen L. de Guevara Muñoz, Laia Miravet Garret 209

Implementing sustainability competences in graphic expression related lectures
Eva Rodríguez Hortelano, Julen Ibarretxe, Maider Iturrondobeitia Ellacuria 216

Improving Interoperability in Civil Engineering: IFC4.3 workflow
Pedro Lastra-González, Borja Arroyo, Cristina Manchado 224

Dynamo based methodology for checking networks after construction vs BIM models
Borja Aroyo, Pedro Lastra-González, Cristina Manchado 232

Coupled Hydrodynamic and Structural Design Methodology for a Low-Cost Remotely Operated Vehicle
Gaizka Erkizia, Idoia San Sebastian, Erik Vadillo, Xabier Amezua, Mikel Iturrate, Xabier Garikano 240

Graphic Design for One Health: Enhancing Student Engagement and Learning through AI-Assisted Visual Communication
Benyamin Soleimani, Larisa Dunai 247

Design for Healthy Urban Environments: Analysis and a Combined Empirical and Perceptual Methodology in Cartagena's Historic Squares
Eva M. Sánchez-García, Mar Melgarejo-Torralba, Victoria Artés-Hernández, Álvaro Ochoa Castillo, Emilio López Salmerón, Dolores Parras-Burgos 254

Improving the design of a day-care service provided in a rural environment
Laura Diago-Ferrer, Natalia Muñoz, Santiago Osnaya, José Luis Santolaya 262

Development of a model for predicting the maximum stress of FDM-modeled PLA specimens
Silvia Losada-Pérez, Ana Isabel García-Díez, Rosa Devesa-Rey, Miguel Ángel Álvarez-Feijoo, María Elena Arce Fariña 269

Advantages and disadvantages of using automatic geometric and dimensioning tolerance tools in 3D CAD systems: A case study of a mechanical guidance device
Fernando Brusola, Antonio Valín, Ignacio Tortajada, María Ángeles Esandi, Jorge Montalvá 278

Development of a Web-Based Digital Twin of a Two-Stroke Motorbike Engine Using Reverse Engineering
Ricard Barberà-Guillem, Andrés Crespo Montalvá, Beatriz Defez, María Moncho Santonja 286

Towards an efficient interaction between learners and conversational artificial intelligence tools in graphic engineering courses
Diego-José Guerrero-Miguel, María-Belén Prendes-Gero, Marta Menéndez Fernández, Martina-Inmaculada Álvarez-Fernández, Ruth Fernández García, Juan Carlos Ríos-Fernández 294

AI-assisted scaffolding for the initial analysis of mechanical drawings in engineering graphics education
Lara García Calvo, María Consuelo Sáiz-Manzanares, Raúl Marticorena Sánchez, Arturo de Román Miguel, Álvaro Alonso Díez 301

CAPRIA methodology and critical use of generative artificial intelligence in initial training in graphic engineering
Diego Francisco García-Molina, Jorge Manuel Mercado-Colmenero, Juan Manuel Montalvo-Gil, Francisco Javier Gallego Álvarez, Cristina Martín-Doñate 307

Service design methodologies: A framework to transform healthcare systems
Laura Aguado-González, Yeray Sañudo, Jorge Sierra-Pérez. 315

Analysis and Application of Generative Artificial Intelligence in 3D Modeling
Eneko Solaberrieta, Xabier Amezua, Gaizka Erkizia, Xabier Garikano 323

Analysis of Tool Wear Measurement in Turning Using 2D and 3D Methods
Marcos Pueo, Raquel Acero, Sergio Aguado, Ana Cristina Majarena, Jorge Santolaria. . 330

Graphical Application for the Morphological Characterization and Geometric Modeling of Real Milling Cutter Edges
Yasser Zekalmi, José Antonio Albajez, María José Oliveros, Sergio Aguado 337

Digital Eco-Design and Parametric Optimization of 3D Assets: A Hybrid Workflow for Sustainable Virtual Fashion Environments
Aida Vidal-Fernández, Cristina Prado-Acebo, Anabel Díaz-Labrador, Francisco Zayas-Gato, Elena Arce Fariña 343

Designing Effective Bar Charts for Global Health Data
Antonio Fernández, Francesco Bianconi 350

A multimodal AI-assisted methodology for the repair-oriented reconstruction and additive remanufacturing of plastic parts
Jorge Manuel Mercado-Colmenero, Ismael Majdoubi-García, Diego Francisco García-Molina, Cristina Martín-Doñate. 357

When Senses Decide: Integrating Multisensory Evaluation into the Design Process
María Alonso-García, Amada Blanco-Spadavecchia, Manuel Damián Marían-Granados 365

From Material to Form: Experimental analysis of Kerfing in MDF for flexible furniture design
Javier Martín-Domínguez, Laura Barrera-Muñoz, Aida López-López, María Alonso-García. 371

From Mental Abstraction to Sustainable Prototyping: A Five-Phase Design Thinking Workflow for Graphical Engineering Education
Julio César Rivera-Pedroza, Marcelo Javier Leslabay Martínez. 379

Comparison of different Experimental Methods for Measuring the of Parameter in Small Punch Tests
Ander Escolar Fernández, Ibon Miguel González de Belandia, Garikoitz Artola Beobide 387

Innovation in contract furniture: A University-Industry collaboration with Alutec on folding chair
Aída López-López, Miriam Fernández-Vida, María Alonso-García, Javier Martín-Domínguez. 395

Exploration of Speculative Scenarios at the Intersection of AI and Collaborative Design
Ilie-Ion Bona-Zaicu, Aiur Retegi-Uria, Mónica Elices-Zabala 402

Comparative Study of Piping Route Software for engineering companies
Fernando Freijo-Guerrero, Carolina Cruz-Villazón 410

A Structured Peer-Review Methodology for Active Learning in Engineering Graphics Courses
Carolina Cruz-Villazóna, Fernando Freijo-Guerrero 418

Situated Concurrent Think-Aloud Evaluation of a Mobile App within a Youth Digital Mental Health Ecosystem
Eva Tausiet, Marta Siguín, Sara Siddi, Concepción de la Cámara, David Vaquero, Teresa Blanco 424

Methodology for Harmonising Historical Data Records from Legacy Industrial Climate-Control Systems in Livestock Facilities
P. Bosque Obón, M. A. Torres Portero, I. Martínez Ruiz, J. Sierra-Pérez 432

Human-Centered Additive Manufacturing of Personalized Assistive Devices for Individuals with Cerebral Palsy
Aitor Tejo-Otero, Haritz Uriarte Larizgoitia, Alberto Martínez, Egoi Azkarraga . . . 439

A reproducible workflow for open-data-based 3D urban modelling for urban climate analysis
Maider Rekondo, Irantzu Alvarez, Rikardo Minguez, Leire Garmendia. 445

Monte Carlo simulation of PHBV film disintegration in compost
Idoia San Sebastian, Gaizka Erkizia, Eva Rodriguez, Maider Iturrondobeitia. 453

Gender study on motivation with the use of virtual reality in learning representation systems in engineering degree programs
Paula Triviño-Tarradas, Carlos Ruiz-Díaz, Pilar Carranza-Cañadas, Rafael Hidalgo-Fernández, María M. Serrano-Baena. 460

Competence Development in Aerospace Engineering Students through Project-Based Learning
Rebeca Martínez García, Fernando J. Fraile Fernández, Covadonga Palencia, Víctor Baladrón Blanco, Jesús de Prado Gil. 468

Adaptive Support System for Reducing Resin Consumption in DLP 3D Printing Systems
Teresa Carranza, Iraia Osquila, Maialen Zelaia, Francesca Perin, Mireia Andonegi. . 475

3D-Printed Mechanical Assemblies from Recycled PET as Sustainable Teaching Resources in Graphical Engineering
Lorena Ugarte, María Lozano, Kizkitza Gonzalez. 483

Improving the design of a laboratory-scale membrane reactor to produce hydrogen by reforming of biomass derivatives
José Valecillos, Negin Karim Zadeh Bajgiran, Gorka Elordi, Aingeru Remiro, Ana G. Gayubo 490

Detecting the Invisible: An Automated Approach to Identifying Plagiarism in Autodesk Inventor Files in Engineering Education
Valentin Gómez-Jáuregui, José-Andrés Díaz-Severiano, Noemi Barral-Ramón 498

Geometry-driven design and additive manufacturing of mycelium-based biocomposites for sustainable applications
Kizkitza González, Unai Ortega, Nerea Zaldua, Lorena Ugarte 506

Topologically Consistent 3D Reconstruction of Polyhedral Objects from Orthographic Projections using Graph Analysis and Winged-Edge Representation
Gerardo Martín-Lorenzo, José Pablo Suárez, Pedro Miguel González. 513

Comparative Design and FEM-Based Structural Assessment of Type IV Green Hydrogen Pressure Vessels for Fuel Cell Vehicle Applications
Miguel Suffo, José Manuel Devís 521

Multimodal Biomechanical Assessment of Untreated and Cross-Linked Corneas for the Optimization of Keratoconus Therapies
Lourdes Quilez, Alejandro Roca, Erwan Bentaib, Carmelo Gómez, José González, Francisco Cavas 529

Enhancing Spatial Vision in Industrial Drawing through VR Integration: A Multidisciplinary Approach for Mechanical Assemblies
Xabier Sandua, Laura Carlosena, Josu Irisarri, Miguel Ángel Martín, Sara Marcelino, Fernando Veiga, Amaia Pérez 536

AI in Engineering Graphics: Changing Teacher's Role
G. Peris Fajarnés, M. Moncho Santonja, I. Lengua, E. Burguera-Sierra, R. Barberà-Guillem, B. Defez 542

State of the Art of Non-Pneumatic Tyres (NPTs) Applied to the Front Caster Wheels of Wheelchairs for Improved Suspension Performance
Bernardo Pajares Moreno, Guillermo Peris Fajarnés, R. Barberà-Guillem, María Moncho Santonja 550

Foreword

It is a great pleasure for all the members of the Organizing Committee to present the Proceedings of the 35th INGEGRAF International Technical Conference, held in Bilbao on 11 September 2026 under the theme "DESIGN FOR ONE HEALTH".

For more than three decades, INGEGRAF has provided a valuable forum for the exchange of knowledge, experience, and innovative ideas among university lecturers, researchers, and professionals working in the field of Graphic Engineering. This 35th edition continues that tradition while addressing one of the key challenges facing contemporary society: the need to rethink the ways in which we design, develop, manufacture, use, and manage the products, systems, infrastructures, and environments that shape our world.

The One Health approach reminds us that human health, animal health, and the health of our planet are deeply interconnected. Design, therefore, cannot be regarded as an isolated technical activity. Every design decision has consequences that extend across environmental, social, economic, and health-related dimensions. In this context, Graphic Engineering has a crucial role to play. Through digital modelling, visualisation, simulation, product development, advanced manufacturing technologies, life-cycle thinking, and emerging tools such as artificial intelligence, our discipline can contribute to the creation of safer, more sustainable, more resilient, and more inclusive solutions.

The contributions gathered in these Proceedings reflect the diversity and vitality of the research and educational activities undertaken within our field. They demonstrate how innovation in engineering graphics and design can support the transition towards more responsible practices and help address complex global challenges through interdisciplinary collaboration.

We would like to express our sincere gratitude to all the authors, reviewers, members of the Scientific and Organising Committees, and institutions whose commitment has made this conference possible. We are proud to have welcomed all participants to Bilbao, a city where industrial heritage, technological innovation, culture, and a strong commitment to sustainability come together.

We hope that this conference has provided an inspiring space for discussion, collaboration, and the generation of new knowledge, thereby reinforcing our shared commitment to designing a healthier future for people and the planet.

Organising Committee of the 35th INGEGRAF International Technical Conference

Prólogo

Es un gran placer presentar las Actas del 35.º Congreso Técnico Internacional de INGEGRAF, celebrado en Bilbao el 11 de septiembre de 2026 bajo el lema "Design for One Health".

Desde hace más de tres décadas, INGEGRAF constituye un valioso foro para el intercambio de conocimientos, experiencias e ideas innovadoras entre profesorado universitario, personal investigador y profesionales del ámbito de la Ingeniería Gráfica. Esta trigésima quinta edición da continuidad a dicha trayectoria, abordando al mismo tiempo uno de los grandes retos de la sociedad contemporánea: la necesidad de replantear la forma en que diseñamos, desarrollamos, fabricamos, utilizamos y gestionamos los productos, sistemas, infraestructuras y entornos que configuran nuestro mundo.

El enfoque One Health (Una Sola Salud) nos recuerda que la salud humana, la salud animal y la salud del planeta están profundamente interrelacionadas. En consecuencia, el diseño no puede entenderse como una actividad exclusivamente técnica o aislada. Cada decisión de diseño genera efectos que trascienden el propio producto y repercuten en las dimensiones ambiental, social, económica y sanitaria. En este contexto, la Ingeniería Gráfica desempeña un papel fundamental. Mediante el modelado digital, la visualización, la simulación, el desarrollo de productos, las tecnologías avanzadas de fabricación, el análisis del ciclo de vida y nuevas herramientas como la inteligencia artificial, nuestra disciplina puede contribuir al desarrollo de soluciones más seguras, sostenibles, resilientes e inclusivas.

Los trabajos recopilados en estas Actas reflejan la diversidad, el dinamismo y la excelencia de la investigación y de las actividades docentes desarrolladas en nuestro ámbito de conocimiento. Asimismo, ponen de manifiesto cómo la innovación en Ingeniería Gráfica y Diseño puede favorecer la transición hacia prácticas más responsables y contribuir a afrontar los complejos desafíos globales mediante la colaboración interdisciplinar.

Deseamos expresar nuestro más sincero agradecimiento a todas las personas autoras, revisoras, integrantes de los Comités Científico y Organizador, así como a las instituciones cuyo compromiso y dedicación han hecho posible la celebración de este congreso. Nos sentimos especialmente orgullosos de haber dado la bienvenida a todas las personas participantes en Bilbao, una ciudad en la que confluyen el patrimonio industrial, la innovación tecnológica, la cultura y un firme compromiso con la sostenibilidad.

Confiamos en que este congreso haya constituido un espacio inspirador para el intercambio de ideas, la colaboración y la generación de nuevo conocimiento, reforzando así nuestro compromiso compartido con el diseño de un futuro más saludable para las personas y para el planeta.

Comité Organizador de la del 35.º Congreso Técnico Internacional de INGEGRAF

Hitzaurrea

Plazer handia da Bilbon 2026ko irailaren 11n ospatu den INGEGRAFen 35. Nazioarteko Konferentzia Teknikoaren aktak aurkeztea, “Design for One Health” lelopean.

Duela hiru hamarkada baino gehiagotik, INGEGRAF foro baliotsua da unibertsitateko irakasleen, ikertzaileen eta Ingeniaritza Grafikoaren eremuko profesionalen artean ezagutzak, esperientziak eta ideia berritzaileak trukatzeko. Hogeita hamabosgarren edizio honek jarraipena ematen dio ibilbide horri, eta, aldi berean, gizarte garaikidearen erronka handienetako bati heltzen dio: gure mundua osatzen duten produktuak, sistemak, azpiegiturak eta inguruneak diseinatzeko, garatzeko, fabrikatzeko, erabiltzeko eta kudeatzeko modua birplanteatzeko beharrari.

One Health (Osasun Bakarra) ikuspegiak gogorarazten digu giza osasuna, animalien osasuna eta planetaren osasuna elkarri lotuta daudela. Ondorioz, diseinua ezin da jarduera tekniko edo isolatu moduan ulertu. Diseinu-erabaki bakoitzak produktua bera gainditzen duten eta ingurumen-, gizarte-, ekonomia- eta osasun-dimentsioetan eragina duten efektuak sortzen ditu. Testuinguru horretan, Ingeniaritza Grafikoak funtsezko eginkizuna betetzen du. Modelatze digitala, bistaratzea, simulazioa, produktuen garapena, fabrikazioko teknologia aurreratuak, bizi-zikloaren analisia eta adimen artifiziala bezalako tresna berrien bidez, gure diziplinak konponbide seguruagoak, jasangarriagoak, erresilienteagoak eta inklusiboagoak garatzen lagun dezake.

Akta hauetan bildutako lanek gure jakintza-esparruan garatutako ikerkuntzaren eta irakaskuntza-jardueren aniztasuna, dinamismoa eta bikaintasuna islatzen dute. Era berean, agerian uzten dute Ingeniaritza Grafikoaren eta Diseinuaren arloko berrikuntzek praktika arduratsuagoetarako trantsizioan eta erronka global konplexuei aurre egiten lagun dezaketela, diziplinarteko lankidetzaren bidez.

Eskerrik beroenak eman nahi dizkiegu Batzorde Zientifiko eta Antolatzaileetako kideei, egileei, zuzentzaileei, bai eta kongresu hau egiteko konpromisoa eta ardura hartu duten erakundeei ere. Bereziki harro gaude Bilbon parte hartu duten pertsona guztiei ongietorria eman diegulako, industria-ondarea, berrikuntza teknologikoa, kultura eta jasangarritasunarekiko konpromiso sendoa biltzen dituen hirian.

Kongresu hau ideiak trukatzeko, lankidetzan aritzeko eta ezagutza berria sortzeko gune inspiratzailea izango delakoan gaude, eta, horrela, pertsonentzat eta planetarentzat etorkizun osasuntsuagoa diseinatzeko konpromisoa indartuko dugu.

INGEGRAFen 35. Nazioarteko Kongresu Teknikoaren Batzorde Antolatzailea

Geometric fitting of column cross-sections from noisy point clouds using constrained minimization

Patricia González-Cabaleiro, Lucía Díaz-Vilariño*, Antonio Fernández

CINTECX, Universidade de Vigo, GeoTECH Group, 36310 Vigo, Spain

* e-mail: lucia@uvigo.gal

Abstract: This paper presents a Scan-to-BIM methodology for the precise geometric characterization of structural columns from 3D point clouds. Despite the importance of columns for structural monitoring and Digital Twin modelling, their automated extraction is frequently hindered by noise, outliers, and partial occlusions caused by intersections with beams or masonry. To address these challenges, we propose a constrained minimization fitting approach grounded on Manhattan-World assumptions. The core methodology models column cross-sections as axis-aligned rectangles, where boundary parameters are optimised through Sequential Least-Squares Quadratic Programming (SLSQP). This process integrates linear constraints derived from percentile ranges and a local nearest-neighbour density criterion to filter outliers effectively. Validation across residential sites in Lugo and Bilbao yielded a fitting error of 4.0-4.5 mm, with dimensional deviations of 2.5-5.0 cm, compared to on-site measurements. These results indicate the method's robustness in extracting key features for Digital Twin modelling and structural monitoring. This automated workflow effectively transforms cluttered spatial data into semantically rich components, supporting advanced urban health assessments and volumetric analysis.

Keywords: *Scan-to-BIM, as-built modelling, structural element segmentation, SLSQP.*

1. INTRODUCTION

Scan-to-BIM workflows transform raw 3D point cloud data of existing buildings into semantically rich Building Information Models (BIM), enabling accurate digital representations for design, maintenance, and analysis [1,2]. These workflows typically involve segmentation, classification, and geometric reconstruction, where accurately parametrising structural elements, especially columns, is essential for reliable modelling, volumetric analysis, and applications such as One Health urban models, linking the built environment with human and environmental health. This process is particularly relevant for existing infrastructure, where missing documentation and unrecorded modifications, combined with labour-intensive and error-prone manual surveys, highlight the need for automated Scan-to-BIM approaches [3,4]. However, point cloud data capture only visible surfaces, and occlusions often cause columns and other concealed elements to be neglected [5,6], emphasising the need for robust methods capable of accurately extracting and parametrising columns for precise as-built BIMs and reliable structural analysis.

Reconstructing columns in Scan-to-BIM workflows requires extracting key geometric parameters such as cross-sectional dimensions, height, orientation, and alignment. Previous studies have achieved this for isolated columns using surface-based or volumetric approaches with bounding shapes, axis-aligned extents, or profile extrusions [7-9]. Surface-based methods [7] typically segment the point cloud into planar or curved patches and fit geometric primitives directly to these surfaces, enabling the estimation of dimensions and orientation. Volumetric approaches [8,9], in contrast, construct solid representations of the column by extruding 2D profiles or using voxel-based approximations, which allows computation of height, cross-section, and alignment parameters even when partial occlusions exist. Fully or partially occluded columns remain challenging, as existing methods rarely provide reliable parameter estimation under severe data sparsity. Some studies combine geometric analysis with machine learning, applying clustering and normal vector analysis on horizontal layers to infer height, orientation, and alignment even when intersected by beams or walls [10-12], while per-point descriptors and dynamic graph convolutions refine local geometry in complex or partially occluded environments [13,14]. These limitations highlight the need for formulations that can operate directly on incomplete geometric observations.

To address these challenges, within our complete Scan-to-BIM workflow, this work formulates footprint extraction as a constrained geometric optimization problem on 2D projections. The proposed approach introduces a side-constrained representation that explicitly encodes geometric consistency for rectangular cross-sections, enabling stable recovery from incomplete point cloud observations. The optimization is solved using Sequential Least Squares Programming (SLSQP) as a numerical tool, and the resulting geometry is evaluated using fitting and dimensional error metrics.

2. METHOD

This section presents the proposed methodology for estimating column cross-sections from segmented point clouds, structured into three stages: pre-processing (Figure 1.a), constrained minimization (Figure 1.b) and fitting verification (Figure 1.c).

2.1. Pre-processing

The input of the proposed workflow consists of a set of M segmented point clouds $\{P_k\}_{k=1}^{M}$, previously aligned with the principal building main axes according to the Manhattan-World assumption adopted in this work, each corresponding to an individual column and defined as $P_k = \{(x_i, y_i, z_i) \in \mathbb{R}^3\}_{i=1}^{N_k}$ [15]. For each column candidate, a region of interest (ROI) is defined as a vertical segment centred along the column's height with a predefined thickness (Figure 1.a). This step focuses the analysis on the main portion of the column and reduces the influence of geometric irregularities occurring at the base or top.

To enhance robustness and prevent sparse noise from biasing the estimation of column boundaries, a nearest-neighbour filtering is applied to identify and remove isolated points that do not belong to the main structural surface. Finally, the filtered 3D points are projected onto the XY plane as 2D points, effectively transforming the 3D data into a 2D footprint estimation task, as shown in Figure 1.a.

2.2. Constrained minimization-based approach

The column cross-section is modelled as an axis-aligned rectangle defined by four parameters, $\Theta = [x_{left}, x_{right}, y_{bottom}, y_{top}]$ (orange dashed rectangle in Figure 1.b), representing the rectangle edges enclosing the column footprint. To determine the optimal geometry, the model minimizes the sum of squared minimum distances from each projected point p_i to its closest rectangle side, as formulated in equation (1). To ensure a precise fit, the optimization considers only points $\mathcal{P}$, whose minimum distance to the rectangle boundary is below a threshold $d_{\max}$. This prevents points belonging to one face of the column from erroneously influencing the optimization of other sides while simultaneously protecting the fit from being dominated by outliers.

$$\min \sum_{p_i \in \mathcal{P}} \left[\min \left(|x_i - x_{left}|, |x_i - x_{right}|, |y_i - y_{bottom}|, |y_i - y_{top}| \right) \right]^2$$

To ensure a robust and realistic fit, the optimization is strictly bounded and constrained. Initial bounds for the variables are derived from percentile ranges of the projected coordinates, which provides a stable starting region and minimizes sensitivity to extreme values. Within these bounds, the optimization is further subject to linear constraints on both position (grey rectangle in Figure 1.b), equation (2), and dimensions (pink lines in Figure 1.b), equation (3), ensuring rectangle aligns with the observed distribution while maintaining structural proportions.

$$\begin{aligned} x_{min} &\le x_{left} \le x_{max} \\ x_{min} &\le x_{right} \le x_{max} \\ y_{min} &\le y_{top} \le y_{max} \\ y_{min} &\le y_{bottom} \le y_{max} \end{aligned} \qquad (2)$$

$$\begin{aligned} w_{min} &\le x_{right} - x_{left} \le w_{max} \\ w_{min} &\le y_{top} - y_{bottom} \le w_{max} \end{aligned} \qquad (3)$$

The resulting constrained optimization problem is solved using Sequential Least-Squares Quadratic Programming (SLSQP) [16], which efficiently manages nonlinear objectives with linear constraints while ensuring convergence within the feasible region.

2.3. Fitting verification

Following the optimization, the resulting rectangle is evaluated to assess geometric consistency with the observed point cloud. This step shifts from global distance minimization to a side-assignment procedure, where points are assigned to one of the four rectangle sides based on a proximity tolerance (green: left, purple: top, blue: right and yellow: bottom; Figure 1.c). If a side has insufficient point support, points are reassigned to adjacent sides.

Once the point sets N_j for each side $j \in \{left, right, top, bottom\}$ are finalised, the edge-wise residual error (e_j) is computed as the mean orthogonal distance between the assigned points and the corresponding rectangle side by s_j, as given in equation (4). Here, $|N_j|$ denotes the number of points assigned to side j, and c_i denotes the coordinate of point i along the axis orthogonal to side j (i.e., the x-coordinate for vertical sides and the y-coordinate for horizontal sides). The overall performance is summarised by the mean fitting error ($\bar{e}$) in equation (5), providing a compact measure of how closely the optimized rectangle aligns with the actual column boundaries.

Complementing the geometric fitting, the method evaluates the dimensional accuracy of the fitted cross-section by comparing the final optimized dimensions against ground-truth measurements obtained on-site. This evaluation is performed independently for each principal axis to allow for a decoupled assessment. The dimensional error Δ for a given axis x or y is defined in equation (6) as the absolute difference between the real measurement (D) and the fitted value (d).

$$e_j = \frac{1}{|N_j|} \sum_{i \in \square_j} |c_i - s_j| \quad (4) \qquad \bar{e} = \frac{1}{4} \sum_{j=1}^{4} e_j \quad (5) \qquad \Delta = | D - d | \quad (6)$$

3. RESULTS

The performance of the proposed constrained minimization method was evaluated on three residential buildings. The first site, located in Lugo, consists of two towers: Case L2 has 2 storeys with 7 columns each, while Case L1 has 5 storeys with 24 columns per level. The second site in Bilbao, Case B, includes 5 storeys; the ground floor (B_0) contains 10 columns, whereas levels B_1 to B_4 each contain 8 columns. Fitting precision was high, with median errors between 4.0 and 4.5 mm (Figure 2.b), indicating stable convergence of the optimization towards observed point cloud surfaces. Dimensional accuracy (Figure 2.a) showed broader variance (2.5–5.0 cm) and anisotropy, particularly between X and Y axes.

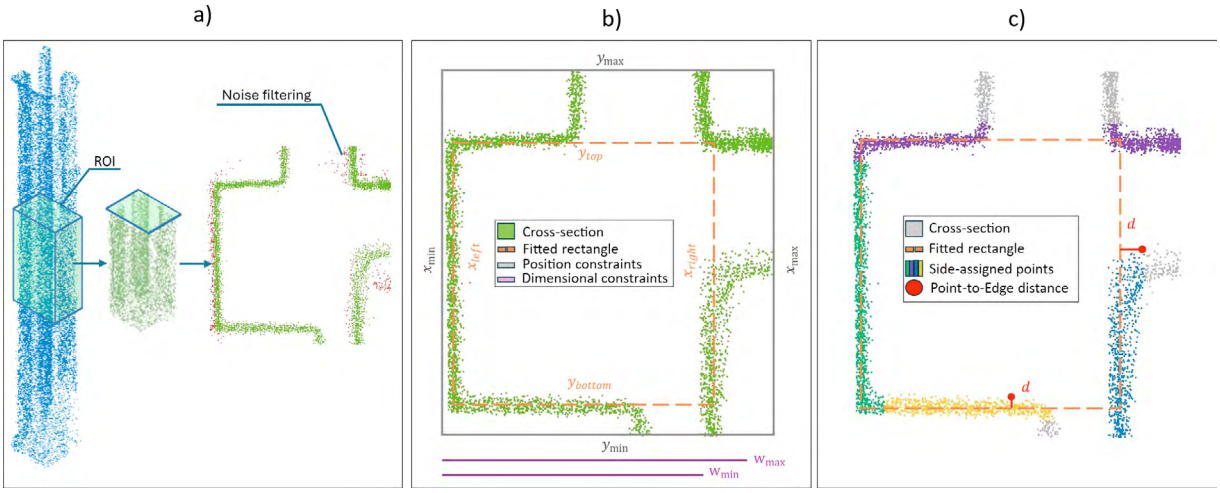


FIG. 1

Methodology: a) Pre-processing, b) Constrained minimization, and c) Verification

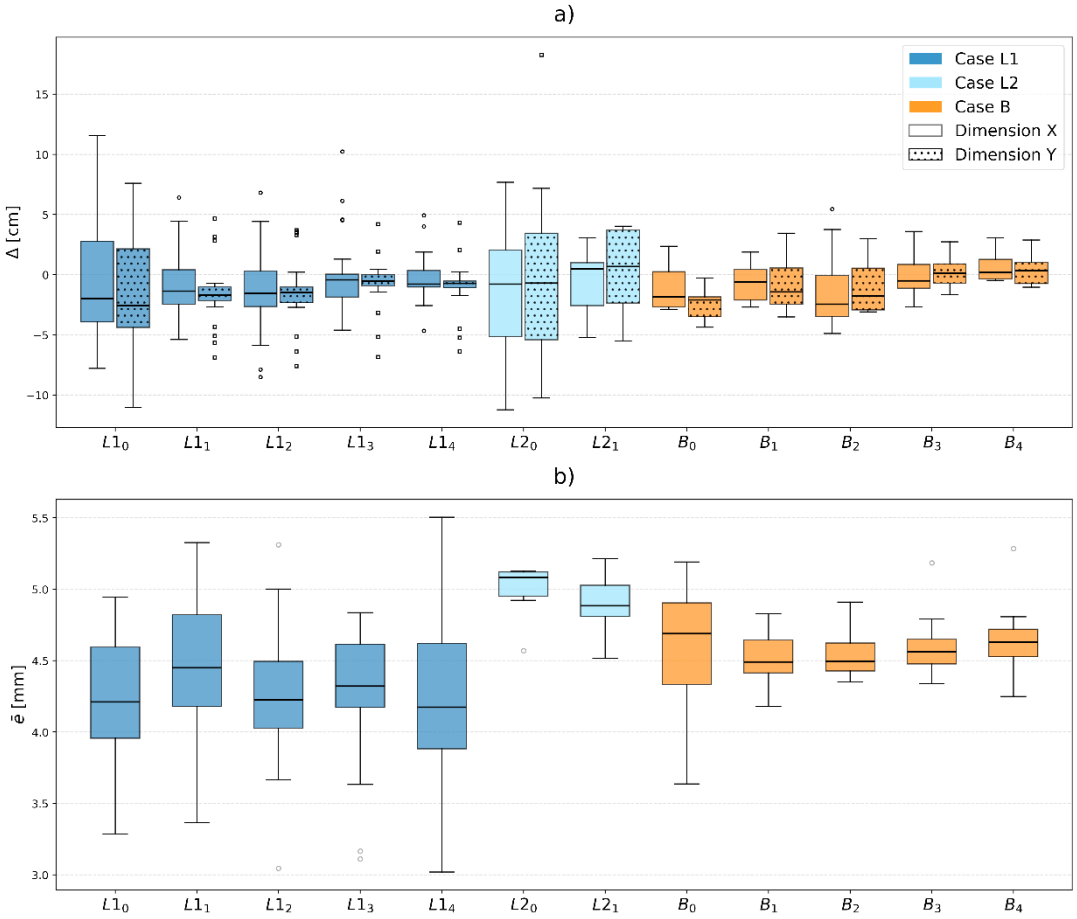


FIG. 2

Error boxplots of all storeys for all case studies (subscripts indicates the corresponding level): a) Dimensional error (Δ) for X and Y axes and b) Mean fitting error ($\bar{e}$)

These discrepancies can be explained by several factors. Conventional surveying practices often rely on a limited number of representative measurements per floor, assuming geometric uniformity that rarely holds in practice. As evidenced in the high-resolution results in Figure 3, local deviations due to construction tolerances and formwork deformations are captured by the proposed method but are typically neglected in manual surveys.

In addition, severe data sparsity caused by occlusions reduces the geometric constraints available for reliable boundary estimation, occasionally leading to deviations in the reconstructed footprint despite low point-wise fitting error. Finally, an additional source of variability comes from the inherent noise of the mobile laser scanner system (±3 mm range noise, ±10 mm nominal precision) contributing to the observed dimensional discrepancies.

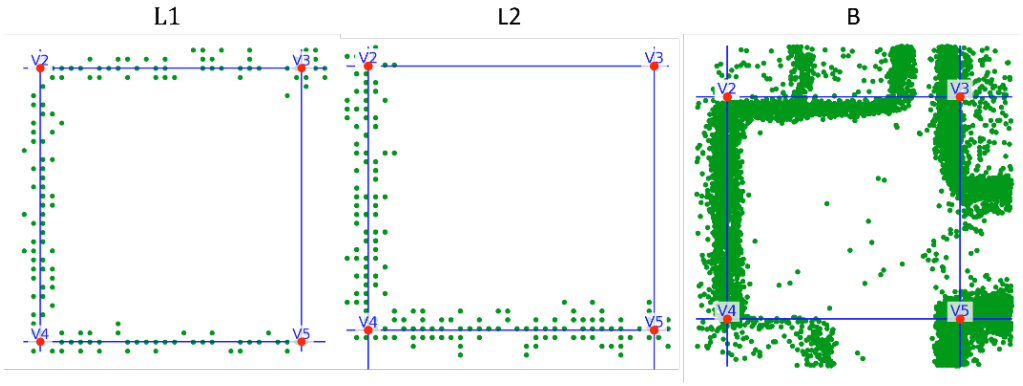


FIG. 3
Examples of fitted rectangles on three different case studies

Overall, the proposed method provides a more detailed and consistent representation of column geometry compared to traditional surveying practices, enabling the capture of as-built variability in complex residential environments.

4. CONCLUSIONS

This study presents a constrained optimization approach for the automated reconstruction of column geometries from point clouds in real-world residential environments. By reducing the 3D data to a 2D footprint through vertical ROI isolation and applying an SLSQP-based fitting, the method achieves a high level of geometric fidelity. The experimental results, validated across three distinct residential sites, consistently showed a mean fitting error of 4.0 to 4.5 mm, confirming that the algorithm accurately aligns with the actual physical surfaces of the structural elements.

A key finding of this research is the discrepancy between automated measurements and traditional manual surveys. While deviations of 2.5 to 5.0 cm were recorded, these differences highlight the limitations of manual extrapolation and the impact of construction tolerances. However, the study also identified that extreme data sparsity due to occlusions remains a physical constraint that can affect dimensional accuracy despite a low geometric fitting error.

The proposed fitting algorithm operates on individual column point clouds. Therefore, rotated columns can be processed after estimating their dominant orientation and locally aligning the point cloud prior to optimization. The current formulation assumes such a step, reflecting a Manhattan-world constraint, and is independent of the global building orientation. However, this assumption limits applicability to orthogonal layouts. Extending the method to automatically estimate orientations and handle non-rectangular cross-sections remains future work.

Acknowledgements: This work has been supported by the Spanish Ministry of Science, Innovation and Universities through the ALLEGRO project Ref. PID2021-123475OA-I00 funded by MCIN/ AEI /10.13039/501100011033/ and by FEDER "Una manera de hacer Europa". P. González-Cabaleiro acknowledges the Grant PRE2024-PRAZA 10 for the training of predoctoral researchers, associated with the project PID2024-157803OB-I00 funded by MICIU/AEI/10.13039/501100011033. The statements made herein are solely the responsibility of the authors.

REFERENCES

[1] Yang, T., Zou, Y., Castillo, E. del R., Hou, L., Zhong, J.: Enhancing Scan-to-BIM for reinforced concrete bridges using point cloud completion techniques. Automation in Construction 181, 106606 (2026).

[2] Luo, J., Yang, Z., Shi, P., Ye, Q.: Indoor scan-to-BIM automation: From mobile perception to 3D building modelling. Automation in Construction 182, 106731 (2026).

[3] Algadi, A., Uluutku, B., Cano, J.A., Walters, L., Alqurashi, I., Luleci, F., Catbas, F.N.: Digital twin-oriented generation of structural data and models with LiDAR scan point clouds. Journal of Infrastructure Preservation and Resilience 6, 32 (2025).

[4] Jarząbek-Rychard, M., Maas H.-G.: Modeling of 3D geometry uncertainty in Scan-to-BIM automatic indoor reconstruction. Automation in Construction 154, 105002 (2023).

[5] Xiong, X., Adan, A., Akinci, B., Huber, D.: Automatic creation of semantically rich 3D building models from laser scanner data. Automation in Construction, 31, 325-337 (2013).

[6] Truong-Hong, L., Lindenbergh, R.: Extracting structural components of concrete buildings from laser scanning point clouds from construction sites. Advanced Engineering Informatics, 51, 101490 (2022).

[7] Romanengo, C., Raffo, A., Biasotti, S., Falcidieno, B., Fotis, V., Romanelis, I., Psatha, E., Moustakas, K., Sipiran, I., Nguyen, Q.-T., Chu, C.-B., Nguyen-Ngoc, K.-N., Vo, D.-K., To, T.-A., Nguyen, N.-T., Le-Pham, N.-Q., Nguyen, H.-D., Tran, M., Qie, Y., Anwer, N. SHREC 2022: Fitting and recognition of simple geometric primitives on point clouds. Computers & Graphics 107, 32-49 (2022).

[8] Nurunnabi, A., Sadahiro, Y., Laefer, D.F.: Robust statistical approaches for circle fitting in laser scanning three-dimensional point cloud data. Pattern Recognition 81, 417-431 (2018).

[9] Son, H., Kim, C.: Semantic as-built 3D modelling of structural elements of buildings based on local concavity and convexity. Advanced Engineering Informatics 34, 114-124 (2017).

[10] Mirzaei, K., Arashpour, A.P.M., Asadi, E., Masoumi, H., Mahdiyar A., Gonzalez V.: End-to-end point cloud-based segmentation of building members for automating dimensional quality control. Advanced Engineering Informatics 55, 101878 (2023).

[11] Romero-Jarén, R., Arranz J.J.: Automatic segmentation and classification of BIM elements from point clouds. Automation In Construction 124, 103576 (2021).

[12] Mirzaei, K., Arashpour, M., Asadi, E., Masoumi, H., Li H.: Automatic generation of structural geometric digital twins from point clouds. Scientific Reports 12(1), 22321 (2022).

[13] Son, H.: Semantic as-built 3D modeling of structural elements of buildings based on local concavity and convexity. Advanced Engineering Informatics 34, 114-124 (2017).

[14] Kim, H., Kim, C.: 3D as-built modeling from incomplete point clouds using connectivity relations. Automation in Construction 130, 103855 (2021).

[15] González-Cabaleiro, P., Albadri, M.S.A., Fernández, A., Vilariño, L.D.: Revealing the Hidden Framework: Reconstructing Occluded Structural Elements from Indoor Point Clouds. SSRN Preprint, http://dx.doi.org/10.2139/ssrn.5771682 (2026).

[16] The SciPy Community, https://docs.scipy.org/doc/scipy/reference/optimize.minimize-slsqp.html, last accessed 2026/04/09.

Multiplayer Virtual Reality for Collaborative Product Evaluation in Industrial Design: Comparing Group and Individual Assessments

Almudena Palacios-Ibáñez*, Carlos García-García, Laura Ruiz-Pastor, Francisco Felip-Miralles, Julia Galán

Universitat Jaume I, Avinguda de Vicent Sos Baynat, s/n, 12006 Castelló de la Plana, Castelló

* e-mail: almudena.palacios@uji.es

Abstract: Virtual Reality (VR) has become increasingly relevant in industrial design for evaluating digital prototypes. However, most studies focus on individual experiences, despite the inherently collaborative nature of design. In this context, this study compares a synchronous collaborative approach where groups of three users interacted in a shared multiplayer virtual environment with an individual approach for product evaluation. Here, participants assessed a children's rocking toy using a Semantic Differential composed by 12 scales while additional measures were collected—i.e., confidence in responses, evaluation time, presence (IPQ), and workload (NASA-TLX). Results revealed no significant differences between conditions in product evaluation or confidence levels. However, evaluation time was significantly longer in the group condition, with NASA-TLX also indicating higher temporal demand in this setting. In contrast, participants reported a greater sense of presence during the collaborative experience. Overall, these findings suggest that, although VR multiplayer environments may increase decision-making time, it does not alter evaluation outcomes while enhancing the sense of presence, thereby supporting its potential to enrich collaborative design processes.

Keywords: *Virtual Reality, Collaborative Experience, Multiplayer Interaction, Product Evaluation, Semantic Differential, Immersive Environments.*

1. INTRODUCTION

In recent years, digital transformation has reshaped how people collaborate, enabling work and decision-making without sharing a physical space [1]. Despite the use of videoconferencing and collaborative tools, these solutions often present limitations for tasks involving spatial understanding and interaction with three-dimensional objects [2]. For instance, the incorporation of physical presence and natural interaction in design activities can enhance communication and increase engagement [3], what may improve the perception of product attributes such as form, scale, and detail.

In this context, immersive technologies foster co-presence and support natural interaction with virtual objects by enabling virtual shared environments [4], making Virtual Reality (VR) a promising solution for remote collaborative design activities. Additionally, advances in technology have made multiplayer VR systems more accessible, opening new opportunities for collaborative work in design processes.

Considering that product evaluation is a key stage in industrial design [5] —traditionally conducted individually or in co-located settings—, multiplayer VR environments now allow remote collaborative evaluation of Virtual Prototypes (VPs). However, while VR has been widely studied for individual evaluation, less is known about how collaborative dynamics in Virtual Environments (VEs) influence user perception and judgment.

Therefore, this study investigates the role of collaboration in immersive product evaluation by comparing individual and group-based assessments in a multiplayer VR environment, aiming to better understand how social context affects perception and decision-making.

2. AIM AND HYPOTHESES

The aim of this study is to investigate how the evaluation of a product is influenced by the social context in which it is performed, specifically comparing individual and multiplayer conditions within an immersive VR environment. To this end, participants assessed a VP using a Semantic Differential [6], while additional measures were collected to capture different aspects of the user experience, including confidence in responses, evaluation time, perceived presence, and cognitive workload.

The study seeks to determine whether collaborative interaction in a shared VE leads to differences in product perception and evaluation outcomes compared to individual assessment. Furthermore, it explores how the presence of other users may influence decision-making processes, subjective confidence, and overall user experience. Based on this, several hypotheses are proposed. Product evaluation (H1) and confidence in the response (H2) may differ between conditions, reflecting the influence of social interaction. Differences are also anticipated in evaluation time, as collaborative settings may prolong decision-making processes (H3). In addition, higher levels of presence are expected in the multiplayer condition due to the shared immersive experience (H4). Finally, perceived workload may differ between conditions, potentially increasing in collaborative environments due to social interaction (H5).

3. METHODS AND MATERIALS

The study followed a within-subject design with two experimental conditions: (1) individual and (2) multiplayer evaluation. Each participant completed both conditions—counterbalanced across participants to control for order effects—separated by a one-week interval to reduce potential memory effects. In the multiplayer condition, participants evaluated the product collaboratively in groups of three users within the same VE, whereas in the individual condition, participants performed the evaluation alone, without the presence or influence of other users.

A total of 15 participants were included—who were required to be of legal age—, as this study was designed as a pilot to explore preliminary effects. The sample included 53,33% female and 46.67% male participants, with a mean age of 31,40 years. Regarding prior experience with VR, 13% reported no previous experience, 27% had occasional experience, and 60% indicated frequent use of VR systems.

The experimental application was developed using Unity (version 6000.3.8f1) with some integrated SDKs to enable the required functionalities. In this sense, the Meta All-in-One SDK (version 85.0.0) was used to ensure compatibility with the HMDs, including interaction and system integration. Additionally, Photon Fusion (version 2.0.9) was implemented for network synchronization, and Photon Voice 2 (version 2.62) was used to enable real-time voice communication between participants. Moreover, the application was displayed in a Meta Quest Pro device, an HMD that provides an immersive VR experience with a resolution of 1800 × 1920 pixels per eye, a refresh rate of up to 90 Hz, and a wide field of view.

The product selected for the evaluation task was a virtual model of a rocking horse toy (Fig. 1.a). This product was chosen due to its combination of functional and aesthetic attributes, making it suitable for assessment using semantic scales. The 3D model was obtained from CGTrader, while materials were created and adjusted within Unity, using textures from AmbientCG. Furthermore, the VE (Fig. 1.a) was designed as a neutral space to avoid external influences on product perception. It consisted of an empty room with a floating round table placed in front of the user. On the table, a virtual button allowed participants to initiate the evaluation process. Once activated, the product and the evaluation interface appeared simultaneously. The product could be freely inspected and manipulated by the user, i.e., the user could pick up the product with their hands and rotate it in any position in space, as well as move it around within the environment. However, gravity was disabled to ensure consistency and avoid synchronization issues in the multiplayer condition. Furthermore, participants were represented by avatars, allowing visibility of other users in the shared VEs during the multiplayer sessions.

3.1. Procedure

Participants were scheduled in groups of three, regardless of the condition they were assigned to perform first. Upon arrival, they were welcomed and provided with a brief explanation of the experiment. Prior to the main task, participants received instructions on how to interact within the VE to ensure familiarity with the system.

In the multiplayer condition (Fig. 1.b and 1.c), one participant was assigned the role of leader. This participant was responsible for entering the responses in the Semantic Differential questionnaire and navigating between scales. This procedure ensured consistent data collection across participants. The remaining participants contributed to the evaluation and were responsible for reporting their confidence in the responses.

During the task, participants observed and evaluated the VP using the provided interface. Interaction with the system was performed using the VR controllers. Once the evaluation was completed, participants removed the HMD and proceeded to complete the post-experiment questionnaires. Finally, they were debriefed and thanked for their participation.



a b c

FIG. 1

Participants interacting within the VE under the multiplayer condition: (a) virtual scene, (b) real-world setting alongside the VE, and (c) real-world setting with two of the three users

3.2. Measures

Product evaluation was conducted using a Semantic Differential composed of 12 attributes (Table 1). Additionally, participants were asked to rate their confidence in each response. These were measured on a 7-point Likert-type scale ranging from –3 to 3, with 0 representing a neutral value. Additionally, the total time required to complete the evaluation task was also recorded.

Before the VR experience, participants completed a demographic questionnaire, and after each session, participants completed the NASA Task Load Index (NASA-TLX) [7] to evaluate perceived workload, and the iGroup Presence Questionnaire (IPQ) [8] to assess the level of presence experienced in the VE. Finally, these data were analysed using Jamovi 2.7.18 [9] and Excel.

4. RESULTS

The Shapiro–Wilk normality test indicated that the different datasets did not meet parametric assumptions, leading to the use of non-parametric methods. Accordingly, the Wil-

coxon signed-rank test was used to both the Semantic Differential measures and confidence in the response (Table 1), total evaluation time, NASA-TLX and IPQ.

In this context, although SD2 yielded a p-value below .05, it was not considered statistically significant after applying the Holm-Bonferroni correction ($\alpha = .004$). Likewise, no significant differences were found in response confidence between conditions. In contrast, evaluation time was significantly affected by the experimental condition ($W = 0.00$, $p < .001$), being higher during the multiplayer experience ($M_{INDIVIDUAL} = 170$ seconds; $M_{MULTIPLAYER} = 655$ seconds).

Regarding the NASA-TLX, the Wilcoxon test revealed significant differences for the "Temporal demand" subscale ($W = 0.00$, $p = .003$), being higher during the multiplayer experience ($M_{INDIVIDUAL} = 2.07$; $M_{MULTIPLAYER} = 3.70$).

Finally, the results of the IPQ indicated moderate to high levels of perceived presence in both conditions according to the scale by Melo *et al.* [10]. At the individual condition, overall presence was rated as very good (M = 4.27, grade B), while spatial presence (M = 4.31, grade D) and involvement (M = 3.88, grade D) evaluated as marginal. In contrast, experienced realism received a lower rating (M = 2.72, grade E), indicating an unsatisfactory level. At the group condition, overall presence was rated as excellent (M = 4.93, grade A), with spatial presence reaching a very good level (M = 4.74, grade B) and involvement considered satisfactory (M = 4.18, grade C). However, experienced realism again obtained the lowest score (M = 2.57, grade F), indicating a not acceptable level.

Table 1

Wilcoxon test for the Semantic Differential and confidence in the response between experimental conditions

	Semantic scales		Semantic Differential		Confidence in the response	
			Statistic	p	Statistic	p
SD1	Small	Large	24.00	.901	14.00	1.000
SD2	Uncomfortable	Comfortable	62.00	.009	8.00	.152
SD3	Unstable	Stable	24.00	.750	7.50	.590
SD4	Boring	Fun	44.50	.690	56.00	.033
SD5	Difficult to use	Easy to use	6.00	.850	2.00	.345
SD6	Dangerous	Safe	29.00	.454	25.50	.763
SD7	Traditional	Innovative	10.00	.072	0.00	.089
SD8	Industrial	Handmade	42.50	.857	11.00	.178
SD9	Unsustainable	Sustainable	10.50	.084	23.00	1.000
SD10	Common	Distinctive	16.00	.792	27.00	.608
SD11	Unpopular	Popular	7.00	.069	13.50	.275
SD12	Economical	Exclusive	8.50	.386	0.00	.012

5. DISCUSSION

Firstly, results in Table 1 indicate that collaboration does not alter product evaluation or response confidence in VR, suggesting that participants' judgments remained stable regardless of the presence of others. This may be partly explained by the participants' background (most of them had a background in industrial design, which constitutes a limitation of this study). In this context, people evaluate design depending on their expertise and experience [11], hence, this may have contributed to more consistent and internally grounded evaluations, as individuals with domain-specific expertise tend to give evaluations closer to the true score of a design [12]. As a result, H1 and H2 are rejected.

Secondly, the Wilcoxon test showed significantly longer evaluation times in the multiplayer setting, supporting H3. This pattern is further supported by the NASA-TLX results, where the "Temporal demand" dimension was also significantly higher in the collaborative condition. This increase may be partly explained by the time required for external users to integrate into a team, as suggested by Hanahara (2021). In this context, users appeared to need time to engage with one another and establish a smoother interaction flow, particularly when they were not previously acquainted.

Regarding H4, higher levels of presence were expected in the multiplayer condition due to the shared immersive experience. The IPQ results support this assumption, hence, H4 is accepted. In this condition, participants could observe fully embodied avatars of their colleagues, which has been shown to influence the perception of "being there" [14]. At the same time, although "Experienced realism" in the IPQ was slightly lower in the multiplayer condition (non-significant), this may be related to the relatively low-fidelity, cartoon-like design of the avatars.

Finally, H5 proposed that perceived workload would differ between conditions, potentially increasing in collaborative environments due to social interaction. However, only the third item of the NASA-TLX showed significant differences, not supporting H5. This suggests that participants did not perceive the task as more cognitively demanding, but rather as more time constrained. One possible explanation is that the collaborative process redistributed cognitive effort across participants, reducing individual workload while increasing the time required to reach a shared decision.

These findings have relevant implications for real-world collaborative design workflows. Multiplayer VR environments such as the one proposed here could support distributed design teams in conducting synchronous product evaluations without physical co-location. Furthermore, the absence of significant differences between conditions suggests that multiplayer VR could be reliably integrated into collaborative product review pipelines. Future implementations could explore its use in cross-disciplinary or geographically distributed teams, where immersive co-presence may be particularly valuable.

6. CONCLUSIONS

In conclusion, the findings indicate that product evaluation in VR does not significantly differ between individual and collaborative contexts in terms of perception and confidence. However, the collaborative condition leads to longer evaluation times and higher tempo-

ral demand, suggesting that group interaction slows down decision-making processes. At the same time, participants reported a stronger sense of presence in the multiplayer environment. Overall, these results highlight that collaborative VR can enrich the design evaluation experience without altering outcomes, although it introduces more time-intensive dynamics in decision-making.

Acknowledgements: This work has been developed within the framework of the research project UJI-2025-01, funded by Universitat Jaume I.

REFERENCES

[1] Arkouli, Z., Tompoulidis, I., Kontos, M., Michalos, G., Makris, S.: Collaborative human-centered design of manufacturing tasks: a multi-user immersive VR experience. Procedia CIRP. 128, 597-602 (2024). https://doi.org/10.1016/j.procir.2024.07.056.

[2] Anton, D., Kurillo, G., Bajcsy, R.: User experience and interaction performance in 2D/3D telecollaboration. Future Generation Computer Systems. 82, 77-88 (2018). https://doi.org/10.1016/j.future.2017.12.055.

[3] Sateei, S., Roupé, M., Johans-Son, M.: Collaborative Design Review Sessions in Virtual Reality: Multi-scale and Multi-user. In: Proceedings of the International Conference on Computer-Aided Architectural Design Research in Asia. pp. 29-38. The Association for Computer-Aided Architectural Design Research in Asia (2022). https://doi.org/10.52842/conf.caadria.2022.1.029.

[4] Yin, J., Zheng, W., Wang, Y., Tong, X., Yan, Y.: A Comparison Study Understanding the Impact of Mixed Reality Collaboration on Sense of Co-Presence. In: 2025 IEEE Conference Virtual Reality and 3D User Interfaces (VR). pp. 580-590. IEEE (2025). https://doi.org/10.1109/VR59515.2025.00081.

[5] Bordegoni, M., Cugini, U., Ferrise, F., Graziosi, S.: A method for bringing user experience upstream to design: This paper intends to correlate human emotional response to product physical characteristics. Virtual Phys. Prototyp. 9, 181-194 (2014). https://doi.org/10.1080/17452759.2014.934574.

[6] Osgood, C.E., Suci, G.J., Tannenbaum, P.H.: The Measurement of Meaning. University of Illinois Press (1957).

[7] G. Hart, S., E. Staveland, L.: Development of NASA-TLX (Task Load Index): Results of Empirical and Theoretical Research. Advances in Psychology. 52, 139-183 (1988). https://doi.org/10.1016/S0166-4115(08)62386-9.

[8] Friedmann, F., Regenbrecht, H.: The Experience of Presence: Factor Analytic Insights. (2001).

[9] jamovi: The jamovi project, https://www.jamovi.org/, last accessed 2025/03/25.

[10] Melo, M., Gonçalves, G., Vasconcelos-Raposo, J., Bessa, M.: How Much Presence is Enough? Qualitative Scales for Interpreting the Igroup Presence Questionnaire Score. IEEE Access. 11, 24675-24685 (2023). https://doi.org/10.1109/ACCESS.2023.3254892.

[11] Lawson, B., Dorst, K.: Design Expertise. Routledge (2013). https://doi.org/10.4324/9781315072043.

[12] Hu, L., Boggess, M., Shepley, M.M.: Comparing Expert, Quasi-Expert, and Novice Evaluations of Award-Winning Design Products Using the Consensual Assessment Technique. Creat. Res. J. 35, 730-748 (2023). https://doi.org/10.1080/10400419.2022.2157591.

[13] Hanahara, S.: How collaboration between industrial designers and other members related to product development affect innovation and efficiency. Annals of Business Administrative Science. 20, 47-62 (2021). https://doi.org/10.7880/abas.0210127a.

[14] Suk, H., Laine, T.H.: Influence of Avatar Facial Appearance on Users' Perceived Embodiment and Presence in Immersive Virtual Reality. Electronics (Switzerland). 12, (2023). https://doi.org/10.3390/electronics12030583.

Advanced structural design and WAAM additive manufacturing as a strategy for sustainability in metallic components

Ainara Cervera, Virginia Uralde*, Fernando Veiga

Universidad Pública de Navarra, Campus de Tudela, Avenida Tarazona s/n, Tudela 31500 (Navarra), SPAIN

* e-mail: virginia.uralde@unavarra.es

Abstract: The transition towards more sustainable manufacturing systems is a major challenge for modern engineering. This study investigates the potential of combining advanced structural design strategies with Wire Arc Additive Manufacturing (WAAM) to reduce the environmental impact of metallic components. Specifically, the integration of topology optimization and lattice structures is evaluated in comparison with conventional CNC machining processes. The main objective is to assess the environmental performance of WAAM manufacturing relative to traditional subtractive machining in aluminum components. Functionally equivalent specimens were designed and manufactured using two different production routes: (i) CNC machining from a solid block and (ii) WAAM additive manufacturing with optimized geometry. Material consumption, energy use, and processing requirements were analyzed to identify the most influential factors affecting environmental performance. A cradle-to-gate Life Cycle Assessment (LCA) was conducted, including raw material extraction, manufacturing, and post-processing stages. The life cycle inventory was developed using GaBi software and its professional database, while environmental impacts were quantified through the Person Equivalent (PE) indicator. The results demonstrate substantial differences between the two manufacturing routes. CNC machining, starting from a 5 kg aluminum block to obtain a 3 kg component, generated a total environmental impact of 6.12 PE. In contrast, the WAAM process required only 2.95 kg of deposited material to produce an optimized 2.5 kg component, resulting in an impact of 3.87 PE, equivalent to a reduction of approximately 37%. Contribution analysis revealed that raw material extraction and processing accounted for 74.6% of the total environmental impact, highlighting material consumption as the dominant factor.

Keywords: *WAAM (Wire Arc Additive Manufacturing), Topology Optimization, Structural Design, Life Cycle Assessment (LCA), Sustainability.*

1. INTRODUCTION

The transition towards more sustainable production models is one of the key challenges currently facing the fields of engineering and advanced manufacturing. Against this backdrop, the manufacturing industry accounts for a significant proportion of global energy consumption and greenhouse gas emissions, which has driven the development of new technologies aimed at reducing environmental impact [1].

In particular, conventional subtractive machining processes, such as CNC machining, are inefficient in their use of materials, as they start with solid blocks that generate large volumes of waste. Various studies have shown that this approach entails a high environmental impact, particularly for materials such as aluminium, the primary production of which is highly energy-intensive [2].

In response to this problem, metal additive manufacturing has emerged as a promising alternative due to its ability to produce components through the controlled addition of material, significantly reducing waste. In particular, WAAM (Wire Arc Additive Manufacturing) technology stands out for its high deposition rate, its suitability for large parts and its potential to improve material efficiency compared to other manufacturing processes [3], [4].

However, numerous authors agree that the true potential of additive manufacturing lies not solely in the process itself, but in its integration with advanced design methodologies. In this regard, topological optimisation and the use of lattice structures enable the mass of components to be reduced whilst maintaining their mechanical performance, which translates into significant improvements from an environmental perspective [5].

From a Life Cycle Assessment (LCA) perspective, various studies have shown that reducing primary material usage is the most decisive factor in lowering the environmental impact of metal components. Comparative studies between additive manufacturing and conventional processes show significant reductions in environmental indicators when optimised design strategies are applied [6], [7].

In this context, this study proposes an integrated approach that combines advanced structural design and additive manufacturing using WAAM technology, with the aim of assessing its environmental impact compared to conventional CNC machining processes. Through the application of a 'cradle-to-door' Life Cycle Assessment methodology, the aim is to quantify the differences between both production routes and identify the key factors influencing the sustainability of the process, in line with recent research on sustainable manufacturing.

1.1. Objectives

The main objective of this study is to evaluate the potential of WAAM additive manufacturing, combined with advanced structural design techniques, as a tool for reducing the environmental impact of metal components. Specifically, the following objectives are set out:

— To identify the most critical stages of the life cycle from an environmental perspective.

— To compare the environmental impact of parts manufactured using CNC machining and WAAM.

2. METHODOLOGY

This study was conducted using a comparative approach between two manufacturing routes for aluminum metal components: a conventional route based on CNC machining from solid stock and an additive route using WAAM technology combined with optimized structural design. The methodological objective was to quantitatively evaluate the differences in environmental impact between the two production strategies, ensuring functional equivalence of the analyzed components at all times.

Figure 1 schematically shows the conceptual framework of the study, including both the theoretical foundations (additive manufacturing and structural optimization) and the two manufacturing routes analyzed, as well as the material flows associated with each process.

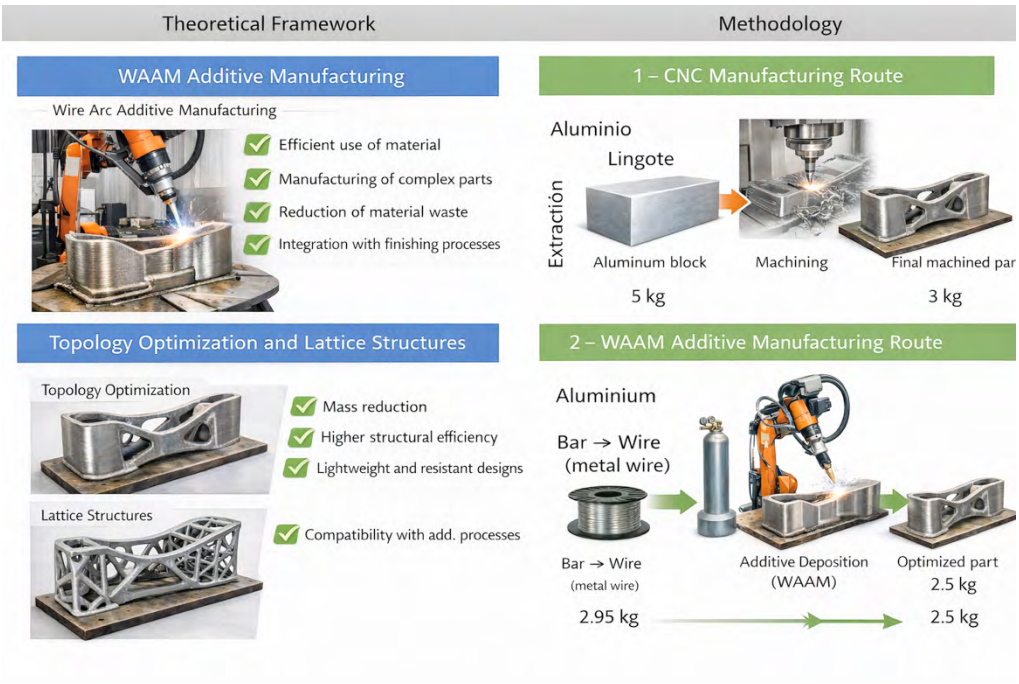


FIG. 1

An overview of the theoretical framework and methodology used, including WAAM additive manufacturing, optimised structural design, and a comparison between the conventional CNC route and the additive route

2.1. Experimental design and definition of case studies

To ensure the validity of the comparison, functionally equivalent structural specimens were designed so that both met the same mechanical and geometric requirements. In the case of the conventional route, the parts were obtained via CNC machining from a solid aluminum block, while the additive route employed WAAM technology, integrating topological optimization criteria and lattice-type structures to minimize the component's total mass.

As shown in Figure 1, the conventional route starts with an aluminium ingot transformed into a block weighing approximately 5 kg, from which a final part weighing 3 kg is obtained through material removal. This process therefore involves a significant loss of material in the form of chips. In contrast, the WAAM additive route is based on the transformation of the filler material (aluminium wire) through controlled deposition, starting with approximately 2.95 kg of material to obtain an optimized part weighing 2.5 kg. This difference reflects a substantial improvement in material efficiency, as it reduces both the initial volume required and the amount of waste generated.

2.2. System definition and LCA

The environmental analysis was conducted using the Life Cycle Assessment (LCA) methodology, following the guidelines established by ISO 14040/44. A "cradle-to-gate" approach was adopted, which includes the following life cycle stages:

1. Extraction and processing of raw materials (aluminum).
2. Material transformation (ingot in CNC and rod/wire in WAAM).
3. Manufacturing processes (CNC machining and WAAM deposition).
4. Finishing and post-processing operations.

The functional unit was defined as the manufacture of one aluminium structural component providing equivalent mechanical performance. The values of 5 kg (CNC route) and 2.95 kg (WAAM route) correspond to the material input required for each manufacturing process and are inventory parameters rather than the functional unit itself.

The LCA model was developed using Sphera GaBi 10 software and the Ecoinvent 3.10 database. Environmental impacts were assessed using the ReCiPe 2016 Midpoint (H) methodology.

The life cycle inventory was compiled using experimental data obtained during the manufacture of the test specimens and information from recognized databases. Specifically, GaBi software was used in conjunction with its database (Ecoinvent) to collect and model the system's input and output flows. Consistent with the flows shown in Figure 1, the following variables were recorded for each production route:

— Initial material mass (5 kg for CNC vs. 2.95 kg for WAAM).

— Final part mass (3 kg for CNC vs. 2.5 kg for WAAM).

— Amount of material removed or unused.

— Energy consumption during the manufacturing process.

— Process time.

— Post-processing requirements.

In the case of CNC machining, the volume of material removed as waste was considered, while in the WAAM route, the efficiency of the deposition process and the reduced need for subsequent machining were taken into account. Likewise, the impacts associated with the transformation of the material (block versus metal wire) were included.

3. RESULTS

The results obtained highlight substantial differences between the conventional route based on CNC machining and the additive route using WAAM with an optimised design. As shown in Fig. 2 (left), the CNC process, which starts with an initial block of 5 kg to produce a final part weighing 3 kg, results in a total environmental impact of 6.12 Person Equivalent (PE). This high value is mainly due to the high consumption of raw materials and the waste generation inherent in subtractive processes.

In contrast, the WAAM route, based on the deposition of 2.95 kg of metal wire to manufacture an optimised part weighing 2.5 kg, has a total impact of 3.87 PE, representing an approximate reduction of 37% compared to the conventional route. This improvement is directly related to greater efficiency in material use and the reduction of subsequent machining operations.

The analysis by impact category, shown in Fig. 2 (right), demonstrates that the reduction occurs consistently across the various environmental indicators, with particular emphasis on the categories related to climate change, the depletion of fossil resources and water consumption, confirming the cross-cutting nature of the environmental improvement introduced by additive manufacturing.

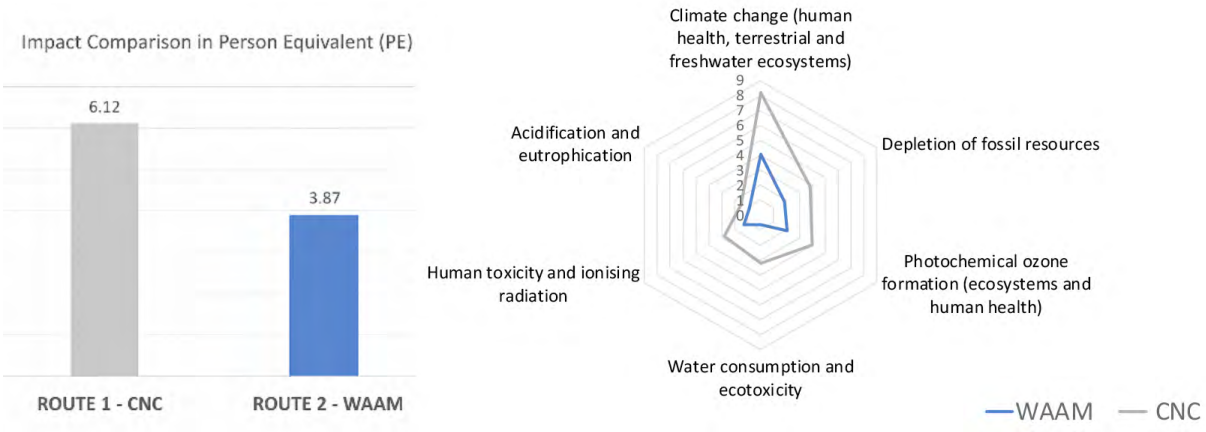


FIG. 2

Left: Comparison of the impact per person.
Right: Comparison of the distribution of environmental impact across six categories

Furthermore, the contribution analysis reveals that the aluminium extraction and processing phase constitutes the main source of environmental impact, accounting for approximately 74.6% of the total in terms of PE. This is clearly illustrated in Fig. 3, which shows

the distribution of impact across the sub-processes of the WAAM route, with the aluminium ingot being the dominant contributor. Consequently, reducing the initial mass and the volume of primary material used is the most decisive factor in improving the process's environmental performance.

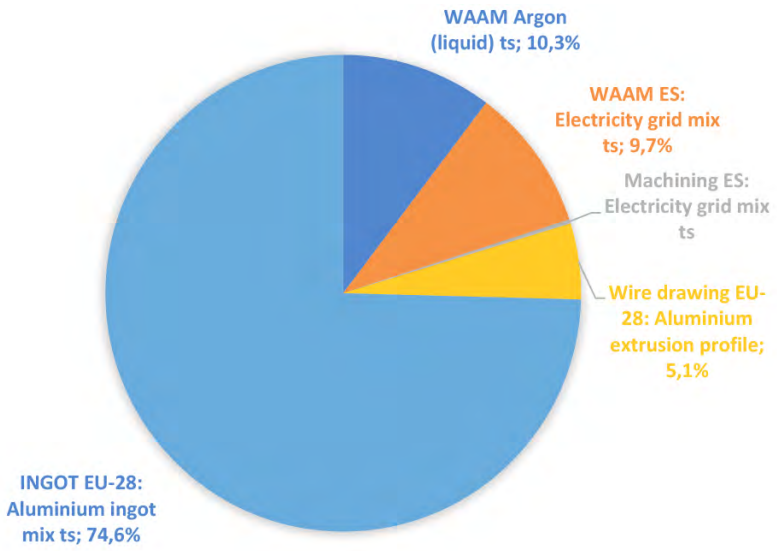


FIG. 3
Weight distribution across sub-processes (WAA route)

In this context, it can be stated that the environmental impact of metal components does not depend exclusively on the manufacturing process itself, but fundamentally on the quantity of primary material required for their production. Therefore, the combination of topological optimisation, lattice structures and additive manufacturing via WAAM acts as a multiplier of environmental benefits, as it directly influences the most intensive phase of the life cycle.

4. CONCLUSIONS

The findings of this study show that additive manufacturing using WAAM technology, when combined with advanced structural design strategies, represents a clearly more environmentally efficient alternative to conventional CNC machining. The approximate 37% reduction in overall environmental impact demonstrates that this improvement is not solely due to the change in production process, but, more significantly, to a substantial optimisation in material usage.

In this regard, the analysis confirms that the aluminium extraction and processing phase accounts for the largest contribution to the environmental impact, making the quantity of primary material used the key factor in the system's sustainability. Thus, mass reduction, rather than the manufacturing technology itself, emerges as the most influential variable in improving environmental performance.

The application of design methodologies such as topological optimisation and the use of lattice-type structures allows direct action to be taken on this critical variable, achieving lighter components without compromising their mechanical performance. In turn, WAAM technology enables the manufacture of geometries close to the final shape, reducing the need for subsequent subtractive operations, as well as the consumption of resources and the generation of associated waste.

REFERENCES

[1] X. Kang *et al.*, "Wire-Based Additive Manufacturing of Multi-Material Structures: A Review", *J. Compos. Sci.*, vol. 9, n.º 10, p. 534, oct. 2025, doi: 10.3390/jcs9100534.

[2] C. Cambon, I. Bendaoud, S. Rouquette, y F. Soulié, "A WAAM benchmark: From process parameters to thermal effects on weld pool shape, microstructure and residual stresses", *Materials Today Communications*, vol. 33, p. 104235, dic. 2022, doi: 10.1016/j.mtcomm.2022.104235.

[3] K. Agrawal y A. R. Bhat, "Advances in 3D printing with eco-friendly materials: a sustainable approach to manufacturing", *RSC Sustainability*, vol. 3, n.º 6, pp. 2582-2604, 2025, doi: 10.1039/D4SU00718B.

[4] C. J. Ejeh, I. Barsoum, A. M. Abou-Ali, y R. K. Abu Al-Rub, "Combining multiple lattice-topology functional grading strategies for enhancing the dynamic compressive behavior of TPMS-based metamaterials", *Journal of Materials Research and Technology*, vol. 27, pp. 6076-6093, nov. 2023, doi: 10.1016/j.jmrt.2023.10.247.

[5] S. Polo, A. García-Domínguez, E. M. Rubio, y J. Claver, "Lattice Structures in Additive Manufacturing for Biomedical Applications: A Systematic Review", *Polymers*, vol. 17, n.º 17, p. 2285, ago. 2025, doi: 10.3390/polym17172285.

[6] F. Rossi, C. De Bernardi, M. Frey, y M. Niero, "From past critiques to present challenges: A review of LCA approaches and results in the aluminum industry", *Waste Management*, vol. 204, p. 114900, ago. 2025, doi: 10.1016/j.wasman.2025.114900.

[7] T. Lotwala, J. Schoop, y N. Khanna, "Life Cycle Assessment to Achieve Sustainability in Pre- and Post-Processing: WAAM Vs. Wrought Ti-6Al-4V", presentado en ASME 2025 International Mechanical Engineering Congress and Exposition - India, American Society of Mechanical Engineers Digital Collection, dic. 2025. doi: 10.1115/IMECE-INDIA2025-160694.

AI-Assisted CAM for DED-Arc: Intelligent Toolpath Planning and Process Optimization

Juan Sustacha, Fernando Veiga*, Virginia Uralde, Alvaro Rodríguez

Universidad Pública de Navarra, Campus de Tudela, Avenida Tarazona s/n, Tudela 31500 (Navarra), SPAIN

* e-mail: fernando.veiga@unavarra.es

Abstract: This work presents a preliminary AI-assisted computer-aided manufacturing (CAM) framework for arc-based Directed Energy Deposition (DED-arc), developed on top of FreeCAD. The proposed system combines a deterministic slice-first planning workflow with an experimental runtime that enables the generation of alternative toolpath strategies from natural-language manufacturing objectives. FreeCAD is adopted as the geometric and computational backbone due to its open-source architecture, parametric modelling capabilities, and scripting-oriented extensibility. The framework generates structured intermediate representations that support traceable and reproducible toolpath generation while enabling controlled modification of planning strategies. In addition, a preliminary integration of OpenClaw has been implemented to explore AI-assisted planning, allowing user-defined manufacturing objectives to be translated into alternative planning configurations and experimental NC programs that can be compared with a deterministic baseline solution. The framework is specifically oriented to DED-arc processes, where toolpath generation is strongly influenced by geometric and process constraints. Although the AI-assisted functionality remains at an exploratory stage and has only been validated at software level, the proposed approach establishes the foundations for future intelligent and adaptive CAM systems for arc-based additive manufacturing.

Keywords: *AI-assisted CAM; Directed Energy Deposition (DED-Arc); FreeCAD; Toolpath Generation; Slicing Strategies; Conversational AI.*

1. INTRODUCTION

Wire Arc Additive Manufacturing (WAAM), as a wire-based implementation of arc-based Directed Energy Deposition (DED-arc), has consolidated its position as a key technology for the fabrication and repair of medium- and large-scale metallic components. Its relevance stems from its high deposition rates, relatively low equipment and feedstock costs, and its capability to manufacture large structures that are not feasible with powder-based processes [1, 2]. However, DED-arc processes are intrinsically complex due to the strong coupling between thermal, metallurgical, and mechanical phenomena. As a result, part quality is highly sensitive to process planning decisions, including toolpath generation, layer sequencing, deposition continuity, and heat accumulation, all of which directly influence bead geometry, residual stress development, and defect formation [3].

From a process-planning perspective, toolpath generation is a critical stage in DED-arc, directly affecting geometric accuracy, process stability, and manufacturability. Conventional CAM approaches rely on geometry slicing, contour extraction, and infill generation [4-6], ranging from raster-based to feature-aware strategies [7, 8]. However, DED-arc also requires optimized deposition direction, bead overlap, interpass temperature, and path continuity, while most current planning methods remain geometry-driven and heuristic-based.

Artificial intelligence (AI) offers a promising alternative to overcome these limitations. Recent developments in machine learning and hybrid physics-informed models have shown significant potential for process optimization, defect prediction, monitoring, and digital twin development [9, 10]. Likewise, advances in multisensor monitoring and data fusion have enabled more effective process awareness and adaptive control [11-13].

The contribution of this work is twofold. First, it provides a FreeCAD-native implementation of a slice-first planning framework for DED-arc, including explicit intermediate representations and a controlled experimental runtime for part-specific reconfiguration. Second, it introduces an AI-assisted paradigm in which toolpath generation is no longer predefined but can be iteratively adapted through interaction between user intent and algorithmic decision-making. This approach aims to bridge the gap between traditional CAM workflows and intelligent manufacturing systems, establishing the basis for more flexible, transparent, and adaptive toolpath planning in DED-arc processes.

2. WAAM SLICE-FIRST CAM FRAMEWORK

Wire Arc Additive Manufacturing (WAAM), as a wire-based implementation of arc-based Directed Energy Deposition (DED-arc), is widely adopted for the fabrication of medium- and large-scale metallic components due to its high deposition rate, scalability, and relatively low cost. However, process quality is strongly dependent on toolpath planning, layer sequencing, and thermal management. In particular, bead geometry, heat accumulation, and residual stress development are directly influenced by the strategy used to convert CAD geometry into executable NC instructions. The system proposed in this work is implemented as a FreeCAD workbench that follows a slice-first planning para-

digm, as shown in Figure 1. The workflow is structured as a sequential pipeline: (i) definition of a Work Coordinate System (WCS), (ii) export of visible solids to a managed STEP file, (iii) slicing of the geometry into WCS-local XY layers, (iv) generation of a structured planning representation, and (v) emission of a baseline NC program. This intermediate representation, stored in JSON format, acts as a contract between geometric processing and NC generation, enabling traceability and inspection. A key design decision is the explicit separation between a baseline pipeline and an experimental runtime. The baseline pipeline produces a stable and reproducible NC program, while the experimental runtime allows controlled modification of planning strategies without overwriting the reference output. This ensures that experimentation is bounded and auditable, which is particularly relevant in process-planning research. The system also enforces a consistent artefact structure, including STEP inputs, feature metadata, slice plans, and NC outputs, improving reproducibility and facilitating debugging. The overall workflow is illustrated below.

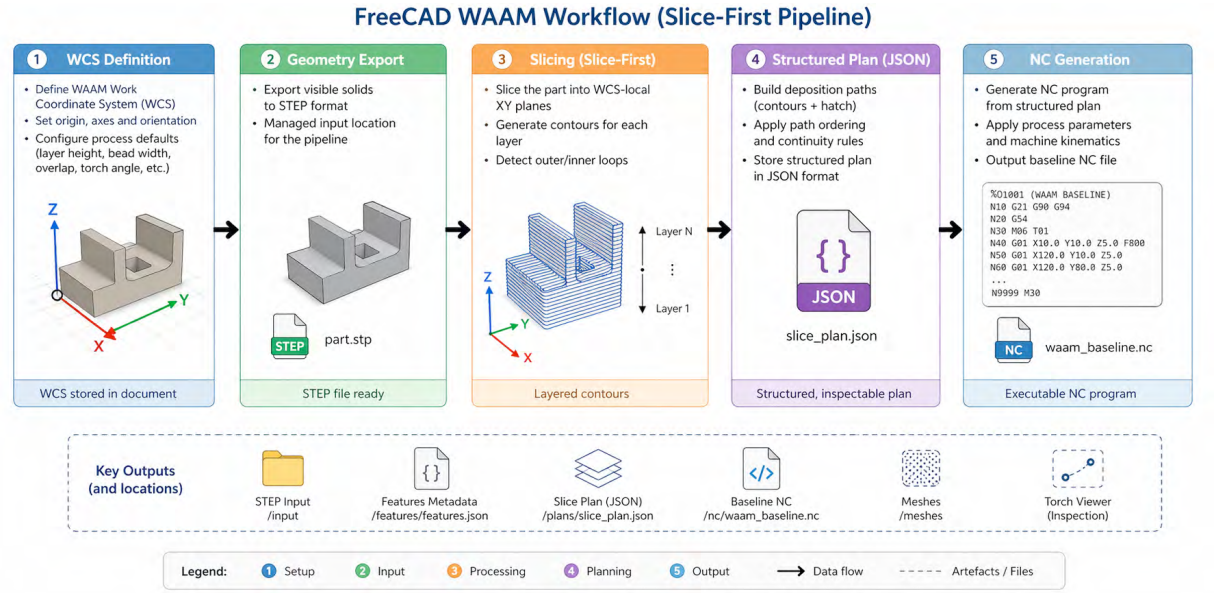


FIG. 1
FreeCAD FreeCAD WAAM workflow

The command interface exposed to the user reflects this structured approach, providing a minimal but complete pipeline from setup to inspection. This avoids the fragmentation typical of generic CAM environments and focuses on a reproducible WAAM-oriented workflow. The planning method follows a deterministic slice-first formulation in which the input geometry is transformed into the WCS-local coordinate frame and discretized into planar layers. Each layer is processed independently as a 2D cross-section, from which deposition paths are generated. Contours are extracted from each slice and classified as outer or inner based on orientation and containment relationships. Outer contours define deposition regions, while inner contours represent holes. This classification enables region-aware path planning, ensuring correct material deposition and

hole preservation. A decision rule determines whether a region is processed using contour-only or contour-plus-hatch strategies. This decision is based on the geometric span relative to bead width and overlap. For sufficiently large regions, hatch infill is generated using scanline-based intersection, producing geometry-conforming paths rather than simple raster approximations.

Path ordering is designed to preserve continuity and minimize non-productive movements. Closed contours can be reoriented to match preferred start points, and infill directions can be alternated between layers to improve deposition stability. The resulting representation is a structured set of toolpaths, each tagged according to its role (outer, inner, infill). The planner generates several intermediate artefacts, summarized in Table 1, which define the execution context for NC generation.

TABLE 1
Principal artefacts generated by the WAAM pipeline

Artefact	Purpose
input_step/part.step	Managed STEP export of visible solids from the active FreeCAD document.
output/features/features.json	Part and WCS metadata; compact descriptive record of the run.
output/operations_mesh/waam_slice_plan.json	Main structured planning artefact: process metadata, layer/path data.
output/dsl_waam/part.llm_waam	Compact WAAM artefact for LLM-oriented or downstream summarization workflows.
output/nc_files/waam_baseline.nc	Baseline control NC program produced from the structured plan.
output/nc_files/waam_baseline_experimental.nc	Experimental NC program; does not overwrite the baseline control output.

This approach transforms the planning problem into a 2.5D representation, where 3D geometry is reduced to ordered 2D paths with layer metadata. This simplification enables efficient computation while preserving essential geometric and process information.

3. EXPERIMENTAL RUNTIME AND VALIDATION

The framework includes a bounded experimental runtime that generates alternative NC programs in an isolated workspace without modifying the baseline output. Experimental changes are fully traceable and reproducible, and are applied at the planning level rather than directly to the NC code. Software-level validation showed that different planning strategies produce measurable changes in path count, deposition length, NC file size, and execution time.

TABLE 2
Quantitative fields present in the uploaded runtime notes for part SCC_908

Observed Field	Value Recorded in Runtime Files
Active part label	SCC_908
Experimental goal	Preserve 4 holes and add material deposition in the base region
Outer contours kept	53
Inner contours kept	0
Fill / link paths generated	216
Hole crossings inserted	0

TABLE 3
Path-level comparison for the two executable worked cases (B = Baseline, E = Experimental)

Case	Layers	Paths B	Paths E	LINK	Torch B/E	Dep. l B/E (mm)
Rectangular block	8	64	72	0	64 / 72	9,600 / 6,720
Four-hole plate	8	208	168	32	208 / 136	16,935 / 10,541

TABLE 4
Mean execution times and NC output sizes over 15 repeated runs

Case	Planning (ms)	Baseline NC (ms)	Exp. NC (ms)	Baseline (kB)	Exp. (kB)
Rectangular block	7.23 ± 0.56	18.76 ± 3.26	10.94 ± 2.94	13.27	14.83
Four-hole plate	20.32 ± 1.23	479.68 ± 8.00	35.93 ± 12.58	62.73	54.53

The results presented in Tables 3 and 4 demonstrate that modifications to the planning strategy are consistently propagated through the complete CAM workflow, affecting both the structure of the generated toolpaths and the resulting NC program. For the rectangular block, the experimental planner increases the number of generated paths while reducing the total deposition length, indicating a different path segmentation strategy rather than a simple reordering of trajectories. In the four-hole plate, the introduction of LINK paths and the reduction in torch ignition events illustrate how the planner can explicitly separate deposition and travel motions, providing greater flexibility for accommodating process-specific constraints such as hole preservation, accessibility, or future thermal management strategies.

From a computational perspective, both planning approaches exhibit execution times compatible with interactive CAM applications, even for the more complex geometry. The relatively small planning overhead demonstrates that alternative toolpath strategies can be evaluated rapidly within the same software environment, supporting iterative process planning without compromising workflow efficiency. Nevertheless, these results should be interpreted strictly as software-level validation. While they confirm the capability of the proposed

framework to generate and compare alternative planning strategies in a reproducible manner, they do not demonstrate improvements in manufacturing quality, deposition efficiency, or mechanical performance. Experimental validation on physical DED-arc components remains necessary to establish the relationship between the generated trajectories and the final characteristics of the manufactured parts. The integration within FreeCAD also enables interactive inspection of toolpaths and NC programs. This facilitates rapid identification of inconsistencies such as missing paths or incorrect ordering.

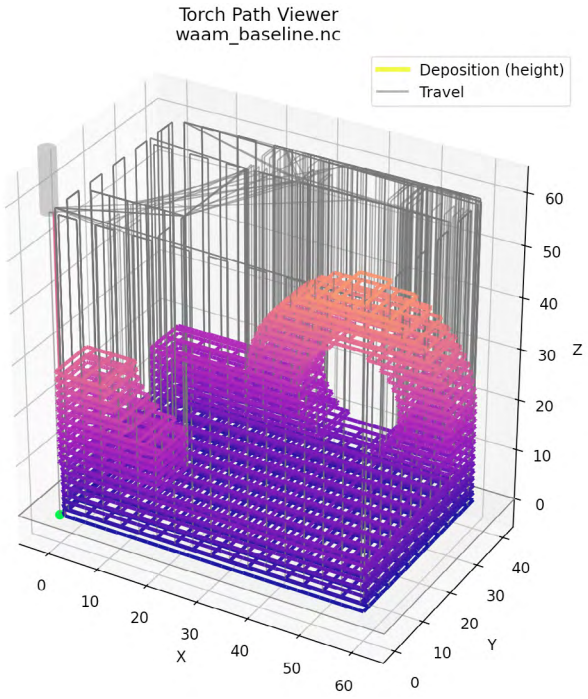


FIG. 2
FreeCAD interface showing slicing and toolpath visualization

4. PRELIMINARY AI-ASSISTED PLANNING INTEGRATION

In addition to the deterministic planning workflow described in this work, a preliminary AI-assisted planning capability has been implemented through OpenClaw. The proposed approach allows the user to define manufacturing objectives using natural-language prompts, which are interpreted to generate alternative planning configurations within the experimental runtime. Rather than modifying the baseline workflow, the system produces an independent experimental NC program that can incorporate changes in deposition regions, path sequencing, contour preservation, infill generation, or other planning rules derived from the user instructions. This architecture enables the exploration of alternative manufacturing strategies while maintaining the traceability and reproducibility of the reference solution. The current implementation demonstrates the feasibility of integrating conversational AI with the proposed CAM framework for adaptive DED-arc toolpath planning. Future work will evaluate the quality of AI-generated strategies through manufacturing experiments and develop more advanced agent-based planning capabilities.

5. CONCLUSIONS

This work presents a FreeCAD-based CAM framework for WAAM that integrates a slice-first planning strategy with a structured and inspectable workflow for toolpath generation. The separation between baseline and experimental planning enables controlled exploration of alternative strategies without compromising the reference solution.

The proposed approach improves transparency and reproducibility by explicitly storing intermediate representations and exposing the planning process to the user. Software-level validation shows that different planning strategies lead to significant variations in toolpath structure and NC output, highlighting the importance of flexible and inspectable CAM systems for DED-arc technologies.

The framework also provides a basis for future integration of AI-assisted planning methods and conversational interfaces, to be further explored and validated through physical WAAM experiments. A preliminary AI-assisted planning capability has also been integrated through OpenClaw, enabling the generation of alternative NC programs from natural-language manufacturing objectives. Although only demonstrated at software level, this functionality establishes the basis for future validation of AI-driven planning strategies in WAAM environments.

REFERENCES

[1] Williams, S.W., Martina, F., Addison, A.C., Ding, J., Pardal, G., Colegrove, P.: Wire + Arc Additive Manufacturing. Materials Science and Technology. 32, 641-647 (2016). https://doi.org/10.1179/1743284715Y.0000000073.

[2] Veiga, F., Villabona, E., Suárez, A., Rivero, P., Aldalur, E.: LFAM with Metallic Materials–Applications. In: Large Format Additive Manufacturing. pp. 393-438. John Wiley & Sons, Ltd (2026). https://doi.org/10.1002/9783527844807.ch14.

[3] Svetlizky, D., Das, M., Zheng, B., Vyatskikh, A.L., Bose, S., Bandyopadhyay, A., Schoenung, J.M., Lavernia, E.J., Eliaz, N.: Directed energy deposition (DED) additive manufacturing: Physical characteristics, defects, challenges and applications. Materials Today. 49, 271-295 (2021). https://doi.org/10.1016/j.mattod.2021.03.020.

[4] Piscopo, G., Atzeni, E., Saboori, A., Salmi, A.: An Overview of the Process Mechanisms in the Laser Powder Directed Energy Deposition. Applied Sciences. 13, 117 (2023). https://doi.org/10.3390/app13010117.

[5] Rauch, M., Hascoet, J.-Y.: Opening New Opportunities For Aeronautic, Naval And Train Large Components Realization With Hybrid And Twin Manufacturing. Journal of Machine Engineering. (2022). https://doi.org/10.36897/jme/155812.

[6] Sookchanchai, K., Promoppatum, P., Uthaisangsuk, V.: Load-carrying capacity of additively manufactured part using graded-topology infilled lattices structures. Mechanics of Advanced Materials and Structures. 31, 1313-1331 (2024). https://doi.org/10.1080/15376494.2022.2135145.

[7] Uralde, V., Suárez, A., Veiga, F., Villanueva, P., Ballesteros, T., Uralde, V., Suárez, A., Veiga, F., Villanueva, P., Ballesteros, T.: Advancements and Methodologies in Directed Energy Deposition (DED-Arc) Manufacturing: Design Strategies, Material Hybridization, Process Optimization and Artificial Intelligence. In: Additive Manufacturing - Present and Sustainable Future, Materials and Applications. IntechOpen (2024). https://doi.org/10.5772/intechopen.1006965.

[8] Ding, D., Pan, Z., Cuiuri, D., Li, H.: A multi-bead overlapping model for additive manufacturing of thin-walled structures. The International Journal of Advanced Manufacturing Technology. 95, 1999-2009 (2019). https://doi.org/10.1007/s00170-017-1283-0.

[9] Özel, T.: Deep learning-based applications in metal additive manufacturing processes: Challenges and opportunities-A review. International Journal of Lightweight Materials and Manufacture. 8, 453-468 (2025). https://doi.org/10.1016/j.ijlmm.2025.04.001.

[10] Fernández-Zabalza, A., Rodriguez A., Veiga, F., Suarez, A., Uralde, V., Ballesteros, T., Alfaro, J.R.: AI-driven predictive modeling of homogeneous bead geometry for WAAM processes. Int J Adv Manuf Technol (2025). https://doi.org/10.1007/s00170-025-16061-1

[11] Bestard, G.A., Sampaio, R.C., Vargas, J.A.R., Alfaro, S.C.A.: Sensor Fusion to Estimate the Depth and Width of the Weld Bead in Real Time in GMAW Processes. Sensors. 18, 962 (2018). https://doi.org/10.3390/s18040962.

[12] Ahsan, M.M., Liu, Y., Raman, S., Siddique, Z.: Digital Twins in Additive Manufacturing: A Systematic Review. arXiv preprint arXiv:2409.00877. (2024).

[13] Liu, N., Li, X., Rajanna, M.R., Reutzel, E.W., Sawyer, B., Rao, P., Lua, J., Phan, N., Yu, Y.: Deep Neural Operator Enabled Digital Twin Modeling for Additive Manufacturing, http://arxiv.org/abs/2405.09572, (2024). https://doi.org/10.48550/arXiv.2405.09572.

Animal-centered design of monitoring system enclosures in livestock environments under a One Health framework

Ian Frega Molina*, Enrique Samperio, Elena Heras-Romanos, Iván Lidón, Rubén Rebollar, Ignacio Gil-Pérez

Universidad de Zaragoza, C. María de Luna, 3, 50018 Zaragoza

* e-mail: ifrega@unizar.es

Abstract: Environmental monitoring in intensive livestock systems is a key component of the One Health framework, as air quality, temperature, and humidity directly affect animal welfare, worker health, and environmental sustainability. While sensing technologies are increasingly available, the physical design of the enclosure that houses these systems remains largely underexplored as a product design problem, despite its direct influence on device performance and environmental interaction. In harsh livestock environments, the enclosure cannot be considered a passive container, but a critical interface that mediates between the sensing system and surrounding conditions. This paper presents the CAD-based design of a monitoring system enclosure developed for lamb fattening pens, addressing competing requirements related to environmental coupling, mechanical protection, animal-centred deployment, manufacturability, maintenance, and cost. Through iterative prototyping and field deployment, the proposed solution formalises enclosure design as a multi-constraint engineering problem and provides transferable design guidelines for environmental monitoring systems operating in harsh, resource-constrained agricultural environments.

Keywords: *Product design, Enclosure design, CAD, One Health.*

1. INTRODUCTION

The One Health framework recognises that human health, animal health, and environmental conditions are deeply interconnected, and that decisions in one domain propagate consequences through the others [1]. In intensive livestock systems this interconnection is especially tangible: indoor air quality parameters, including temperature, relative humidity, and gaseous pollutants such as ammonia (NH_3), directly influence animal welfare, productivity, and farm-worker exposure. Continuous environmental monitoring is therefore a key component of Precision Livestock Farming (PLF) [2,3], providing the data required to characterise health-relevant exposures, detect anomalies, and support management decisions. Recent work has demonstrated the feasibility of low-cost IoT architectures combining single-board computers, commercial sensors, and wireless connectivity for agricultural monitoring [4,5].

A consistent gap in this literature is the treatment of the physical enclosure that houses the sensing system. In most published designs, the enclosure is mentioned only as a protective box, with no documented trade-off analysis. This overlooks its role as a critical design element whose geometry governs measurement representativeness, resistance to mechanical and chemical degradation, and compatibility with the animals' behavioural space. Here, enclosure design is addressed as a multi-constraint product design problem for deployment in lamb fattening pens, using parametric CAD (Autodesk Inventor) and iterative additive manufacturing to guide successive design iterations before field deployment.

Commercial industrial enclosures do not fully address livestock monitoring needs. Although IP-rated solutions provide effective protection, they generally lack the environmental coupling required for representative sensing, are not intended to integrate multiple sensing and computing components, and are often cost-prohibitive for sheep farming systems. Tailored enclosures are therefore required to balance protection, measurement performance, integration, and affordability.

2. DESIGN REQUIREMENTS

The design space was defined by four interdependent requirement families. Regarding environmental constraints, lamb fattening pens expose electronics to continuous particulate matter from straw bedding, sustained relative humidity in the range 70-80%, ammonia concentrations that vary between background levels and episodic peaks, and the risk of mechanical impact from direct animal contact [6,7]. In practice, this means the enclosure has to withstand all four stressors simultaneously.

Protection requirements are in direct conflict with measurement requirements. A hermetically sealed enclosure would block contamination but would also decouple the internal sensor environment from the pen atmosphere being monitored. Sufficient passive air exchange is therefore a functional requirement, not an optional feature, and ventilation geometry acts simultaneously as a structural parameter and as an environmental-coupling parameter. A further representativeness constraint concerns sensor height: concentrations and microclimate conditions vary vertically within the pen, with higher values near the bedding

surface where animals breathe [6], making proximity to the animal breathing zone a design objective.

Animal-centred constraints further shape the design space. The device must be installed at a height that precludes direct animal contact, and crucially, no supplementary fencing or barriers may be used around the installation point, as these would alter pen geometry and the very microenvironment being measured. Installation height and spatial accessibility are therefore treated as primary geometric constraints rather than experimental variables. Finally, economic and operational constraints are particularly relevant in sheep farming systems, which typically operate under tighter margins. As a result, the enclosure must be manufacturable with widely available FDM equipment, rely on off-the-shelf components, and allow maintenance without specialised tools.

3. CAD-BASED ENCLOSURE DESIGN

3.1. Design methodology

Parametric CAD modelling in Autodesk Inventor served as the central tool for geometric exploration and decision-making. Each iteration evaluated the combined effect of ventilation layout, opening geometry, wall thickness distribution, and sub-assembly architecture on the full set of competing requirements. Physical prototypes were produced on a Bambu Lab H2S FDM printer, enabling immediate assessment of printability, structural integrity, and assembly feasibility before committing to the next design iteration. Prototypes were manufactured by material extrusion (FDM) using 1.75 mm PLA filament, a 0.4 mm nozzle and 0.12 mm layer height. No CFD or thermal simulations were performed; ventilation geometry was refined through successive CAD iterations and prototype testing under real conditions.

3.2. Exploration of design configurations

Three enclosure configurations were explored during development (Figure 1), each derived from successive design iterations and each exposing a specific constraint conflict that drove the transition to the next. The first configuration relied on a sealed body with lateral micro-vents, providing good particle protection but causing thermal accumulation and poor environmental coupling, making it unsuitable for reactive gas sensing. The second configuration introduced an upward-facing open grille, improving thermal management and air exchange but allowing particle ingress that fouled the sensor and obstructed the ventilation path in straw-bedding environments [6,7]. The adopted configuration resolved this conflict using a downward-facing recessed opening protected by angled deflecting walls that channel air while blocking direct particle trajectories. A secondary anti-particle mesh provides additional filtration without active components. Table 1 presents the qualitative decision matrix used to compare the three concepts against the principal design criteria; as summarised in Table 1, this configuration achieves the best overall balance across all relevant design criteria.

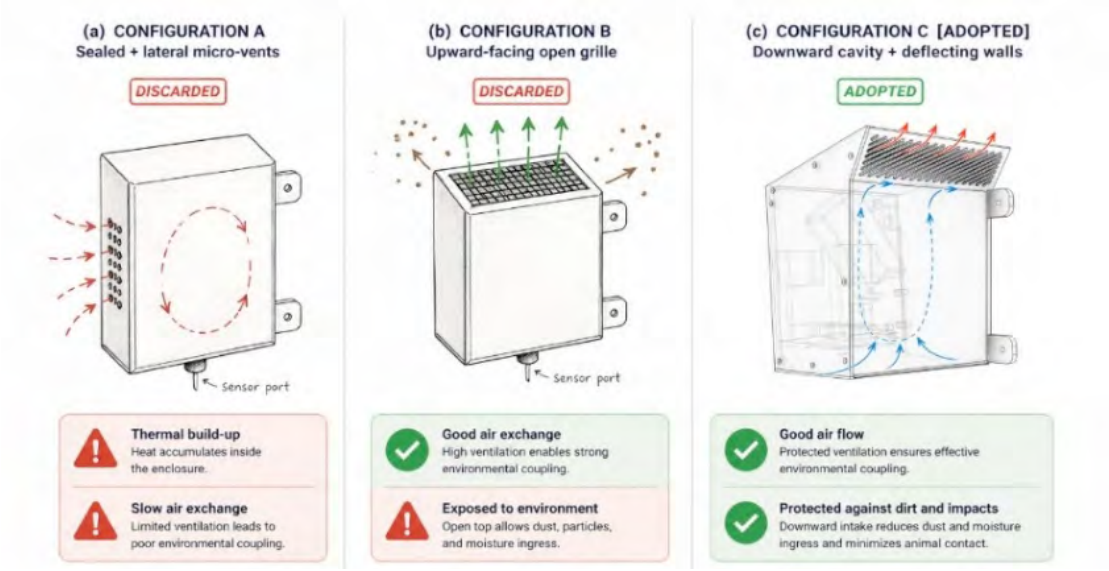


FIG. 1
Design configurations explored during enclosure development

TABLE 1
Comparison of enclosure design configurations across principal design criteria

Criterion	Config. A	Config. B	Config. C	Rationale for Config. C
Dust protection	High	Very low	High	Downward cavity blocks direct particle ingress
Air exchange	Low (heat build-up)	Very high	Medium–high	Protected convective flow, no active ventilation required
Thermal management	Poor (overheat)	Adequate	Good	Angled wedge redirects exhaust upward from wall
Sensor proximity	Low	Medium	High	Variable base thickness minimises air gap at sensor port
Animal safety	Adequate	Risk	High	Flush geometry, no external protrusions
Field maintainability	Poor (full removal)	Medium	High	Two-face access and rail-guided modules
FDM printability	Easy	Complex	Optimal	Modular print, grille independent, no supports

3.3. Detailed geometric decisions

The selection of Configuration C opened a second tier of design decisions. The overall enclosure profile was shaped by the need to reconcile two simultaneous requirements: the active cooling fan of the Raspberry Pi 5 is oriented upward, requiring a clear thermal path, while the rear mounting face must remain flat and free of openings for flush wall contact. An angled upper wedge profile resolves both conditions by creating a thermal chimney effect that redirects warm air upward and away from the mounting surface, enabling passive thermal regulation without additional components (Figure 2).

At the lower part of the enclosure, sensor positioning introduced a further constraint. Proximity to the animal breathing zone improves measurement representativeness but increases the structural demands on the base wall. This was addressed through a variable-thickness design: the perimeter zones retain full material depth for rigidity, while the area around the sensor port is tapered to the minimum printable thickness, minimising the air-gap between sensor and environment without compromising mechanical integrity. The ventilation grille required a separate solution due to the manufacturing limitations of fine lattice geometries. Printing it as part of the main body would have required extensive support material and prevented integration of the anti-particle mesh. The grille was designed as an independent rail-guided component, allowing optimal print orientation and mesh integration without adhesives.

Maintenance requirements shaped the assembly architecture. Since full disassembly in field conditions is not practical, the design incorporates a two-face access strategy: one lateral face provides direct access to sensors, connectors, and status elements for routine operations, while the opposite face enables extraction of the Raspberry Pi sub-assembly via a guided rail without disturbing the wiring harness. All retention is screw-based on these two faces; all other surfaces remain fastener-free. The Raspberry Pi mounting bracket required a specific solution because standard brackets restrict access to the GPIO header used by the ammonia sensor. A three-point cantilevered support was developed, providing mechanical stability while leaving the interface fully exposed and accessible. Throughout the assembly, soldered connections were replaced by crimped ferrules and push-in terminals, allowing component replacement without specialised tools and ensuring full reversibility of all electrical connections.



FIG. 2
Enclosure prototype: exterior and interior views

4. DEPLOYMENT AND DESIGN VALIDATION

The enclosure was deployed in a working lamb fattening pen under real farming conditions. Two units were installed on the same structural column at different heights: one positioned as low as safely possible, approaching the animal breathing zone while remaining out of reach, and one at approximately 1.7 m (Figure 3). This dual-height installation serves as a validation of the animal-centred design constraints and the intended environmental coupling.



FIG. 3
Dual-height deployment in lamb fattening pen

Operational deployment indicated that the geometric decisions successfully balanced the competing requirements over an extended monitoring period. Although no quantitative airflow measurements were performed, no particle accumulation or maintenance issues attributable to the enclosure geometry were observed during the deployment period. The downward-facing ventilated cavity with deflecting walls prevented particle ingress despite continuous straw movement and animal activity, and no sensor fouling attributable to enclosure design was observed. Thermal performance of the internal components remained within operating bounds throughout, supported by the passive wedge-profile chimney. The two-face access architecture enabled maintenance without full device removal. Animal behaviour in the pen showed no response to the device presence, and the compact form integrated naturally into the pen geometry without requiring supplementary barriers. The lower installation confirmed greater proximity to the animal breathing zone as the metrologically superior position, while both installations used the same enclosure, validating the generality of the geometric solution. Table 2 summarises the principal design trade-offs and their geometric resolutions.

TABLE 2
Principal design trade-offs and their geometric resolutions

Decision	Conflict	Resolution	Geometric solution
Ventilation orientation	Airflow vs. dust ingress	Downward cavity	Recessed grille with deflecting walls and mesh
Mounting face	Flush contact vs. penetrations	Closed rear face	Cables and vents routed to lateral faces
Sensor positioning	Breathing-zone proximity vs. wall strength	Variable-thickness base	Thick perimeter, minimal thickness at sensor port
Maintenance access	Easy service vs. compactness	Two-face screw access	Primary service face + secondary RPi rail extraction
Grille sub-component	Print quality vs. mesh integration	Detachable rail-guide grille	Independent print, mesh inserted post-print
Thermal profile	RPi fan direction vs. flat mounting face	Angled upper wedge	Exhaust guided upward, away from wall
RPi bracket	Board support vs. GPIO access	Cantilevered bracket	GPIO fully accessible without board removal

5. DISCUSSION

From a One Health perspective, enclosure design decisions propagate directly through the measurement chain. A well-designed enclosure does not only protect electronics, but also determines whether the collected data reflect the actual environmental conditions experienced by animals and workers. Poorly resolved trade-offs, whether excessive sealing, misoriented ventilation, or large sensor offsets, introduce systematic bias that undermines the validity of health-related inferences drawn from the data, even when the data appears statistically complete and continuous [6,8]. The animal-centred approach adopted here, which treats installation height, spatial accessibility, and behavioural compatibility as primary geometric constraints, enables monitoring systems to be deployed safely and at scale without altering pen layout or animal behaviour, a necessary condition for obtaining representative environmental data. The CAD-driven trade-off framework demonstrated in this article makes enclosure design decisions explicit, traceable, and easier to replicate [4,5]. The proposed design was validated in a single lamb fattening facility and without computational flow simulations; therefore, additional validation in other livestock systems and operating conditions is required before broader generalisation. Commercial IP-rated enclosures offer strong protection but are not tailored to livestock monitoring needs, and their cost is often prohibitive for sheep farming systems.

6. CONCLUSIONS

This paper demonstrates that the physical enclosure of an environmental monitoring system is a first-order design element in livestock environments, not a secondary container. By formalising enclosure design as a multi-constraint problem and resolving trade-offs through parametric CAD and iterative additive manufacturing, the study produced a robust, maintainable, and metrologically sound device suitable for real farming conditions under tight economic constraints. The principal contributions are the formalisation of enclosure design as an explicit trade-off problem; the demonstration that targeted geometric decisions can simultaneously satisfy conflicting requirements across protection, sensing, maintenance, and animal-centred constraints; and a transferable framework with practical guidelines for researchers and engineers working in harsh, resource-constrained agricultural environments. The enclosure should therefore be considered a first-order design variable in environmental monitoring systems, rather than an implementation detail. Future work will extend the design to additional species and production systems, evaluate alternative materials (e.g. PETG, ASA) for improved resistance to humidity and ammonia exposure, and will investigate quantitative relationships between enclosure geometric parameters and measurement representativeness across deployment contexts.

REFERENCES

[1] Halachmi, I., Guarino, M.: Precision livestock farming: A “per animal” approach using advanced monitoring technologies. Animal 10(9), 1482-1483 (2016). https://doi.org/10.1017/S1751731116001142

[2] Norton, T., Chen, C., Larsen, M.L.V., Berckmans, D.: Precision livestock farming: Building digital representations to bring animals closer to the farmer. Animal 13(12), 3009-3017 (2019). https://doi.org/10.1017/S175173111900199X

[3] Morrone, S., Dimauro, C., Gambella, F., Cappai, M.G.: Industry 4.0 and precision livestock farming: An overview across animal productions. Sensors 22(12), 4319 (2022). https://doi.org/10.3390/s22124319

[4] Morgan-Davies, C., *et al.*: Exploring precision livestock farming for small ruminant welfare management. Animal 18, 101233 (2024). https://doi.org/10.1016/j.animal.2024.101233

[5] Wolfert, S., Ge, L., Verdouw, C., Bogaardt, M.J.: Big data in smart farming: A review. Agricultural Systems 153, 69-80 (2017). https://doi.org/10.1016/j.agsy.2017.01.023

[6] García-Ramos, F.J., Aguirre, A.J., Barreiro, P., Horcas, E., Boné, A., Vidal, M.: Applicability of ammonia sensors for environmental control in lamb fattening. Journal of Sensors 2018, 4032043 (2018). https://doi.org/10.1155/2018/4032043

[7] Seedorf, J., Hartung, J.: Survey of ammonia concentrations in livestock buildings. Journal of Agricultural Science 133(4), 433-437 (1999). https://doi.org/10.1017/S0021859699007170

[8] Williams, T., Wilson, C., Wynn, P., Costa, D.: Opportunities for precision livestock management under climate change. Animal Frontiers 11(5), 63-68 (2021). https://doi.org/10.1093/af/vfab065

BIM-Integrated Energy Simulation of Radiative Cooling Envelopes in Office Buildings

Laura Carlosena[a, c, *], Xabier Sandúa[b, c], Alicia Elena Torres-García[a, d], Amaia Pérez[c], Sara Marcelino[a, c], Miguel Beruete[a, d]

[a] Institute of Smart Cities (ISC), Public University of Navarre (UPNA), Campus de Arrosadia, 31006 Pamplona, España

[b] Institute for Advanced Materials and Mathematics (INAMAT²), Public University of Navarre (UPNA), Campus de Arrosadia, 31006 Pamplona, España

[c] Department of Engineering, Public University of Navarre (UPNA), Campus de Arrosadia, 31006 Pamplona, España

[d] Department of Electrical, Electronic and Communications Engineering, Public University of Navarre (UPNA), Pamplona 31006 Spain

* e-mail: laura.carlosena@unavarra.es

Abstract: Buildings significantly affect human health and energy consumption. In office environments, poor thermal conditions reduce productivity and increase absenteeism, while buildings themselves contribute substantially to greenhouse gas emissions and urban heat island effect. Improving building thermal performance is therefore both an energy efficiency challenge and a public health priority. This study investigates radiative cooling as a passive building strategy. These materials dissipate heat to the atmosphere without consuming energy, reducing surface temperatures and lowering indoor cooling demand. To assess their potential, a workflow combining Building Information Modelling (BIM) and dynamic energy simulation (EnergyPlus) was developed, testing three envelope configurations across three climate zones: temperate (Brussels), hot and dry (Phoenix), and tropical (Singapore). Results were also analyzed under a future RCP 4.5 climate scenario. Outcomes reveal a strong climate dependency. Singapore showed the greatest benefit, with a 38.4% reduction in annual cooling energy when radiative cooling covered the full envelope. Phoenix achieved a 32.6% reduction, though winter heating penalties limited gains. Brussels showed limited applicability, as heating demand increases outweighed cooling savings. Future climate projections consistently show rising cooling demands, reinforcing the long-term relevance of passive cooling strategies, especially in warm and tropical regions. Overall, BIM-integrated simulation proves to be a robust design tool for evaluating envelope strategies with direct implications for occupant health, energy performance, and climate resilience.

Keywords: *Radiative cooling, BIM, energy efficiency, built environment, energy simulation.*

1. INTRODUCTION

Buildings play a critical role in both human well-being and global energy consumption. In office environments, inadequate thermal conditions can negatively affect occupant comfort, productivity, and attendance, while the building sector remains a major contributor to energy demand, greenhouse gas emissions, and the intensification of urban heat island effects [1]. Consequently, enhancing the thermal performance of buildings is essential not only for improving energy efficiency but also for promoting healthier and more comfortable indoor environments. In this context, passive cooling technologies have attracted increasing attention as sustainable alternatives to conventional mechanical systems. Among these strategies, radiative cooling has emerged as a promising approach for reducing cooling loads and mitigating overheating in buildings. Recent advances in passive daytime radiative cooling (PDRC) materials have expanded their potential applications beyond coatings and films to structural building materials. In particular, a newly developed Roman-inspired radiative cooling concrete [2] combines the mechanical functionality of conventional concrete with high solar reflectance (≈0.95) and thermal emissivity (≈0.91), achieves daytime radiative cooling powers above 45 W m^{-2}, remaining up to 2°C below ambient temperature under strong solar irradiance. Simulations indicate potential reductions of ~50% in building energy use and CO_2 emissions, lowering urban surface temperatures by up to 10°C during heat waves. These developments highlight the potential of integrating radiative cooling technologies directly into building envelopes as a scalable strategy for improving energy efficiency and climate resilience in the built environment.

Moreover, the built environment increasingly relies on novel materials and coatings, BIM, and energy simulation to improve energy efficiency in the built environment and as a decision led tool. Recent work focuses on accurate physical modeling and digital integration across the whole building life cycle. Together, these approaches support low carbon design by coupling advanced materials, detailed 3D information models, and dynamic performance simulations. Recent reviews highlight daytime radiative cooling as a “zero energy” passive cooling strategy, enabled by spectrum selective and broadband emitters integrated into roofs and facades for sub ambient temperatures and cooling load reduction [3]. Building studies show roofs based on radiative cooling (RC) materials can cut annual cooling energy by ~7–9% in cooling dominated climates and significantly lower roof and indoor temperatures [4,5].

On the one hand, new models couple spectral dependent radiative properties with whole building simulation tools (EnergyPlus, DeST) to improve accuracy and reduce computation time [6]. On the other hand, BIM has evolved into a core digital platform for energy-efficient building design, enabling 3D, data rich models that support energy analysis, optimization of envelopes and HVAC, and lifecycle decision making [7,8,9]. Systematic reviews show strong interest in BIM–BEM integration for performance based design, while emphasizing continuing interoperability and data exchange challenges between BIM tools (e.g., Revit) and simulation engines (EnergyPlus, DesignBuilder, IES, GBS) [9,10,11]. Dynamic thermal and building energy simulations are central to quantifying performance, such as testing advanced materials such as radiative coolers, and guiding retrofit and early stage design decisions within BIM workflows [11,12]. Radiative cooling materials, when coupled with robust energy simulation, offer promising passive cooling potential for building envelopes.

2. METHODOLOGY

Building energy simulations were performed to evaluate the impact of radiative cooling (RC) materials on annual heating and cooling energy demand. Results are reported in kWh/m² for three climatic locations. The simulations provided annual heating and cooling energy demands for each building configuration.

2.1. Workflow

The workflow consisted of three sequential stages 1) climate selection, 2) building modelling, and 3) energy simulation. First, representative climates were selected to evaluate the performance of radiative cooling materials under different environmental conditions. For that purpose, we used the methodology proposed in [13]. Hourly meteorological datasets were generated using Meteonorm v8.2 based on Typical Meteorological Year (TMY) data, including models for solar radiation, diffuse sky irradiance, sky temperature, and solar geometry. The selected locations correspond to different Köppen-Geiger climate classifications. Singapore (Af) represents a humid equatorial climate characterized by high temperatures, elevated humidity levels, and frequent cloud cover, conditions that are challenging for radiative cooling technologies. Phoenix (BSh) represents a hot semi-arid climate with high solar irradiance, low humidity, and predominantly clear skies, conditions that are highly favorable for radiative cooling. Brussels represents a temperate climate with significant seasonal heating requirements, allowing the evaluation of potential heating penalties associated with radiative cooling. Finally, to evaluate the influence of future climate conditions on building energy performance, simulations were also conducted using the Representative Concentration Pathway (RCP) 4.5 scenario. This scenario represents a moderate stabilization scenario in which greenhouse gas emissions are partially mitigated, leading to an intermediate level of climate change.

The building model was developed using Autodesk Revit 2025 to ensure compatibility with a BIM-based simulation workflow. Revit was selected as it provides robust interoperability through the gbXML schema, which is directly supported by DesignBuilder. This workflow enables the transfer of geometric and construction information from BIM environments into building energy simulation tools while preserving consistency throughout the design process.

Energy simulations were performed using EnergyPlus 9.4 through the DesignBuilder 7.3.1.003 graphical interface. The BIM model was initially exported from Revit using the gbXML format and imported into DesignBuilder. However, limitations associated with geometry translation and interoperability between software platforms were identified during the import process. Although the case-study building consisted of a relatively simple geometry, discrepancies were observed in the imported model, requiring the geometry to be reconstructed directly within DesignBuilder to ensure simulation reliability and consistency. Consequently, the final energy simulations were conducted using a manually recreated DesignBuilder model while maintaining the same geometric and construction characteristics defined in the BIM environment. This additional step reduced potential errors associated with data exchange and ensured that the simulation results were not influenced by interoperability issues between software platforms.

2.2. Cases

A three-story office building with a total conditioned floor area of 1605 m² was modeled and simulated for all climatic locations. Building dimensions are 15.4 by 2.8 and a total height of 10.5 m. The building envelope consisted of 20 cm-thick walls and roof, representing a typical heavyweight construction with high thermal inertia. The building was assumed to operate continuously (24/7), maintaining stable internal conditions throughout the year of 21°C. The building façade included 30% glazing, evenly distributed across orientations. All envelope characteristics, internal gains, and operational schedules were kept constant across simulations, ensuring that performance variations were attributable solely to climatic differences between locations. Three envelope configurations were used a reference case with conventional concrete construction and no insulation, a variant with RC —solar reflectance (0.95) and thermal emissivity (0.91)— applied to the roof only, and a variant covering both walls and roof (Table 1).

Table 1
Building scenario configuration

Scenario	Name	Wall composition	Roof composition
S1	Reference (Ref)	20 cm concrete	20 cm concrete
S2	RC_roof	20 cm concrete	20 cm concrete RC
S3	RC_envelope	20 cm concrete RC	20 cm concrete RC

3. RESULTS

Table 2 presents the total annual building energy demand, expressed as the sum of heating and cooling loads normalized by floor area (kWh/m²·year), for the reference case and the two radiative cooling configurations as shown in Table 1. Results are reported for three representative climate zones under current climatic conditions and the future RCP4.5 scenario. This comparison enables the assessment of the overall energy impact of radiative cooling technologies and their sensitivity to different climatic conditions and projected climate change.

Table 2
Total Energy Demand (Heating + Cooling) [kWh/m²·year] in each location

Location	Scenario	Reference	RC_roof	RC_envelope	Δ vs Ref (RC_roof)	Δ vs Ref (RC_envelope)
Brussels	Present	100.46	105.34	112.44	+4.8%	+11.9%
Phoenix	Present	103.21	94.05	91.75	−8.9%	−11.1%
Singapore	Present	270.33	190.59	166.59	−29.5%	−38.4%
Brussels	RCP4.5	100.04	104.22	110.83	+4.2%	+10.8%
Phoenix	RCP4.5	106.85	96.88	93.92	−9.3%	−12.1%
Singapor	RCP4.5	280.52	200.37	175.11	−28.6%	−37.6%

3.1. Brussels

In Brussels, the application of radiative cooling materials decreases cooling demand substantially but simultaneously increases heating demand. As a result, the heating penalty outweighs the cooling benefit, leading to a net increase in annual energy consumption. Under the present climate, total energy use rises from 100.46 kWh/m²·year for the reference building to 105.34 kWh/m²·year with the radiative cooling roof and 112.44 kWh/m²·year with the radiative cooling envelope. Similar trends are observed under the RCP4.5 scenario, where total energy demand reaches 104.22 kWh/m²·year and 110.83 kWh/m²·year for the roof and envelope configurations, respectively. Climate warming slightly reduces the penalty because heating requirements decrease, but radiative cooling remains disadvantageous in this climate.

3.2. Phoenix

In Phoenix, the reduction in cooling demand more than compensates for the increase in heating demand, resulting in lower overall energy consumption. Under present climatic conditions, annual energy demand decreases from 103.21 kWh/m²·year in the reference case to 94.05 kWh/m²·year with the radiative cooling roof and 91.75 kWh/m²·year with the radiative cooling envelope. Under the RCP4.5 scenario, the total demand increases for all configurations because of higher cooling requirements, yet radiative cooling remains beneficial. Energy use falls from 106.85 kWh/m²·year in the reference building to 96.88 kWh/m²·year and 93.92 kWh/m²·year for the roof and envelope configurations, respectively. The full-envelope application consistently provides the largest savings, demonstrating the suitability of radiative cooling materials in hot-arid climates.

3.3. Singapore

Singapore exhibits the strongest benefits from radiative cooling because cooling dominates building energy consumption and heating demand is essentially negligible. In the present climate, annual energy demand decreases from 270.33 kWh/m²·year in the reference building to 190.59 kWh/m²·year with a radiative cooling roof and 166.59 kWh/m²·year with a radiative cooling envelope. Under the RCP4.5 scenario, cooling requirements increase, raising the reference demand to 280.52 kWh/m²·year. Nevertheless, the radiative cooling strategies continue to provide substantial reductions, lowering consumption to 200.37 kWh/m²·year and 175.11 kWh/m²·year for the roof and envelope configurations, respectively. The envelope configuration consistently achieves the highest savings, confirming that radiative cooling is particularly effective in hot-humid climates where cooling loads dominate year-round.

3.4. Comparison between climates

The results highlight the strong climate dependence of radiative cooling technologies. In Brussels, both radiative cooling configurations increase total annual energy demand due to higher heating requirements, despite significant reductions in cooling loads. In contrast, Phoenix and Singapore benefit from net energy savings, as cooling-demand reductions out-

weigh the associated heating penalties. The greatest improvements are observed in Singapore, where the radiative cooling envelope reduces total energy consumption by nearly 40% under both present and future climate conditions. The RCP4.5 scenario generally increases total energy demand in the warm climates because of higher cooling needs, but it does not alter the overall trends: radiative cooling remains beneficial in hot climates and less suitable in colder regions. Among the evaluated strategies, the full-envelope application consistently delivers the largest energy savings.

4. CONCLUSIONS

The simulation results demonstrate that the effectiveness of radiative cooling materials depends strongly on climatic conditions. For all locations, radiative cooling materials reduced cooling demand, with the largest reductions consistently obtained when radiative cooling materials were applied to both roofs and walls. The RC_envelope configuration achieved cooling demand reductions of 47.1% in Brussels, 32.6% in Phoenix, and 25.5% in Singapore relative to the uninsulated reference buildings.

The application of radiative cooling materials also increased heating demand in climates where heating loads were present. This effect was observed in both Brussels and Phoenix and was more pronounced when radiative cooling materials were applied to the entire envelope. The incorporation of mineral wool insulation substantially reduced heating demand in Brussels and Phoenix and reduced cooling demand in Phoenix and Singapore. The results indicate that radiative cooling materials are effective in reducing cooling loads across all examined climates. However, their impact on annual building energy performance depends on the balance between heating and cooling requirements.

Although the initial workflow was intended to use a BIM-based approach, where the building geometry would be modeled in Revit and subsequently imported into Energy simulations software for simulations, several limitations were encountered during the data exchange process. As a result, the building had to be remodeled directly in the energy simulation software to ensure reliable simulation results and full compatibility with the analysis requirements. These challenges highlight that there is still room for improvement in the interoperability between BIM and building performance simulation tools, particularly regarding the accurate transfer of geometric information, material properties, and model data during the conversion and import processes.

REFERENCES

[1] Santamouris, M.: Recent progress on urban overheating and heat island research. Integrated assessment of the energy, environmental, vulnerability and health impact. Synergies with the global climate change. Energy and Buildings 207, 109482 (2020). https://doi.org/10.1016/j.enbuild.2019.109482.

[2] Dolado, J.S., Goracci, G., Moutaoukil, G., Agbaoye, R.O., Beruete, M., Torres-García, A.E., Carlosena, L., Prabhu, A., Ibáñez, J.A., Adams, N., van Lipzig, N., Allacker, K.: A Modern Roman-Inspired Concrete with Daytime Radiative Cooling Capacity. Advanced Science n/a(n/a), e11691 (2025). https://doi.org/10.1002/advs.202511691.

[3] Wang, Z., Pian, S., Zhang, Y., Ma, Y.: Fundamental concepts, design rules and potentials in radiative cooling. Reports on Progress in Physics 88(4), 045901 (2025). https://doi.org/10.1088/1361-6633/adc69d.

[4] Chen, J., Lu, L.: Comprehensive evaluation of thermal and energy performance of radiative roof cooling in buildings. Journal of building engineering 33, 101631 (2020). https://doi.org/10.1016/j.jobe.2020.101631.

[5] Belotti, C., Manara, J., Vidi, S., Pattelli, L., Hameury, J.: Spectral longwave atmospheric irradiance determination for site- and date-specific passive radiative cooling modeling. Sustainable Energy Technologies and Assessments 91, 105046 (2026). https://doi.org/10.1016/j.seta.2026.105046.

[6] Xuan, Q., Lei, L., Wang, T., Jiang, B., Zhao, B., Li, G., Pei, G., Dai, J.-G.: Analysis of the thermal and energy saving performance of the concrete roof with radiative cooling coating. Journal of Building Engineering 106, 112578 (2025). https://doi.org/10.1016/j.jobe.2025.112578.

[7] Zhao, T., Qu, Z., Liu, C., Li, K.: BIM-based analysis of energy efficiency design of building thermal system and HVAC system based on GB50189-2015 in China. International Journal of Low-Carbon Technologies (2021). https://doi.org/10.1093/ijlct/ctab051.

[8] Pereira, V., Santos, J., Leite, F., Escórcio, P.: Using BIM to improve building energy efficiency - A scientometric and systematic review. Energy and Buildings 250, 111292 (2021). https://doi.org/10.1016/j.enbuild.2021.111292.

[9] Alhammad, M., Eames, M., Vinai, R.: Enhancing Building Energy Efficiency through Building Information Modeling (BIM) and Building Energy Modeling (BEM) Integration: A Systematic Review. Buildings 14(3), 581 (2024). https://doi.org/10.3390/buildings14030581.

[10] Luong, D.L., Truong, N.-S., Ngo, N.-T., Nguyen, N.-Q.: Developing the hybrid BIM-BEM and jellyfish search optimization system for optimizing energy consumption and building installation costs. Scientific Reports 14(1), 17186 (2024). https://doi.org/10.1038/s41598-024-68021-6.

[11] Hosseini, S.M., Shirmohammadi, R., Kasaeian, A., Pourfayaz, F.: Dynamic thermal simulation based on building information modeling: A review. International Journal of Energy Research 45, 14221-14244 (2021). https://doi.org/10.1002/er.6740.

[12] Carrasco, C., Lombillo, I., Balbas, F.J.R., Aranda, J.R., Villalta, K.: Building Information Modeling (BIM 6D) and Its Application to Thermal Loads Calculation in Retrofitting. Buildings (2023). https://doi.org/10.3390/buildings13081901.

[13] Carlosena, L., Ruiz-Pardo, Á., Rodríguez-Jara, E.Á., Santamouris, M.: Worldwide potential of emissive materials based radiative cooling technologies to mitigate urban overheating. Building and Environment 243, 110694 (2023). https://doi.org/10.1016/j.buildenv.2023.110694.

Sustainable 3D printing of biomass-based biosensors with tunable electrical and biological properties

Jesús M. Rodríguez-Rego[a], *, Laura Mendoza-Cerezo[a], Alfonso C. Marcos-Romero[a], Paulo S. Duque-de Brito[b], Eva M. Hernández-Preciado[c]

[a] Graphic Expression, School of Industrial Engineering, University of Extremadura, 06006, Badajoz

[b] Valoriza-Research Centre for Endogenous Resources Valorization, Portalegre Polytechnic University, 7300-555, Portugal

[c] Nursing, Faculty of Nursing and Occupational Therapy, University of Extremadura, 10003, Cáceres

*e-mail: jesusrodriguezrego@unex.es

Abstract: Sustainable conductive materials are increasingly relevant for the development of flexible biosensors with reduced environmental impact. In this work, biomass-derived carbon obtained from peach peel pyrolysis was incorporated into a K-carrageenan (KC) hydrogel matrix to produce a printable conductive formulation for extrusion-based 3D printing. The study evaluated the relationship between rheological behaviour, printability, electrical response, and cytocompatibility. The developed formulation showed predominantly elastic behaviour and clear shear-thinning response, supporting stable extrusion through a 22G nozzle. Printed structures maintained their geometry after deposition, achieving a shape fidelity of 94.04% based on the comparison between the CAD-defined area and the measured printed area. Electrical characterization showed a stable response within the analysed temperature range and a marked resistance increase under bending, indicating piezoresistive behaviour. In vitro assays using MSC 181TT cells showed no significant reduction in cell viability after 24 h exposure to biomass-containing extracts. These results suggest that peach-peel-derived carbon can be used as a sustainable conductive filler for hydrogel-based inks, providing a promising route for the additive manufacturing of flexible, cytocompatible biosensing platforms.

Keywords: *Biomass-derived hydrogel, Extrusion-based 3D printing, Piezoresistive sensor, Rheological behaviour, Sustainable bioelectronics.*

1. INTRODUCTION

Biosensors are devices that convert a biological, chemical, or physical interaction into a measurable signal, commonly electrical, optical, or mechanical. In flexible biosensing platforms, device geometry, material distribution, and signal stability are key design factors, making extrusion-based 3D printing a useful route for fabricating customized sensor structures with controlled dimensions. Conventional bioelectronic devices often rely on synthetic conductive polymers, metallic components, and nanomaterials that may involve limited degradability, high cost, or environmental concerns [1].

Biomass-derived carbon materials have emerged as attractive conductive fillers due to their electrical functionality, tunable surface chemistry, and potential for waste valorisation. In parallel, natural biopolymers offer biodegradability and biocompatibility, although they usually require conductive fillers to achieve efficient charge transfer [2].

Extrusion-based 3D printing enables the fabrication of functional hydrogel structures with controlled geometry and material distribution [3]. However, printable hydrogel inks must combine shear-thinning behaviour during extrusion with sufficient recovery after deposition, and the incorporation of conductive carbon fillers can affect printability, shape fidelity, and cell viability [4].

Despite these advances, the integration of biomass-derived carbon into printable hydrogel matrices still requires further study, particularly regarding the relationship between processing conditions, charge transport, shape fidelity, and biological response [5].

This work addresses this challenge by developing a KC hydrogel loaded with carbonized peach peel for extrusion-based 3D printing. The formulation was evaluated in terms of rheological behaviour, CAD-based shape fidelity, electrical resistance under temperature and bending conditions, and in vitro cytocompatibility.

2. MATERIALS AND METHODS

2.1. Method for hydrogel fabrication

The ink was formulated using a KC matrix and biomass-derived carbon obtained from peach peel pyrolysis at 900 °C. KC was dissolved at 2% (w/v) in distilled water at 80 °C under constant stirring, followed by the addition of 2% (w/v) biomass-derived carbon. Mechanical stirring was used to promote homogeneous dispersion and reduce aggregate formation before printing. After pyrolysis, the carbonized peach peel was mechanically ground to obtain a fine carbonaceous powder before incorporation into the hydrogel matrix. The powder was dispersed under mechanical stirring to reduce agglomeration and avoid nozzle obstruction during extrusion.

2.2. Rheological analysis

Rheological behaviour was evaluated using a Kinexus Pro rotational rheometer with a 40 mm parallel-plate geometry and a fixed gap of 0.2 mm. Temperature sweeps were per-

formed from 26 to 40 °C within the linear viscoelastic range. Storage modulus (G'), loss modulus (G''), and viscosity as a function of shear rate were recorded to assess the suitability of the formulation for extrusion-based printing.

2.3. Printability analysis

Printability was evaluated using a CELLINK Bio X extrusion system under constant printing parameters: 40 kPa, 9 mm/s, and 22G nozzle. Shape fidelity was assessed by comparing the projected area of the CAD model with the area of the printed geometry measured in AutoCAD. The printed specimen was photographed, imported into AutoCAD, scaled using a known reference dimension, and its external contour was measured. Shape fidelity was calculated as indicated in equation (1):

$$SF(\%) = \frac{\min\left(A_{CAD}, A_{printed}\right)}{\max\left(A_{CAD}, A_{printed}\right)} \times 100 \quad (1)$$

where A_{CAD} is the theoretical area defined in the CAD model and $A_{printed}$ is the projected area measured from the printed specimen.

2.4. Characterisation of electrical resistance

Electrical resistance was measured on printed specimens using a Keithley 197 Autoranging Microvolt DMM. Measurements were performed at 25, 30, and 40 °C and under controlled bending conditions. The same contact configuration was maintained throughout the tests to reduce variability associated with electrode positioning. Resistance values were used to evaluate thermal stability and piezoresistive response.

Electrical measurements were performed on three independently printed specimens, and three consecutive readings were recorded for each condition after signal stabilization. This procedure was used to assess the repeatability of the electrical response and to reduce the influence of contact-related variability.

2.5. Cytotoxicity assay

For the cytotoxicity assays, the MSC 181TT cell line (kindly provided by INIBIC, A Coruña, Spain) was seeded in 96-well plates at a density of 5,000 cells per well and incubated for 24 h to reach subconfluence in complete DMEM (supplemented with 10% FBS and 1% pen/strep) under standard culture conditions (37 °C, 5% CO_2). The hydrogel was incubated in complete DMEM for 24 h to obtain the extract (0.2 g of hydrogel per 1 mL). The extract was then filtered and placed in contact with the cell cultures at various concentrations (25, 50, 75 and 100%) for an additional 24 h.

Cell viability was quantified using the MTS assay (CellTiter 96® AQueous One Solution, Promega) by measuring absorbance at 490 nm with an HiPo MPP-96 microplate

reader. All assays were performed in triplicate (n = 3), and data are presented as mean ± standard deviation. Student's t-test was used as a preliminary comparison between treated groups and the untreated control, with statistical significance set at $p < 0.05$.

3. RESULTS AND DISCUSSION

3.1. Rheological behaviour

Both formulations showed predominantly elastic behaviour over the analysed temperature range, with G' remaining higher than G'' (Figure 1A), which is consistent with hydrogel systems suitable for maintaining structural stability after deposition [6]. The incorporation of biomass-derived carbon slightly reduced the viscoelastic moduli, suggesting a moderate effect of the carbon phase on the KC network.

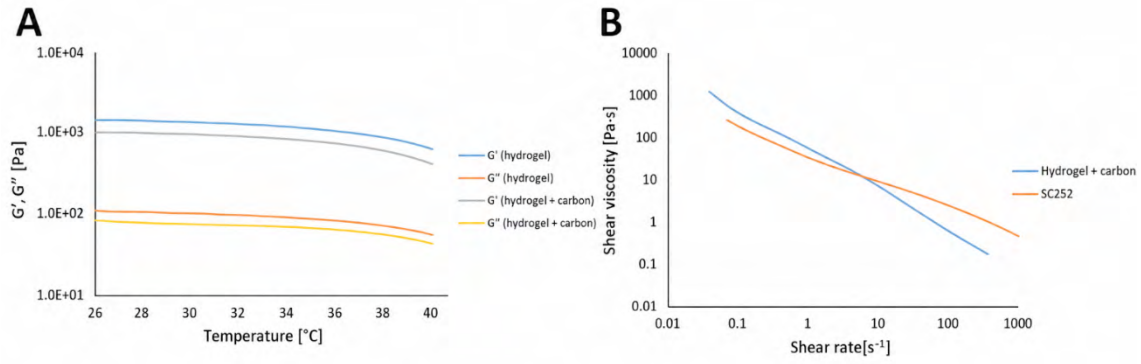


FIG. 1

Rheological characterization of KC-based hydrogel and biomass-loaded system: A) temperature-dependent viscoelastic properties (G' and G'') and B) shear-thinning behaviour as a function of shear rate

Both formulations showed predominantly elastic behaviour over the analysed temperature range, with G' remaining higher than G'' (Figure 1A), which is consistent with hydrogel systems suitable for maintaining structural stability after deposition [6]. The incorporation of biomass-derived carbon slightly reduced the viscoelastic moduli, suggesting a moderate effect of the carbon phase on the KC network.

Viscosity decreased with increasing shear rate in both systems, confirming shear-thinning behaviour suitable for extrusion-based 3D printing (Figure 1B) [7]. The biomass-loaded formulation maintained sufficient viscosity at low shear rates for shape retention, while its lower viscosity under shear favoured extrusion through the nozzle.

3.2. Printability and Shape Fidelity

The biomass-loaded hydrogel was successfully extruded through a 22G nozzle under controlled pressure conditions, producing continuous filaments without noticeable disconti-

nuities or clogging. The printed specimens showed good dimensional stability, with no significant collapse or spreading after deposition.

The area-based comparison showed a slight over-deposition of the material, with an experimental area of 11.75 mm² compared with the theoretical CAD area of 11.05 mm². Using the defined shape fidelity equation, the printed geometry reached 94.04% (Table 1), indicating good agreement between the CAD model and the fabricated specimen. This deviation may be associated with filament spreading after deposition and viscoelastic relaxation of the hydrogel. Future work should include digital inspection techniques, such as calibrated image analysis, 3D scanning, or contour deviation maps, to obtain a more complete evaluation of dimensional accuracy.

TABLE 1
Shape fidelity assessment based on CAD and printed areas

Theoretical area [mm²]	Actual area [mm²]	% of Similarity
11.05	11.75	94.04

3.3. Electrical Response of the Printed Biosensor

The electrical response of the printed hydrogel was evaluated under temperature variation and bending deformation (Figure 2 and Table 2). Resistance showed only a slight decrease with temperature, from 55.01 kΩ at 25 °C to 54.66 kΩ at 40 °C, indicating a relatively stable electrical response within the analysed range, which is advantageous for biosensing applications where signal stability is required [8].

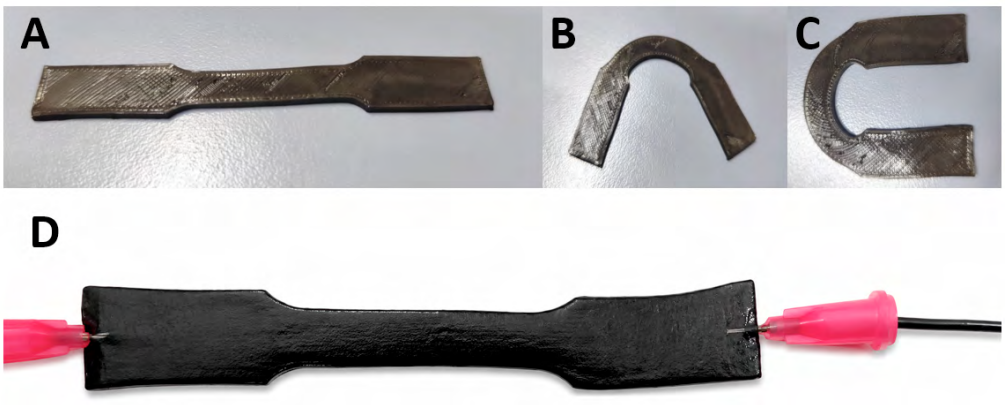


FIG. 2
Printed biomass-based hydrogel specimens used for electromechanical evaluation: A) undeformed specimen, B) specimen under moderate bending, and C) specimen under higher bending deformation. D) Sample connected to the voltmeter

TABLE 2
Electrical resistance under temperature and bending conditions

Condition	Value	Electrical resistance [kΩ]
Temperature (°C)	25	55.01
	30	54.78
	40	54.66
Bending angle (°)	0	55.01
	23	63.24
	60	64.92

In contrast, bending produced a clear increase in resistance, from 55.01 kΩ in the undeformed state to 64.92 kΩ at 60°. This behaviour suggests a piezoresistive response associated with deformation-induced changes in the conductive network, in agreement with the operating principle of flexible strain-sensitive materials [9]. However, complete sensor validation will require cyclic loading tests, sensitivity quantification, and long-term stability analysis.

3.4. Cytotoxicity assay

Exposure of MSC 181TT cells to biomass-containing extracts did not reduce cell viability at any of the tested concentrations after 24 h (Figure 3). Viability values remained comparable to the untreated control, with no statistically significant differences between groups (Student's t-test, $p > 0.05$). These results indicate that the developed formulation did not show cytotoxic effects under the evaluated extraction conditions.

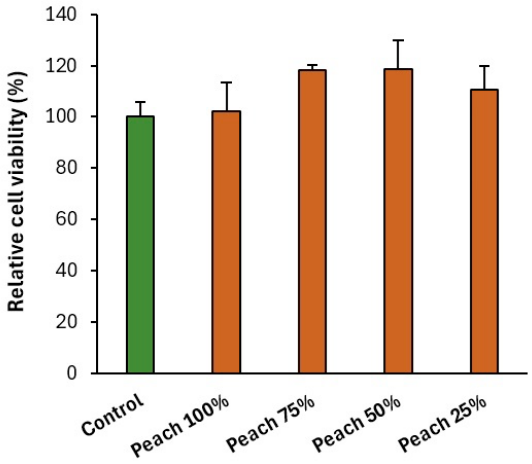


FIG. 3
Relative cell viability (%) of MSC 181TT cells following 24 h exposure to peach peel biomass extracts at concentrations of 25, 50, 75, and 100%. Cell viability was determined by MTS assay and expressed as a percentage relative to the untreated control (set at 100%). Data are presented as mean ± SD (n = 3). No statistically significant differences were observed between treatment groups and the control (Student's t-test, $p > 0.05$)

4. CONCLUSIONS

This work demonstrates the feasibility of using peach-peel-derived carbon as a sustainable conductive filler in a KC hydrogel matrix for extrusion-based 3D printing of flexible biosensing platforms. The formulation showed shear-thinning behaviour and predominantly elastic response, enabling stable extrusion and shape retention after deposition. The printed structures achieved a good shape fidelity of 94.04% based on the comparison between CAD and printed areas. Electrical characterization showed a stable response to temperature variations and a clear piezoresistive behaviour under bending deformation, while cytotoxicity assays confirmed no significant reduction in MSC 181TT cell viability after 24 h exposure to the extracts.

Overall, the results support the potential of biomass-derived hydrogel inks for sustainable additive manufacturing of cytocompatible sensing platforms. Future work should focus on improving dimensional inspection, quantifying sensor sensitivity under cyclic loading, and evaluating long-term electrical and biological stability.

Acknowledgements: The authors would like to thank the BIOIMP_ACE_MAS_6_E project, co-funded by the European Union through the Interreg VI-A Spain-Portugal Programme (POCTEP) 2021-2027.

REFERENCES

[1] Feig, V.R., Tran, H., Bao, Z.: Biodegradable Polymeric Materials in Degradable Electronic Devices. ACS Cent. Sci. 4, 337-348 (2018). https://doi.org/10.1021/acscentsci.7b00595.

[2] Serafin, A., Casanova, C.R., Chandel, A.K.S., Reis, R.L., Oliveira, J.M., Collins, M.N.: Conductive biological materials for in vitro models: properties and sustainability implications. In Vitro Model. 4, 89-110 (2025). https://doi.org/10.1007/s44164-025-00088-5.

[3] Chen, X.B., Fazel Anvari-Yazdi, A., Duan, X., Zimmerling, A., Gharraei, R., Sharma, N.K., Sweilem, S., Ning, L.: Biomaterials / bioinks and extrusion bioprinting. Bioact Mater. 28, 511-536 (2023). https://doi.org/10.1016/j.bioactmat.2023.06.006.

[4] Cong, C., Subramanian, S., Bodkhe, G.A., Wang, G., Li, Z., Wang, R., Li, X., Kim, M., Kim, S.H.: 3D Carbon-Based Conductive Network Printed for Glucose Sensors on Curved and Flexible Substrates. ACS Appl. Mater. Interfaces. 16, 7543-7553 (2024). https://doi.org/10.1021/acsami.3c14757.

[5] Li, Y., Xu, R., Wang, H., Xu, W., Tian, L., Huang, J., Liang, C., Zhang, Y.: Recent Advances of Biochar-Based Electrochemical Sensors and Biosensors. Biosensors. 12, (2022). https://doi.org/10.3390/bios12060377.

[6] Ata, O., Yazar, G., Tavman, S., Kokini, J.L.: Linear and nonlinear rheological properties of gelatin-chitosan hydrogels: Evaluation of crosslinker concentration and temperature effects. Food Hydrocolloids. 163, 111130 (2025). https://doi.org/10.1016/j.foodhyd.2025.111130.

[7] Mendoza-Cerezo, L., Rodríguez-Rego, J.M., Macias-García, A., Iñesta-Vaquera, F. de A., Marcos-Romero, A.C.: Study of Printable and Biocompatible Alginate-Carbon Hydrogels for Sensor Applications: Mechanical, Electrical, and Cytotoxicity Evaluation. Gels. 11, (2025). https://doi.org/10.3390/gels11060389.

[8] Naresh, V., Lee, N.: A Review on Biosensors and Recent Development of Nanostructured Materials-Enabled Biosensors. Sensors. 21, (2021). https://doi.org/10.3390/s21041109.

[9] Li, F., Liu, Y., Shi, X., Li, H., Wang, C., Zhang, Q., Ma, R., Liang, J.: Printable and Stretchable Temperature-Strain Dual-Sensing Nanocomposite with High Sensitivity and Perfect Stimulus Discriminability. Nano Lett. 20, 6176-6184 (2020). https://doi.org/10.1021/acs.nanolett.0c02519.

Horizontal extrusion bioprinting for tubular structure fabrication: design and preliminary feasibility assessment of a rotating-axis system

Jesús M. Rodríguez-Rego*, Laura Mendoza-Cerezo, Alfonso C. Marcos-Romero, Juan P. Carrasco-Amador, David Picado-Tejero

Graphic Expression, School of Industrial Engineering, University of Extremadura, 06006, Badajoz

*e-mail: jesusrodriguezrego@unex.es

Abstract: The fabrication of functional tubular structures remains one of the major challenges in 3D bioprinting, due to the need to simultaneously achieve geometric precision, structural stability, and cell viability. Conventional strategies, such as layer-by-layer deposition, coaxial extrusion, and bioprinting within support media, present limitations in terms of operational complexity, architectural control, and dependence on specific gelation conditions. In this work, a bioprinting system based on horizontal extrusion with a rotating axis is proposed, developed through the modification of a commercial 3D printer. This approach introduces a paradigm shift in the fabrication process by replacing vertical deposition with a continuous radial deposition mechanism onto a dynamic cylindrical support. The system enables the direct formation of tubular structures through the synchronization of extrusion flow rate and rotational speed, providing precise control over wall thickness and final geometry. The system architecture, implemented mechanical modifications, and key operational parameters are described, along with the implications of the design in terms of process stability and bioink selection. The proposed system reduces the need for support materials and improves stability during fabrication, constituting an accessible and potentially scalable alternative for the generation of tubular structures. Finally, the limitations of the approach and future perspectives are discussed, including its integration with advanced bioprinting strategies and its application in vascular tissue engineering and other cylindrical biological systems.

Keywords: *Horizontal extrusion bioprinting, Tubular structure fabrication, Biofabrication, Hydrogel bioinks, Vascular tissue engineering.*

1. INTRODUCTION

3D bioprinting has emerged as one of the most promising technologies in tissue engineering and regenerative medicine, as it enables the precise placement of living cells and biomaterials to fabricate structures that mimic human tissues and organs [1]. However, despite its widespread adoption, this technique presents significant limitations when applied to the fabrication of hollow structures, particularly those with small diameters [2].

The main challenge in layer-by-layer fabrication lies in maintaining structural stability throughout the deposition process. In conventional layer-by-layer 3D printing, cylindrical or hollow geometries typically require additional support structures, which complicates the process and limits material selection [3].

Currently, one of the most widely used approaches is embedded printing within support baths. This technique enables the fabrication of complex structures without conventional supports, using the surrounding medium itself as a temporary scaffold [4]. Among its main advantages, the support bath eliminates the need for additional support structures and enables the fabrication of closed cavities and complex internal channels [5]. Some of the main limitations lie in the rheological interactions between the bioink and the support bath, which can affect shape fidelity and structural stability. In addition, tuning the crosslinking kinetics and the properties of the support bath for each bioink is complex and, in some cases, insufficiently addressed in the literature [6, 7].

In this context, there is a clear need to explore new biofabrication strategies that enable the direct generation of tubular structures without relying on external supports or complex material interactions. An emerging approach involves reconfiguring the deposition system into a horizontal extrusion scheme, in which the material is deposited around a central axis or rod acting as a dynamic support. This configuration leverages the system geometry to guide material deposition, facilitating the formation of continuous structures with circular cross-sections while reducing issues associated with gravitational collapse.

In this work, the conceptual and functional design of a horizontal extrusion-based bioprinting system is proposed, based on the use of a central axis as a dynamic support for the fabrication of tubular structures. The underlying principles of the system, key operational parameters, and their implications in terms of structural stability and cell viability are analyzed, with the aim of establishing a solid foundation for the development of bioprinting devices oriented toward vascular applications and other cylindrical tissue constructs.

2. CONCEPT OF THE PROPOSED SYSTEM AND MODIFICATION OF THE BASE PRINTER

The proposed system is based on the reconfiguration of a conventional extrusion-based 3D printer into a horizontal deposition architecture, specifically designed for the fabrication of tubular structures via bioprinting. Unlike traditional layer-by-layer systems operating in the vertical direction, this approach introduces a central rotating axis

acting as a dynamic support, enabling the controlled deposition of bioink around a cylindrical surface.

This structural modification transforms the fabrication process from a sequential layer-stacking scheme into a continuous radial deposition mechanism, in which the tubular geometry is generated through the synchronized combination of extrusion and rotation.

The system consists of three main subsystems:

—Horizontal syringe-based extrusion system.

—Central rotating axis with speed control.

—Motion control and synchronization platform.

The bioink is continuously extruded through a horizontally oriented nozzle, while the central axis rotates at a controlled speed, enabling the progressive deposition of material onto its surface. The combination of both motions allows the formation of concentric layers that define the wall thickness of the tubular structure.

From a functional perspective, the thickness of the generated structure depends on the relationship between the extrusion flow rate (Q) and the rotational speed of the axis (ω), as well as the distance between the nozzle and the mandrel surface. This coupling introduces a new degree of control over the final geometry, not present in conventional systems.

2.1. Base platform and mechanical reconfiguration

The system was implemented using a commercial cartesian 3D printer, Ender 3 Pro (Creality 3D, Shenzhen, China), originally designed for thermoplastic filament deposition. This platform provides a robust structure, precise positioning systems along the Cartesian axes, and widely accessible control electronics.

The main modification consists of replacing the conventional extrusion head with a syringe-based extrusion system adapted for processing bioinks. This change enables the handling of hydrogels and biological materials while maintaining flow control through a stepper motor.

Additionally, the extrusion system has been reoriented to operate in the horizontal direction, allowing alignment of the nozzle with the deposition axis and facilitating the formation of cylindrical structures without the need for additional support. The proposed modifications are illustrated in Figure 1.

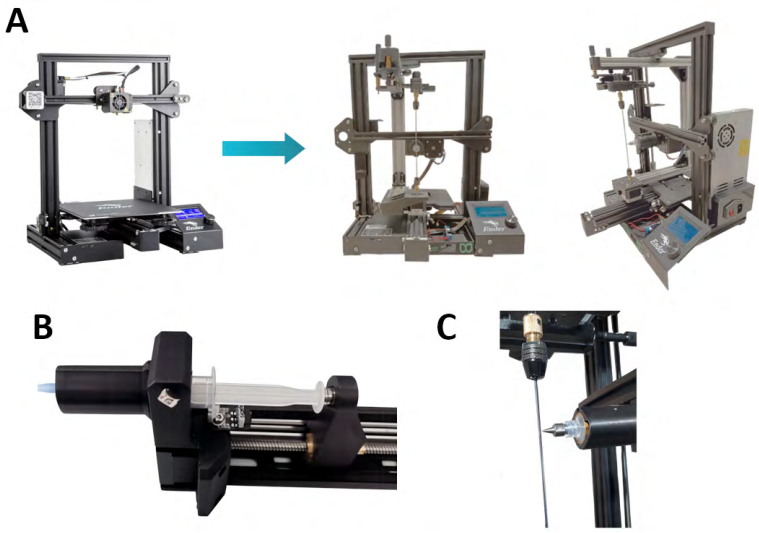


FIG. 1
Design and implementation of the horizontal extrusion bioprinting system. A) Commercial base printer and modified prototype. B) Configuration of the syringe-based extrusion system. C) Schematic of the rotating axis system used as dynamic support for tubular structure fabrication

2.2. Adapted extrusion system

The extrusion system is based on a stepper motor-driven pushing mechanism acting on the plunger of a syringe loaded with bioink. This approach enables precise regulation of the extrusion flow rate, allowing it to be tailored to the specific requirements of the process.

The horizontal configuration introduces additional considerations, such as the stability of the extruded filament and its initial adhesion to the rotating axis. These factors depend on both the rheological properties of the bioink and the deposition distance and extrusion speed.

2.3. Rotating axis system

The central component of the system is the rotating axis, which serves as both a physical support and a geometric reference for lumen formation. This axis is coupled to a stepper motor that enables precise control of its rotational speed.

The stability of the axis, its alignment with the nozzle, and the uniformity of rotation are critical factors to ensure homogeneity of the inner diameter and wall thickness. Additionally, the system must be designed to allow mandrel removal without compromising the structural integrity of the fabricated construct.

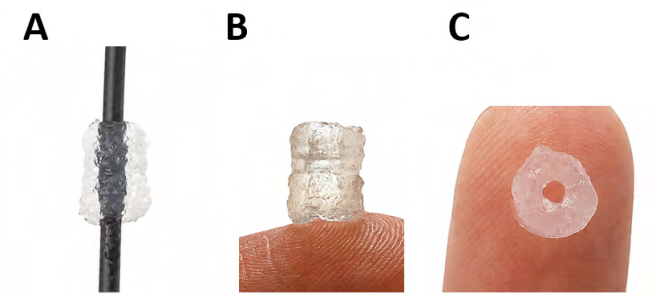


FIG. 2

Production of a tubular hydrogel structure using the newly developed bioprinting technology. A) Tubular hydrogel structure on the rotating axis. B) Side view of the hydrogel removed from the rotating axis. C) Top view of the hydrogel removed from the rotating axis

The proposed configuration enables the transformation of a conventional printer into a system capable of directly fabricating tubular structures (Figure 2), reducing reliance on support materials and improving stability during the deposition process.

The printing process is carried out in four sequential steps. First, the syringe containing the bioink is mounted horizontally and aligned with the rotating mandrel. Second, the nozzle-to-mandrel distance is adjusted to ensure initial contact between the extruded filament and the mandrel surface. Third, the mandrel rotation and the syringe extrusion are activated simultaneously, so that the bioink is deposited radially around the cylindrical support. Finally, the wall thickness is controlled by adjusting the extrusion flow rate, rotational speed, and number of deposited passes. After deposition, the construct can be crosslinked and the mandrel can be removed depending on the selected bioink and gelation strategy. The preliminary construct preserved the intended tubular configuration and a visible lumen after mandrel removal. Future work will include dimensional measurements of inner diameter, outer diameter, and wall thickness to quantify fabrication accuracy.

The use of a rotating axis introduces the possibility of generating structures with controlled anisotropic properties and, potentially, incorporating radial gradients through modulation of the extrusion process.

However, this approach also presents challenges related to process control, the selection of suitable bioinks, and the optimization of operational parameters, all of which must be addressed to ensure the reproducibility and applicability of the system.

3. PRELIMINARY FEASIBILITY ASSESSMENT AND VALIDATION PLAN

As a preliminary feasibility assessment, a non-cell-laden hydrogel construct was fabricated using the rotating-axis configuration. The material was successfully deposited around the mandrel, and the resulting tubular structure could be removed while preserving a visible hollow geometry, as shown in Figure 2. This preliminary result supports the technical feasibility of the proposed horizontal extrusion approach, although further dimensional and biological validation is still required.

Future validation will be organized in three stages: first, non-cell-laden hydrogel printing to determine the operational window of the system; second, dimensional characterization of the printed tubes by comparing the target and fabricated geometries; and third, biological validation using cell-laden bioinks to assess post-printing cell viability and distribution. The expected outcome is the identification of combinations of extrusion flow rate, rotational speed, nozzle-to-mandrel distance, and bioink rheology that allow continuous tubular deposition with controlled wall thickness.

In the first stage, non-cell-laden hydrogel formulations will be used as model materials to establish the initial printing conditions without introducing biological variability. The tests will focus on the practical aspects that determine whether the process can be executed reliably, including the initial adhesion of the extruded filament to the mandrel, the stability of the deposited material during rotation, and the preservation of the cylindrical geometry after deposition. Once stable printing conditions are identified, these parameters will be used as the starting point for the subsequent dimensional and biological validation stages.

4. CONCLUSIONS

This work presents the design and implementation of a horizontal extrusion bioprinting system based on a rotating axis for the fabrication of tubular hydrogel structures. The system was developed by modifying a commercial Cartesian 3D printer and integrating a syringe-based horizontal extrusion unit with a controlled rotating mandrel. A preliminary non-cell-laden hydrogel construct was fabricated, demonstrating that the proposed configuration can generate tubular deposits and preserve a visible lumen after mandrel removal.

The results support the technical feasibility of the approach as a low-cost and accessible platform for tubular biofabrication. Further work will focus on optimizing the relationship between extrusion flow rate, rotational speed, nozzle-to-mandrel distance, and bioink rheology, as well as performing quantitative dimensional characterization and biological validation with cell-laden bioinks.

Acknowledgements: The authors would like to thank the BIOIMP_ACE_MAS_6_E project, co-funded by the European Union through the Interreg VI-A Spain-Portugal Programme (POCTEP) 2021-2027.

REFERENCES

[1] Matai, I., Kaur, G., Seyedsalehi, A., McClinton, A., Laurencin, C.T.: Progress in 3D bioprinting technology for tissue/organ regenerative engineering. Biomaterials. 226, 119536 (2020). https://doi.org/10.1016/j.biomaterials.2019.119536.

[2] Kirillova, A., Maxson, R., Stoychev, G., Gomillion, C.T., Ionov, L.: 4D Biofabrication Using Shape-Morphing Hydrogels. Adv. Mater. 29, 1703443 (2017). https://doi.org/10.1002/adma.201703443.

[3] Wu, Q., Song, K., Zhang, D., Ren, B., Sole-Gras, M., Huang, Y., Yin, J.: Embedded extrusion printing in yield-stress-fluid baths. Matter. 5, 3775-3806 (2022). https://doi.org/10.1016/j.matt.2022.09.003.

[4] Hinton, T.J., Jallerat, Q., Palchesko, R.N., Park, J.H., Grodzicki, M.S., Shue, H.-J., Ramadan, M.H., Hudson, A.R., Feinberg, A.W.: Three-dimensional printing of complex biological structures by freeform reversible embedding of suspended hydrogels. Sci. Adv. 1, e1500758 (2015). https://doi.org/10.1126/sciadv.1500758.

[5] Zhao, J., He, N.: A mini-review of embedded 3D printing: supporting media and strategies. J. Mater. Chem. B. 8, 10474-10486 (2020). https://doi.org/10.1039/d0tb01819h.

[6] Lei, I.M., Zhang, D., Gu, W., Liu, J., Zi, Y., Huang, Y.Y.S.: Soft Hydrogel Shapeability via Supportive Bath Matching in Embedded 3D Printing. Adv. Mater. Technol. 8, 2300001 (2023). https://doi.org/10.1002/admt.202300001.

[7] Tisato, S., Vera, G., Song, Q., Nekoonam, N., Helmer, D.: Additive manufacturing of multi-material and hollow structures by Embedded Extrusion-Volumetric Printing. Nat. Commun. 16, 6730 (2025). https://doi.org/10.1038/s41467-025-62057-6.

Redesign of an Electric Scooter through the Application of TPMS Structures

Ramón Miralbes-Buil*, David Ranz-Angulo, Clara Luna Martín-Compaired, José Antonio Gómez-García

University of Zaragoza, DIDYF-EINA C/María de Luna n.4. 50018 Zaragoza

* e-mail: miralbes@unizar.es

Abstract: Triply Periodic Minimal Surface (TPMS) structures enable the fabrication of lightweight components through additive manufacturing, allowing geometries and design configurations that cannot be achieved using conventional processes. This work focuses on the redesign of a Xiaomi M365 electric scooter, originally featuring an aluminium structure, by incorporating lattice architectures of different types, namely gyroid and diamond. First, a computer-aided design (CAD) model of the original aluminium scooter was obtained through reverse engineering. Subsequently, the structure was redesigned considering the constraints of the additive manufacturing process and material limitations. TPMS architectures were integrated into the scooter base to develop a monomaterial sandwich structure. The redesigned structure was analysed in accordance with the UNE-EN 17128:2020 standard using the finite element method (FEM), and iterative modifications were carried out to ensure compliance with structural requirements. Finally, a prototype was manufactured via additive processes and experimentally tested using an INSTRON testing machine, following an adapted application of the ASTM C393 standard. Both numerical simulations and experimental results demonstrate that a scooter structure manufactured via additive manufacturing and incorporating TPMS architectures can achieve strength levels comparable to those of the original metallic configuration. However, the final design exhibits a significantly higher weight and reduced global stiffness.

Keywords: *redesign, TPMS, lattice, CAD, FEM, scooter.*

1. INTRODUCTION

Triply Periodic Minimal Surface (TPMS) structures enable the generation of designs with a high proportion of void regions and a thin-walled internal architecture, allowing optimal stiffness and strength to be achieved [1]. These structures are defined by a mathematical function which, for a unit cell repeated throughout the structure, determines the three-dimensional geometry of the surface such that the total surface area is minimised and, consequently, the specific mechanical properties are maximised. A solid structure is subsequently generated by assigning thickness to this surface, typically controlled through the volume fraction.

Several studies have analysed different TPMS topologies and concluded that the most efficient structures are the gyroid and diamond configurations [2,3]. These structures are primarily used for structural light weighting in components manufactured via additive manufacturing (AM), enabling optimisation of stiffness and strength by varying both geometric dimensions and local thickness throughout the design.

Traditionally, many products—such as the electric scooter considered in this study have been designed using load-bearing structures made from materials such as steel, aluminium, or composite materials. These designs were constrained by conventional manufacturing processes, which typically resulted in solid structures with suboptimal material utilisation. With the advent of AM, it is now possible to generate virtually any geometry, ensuring structural optimisation through the precise placement of material only where required [3].

Accordingly, this study focuses on the redesign of a common structural product, namely an aluminium electric scooter, such that a material with significantly lower mechanical properties, namely ABS, can be used to achieve a product with comparable weight and strength, albeit with reduced stiffness.

2. MATERIALS AND METHODS

The first step in the redesign process involved generating a CAD model of the scooter through reverse engineering. Starting from a Xiaomi M365 scooter, the “HP 3D Scan” 3D scanner (….) and callipers were used to obtain the external geometry. The surface was initially generated within the scanning software and subsequently imported into SolidWorks, where the geometry was refined, features were identified, and scanning errors were corrected until an accurate model was obtained (see Figure 1).

The material of the original scooter, aluminium 6061-T6, was identified based on manufacturer specifications.

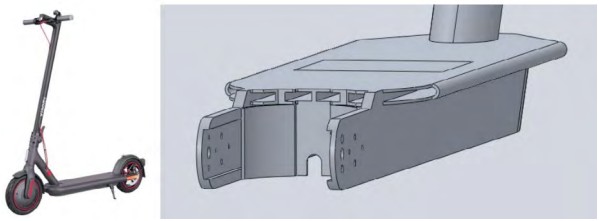


FIG. 1
Left: Xiaomi M365 scooter. Right: CAD model of the scooter

The original scooter was then analysed using the finite element method (FEM) in SolidWorks Simulation to determine its stiffness and strength. The analysis was conducted in accordance with the UNE-EN 17128:2020 standard [5], which specifies that such devices must withstand a force of 3000 N applied over a central area of 100 × 100 mm.

Regarding boundary conditions, the rear wheel region was modelled as a bi-supported constraint allowing rotational freedom corresponding to the wheel, while the central stem region was constrained to prevent rotation and displacement normal to the surface, while allowing in-plane displacements (see Figure 2).

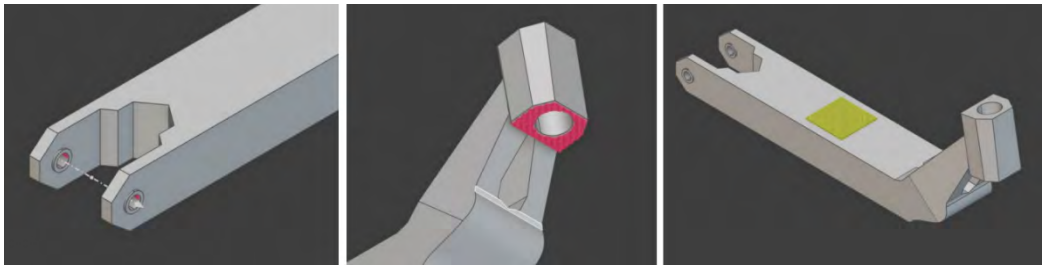


FIG. 2
Loads and boundary conditions for the FEM simulation

Due to limitations in physically testing the full structure—specifically, the lack of testing machines capable of accommodating the scooter—an equivalent experimental test was conducted using an INSTRON 8062 universal testing machine. A three-point bending test, similar to that described in ASTM C393 [6], was performed with a support span of 260 mm and a central load applied via a 100 × 100 mm plate. These tests enabled experimental comparison of stiffness and strength between the original scooter and the redesigned prototype in the central region (see Figure 3).



FIG. 3
Left and centre: test of the aluminium electric scooter. Right: test of the AM specimen

For the TPMS-based redesign, the software n-Topology was used, as it enables both CAD modelling and the application and simulation of TPMS structures. Through multiple

iterations of analysis and optimisation, the scooter was redesigned to achieve strength comparable to the original aluminium structure. Two designs were generated: one based on a gyroid structure and the other on a diamond structure (see Figure 4).

Due to manufacturing constraints, only half of the central section of the scooter was prototyped, with dimensions of 100 × 280 × 90 mm. Full-scale prototyping was not feasible due to size limitations of the available AM equipment. Additionally, FEM analyses of the rectangular sandwich panel section were conducted using n-Topology to validate the simulation results.

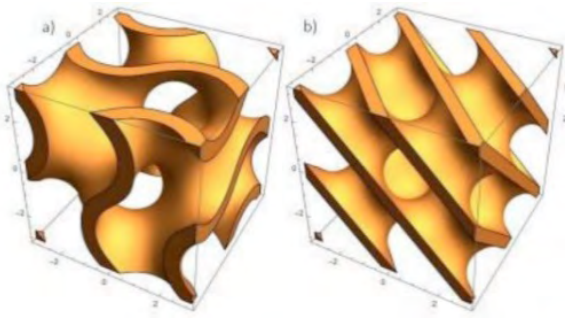


FIG. 4
Left: gyroid structure. Right: diamond structure

3. RESULTS

Analysis of the original scooter (see Figure 5) showed a deformation of 0.978 mm under the standard test load, with a safety factor of approximately 5.

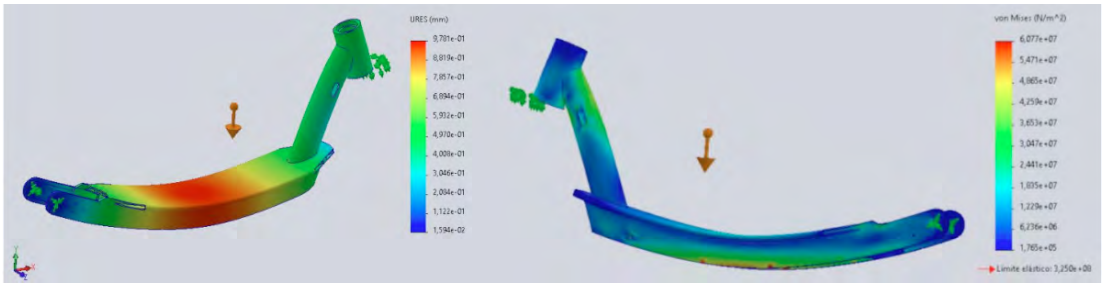


FIG. 5
Left: deformation of the Xiaomi scooter. Right: stress distribution

The scooter was then redesigned using both diamond and gyroid internal structures, while maintaining a solid shell with a thickness of 2.25 mm and a volume fraction of 20%. After iterative optimisation aimed at reducing weight while maintaining comparable strength, two designs were obtained with masses of 4.49 kg (gyroid) and 3.74 kg (diamond), compared to 2.79 kg for the original aluminium structure.

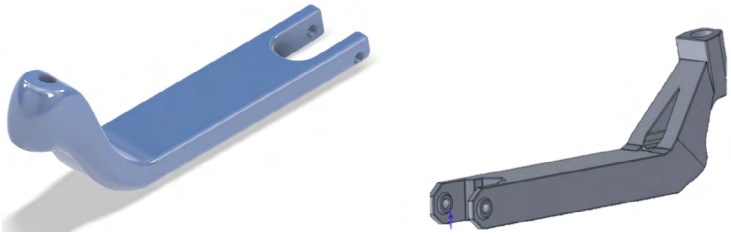


FIG. 6
Left: diamond prototype. Right: gyroid prototype

In terms of stiffness and strength, it should be noted that stiffness was significantly reduced despite the use of a lightweight sandwich-type structure, with deformations of 1.8 mm and 5 mm, respectively (see Figure 7)

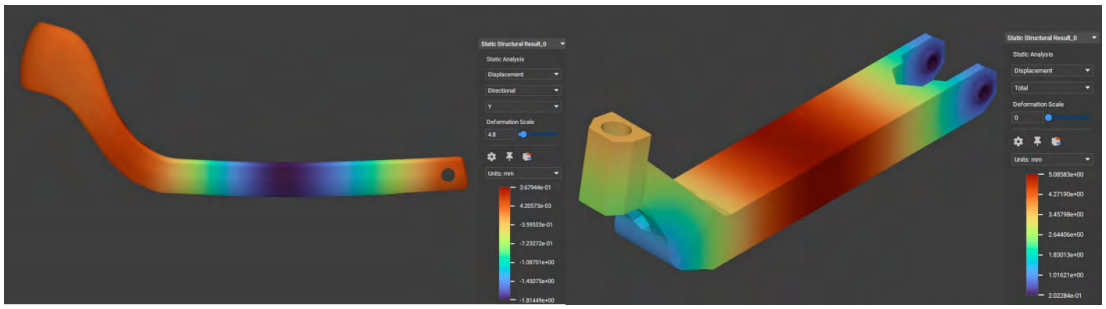


FIG. 7
Displacement obtained from FEM analysis of the final prototypes

Regarding strength, due to the lower yield strength of ABS (42 MPa) compared to aluminium (280 MPa), a significantly greater amount of material and a more optimised distribution were required to achieve a comparable safety factor. Additionally, geometric optimisation was necessary in certain regions to minimise stress concentrations (see Figure 8). As a result, a prototype with a safety factor of approximately 5 was achieved.

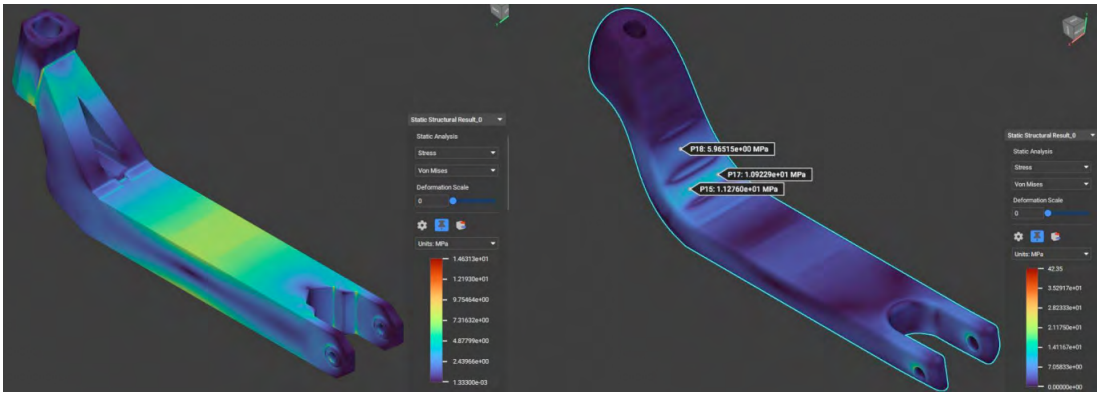


FIG. 8
Stress results from FEM analysis

Finally, several sandwich panels representing the central region of the scooter, as well as the central scooter section itself, were tested using the INSTRON machine to compare stiffness and strength. While the aluminium scooter was not tested to failure, the sandwich prototypes were (see Figure 9). Failure occurred at approximately 22 kN in both cases, with displacements of 11 mm for the diamond structure and 21 mm for the gyroid structure.

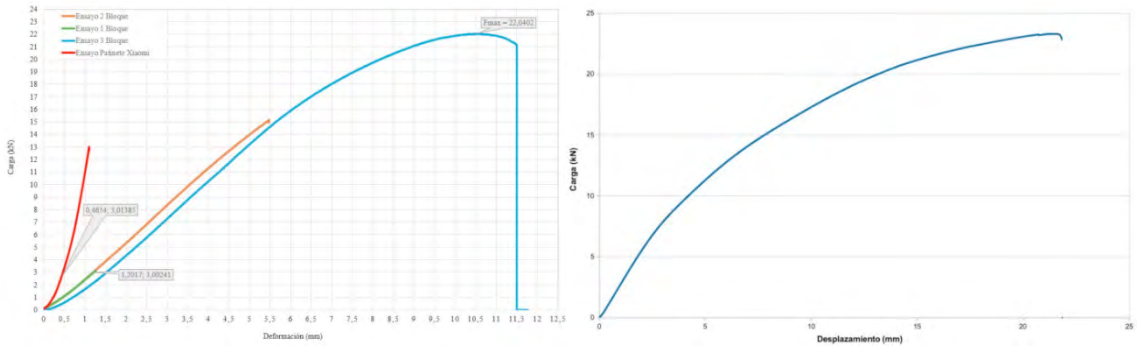


FIG. 9
Force-displacement curves for diamond and aluminium scooters (left) and gyroid scooter (right)

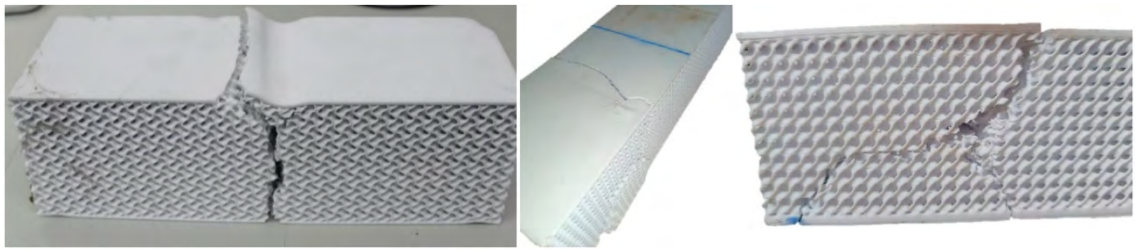


FIG. 10
Fracture of the different structures

4. CONCLUSIONS

The main conclusions of this study indicate that, although it is feasible to redesign a conventional structural product such as an electric scooter for additive manufacturing, the significantly lower mechanical properties of typical AM materials compared to conventional metallic materials necessitate the use of a substantially greater amount of material to achieve comparable strength. However, stiffness is generally reduced.

On the other hand, additive manufacturing enables production in virtually any location using relatively simple equipment. Furthermore, it allows the fabrication of monomaterial components, which facilitates improved recyclability.

Acknowledgements: This research was supported by a grant from the Spanish Agency of Research (Grant No. PID2022-137134NB-I00) and by the Aragon Government (Grant No. T38_23R).

REFERENCES

[1] Zhao, M., Liu, F., Fu, G., Zhang, D.Z., Zhang, T., Zhou, H.L.: Improved Mechanical Properties and Energy Absorption of BCC Lattice Structures with Triply Periodic Minimal Surfaces Fabricated by SLM. Materials 11(12), 2411 (2018).

[2] Miralbes, R., Ranz, D., Pascual, F.J., Zouzias, D., Maza, M.: Characterization of additively manufactured triply periodic minimal surface structures under compressive loading. Mechanics of Advanced Materials and Structures 29(13), 1-13 (2022).

[3] Xu, C.Y., Daynes, S., Das, R., Kabaliuk, N.: Anisotropic mechanical properties and energy absorption of TPMS structures: a comparative study of polylactic acid and thermoplastic polyurethane materials. Thin-Walled Structures 217(B) (2025).

[4] Toshev, R., Kolatsis, N., Shamzzuzoha, A., Helo, P.: The economics of additive manufacturing ikand topology optimisation - a case analysis of the electric scooter. Journal of Engineering Design 34(4), 313-338 (2023).

[5] UNE-EN 17128:2020. Vehículos ligeros motorizados para el transporte de personas y mercancías e instalaciones relacionadas y no sujetos a homologación para uso en carretera. Vehículos eléctricos ligeros personales (PLEV). Requisitos de seguridad y métodos de ensayo. AENOR (2020).

[6] ASTM C393/C393M-20. Standard Test Method for Core Shear Properties of Sandwich Constructions by Beam Flexure. ASTM (2020).

Parametric 3D Modeling and Digital Twin Development for Modular Sofa Design

María Matías[a], José Manuel Auría[a], Raquel Acero[a, b], Carmelo Pina[a, b, *]

[a] Design and Manufacturing Engineering Department, University of Zaragoza, María de Luna 3, 50018, Zaragoza, Spain

[b] Aragón Institute for Engineering Research (I3A), University of Zaragoza, Mariano Esquillor Gómez s/n, 50018, Zaragoza, Spain

* e-mail: carpina@unizar.es

Abstract: The upholstered furniture sector in Spain, rooted in artisanal traditions and fragmented business structures, faces the urgent challenge of digital transformation under the Industry 4.0 framework. This research demonstrates the practical utility of parametric CAD tools within a sector SME by creating a digital twin of a representative sofa model to optimize design and manufacturing processes. The methodology followed five phases: on-site data collection, sectoral research, 3D parametric modelling (utilizing silhouette scanning for complex organic geometries), the definition of a modular alphanumeric coding system, and the generation of comprehensive technical documentation. The primary result is a high-fidelity digital twin organized into five reconfigurable modules (fixed/folding armrests, fixed/relax modules, and chaise longue). This model integrates structural elements, such as pine frames and metallic mechanisms, with comfort components like springs and foams. Validation tests confirmed that this digital approach enables early interference detection and agile dimensional adjustments through embedded parameters. The study concludes that digitalization via parametric CAD is a viable and effective solution for SMEs. It replaces traditional physical patterns with high-precision technical drawings, facilitating the future implementation of CAM/CNC technologies. Ultimately, this transition minimizes material waste and streamlines the development of flexible, customizable catalogues, significantly enhancing sectoral competitiveness and sustainability.

Keywords: *Digital Twin, Upholstered Furniture Industry, SME Digitalization, Modular Design.*

1. INTRODUCTION

In recent years, the concept of Industry 4.0 has redefined the industrial landscape through digital transformation, powered by automation, the Internet of Things (IoT), and artificial intelligence. These technologies facilitate real-time decision-making and provide unprecedented levels of productivity and flexibility.

The furniture sector is no exception to these impacts, where new technologies offer a path to increased production efficiency and enhanced product personalization [1]. This research focuses on a Spanish sofa manufacturer that, despite its promising trajectory, largely relies on traditional, artisanal manufacturing methods. Currently, their designs are created on paper, using physical patterns to mark and cut structural components. Transitioning to digitalization offers a significant opportunity to optimize production, reduce material waste, and streamline the creation of design variations.

The primary objective of this research is to practically demonstrate the functionality of 3D CAD tools in an upholstery SME. By creating a digital twin of one most representative sofa with chaise lounge, this study illustrates how digital tools can modernize traditional design and manufacturing workflow [2][3].

2. SECTORAL AND INSTITUTIONAL CONTEXT

The Spanish wood and furniture industry is a vital national economic engine [4], having invoiced over 4,000 million euros in 2024 [5]. The sector is highly fragmented, with over 87% of companies classified as micro-SMEs. Despite this fragmentation, the industry remains resilient, with a growing international presence and a 3.8% increase in exports during the first half of 2025.

Upholstered furniture, particularly sofas, represents a core segment of this industry, blending traditional woodworking and upholstery techniques with modern comfort technologies. Current trends emphasize ergonomics, sustainability, and modularity [6]. Consumers increasingly demand flexible catalogues that can be tailored to specific needs without significantly increasing costs or delivery times.

For Spanish SMEs, digitalization is no longer optional but a requirement for remaining competitive against low-cost imports and large multinationals. The implementation of integrated CAD/CAM systems allows for a bidirectional flow of information, where design changes are automatically reflected in production.

3. METHODOLOGY

The research followed a structured five-phase methodology designed to transition from a physical product to a digital representation.

1. On-site Data Collection: Multiple factory visits were conducted to document production processes and technical specifications for the selected sofa model, as shown in Fig. 1. This involved taking detailed photographs, measurements, and creating hand-drawn sketches of individual components and assemblies. See Fig. 2



FIG. 1
Assembly and upholstery workshop

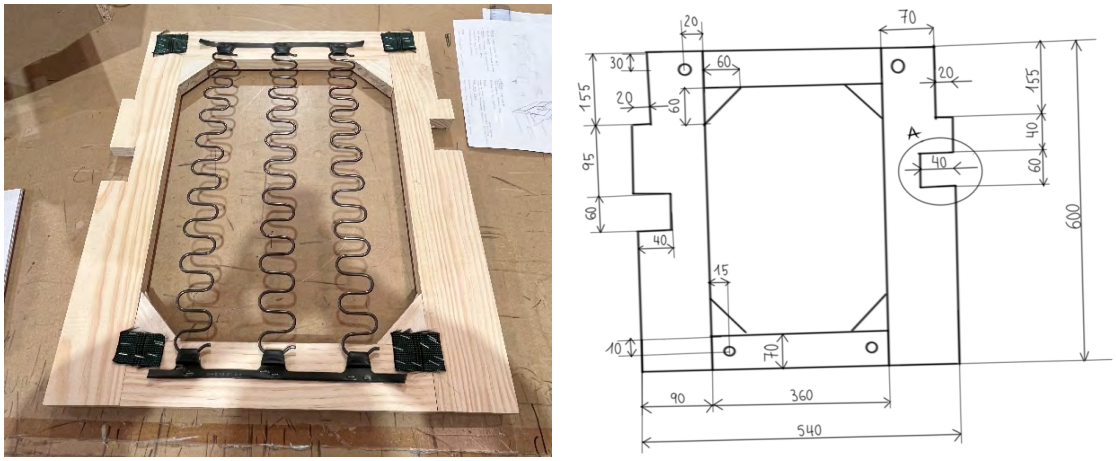


FIG. 2
Relax module seat (part and sketch)

2. Sectoral Research: An in-depth analysis of the Spanish furniture industry and current technological trends (Industry 4.0) was performed in parallel with technical tasks.
3. 3D Parametric Modelling: Using advanced CAD software, each component was digitally recreated. This phase addressed the complexity of furniture modelling, which includes numerous hidden elements such as frames, suspensions, and varied foam layers. One example is shown in Fig. 3

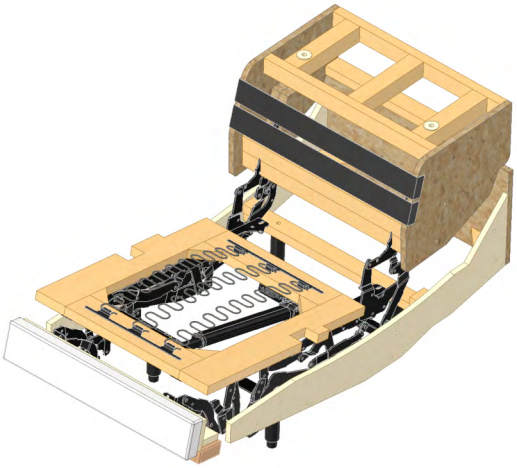


FIG. 3
3D Relax module

4. Modular Architecture Definition: A modular structure was established in Excel, accompanied by an alphanumeric coding system (XXYYZZ_WW) to organize the assembly and ensure factory-level traceability.
5. Technical Documentation: The final phase involved generating comprehensive assembly and part drawings to define the product geometrically, as show in Fig. 4.

4. TECHNICAL DEVELOPMENT AND IMPLEMENTATION

4.1. Modelling Complex Geometries

The selected sofa is a sophisticated product consisting of a fixed module, a recliner (relax) module, and a chaise longue with a folding armrest. While rectilinear components were straightforward to model, parts with organic, curved profiles, such as the backrest side panels, posed a challenge. Standard photography proved insufficient due to perspective distortion. To achieve high fidelity, physical silhouettes were scanned and imported into CAD Software. Spline operation was then used to interpolate and recreate these organic forms with precision.

4.2. Assemblies and Sub-assemblies

Modelling followed an iterative process, building sub-assemblies such as wooden frames before integrating them into larger modules. Structural frames utilize pine wood, particleboard, and MDF, joined via gluing and stapling. Suspension elements like springs and webbing were also modelled; for the seat springs, a 3D sketch and a sweep operation were employed to capture their complex arc and zigzag geometry. The relax module presented the highest technical complexity, integrating a metallic articulated structure with an electric motor. The mechanism required significant modelled work and modification to match the physical model's specific dimensions and wooden frame constraints.

4.3. Modular Architecture and Coding

The global assembly was structured into five primary modules: fixed armrest, folding armrest, fixed module, relax module, and chaise longue. Each module was further subdivided into second-level sub-assemblies (e.g., frames, headrests). A structured alphanumeric system (XXYYZZ_WW) is proposed to uniquely identify every product part:

—XX (Module): Identifies the section (e.g., MF for Fixed Module, AR for Armrest).

—YY (Part Type): Defines material or function (e.g., AG for particleboard, LI for wooden strip).

—ZZ (Sequence): A unique identifier within the category.

—WW (Variant): Distinguishes dimensions or finishes.

This coding is integrated into the Bill of Materials (BOM), which is automatically generated from the CAD model, allowing precise cost tracking and optimized raw material purchasing [7]. Additionally, this organization allows to reuse modules across different sofa ranges, significantly reducing design time for new catalogue entries.

Under the artisanal method, creating a variation of a sofa (e.g., changing a 3-seater to a 2-seater or modifying armrest width) required manual measurements, the creation of new physical paper patterns, and physical prototyping to test fitment. By reusing the Digital Twin assets, the time required to generate a new catalogue entry is reduced by approximately 60% to 75%. Tasks that previously took days, such as redefining the internal wooden frame, are now executed in minutes through parametric adjustment.

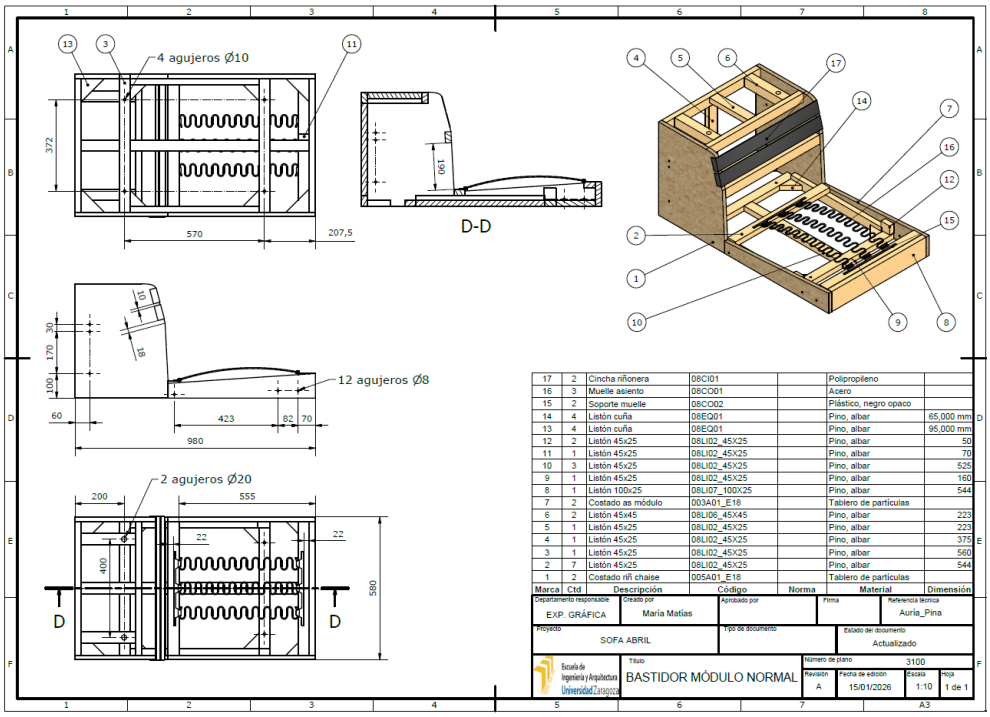


FIG. 4
Fixed module technical drawing

5. RESULTS AND DISCUSSION

The primary output is a high-fidelity digital twin of the sofa. This model allows for the visualization of the product from any perspective and provides absolute control over its constituent materials and costs. The generated technical documentation includes numerical marking for every part in assembly drawings and detailed geometric definitions in part drawings. These digital drawings can directly replace traditional physical patterns, ensuring that every manufactured piece is identical and meets quality standards.

Furthermore, the parametric nature of the model facilitates agile customization. Dimensions or aesthetic features (such as fabric textures and colours) can be adjusted virtually, eliminating the need for expensive physical prototypes during the early stages of design modification.

Another significant advantage discovered is the potential for design simulation. CAD tools allow manufacturers to detect interferences and simulate physical stresses on the sofa's structure. This ensures that the design can withstand required loads and identifies critical sections prone to failure before manufacturing begins.

6. CONCLUSIONS

This project demonstrates that the transition from artisanal methodologies to parametric 3D modelling represents a critical milestone for the competitiveness of Spanish upholstered furniture SMEs. The implementation of a digital twin, using 3D CAD tools, has proven to be a highly effective solution for managing the complexity of upholstered furniture, which involves numerous hidden structural and comfort components.

The most significant impact of this work is the drastic reduction in design-to-manufacturing lead times. Under traditional methods, every modification to a model required the manual creation of physical paper patterns and the construction of physical prototypes to detect assembly errors. Through the digital twin approach, the generation of technical documentation, including precise assembly plans and detailed part drawings, is now automated and agile:

—Assembly interferences and structural stresses are now detected virtually before any material is cut, eliminating the 100% cost associated with discarded physical prototypes during early-stage errors.

—The established modular architecture and alphanumeric coding system (XXYYZZ_WW) allow for the rapid configuration of new catalogue variants by reusing existing digital modules, potentially reducing the development time of new sofa ranges by up to 60-70% compared to starting from scratch on paper.

From a financial standpoint, the project directly addresses the challenge of rising energy and raw material costs that have historically hampered the sector. The ability to generate optimized cut lists directly from the 3D model ensures maximum material utilization of pine wood, particleboard, and fabrics. By replacing traditional manual marking with digital definitions, the company minimizes the human error margin in material consumption, which is essential for maintaining margins against low-cost imports.

In conclusion, this pilot project proves that digitalization is not merely an option but a requirement for artisanal firms to survive in a globalized market. The work provides a scalable methodology to digitize the entire portfolio, enabling future vertical integration through CAD/CAM technologies [8]. Furthermore, these digital assets open new commercial avenues, such as real-time web-based 3D configurators for customers, aligning the company with modern consumption trends.

REFERENCES

[1] J. José, O. Gras, C. Mahier, E. Mouazan, M. Victoria Gómez Gómez, and P. Dufkova, Twin transition in the manufacturing sector. A blueprint, 2022.

[2] A. A. Neto, F. Deschamps, E. R. Da Silva, and E. P. De Lima, Digital twins in manufacturing: an assessment of drivers, enablers and barriers to implementation, Procedia CIRP, vol. 93, pp. 210-215, Jan. 2020, doi: 10.1016/J.PROCIR.2020.04.131.

[3] H. A. Babty, B. Eynard, M. Bricogne, and E. Pansart, Digital Twin for Railway Sector: Cutting Through the Plethora of Terms and Classification of Use Cases, in Lecture Notes in Mechanical Engineering, 2025. doi: 10.1007/978-3-031-72829-7_54.

[4] Spaniens Ratio-Möbel. Binnenmarkt kompensiert Exportverluste, in Holz - Kurier, Oct. 2000, pp. 20-21.

[5] La industria del mueble en España. Edición 2025, Paterna, 2025.

[6] P. Bolzan, M. Bianchini, M. Ronchi, B. Chiti, and ..., Exploring Design Strategies in Upholstered Furniture: An In-Depth Exploration through Case Studies, … /ISDRS SERIES IN …, 2024.

[7] K. Aidinli, P. Minaoglou, P. Kyratsis, and N. Efkolidis, Automating Product Design and Fabrication Within the Furniture Industry, Designs (Basel)., vol. 9, no. 5, 2025, doi: 10.3390/designs9050116.

[8] C. Hu and J. Zhu, A review of digital twin-enabled intelligent manufacturing with a focus on the wooden furniture industry, 2025. doi: 10.1080/17480272.2025.2551742.

Pressure Measuring Device for Shoulder Loads during Holy Week Processions

David Sánchez-Murcia, José Macías-García, Óscar D. de-Cózar-Macías*, Francisca J. Castillo-Rueda, Laia Miravet-Garret

Universidad de Málaga, Dpto. de Expresión Gráfica, Diseño y Proyectos.
Escuela de Ingenierías Industriales

* e-mail: odecozar@uma.es

Abstract: The increasing professionalization of load-bearing roles in physically demanding cultural contexts, such as Holy Week processions in southern Spain, has highlighted the lack of objective, quantitative tools to assess and manage the physical strain experienced by float bearers. This paper presents the design and development of a portable, non-intrusive device to measure shoulder pressure during load-bearing activities, thereby improving ergonomics, preventing injuries, and supporting data-driven organizational decisions. The methodology follows a user-centered design approach combined with engineering development and real-world validation. Initially, qualitative research was conducted through structured interviews with key stakeholders to identify ergonomic and functional requirements. Based on these findings, a wearable system (SLMD) was developed, integrating piezoresistive sensors, an ESP32 microcontroller, GPS tracking, and wireless communication within an ergonomic textile structure. A web-based platform was also implemented for real-time visualization and post-event analysis. The prototype was tested under realistic conditions, demonstrating its ability to measure and transmit pressure data accurately. Results indicate that the system effectively detects load imbalances and critical effort points, enabling improved load distribution and injury prevention. Additionally, the system has been formally protected through its registration as a utility model, reinforcing its innovation potential. The proposed solution contributes to the "Design for One Health" paradigm by integrating human well-being, technological innovation, and cultural sustainability, offering potential applications beyond the cofrade context.

Keywords: *Wearable sensors, Ergonomics, Load monitoring, Pressure measurement, One Health.*

1. INTRODUCTION

The concept of "Design for One Health" promotes the development of solutions that integrate human well-being, environmental sustainability, and technological innovation. Within this framework, physically demanding cultural practices constitute a relevant yet often overlooked domain in which design can play a critical role.

Holy Week processions in southern Spain involve prolonged manual handling of heavy religious structures, with participants carrying them on their shoulders for extended periods. These activities impose high biomechanical demands, including static loading, repetitive movements, and constrained postures. Previous studies have demonstrated that improper load distribution during manual carrying tasks significantly increases musculoskeletal stress and fatigue [1-5].

Despite the increasing professionalization of these activities, load management remains largely based on empirical knowledge and subjective perceptions. This lack of objective measurement tools limits the ability to optimize load distribution and prevent injuries.

The objective of this work is to design and validate a wearable device capable of measuring shoulder pressure in real time, thereby improving ergonomic conditions, supporting decision-making, and contributing to the One Health approach.

From a One Health perspective, the proposed system contributes to human health through the prevention of musculoskeletal disorders and the promotion of ergonomic practices. Furthermore, by supporting the safe development of cultural and social activities, the device contributes to community well-being and the preservation of cultural heritage. The integration of sensing technologies and digital monitoring tools also promotes technological innovation aimed at improving quality of life.

2. METHODOLOGY

The methodology follows a comprehensive product development framework integrating user-centered design, engineering development, and experimental validation.

2.1. User-Centered Design

A qualitative study was conducted through structured interviews with key stakeholders, including float bearers, forepersons, and organizers. This phase enabled the identification of critical requirements, including comfort, non-intrusiveness, real-time data access, and compatibility with traditional attire.

These requirements are aligned with ergonomic design principles established in human-system integration standards [6], ensuring the system's usability and acceptance.

2.2. System Design

Based on the identified requirements, the Shoulder Load Monitoring Device (SLMD) system was developed. The device integrates piezoresistive pressure sensors for load meas-

urement [7, 8], an ESP32 microcontroller for data acquisition and processing, a GPS module for spatial tracking, and wireless communication modules for real-time data transmission. These components are embedded in an ergonomic textile structure made of flexible and breathable materials. The integration of these components follows design criteria established in the development of embedded monitoring systems [5].

The final design ensures adaptability to different users while minimizing interference with movement and aesthetics. Figure 1 illustrates the conceptual design.

Unlike conventional wearable pressure monitoring systems developed for industrial ergonomics or medical applications, the proposed DMCH system has been specifically designed for shoulder-borne load carrying in cultural processions. Its distinctive features include the integration of pressure sensing, geolocation, real-time wireless communication, and a non-invasive wearable structure adapted to the operational requirements of float bearers. This combination enables both ergonomic assessment and route-based analysis within a single platform.

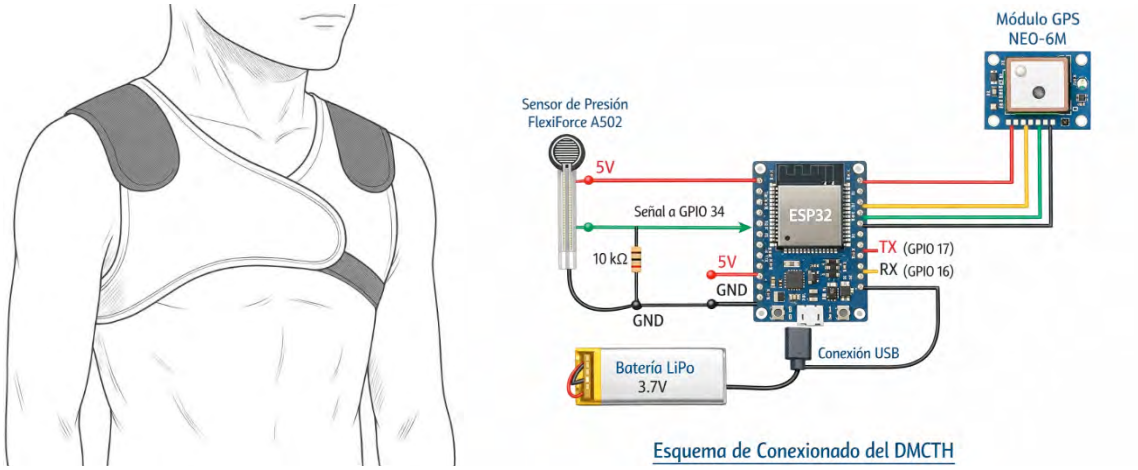


FIG. 1
Final design

2.3. Data Management Platform

A web-based application was developed to visualize and analyze the collected data. The platform enables real-time monitoring, historical data storage, and identification of critical load peaks.

The platform allows:

—Monitoring of pressure distribution during activity.

—Identification of peak load conditions.

—Post-event analysis for decision-making.

2.4. Experimental Validation

The system was tested through controlled tests and real-world trials. Measurements were collected during load-bearing activities, and system performance was evaluated based on measurement accuracy, system reliability, and user experience.

Sensor calibration procedures were conducted following standardized methodologies for force measurement systems [9], ensuring the reliability of the collected data.

The validation process was carried out through a series of controlled tests designed to reproduce the operational conditions experienced during Holy Week processions. Several load-bearing scenarios were considered, including static standing positions, continuous walking, turning manoeuvres, and start-stop transitions. Pressure data were collected continuously through the piezoresistive sensors while the ESP32 module transmitted the information in real time to the monitoring platform. The recorded data were subsequently analysed to identify pressure peaks, load asymmetries, and variations associated with different movement conditions.

3. RESULTS

The experimental validation demonstrated that the SLMD system accurately measures and transmits pressure data in real time.

As shown in Table 1, the system achieved consistent measurements under varying load conditions, with acceptable error margins for ergonomic applications.

TABLE 1
Summary of shoulder pressure measurements under different conditions

Condition	Mean Pressure (N)	Max Pressure (N)	Std. Deviation (N)	Observations
Static load (standing)	120	135	8	Stable distribution
Walking (steady pace)	145	165	12	Moderate variability
Turning manoeuvres	170	210	18	High asymmetry detected
Start/stop transitions	185	230	22	Peak loads observed
Uneven terrain	160	200	20	Load imbalance

The results highlight:

—Identification of load imbalances among participants.

—Detection of peak pressure zones during specific moments.

—Correlation between route conditions and physical demand.

Figure 2 presents an example of load distribution across participants in a short period. The system successfully identified critical segments of the route where physical demand increased significantly.

A key outcome of this work is the formal protection of the developed system as an industrial property asset. The device has been registered as a utility model (application number: U202532155) at the Spanish Patent and Trademark Office (OEPM), confirming its novelty and applicability.

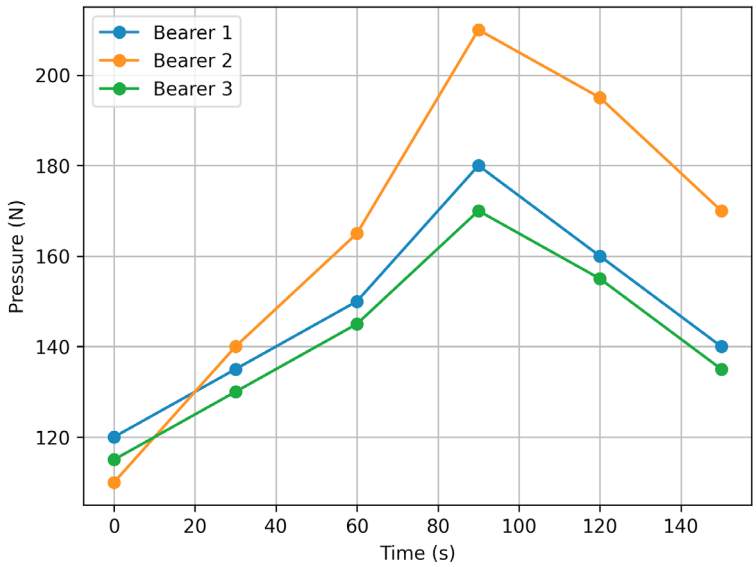


FIG. 2
Shoulder pressure distribution recorded during a simulated load-bearing test

This registration [10] reinforces the technological innovation of the proposed solution and supports its potential for transfer, commercialization, and further development.

Additionally, the device's ergonomic integration proved effective, with users reporting high levels of comfort and minimal interference with their activities, consistent with previous studies on load carriage biomechanics [1-3].

4. CONCLUSIONS

The developed DMCH system demonstrates the feasibility of using wearable sensing technologies to objectively measure shoulder loads during Holy Week processions. The obtained results confirm the ability of the device to identify load imbalances, detect pressure peaks, and provide real-time information about the physical demands experienced by participants.

The importance of this work lies in the lack of objective tools currently available for evaluating ergonomic conditions in this type of cultural activity. By providing quantitative information, the proposed system can contribute to reducing the risk of musculoskeletal injuries and improving load distribution strategies.

The usefulness of the device extends beyond data collection. The generated information can support decision-making processes by organizers and coordinators, helping to improve participant safety and operational planning. Furthermore, the technological approach presented in this work may be adapted to other contexts involving manual load handling, occupational ergonomics, and health monitoring applications.

From a One Health perspective, the proposed solution contributes to human well-being, technological innovation, and the sustainable preservation of cultural traditions, demonstrating the value of design-driven engineering solutions for addressing real societal challenges.

Future work will focus on improving calibration methods [9], expanding analytics capabilities, and exploring applications in other sectors such as occupational safety and healthcare.

REFERENCES

[1] Bini, R.R., Hume, P.A., Croft, J.L.: Effects of load carriage on human biomechanics. Journal of Applied Biomechanics 34(2), 99-110 (2018). https://doi.org/10.1123/jab.2016-0339

[2] Crea, S., Donati, M., De Rossi, S.: Commercially available pressure sensors for sport and health applications: A comparative review. Foot 57, 101984 (2023). https://doi.org/10.1016/j.foot.2023.101984

[3] Zhang, M., Wang, R., Li, X.: A wearable electronic system based on flexible pressure sensors for running motion monitoring. Discover Nano 18(1), 45 (2023). https://doi.org/10.1186/s11671-023-03788-7

[4] Cutti, A.G., Giovanardi, A., Rocchi, L., Davalli, A.: Wearable systems for shoulder kinematics assessment: a systematic review. BMC Musculoskeletal Disorders 20(1), 546 (2019). https://doi.org/10.1186/s12891-019-2890-6

[5] Simpson, L., Maharaj, M., Mobbs, R.: Use of a shoulder-mounted wearable sensor prototype for monitoring upper body biomechanics. Journal of Medical Internet Research 27, e73566 (2025). https://doi.org/10.2196/73566

[6] NASA: Man-Systems Integration Standards. NASA Publications (2010).

[7] Jin, H., Park, S., Lee, K., Kim, J.: Advances in flexible wearable pressure/strain sensors for motion monitoring in orthopaedic sports medicine. Journal of Orthopaedic Translation 45, 1-15 (2026). https://doi.org/10.1016/j.jot.2025.12.003

[8] Tekscan Inc.: FlexiForce Sensors User Manual. Tekscan, Boston (2023).

[9] ISO 376: Metallic materials – Calibration of force-proving instruments used for the verification of uniaxial testing machines (2011).

[10] Universidad de Málaga: Sistema de monitorización de la carga soportada sobre al menos un hombro de una persona. Utility Model Application U202532155, Oficina Española de Patentes y Marcas (OEPM), Madrid (2025).

A Blended Learning Approach to Teaching Graphical Expression in Engineering

José S. Velázquez[a, b], Francisco L. Sáez[a, b], José González-Cabrero[a, b], Lucas Díaz-Moreno[a, b], Carmelo Gómez[a, b,*], Francisco Cavas[a, b]

[a] Department of Structures, Construction and Graphical Expression, Technical University of Cartagena member of European University of Technology EUT+, 30202 Cartagena, Spain

[b] Bioengineering and Applied Computational Simulation Research Group, Technical University of Cartagena member of European University of Technology EUT+, 30202 Cartagena, Spain

* e-mail: carmelo.gomez@upct.es

Abstract: Blended Learning (BL) combines online educational materials with traditional face-to-face instruction, offering a flexible and personalized learning experience. This teaching innovation project applied a BL model to the Graphical Expression subject across the Electronics and Automation, Chemical, and Electrical Engineering degrees at the Technical University of Cartagena (UPCT), involving 240 potential students. The primary objective was to improve content comprehension and provide support particularly to those facing attendance difficulties. Multimedia packages were developed to complement each theoretical session, consisting of 12 one-hour video lessons narrated by the instructor (activated 7-10 days after each face-to-face class to encourage attendance) and 13 self-assessment quizzes integrated into Moodle with formative feedback. The platform also enabled the instructor to monitor student engagement and identify the most challenging concepts. The results were notably positive: the average score on the second partial exam rose from 3.97 to 4.26, the failure rate dropped by 8.9%, and the proportion of students achieving a "Merit" grade increased by 21.4%. Class attendance remained consistently high at 60-65%, compared to the previous 30-35%, and the number of students absent from the final exam fell from 4 to just 1. Between 11% and 25% of enrolled students actively used the video resources, and 61.8% of survey respondents strongly agreed that the videos facilitated subject follow-up. In conclusion, this zero-cost innovation improved academic performance, student motivation, and course retention, confirming the value of BL in complex technical disciplines.

Keywords: *Autonomous Learning, Academic Performance, Formative Feedback, Moodle, Student Engagement.*

1. INTRODUCTION

University-level engineering education has progressively incorporated hybrid models and digital environments in response to two converging needs: the expansion of instructional flexibility and the adaptation to a student profile increasingly accustomed to digital technologies. In the Spanish context, this shift has materialized relatively early as a transition from traditional face-to-face instruction toward hybrid formats supported by ICT, in line with the new teaching-learning paradigm promoted by the European Higher Education Area (EHEA) [1, 2].

In this context, the Blended Learning (BL) methodology has gained particular interest in Engineering degree programs due to its capacity to combine face-to-face activities with virtual work, continuous monitoring, and more autonomous learning. Published experiences in Spain show that this approach is not limited to transferring content onto a platform, but is typically accompanied by active learning strategies, such as project-based learning, the use of CAD/DAO tools, spatial visualization, tutored work, and the flipped classroom model [3].

This orientation proves particularly relevant in Graphical Expression, a core subject in multiple Engineering degree programs due to its connection with technical representation, blueprint reading, and the development of spatial and professional competencies. At the University of Alicante, a virtual learning environment was already proposed specifically for Graphical Expression, with the aim of enabling students to develop the knowledge and skills required to interpret and produce drawings for real-world projects; similarly [2], other studies describe the shift from traditional lecture-based instruction toward a greater emphasis on Computer-Aided Design (CAD) lab sessions and interactive resources for spatial visualization [4, 5]. Taken together, the available literature suggests that BL is not only viable in this area, but particularly well-suited to both the competencies to be developed and the visual and procedural nature of Graphical Expression.

Considering current trends, the direction does not appear to be toward replacing face-to-face instruction, but rather toward its reconfiguration: hybrid formats are used to reserve in-person interaction for tasks of higher pedagogical value, while transferring part of the training, monitoring, and guided practice to the digital environment. This is precisely the direction taken by several Spanish studies in Graphical Engineering and related fields, where the incorporation of new methodologies has led to improved academic outcomes and student competencies, while simultaneously reinforcing autonomy, motivation, and digital skills [3, 6]. This teaching innovation project applied a BL model to the Graphical Engineering subject across the Electronics and Automation (GIEIA), Chemical (GIQI), and Electrical (GIE) Engineering degrees at the Technical University of Cartagena (UPCT), during the first quarter of the course 2025-2026.

2. MATERIALS AND METHODS

2.1. Main objectives

The project primarily pursued two objectives: on the one hand, to improve students' comprehension and application of Graphical Engineering concepts through a blended learn-

ing approach that combines in-person and digital resources; and on the other, to foster student autonomy through the use of digital resources (such as videos and formative quizzes) to reinforce classroom content.

2.2. Methodology

In this project, a set of online multimedia content "packages" was created for each lecture session or "topic" delivered in the Graphical Expression subject (1st year) across the previously mentioned degree programs, serving as a complement and reinforcement tool for students who were unable to attend class or simply needed to review the covered concepts (see Figure 1a).

These content packages consisted of a total of 12 video lessons of approximately one hour each, narrated by the instructor based on the class notes, using PowerPoint with voice-over and a virtual pointer (see Figure 1b). These videos were made available a few days after each corresponding face-to-face session (between 7 and 10 days), in order to encourage class attendance, but without an excessively long delay, so as to prevent course dropout among students who had missed a session.

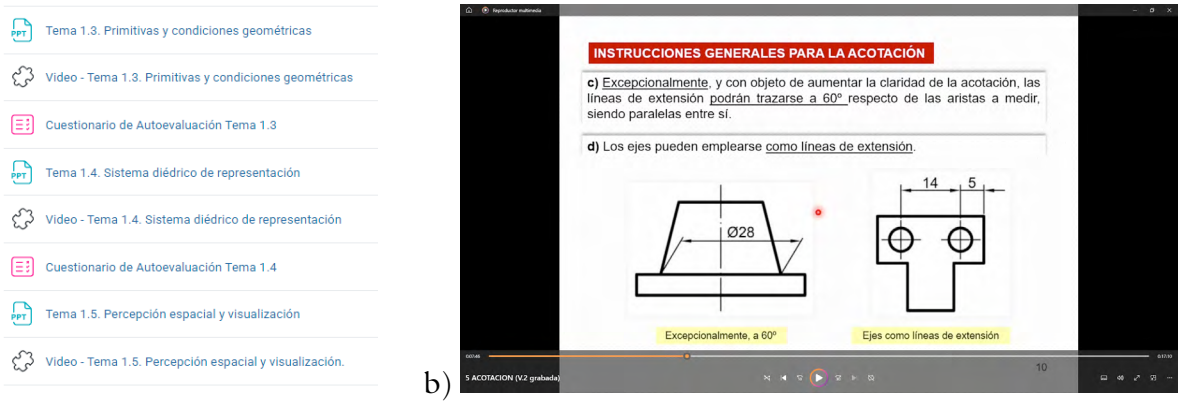
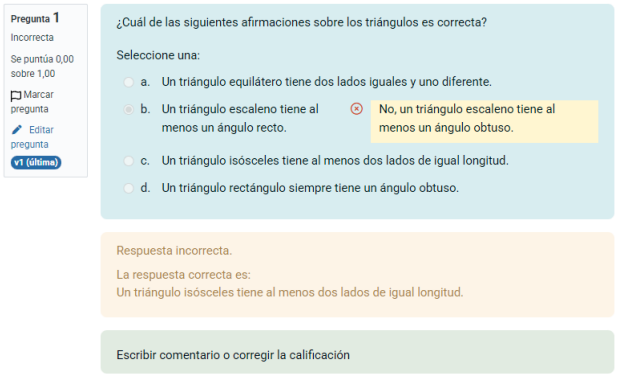


FIG. 1
a) Overview of tools in the Virtual Classroom;
b) Example of video lesson

Additionally, a total of 13 self-assessment quizzes were created and integrated into the subject's Virtual Classroom under the Moodle platform (Figure 2a), one for each theory topic, highlighting the key concepts covered in each session. These quizzes, although providing an indicative score out of 10 points, served a primarily formative purpose, as they did not contribute to the final course grade. Upon completion, students were shown the errors made along with the correct answers, some of which included detailed explanations of why they were correct —or incorrect— with the ultimate goal of enabling students to identify their mistakes and assess their level of understanding once the topic had been studied.

a)



b)

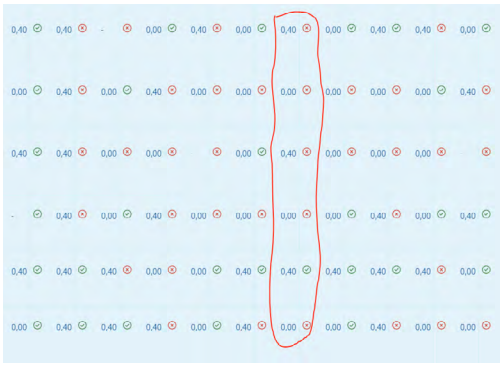


FIG. 2

a) Example of a question with an incorrect answer marked;
b) Detection of a question with a high failure rate

The integration of these new tools allowed the instructor to detect gaps or weaknesses in students' grasp of the concepts, by quickly visualizing which questions were causing the most difficulty (see Figure 2b), and subsequently reinforcing the explanation of those concepts in later class sessions.

Finally, in order to assess student satisfaction with the new tools, a feedback survey evaluating the "Video Lessons and Self-Assessment Quizzes" was activated in the Virtual Classroom upon course completion, and responses were recorded.

3. RESULTS

Table 1 shows the grading results obtained following the second partial exam of the course, comparing them with those from the immediately preceding academic year.

TABLE 1

Comparison of results: Academic Year 25-26 vs. 24-25

ACADEMIC YEAR 25-26 (2nd Partial Exam)			**ACADEMIC YEAR 24-25 (2nd Partial Exam)**			
Category	**No. of students**	**%**	**Category**	**No. of students**	**%**	**Gain/ loss (%)**
Failing grades (<4)	16	27.10	Failing grades (<4)	21	37.50	–10.4
Compensable grades (4.00-4.99)	12	20.30	Compensable grades (4.00-4.99)	14	25.00	–4.7
Pass (5.00-6.99)	14	23.70	Pass (5.00-6.99)	12	21.40	2.3
Merit (7.00-8.99)	16	27.10	Merit (7.00-8.99)	4	7.10	20.0
Distinction (≥9)	0	0.00	Distinction (≥9)	1	1.80	–1.8
Absent	1	1.70	Absent	4	7.10	–5.4
Total	59	100.00	Total	56	100.00	
Average score	4.26 (/10)		Average score	3.97 (/10)		

Table 2 shows the results of the "Satisfaction Survey" evaluating the tool, broken down by degree program, based on Likert-type items ranging from 1 to 5, where 1 means "strongly disagree" and 5 means "strongly agree" with each statement.

Table 2
Satisfaction Survey Results by Degree Program

Degree	Question	Did not use (%)	1 (%)	2 (%)	3 (%)	4 (%)	5 (%)	Average score (1-5)	% High rating (4 or 5)
GIE (n = 19)	Quizzes: Help with comprehension	31.6	0.0	0.0	15.8	15.8	36.8	~3.9	52.6
	Quizzes: Clarity/adequacy	31.6	0.0	0.0	5.3	31.6	31.6	~3.9	63.2
	Videos: Facilitate follow-up	26.3	0.0	0.0	5.3	15.8	52.6	~4.4	68.4
	Videos: Complement balance	26.3	0.0	0.0	5.3	15.8	52.6	~4.4	68.4
GIEIA (n = 4)	Quizzes: Help with comprehension	25.0	0.0	0.0	0.0	25.0	50.0	4.0	75.0
	Quizzes: Clarity/adequacy	25.0	0.0	0.0	0.0	50.0	25.0	3.5	75.0
	Videos: Facilitate follow-up	50.0	0.0	0.0	25.0	25.0	0.0	2.5	25.0
	Videos: Complement balance	50.0	0.0	25.0	0.0	0.0	25.0	2.5	25.0
GIQI (n = 11)	Quizzes: Help with comprehension	18.2	9.1	9.1	9.1	36.4	18.2	~3.3	54.5
	Quizzes: Clarity/adequacy	18.2	9.1	18.2	9.1	27.3	18.2	~3.1	45.5
	Videos: Facilitate follow-up	27.3	0.0	9.1	0.0	0.0	63.6	~4.4	63.6
	Videos: Complement balance	27.3	0.0	9.1	0.0	0.0	63.6	~4.4	63.6
TOTAL (n = 34)	Quizzes: Help with comprehension	26.5	2.9	2.9	8.8	23.5	35.3	~3.7	58.8
	Quizzes: Clarity/adequacy	26.5	2.9	5.9	5.9	32.4	26.5	~3.6	58.9
	Videos: Facilitate follow-up	29.4	0.0	2.9	8.8	14.7	44.1	~4.1	58.8
	Videos: Complement balance	29.4	0.0	8.8	5.9	14.7	41.2	~4.1	55.9

Figure 3 shows the peaks of activity in the Virtual Classroom prior to the partial exams, which has allowed us to verify student usage of the new tools made available to them



FIG. 3
Activity peaks in the use of videos and quizzes prior to the partial exams

4. DISCUSSION

Regarding the achievement of the primary objective, the tools incorporated into the Virtual Classroom have clearly contributed to improving students' comprehension of Graphical Expression concepts. As shown in Table 1, comparing the results of the 2nd partial exam (the longest and most complex in the course) in the final ordinary examination session between academic years 24-25 (previous year) and 25-26 (current year). All the evaluation criteria, the type of exercises, and the difficulty level of this partial exam remained consistent and identical between both academic years. Results show that not only has the average score improved following the implementation of the tools (rising from 3.97 to 4.26) but the number of failing grades has also decreased by 10.4%, 4.7% of students moved from "compensable" to a full "Pass," and the percentage of students achieving a "Merit" grade improved by 20.0%.

Regarding the achievement of the secondary objective, it should be noted that the tools developed have allowed students to reinforce concepts at the moments they need it most, as shown in Figure 3, which illustrates access to Virtual Classroom resources in the days immediately preceding the partial exams (November 7 and December 14).

According to data extracted from Moodle, the number of students who used the video lessons ranges between 7 and 15 users depending on the video (11-25% of total enrolled students), which can be considered a notably high percentage. It has also been observed that, following the implementation of the tool, class attendance remained consistently around 60-65% through the final session of the course, whereas it had previously hovered around 30-35%. This appears to indicate that student motivation toward the subject has also increased, and that "disengagement" and subsequent course dropout have been successfully prevented. This is further supported by the data in Table 1, which shows that the number of students absent from the second partial exam in the final ordinary session decreased from 4 in 2025 to 1 in 2026 (a reduction of 5.4% of total enrolled students), confirming that the toolkit helps prevent students from dropping out of the course.

In terms of academic performance, the data presented in Table 1 allow us to state that the implementation of this tool has not only improved the group's average score (from 3.97 to 4.26) but has also enabled 73% of students to have the possibility of passing after the ordinary examination session, compared to 62.4% in academic year 24-25, thus clearly contributing to improved academic outcomes.

With respect to the final satisfaction survey, as shown in Table 2, it was completed by 34 students (19 from GIE, 4 from GIEIA, and 11 from GIQI). Overall, the tool showed high acceptance, particularly the recorded video sessions, which were rated very positively for their ability to facilitate course follow-up (61.8%) and complement other learning activities (61.8%). It is worth noting that approximately 1 in 4 students did not use the quizzes. Among those who did, the perception was positive, with a mean score of 3.7/5 and more than half (57.4%) giving a high rating (4 or 5). The videos were very well received in GIE and GIQI, with mean scores above 4.4. In GIEIA, the rating was lower (2.5), but with only 4 responses and 50% of respondents having not used them. These results align with previous Spanish BL experiences in Graphical Engineering, where comparable approaches improved performance, motivation, and autonomy [3, 6], and support earlier calls for virtual environments suited to this visual, procedural subject [2, 4, 5].

5. CONCLUSIONS

As demonstrated, the set of tools developed has enabled the integration of the benefits of both face-to-face and digital instruction, which proves especially valuable in the teaching of complex disciplines such as Engineering. By incorporating resources such as explanatory videos and self-assessment quizzes, students have been able to learn at their own pace, autonomously reinforcing concepts and skills. Furthermore, this tool has facilitated immediate feedback (since the entire proposal is fully integrated into Moodle, usage statistics and metrics can be reviewed in real time) and has enabled closer monitoring of each student's progress, improving comprehension and problem-solving at zero investment cost, as the Moodle platform is free of charge.

The BL tools developed are fully transferable to other degree programs, and by adapting the video lesson content and creating self-assessment quizzes linked to different subject matter, they could clearly be adapted to other courses. However, the study also presents some limitations. For example, the possible influence of differences between academic cohorts must be considered, thus further comparison with successive promotions is recommended. Furthermore, the absence of a control group within the same cohort (the comparison instead relying on two consecutive academic years) limits the extent to which the observed improvements can be attributed solely to the BL intervention.

Acknowledgements: The authors would like to thank all the members of the Graphical Expression area at UPCT who contributed to the elaboration and implementation of this teaching innovation experience, as well as to all the students who voluntarily provided their feedback, helping to improve the experience for future academic years.

REFERENCES

[1] Vidal, Ó.F. and N.O. Torre. El influjo de las tecnologías de la información y la comunicación enel aprendizaje de la ingeniería gráfica en España. 2013.

[2] Prieto, J.F., *et al.* Elaboración de una plataforma e-learning para la enseñanza aprendizaje de la Expresión Gráfica. 2007.

[3] Olmedo-Torre, N., M.M. Martínez, and M. Peña, Effectiveness of blended instructional design based on active learning in a graphic engineering course. Computer Applications in Engineering Education, 2021. 29(4): p. 810-837.

[4] Torre, N.O. and J.I. Cacho. Incorporación de nuevas metodologías de enseñanza - aprendizaje en la asignatura de expresión gráfica. 2019.

[5] García, J.C.A., M.L.S. García, and A.D. Olmos. Metodologías innovadoras en la enseñanza y el aprendizaje de la Ingeniería Gráfica. 2016.

[6] Alducin-Ochoa, J.M. and A.I. Vázquez-Martínez, Improving performance in Engineering through blended-learning. Digital Education Review, 2014: p. 87-107.

Graph-based Structural Characterization of Urban bus Transport Networks Using a Cycle Interaction Approach

Marina Díaz-Jiménez[a], *, Yoann Pigné[b], Patricia Ruiz[a], Pablo Pavón-Domínguez[a]

[a] Department of Mechanical Engineering and Industrial Design, University of Cádiz

[b] Laboratoire LITIS, UFR des Sciences et Techniques, Université Le Havre Normandie

* e-mail: marina.diaz@uca.es

Abstract: Urban public transport networks play a key role in sustainable mobility and require robust analytical frameworks to understand their structural organization. This work presents a graph-based methodology for the structural characterization of urban bus transport networks, using the Barcelona metropolitan bus network as a case study. The network is modelled as a directed graph following the Space-L representation, where nodes correspond to bus stops and intermediate points along the routes, and edges represent connections between consecutive stops/points. In addition, a complementary cycle-based interpretation is introduced, where each bus line is modelled as a closed cycle. Based on this approach, a meta-graph representation (Space-C) is constructed, in which nodes represent bus lines and edges capture the interactions through shared stops/points. The results show that the network can be described as a system of interconnected cycles, where most interactions between lines occur through a small number of shared stops/points. Despite this localized interaction pattern, the meta-graph exhibits significant clustering, indicating the presence of structured groups of routes. The proposed characterization provides a consistent basis for the generation of synthetic transport networks that reproduce the structural properties of real urban systems. This contributes to the development of graph-based visualization and digital tools for spatial data analysis, urban infrastructure design, and transport planning.

Keywords: *Urban Bus Transport Networks, Complex Networks, Graph Theory, Graphical Visualization, Sustainable Transport.*

1. INTRODUCTION

Urban public transport systems are essential for sustainable urban mobility, contributing to spatial planning, accessibility, and environmental impact mitigation [1]. Understanding their structural organization is crucial for developing analytical tools and designing efficient transport systems. In this context, graph theory and complex network analysis provide a powerful framework for modelling and studying transport infrastructures [2-4].

Public transport networks have been extensively studied in graph theory using different approaches. Sienkiewicz and Hołyst [5] introduced a network typology based on two representations: the Space-L, which directly reflects the structure of the system, and the Space-P, which captures the transfer structure. Using these representations, several graph properties are analysed, e.g. degree distribution and path length. Subsequent works further extended these approaches. For instance, von Ferber *et al.* [6] introduced the Space-C representation, where nodes correspond to routes and edges represent shared stops between them. Similarly, Xu *et al.* [7] analysed bus transport networks using weighted representations, where lines are nodes and edge weights represent the number of shared stations. Other studies, such as Derrible and Kennedy [8], analysed the robustness of the network and highlighted the role of loop structures in network resilience. Within this context, this work proposes a graph-based structural characterization of urban bus transport networks by means of a cycle interaction approach. The Barcelona metropolitan bus network is analysed through two complementary representations: a node-level model using the Space-L representation and a cycle-level meta-graph in Space-C. This dual perspective enables the study of both local connectivity patterns and global interactions between routes. Beyond network analysis, these representations provide a graphical abstraction of transport infrastructures that facilitates the visual analysis and interpretation of complex spatial interactions between routes.

This work is structured as follows. Section 2 presents the proposed methodology, including the graph-based modelling and the cycle interaction approach. Section 3 describes the experimental setup and the dataset used. Sections 4 reports and discusses the main results of the structural analysis. Finally, Section 5 summarises the main conclusions and outlines the potential future works.

2. METHODOLOGY

This section presents the methodology used to model and analyse the Barcelona metropolitan bus network. It is first represented as a directed graph (Space-L), and then, a cycle-based interpretation is introduced, leading to a meta-graph representation (Space-C). Finally, a set of structural metrics is defined to characterise the network at both node and cycle levels.

2.1. Graph representation of the transport network, Space-L

The transport network is first modelled as a directed graph $G = (V, E)$, where V corresponds to nodes representing bus stops and intermediate points along the routes, and E are the directed edges representing connections between consecutive points where the bus stops along the route. The directed edges reflect the operational sense of the direction of the bus. The analysis focuses

on the unweighted version of the graph to study its structural properties. This graph-based representation ensures that the network topology is accurately described and provides the basis for its analysis, enabling the computation of structural properties such as connectivity, degree distribution, and path-related metrics.

2.2. Cycle-based meta-graph representation, Space-C

A complementary interpretation of the transport network is proposed based on the structure of bus routes. In this approach, each bus line is interpreted as a cycle within the network. This assumption is supported by the fact that bus routes are defined as continuous sequences of bus stops that typically start and end at the same location, forming closed paths. To validate this interpretation, each route is analysed individually to verify both its continuity and closure. Continuity is ensured by checking that consecutive segments of a route are spatially connected, while closure is assessed by evaluating the proximity between the final and initial stops of the route. This cycle-based interpretation provides a higher-level abstraction of the transport system, where the network can be understood as a set of interconnected cycles. This perspective enables the analysis of structural properties at the route level and establishes the basis for modelling the interactions between bus lines.

Using this cycle-based representation of bus routes, a meta-graph $H = (V_c, E_c)$ is built following the Space-C approach to analyse interactions between lines. The node set V_c represents bus lines, while edges in E_c connect pairs of lines that share at least one bus stop. The meta-graph H is undirected and weighted, with edge weight defined as $W_{ij} = |S_i \cap S_j|$, where S_i and S_j denote the sets of bus stops belonging to bus lines i and j, respectively. This representation enables the transport network to be interpreted as a system of interacting cycles, providing a higher-level description of the network structure. It allows analysing how bus lines are interconnected, identifying highly connected routes, clusters of interacting lines, and patterns of shared infrastructure within the system. Figure 1 illustrates a conceptual example of the proposed methodology.

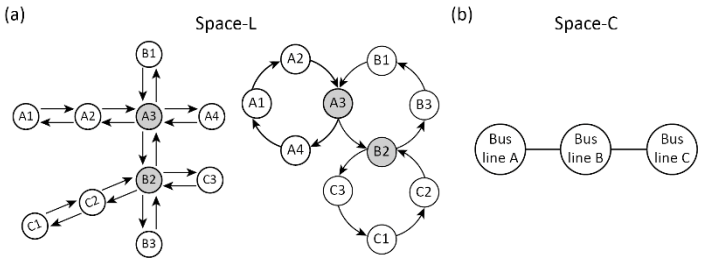


FIG. 1

Conceptual illustration of the proposed methodology, (a) Space-L representation of bus lines and cycle-based interpretation (shared stops highlighted in grey), (b) Space-C meta-graph

2.3. Structural characterization

Based on the previous representations, the network structure is analysed at two complementary levels using graph-theoretic metrics for both the node-level (Space-L) and the cycle-level (Space-C) representations.

2.3.1. *Node-level network, Space-L*

At the node level, structural properties are analysed using the Space-L representation, including basic topological metrics such as the number of nodes and edges, network density, diameter, and average path length. In addition, the degree distribution is evaluated to characterise connectivity patterns. Furthermore, transport-specific measures are considered, such as the distribution of nodes per line and the number of lines serving each point. These metrics provide insight into the network organisation and the presence of highly connected transfer points.

2.3.2. *Cycle-level network, Space-C*

At the cycle level, structural properties are analysed through the meta-graph representation (Space-C). Several metrics are computed to characterise the interaction between cycles. These include the node degree (number of lines connected to a given route), and the strength, defined as the total number of shared nodes between a line and all its connected lines. In addition, clustering coefficients are evaluated to identify groups of strongly interconnected routes. The distribution of shared nodes between pairs of lines is also analysed to assess the intensity of interactions within the network. Additionally, the interaction between lines is further analysed using normalized measures such as the Jaccard index, which quantifies the relative overlap between routes. In summary, these metrics allow characterising both the internal structure of individual routes and the interconnection patterns between them, providing a comprehensive description of the transport network. These properties define a structural signature of the network, being particularly useful as a reference for the generation of synthetic transport networks that aim to reproduce the structural characteristics of real systems.

3. EXPERIMENTAL SETTING

The case study focuses on the urban bus transport network of Barcelona, operated by Transports Metropolitans de Barcelona (TMB) [9]. TMB provides open-access data describing the public transport system, including information of bus stops and routes, as well as the geographical coordinates of stops expressed in terms of longitude (X) and latitude (Y).

The data was preprocessed to remove duplicates, correct inconsistencies, and ensure route continuity. In addition, spatial data was transformed into a consistent coordinate system to enable an accurate geometric representation of the network. The current Barcelona bus network consists of 103 bus lines. However, this study considers 101, excluding two isolated routes (101 and 111 bus lines) that do not connect to the main network, as they do not contribute meaningful information to the proposed analysis. This process results in a consistent dataset for graph-based modelling and structural analysis of the transport network. Detailed geographical information on the Barcelona bus network, including the spatial distribution of routes and stops, is publicly available through the official TMB platform [9].

4. RESULTS

This section presents the main results obtained from the structural analysis of the Barcelona bus transport network. First, the properties of the network at the level of stops/

points are described. Then, the interaction between bus lines is analysed through the meta-graph representation. Finally, the main structural patterns observed in the network are discussed.

4.1. Node-level analysis, Space-L

The resulting directed graph consists of 4,015 nodes and 6,894 edges. Due to the presence of multiple interconnected routes, the resulting graph is strongly connected, meaning that any node can be reached from any other node through directed paths.

Although the network is directed, the in-degree and out-degree are identical for all nodes; therefore, a single degree measure is considered. The degree distribution is shown in Figure 2(a), ranging from 1 to 9. These results suggest that most nodes have low degree, and the proportion of nodes decreases as the degree increases, with only a small proportion exhibiting high connectivity. These highly connected nodes correspond to major transfer points within the network, where multiple bus lines intersect. In addition, the number of lines serving each node is analysed and shown in Figure 2(b), where the distribution is expressed in terms of the proportion of nodes. The results indicate that most nodes are served by a single line, while a smaller proportion of nodes are shared by multiple lines, with a maximum value of 7. These shared points play a key role in the connectivity of the network, acting as transfer points between routes. Additional descriptive parameters indicate a sparse network structure, with an average degree of 1.717, a density of 0.00043, a diameter of 180, and an average path length of 46.190.

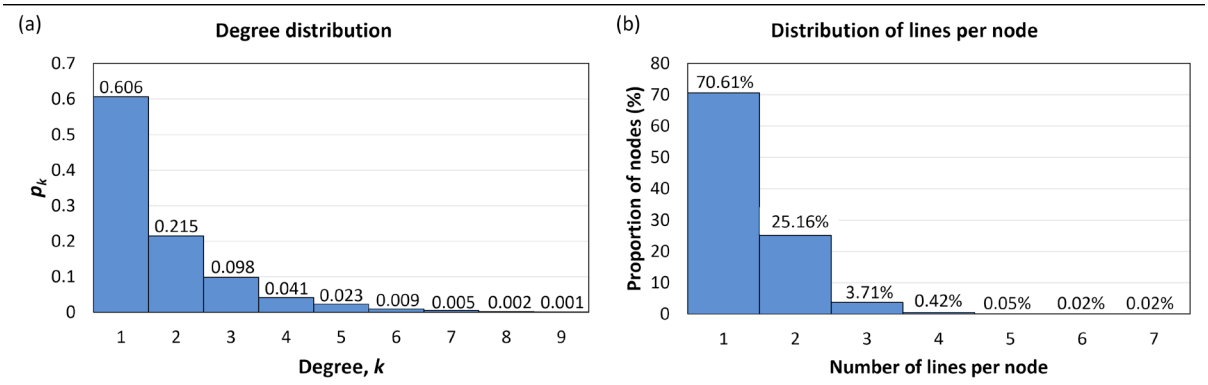


FIG. 2

Node-level properties of the Space-L network, (a) Degree distribution of the Barcelona bus transport network, (b) Distribution of lines per node

4.2. Node-level analysis, Space-L

At the cycle level, each bus line is interpreted and analysed as an individual closed cycle. The distribution of cycle sizes (see Figure 3(a)), measured as the number of nodes per line, shows that most lines concentrate around an average of approximately 68.2 nodes, within a range from 19 to 127. Only a small proportion of lines exhibit very low

or very high values. This indicates a relatively concentrated distribution, with a tendency towards a unimodal shape, reflecting a certain level of homogeneity in route sizes across the network. This variability plays an important role in the structural organisation of the network.

4.3. Meta-graph structure and interactions

The interaction between bus lines is analysed through the meta-graph representation (Space-C). The resulting meta-graph consists of 101 nodes, corresponding to each bus line, and 817 edges representing shared nodes between lines. The analysis shows that the meta-graph is connected, indicating that all bus lines are linked through shared nodes. The average degree of the meta-graph is 16.178, suggesting that each line interacts with more than 16 lines. The strength, defined as the total number of shared nodes with other lines, reveals that some routes are significantly more interconnected than others, with a minimum of 5 and a maximum of 95 nodes. These highly connected lines play a central role in the structure of the network. Figure 3(b) presents the distribution of shared nodes between pairs of lines, showing that most interactions involve a small number of shared nodes, typically one or two. This indicates that line intersections are generally localized rather than extended across long segments.

Additionally, the Jaccard index, ranging from 0 to 1, is used to measure the relative overlap between routes. The results indicate that the proportion of shared nodes between lines is generally low (with a maximum value of 0.092), reinforcing the idea of localized interactions. This suggests that bus lines exhibit very limited overlap. Furthermore, the clustering coefficient indicates the presence of some groups of strongly interconnected lines, with a mean value of 0.377 and a maximum of 1. Only one line reaches this maximum, while 13 lines exhibit clustering values above 0.5, suggesting that such structures exist but are not widespread across the network. This indicates that the network is not purely randomly organised but presents localized clusters of routes that share common infrastructure.

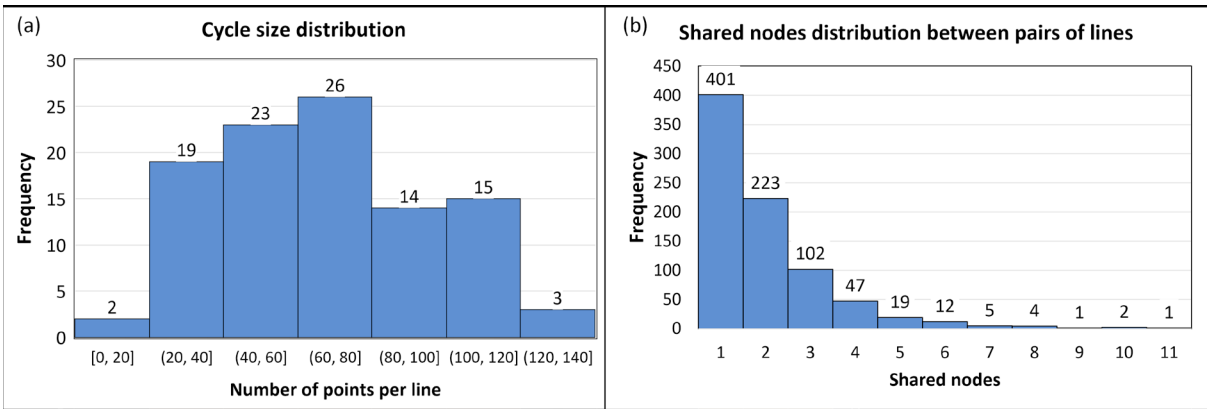


FIG. 3

Cycle-level and interactions, (a) Cycle size distribution, (b) Shared nodes distribution

5. CONCLUSIONS

This work presents a graph-based structural characterization of the Barcelona bus transport network by combining a node-level representation (Space-L) with a cycle-based interpretation (Space-C). This dual approach enables the analysis of both local connectivity patterns and interactions between transport routes. The results show that the network can be effectively described as a system of interconnected cycles, where each bus line forms a closed structure and interactions between lines occur at specific transfer points. These interactions are typically limited to a small number of shared nodes, indicating a highly localized connectivity pattern. The meta-graph exhibits clustering, revealing the presence of some localized groups of routes rather than random interconnections. The combination of variability in cycle sizes and non-uniform interaction patterns leads to a complex but organized network topology. These findings support the validity of the proposed cycle-based interpretation and provide a compact structural characterization of the system. From a practical perspective, the identified interaction patterns may support transport planning by facilitating the identification of transfer points, groups of highly interconnected routes, and structural features that influence network organization. This characterization also establishes a consistent basis for the development of synthetic transport network models that reproduce the structural behaviour of real urban systems, including cycle-size distributions, route interaction patterns, node connectivity, and clustering characteristics. Future work will focus on the generation of such models and on extending the analysis to other transport networks to assess its applicability. Furthermore, the adaptation to multimodal transport systems, where different transport modes (e.g., buses, metro, and commuter rail) are represented within a unified cycle-based interaction framework is also foreseen.

Acknowledgements: This publication is part of PID2022-137858OB-I00 project (eMob), funded by Spanish MCIN, the AEI and the ERDF on MCIN/AEI/10.13039/5011 00011033/FEDER, UE, we would also like to acknowledge the Spanish Ministerio de Ciencia, Innovación y Universidades for the support through PREP2022-000333 grant.

REFERENCES

[1] European Commission. Strategic Transport Research and Innovation Agenda (STRIA). 2Zero Partnership 2021-2027. 2021, https://www.2zeroemission.eu/wp-content/uploads/2023/01/2Zero-SRIA-webversion-2022.pdf, last accessed 2026/06/18.

[2] Newman, M. E. J.: The Structure and Function of Complex Networks. SIAM Review 45(2), 167-256 (2003).

[3] Barabási, A.-L. Pósfai, M.: Network science. Cambridge University Press, Cambridge (2016).

[4] Costa, L. d. F., Oliveira, O. N., Travieso, G. *et al.*: Analysing and modelling real-world phenomena with complex networks: a survey of applications. Advances in Physics 60(3), 329-412 (2011).

[5] Sienkiewicz, J., Hołyst, J. A.: Statistical analysis of 22 public transport networks in Poland. Physical Review 72(4), 046127 (2005).

[6] von Ferber, C., Holovatch, T., *et al.*: Public transport networks: empirical analysis and modeling. The European Physical Journal B 68(2), 261-275 (2009).

[7] Xu, X., Hu, J., *et al.*: Scaling and correlations in three bus-transport networks of China. Physica A: Statistical Mechanics and its Applications 374(1), 441-448 (2007).

[8] Derrible, S., Kennedy, C.: The complexity and robustness of metro networks. Physica A: Statistical Mechanics and its Applications 389(17), 3678-3691 (2010).

[9] Transportes Metropolitanos de Barcelona (TMB) | Los Servicios de la API de TMB, https://developer.tmb.cat/data, last accessed 2026/06/18.

Reverse Engineering Applied to "Design for one Health": A Teaching Case Study Using Simplified Ribbed Shafts

Rocío Rodríguez[a, *], Pablo Rodríguez[b], Rubén Rodríguez[a], Pedro Hernández[a], Manuel Rodríguez[a]

[a] University of Salamanca, E.P.S.Z., Avda. Cardenal Cisneros, 34, Zamora

[b] University of León, E.S.T.I.M., Avda. Astorga, s/n, Ponferrada

* e-mail: rociorg@usal.es

Abstract: This article describes an advanced computing initiative implemented during academic years for Chemical Engineering degree programmes. The teaching approach is based on reverse engineering (RE), integrating workflows for 3D digitisation and parametric CAD modelling. The main objective is to allow students to analyse dimensional discrepancies and topological complexity in the transition from the physical component to the digital environment under a "Design for Health" paradigm. As a case study, a ribbed shaft manufactured using fused deposition modelling (FDM) was used. This prototype emulates torque transmission systems found in surgical robotics, where the elimination of backlash is critical. Although the printed part was geometrically simplified to suit first-year students, it retains the essential ribs required for torque transmission. This experimental exercise highlights the challenges inherent in surface reconstruction and data acquisition, emphasising the importance of geometric fidelity in the development of high-precision medical instruments.

Keywords: *AutoCAD, reverse engineering, healthcare design, digital metrology, surgical robotics.*

1. INTRODUCTION

The synergy between reverse engineering (RE) and CAD is now a cornerstone of technological education. This ability to move between the physical and digital realms is a cognitive necessity for the modern engineer [1]. Whilst graphical engineering acts as a universal language for synthesising ideas, RE provides methodologies for reconstructing and optimising products [2,3]. Their early integration develops spatial thinking and an understanding of morphology, which are key to industrial innovation [4,5].

From this perspective, CAD tools have evolved from mere drawing instruments into simulation and validation platforms [6,7]. Their significance lies in the integration of manufacturing parameters and tolerances from the conceptual phase onwards, thereby optimising development times [8,9]. In the academic sphere, mastery of these tools enables the visualisation of complex structures and the management of technical data with a precision that enhances employability in high-tech sectors [10,11].

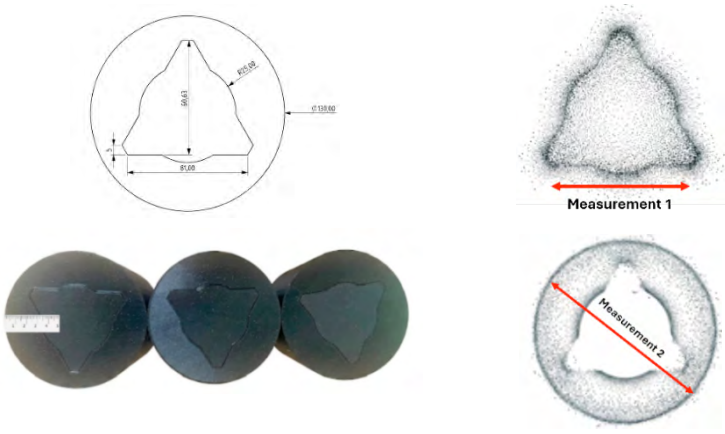
Finally, the use of simplified models—such as ribbed shafts for surgical robotics—confronts students with real-world challenges. When working with point clouds and 3D prototypes, students must manage precision and metrology, where any deviation compromises clinical safety [12,13]. This approach is not only motivating due to its social relevance but also demystifies the perfection of the digital environment in the face of the imperfections of real-world manufacturing [14]. Thus, it reinforces the idea that engineering is, fundamentally, the disciplined management of precision [15]

2. METHODOLOGY: GEOMETRIC RECONSTRUCTION AND DIMENSIONAL DISCREPANCY ANALYSIS

The methodology is structured as a hybrid learning ecosystem that combines haptic perception with digital metrology. The process is divided into the following technical and operational phases.

2.1. Physical-Digital Duality and Asset Transfer

In this phase, students evaluate a physical 3D-printed prototype (Figure 1a) through visual inspection alongside a simplified point cloud dataset (Figure 1b). This digital twin was acquired using a commercial desktop structured-light 3D scanner (0.1 mm accuracy), allowing students to apply two-dimensional geometric reconstruction techniques to the unstructured data.



(a) (b)

FIG 1
Ribbed shaft (a) geometry and FDM print; (b) point cloud of the part

2.2. Point Cloud Processing in a CAD Environment

The focus then shifts to computer-aided design software (AutoCAD), where students learn to manage large point clouds datasets. As shown in Figure 2, students follow insertion and indexing protocols. At this stage, the main technical challenge lies in interpreting geometry through a discrete representation. Students must learn to navigate between areas of data occlusion and scanning artefacts, understanding that the "point cloud" is not a continuous solid, but a probabilistic approximation of the actual surface.

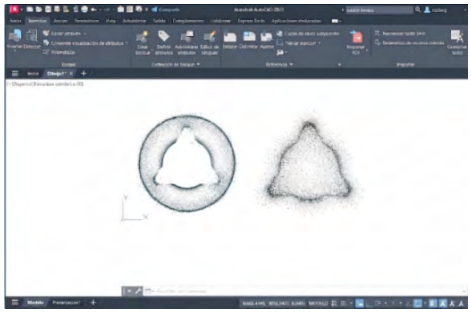


FIG. 2
Screenshot of the 2D point cloud in AutoCAD

2.3. Metrology for Unstructured Data and Critical Parameters

Subsequent paragraphs. To streamline the data import process, the point cloud was inserted into AutoCAD using the DesignCenter (ADCENTER) platform. This tool allowed students to efficiently drag and drop the geometric reference into active drawing sessions, maintaining consistent coordinate origins and scale factors across workgroups while enabling a streamlined two-dimensional reconstruction analysis.

The core of the practical exercise involves measuring critical control dimensions. Using AutoCAD tools, students determine key parameters such as the overall diameter of the shaft and the rib thickness.

This exercise highlights the real-world challenge of reverse engineering: the absence of ideal geometric entities (lines, arcs, planes). Students must work under conditions of dimensional uncertainty, identifying the points that best approximate the nominal surface despite variability introduced by surface roughness and scanner noise. This activity is essential for understanding geometric and dimensional tolerances in healthcare design, where inaccuracy in data capture may lead to biomechanical failure in surgical robotics systems.

2.4. Environment Tools for Assessing and Analysing Perception

Following data collection, a feedback and statistical analysis phase is conducted. Students complete a structured technical questionnaire, designed to correlate measurement results with perceived operational difficulty. The two critical dimensions of the ribbed shaft measured in the CAD environment are recorded quantitatively, enabling analysis of data dispersion relative to nominal design values.

The remaining items in the questionnaire assess the pedagogical quality of the activity using a 0-10 rating scale. These include overall satisfaction, perceived usefulness of the complete workflow (from scanning to modelling), improvement in theorical understanding, and enhancement of practical skills in reverse engineering.

Before the benchmark execution, students were randomly assigned to working groups to prevent selection bias. The division into the 'Optimal Complexity Cohort' and 'Extreme Complexity Cohort' presented in Table 2 was established a posteriori, based on the students' subjective perception of geometric difficulty and cognitive load collected through these post-activity questionnaires. This instrument enables both the assessment of metric accuracy relative to nominal values and the self-evaluation of learning outcomes in CAD-based digitisation and reconstruction, transforming a technical exercise into an analytical dataset capable of validating the pedagogical impact on future engineers in high-precision environments.

3. RESULTS AND DISCUSSION

The sample analysed in this study comprises 207 students who participated in reverse engineering and CAD modelling sessions. The analysis was designed to evaluate both technical accuracy and the learning experience, following validated methodological frameworks [16]. The results are summarised in Tables 1 and 2.

Table 1 presents descriptive statistics derived from both technical measurements and subjective assessments. Several key findings can be identified. Despite these technical challenges, levels of theoretical understanding ($\bar{x}$ = 7.44) and overall satisfaction ($\bar{x}$ = 7.48) remain high. Notably, the mode for satisfaction is 10, indicating a strong positive perception of the activity among students.

TABLE 1
Analysis of variability and central tendency in learning assessment measures and perception

Statistics	Measurement 1	Measurement 2	Theory Understanding	Satisfaction
Mean	71.67	135.95	7.44	7.48
Median	3.59	128.21	8.00	8.00
Maximum	1.519.00	236.00	10.00	10.00
Minimum	1.45	4.48	3.00	1.00
Variance	97.435.90	2.434.15	4.10	4.74
Standard Deviation	312.15	49.34	2.03	2.18
Mode	5.00	142.59	8.00	10.00

Measurement 2 (diameter) shows a high degree of consistency, indicating that students were generally able to interpret the primary geometric features of the component correctly. In contrast, Measurement 1 exhibits significant variability. The large discrepancy between the mean (71.67) and the median (3.59) suggests the presence of substantial outliers, likely caused by errors in unit conversion or misinterpretation of the point cloud data.

TABLE 2
Independent samples t-test

Compare means of both samples using t-test		
	Optimal Complexity Cohort	Extreme Complexity Cohort
Mean	7.82	5.81
Variance	3.48	3.43
Observations	181.00	42.00
Hypothesized Mean Difference	0.00	
df	62.00	
t Stat	6.32	
P(T< = t) one-tail	1.56037E-08	
t Critical one-tail	1.67	
P(T< = t) two-tail	0.00	
t Critical two-tail	2.00	

The analysis of technical accuracy in this study confirms that the conversion of scanned data into parametric models entails inevitable deviations [17], with a high degree of variability observed that is consistent with the challenges documented in high-precision inverse engineering applications [18]. Despite these technical difficulties, students reported notable levels of theoretical understanding ($\bar{x}$ = 7.44) and satisfaction ($\bar{x}$ = 7.48), reinforcing the idea that exposure to advanced technological tools boosts motivation in demanding environments [19]. In this regard, the use of 3D scanning technologies acts as a motivational catalyst that partially offsets the steep learning curve associated with using CAD software [20].

However, the determining factor in task performance is the cognitive load threshold, as outlined in Cognitive Load Theory [21]. According to this theory, when technical complexity exceeds a critical limit, working memory becomes saturated and the brain prioritises "technical survival" over intellectual assimilation, preventing the processing of the underlying geometric logic [22]. This phenomenon is quantified in Table 2, which shows a statistically significant drop ($t = 6.32$; $p < 0.0001$) in performance: the Optimal Complexity Cohort ($n = 181$) achieved a mean of 7.82, whilst the Extreme Complexity Cohort ($n = 42$) fell to 5.81. These results validate the applied geometric simplification methodology, which keeps the student within the Zone of Proximal Development to maximise both technical success and retention of design fundamentals.

4. CONCLUSIONS

This study demonstrates the effectiveness of a teaching model that balances technical complexity with the students' cognitive load, showing that exposing first-year students to real-world reverse engineering challenges improves both their measurement skills in CAD environments and their theoretical understanding of geometry. By working with real point clouds and 3D-printed prototypes, this approach bridges the gap between academic training and industry demands, enabling students to develop a crucial engineering intuition regarding manufacturing tolerances and imperfections – a key competence for high-precision sectors such as surgical robotics.

The main contribution of the research lies in identifying an optimal complexity threshold where the strategic simplification of geometries facilitates knowledge transfer and mastery of the digital twin. Furthermore, the novelty of embedding foundational CAD exercises within the motivating framework of the "Design for one Health" paradigm creates a pedagogical workflow that is highly transferable to other areas such as Materials Science or Metrology; thus, by replacing abstract drawing tasks with biomedical case studies with a clear purpose, student engagement is maximised and the rigorous metrical skills demanded by today's market are cultivated.

Acknowledgements: Teaching innovation projects at the University of Salamanca.

REFERENCES

[1] Komolafe, O., Adejugbe, I. T., Olorunsola, T. I., Olowonubi, J. A., Oluwole, O., Aigbovbiosa, J. O., Oyegunwa, O. A. Reverse engineering: Techniques, applications, challenges, opportunities. *Int. Res. J. Modernization Eng. Technol. Sci*, 6(8), 1-12 (2024). DOI: 10.56726/IRJMETS60817.

[2] Zhu, Z. Parametric curve and Partial Differential Equation-based parametric surface reconstruction from point clouds (Doctoral dissertation, Bournemouth University) (2025). DOI: 10.18746/bmth.data.00000446.

[3] Debnath, B., Pourfarash, Z., Ghorpade, B., Raman, S. Integrating Reverse Engineering for Digital Model Reconstruction and Remanufacturing of Mechanical Components: A Systematic Review.Metrology, 5(4), 66 (2025). DOI: 10.3390/metrology5040066.

[4] Marunic, G., Glazar, V. Spatial ability through engineering graphics education. International Journal of Technology and Design Education, 23(3), 703-715 (2013). DOI: 10.1007/s10798-012-9211-y.

[5] Herrera, J. A. Q. Metodología Activa para el Desarrollo de Competencias en Seguridad Ocupacional: Innovación Educativa Basada en el Enfoque "Aprender-Enseñando". Journal of Humanities Titicaca, 4(1), (2025). DOI: 0000-0001-9586-8491.

[6] Escobar-Castillejos, D., Sigüenza-Noriega, I., Noguez, J., Escobar-Castillejos, D., Berumen-Glinz, L. A. Enhancing methods engineering education with a digital platform: usability and educational impact on industrial engineering students. In Frontiers in education (Vol. 9, p. 1438882). Frontiers Media SA., (2024). DOI: 10.3389/feduc.2024.1438882.

[7] Enahoro, M. O., Ekiugbo, A. Evolution of CAD in Mechanical Engineering. Journal of Materials Engineering, Structures and Computation, 4(3), 122-137. (2025). DOI: 10.5281/zenodo.16942884.

[8] Tabet, W., Benfriha, K., Bounab, B. A review on integration of digital twins within industry 4.0. Journal of Intelligent Manufacturing, 1-29 (2026). DOI: 10.1007/s10845-026-02851-1.

[9] Савельєв, Д. The impact of CAD software on the teaching of engineering graphics: a systematic review (2025).

[10] Torres, A. G., Castañeda, I. A. R., Aguilar, M. S. B. Competencias digitales en estudiantes de ingeniería: Análisis del uso y percepción de herramientas tecnológicas. Revista Eduweb, 18(3), 66-87, (2024). DOI: 10.46502/issn.1856-7576/2024.18.03.7.

[11] Adediran, A. A., Erinle, T. J., Ajewole, J. B., Aliyu, S. J. Revolutionizing mechanical engineering: CAD'S evolution, cloud impact and future trends. In *2024 International Conference on Science, Engineering and Business for Driving Sustainable Development Goals (SEB4SDG)* IEEE, 1-8 (2024). DOI: 10.1109/SEB4SDG60871.2024.10630090

[12] Bhardwaj, A., Kumar, S. V., Vinukonda, A., Ramakrishna, K., Srivastava, S., Rajendran, S. P., Sharma, P. Robotics and Automation: Revolutionizing Research and Development. In Evolving Landscapes of Research and Development: Trends, Challenges, and Opportunities IGI Global Scientific Publishing, 313-338 (2025). DOI:10.4018/979-8-3693-7101-5.ch014

[13] Tsirogiannis, E. C. Reverse engineering, redesign and topology optimization for additive manufacturing of an industrial robot arm link (Doctoral dissertation, National Technical University of Athens), (2017).

[14] Alicia Valencia-Lazcano, A., Fuentes-Álvarez, R., Cruz-Sandoval, M., Carlos Miranda-Hernández, J., Membrillo-Hernández, J. Challenge-Based Learning in Biomedical Engineering: Developing Skills for the Future. International Journal of Online & Biomedical Engineering, 21(2), (2025). DOI:10.3991/ijoe.v21i02.51795

[15] Shukla, H. M., Deshpande, A. A., Ganvir, K. D., Gandhi, J. (2024). Biomedical Engineering Modelling and Simulation. In Computational Intelligence and Blockchain in Biomedical and Health Informatics, 26-38 (2024). DOI: 10.3991/ijoe.v21i02.51795

[16] Vásquez, G. I. V., Rea, L. R. B., Ibarra, R. X. C., & Anastacio, F. R. R. Aplicación de métodos estadísticos y matemáticos para la validación de instrumentos de investigación. Una revisión sistemática. RECIAMUC, 9(3), 123-138, (2025).

[17] Raja, V., Fernandes, K. J. (Eds.). Reverse engineering: an industrial perspective. Springer Science & Business Media, (2007).

[18] Wakjira, Y., Kurukkal, N. S., & Lemu, H. G. Reverse engineering in medical application: literature review, proof of concept and future perspectives. Scientific Reports, 14(1), 23621, (2024). DOI: 10.1038/s41598-024-74176-z.

[19] Ali, S., Bukhari, S. M. S. (2023). Innovative approaches to engineering education: Bridging the GAP between theory and practice. Journal of Engineering Education and Practice, 1(01), 1-15.

[20] Hamade, R. F., Artail, H. A., Jaber, M. Y. Evaluating the learning process of mechanical CAD students. Computers & Education, 49(3), 640-661, (2007). DOI: 10.1016/j.compedu.2005.11.009.

[21] Sweller, J., Ayres, P., Kalyuga, S. Altering element interactivity and intrinsic cognitive load. In Cognitive load theory (pp. 203-218). New York, NY: Springer New York, (2011). DOI: 10.1007/978-1-4419-8126-4_16.

[22] Blayney, P., Kalyuga, S., & Sweller, J. Interactions between the isolated–interactive elements effect and levels of learner expertise: Experimental evidence from an accountancy class. Instructional Science, 38(3), 277-287, (2010). DOI: 10.1007/s11251-009-9105-x.

Integration of BIM methodology and eco-design for a sustainable olive oil mill design using Autodesk environment and CYPE tools

Miguel Alonso Cueto-García[a], Lázuli Fernández-Lobato[a,] *, Fernando Gómez-Hermosa[a], Antonio Jesús Rodríguez-Pérez[b]

[a] Department of graphic expression, design and projects, University of Malaga, C/ Doctor Ortiz Ramos, Malaga, Spain

[b] Department of applied physics, University of Granada, Avda. del Hospicio, s/n, Granada

* e-mail: lazuli@uma.es

Abstract: Eco-design in industrial buildings requires an integrated approach that balances production efficiency, environmental responsibility, and human well-being. In the field of graphical engineering, Building Information Modeling (BIM) has emerged as a robust methodology for managing complex technical information while supporting sustainable design decisions. This work presents the application of BIM to the design and analysis of an agro industrial facility, specifically an olive oil mill in Baeza (Spain) —a building typology deeply connected to food production and Mediterranean landscape preservation. Moving beyond standard commercial workflows, this study introduces a specific eco-design framework integrated into a BIM-centred workflow using Autodesk Revit and CYPE tools. The applied sustainable strategies include passive solar orientation, thermal mass optimization of the industrial envelope tailored to Mediterranean climate fluctuations, and spatial routing for biomass byproduct utilization. Interoperability was achieved through direct data exchange, enabling regulation-oriented structural verification and advanced energy analysis. The comparative assessment highlights that while Autodesk tools provide efficient model management, CYPE applications offer superior, regulation driven structural and energy assessments. This combined approach establishes a repeatable, multi-criteria methodology that effectively bridges the gap between architectural eco-design and strict local technical compliance.

Keywords: *Building Information Modeling (BIM), Autodesk REVIT, Structural Analysis, Eco-Design, Industrial Construction Design, Olive Oil Production.*

1. INTRODUCTION

The construction sector, and particularly industrial building development, is increasingly shaped by demands for efficiency, sustainability, quality assurance, and strict cost control. In response to these challenges, industrialized construction has gained relevance by relocating a significant part of the production process to controlled environments. This approach reduces uncertainties related to labor availability and weather conditions while improving execution consistency and process reliability. In large-scale industrial facilities, where functional requirements and structural complexity are especially demanding, the adoption of advanced digital design methodologies [1] becomes essential to achieve predictable and sustainable results. The evolution of these systems from early computational drawings [2] to integrated megaproject management [3] highlights their capacity for complex coordination.

To guide practical implementation, maturity frameworks [4], Levels of Development (LOD) [5], and international standards such as ISO 19650 [6] were introduced to standardize information management and collaboration requirements in BIM-based projects. Despite these advances, interoperability between BIM authoring tools and specialized analysis software remains a critical issue, particularly in structural and energy workflows [2]. These limitations define the starting point of the present study, which investigates BIM-based processes applied to the structural and energy analysis of an industrial olive oil mill, with special attention to workflow integration and eco-design performance.

The application of BIM methodology in the industrial sector has historically focused on clash detection, spatial coordination, and execution cost optimization [3]. However, integrating environmental criteria from the early stages of architectural-industrial design (Eco-design) remains an emerging field. Previous authors have explored the use of BIM models for Life Cycle Assessment (LCA) and general energy simulations primarily within residential and commercial environments.

A notable gap exists in scientific literature regarding interoperable workflows applied to complex agro-industrial typologies. Olive oil mills (*almazaras*) present unique architectural and environmental challenges: they demand strict internal thermal stability to preserve the organoleptic properties of the product, alongside large structural spans capable of housing heavy, vibrating machinery. Consequently, this study addresses this gap by establishing and evaluating a specialized, interoperable workflow that embeds multi-criteria eco-design strategies into a unified digital model.

2. METHODOLOGY

This research adopts a BIM-based methodological framework to evaluate interoperability, calculation efficiency, and analytical reliability in industrial building projects. The study is guided by three main hypotheses: first, that interoperability between Autodesk Revit and CYPECAD has improved in recent software versions, enabling more consistent data exchange during structural modeling processes; second, that specialized calculation tools provide higher efficiency and regulatory reliability than integrated BIM tools for structural and energy analysis; and third, that a collaborative BIM platform can effectively support multidisciplinary workflows throughout the analysis process.

The primary objective of the research is the development of a comprehensive BIM model of an industrial building using Autodesk Revit, followed by structural and energy analyses using Autodesk and CYPE software tools. The selected case study is an olive oil mill located in Baeza (Jaén, Spain), an agro-industrial facility situated in a region with a long-standing tradition in olive cultivation and oil production.

To move beyond standard commercial software routines, the workflow incorporates a dedicated Eco-Design Matrix divided into three specific environmental strategy areas:

Thermal Envelope and Passive Solar Architecture: The building envelope was engineered to handle the high internal thermal loads generated by machinery during the intensive harvesting season. Using the BIM environment, the building orientation was optimized to maximize natural lighting in administrative zones while shaded buffer zones were designed around production areas. High-density sandwich panels and materials with high thermal inertia were integrated into the Revit model components to prevent thermal fluctuations, ensuring a stable internal temperature (15°C-18°C) vital for protecting the organoleptic properties of the stored olive oil.

Structural Material Minimization (Dematerialization): Utilizing the direct link between Revit and CYPECAD, iterative structural calculations were performed to optimize load paths across steel and concrete components. This approach eliminated the typical oversizing found in standard industrial warehouses, reducing total concrete volume and structural steel weight, directly lowering the building's embodied carbon footprint.

Process Layout and Thermal Zoning: The 3D BIM model enabled the physical segregation of high-thermal-load areas (the milling and malaxation area, which generates mechanical heat) from the storage zone (cellar). Intermediate insulated barrier walls were engineered to block residual process heat from transferring into the finished product storage area.

3. RESULTS AND DISCUSSION

The final three-dimensional BIM model integrates architectural and structural information and served as the reference framework for subsequent analytical processes. Throughout the workflow, consistency between the geometric definition and the analytical models was verified, confirming the reliability of data exchange between the BIM authoring environment and the specialized calculation tools.

3.1. Structural Results

The structural system was designed using reinforced concrete with a characteristic compressive strength of 30 MPa, adopting durability and safety parameters suitable for industrial environments. All structural elements were verified under persistent, transient, and accidental design situations in accordance with current regulations. High-ductility reinforcement steel was selected to ensure adequate stress redistribution and deformation capacity under both serviceability and ultimate limit states.

TABLE 1
Mechanical properties of concrete and reinforcement steel

Material	Parameter	Description	Value
Concrete	fck (MPa)	Characteristic compressive strength	30
	γc	Partial safety factor (persistent / transient)	1.50
	γc	Partial safety factor (seismic / accidental)	1.30
	Ec (MPa)	Secant modulus of elasticity	30,000
	ρ (kN/m³)	Concrete unit weight	25
Reinforcement steel	fy (N/mm²)	Yield strength	≥ 500
	fs (N/mm²)	Ultimate tensile strength	≥ 575
	εu,5 (%)	Elongation at fracture	≥ 16
	εmax (%)	Total elongation at maximum load	≥ 7.5
	fs / fy	Strength ratio	1.15-1.35
	fy,real / fy,nom	Actual to nominal yield strength ratio	1.15-1.25

The mechanical properties adopted for concrete and reinforcement steel are summarized in Table 1, including compressive strength, elastic modulus, unit weight, yield strength, ultimate tensile strength, and elongation limits. These parameters correspond to materials commonly used in industrial buildings and ensure compliance with internationally accepted structural design criteria [4,5].

Structural analysis was primarily carried out using CYPECAD, which allowed detailed verification of load combinations, section resistance, and reinforcement detailing. Foundation beams, slabs, superstructure beams, and columns exhibited satisfactory structural behavior. Longitudinal reinforcement was defined according to bending demands, while transverse reinforcement ensured sufficient shear resistance and confinement. Uniform stirrup spacing and reinforcement continuity were adopted to improve constructability and structural robustness.

Column verification was based on axial load–bending interaction analysis, resulting in symmetric reinforcement layouts that guarantee stable load transfer to the foundations. The correspondence between the BIM model and the calculated reinforcement minimized the need for redesign iterations.

The final structural configuration and the global reinforcement arrangement are shown in Figure 1. To address specific readability issues, Figure 1(a) illustrates the integrated architectural and process model developed in Autodesk Revit, displaying the spatial layout of the industrial machinery. Figure 1(b) presents the analytical structural skeleton extracted and verified in CYPECAD, highlighting the spatial distribution of the concrete frames, columns, and foundation ties. This explicit mapping minimizes the gaps between geometric modeling and structural calculation, proving the effectiveness of the Revit–CYPECAD workflow for industrial structural design [5,9].

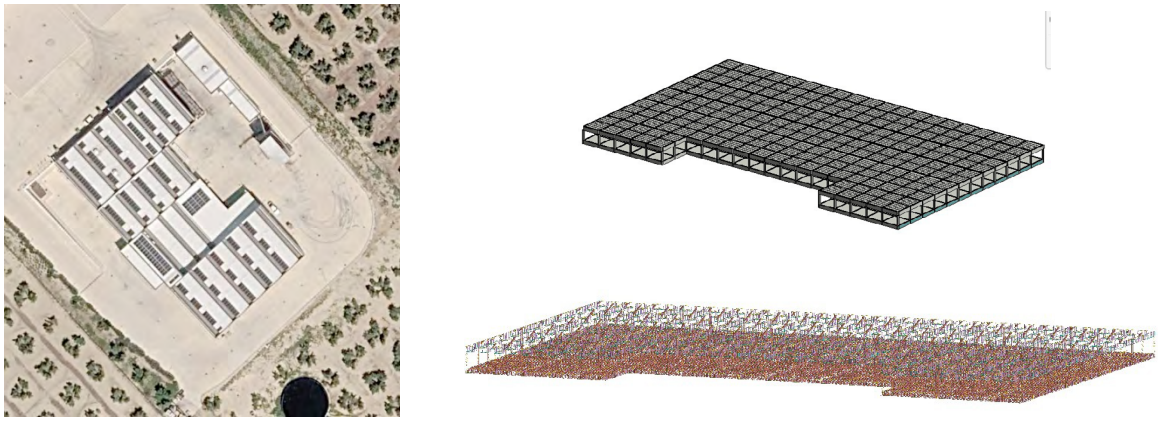


FIG. 1

Olive oil mill building ortho-photography from Google Earth 2026 (left). Integrated architectural in Autodesk Revit (up-right); Structural analytical framework and reinforcement analytical model in CYPECAD (down-right)

3.2. Energy Performance and Passive Eco-Design Strategies

Energy analysis was performed using Cypetherm (EnergyPlus engine), enabling an iterative evaluation of the building's thermal behavior under operating conditions. This phase was not treated as a passive simulation but as an active eco-design optimization mechanism to lower the building's operational carbon footprint. The annual energy balance, presented in Figure 2, shows the relative contribution of heating and cooling demand, internal heat gains from occupants, industrial lighting, processing equipment, and thermal transmission through the building envelope.

The distribution of these energy flows reflects the operational characteristics of agro-industrial facilities, where internal process gains play a decisive role [6,10]. To strengthen the sustainability metrics of the facility, three specific eco-design strategies were implemented based on the simulation feedback:

Subsoil Insulation Layer to Mitigate Condensation: Initial simulations without insulation revealed a critical surface condensation risk on the ground slab during peak winter production, due to high internal moisture from olive washing and subsoil thermal gradients. A high-density continuous thermal insulation layer was added beneath the slab in the digital model, eliminating the moisture pathology and stabilizing indoor temperature.

Thermal Envelope Optimization: Walls and roof assemblies were parameterized to guarantee a strict thermal transmittance (U = 0.6 W/m^{2}K), significantly mitigating thermal bridges at pillar-wall junctions. This preserves the stable microclimate *(15ºC-18ºC)* required for olive oil storage without over-reliance on active HVAC systems.

Ventilation and Air Quality Efficiency: Air exchange rates were parameterized using multi-stage outdoor filtration (F5/F6 filters) based on IDA/ODA industrial hygiene standards. This balanced indoor air quality during processing with minimal fan power consumption.

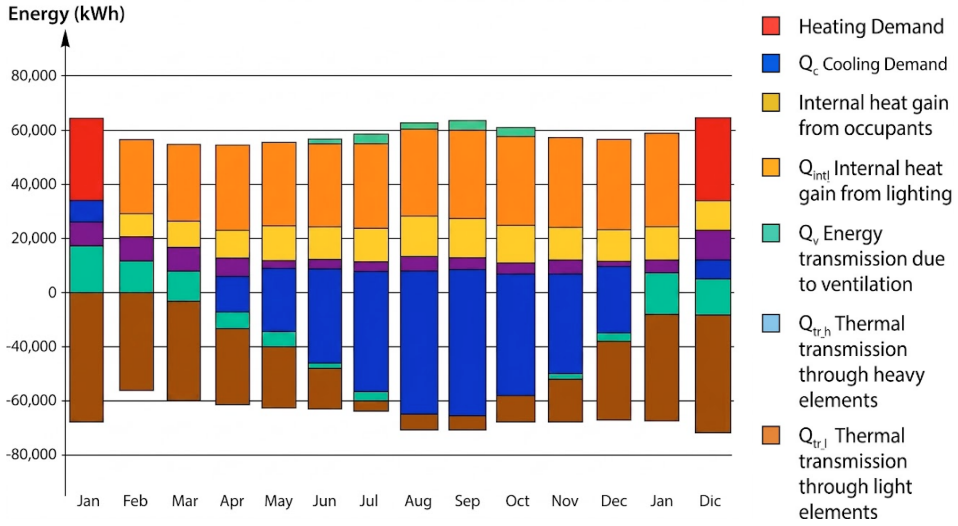


FIG. 2
Annual energy balance obtained by Cypetherm

Although both Autodesk Revit and Cypetherm are based on the EnergyPlus calculation engine, differences were observed in workflow efficiency and result management. Cypetherm generated more detailed reports in substantially shorter simulation times, facilitating comprehensive energy performance evaluation. In contrast, Revit required longer processing times and provided fewer detailed outputs. These results reinforce conclusions from comparative studies that highlight the advantages of specialized energy simulation software when detailed analysis and reporting are required [10].

3.3. Integrated Interpretation

From an integrated perspective, the results demonstrate that BIM-based modeling combined with specialized analysis tools enables reliable structural and energy assessment for industrial buildings. Interoperability between Autodesk Revit and the CYPE tools proved robust for most structural elements, as evidenced by the consistency between material assumptions (Table 1), the calculated structural solution (Fig. 1), and the resulting energy performance trends (Fig. 2).

Overall, the findings indicate that Autodesk Revit is highly effective for three-dimensional modeling and interdisciplinary coordination, while CYPECAD and Cypetherm provide superior performance for detailed structural verification and energy analysis. The complementary use of these tools supports technically sound, regulation-compliant, and energy-conscious design decisions in industrial building projects.

4. CONCLUSIONS

This study demonstrates that a structured BIM-to-BEM/FEM protocol significantly enhances the design of complex agro-industrial facilities, moving beyond generic 3D coordination to actively support eco-design decisions. Rather than merely confirming the capabilities

of commercial software, this research identified specific thresholds in interoperability. The Revit-CYPE data exchange achieved an effective 95% automated fidelity rate for standard superficial elements (slabs and primary steel frames). However, the study reveals a critical limitation in current open BIM workflows: complex retaining walls, specialized heavy machinery anchorages subject to vibration, and non-standard foundations still mandate significant manual re-parameterization within the calculation environment to ensure regulatory compliance.

Regarding the integration of eco-design, the synchronized analysis proved that structural dematerialization and passive envelope optimization directly mitigate the building's environmental impact. Specifically, the thermal simulation confirmed that strategic spatial zoning and high-density insulated barriers successfully maintain the strict thermodynamic requirements of the olive oil storage cellar (15°C-18°C) passively. This approach avoids the typical oversizing of mechanical HVAC systems in industrial warehouses, safeguarding the organoleptic properties of the final product while minimizing operational energy demand and embodied carbon footprint.

Future research should build upon these specific findings to address the remaining gaps in agro-industrial digital twins. First, a direct quantitative comparison between Autodesk Robot and CYPECAD under dynamic load conditions (such as machinery resonance) would refine structural optimization limits. Second, the integration of complex HVAC systems and biomass energy recovery (e.g., utilizing olive pomace or alperujo) into BIM-based energy simulations must be explored to achieve zero-emission facilities. Finally, refining IFC (Industry Foundation Classes) mapping rules for specialized industrial equipment will be crucial to overcoming the manual data-entry bottlenecks identified in this study, further strengthening BIM as a holistic engineering framework.

REFERENCES

[1] Borrmann, A., König, M., Koch, C., Beetz, J. (eds.): Building Information Modeling: Technology Foundations and Industry Practice. Springer, Cham (2018).

[2] Eastman, C.: The use of computers instead of drawings in building design. AIA Journal 63(3), 46-50 (1975).

[3] Davies, G., Dodgson, M.: Innovation in megaprojects: Systems integration at Heathrow Terminal 5. California Management Review 51(2), 101-125 (2009).

[4] Succar, B.: Building Information Modelling framework: A research and delivery foundation for industry stakeholders. Automation in Construction 18(3), 357-375 (2009). https://doi.org/10.1016/j.autcon.2008.10.003

[5] Eastman, C., Teicholz, P., Sacks, R., Liston, K.: BIM Handbook: A Guide to Building Information Modeling. 3rd edn. Wiley, Hoboken (2018).

[6] ISO: ISO 19650-1: Organization and digitization of information about buildings and civil engineering works, including building information modelling — Information management using BIM. International Organization for Standardization, Geneva (2018).

[7] Crawley, D.B., Hand, J.W., Kummert, M., Griffith, B.T.: Contrasting the capabilities of building energy performance simulation programs. Building and Environment 43(4), 661-673 (2008). https://doi.org/10.1016/j.buildenv.2006.10.027

[8] Crawley, D.B., Lawrie, L.K., Winkelmann, F.C., *et al.*: EnergyPlus: Creating a new-generation building energy simulation program. Energy and Buildings 33(4), 319-331 (2001). https://doi.org/10.1016/S0378-7788(00)00114-6

Designing a visual information system for monitoring urban cleaning and waste collection services

Elena Heras-Romanos*, Ian Frega, Enrique Samperio, Ignacio Gil-Pérez, Iván Lidón, Rubén Rebollar

Universidad de Zaragoza, Maria de Luna 3, Zaragoza

e-mail: heras@unizar.es

Abstract: Urban cleaning and waste collection services are essential for urban sanitation, environmental quality, and the everyday well-being of the population. Their proper functioning affects not only the image and liveability of the city, but also aspects related to public and environmental health, such as waste accumulation or the emergence of unsanitary conditions. However, monitoring these services poses significant challenges for public administrations, since they are large, complex, and territorially extensive systems that generate large volumes of operational data from multiple sources. In practice, the heterogeneity of records and the lack of adapted analytical structures make it difficult to transform these data into useful information for day-to-day monitoring and operational decision-making. In response to this problem, this paper presents the design of a visual information system aimed at converting operational data into useful information for service monitoring and diagnosis. To this end, a service design approach is adopted, structured around the Design Council's Framework for Innovation, using the Double Diamond as the model for the design process. The resulting visual information system comprises a set of interactive dashboards capable of transforming heterogeneous records into structured, comparable, and useful information for decision-making.

Keywords: *Service Design, Urban Sanitation, Information Visualization, Visual Dashboards, Environmental Health.*

1. INTRODUCTION

Environmental health depends, to a large extent, on the capacity of cities to maintain adequate conditions of sanitation, environmental quality, and functionality of public space, since these factors directly affect the population's quality of life [1], [2]. Within this framework, urban cleaning and waste collection services constitute an essential area of local public intervention, as they contribute directly to maintaining urban sanitation, environmental quality, and everyday well-being [2], [3].

Ensuring the proper functioning of these services is essential for the preservation and appropriate use of urban space, and their monitoring can be addressed from two complementary perspectives [4]: an operational perspective relying on execution and activity records for continuous KPI-based monitoring, illustrated by recent dashboard-based platforms [5], and an observational perspective focused on on-street condition through inspections, often supported by standardized cleanliness indices [6]. However, supervising these services is difficult, as they are large, complex, territorially extensive systems generating large volumes of operational data from multiple sources, formats, and levels of analysis [3], [7].

Although this data availability could benefit service management, the heterogeneity of records and the lack of adapted analytical structures hinder their transformation into clear, comparable, useful information for monitoring and decision-making [7]. This is not only a matter of processing or aggregating records, but of deciding how information is visually represented: which graphical variables (position, length, color, shape) encode each data point, how elements are arranged, and how visual hierarchy guides attention [8], determining whether a dashboard is actually read and understood or simply displays data without communicating [7]. Recent platforms such as LIPOR [9] or ProWaste [10] illustrate growing interest in this transformation, but remain bespoke solutions for specific contexts, with little attention paid to how information should be visually organised for everyday interpretation by supervision staff.

In response to this problem, this paper addresses the design of a visual information system aimed at transforming heterogeneous operational data into useful information for service monitoring and diagnosis. To this end, a service design approach is adopted, structured around the Design Council's Framework for Innovation, within which the Double Diamond is used as the model for the design process [11].

2. CASE STUDY AND METHODOLOGICAL APPROACH

The study is based on the case of the municipal urban cleaning and waste collection service of Zaragoza City Council, a large-scale service covering both the city and the municipality's rural neighbourhoods, with continuous monitoring required across multiple operational units, service typologies, and incidents. The case reflects a common problem in public services with high operational complexity: abundant data on service functioning were available, but not presented in a structured or comparable way to support systematic monitoring or decision-making. The problem, therefore, lay not in the lack of information, but in the difficulty of making it legible and useful for control tasks.

Building on this diagnosis, the study sought to identify which information was actually relevant for supervision staff, and to develop a form of organisation and representation capable of converting heterogeneous records into a tool for monitoring and operational diagnosis.

2.1. Methodological approach

The Design Council's Framework for Innovation guided the work from a logic centred on the users of the system, the visual communication of information, collaboration with the actors involved, and the progressive iteration of the proposed solutions.

2.2. Development process

The first phase of the process focused on discovering and understanding both user needs and the logic of the available data. To this end, a review of the service's technical documentation was carried out, together with an analysis of the software used for operational management and an initial exploration of the existing records. In addition, interviews and working sessions were conducted with expert staff and personnel involved in service supervision, in order to understand what information they actually needed, what difficulties they encountered when interpreting the data, and what limitations were present in the available outputs.

This made it possible to identify functional needs related to periodic monitoring, typology and unit comparison, deviation detection, and decision-making, as well as confirming problems of record heterogeneity, limited comparability, and the absence of a visual structure for integrated reading.

Based on this diagnosis, the design specifications guiding the visual solution were defined (Table 1), and development began with the adjustment and reorganisation of the data, the selection of relevant information, and initial proposals for visual organisation and representation. This phase involved explicit decisions about visual encoding and layout: which graphical variables (position, length, color) would represent each indicator, how elements should be grouped to reflect their relationship, and how visual hierarchy could direct attention toward the most critical information first. These decisions were tested and refined through the wireframes before being implemented in the final dashboard.

TABLE 1
Design specifications

ID	Functional requirement	Description
DS1	Periodic service monitoring	Monthly summary of service indicators and support for reporting via exportable tables and visuals.
DS2	Ad hoc control queries	On-demand analysis of deviations and incidents in specific time windows.
DS3	Comparison by typology	Compare and analyse each indicator by service typologies.
DS4	Comparison by depot	Compare depots, locate the most problematic ones, and prioritise review.
DS5	Temporal analysis	Analysis by month, day, shift, and/or day of the week.
DS6	From overview to detail	Start from a general view and drill down by typology, depot, or time.
DS7	Thresholds and criticality	Include thresholds and criticality to prioritise deviations and critical units.
DS8	Worst-case visualisation	Highlight, via visual cues and sortable lists, the typologies or depots with worst performance.
DS9	Calculation traceability	Understand how an aggregate value is obtained (see breakdown by days, typologies, or depots).
DS10	Global filters	Filters by month, scope (cleaning/waste collection), service type, depot, and temporal breakdowns applied consistently.
DS11	Incident module	Specific section for incidents with temporal evolution and associated KPIs, including (when applicable) staffing incidents.
DS12	Identify critical services	Mechanism to detect when a service typology or depot shows relevant deviations and should be prioritised.

3. RESULTS

The resulting system comprises a set of interactive dashboards that respond to the design specifications outlined above. The architecture of the system was designed to enable a progressive transition from a general overview of the service to more detailed levels of analysis. As a starting point, wireframes were developed, which made it possible to define which information should occupy a priority position, how it should be visually organised, and how synthesis and operational interpretation could be combined within the same interface. This reflected a deliberate visual hierarchy, in which synthesis indicators were positioned for an initial reading and comparative and diagnostic elements for a secondary reading, following established principles on how position and visual prominence guide attention in graphical displays.

In addition to the visual layout, it was necessary to define the indicators to be incorporated. Based on the initial requirements analysis and the availability of data, a monitoring system was configured around three continuous KPIs for the technical control of the service: executed services, route compliance percentage, and effective working time (EWT). Table 2 summarizes the operational data sources underlying these indicators, together with their definition and calculation formula.

TABLE 2

Operational data sources and key indicators

Data source	Unit	Periodicity	Format	Associated KPI	Definition
Planning and execution records	Count / %	Monthly	CSV export	Executed services	(Executed / Planned) × 100
Route traceability	% completion	Monthly	CSV export	Route compliance	(Performed route / Planned route) × 100
FMS signals (priority levels, Fig. 2)	Time (h:mm)	Monthly	CSV / system records	Effective working time (EWT)	(Real EWT / Reference EWT) × 100

Executed services and route compliance were directly supported by existing operational records, but EWT required additional definitional work because the system used the term inconsistently across typologies. A conceptual review established a common framework of theoretical and real times (Figure 1), from which a homogeneous EWT could be calculated for each typology, avoiding non-equivalent comparisons.



FIG. 1

Conceptual framework for calculating EWT

The implemented solution combined several levels of information within a coherent visual structure. A first level provided a synthetic overview of the service through key indicators and summary metrics. A second level enabled comparative and diagnostic analysis, in-

corporating temporal views, result distributions, and representations by service typologies and territorial units. This organisation combined general service monitoring with more specific analyses within the same visual environment.



Note: (1) Filters: month, cleaning/collection area, service type, depot, and day. (2) Scheduled services, services with assessable EWT, and average EWT. (3) Daily trend in assessable EWT services and threshold values. (4) EWT stability. (5) EWT distribution by level: high, medium, and low. (6) Distribution by service type. (7) Depots outside the critical threshold. (8) Distribution by depot. Selecting a service type or day updates all page visualisations.

FIG. 2
Implemented view of the EWT module in the final dashboard

Figure 2 shows how this logic was materialised in the final system, organising synthesis, comparison, and detail elements to facilitate operational reading, identify problematic cases, and support everyday interpretation of the service. EWT and route compliance values are classified into performance levels, defined as high (above 90% of the reference value), medium (80-90%), and low (below 80%), to enable comparison across typologies and depots. A typology or depot is flagged as critical when the proportion of high-level results falls below, or the proportion of low-level results exceeds, predefined thresholds, or when executed services remain below a 95% reference threshold for more than four days within a month. Color and position were used as primary graphical variables to encode performance levels and prioritize critical cases, helping users identify deviations at a glance.

In addition to the visual organisation of information, the system incorporated an interaction logic aimed at facilitating its use in supervision tasks. To this end, a coherent structure was maintained across screens, with global filters placed in constant positions and navigation that allowed users to move from a general overview to more detailed levels of analysis. In addition, resources such as comparative views, temporal breakdown options, and visual prioritisation mechanisms were incorporated, designed to speed up the identification of critical cases and promote a more operational reading of the available information. This demon-

strates how heterogeneous operational records can be systematically transformed into a structured and interpretable visual tool to support day-to-day service control.

3.1. Validation with expert users

The system was iteratively reviewed by six professionals involved in service supervision: three technical control operators, the managers responsible for street cleaning and waste collection, and the general director of the service. Compared with the original software, which was perceived as overly complex, the new system enabled faster, more visual, and easier-to-understand monitoring, supporting quicker and more detailed monthly reporting. Users also reported time savings and access to aggregated information that had previously only been available at a container-by-container level.

This analysis also confirmed the relevance of the conceptual review of EWT described above (Figure 1): the start of effective working time had previously been recorded differently across service typologies, preventing consistent comparisons. Homogenising this definition ensured indicator coherence and revealed previously undetected measurement inconsistencies in how certain services were recorded.

4. CONCLUSIONS

This paper presents a visual information system for monitoring and diagnosing Zaragoza's urban cleaning and waste collection service, showing that the main challenge is not data availability but transforming data into clear, comparable, and useful information for supervision.

Based on a service design approach structured through the Design Council's Framework for Innovation, the process identified user needs, clarified comparability issues, and developed a visual solution combining summary indicators, comparative views, temporal analysis, and interaction mechanisms for monitoring and operational diagnosis. Overall, the work shows how visual encoding and hierarchy can transform heterogeneous operational data into legible, decision-oriented dashboards for public services.

On the other hand, this work has limitations: the proposed system addresses the operational dimension of technical control, based on execution and activity records, but does not incorporate the observational perspective of on-street service condition obtained through inspections or audits. Prior literature shows that these two perspectives capture different dimensions of service quality and may diverge if used in isolation [4]. In addition, the visual design of the dashboard was validated through iterative feedback from expert users rather than a systematic usability evaluation, such as task-based testing or standardized metrics.

Overall, the proposal highlights the value of information design in improving the practical usefulness of operational data in complex public services, strengthening the capacity of local administrations to interpret service performance, detect critical situations, and support decision-making in urban services linked to environmental health.

REFERENCES

[1] Zhou, X., *et al.*: Review of global sanitation development. Environment International (2018). doi: 10.1016/j.envint.2018.07.047.

[2] Konteh, F.H.: Urban sanitation and health in the developing world: Reminiscing the nineteenth century industrial nations. Health Place 15(1), 69-78 (2009). doi: 10.1016/j.healthplace.2008.02.003.

[3] Giusti, L.: A review of waste management practices and their impact on human health. Waste Management (2009). doi: 10.1016/j.wasman.2009.03.028.

[4] López, I., Gutiérrez, V., Collantes, F., Gil, D., Revilla, R., Gil, J.L.: Developing an indicators plan and software for evaluating Street Cleanliness and Waste Collection Services. Journal of Urban Management 6(2), 66-79 (2017). doi: 10.1016/j.jum.2017.06.002.

[5] Matheus, R., Janssen, M., Maheshwari, D.: Data science empowering the public: Data-driven dashboards for transparent and accountable decision-making in smart cities. Government Information Quarterly 37(3), 101284 (2020). doi: 10.1016/j.giq.2018.01.006.

[6] Sevilla, A., Rodríguez, M.L., García-Maraver, Á., Zamorano, M.: An index to quantify street cleanliness: The case of Granada (Spain). Waste Management 33(5), 1037-1046 (2013). doi: 10.1016/j.wasman.2013.01.012.

[7] Munir, M.T., Li, B., Naqvi, M., Nizami, A.S.: Green loops and clean skies: Optimizing municipal solid waste management using data science for a circular economy. Environmental Research (2024). doi: 10.1016/j.envres.2023.117786.

[8] Cleveland, W.S., McGill, R.: Graphical perception: Theory, experimentation, and application to the development of graphical methods. Journal of the American Statistical Association 79(387), 531–554 (1984). doi: 10.1080/01621459.1984.10478080.

[9] Prata, J., Simões, C.L., Simoes, R.: Improvements to Municipal Solid Waste Collection Systems Using Real-Time Monitoring. Sustainability 17(4), 1405 (2025). doi: 10.3390/su17041405.

[10] Stephan, T., Hari Krishna, S.M., Lin, C.C., Sumesh, U., Agarwal, S., Kim, H.: ProWaste for proactive urban waste management using IoT and machine learning. Scientific Reports 15(1), 27790 (2025). doi: 10.1038/s41598-025-08452-x.

[11] Design Council: Design Council: Framework for Innovation. https://www.designcouncil.org.uk/resources/framework-for-innovation/, last accessed 2026/06/21.

Ecodesign using marine seafloor waste from the Cantabrian Coast

Carlota Alfaro-Ortega[a], Amaia Garrrido[a], Julen Ibarretxe[a, b], Maider Iturrondobeitia[a, b, *]

[a] Life Cycle Thinking Group, Department of Graphic Design and Engineering Projects, School of Engineering of Bilbao, Building 2-I, University of the Basque Country (EHU), Rafael Moreno Pitxitxi 3, 48013 Bilbao, Spain

[b] Research Centre for Experimental Marine Biology and Biotechnology (PiE-EHU), University of the Basque Country (EHU), Plentzia, Basque Country, Spain

* e-mail: maider.iturrondobeitia@ehu.eus

Abstract: Marine litter, particularly plastics, has emerged as a major global environmental challenge due to its persistence, widespread distribution, and inadequate end-of-life management. An estimated 4.8 to 12.7 million metric tons of plastic entered the ocean in 2010, representing up to 79% of all marine debris. High-density polymers and plastics that accumulate biological fouling tend to settle in deep-sea environments, where recent estimates indicate the presence of 3 to 11 million metric tons of plastic pollution. The distribution of this debris is influenced by hydrodynamic conditions, geomorphology, and human activities, with shallow coastal areas, especially those with intense fishing and tourism, showing the highest accumulation. Given that most marine litter consists of thermoplastics with high recovery potential, particularly abandoned, lost, or discarded fishing gear (ALDFG), Circular Economy strategies offer promising pathways for valorisation. Transforming marine litter into new materials can reduce pressure on ecosystems and fossil resources while simultaneously strengthening community engagement and promoting local responsibility when carried out at a local scale. In this context, the present study develops two kayak drain-plug prototypes using additive manufacturing (3D printing) and ecodesign through Siemens Solid Edge software. The prototypes are produced from recycled polyethylene (PE) and polypropylene (PP) fishing nets recovered from the seafloor of the Bay of Bizkaia, demonstrating a replicable model for aquatic sports associations interested in converting collected marine litter into functional products.

Keywords: *Marine plastic-litter, Seafloor debris, Circular Economy, 3D printing, Ecodesign, Bay of Bizkaia.*

1. INTRODUCTION

Marine litter is a major global environmental concern, with plastics representing the most abundant and persistent component. More than 310 million tons of plastics were produced worldwide in 2023, and this volume is projected to reach 710 million tons by 2040 [1] [2]. Their extensive use, combined with inadequate waste management systems, has led to the rapid accumulation of plastics, making them a pervasive pollutant across marine environments [3]. Due to their widespread distribution, durability, and low biodegradability, marine plastics significantly affect marine life, threatening biodiversity and the integrity of natural ecosystems [5].

Marine litter composed of high-density polymers, or materials that gain additional weight through biofouling, tends to sink and accumulate on the seafloor. It is estimated that between 3 and 11 million metric tons of plastic pollution currently reside on the ocean floor [7]. Its distribution is strongly influenced by hydrodynamic conditions, geomorphology, and human activities [8]. For instance, shallow coastal areas typically exhibit much higher concentrations of marine litter than the continental shelf [9], largely due to fishing and tourism activities that contribute substantially to seabed pollution. Over time, plastics deposited on the seafloor degrade into secondary microplastics, consisting of increasingly smaller fragments generated through the embrittlement and fragmentation of larger plastic items [10].

Marine litter is largely composed of thermoplastic materials with high recycling potential, including abandoned, lost, or otherwise discarded fishing gear (ALDFG). In line with Circular Economy principles, the conversion of waste into secondary raw materials offers an effective strategy to reduce pressure on marine ecosystems and fossil resources while diverting waste from landfill and incineration. Although several studies have investigated the recycling of marine plastics through additive manufacturing [4] [5], most have focused on polyamide-based materials or beach-collected litter. In contrast, the valorisation of ALDFG recovered directly from the seafloor remains largely unexplored, despite its significant contribution to persistent marine pollution.

Beyond the environmental benefits, locally driven initiatives that actively engage communities in addressing marine litter are essential for achieving long-term sustainability. Converting waste into valuable resources at the local scale not only reduces the carbon footprint associated with transport and external treatment processes, but also strengthens social participation, environmental awareness, and collective responsibility. In this context, waste is no longer perceived solely as an environmental burden, but as an opportunity to generate social, economic, and ecological value. This approach, consistent with the principle *Think global, act local,* empowers communities to take an active role in the restoration of their environment while fostering circular economy opportunities based on locally recovered materials.

The present study develops a kayak drain-plug prototype using additive manufacturing (3D printing) and ecodesign through Siemens Solid Edge CAD software. The prototype is produced from recycled polyethylene (PE) and polypropylene (PP) fishing nets recovered from the seafloor of the Bay of Bizkaia. Its novelty lies in combining: the recovery of seafloor ALDFG, a local circular workflow that transforms waste into a functional product within the same coastal region, and ecodesign principles integrated with additive manufacturing. This approach demonstrates the potential of locally recovered marine litter to generate value-added products while supporting environmental restoration and circular economy goals.

2. METHODOLOGY

2.1. Ecodesing methodology

In addition to the functional requirements, ecodesign principles guided the development of the component. The drain plug was conceived as a single-piece, mono-material product to facilitate end-of-life recycling and simplify manufacturing. The use of locally recovered recycled polymers reduces the environmental impacts associated with virgin raw material extraction and transportation. Furthermore, the design was optimized for additive manufacturing by avoiding unnecessary overhangs, reducing the need for support structures, and optimizing wall thicknesses to ensure proper extrusion of the recycled material.

In addition, the geometry was modelled parametrically to adjust dimensions and tolerances, incorporating a slight taper to improve fitting, an external flange to ensure sealing, and reinforcement zones that increase stiffness without significantly increasing material volume. Subsequently, to confirm that the proposed geometry was suitable for the selected materials, a structural validation was performed through finite element simulation. Two drain plug prototypes were manufactured using recycled thermoplastic materials: one produced from recycled polypropylene (PP) and the other from polyethylene (PE). To assess their structural performance under service conditions, the mechanical behaviour of both components was evaluated through finite element analysis (FEA). The simulations were carried out using Solid Edge (v. 226.00.01.004 x64) for geometric preparation and Femap (v. 2401.0.0) as the pre- and post-processing environment, employing the NX Nastran solver (v. 2312.0) for numerical computation. Both studies consisted of linear static analyses using a full tetrahedral mesh composed of approximately 15,117 elements and 25,362 nodes. The analysed component corresponded to a drain plug geometry with a total volume of 7541.814 mm^3. The polypropylene model included a density of 913 kg/m^3, Young's modulus of 1103 MPa, Poisson's ratio of 0.35, and a yield strength of 33.1 MPa. The polyethylene model presented a density of 886 kg/m^3, Young's modulus of 144.8 MPa, Poisson's ratio of 0.35, and a yield strength of 9.65 MPa. Thermal and mechanical properties provided by the material database were incorporated into the analyses. The loading conditions included hydrostatic pressure corresponding to a water density of 997 kg/m^3 together with an external force of 100 N applied along the vertical axis of the component. To reproduce the real operating conditions of the drain plug, two fixed constraints were applied to specific regions of the geometry, fully restricting all degrees of freedom and simulating the anchoring of the component during service conditions.

2.2. Material processing methodology

On 24 September 2024, a citizen-science initiative was carried out in the Port of Pasaia (Bay of Biscay), during which volunteer divers conducted a seafloor cleanup and recovered 79 kg of marine litter, 51.4% of which corresponded to plastic materials. The ALDFG collected during the activity were analysed using Attenuated Total Reflectance Fourier-Transform Infrared Spectroscopy (FTIR-ATR). The analyses were performed with a PerkinElmer Spectrum™ FTIR spectrometer operating at a resolution of 4.0 cm^{-1} and a wavelength range of 11,000-30 cm^{-1}, equipped with a Golden Gate ATR system with a ZnSe crystal. Sixteen scans were recorded within the spectral window of 4000-650 cm^{-1}. The results confirmed that some of the recovered fishing nets were composed of polyethylene (PE) and polypropylene (PP).

The recovered material was subsequently processed using a Polymix PX-MFC 90D mill operating at 3000 rpm. No prior cleaning treatment was applied in order to assess whether this step could be omitted from the processing workflow. The shredded material was then extruded using an SJSZ10/29 extruder (Wuhan Earon Plastic Machinery) at a feed rate of 30 Hz, an extrusion speed of 45 Hz, and a temperature of 180 °C to produce pellets. Finally, the prototype shown in Figure 1 was manufactured from the recycled pellets using additive manufacturing with a Tumaker Mini Pro Pellet 3D printer. The printing parameters included an inlet and outlet nozzle temperature of 195°C and 165°C, respectively, an extrusion speed of 0.4 mm/s, and a bed temperature of 95°C.

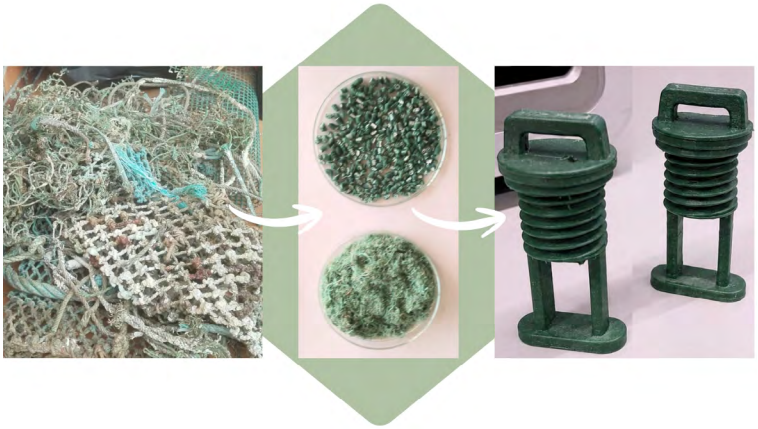


FIG. 1
Kayak drain-plug prototypes using additive manufacturing (3D printing)

3. RESULTS

Chemical characterization of the materials recovered from the seafloor was performed using Attenuated Total Reflectance Fourier Transform Infrared Spectroscopy (FTIR-ATR). As shown in Figure 2, the analysis confirmed that the recovered samples corresponded to polyethylene (PE) and polypropylene (PP) fishing nets.

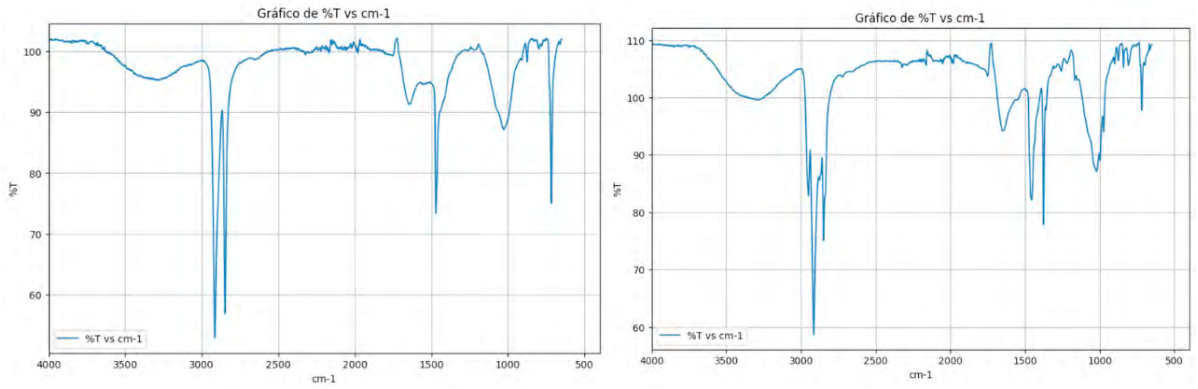


FIG. 2
Chemical analysis results of the polyethylene (PE) (first) and polypropylene (PP) (second) fishing nets

The finite element analyses demonstrated that both materials exhibited very low displacement values under the applied loading conditions. The polypropylene model showed the lowest deformation, with a maximum total displacement of 2.06×10^{-5} mm, whereas the polyethylene model reached a slightly higher displacement of 1.57×10^{-4} mm due to its lower elastic modulus. In both cases, the largest deformations were concentrated in the flexible central section of the drain plug, while the constrained regions remained practically undeformed (Figure 3). The Von Mises stress distributions revealed very low stress levels for both materials. The maximum stress obtained for polypropylene was approximately 0.0017 MPa, while polyethylene exhibited a similar maximum value of 0.0017 MPa. These stresses were significantly below the yield strengths of the materials, indicating safe structural behaviour under the simulated loading conditions. Stress concentrations were mainly located near the constrained areas of the geometry. The safety factor analysis confirmed the structural suitability of both drain plug designs. Polypropylene exhibited extremely high safety factors ranging from 1.95×10^{4} to 1.06×10^{11}, while polyethylene showed values between 5.69×10^{3} and 3.11×10^{10}. Since all safety factor values were well above the acceptable threshold of 1, both materials can be considered mechanically safe under the simulated service conditions.

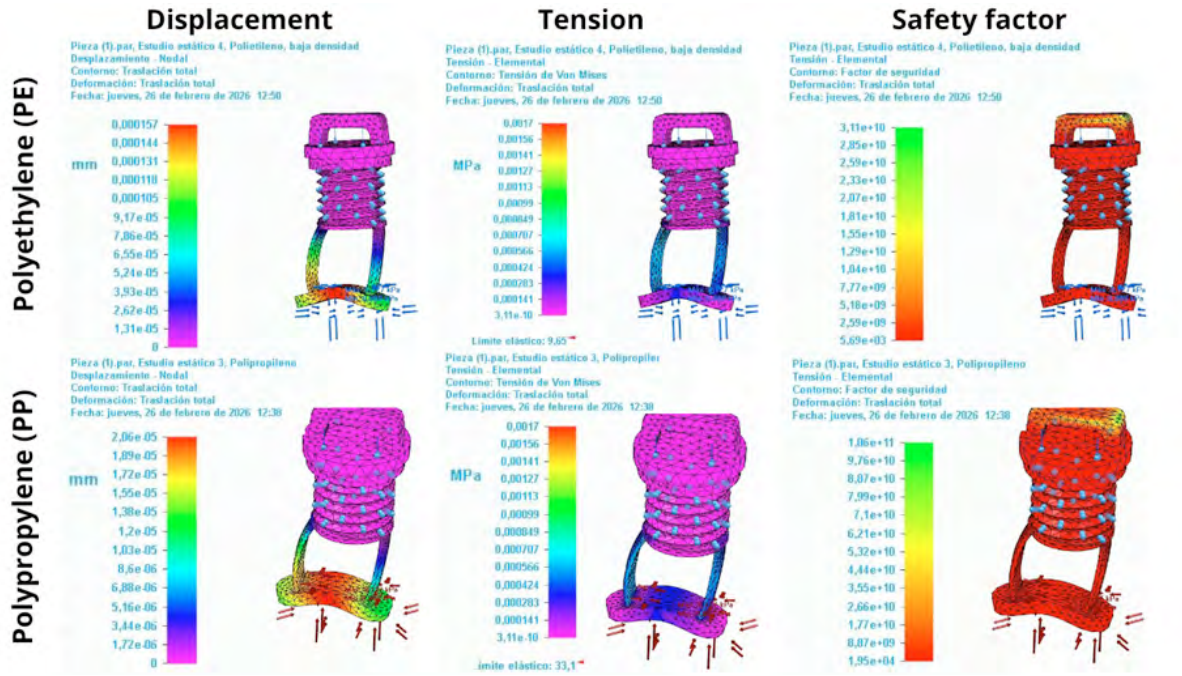


FIG. 3
Results of the simulation performed in Solid Edge for the polyethylene (PE) and polypropylene (PP) nets

4. CONCLUSIONS

This study demonstrates the potential of ecodesign and additive manufacturing as complementary tools for the valorisation of marine litter recovered from the seafloor. The drain plug was developed following ecodesign principles, including the use of locally recovered recycled materials, a mono-material single-piece configuration to facilitate end-of-life recy-

cling, and a geometry optimized to minimize material consumption and avoid support structures during manufacturing. These design decisions improve resource efficiency while supporting circular economy objectives.

Numerical simulations confirmed that both polypropylene (PP) and polyethylene (PE) are suitable materials for kayak drain-plug applications under normal operating conditions involving hydrostatic pressure and moderate mechanical loads. Both materials exhibited minimal displacements, very low stress levels, and high safety factors, indicating reliable structural performance. Polypropylene showed superior mechanical behaviour due to its lower deformation and higher elastic modulus, although polyethylene also performed safely despite its lower stiffness. Overall, the results demonstrate that polymers recovered from the seafloor can be successfully transformed into functional and mechanically reliable products.

Additive manufacturing (3D printing) represents a feasible and economically accessible solution for nautical sports organisations and training centres to produce small functional components and replacement parts on demand. The proposed workflow highlights the potential of locally recovered marine litter as a valuable secondary raw material, reducing dependence on virgin resources while creating local value. Moreover, the approach is potentially scalable to other coastal regions and may help reduce the environmental and economic costs associated with marine litter management. Future research should address long-term durability, environmental ageing, life-cycle performance, and the application of this methodology to other marine litter streams and nautical components.

REFERENCES

[1] Global Plastic Production, 2023. Statista. Annual Production of Plastics Worldwide from 1950 to 2023. https://www.statista.com/statistics/282732/global-producti on-of-plastics-since-1950/ (Accessed date: November 2024).

[2] Lau, W.W.Y., Shiran, Y., Bailey, R.M., Cook, E., Stuchtey, M.R., Koskella, J., Velis, C.A., Godfrey, L., Boucher, J., Murphy, M.B., Thompson, R.C., Jankowska, E., Castillo Castillo, A., *et al.*, 2020. Evaluating scenarios toward zero plastic pollution. Science 369 (6510), 1455–1461. https://doi.org/10.1126/science.aba9475. Author, F., Author, S.: Contribution title. In: CONFERENCE 2026, pp. 1-2. Publisher, Location (2026).

[3] Apete, L., Martin, O., Iacovidou, E. Fishing plastic waste: knowns and known unknowns. Mar. Pollut. Bull. 0 (accepted, in press), pp. 1 (2024).

[4] Farina, I., Singh, N., Colangelo, F., Luciano, R., Bonazzi, G., & Fraternali, F. High-performance nylon-6 sustainable filaments for additive manufacturing. Materials, 12(23), 3955. (2019).

[5] Russell, G. *The properties of glass fiber reinforced polypropylene filaments recycled from fishing gear* (2024).

[6] Bo, M., Bava, S., Canese, S., Angiolillo, M., Cattaneo-Vietti, R., Bavestrello, G.,. Fishing impact on deep Mediterranean rocky habitats as revealed by ROV investigation. Biol. Conserv. 171, 167-176 (2014).

[7] Zhu, X., Rochman, C. M., Hardesty, B. D., & Wilcox, C.. Plastics in the deep sea: A global estimate of the ocean floor reservoir. Deep-Sea Research Part I: Oceanographic Research Papers, 207, 104266 (2024).

[8] Alfaro-Ortega, C., Ibarretxe, J., Iturrondobeitia, M. Marine litter in the south-east of the Bay of Biscay: a review of current methods, standards, databases and challenges. Mar. Pollut. Bull. 213, 117632 (2025).

[9] MSFD Technical Subgroup on Marine Litter, Guidance on Monitoring of Marine Litter in European Seas. Luxembourg: Publications Office of the European Union, 2013.

[10] Yang, H., Chen, G. y Wang, J. Microplastics in the Marine Environment: Sources, Fates, Impacts and Microbial Degradation. Toxics, 9(2), 41 (2021).

An Interoperable Workflow for LiDAR-Based 3D Mesh Generation and Spatial Data Integration in Engineering Design

M. T. Yubero*, E. Bonet, Lluís Sanmiquel

Department of Mining, Industrial and ICT Engineering, Les Bases Avenue 61-73, 08242 Manresa, Spain

* e-mail: maria.teresa.yubero@upc.edu

Abstract: Three-dimensional representations of hydraulic infrastructure and surrounding terrain are increasingly used to support engineering design, inspection and spatial decision-making. However, practical workflows remain fragmented when mobile LiDAR meshes, point clouds, terrain models and GIS layers are processed in different software environments. This paper presents a reproducible workflow for transforming fragmented mobile LiDAR-derived local meshes into a georeferenced, multiresolution and interoperable engineering model. In comparison with conventional scan-to-mesh procedures focused mainly on visualization, the proposed contribution lies in the explicit connection between mobile acquisition, residual-based registration control, terrain integration and GIS-ready engineering reuse. The method combines iPad LiDAR and Polycam acquisition, Python-based three-dimensional similarity transformations, CloudCompare processing, official georeferenced terrain data and QGIS integration. The contribution is demonstrated in a dam and spillway case study. Thirty-three local GLB meshes, containing 2.72 million vertices and 4.55 million triangular faces, were assembled in ETRS89/UTM zone 31N using redundant homologous points. A quantitative registration-control step was introduced: 27 of 28 transformations were accepted, while one inconsistent transformation was rejected before integration. The final model combined a 1 m official terrain surface with LiDAR-derived infrastructure zones approximately thirteen times finer in linear point spacing. The results show improved traceability, quality control and reuse of spatial data within a Design for One Health perspective.

Keywords: *LiDAR, point cloud, 3D mesh, georeferencing, GIS, hydraulic infrastructure.*

1. INTRODUCTION

Accurate three-dimensional (3D) representations of infrastructure and territory have become essential in many engineering design tasks. Digital models derived from LiDAR, photogrammetry and geospatial data support inspection, documentation, design review and the interpretation of spatial constraints [1,2,3]. This is particularly relevant for hydraulic infrastructure, where structural elements, terrain morphology and water-related processes must be considered together.

Within a Design for One Health framework, infrastructure should not be analysed as an isolated object, but as part of a broader system involving built assets, natural environments and human activities. In this context, 3D models can provide a common geometric basis for linking inspection, territorial analysis, environmental constraints and subsequent engineering decisions.

Despite these opportunities, the operational use of 3D spatial data is still limited by interoperability and traceability issues. Mobile LiDAR captures, triangulated meshes, digital terrain models and GIS layers are often produced in different formats and software environments [4,5]. The main contribution of this work is therefore not the use of LiDAR or mesh reconstruction alone, but a documented workflow for assembling fragmented mobile LiDAR-derived meshes into a georeferenced, terrain-integrated and reusable engineering model. The workflow explicitly incorporates redundant control points, quantitative registration checks, multiresolution spatial modelling and GIS-compatible outputs.

Compared with established point-cloud workflows, which often report acquisition, registration, meshing or GIS visualization as separate tasks, the proposed approach addresses the practical transition from fragmented mobile LiDAR captures to an engineering-ready spatial product. Its specific contribution is the combination of four elements in a single traceable workflow: (i) local-to-UTM transformation of non-georeferenced mobile meshes, (ii) rejection of inconsistent registrations using residual indicators, (iii) multiresolution integration with an official terrain model, and (iv) export of functional surfaces and GIS-compatible products for subsequent engineering interpretation.

2. MATERIALS AND METHODS

The methodology was applied to a hydraulic infrastructure case study involving a dam-like structure, an existing lateral spillway and the surrounding valley terrain. The work was organized into six stages: spatial data acquisition, point-cloud and mesh preprocessing, registration and georeferencing, mesh generation, model optimization and export to interoperable products (Fig. 1). Open-source tools were prioritized in order to reduce dependency on proprietary formats and to make the process reproducible in common engineering environments [6,7].

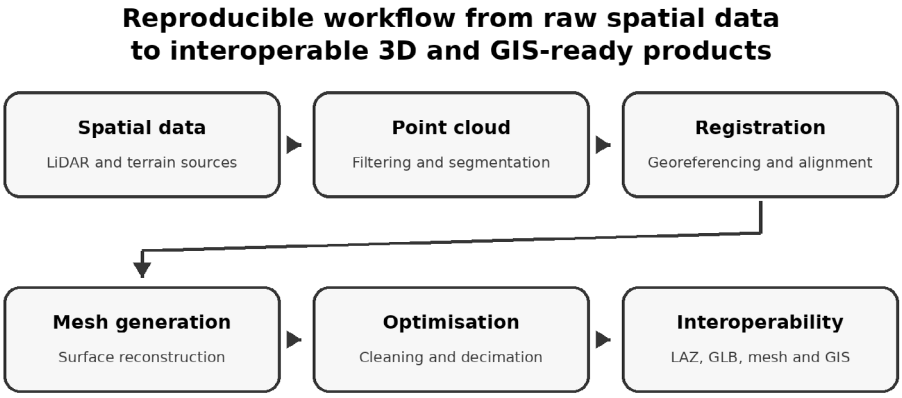


FIG. 1
Proposed workflow from raw spatial data to interoperable 3D and GIS-ready products

The detailed geometry of the infrastructure was acquired by mobile LiDAR using an iPad and processed with Polycam. Because the structure could not be captured reliably as a single model, the survey was divided into local pieces corresponding to the crest, benches, lateral zones, downstream face, spillway and immediate surroundings. This produced local GLB meshes that initially had their own arbitrary coordinate systems. The territorial context was obtained from the official ICGC 1 m surface model, downloaded as GeoTIFF with TFW georeferencing information, clipped to the area of interest and converted into a point-based representation for integration with the LiDAR-derived data.

Preprocessing combined visual inspection, cleaning of non-relevant fragments, manual segmentation of functional areas and local mesh editing in CloudCompare. The workflow did not rely on a single black-box automatic meshing algorithm: Polycam provided the initial local triangulated surfaces, while CloudCompare was used for cleaning, decimation and local editing. The objective was not to generate a closed volumetric object, but to obtain functional geometric surfaces suitable for design review, GIS overlay and later hydraulic interpretation. Surfaces were therefore separated according to their engineering role, including the reservoir context, dam body, downstream channel, wooded/contextual areas and lateral spillway.

Noise removal was performed using a combined geometric and engineering-consistency criterion. Isolated fragments, duplicated surfaces, vegetation artefacts and surfaces unrelated to the hydraulic structure were first removed by visual inspection and local editing. In steep or noisy areas, a local elevation-consistency check was then used: points or triangles showing abrupt vertical jumps were flagged when the surrounding 360-degree neighbourhood did not support the same change in elevation. Flagged elements were not removed automatically; they were inspected and classified either as real discontinuities, such as edges, lips or walls, or as acquisition artefacts to be removed before meshing.

Shadow zones and inaccessible areas were treated separately. Where the LiDAR could not capture continuous geometry, especially near quasi-vertical walls and between dam benches with large height differences, constrained interpolation surfaces were generated from reliable boundary points. This gap-filling step was used only to preserve geometric

continuity between observed areas. Interpolated surfaces were therefore considered auxiliary reconstructed geometry and were not used as independent validation data.

The registration stage used homologous points identified between each local mesh and the target UTM reference. For a local point P and its corresponding georeferenced point Q, a three-dimensional similarity transformation was computed as $Q = sRP + t + e$, where s is the scale factor, R the rotation matrix, t the translation vector and e the residual. Python scripts calculated the transformation parameters and exported a homogeneous 4×4 matrix, which was then applied to the corresponding mesh in CloudCompare. Redundant points were used whenever possible, not only to solve the transformation but also to calculate residuals and detect inconsistent alignments.

After registration, the LiDAR-derived infrastructure model and the official terrain-derived point cloud were integrated in ETRS89/UTM zone 31N. QGIS was used to manage the georeferenced terrain data, clipping limits and GIS-compatible overlays, while CloudCompare was used for point-cloud and mesh manipulation. Final products included ASC and XYZ point clouds for metric processing, STL functional surfaces for design and numerical-preprocessing tasks, and compact mesh representations suitable for visualization and communication.

3. RESULTS AND DISCUSSION

The resulting model assembled fragmented mobile LiDAR captures with a real georeferenced terrain base. Figure 2 shows the point-cloud context used during registration and spatial interpretation, while Figure 3 illustrates an optimized mesh component after cleaning and alignment. The workflow therefore moved beyond a visual reconstruction by introducing a common coordinate system and explicit quality-control checks.

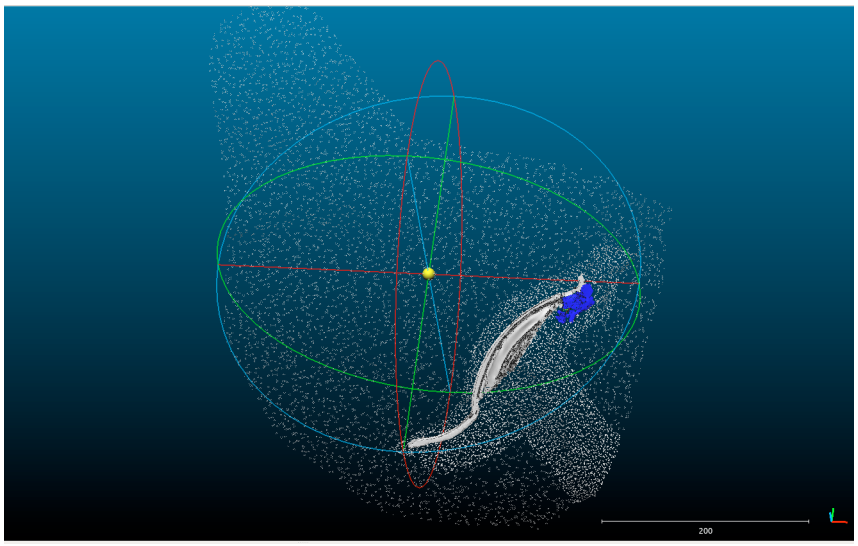


FIG. 2

Point-cloud context used for alignment, registration and spatial interpretation of the hydraulic infrastructure (high density points for dam and spillway (blue))

TABLE 1
Main quantitative indicators of the revised workflow and resulting digital model

Aspect	Indicator	Value
Mobile LiDAR input	Local GLB meshes	33
Mesh complexity	Vertices / triangular faces	2,720,560 / 4,549,363
Registration control	Transformations calculated / accepted	28 / 27
Reference points	Accepted local-UTM correspondences	136
Registration errors	Point-wise 3D residual distance	136 residuals; median 0.368 m; mean 0.436 m; P95 1.085 m
Residual errors / deviations	Component-wise absolute residuals	mean |dX|/|dY|/|dZ| = 0.220 / 0.294 / 0.096 m
RMSE	Per-transformation root mean square error	accepted 0.037-0.991 m; median 0.462 m; mean 0.455 m; rejected 3.458 m
Official terrain	Formal raster resolution	ICGC MDS 1 m GeoTIFF + TFW
Point spacing (not RMSE)	Exterior point model / dam LiDAR / spillway LiDAR	0.5009 / 0.03865 / 0.03730 m
Point models	Exterior / dam / spillway unique points	692,202 / 1,631,912 / 308,912
Hydraulic focus	Relative linear refinement	dam and spillway approx. 13x finer than exterior point model
Interoperable outputs	Main exchange formats	ASC, XYZ, STL and GLB
Preprocessing	Noise / shadow-zone treatment	Local elevation-consistency check and constrained interpolation

The quantitative indicators in Table 1 respond to two methodological requirements: documenting the complexity of the input data and evaluating the consistency of the registration stage. The dataset included 33 local GLB meshes with more than 2.7 million vertices and 4.5 million triangular faces. The registration process involved 28 transformation procedures and 136 accepted local-to-UTM point correspondences. One transformation was rejected because its residual error was clearly excessive. Registration errors were computed as point-wise 3D residual distances between transformed local control points and their target UTM coordinates. For the 136 accepted correspondences, the median residual distance was 0.368 m and the mean residual distance was 0.436 m, with a 95th percentile of 1.085 m. Residual deviations were also checked component-wise, with mean absolute deviations of 0.220 m, 0.294 m and 0.096 m in X, Y and Z, respectively. These residual errors and deviations were summarized at transformation level using RMSE, which allowed inconsistent alignments to be detected before integration into the global model. The point-spacing values reported in Table 1 describe the spatial density of the processed point models and should not be interpreted as registration RMSE: the exterior point model is derived from the official ICGC surface model, whereas the dam and spillway were represented by much denser LiDAR-derived data. The accepted transformations remained within sub-metric residuals, with the maximum accepted RMSE below 1 m.

The additional preprocessing criteria also clarify the role of engineering judgement in the workflow. The local elevation-consistency check helped distinguish real hydraulic or structural discontinuities from acquisition noise, while constrained interpolation was limited to shadow areas where direct LiDAR coverage was not feasible. This makes the workflow more reproducible than a purely visual cleaning process, but still avoids treating uncertain interpolated zones as measured geometry.

A second result is the multiresolution integration of the infrastructure with the surrounding terrain. The exterior terrain, derived from the official 1 m surface model, provides the territorial and hydraulic context, while the dam body and spillway retain a much denser LiDAR-based description. Point-density indicators were computed from unique XYZ coordinates using nearest-neighbour spacing. The median spacing was 0.5009 m in the exterior terrain, 0.03865 m in the dam block and 0.03730 m in the lateral spillway, corresponding to approximately thirteen times finer linear resolution in the hydraulically sensitive areas. This allocation of detail is more efficient than applying a uniform high-density model to the whole domain.

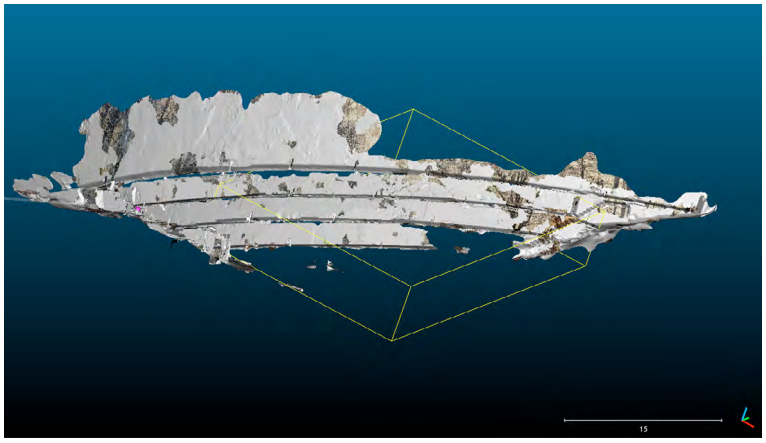


FIG. 3
Reconstructed and optimized 3D mesh of the hydraulic infrastructure (dam) after local cleaning and registration

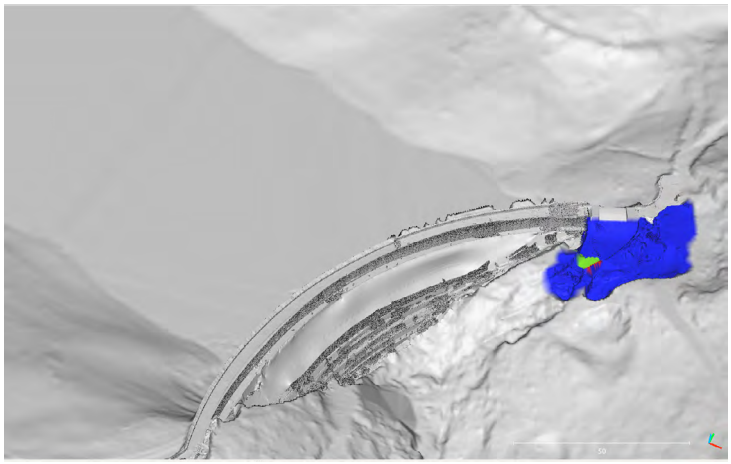


FIG. 4
Integration of the reconstructed infrastructure with the surrounding georeferenced terrain model

The GIS integration was achieved by maintaining all products in the same UTM framework and by exporting point-cloud and mesh products that could be used in both CloudCompare and QGIS. This enabled the reconstructed infrastructure to be interpreted together with terrain, access, environmental and hydrological layers. In practical engineering terms, the same geometric basis can support visualization, plan production, spatial overlay, preliminary hydraulic preprocessing and the definition of areas requiring further inspection.

The workflow also has limitations. Mobile LiDAR acquisition may generate occlusions, incomplete surfaces and local noise, especially in large outdoor infrastructures with vegetation and abrupt changes in slope. Mesh reconstruction and simplification therefore cannot be treated as a fully automatic process.

4. CONCLUSIONS

This paper presented a practical workflow for transforming fragmented mobile LiDAR-derived meshes into a georeferenced and interoperable digital model for hydraulic infrastructure design. The case study demonstrates that the main difficulty is not only mesh generation, but the controlled assembly of multiple local captures, their integration with official terrain data and their preparation for subsequent CAD, GIS and hydraulic-modelling uses.

The revised workflow provides quantitative evidence of this process. A total of 33 local GLB meshes were managed and integrated through Python-based similarity transformations and CloudCompare processing. Of the 28 transformation procedures calculated, 27 were accepted and one was rejected due to excessive residual error. The accepted transformations remained within sub-metric registration residuals, which provided a practical quality-control criterion for detecting inconsistent alignments before incorporating local meshes into the global model.

The results also show the usefulness of a multiresolution strategy. The official ICGC surface model provided the territorial context with a 1 m reference resolution, while the LiDAR-derived dam block and lateral spillway preserved a much finer point spacing, approximately thirteen times denser in linear resolution. This allocation of geometric detail is relevant in hydraulic infrastructure because the spillway, dam body and downstream flow path require higher geometric fidelity than the surrounding terrain.

Compared with a conventional qualitative point-cloud-to-mesh workflow, the proposed approach adds three specific contributions: a documented local-to-UTM registration procedure, quantitative registration control, and a functional separation of outputs for visualization, GIS integration and engineering use. The workflow therefore improves the traceability of geometric decisions made during the preparation of digital infrastructure models.

The main contribution is a practical and traceable bridge between mobile LiDAR acquisition, mesh processing, georeferenced terrain modelling and GIS-based engineering use, rather than a new isolated meshing algorithm. Future work should focus on automated uncertainty mapping, clearer mesh-quality indicators and stronger links between geometric simplification and simulation-oriented hydraulic models.

REFERENCES

[1] Brilakis, I., Fathi, H., Rashidi, A.: Progressive 3D reconstruction of infrastructure with videogrammetry. Automation in Construction 20(7), 884-895 (2011). DOI: 10.1016/j.autcon.2011.03.005

[2] Kim, S., Kim, S., Lee, D.-E.: 3D point cloud and BIM-based reconstruction for evaluation of project by as-planned and as-built. Remote Sensing 12(9), 1457 (2020). DOI: 10.3390/rs12091457

[3] Zhang, Y., Nie, G., Wang, D.: Structural health monitoring based on three-dimensional point cloud technology: A systematic review. Results in Engineering 27, 106552 (2025). DOI: 10.1016/j.rineng.2025.106552

[4] Rantanen, T., Julin, A., Virtanen, J.-P., Hyyppa, H., Vaaja, M.T.: Open geospatial data integration in game engine for urban digital twin applications. ISPRS International Journal of Geo-Information 12(8), 310 (2023). DOI: 10.3390/ijgi12080310

[5] Gura, D., Karamysheva, T.: Using CloudCompare software editing tools for processing a three-dimensional point cloud of an urban development site. ITM Web of Conferences 59, 02008 (2024). DOI: 10.1051/itmconf/20245902008

[6] CloudCompare: 3D point cloud and mesh processing software. Open Source Project, https://www.cloudcompare.org/, last accessed 2026/05/11.

[7] QGIS Development Team: QGIS Geographic Information System User Guide. Open Source Geospatial Foundation Project, https://docs.qgis.org/latest/en/docs/user_manual/index.html, last accessed 2026/05/11.

AI-Driven Tools Across the Product Design Lifecycle. A Systematic Review and Comparative Analysis for Industrial Design Engineering

Flors García-Malet, Fernando Fernández-Lapuente, Óscar Paseta-Martínez, David Ranz-Angulo*

Department of Design and Manufacture Engineering, University of Zaragoza (Spain), C/ María de Luna 3, 50018-Zaragoza

* e-mail: dranz@unizar.es

Abstract: The rapid integration of artificial intelligence (AI) into workflows transforms the Product Design Process, yet its systematic application remains highly fragmented. This study presents a structured, comparative review of AI-based Engineering Design Tools applied across the entire product lifecycle, from problem definition to documentation, evaluating their capabilities and core limitations. Mapping tools across five key stages reveals a heterogeneous landscape. AI demonstrates strong performance in early-stage activities, such as, market research and rendering using natural language and Generative Design models. However, significant limitations persist in conceptualisation and Design Automation, where integration with parametric CAD systems and physical validation remains constrained. No single tool provides comprehensive support, resulting in fragmented workflows requiring manual human expertise to ensure coherence. Rather than replacing designers, AI redefines their role towards supervision and validation. This work provides clear criteria for selecting and integrating Artificial Intelligence in Design, emphasising hybrid approaches that combine human expertise with AI capabilities.

Keywords: *Artificial Intelligence in Design, Product Design Process, Design Automation, Generative Design, Engineering Design Tools.*

1. INTRODUCTION

In recent years, Artificial Intelligence has transitioned from a distant technological promise into a central actor redefining creative workflows [1, 2]. At present, product design and industrial design engineering are integrating the use of various AI-driven tools, radically transforming the way projects are conceptualised, visualised, and developed. In fact, using articulated ecosystems of generative models, it is now possible to shorten the product development life cycle, successfully turning any abstract idea into interactive prototypes and minimum viable product concepts in unprecedented fractions of time [3].

The importance of incorporating these technologies into the design discipline lies in the tangible benefits they offer over conventional methodologies. AI tools can automate repetitive tasks and accelerate visualisation; furthermore, they foster innovation by acting as co-creative partners that stimulate divergent thinking and expand the boundaries of formal and functional exploration [4, 2]. Far from replacing the professional, various leaders in industrial design have demonstrated that AI elevates the process, allowing for more efficient design whilst preserving the designer's creativity and artisanal value, provided there is a thoughtful convergence and combination of traditional techniques and intelligent software [5].

Despite this remarkable potential and the significant increase in the quantity and capability of available applications, the integration of AI across all stages of product design remains fragmented and insufficiently characterised. As emerging literature points out, considerable barriers and dilemmas persist in the designer-AI interaction, particularly regarding the loss of direct control over precise iterations and the imbalance between algorithmic generation and human expertise [1]. Whilst the technology excels in early stages such as research or the generation of visual ideas, severe operational limitations persist in advanced phases, where the transfer of information to parametric CAD environments, industrialisation, and physical validation still present bottlenecks that depend strictly on human intervention [4]. Therefore, it can be concluded that there are insufficient standardised comparative criteria to assist designers in evaluating each tool for the specific stages of the process.

The objective of this study is to present a structured review and a comparative analysis of specific AI-based tools applied throughout all stages of the product design process, from the initial problem definition to the generation of technical documentation. The aim is to accurately identify their capabilities, operational limitations, and practical implications, thereby providing clear criteria to guide their informed adoption within industrial design engineering.

To achieve this objective, the article is structured as follows: firstly, the methodological approach is presented, which combines a literature review with the analysis of representative AI tools, both commercial and research based. Subsequently, a comparative framework is defined that classifies and evaluates the applied software across five fundamental design stages: (1) problem definition and specifications; (2) conceptualisation and selection; (3) technical and formal development; (4) industrialisation and commercial strategy; and (5) documentation generation. Next, the results of their comparison are detailed using variables such as functionality, level of automation, and interoperability. Finally, the findings are discussed from both a practical and a research perspective, emphasising the need to adopt hybrid design approaches that systematise seamless collaboration between human and artificial intelligence.

2. MATERIALS AND METHODS

The methodology was based on the identification, classification, and comparative evaluation of AI tools applicable to the industrial design cycle, divided into five phases: problem definition and PDSs, concept ideation and selection, formal and technical development, industrialization and commercial strategy, and documentation generation. To this end, publicly accessible tools with free availability between January and April 2026 were selected.

To standardize the study, a common prompt structure was used, based on prompt engineering principles and organized into five elements: context, instructions, conditions, limitations, output format [6]. This structure made it possible to standardize interactions, facilitate the comparison of results, and guide the generated responses precisely.

Based on the individual analysis of each tool according to its application in each phase, its main contributions and limitations were identified. This made it possible to assess their actual usefulness and to draw conclusions about the improvements they can introduce into the design process, as well as about those aspects in which the designer's intervention remains essential.

3. RESULTS

3.1. Problem definition and specifications

3.1.1. *Preliminary studies and requirements analysis*

AI	Traceability and real sources	Logical-technical reasoning	Qualitative analysis and empathy	Synthesis and visual modelling
Perplexity	✅	⚠	❌	❌
Claude	⚠	✅	✅	⚠
ChatGPT	⚠	⚠	⚠	✅
Synthetic Users	❌	❌	⚠	✅
Elicit	✅	⚠	❌	❌

FIG. 1
Comparative analysis of AI tools during the preliminary studies and requirements phase

In this initial phase, multiple AIs were combined to address various limitations. Perplexity and Elicit lead the documentary research; they guarantee hallucination-free access to regulations, patents, and real market data. For user understanding, Synthetic Users allow for agile early simulations, but Claude is unsurpassed when processing real interviews, standing out for its empathy and lack of bias. In terms of ideation and strategy, ChatGPT

is the most versatile at generating diagrams, archetypes, and SWOT matrices, although Claude dominates once again when hierarchically structuring complex logical trees. In conclusion, the success of this phase lies in combining the verifiable rigour of Perplexity, the deep analytical logic of Claude, and the generative and synthesising capacity of ChatGPT (Figure 1).

3.1.2. *Generation of the Product Design Specification (PDS)*

IA	Extended context window	Tabular structuring	Collaborative work	Sustained technical rigour
Claude	✅	✅	❌	✅
ChatGPT	⚠	✅	❌	⚠
Notion AI	❌	⚠	✅	❌

FIG. 2
Comparative analysis of AI tools during the Generation of the PDS phase

In the generation of the Product Design Specifications, Notion AI was used to centralize the team's notes and create verification checklists, while ChatGPT assisted in writing the initial drafts of the dimensional and operational specifications. However, Claude was employed for the drafting and compilation of the final technical document. In conclusion, Claude is the optimal AI for this final task. Its enormous context window allows it to simultaneously assimilate the market research, user analysis, functional requirements, and regulations, thereby generating a robust, coherent, and highly professional specifications document without losing the overarching thread (Figure 2).

3.2. Concept ideation and selection

3.2.1. *Ideation techniques, concept development and sketching*

In this phase, AI proved useful for accelerating conceptual exploration, increasing the number of alternatives, and streamlining the description and preliminary visualization of concepts. As shown in Figure 3, Gemini stood out in idea generation and visual support, while ChatGPT achieved better results in technical formulation, particularly in proposing alternatives and developing mechanisms or electronic components, as well as in the structured writing of concepts. Nevertheless, the definition of consistent concepts still depends on the designer's judgment, since it is the designer who selects, combines, and reformulates the generated proposals, while also contributing creativity for innovative solutions. In addition, the designer remains responsible for supervising and guiding the iterations involved in the sketching process.

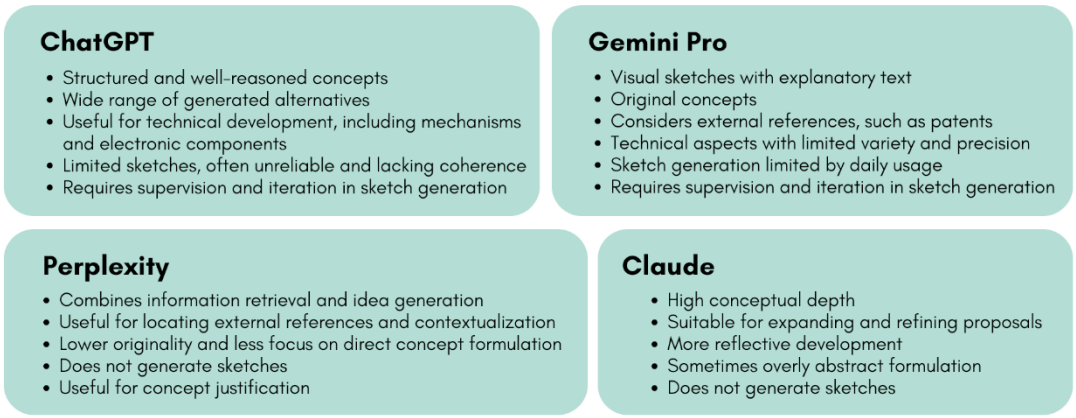


FIG. 3
Tools analysed in the ideation, concept development, and concept sketching phase

3.2.2. *Selection of the concept to be developed*

In this phase, the analysed tools did not rank the concepts in the same way, showing that concept selection cannot be understood as a stage with a single optimal solution. As shown in Figure 4, their main usefulness does not lie in delegating the final decision to AI, but rather in supporting the structuring of criteria, organizing comparisons, and identifying the strengths, weaknesses, and possible improvements of each alternative. Consequently, the final choice still rests with the designer, who interprets the results according to the project context and objectives. Among the evaluated tools, Claude stood out as the most suitable option due to the clarity of its structure, its visual quality, and its writing capabilities.

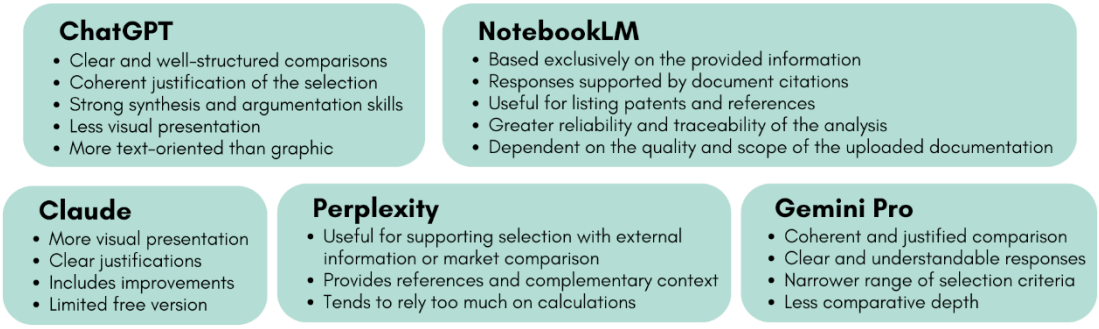


FIG. 4
Tools analysed in the concept selection phase

3.3. Formal and technical development

In this phase, the analysed tools proved useful mainly for generating initial volumes and visualizing concepts quickly, but they still showed significant limitations in shape fidelity, geometric precision, editability, and export options, making their integration into a complete technical CAD workflow unfeasible. As shown in Figure 5, the matrix uses a colour code to distinguish functions available for free (**green**), functions that require payment (**orange**), and un-

available functions (**red**). Based on this comparison, most of the evaluated AIs provide effective support in the early stages of formal exploration, but they still cannot reliably replace precise technical modelling, controlled geometric editing, or a fully operative final 3D development.

AI	Text-to-CAD	Image-to-CAD	Multiview	Part segmentation	Model download	Shape fidelity
Hunyuan 3D	✗	✓	✓	✗	✓	✗
Hitem 3D	✗	✓	✓	✓	✓	✗
Tripo AI	✓	✓	⚠	⚠	⚠	✓
Meshy	✓	✓	✗	✗	⚠	✗
Chat GPT	✓	✓	✗	✓	✓	✗
Rodin	✗	✓	✗	✓	⚠	✓

FIG. 5
Tools analysed in the formal and technical development phase

3.4. Industrialisation and commercial strategy

During the industrialisation and commercialisation phase, a multifaceted AI approach is essential. Autodesk Fusion 360 drives technical viability through topological optimisation, whilst Microsoft Copilot excels in financial modelling by structuring production costs natively within spreadsheets. For supply chain management, Perplexity reliably sources B2B manufacturers and material datasheets. To secure market penetration, ChatGPT effectively drafts commercial strategies, supplier contracts, and persuasive copy. Finally, NanoBanana Pro produces high-impact photorealistic visualisations for promotional campaigns prior to physical manufacturing. This strategic ecosystem minimises manual labour, demonstrating that whilst no single tool covers the entire late-stage spectrum, their combined capabilities seamlessly bridge the gap between engineering and market launch (Figure 6).

AI	Technical and financial modelling	Supply chain and sourcing	Strategy and copywriting	Visual asset generation
Autodesk Fusion 360	✓	✗	✗	⚠
Microsoft Copilot	✓	⚠	⚠	⚠
Perplexity	⚠	✓	⚠	✗
ChatGPT	⚠	⚠	✓	⚠
NanoBanana Pro	✗	✗	⚠	✓

FIG. 6
Comparative of AI tools during the industrialisation and commercial strategy phase

3.5. Document´s generation

During the final documentation phase, the workflow must seamlessly bridge extensive technical writing with precise graphical planimetry. Notion AI serves as the collaborative hub, effectively organising scattered engineering notes and decisions. For the textual narrative, Claude provides unparalleled capability in drafting cohesive and rigorous technical reports, whilst ChatGPT supports this by structuring indices and programming automation scripts for CAD title blocks. On the graphical front, Autodesk Fusion 360 accelerates the extraction of 2D views and component detailing directly from 3D assemblies, supported by BricsCAD AI for pattern recognition and block standardisation. However, whilst these integrated tools significantly reduce manual labour, precise dimensioning and tolerancing still require indispensable human validation (Figure 7).

AI	Technical narrative and synthesis	Workspace and data organisation	Graphical planimetry views	Automation and standardisation
Claude	✅	⚠	❌	⚠
Notion AI	⚠	✅	❌	⚠
ChatGPT	✅	⚠	❌	✅
Autodesk Fusion 360	❌	⚠	✅	✅
BricsCAD AI	❌	⚠	✅	⚠

FIG. 7
Comparative of AI tools during the document's generation phase

4. CONCLUSIONS

This study results show that AI provides especially useful support in design phases such as preliminary analysis, market research, ideation, writing, and preliminary visualization. However, its performance depends on the tool used. The main limitations are found in the formal and technical development phase, where these tools still cannot be effectively integrated into CAD workflows, as well as in industrialization and technical documentation, where expert validation, regulatory accuracy, and detailed human control are still required.

In conclusion, the study confirms that AI does not replace the designer but rather acts as a support tool. A hybrid approach therefore appears to be the most appropriate, with final interpretation, selection, and validation continuing to depend on human judgment.

DATA OPENLY AVAILABLE

The standardized prompts used in this study have been compiled in the github repository to facilitate the transparency, traceability and reproducibility of the proposed methodology. The re-

pository provides access to the prompts used throughout the different stages of the design process. https://github.com/opaseta/Input-prompts-for-AI/blob/main/Prompts.docx

REFERENCES

[1] Sattele, V.: CreAI: visualizar los procesos co-creativos de diseño industrial con IA. Economía Creativa 20, (2024), https://doi.org/10.46840/ec.2024.20.a5

[2] INAIR homepage, https://inairspace.com/blogs/learn-with-inair/benefits-of-ai-design-tools-over-traditional-methods-in-modern-creative-workflows, last accessed 2026/02/07.

[3] Medium homepage, https://medium.com/design-ibm/cracking-ai-toolkit-for-product-design-idea-to-mvp-in-under-1-hour-0eab8e6edac7, John, M. A., last accessed 2026/02/07.

[4] Wang, N., Kim, H., Peng J., Wang, J.: Exploring creativity in human-AI co-creation: a comparative study across design experience. Frontiers in Computer Science 7, (2025), https://doi.org/10.3389/fcomp.2025.1672735

[5] De zeen homepage, https://www.dezeen.com/2025/04/17/blond-harrys-installation-ai-design/, Lindsay, C., last accessed 2026/04/17.

[6] Aprender 21 homepage, https://www.aprender21.com/blog/estructura-de-un-prompt-perfecto, Peiro, E., last accessed 2026/01/03.

From drawn geometry to simulated geometry: a geometric abstraction model in the bim-bem workflow for energy simulation

Ruth Fernández García[a, *], Rafael Rodríguez Galindo Diez[b], Diego José Guerrero Miguel[c], María Belén Prendes Gero[c], Marta Menéndez Fernández[d]

[a] University of Oviedo, School of Mining.
Campus de Mieres C/ Gonzalo Gutiérrez Qurós s/n. C.P: 33600, Mieres. Spain.

[b] University of León, Department of Mining Technology Surveying and Structures.
Campus de Vegazana, s/n. León. Spain.

[c] University of Oviedo, Construction and Manufacturing Engineering Department,
C/ Pedro Puig Adam, Edificio Departamental Oeste 6, C.P: 33204, Gijón (Asturias). Spain.

[d] University of León, Department of Mining Tecnology Surveying and Structures.
Campus de Vegazana, s/n. León. Spain.

* e-mail: UO310274@uniovi.es

Abstract: Energy simulation of buildings is widely used to support decision-making in architectural and engineering design. However, the persistent discrepancy between the predicted and actual energy performance of buildings, known as the "energy performance Gap" (EPG), remains not fully understood. Whilst previous studies have focused primarily on operating conditions, occupant behaviour and uncertainties in input data, less attention has been paid to the modelling process itself, particularly geometric transformations. This article examines the role of geometric abstraction in BIM-BEM workflows and proposes a conceptual framework based on geometric abstraction levels (GAL). A conceptual case study based on a representative single-family residential building is used to analyse the effects of successive levels of abstraction under controlled modelling conditions. Key geometric descriptors, such as the envelope area, volume, compactness and orientation, are compared throughout the abstraction process. The results indicate that geometric deviations are not random artefacts of simplification, but rather structured consequences of modelling decisions. The proposed framework contributes to a better understanding of the relationship between geometric representation and simulation modelling, providing a basis for future research into geometric abstraction and its implications for simulation reliability.

Keywords: *Geometric abstraction, BIM-BEM, Energy Simulation, Geometric Modelling, Deviation in Energy Performance.*

1. INTRODUCTION

Building energy simulation has established itself as a essential tool in architectural and engineering design, supporting decision-making aimed at improving energy efficiency, reducing environmental impact and complying with increasingly stringent regulatory frameworks. However, despite the significant advances made in simulation tools, there remains a substantial discrepancy between the predicted energy performance and the actual energy performance of buildings. This phenomenon, known as the Energy Performance Gap (EPG), remains not fully understood [1,2].

Traditionally, this discrepancy has been attributed to factors relating to user behaviour, operating conditions or uncertainties associated with the input parameters and the simulation models themselves [3,4,5]. Consequently, most studies have focused on the stochastic variability of the system, paying less attention to the deterministic processes involved in the construction and preparation of the models.

Among these processes, geometric modelling has received limited attention as a potential source of deviation. In current BIM-BEM workflows, the building's geometry undergoes a progressive transformation from detailed architectural models developed in BIM (Building information Modeling) environments to simplified representations adapted to the requirements of BEM (Building Energy Modeling) energy models [6,7]. This transformation in not merely a reduction in the level of geometric detail, but a reinterpretation of the original representation that con after relevant parameters such as the envelope area, the built volume, compactness or orientation.

Various studies have shown that geometric simplifications can produce appreciable variations in simulation results, even when the modifications introduced appear relatively minor [9]. However, these simplifications have typically been addressed from an empirical perspective, without explicitly structuring the transformation process or analysing geometric abstraction as a systematic phenomenon within BIM-BEM workflows.

In this context, this paper analyses geometric abstraction as a modelling process that warrants explicit consideration within the construction of energy models. To this end, a conceptual framework based on Geometric Abstraction Levels (GAL) is proposed, the aim of which to characterize the progressive evolution on geometry throughout the BIM-BEM workflow. This approach provides a structured basis for analysing geometric transformations for the modelling process for energy simulation.

2. GEOMETRIC ABSTRACTION IN THE BIM-BEM WORKFLOW

The transition from BIM models to building energy modelling (BEM) involves adapting highly detailed architectural representations into simplified, parameterised structures that are compatible with the requirements of simulation tools, a process that has been extensively documented in the literature [6,7]. This transformation includes operations such as geometric simplification, the definition of thermal zones, model discretisation and the redefinition of energy parameters, and constitutes a critical stage within the BIM-BEM workflow, in which both technological aspects and criteria relating to the structuring of model information play a significant role [8].

In this context, geometric abstraction can be understood as a set of transformations through which the original architectural geometry is translated into a representation suitable for use in simulation models. These transformations are not limited to a reduction in the level of detail, but involve processes of simplification, aggregation and interpretation that may after relevant properties of the building, such as the surface are of the building envelope, volumetric relationships, compactness or orientation.

In order to structure the process, a conceptual framework based on Geometric Abstraction Levels (GAL) is proposed, which sequentially describes the evolution of the geometry throughout the BIM-BEM workflow:

— GAL_0: Detailed architectural model (BIM), characterised by high geometric fidelity.
— GAL_1: Simplified volumetric representation, focusing on the building´s overall form.
— GAL_2: Definition of thermal zones and building envelope adapted to the requirements of energy modelling.
— GAL_3: BEM model ready for simulation.

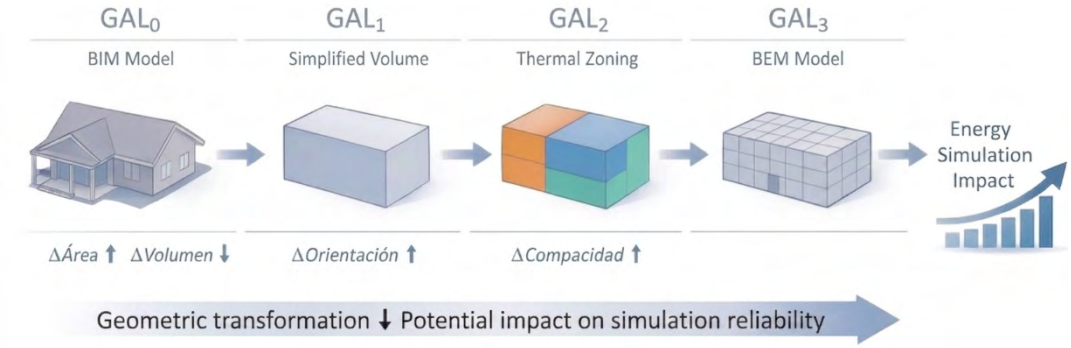


FIG. 1
Summarises the proposed geometric abstraction process, showing the evolution of the building representation across the different GAL levels and its potential implications for the energy simulation modelling process

Each transition between these levels involves specific geometric operations that may introduce differences from the original representation. However, these transformations tend to remain implicit in the modelling process and are rarely described or documented systematically.

Unlike traditional approaches, which regard simplification as a necessary technical adjustment for simulation, the proposed conceptual basis for future studies aimed at its evaluation and characterisation.

3. METHODOLOGY

To analyse the implications of geometric abstraction in modelling for energy simulation. an approach is adopted that involves comparing different geometric representations generated from the same initial geometry and subjected to varying levels of abstraction.

The study is based on a conceptual case study of a representative single-family dwelling, selected for its widespread use in research relating to residential energy simulation and for its suitability for the controlled application of geometric transformations within BIM-BEM workflows.

The initial geometry is developed in a BIM environment using Autodesk Revit. From this model successive representations corresponding to the different defined levels of geometric abstraction (GAL_0-GAL_3) (Table 1) are generated, applying systematic criteria of simplification, aggregation and geometric reorganization. This procedure allows for the controlled reproduction of the transformations typically present in the transition processes from BIM to BEM.

TABLE 1

Changes in geometric descriptors across the GAL levels of abstraction.
The values represent relative changes compared with the reference model (GAL_0)

Nivel	Description
GAL_0	Detailed BIM model with high geometric fidelity.
GAL_1	Simplified volumetric representation focusing on the building´s overall shape.
GAL_2	Definition of thermal zones and building envelope adapted to energy criteria.
GAL_3	BEM model ready for simulation.

In order to insolate the effect of geometric abstraction, the remaining variables in the model are kept constant throughout the entire process. In particular, material properties, climatic conditions and operational assumptions are considered invariant, so that the observed differences can be attributed exclusively to changes in the geometric representation.

To characterise the transformations introduced, a set of relevant geometric descriptors is analysed. The main parameters considered and their evaluation across the levels of abstraction are summarised in Table 2:

TABLE 2

Evolution of geometric descriptors across the GAL levels of abstraction.
The values reflect relative changes compared with the initial architectural model (GAL_0)

Descriptor	GAL_0	GAL_1	GAL_2	GAL_3
Enveloping surface	0%	–4%	–7%	–10%
Volume	0%	–2%	–3%	–5%
Compactness	0%	+3%	+6%	+9%
Orientation	0°	+2°	+5°	+8°

The values set out in Table 2 are intended to illustrate the proposed conceptual framework and to represent geometric variations typically associated with the different levels of abstraction. They should no be interpreted as statistical averages or as generalizable results; consequently, no measures of dispersion or confidence intervals are included.

—Envelope surface area, as an indicator of heat transfer potential.

—Enclosed volume, representative of the building´s special capacity.

—Surface-to-volume ratio (compactness), as a summary descriptor of the geometric configuration.

—Orientation of the envelope elements, relating to solar exposure and heat transfer.

Comparing these descriptors across different levels of abstraction makes it possible to identify and characterise both the magnitude and the nature of the geometric deviations introduced during the modelling process.

The methodological approach adopted allows for the analysis of geometric transformations in a controlled and reproducible manner, whilst maintaining the conceptual mature of the proposed framework. In this way, a structured basis is established for studying the evolution of geometry within the BIM-BEM workflow and its potential implications for the modelling process for energy simulation.

4. RESULTS AND DISCUSSION

The comparison between the different levels of abstraction, illustrated in Figure 2, reveals a progressive and consistent transformation of the main geometric descriptors under consideration. Generally speaking, the surface area of the envelope and the volume tend to decrease as the level of abstraction increases, whilst compactness shows an upward trend as a result of the processes of simplification geometric aggregation.

The magnitude of these variations is not uniform, but increases progressively across the different GAL levels, suggesting the accumulation of geometric effects during the transformation process. This behaviour highlights the existence of systemic patterns associated with the evolution of the geometry, beyond the specific modifications resulting from simplification of the model.

The results obtained indicate that the differences observed cannot be interpreted as random variations, but rather as the consequence of modelling decisions implicit in the BIM-BEM process. From this perspective, geometric abstraction con be considered a relevant aspect in the construction of models intended for energy simulation.

This approach partially shifts the focus of attention from uncertainties associated exclusively generation and transformation.

Consequently, geometric representation ceases to be a mere becomes an element that warrants explicit consideration within the BIM-BEM modelling workflows.

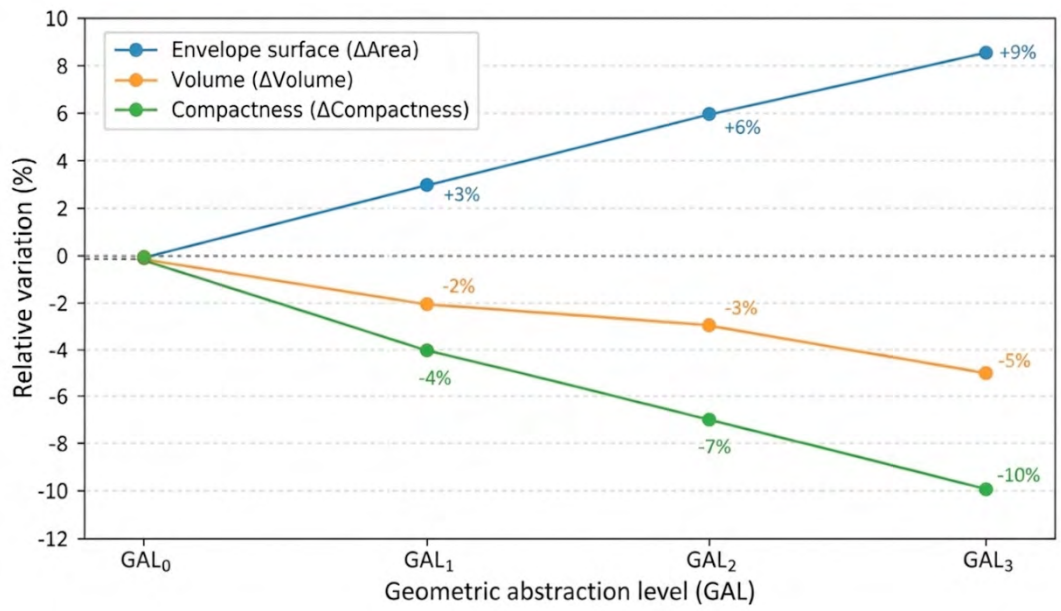


FIG. 2

Evaluation of geometric descriptors across the GAL abstraction levels. The relative variations in envelope area, volume and compactness are shown in relation to the reference model (GAL_0)

5. CONCLUSIONS

This paper proposes a conceptual framework for analysing geometric abstraction in BIM-BEM workflows through the definition of Geometric Abstraction Levels (GAL). The study carried out shows that the transformation of geometry is not a neutral process, but rather involves significant changes to various geometric descriptors relevant to the representation of the building.

The explicitly structuring of these transformations allows the evolution of geometry to be approached as a process capable of analysis and characterization, providing a complementary perspective to traditional approaches focused exclusively on energy parameters or operating conditions.

The results obtained suggest that geometric abstraction is a significant aspect in the construction of models intended for energy simulation and that its explicit consideration can contribute to a better understanding of the modelling processes associated with BIM-BEM workflows.

Finally, the proposed conceptual framework establishes a working basis for future research aimed at studying geometric transformations and their influence on the consistency and reliability of energy models.

REFERENCES

[1] de Wilde, P.: The gap between predicted and measured energy performance of buildings: A framework for investigation. Automation in Construction 41, 40-49 (2014). https://doi.org/10.1016/j.autcon.2014.02.009.

[2] Zheng, Z., Zhou, J., Zhu, J., Yang, Y., Xu, F., Liu, H.: Review of the building energy performance gap from simulation and building lifecycle perspectives: Magnitude, causes and solutions. Developments in the Built Environment 17, 100345 (2024). https://doi.org/10.1016/j.dibe.2024.100345.

[3] Coakley, D., Raftery, P., Keane, M.: A review of methods to match building energy simulation models to measured data. Renewable and Sustainable Energy Reviews 37, 123-141 (2014). https://doi.org/10.1016/j.rser.2014.05.007.

[4] Tian, W., Heo, Y., de Wilde, P., Li, Z., Yan, D., Park, C.S., Feng, X., Augenbroe, G.: A review of uncertainty analysis in building energy assessment. Renewable and Sustainable Energy Reviews 93, 285-301 (2018). https://doi.org/10.1016/j.rser.2018.05.029.

[5] Heo, Y., Choudhary, R., Augenbroe, G.A.: Calibration of building energy models for retrofit analysis under uncertainty. Energy and Buildings 47, 550-560 (2012). https://doi.org/10.1016/j.enbuild.2011.12.029.

[6] Gao, H., Koch, C., Wu, Y.: Building information modelling based building energy modelling: A review. Applied Energy 238, 320-343 (2019). https://doi.org/10.1016/j.apenergy.2019.01.032.

[7] Ciccozzi, A., de Rubeis, T., Paoletti, D., Ambrosini, D.: BIM to BEM for building energy analysis: A review of interoperability strategies. Energies 16(23), 7845 (2023). https://doi.org/10.3390/en16237845.

[8] Raji, B., Tenpierik, M., van den Dobbelsteen, A.: The impact of model simplifications on energy simulation results. Energy and Buildings 163, 308-321 (2018). https://doi.org/10.1016/j.enbuild.2018.03.046.

[9] Farzaneh, A., Monfet, D., Forgues, D.: Review of using building information modeling for building energy modeling during the design process. Journal of Building Engineering 23, 127-135 (2019). https://doi.org/10.1016/j.jobe.2019.01.029.

Development of an interactive book for active learning in Engineering Graphics education

Sandra Munera, Nereida Tarazona, Francisco Albert, Nuria Aleixos, Alejandro Rodríguez-Ortega*

Departamento de Ingeniería Gráfica, Universitat Politècnica de València (UPV), Camino de Vera s/n, 46022, Valencia (Spain)

* e-mail: alrodor@upv.es

Abstract: This paper describes the design and development of an interactive digital resource structured as a solved exercise book focused on technical drawing standardisation in Engineering Graphics, which also supports the three-dimensional modelling of the proposed parts. The resource integrates standardised technical drawings, manipulable 3D models, recommended practices, and multiple annotated solutions for each exercise, allowing students to approach each problem from both a representational and a modelling perspective. The resource is designed to address common learning difficulties in Engineering Graphics, particularly those related to spatial visualisation and the interpretation and generation of technical drawings. Its main objective is to strengthen students' understanding of the relationship between two-dimensional representations and their corresponding three-dimensional models, both when analysing drawings and when constructing them from geometric information. Each exercise includes different commented solutions, enabling learners to compare distinct valid approaches and reinforcing the application of standardisation criteria. The incorporation of interactive 3D models enhances comprehension by allowing users to directly explore geometry and spatial relationships. By combining solved exercises with interactive visualisation, the resource promotes an active and bidirectional learning process between 2D and 3D environments. It is conceived as a complementary teaching tool adaptable to different learning paces. Future work will focus on its implementation in educational settings and on evaluating its impact on student learning, engagement, and skill development through empirical studies.

Keywords: *Standardization, Modelling, Engineering education, Interactive Learning Resource, Student Engagement.*

1. INTRODUCTION

Engineering Graphics is a fundamental component of engineering education, as it supports the development of spatial reasoning, technical communication skills, and the ability to interpret and produce standardised representations of engineering components. Mastery of technical drawing conventions and three-dimensional visualisation is essential for future engineers, as these skills underpin design and manufacturing processes [1, 2]. However, many students experience difficulties when establishing clear relationships between three-dimensional objects and their corresponding two-dimensional representations, especially when learning relies on static materials [2].

Over the past decade, engineering education has incorporated various interactive digital resources, such as virtual laboratories, CAD-based environments, AR/VR systems, and web-based simulations [3]. These tools foster active learning through visualisation, iterative design, and immediate feedback, enhancing both engagement and learning outcomes. In Engineering Graphics, CAD and spatial visualisation tools are particularly relevant, as they support 3D modelling and improve spatial cognition.

Compared to traditional approaches characterised by passive learning and limited practical exposure [4], interactive methodologies promote participation and experimentation, leading to more effective learning environments [5]. Their benefits have been demonstrated across domains such as mechanics, manufacturing, and industrial engineering [6], as well as in areas like automatic control and engineering drawing [7,8]. Their effectiveness is closely linked to their interactive nature, especially in mobile and immersive contexts [9]. For instance, Weis *et al.* [10] reported improved self-directed learning using a web-based application with integrated 3D visualisation.

However, advanced systems, particularly AR/VR and web-based applications, often require specialised skills, dedicated hardware, and internet access, limiting their accessibility [3]. In this context, interactive PDFs offer a low-cost, platform-independent, and offline alternative. They are easy to develop and distribute while still supporting features such as navigation, embedded media, and 3D visualisation, making them a scalable and effective educational solution.

In this context, interactive digital resources have gained relevance in Engineering Graphics due to their potential to enhance engagement and improve conceptual understanding. In particular, the use of manipulable 3D models facilitates the comprehension of spatial relationships and graphical concepts.

This paper presents the development of an interactive digital resource designed to support learning in Engineering Graphics, with a focus on technical drawing standardisation and three-dimensional modelling. The resource is conceived as a solved exercise book that integrates manipulable 3D models, standardised drawings, and annotated alternative solutions. Its main objective is to facilitate a bidirectional learning process between spatial visualisation and normative representation, while promoting deeper understanding and student engagement.

2. DESCRIPTION OF THE RESOURCE

The developed resource consists of an interactive digital book designed to support learning in Engineering Graphics courses. It integrates theoretical explanations and practical exercises within a unified digital environment, combining manipulable three dimensional models, standardised two dimensional technical drawings, and explanatory comments associated with each activity.,

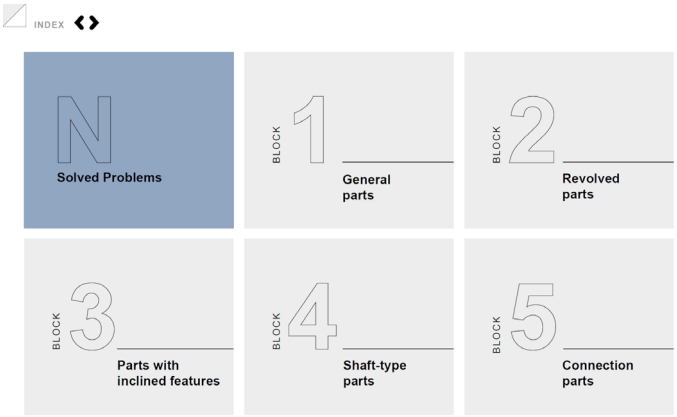


FIG. 1
Classification of the different content blocks in the interactive resource

The overall structure of the resource is organised into several thematic blocks according to the typology of the parts considered. Specifically, the content is divided into generic parts, parts with inclined faces, revolution parts, shaft type components, and connection elements. An overview of these blocks is presented in Figure 1, which illustrates both the classification criteria and the scope of each category. This organisation enables a progressive approach, allowing students to engage with increasing levels of geometric and representational complexity.

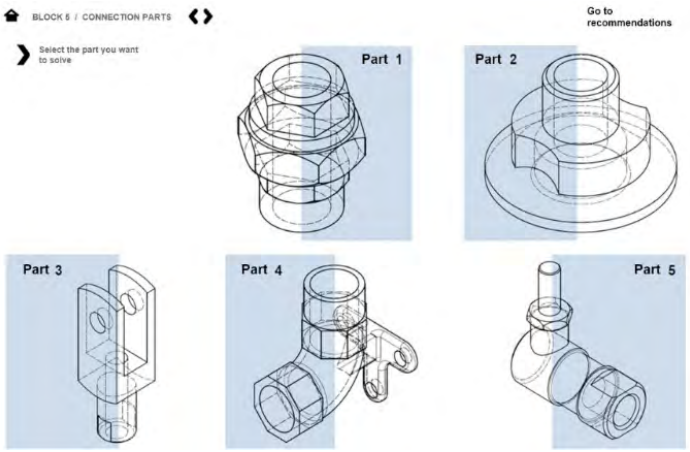


FIG. 2
Example of a set of parts included within a specific content block

To exemplify the content of each block, Figure 2 presents a representative set of parts corresponding to a specific category. These examples reflect the type of exercises included in the resource and highlight the progression in difficulty within each block. Additionally, each section incorporates specific recommendations and best practices related to the correct application of technical drawing standards, as illustrated in Figure 3. These guidelines are intended to support students not only in learning how to represent a part, but also in understanding the rationale behind different representational decisions.

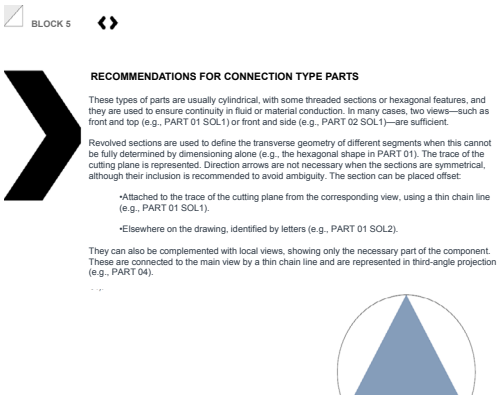


FIG. 3
Example of block-specific recommendations and best practices provided to guide students in the correct application of technical drawing standards

A key feature of the resource is illustrated in Figures 4 and 5, where an individual exercise is presented in detail. For each part, the resource includes a manipulable three-dimensional model that can be interactively explored, allowing students to orient the model, change the visualisation mode, and perform sections or cuts in different directions to analyse its internal geometry and plan the necessary views, cuts, and sections required for its complete definition (Figure 4). Once students have completed their own detailed drawing, they can compare their solution with the different solutions provided, each accompanied by explanatory comments and available with or without dimensions.

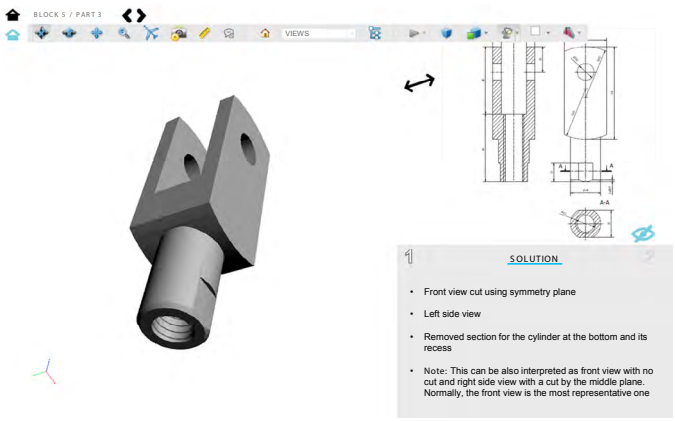


FIG. 4
Detailed example of the manipulable 3D model of an individual exercise

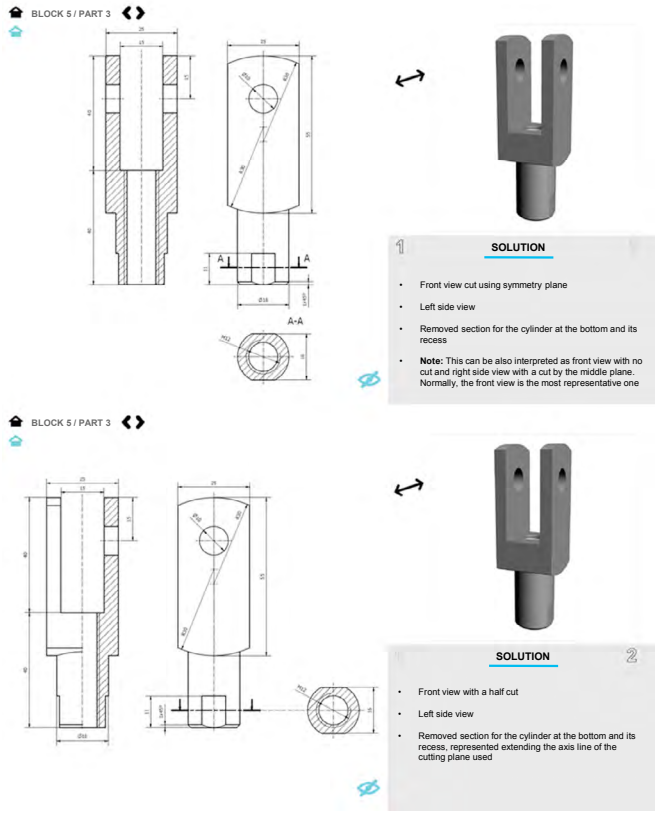


FIG. 5
Example of the standardised views of an individual exercise, and two valid solutions with explanatory comments

This interactive approach is further reinforced by the simultaneous visualisation of the manipulable 3D model and its corresponding standardised technical drawings, including the relevant orthographic views (Figure 5). This dual representation enables students to study and compare both formats in parallel, facilitating a deeper understanding of the dihedral system and significantly improving spatial visualisation skills. Furthermore, the inclusion of multiple valid solutions highlights that technical drawing involves informed decision making rather than a single fixed outcome. Overall, the integration of structured content, advanced interactivity, normative representations, and guided explanations provides a comprehensive learning environment that supports both conceptual understanding and the development of practical skills.

3. DEVELOPMENT OF THE RESOURCE

The development of the resource followed a progressive and iterative process aligned with the learning objectives of Engineering Graphics courses. In an initial phase, a set of representative exercises was selected, encompassing different types of parts and addressing topics that are known to be particularly challenging for students, such as the interpretation of views and sections, dimensioning, and the application of technical drawing standards.

All parts were modelled using Autodesk Inventor 2026, a professional computer-aided design (CAD) tool widely used in engineering contexts. This software was employed to generate accurate three-dimensional models and to derive the corresponding two-dimensional technical drawings, ensuring full geometric and dimensional consistency between both representations, as well as compliance with applicable standards.

Once the graphical content was produced, the models, drawings, and explanatory texts were integrated into an interactive digital book using Adobe InDesign. This tool enabled the structured organisation of content, the incorporation of interactive elements, and intuitive navigation between models, drawings, and associated comments. The resulting resource is a flexible and scalable digital environment that can be easily expanded, updated, or adapted in future iterations.

4. PEDAGOGICAL APPROACH AND TEACHING IMPLEMENTATION

The pedagogical approach of the proposed resource is based on active learning principles, which emphasise the learner's role in constructing knowledge through interaction and exploration [11]. This approach is particularly appropriate in Engineering Graphics, where the development of spatial reasoning requires active engagement with graphical content.

The resource design builds on research highlighting the importance of spatial skills in engineering education and the benefits of linking three-dimensional models with two-dimensional representations [2]. By allowing students to interact with 3D models and compare them with technical drawings, the resource supports a bidirectional learning process that strengthens both interpretation and modelling skills. Additionally, the inclusion of alternative valid solutions with explanatory comments encourages analytical thinking and helps students understand technical drawing as a decision-making process guided by standards, rather than as a purely procedural task [1].

The resource has been conceived as complementary material for face-to-face courses, supporting both classroom activities and autonomous learning. Future work will focus on its implementation and on evaluating its impact on student learning, engagement, and skill development.

5. CONCLUSIONS AND FUTURE WORK

This paper has presented the development of an interactive digital resource conceived primarily as a collection of solved exercises in technical drawing standardisation, while also being suitable for use in three-dimensional modelling activities. The resource integrates manipulable 3D models, standardised technical drawings, and explanatory comments within an interactive digital book format. In doing so, it addresses one of the core challenges in Engineering Graphics education: understanding the relationship between three-dimensional objects and their two-dimensional normative representations.

The dual nature of the resource enables its use from two complementary perspectives. On the one hand, it supports the learning of technical drawing standards through guided, solved exercises that emphasise criteria and decision-making processes. On the other hand,

the availability of associated 3D models allows the same material to be used as a basis for modelling tasks, fostering the connection between graphical interpretation and digital representation. This integrated approach is aligned with active and constructivist learning principles, promoting student engagement, deeper conceptual understanding, and self-regulated learning.

As the resource has not yet been implemented in classroom settings, future work will focus on its empirical evaluation through evidence-based studies, including pre-test–post-test and quasi-experimental designs. These studies will analyse its impact on student performance, engagement, and perception. Additionally, further developments will address the expansion of the exercise set, the gradual increase in complexity, and the enhancement of interactive features based on feedback from both, students and professors.

Acknowledgements: This work was funded by the Educational Innovation and Improvement Project (PIME) PIME/25-26/552, granted by the Universitat Politècnica de València (UPV).

REFERENCES

[1] Bertoline, G. R., Wiebe, E. N., Miller, C. L., Mohler, J. L.: Engineering Graphics Communication. McGraw-Hill (2009).

[2] Sorby, S. A.: Educational research in developing 3-D spatial skills for engineering students. *International Journal of Science Education* 31(3), 459-480 (2009).

[3] Lampropoulos, G., Fernández-Arias, P., de Bosque, A., Vergara, D.: Virtual reality in engineering education: A scoping review. *Education Sciences* 15(8) (2025).

[4] Lai, K.-W., Hong, K.-S.: Technology use and learning characteristics of students in higher education: Do generational differences matter? *British Journal of Educational Technology* 46, 725-738 (2015).

[5] Ho, E., Jeon, M.: Interaction map: A visualization tool for personalized learning based on assessment data. *Psych* 5, 1140-1155 (2023).

[6] Carbonell, V., Romero, C., Martínez, E., Flórez, M.: Interactive simulations as teaching tools for engineering mechanics courses. *European Journal of Physics* 34, 991 (2013).

[7] Pando Cerra, P., Alvarez Peñin, P., Perez Morales, M., Higuera Garrido, A.: Research regarding the implementation of an interactive application for educational improvement of engineering drawing. *Computer Applications in Engineering Education* 19, 183-192 (2011).

[8] Criollo-C, S., Abad-Vásquez, D., Martic-Nieto, M., Velásquez-G, F. A., Pérez-Medina, J.-L., Luján-Mora, S.: Towards a new learning experience through a mobile application with augmented reality in engineering education. *Applied Sciences* 11, 4921 (2021).

[9] Corral Abad, E., Gómez García, M. J., Diez-Jiménez, E., Moreno-Marcos, P. M., Castejón Sisamón, C.: Improving the learning of engineering students with interactive teaching applications. *Computer Applications in Engineering Education* 29, 1665–1674 (2021).

[10] Weis, P., Smetanka, L., Hrček, S., Vereš, M.: Interactive application as a teaching aid in mechanical engineering. *Computers* 13(7) (2024).

[11] Prince, M.: Does active learning work? *Journal of Engineering Education* 93(3), 223-231 (2004).

From conceptual exploration to functional coherence: integrating AI and technical disciplines in industrial design

Victoria Artés[a], Mar Melgarejo-Torralba[a], Eva M. Sánchez-García[a], Alfonso Ramallo-González[b], Juan Manuel Salmerón Núñez[a], Dolores Parras-Burgos[a, *]

[a] Universidad Politécnica de Cartagena member of European University of Technology EUT+, Department of Structures, Construction and Graphic Expression, Higher Technical School of Industrial Engineering. C/ Dr. Fleming, s/n, CP 30202, Cartagena (Murcia)

[b] Universidad Politécnica de Cartagena member of European University of Technology EUT+, Department of Automation, Electrical Engineering, and Electronic Technology, Higher Technical School of Industrial Engineering. C/ Dr. Fleming, s/n, CP 30202, Cartagena (Murcia)

* e-mail: dolores.parras@upct.es

Abstract: The development of graphic engineering skills requires methodologies that integrate advanced digital tools and interdisciplinary collaboration in real project contexts. This paper presents the implementation of a Project-Based Learning (PBL) approach that combines generative AI, interdisciplinary technical integration and parametric CAD modelling in the development of a functional product. The objective is to structure an integrated design process in which AI-assisted conceptual generation is incorporated into an interdisciplinary project, avoiding the traditional fragmentation between formal ideation and technical definition. The experience is implemented in university degree courses through the complete design of a lighting system that requires geometric, structural and electrical consistency. The methodology combines three interdependent levels: conceptual exploration using generative tools, definition of the electrical system and dimensional modelling. The PBL approach allows initial formal decisions, generated with AI support, to be progressively verified in technical terms, establishing constant feedback. AI is incorporated as an initial digital exploration tool, whose proposals must be verified in structural and energy terms within a shared technical environment. The evaluation was based on academic results, analysis of the projects developed, and a perception survey. The results show high academic performance and a positive assessment of the use of AI as a digital tool applied to design, especially as a support for the creative process. In conclusion, the integration of generative AI and interdisciplinary technical validation within a PBL environment strengthens the geometric-functional coherence of the design and provides a replicable methodological framework aligned with the current demands of engineering.

Keywords: *Artificial Intelligence, CAD, Model, Interdisciplinarity, PBL.*

1. INTRODUCTION

In recent decades, product design has transformed from an approach centred on hand tools to processes based on digital technologies [3]. This transformation has made it possible to enhance the creative procedures and improve the capacity for iteration, although the sector continues to face challenges such as the growing complexity of design problems, large-scale customisation and the need to shorten development times [7]. In this context, advances in artificial intelligence (AI) have expanded idea-generation models and introduced new dynamics into creative processes, where collaboration between humans and algorithmic systems requires ensuring interpretability, trust and the evaluation of results [4]. Tools such as Autodesk Generative Design, MidJourney and DALL·E have made it easier to explore alternatives in the early stages of the design process, broadening the range of possible solutions. Recent studies also identify generative AI as a useful tool for concept generation, refinement and iteration in product design education [6]. However, its use has mainly focused on ideation, without systematic integration into the technical definition and functional validation phases. This situation highlights a significant limitation in industrial design, where the separation between the design approach and the product's technical performance can affect its final quality. From a theoretical perspective, design should be understood as an integrated system in which ideation and constructive definition are interrelated processes that must be developed in parallel [2]. In the design of real mechanical components, it is essential that aesthetics, functionality, manufacturability and technical constraints interact simultaneously. The engineering literature indicates that interdisciplinary integration from the initial stages improves product coherence, reduces development times and facilitates more viable solutions that are better suited to the actual realities of manufacturing [1]. However, in higher education, where knowledge is organised into separate subjects, this fragmentation hinders a comprehensive understanding of technical systems and the transfer of knowledge between disciplines [5]. In this context, it is necessary to move beyond compartmentalised approaches to teaching in order to develop methodological frameworks that coherently integrate conceptual development, technical definition and digital tools into a single design workflow. The aim of this study is to analyse and validate a teaching strategy based on the integration of generative AI, interdisciplinary co-design and CAD modelling, using a Project-Based Learning (PBL) approach, in order to assess its impact on design coherence and the functional quality.

To this end, the following hypotheses are proposed: (H1) the use of AI enhances conceptual exploration in the early stages of design by broadening the range of solutions and encouraging more creative proposals; (H2) the simultaneous development of formal and technical constraints early on improves design compatibility; (H3) the availability of interdisciplinary knowledge increases the viability of solutions and their suitability for professional practice; and (H4) the integration of AI tools and an interdisciplinary approach increases student motivation.

The study analyses students' progress through the process of designing a desk lamp, replicating professional practice. The results obtained at different levels of knowledge show that generative AI encourages students to interactively reformulate design criteria and carefully select proposals, rather than just settling for fixed solutions. Furthermore, projects developed by incorporating the electrical component from the product design phase onwards demonstrate higher levels of stability, functionality and technical-constructive coherence.

The integration of real-world limitations during the design process encourages more feasible solutions that are closer to actual manufacturing. Furthermore, the incorporation of contemporary technological tools, in line with current product design practice, has contributed to greater student engagement and motivation throughout the project.

2. MATERIALS AND METHODS

This study is conceived as applied research in the field of graphic engineering education. It adopts a comparative and evolutionary methodological design for a desk lamp, developed over two consecutive academic years (2024-2025 and 2025-2026). The intervention is implemented in the Industrial Design II subject at the Universidad Politécnica de Cartagena Universidad (UPCT), within the Mechanical Engineering (GIM), Industrial Design and Product Development (GIDI) degree programmes, and the combined degree programme integrating both qualifications (PCEO). The total sample comprises 191 students.

The comparison doesn't track the same students over time, but contrasts two consecutive teaching models applied to different cohorts. The research design is structured in two phases. Phase 1 corresponds to the 2024-2025 academic year and involves 145 students. It applies an AI-assisted generative ideation methodology to the design of a desk lamp. Students begin with conceptual exploration using tools such as ChatGPT, Copilot or Gemini, developing increasingly specific prompts to generate alternatives and explore formal and functional solutions. The groups then present their proposals in class, justify their selection criteria and receive feedback. Based on this process, they select a final proposal and develop it through CAD modelling in SolidWorks, including parts, assemblies and technical drawings. Finally, the projects are presented, and each student submits an individual report documenting the design process and the decisions taken. Phase 2 refers to the 2025-2026 academic year and involves 46 students. At this stage, a crossover model is applied to the design of the desk lamp, based on the simultaneous integration of formal and technical criteria. There are two distinct groups: 21 students on the PCEO dual-degree programme, who are studying the Electrical Technology subject in parallel, and 25 GIDI students, who have not yet received this training. This setup allows us to analyse how the availability of technical knowledge influences the design process. At the start of the project, the PCEO students receive a specific session on lighting system design, covering aspects such as the selection of the light source, the type of power supply, the sizing of conductors according to cross-section and length, and the layout of electrical components. Based on this, these students take real-world constraints into account from the very beginning, such as the size of the light heads depending on the luminaire, the layout of the wiring, and the location of the batteries, connections and power supply components. This integration is reinforced in the Electrical Technology subject, where students must carry out detailed calculations for the product's installation, define the power supply system, provide technical justification for the decisions made, and take into account variables such as energy consumption and the system's viability. This approach allows the design process to evolve in parallel with the product's technical resolution, bringing the learning experience closer to a real-world context.

Data collection was based on three sources: the academic assessment of the projects, a qualitative analysis of the projects and the interim and final presentations, and a perception questionnaire aimed at the students. The projects were assessed using a rubric comprising

five criteria: design quality, complexity of CAD modelling, technical and functional coherence, integration of components, and quality of technical documentation. The qualitative analysis focused on the relationship between conceptual exploration, decision-making and the technical resolution of the product. The questionnaire included items on the AI tools used, the perceived usefulness of AI in the ideation phase, its impact on creativity and decision-making, and the overall learning experience. Building on these sources, the study combines quantitative and qualitative analyses. The quantitative analysis focuses on academic results and questionnaire responses, enabling an assessment of students' performance, perceived usefulness and motivation. The qualitative analysis aims to examine the design process, paying particular attention to the consistency between conceptualisation and technical definition, as well as students' ability to anticipate and integrate real-world electrical constraints in initial phases.

3. RESULTS AND DISCUSSION

The results are organised into two levels: the impact of using generative AI during the ideation phase (Phase 1) and the effect of interdisciplinary technical integration on design (Phase 2).

3.1. Phase 1: AI as a tool for ideation

The first phase of the study demonstrated that incorporating AI into the early stages of the design process enhances conceptual exploration, facilitates decision-making and increases student engagement. This approach led to the development of 45 complete lamp design projects, realised through CAD modelling and technical documentation, thereby demonstrating the feasibility of integrating AI into a real-world design workflow.

TABLE 1
Academic results for Phase 1 compared with the previous year

Degree programmes and academic year	Number of students	N.° of students with grade A (≥9)	N.° of students with a grade B (7-8,9)	N.° of students with a grade C (5-6,9)	N.° of students who failed or did not attend
GIDI 2024-25	22	13 (59,09%)	4 (18,18%)	0 (0,00%)	5 (22,73%)
GIDI 2023-24	19	4 (21,05%)	9 (47,37%)	4 (21,05%)	2 (10,53%)
PCEO 2024-25	18	10 (55,56%)	8 (44,44 %)	0 (0,00%)	0 (0,00%)
PCEO 2023-24	19	4 (21,05%)	11(57,89%)	4 (21,05%)	0 (0,00%)
GIM 2024-25	105	54 (51,43%)	32 (30,48%)	10 (9,52%)	9 (8,58%)
GIM 2023-24	60	8 (13,34%)	18(30,00%)	17(28,33%)	17(28,33%)

From an academic perspective, the results of Phase 1 show an improvement in performance. There has been a significant increase in the percentage of top marks compared with the previous academic year and a reduction in low marks, particularly in GIM (Table 1).

These results indicate that the methodology, as well as being compatible with the acquisition of technical skills, promoted effective learning within the project, as analysed by the teaching staff in their evaluation of the practice. In terms of tool usage, ChatGPT was the dominant platform, followed by Copilot and Gemini, although there was also evidence of the combined use of visual and graphic design tools such as DALL·E, Leonardo AI, Stable Diffusion, RunwayML, Canva and Freepik. This highlights a diverse digital ecosystem and a strategic use of available resources, demonstrating advanced digital skills that are well worth fostering. Furthermore, AI is used strategically, tailored to each phase of the design process. A qualitative analysis of the brief revealed two main strategies for interacting with AI. On the one hand, an exploratory approach, aimed at seeking inspiration and expanding formal imagination, with a predominance of modern and minimalist designs alongside futuristic, organic or industrially inspired proposals. On the other hand, a directive approach, focused on requesting proposals with specific characteristics. In subsequent iterations, the students refined their designs, discarding alternatives and simplifying geometries to facilitate their modelling in SolidWorks. Following analysis of the questionnaire (79 responses), there is clear evidence of high acceptance of the use of AI in design: 86.7% rated the experience positively, indicating a favourable reception and increased motivation. Furthermore, over 85% considered it an effective aid to ideation, particularly for generating sketches, exploring alternatives and overcoming creative blocks. Critical assessments relate to expectations of more advanced technical support, which reinforces its role as a complementary tool rather than a substitute for disciplinary knowledge.

This initial phase shows the contribution of AI to ideation. It acted as a creative catalyst by expanding the range of formal alternatives, supporting creative exploration and facilitating early decision-making. However, final decisions remained with the students, reinforcing critical thinking and project autonomy, while the technical-functional coherence of the final design depended on additional disciplinary knowledge.

3.2. Phase 2: simultaneous integration of formal and technical criteria

The second phase examined the impact of simultaneously integrating aesthetic, functional, structural and electrical criteria into the coherence of the design. The interim submission demonstrates a high level of student engagement and greater technical maturity when real-world constraints are incorporated from the early stages (Table 2).

TABLE 2
Academic results for Phase 2 compared with the previous year

Degree programmes and academic year	N.º of students	N.º of students with grade A (≥9)	N.º of students with a grade B (7-8,9)	N.º of students with a grade C (5-6,9)	N.º of students who failed or did not attend
GIDI 2025-26	25	9 (36,00%)	14 (56,00%)	0 (0,00%)	2 (8,00%)
GIDI 2024-25	19	4 (21,05%)	9 (47,37%)	4 (21,05%)	2 (10,53%)
PCEO 2025-26	21	14 (66,67%)	6 (28,57%)	0 (0,00%)	1 (4,76%)
PCEO 2024-25	19	4 (21,05%)	11(57,89%)	4 (21,05%)	0 (0,00%)

The grades of the PCEO group, which carried out the project in parallel with the Electrical Technology subject, were higher than those of the GIDI group: 66,67% achieved an A grade and 28,57% a B grade, reflecting high performance and a greater ability to integrate aspects such as stability, articulation, materials, electrical supply systems and constructability from the earliest stages. In GIDI, without this training, the results were slightly lower: 36% achieved an A grade and 56% a B grade. These projects showed high formal quality but lower technical maturity and a later integration of construction and electrical constraints. Compared with the previous year, the percentage of outstanding grades increased significantly in both groups, with an increase of 45,62 points in PCEO and 14,95 points in GIDI, demonstrating an improvement in performance. The PCEO group's projects demonstrate a greater ability to anticipate real-world industrial constraints right from the product conception phase. Designs such as *FlexTwo* and *Year Light* stand out for their formal and technical coherence, integrating articulated structures, adjustable lighting systems and detailed mechanical solutions. More conceptual proposals, such as *Vida* show a clear effort to connect form, functionality and lighting, despite their greater technical complexity. For their part, the GIDI group's proposals stand out for their formal richness, originality and capacity for conceptual innovation. Projects such as *Lumina*, inspired by the double helix of DNA or *Spineline*, based on a translucent vertebral structure, demonstrate significant design potential. However, during development, construction-related concerns often arise regarding stability, switch placement, cable integration or electrical safety. These aspects are typically addressed as subsequent adjustments, rather than forming part of the initial design.

The results of Phase 2 highlight the role of technical knowledge in achieving functional coherence. Students with parallel training in Electrical Technology integrated stability, articulation, materials, electrical supply and component layout earlier, leading to more viable and technically consistent designs. Overall, the early incorporation of technical constraints helped bridge the gap between ideation and feasibility, improved the anticipation of technical problems and strengthened the link with professional practice.

4. CONCLUSIONS

A comparison of the two phases reveals a clear evolution in the design process. Phase 1 showed that AI supports conceptual exploration and creative divergence (H1), increasing formal diversity, idea exploration and early decision-making, while technical coherence depends on disciplinary knowledge. Feedback from students also confirmed a very positive impact in terms of motivation, engagement and acceptance of the methodology (H4). However, its application in isolation does not guarantee the technical-functional coherence of the product, as this phase was characterised by a more open and exploratory creative approach, with fewer real constraints present from the outset of the process. In Phase 2, thanks to an interdisciplinary crossover learning model that integrated two subjects, the gap between the design concept and its feasibility was significantly reduced. The simultaneous incorporation of technical constraints during project development led to more coherent and functional proposals, closer to the actual manufacturing context (H2). Students demonstrated a greater ability to anticipate problems relating to stability, power supply, component integration and structural solutions. The process shifted from a sequential approach (first conceptualising and then solving problems) to an iterative approach, in which formal and technical decisions continuously feed into one another.

From a methodological perspective, the results highlight the value of project-based learning as a suitable framework for integrating digital tools and interdisciplinary knowledge into contexts closely linked to professional practice (H3). The combination of AI, technical criteria and realistic CAD modelling creates a more comprehensive and realistic learning environment, closely linked to the actual practice of industrial design. Among the study's key findings is the evidence that combining generative tools with technical expertise from the earliest stages is more effective than using them in isolation. Furthermore, it proposes a methodological model that can be applied to other contexts within computer graphics and product design, as it enables the integration of creativity, digital skills and technical problem-solving into a single design workflow. However, the study has some limitations. The distribution of the groups is determined by the curriculum rather than by random assignment, which may introduce bias. Future studies should use standardized statistical analyses and initial diagnostic assessments to verify grade improvements, account for sample-size differences, measure actual student progress and separate prior knowledge from the pedagogical intervention, while also exploring AI beyond ideation for technical validation tasks such as assisted simulation, component selection and compliance checking. Finally, since this study was conducted in a single institutional context, it would be advisable to validate the results in other academic settings.

REFERENCES

[1] Basu, S., Biswas, N. , Biswas, S.N. Sarkar, S.: A study on concurrent engineering-based design and product development. International Journal of Recent advances in Mechanical Engineering 2(1), 1-6 (2013).

[2] de Vere, I., Melles, G., & Kapoor, A.: Product design engineering: interdisciplinary pedagogy integrating engineering science with "designerly ways". In: The 2nd International Conference on Design Education ConnectED. University of New South Wales, (2010).

[3] Fakhry, M., Kamel, M., & Abdelaal, M.: CAD using preference compared to hand drafting in architectural working drawings coursework. Ain Shams Engineering Journal 12(3), 3331-3338 (2021).

[4] Sala, G., & Gobet, F.: Cognitive training does not enhance general cognition. Trends in cognitive sciences, 23(1), 9-20 (2019).

[5] Spelt, E. J. H., Biemans, H. J. A., Tobi, H., Luning, P. A., & Mulder, M.: Teaching and learning in interdisciplinary higher education: A systematic review. Educational Psychology Review, 21(4), 365-378 (2009).

[6] Reynolds, T.J. & Batley, A.: Exploring the impact of generative AI on concept generation, ideation, and design methodology in product design education. In: DS 131: International Conference on Engineering and Product Design Education, pp. 37-42 (2024).

[7] Yang, H., Li, R., He, X., Zhang, H., Wu, F., Liu, J., & Guan, Z.: An intelligent customized design method for complex products under the influence of dynamic uncertainty. Advanced Engineering Informatics, 66, 103480 (2025).

Design and Development of a Musculoskeletal and Cardiovascular Rehabilitation Device for Hospital Environments

I. Sola-Arean*, D. Ranz

Department of Design and Manufacturing Engineering (EINA), University of Zaragoza.
C/María de Luna s/n, 50018 Zaragoza, Spain

* e-mail: ivan.sola.arean@gmail.com

Abstract: This paper presents the design and development of a physical training device for hospital environments, aimed at the rehabilitation of patients with mobility limitations derived from musculoskeletal injuries or prolonged periods of inactivity. The primary objective of the project is to facilitate functional recovery through a system that enables more natural walking and running patterns, offering greater safety and autonomy to the user during rehabilitation. The project stems from a comparative analysis between professional and domestic equipment, identifying the need for a system that combines safety, ergonomics, and versatility within a controlled environment. Based on this study, the functional requirements of the device were defined, incorporating the capability to regulate speed via the user's own movement and allowing multi-directional displacement without the need to adjust body orientation. The development of the device was carried out using CAD modelling, functional prototyping, and simulations. The final device facilitates therapeutic exercises aimed at restoring joint mobility, strengthening atrophied musculature, and improving cardiovascular endurance, thereby contributing to comprehensive rehabilitation. Although the product does not replace conventional treadmills, it offers significant improvements in user experience, safety, and exercise versatility.

Keywords: *Rehabilitation, Hospital environments, Injuries, Sport, Treadmill.*

1. INTRODUCTION

Currently, the market offers a wide variety of treadmill and walking devices for both professional and domestic environments. While the available equipment differs in terms of technical specifications, none introduces significant innovation. This project focuses on the design of a device for hospital environments that enables patients to perform a series of exercises more naturally within a controlled setting for musculoskeletal and cardiovascular rehabilitation. This is particularly relevant since "the sequelae of chronic diseases and prolonged bed rest in hospitalised patients lead to a deterioration in quality of life, physical deconditioning, and neurological sequelae, as well as an increased burden on caregivers, the healthcare system, and society in general [1]". Similarly, other studies conducted on patients who present with respiratory and/or cardiovascular deficiencies, or who have undergone surgery for these conditions, conclude that aerobic exercise programmes should be implemented in severe cases for rehabilitation within a controlled hospital environment [2, 3, 4, 5].

At the outset of the project, an in-depth analysis was performed on the characteristics of various types of professional and domestic treadmills, examining their constituent components, embedded technologies, potential technological applications. The vast majority of walking and running treadmills operate in a very similar manner: the deck where the user exercises consist of a running bed covered by a rubber belt. At either end of the deck, two rollers tension and drive the belt, allowing the user to walk or run without changing their physical location. These rollers are driven either by an electric motor, with speed variations controlled via a user interface on the machine, or by the user's own exertion, meaning the individual regulates the exercise speed themselves. The product design developed in this work focuses on a treadmill that allows the user to move in any direction in a far more natural manner, preventing them from having to make unnatural movements or halt the exercise to change position. This effect is achieved by utilising a concave platform and conveyor omnidirectional spheres capable of rotating in any direction. The user positions themselves at the centre and begins to walk or run on these conveyor spheres.

2. MARKET RESEARCH

A comprehensive market research study was conducted to examine the different types of walking and running treadmills. This involved interviews with fitness centres and end-users regarding product utilisation, alongside an analysis of the European and Spanish regulatory frameworks governing such equipment. Finally, virtual prototyping methodologies were employed to verify compliance with these requirements.

Two distinct categories of treadmills are clearly identifiable within the current market (figure 1): professional models designed for sports facilities and rehabilitation clinics, characterised by ample surface areas and adjustable speeds; and domestic devices, which prioritise compactness at the expense of limiting both operating speed and the range of feasible exercises. Within the professional segment, equipment can be further sub-categorised into motorized systems—where an electric motor drives the running belt—and non-motorized (manual) machines, where the user drives the belt through their own physical exertion. In the former option, belt speed can be modified by the user via the machine's control console, whereas in the latter, the individual establishes the exercise velocity through their own physical power and stamina.



FIG. 1
Treadmills on the Current Market

Regardless of whether the treadmills are intended for professional or domestic use, the overarching legislation applicable to all such devices is Directive 2001/95/EC of the European Parliament and of the Council of 3 December 2001 on general product safety [6].

2.1. Common Requirements and Proposed Solution

Various concept designs were generated to address the versatility requirements of devices destined for hospital environments, specifically focusing on the recovery and rehabilitation of users with reduced mobility. These distinct concepts were evaluated against key primary requirements, such as ease and speed of manufacturing; simplicity and speed of assembly, maintenance, and repair; ease and speed of user onboarding; whether the concept could be successfully developed from a technical and technological standpoint; and product innovation—evaluating whether similar products already exist on the market or if the intended activity could be performed using a comparable machine.

Among all the proposed solutions, an omnidirectional walking and running platform was selected (Figure 2). This option represented the most innovative product, as the user is not restricted to running in a single direction, but can instead run forwards, backwards, sideways, and even diagonally. Although the product is susceptible to improvement regarding assembly, repair, and maintenance—owing to its complex mechanical assemblies—the concept compensates for these limitations through its high feasibility and manufacturability.

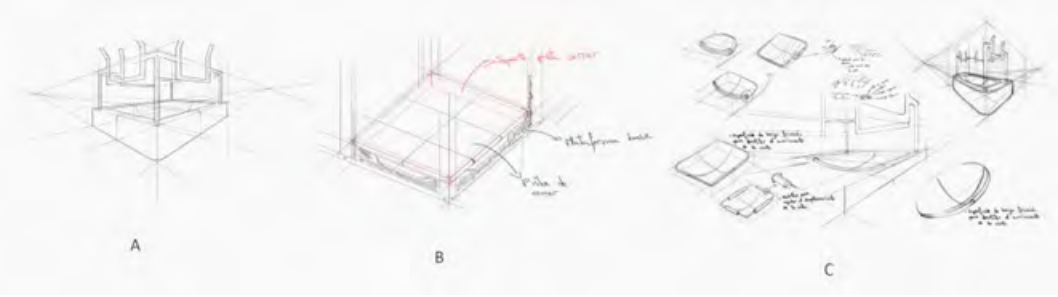


FIG. 2
Selected Design Concept

2.2. Concept Development

With the chosen concept established, its technical feasibility was evaluated across several phases. In the first phase, all proposed solutions were analysed from multiple perspectives, including their capacity for efficient and cost-effective manufacturing, weight, component safety, and ease of assembly and maintenance. Different solutions were generated for the constituent parts of the device.

In the second phase, the technical feasibility of the platform was evaluated using a system similar to the previous analysis, but employing different parameters to determine the optimal solution for the motion transmission system, the coupling between the transmission system and the support, and the assembly method of the exercise platform. For this study, conveyor omnidirectional spheres were specified as the elements to transmit omnidirectional motion. The final analysis was conducted to determine the number of conveyor spheres required to transmit motion efficiently while preventing the product from becoming excessively heavy. To ascertain the number of conveyor spheres, an equation was initially utilised (Figure 4) which divides the shortest dimension of the object's surface by a safety factor (2.5 or 3.5) to find the minimum pitch between spheres, subsequently yielding the total number of spheres required for that specific surface area.

A prototype simulating the surface of the running track was fabricated, featuring spheres of various dimensions to replicate as closely as possible the surface available to the patient when using the product. To ensure a broader range of options, supports with varying sphere densities per surface area and different sphere sizes were tested. Through a questionnaire administered to several users regarding the activities performed on the different supports, the necessity to develop a new conveyor sphere design was identified, as those currently available on the market excessively increased the overall weight of the product.

Various conveyor sphere concepts were generated and analysed from different standpoints to select the optimal design, including manufacturability, weight, total number of spheres on the running track and their cumulative weight, maximum stress, and deformation, among others. The selected conveyor sphere (Figure 4) utilises 6066 aluminium for all its components, except for the internal bushing, which is made of Teflon.



FIG. 3
Experimental Method

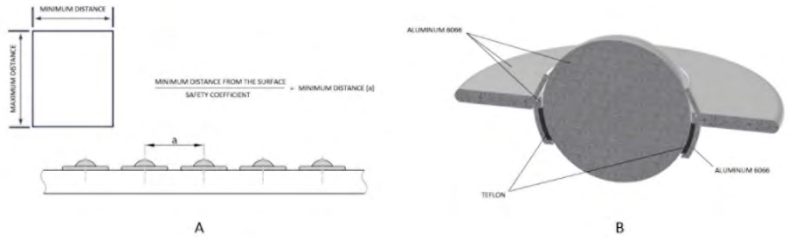


FIG. 4
Minimum Pitch Equation Between Conveyor Spheres and Selected Concept

2.3. Structural Analysis

The behaviour of systems subjected to stress during machine operation was simulated through a displacement study under load conditions using Autodesk Inventor software [7], as illustrated in Figure 5. This structural analysis was applied to the most highly stressed components, namely the conveyor omnidirectional spheres, the damper fixture base on the frame assembly, and the platform deck. The load applied for the running track analysis was 120 kg (corresponding to the approximate 92 kg weight of a heavyweight boxer plus the dynamic force exerted during a maximum-velocity sprint) in addition to the weight of the conveyor spheres. For the individual conveyor spheres, only the aforementioned user weight and dynamic exertion force were applied, whereas for the dampers, the user weight, exertion force, and the cumulative weight of the remaining product components were factored in.

This Computer-Aided Engineering (CAE) software enabled the virtual simulation of the concept. As shown in Figure 5, after implementing various solutions to the running track, a von Mises stress of 0 MPa was achieved across the entire surface of the component, with a maximum displacement of 0.08 mm located at the centre of the track. These data indicate that one of the components most susceptible to fatigue during exercise can withstand the applied loads without exceeding its yield strength, maintaining a safety factor of 28.94.

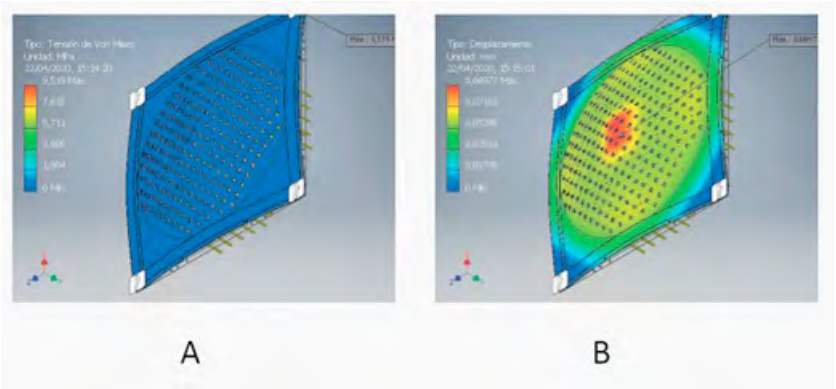


FIG. 5
Von Mises Stress and Displacement Analysis

3. MUSCULOSKELETAL AND CARDIOVASCULAR REHABILITATION DESCRIPTION

Once the final design solution was achieved, it was represented through 3D models, performing the complete modelling of the machine using the commercial software Autodesk Inventor [7]. This model was utilised to define the appropriate assembly process and to generate the engineering drawings for manufacturing.

3.1. Technical Specifications

The musculoskeletal and cardiovascular rehabilitation device (Figure 6) has dimensions of 1213 × 1890 × 1890 mm (height x length x depth). It is primarily manufactured from 1020 steel, whilst the covers and fairings are fabricated from polycarbonate.

The product features a main base structure to which the dampers, pillars, and braking system are secured. The running track is attached to the dampers to absorb the impacts generated by patients during exercise. The conveyor omnidirectional spheres are positioned within the orifices of the running track and secured with a housing using fasteners, creating a sandwich configuration. Hidden inside, between the running track and the main base, is the braking system that acts upon the conveyor spheres. This system features a series of springs that push upwards against a platform lined with polyurethane foam. The height of this platform is regulated via a ratchet-and-pulley system attached to the frame assembly, ensuring quick and easy access for both the physiotherapist and the patient.

The device's frame assembly is secured to four pillars, which are bolted to the main base. This handrail structure allows the patient to grip it quickly if they become fatigued or lose their balance, and it also serves to attach additional accessories, such as a cup holder. Furthermore, resistance bands, elastic straps, or a safety harness can be anchored to this element, providing the patient with exercise variety and enhanced safety.

To conceal the internal mechanisms—preventing accidents and reducing wear and tear—polycarbonate casings are bolted over the running track and onto the sides of the product. This device is designed to withstand a maximum load of approximately 120 kg. To support a higher load capacity, a comprehensive re-evaluation and redesign of all its components would be required. Since it does not incorporate any electronic components, electrical safety considerations are non-applicable in this setting, as there is no risk of electrocution to the physiotherapist or the patient. For this category of product, only the European CE certification is required.

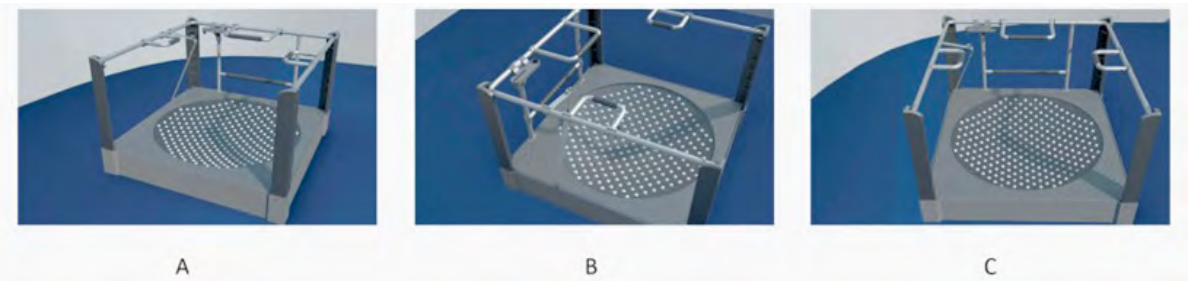


FIG. 6
3D Model of the Musculoskeletal and Cardiovascular Rehabilitation Device

4. CONCLUSIONS

In conclusion, the design developed in this project is not intended to replace the manual walking and running treadmills currently available on the market. Instead, the devised product enables a wider variety of rehabilitation exercises, as it allows users to change direction without executing movements that could cause an accident. Owing to its frame assembly, the device permits physiotherapists to attach resistance bands to the bars, increasing the workload the patient must overcome during exercise and thereby intensifying the exertion. Furthermore, to enhance safety, a belt or harness can be secured to the patient and anchored to the frame structure. The braking system provides an additional method to increase resistance and patient exertion; this consists of a platform that the physiotherapist or patient can raise or lower using a mechanism installed on the frame assembly. To increase resistance, the braking platform is raised to act upon the conveyor omnidirectional spheres of the running track. The greater the contact between the braking platform and the conveyor spheres, the more effort the patient must exert to move across the track. Another feature that fosters exercise diversity is the adjustable bar system integrated into the frame. This element can be adjusted both angularly and longitudinally to accommodate different patient heights or to facilitate exercise in various positions.

REFERENCES

[1] Carvajal Tello, N., González Marmolejo, W., Segura Ordoñez, A.: Diseño y desarrollo tecnológico de un dispositivo terapéutico para la rehabilitación física en el ámbito hospitalario. Revista Salud Uninorte, Vol. 35, núm. 2, 2019 (https://doi.org/10.14482/sun.35.2.617.1).

[2] Joanne Price, K., Ashley Gordon, B., Richard Bird, S., Clare Benson, A.: A review of guidelines for cardiac rehabilitation exercise programmes: Is there an international consensus, European Journal of Preventive Cardiology, Volume 23, Issue 16, 1, 1715-1733, 2016 (https://doi.org/10.1177/2047487316657669).

[3] Azevedo, P., Gomes, B., Macedo, J., Ferreira, S., Pereira, J., Pires, A.: Debilidad muscular en pacientes críticos: efectos de un programa de rehabilitación sistematizado de enfermería, Enfermería Clínica, Volumen 33, Issue 3, Pages 216-222, 2023 (https://doi.org/10.1016/j.enfcli.2022.11.001).

[4] Vicuña Q., M. J., Paredes G., D., Gutiérrez G., C., Valenzuela, R., Vergara F., N., Álvarez M., H., Azarola, M., Pérez C., P., Valenzuela M., R.: Efectos de un programa de rehabilitación pulmonar perioperatoria en pacientes sometidos a cirugía torácica: estudio de corte observacional retrospectivo. Revista Chilena De Enfermedades Respiratorias, 42(1), 27-36, 2026.

[5] Khan, A. A., Naseer, O., Iliescu, D., Hines, E.: The International Journal of Soft Computing and Software Engineering [JSCSE], Vol. 3, No. 3, pp. 30-37, 2013 (https://doi.org/10.48550/arXiv.1401.7249).

[6] Agencia Estatal Boletín Oficial del Estado, www.boe.es/buscar/doc.php?id=DOUE-L-2011-81464, last accesed 2026/05/01.

[7] Autodesk Inventor help homepage, https://help.autodesk.com/view/INVNTOR/2026/ES-P/?guid=GUID-4DFDDCD8-FF43-4B90-8EF6-82E8A76ED6BC.

Sustainability and structural assessment of urban bicycle frames manufactured using different material systems

Mauricio López-Gutiérrez, David Ranz-Angulo*, Carmelo Pina-Gadea, José Antonio Gómez-García

Department of Design and Manufacture Engineering, University of Zaragoza (Spain), C/ María de Luna 3, 50018-Zaragoza

* e-mail: dranz@unizar.es

Abstract: This study evaluates the environmental performance of urban bicycle frames manufactured using different material systems while ensuring equivalent structural functionality: carbon fiber reinforced polymer composites, natural fiber composites based on flax fibers, aluminium alloy, and structural steel. The functional unit is a complete urban bicycle frame capable of fulfilling identical structural requirements according to ISO 4210-6. Structural analyses are performed using finite element analysis to ensure that each design meets the required stiffness and strength criteria. The environmental assessment is conducted using the Life Cycle Assessment methodology in accordance with ISO 14040 and ISO 14044 standards. The system boundaries include raw material extraction, material processing and frame manufacturing. The results highlight the influence of material production intensity, manufacturing complexity, and recyclability on the overall environmental performance. Particular attention is given to the balance between the mechanical performance of advanced composites and the environmental impact associated with the production of fibres and polymer matrices.

Keywords: *Life Cycle Assessment, Urban Bicycle Frame, Sustainable Design, Multi-Material LCA, Bio-Based Composites, Finite Element Analysis.*

1. INTRODUCTION

Urban mobility is undergoing a rapid transformation driven by the need to reduce greenhouse gas emissions, energy consumption, and material intensity in transportation systems. Bicycles play a central role in this transition due to their low operational environmental impact and high efficiency in short-distance travel. However, the environmental footprint associated with the manufacturing of bicycle components remains significant and depends strongly on material selection and production processes. This study evaluates the environmental performance of urban bicycle frames manufactured using different material systems while ensuring equivalent structural functionality. The objective of this research is to assess and compare the sustainability performance of bicycle frames produced with representative material systems widely used or proposed in the bicycle industry: carbon fiber reinforced polymer composites, natural fiber composites based on flax fibers, aluminium alloys, and structural steel.

The functional unit defined in the study is a complete urban bicycle frame capable of fulfilling identical structural requirements according to ISO 4210-6. The developed frame consists of two half-shells bonded along their mid-plane, which simplifies the manufacturing process. Structural analyses are performed using finite element analysis (FEA) to ensure that each design meets the required stiffness and strength criteria. This approach establishes functional equivalence between alternatives and allows a consistent environmental comparison. The environmental assessment is carried out using the Life Cycle Assessment (LCA) methodologies methodology in accordance with ISO 14040 [1] and ISO 14044 [2] standards.

2. FRAME DEVELOPMENT

2.1. Design

The frame design approach is oriented towards enabling its manufacture using a two-shell construction, as opposed to the traditional method of producing monocoque carbon fibre frames. This method offers notable advantages: it reduces tooling costs by simplifying mold construction, improves accessibility during the lamination process and visual inspection, shortens preparation times and, in short, simplifies the overall manufacturing process. As a counterpart, it only guarantees a quality surface finish on the face in contact with the mold, and result in a bond line between the shell halves that represents a greater challenge from a mechanical performance standpoint.

In this context, various design solutions have been adopted, consistent with the objective of producing a frame with an urban aesthetic while meeting structural safety requirements. First, a continuous outer face has been maintained along the entire frame in order to integrate chainstay and seatstays and simplify the lamination process as shown in Fig. 1A. At the junction between the two shell halves, this continuity is achieved through a perimeter flange that maximizes the adhesive contact area between both faces. Furthermore, in order to limit the displacements caused by buckling loads in the rear triangle, a PVC foam core has been incorporated, giving the assembly a sandwich type structure. This same methodology has been applied in critical interface zones with commercial components: the head-

set cup, seat post, and bottom bracket conduits are defined by foam inserts over which the laminate is applied, thereby ensuring the correct integration of these components into the frame (Fig. 1B). The design corresponds to an adult size L bicycle with a wheel size of twenty-eight inches; this approach allows a direct comparison with other frames on the market. Finally, the 3D model was developed in SOLIDWORKS® 2025.

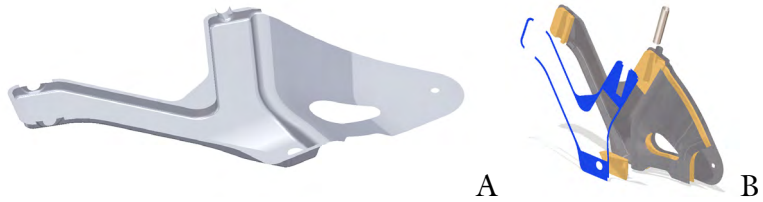


FIG. 1
A: Half shell. B: Structure of a half shell, Blue: Adhesive, Orange: Foams

2.2. Finite Element Analysis

The Structural analysis was conducted using SOLIDWORKS® 2025 Simulation, a tool that enables static mechanical analyses based on the finite element method. In accordance with ISO 4210-6:2023. However, sections 4.1 and 4.2 correspond to energy-based tests that could not be replicated due to the inherent limitations of the software used. Regarding fatigue resistance, will be carried out in a subsequent phase. In the interim, a static analysis replicating the loading conditions specified for the fatigue test has been performed, incorporating a safety factor of 2.5.

The most representative test is that defined in section 4.5, which simulates the load exerted by the weight of a cyclist in the pedalling position. In this case, 2,5 kN were applied offset 70 mm rearward from the central axis of the seat post, with a post length of 250 mm. The boundary conditions of the model restrict axial displacements along the front fork axis and displacements in all three spatial directions at the rear axle. Regarding to the mesh, the maximum element size is 4 mm. In Fig. 2 and Fig. 3 the results of the analyses are shown.

As shown in Fig. 2A, the maximum global displacement obtained is 1,71 mm due to buckling stress. Regarding the stress state, the fiber laminate remains within admissible limits even under the amplified load, with the most stressed regions being the rear axle and the upper junction between the central body and the rear triangle.

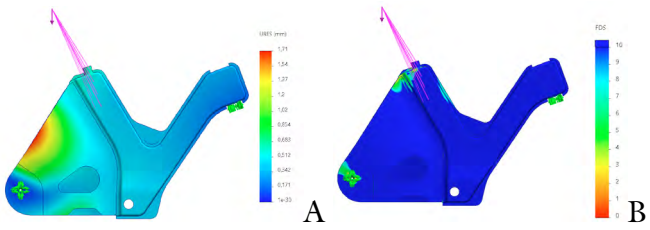


FIG. 2
A: Global displacements, B: Safety factor with Tsai-Wu error criterion

Finally, given that the frame consists of two bonded halves, it is particularly relevant to verify that the foam cores remain below their elastic limit of 1 MPa and that the adhesive does not exceed its maximum shear strength of 17 MPa. As shown in Fig. 3, both conditions are satisfactorily met. Nevertheless, the influence of temperature on the behaviour of the adhesive should be also investigated in future works.

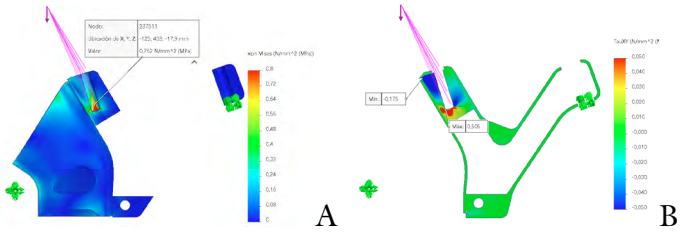


FIG. 3
A: Von Misses stress in the cores, B: Shear stress in the adhesive

3. LIFE CYCLE ASSESSMENT

3.1. Goal and Scope Definition

The main objective of this analysis, defined in accordance with ISO 14040 [1] and ISO 14044 [2], is to compare the carbon footprint of two material families applied to a bicycle frame, composite and metallic materials, using the LCA methodology. In the case of composite materials, the environmental impact of the carbon fiber prototype frame is evaluated alongside a hypothetical variant manufactured entirely from flax fiber. For metallic materials, a frame with equivalent performance is designed in order to compare its environmental impact considering two representative alloys: 6061-T6 aluminium and annealed AISI 4130 steel.

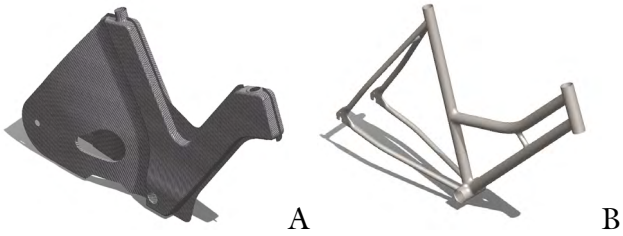
3.2. Functional Unit

The mechanical equivalence criterion requires that all frames must operate under a safety factor of 2.5 and have similar displacements at the crankset under the vertical force test (Table 1).

TABLE 1
Structural equivalence of frames in function of the material

Parameters	Weight [g]	Δy [mm]
Carbon Fiber	2.824	–0,387
Flax Fiber	5.805	–0,402
Aluminium 6061-T6	2.312	–0,347
Steel AISI 4130	3.676	–0,395

It should be noted that the frame geometry varies depending on the material used, given that the manufacturing processes for a composite frame and a metallic one are different. For this reason, a tubular geometry representative of commercially available frames has been modelled in 3D for the metallic cases (Fig. 4B) and maintaining the external dimensions of the composite frame as a common geometric reference (Fig. 4A).



A B

FIG. 4
A: Composite frame structure, B: Metallic frame structure

3.3. System Boundaries

This study boundaries encompass the life cycle stages from cradle to gate, including raw material extraction, processing, transportation, and the manufacturing processes associated with frame production, accounting for energy consumption and consumable materials. For the composite infusion process, the cutting waste generated during layup on the mould, trimmings and flash resulting from the deflashing phase, resin waste remaining in the injection circuits and auxiliary materials such as release agents were considered.

3.4. Assumptions

Inventory data were sourced from the EcoInvent V3.11 database, and the LCA model was developed using SimaPro 10.4.0.0. As for environmental indicators ReCiPe 2016 Endpoint (H) V1.12 / World (2010) H/A was selected as the primary impact assessment methodology. Although the single score approach simplifies the overall interpretation of results by aggregating multiples indicators into a single weighted value, it introduces additional uncertainty. For this reason, the carbon footprint was additionally calculated using the IPCC 2021 GWP100 methodology, given its relevance in the current context and its alignment with international greenhouse gas emission.

The vacuum infusion process losses result in a manufacturing yield of 82%, meaning that 1,22 kg of fibre and resin are required to produce 1 kg of finished composite material [3]. Since EcoInvent does not include an entry for carbon fiber, this material was modelled by accounting for all processes associated with its manufacturing [4]. It should be also noted that the resin used in the flax fiber frame contains 35% bio-based content; however, since no specific entry exists in EcoInvent to model this bio-based fraction, its environmental impact was reduced proportionally by 35%. Finally, for the aluminium and steel frame, the inventory data was adapted with a correction factor to establish the mechanical equivalence with the frame under analysis [5].

3.5. Inventory Data

The inventory for the frames is detailed in Table 2, Table 3, Table 4 and Table 5. It includes a 15% waste of the raw material in the adhesive and the PVC foam and in all materials for the steel and aluminium frame. Also, the final weight of resin and fibre is employed as an input for the raw material, but a waste of 18% is considered in the input weight for the entry of the vacuum infusion moulding for composite production (GLO), as explained before with the manufacturing yield of 82%.

TABLE 2
Inventory for a carbon fibre bicycle frame

Parameters	Input	Weight [g]
Epoxy Resin	Epoxy resin (GLO)| market for epoxy resin | Cut-off, S	1.250,0
Epoxy Adhesive	Polyurethane adhesive (GLO)| market for (…)	45,3
PVC Foam Core	Polyvinylchloride, suspension polymerised (GLO)| market for (…)	330,0
Carbon Fiber	Modelled [4]	1.250,0
Infusion with waste 18%	Vacuum infusion moulding for composite product (GLO) (…)	3.046,0

TABLE 3
Inventory for a flax fibre bicycle frame

Parameters	Input	Weight [g]
Bio Epoxy Resin	Epoxy resin (GLO)| market for epoxy resin | Cut-off, S	2.740,0
Epoxy Adhesive	Polyurethane adhesive (GLO)| market for (…)	45,3
PVC Foam Core	Polyvinylchloride, suspension polymerised (GLO)| market for (…)	330,0
Flax Fiber	Market for fibre, flax, long, scutched RER	2.740,0
Infusion with waste 18%	Vacuum infusion moulding for composite product (GLO) (…)	6.682,0

TABLE 4
Inventory for an AISI 4130 steel bicycle frame

Parameters	Input	Unit	Value
Steel	Steel, low-alloyed (GLO)| market for (…)	[g]	4.227,00
Tap water	Tap water (GLO)| market group for tap water | Cut-off, S	[g]	1.267,00
Powder coat	Powder coat, steel (GLO)| market for (…)	[m^2]	0,38
Welding, arc	Welding, arc, steel (GLO)| market for (…)	[m]	2,10
Steel waste	Steel and iron (waste treatment) (GLO)| recycling of (…)	[g]	551,00
Wastewater	Wastewater, average (GLO)| market for | Cut-off, S	[g]	1.267,00

TABLE 5
Inventory for a 6061-T6 aluminium bicycle frame

Parameters	Input	Unit	Value
Aluminium	Aluminium, wrought alloy (GLO)| market for (…)	[g]	2.658,00
Extrusion	Powder coat, aluminium sheet (GLO)| market for (…)	[g]	2.658,00
Welding arc	Impact extrusion of aluminium, 3 strokes (GLO)| market for (…)	[m]	1,33
Powder coat	Welding, arc, aluminium (GLO)| market for (…)	[m^2]	0,38
Electricity	Electricity, medium voltage, aluminium industry (…)	[kWh]	48,55
Aluminium, waste	Aluminium (waste treatment) (GLO)| recycling of aluminium (…)	[g]	346,00

3.6. Results and discussion

As shown in Fig. 5. Results for each frame composite materials have a lower environmental impact under the ReCiPe methodology, whereas metallic materials exhibit a higher overall impact. However, in terms of carbon footprint, carbon fiber performs the worst, closely followed by aluminium, which is likely due to the high energy demand associated with raw material production in both cases. Steel shows a better carbon footprint than both aluminium and carbon fiber, while flax fiber presents a considerable impact as well, although this is mainly driven by the manufacturing process because of the large number of consumables required during the vacuum infusion process.

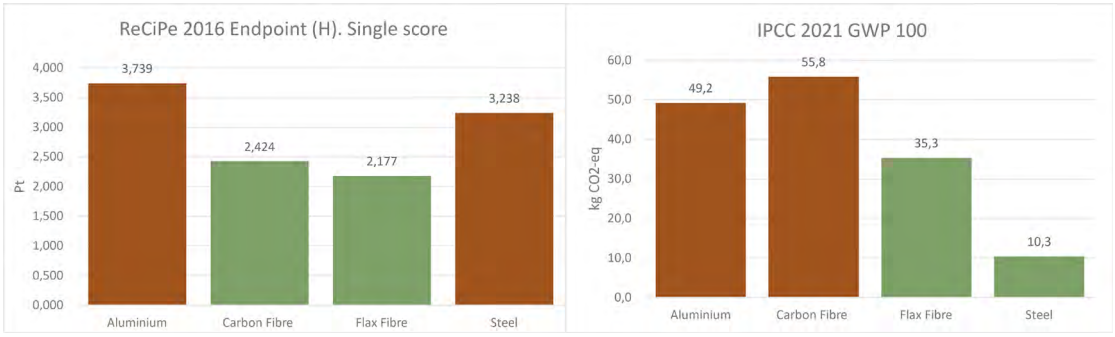


FIG. 5
Results for each frame

To compare, the results reported in the literature by other authors were used as a reference [6]. These values were adjusted by means of mass-based correction factor in order to establish a functional equivalence with the CFRP frame under analysis. An aluminium 6061-T6 frame, manufactured with an 80% recycled content, yields a global warming potential of 12,61 kg CO_2 eq., while a frame produced from AISI 4130 steel, with a 20% recycled content, results in an impact of 8,45 kg CO_2 eq. In contrast, a conventionally manufactured car-

bon fiber reinforced polymer frame represents an estimated impact of 51.45 kg CO_2 eq. The carbon fiber value is similar to the value obtained [6], and when the percentages of recycled material used by the author area considered, the results are consistent.

4. CONCLUSIONS

The manufacture of a carbon fiber frame using a two-shell construction is mechanically feasible. However, due to this manufacturing approach, geometric modifications are required, which increase the frame weight compared with conventional frames. This is mainly because the chain stays and seat stays are integrated as a continuous surface, as well as because of the larger overall frame area compared with a tubular frame. Even so, since this is still a prototype, further optimization can be studied. With regard to environmental impact, a flax fiber frame, although heavier, shows a global impact that is 41,77% lower than an aluminium frame and 32,76% lower than that of an equivalent steel frame under ReCiPe methodology. The same trend is observed, to a lesser extent, for carbon fiber. Nevertheless, when only greenhouse gas emissions are considered, composite materials can be more than five times more harmful than a steel frame. It is worth noting that the two-shell manufacturing process doubles the infusion operations required per frame, which negatively affects its environmental performance. In conclusion, this study shows that composite materials for structural components can be botch technically viable and compatible with a sustainable approach, while also underscoring the importance of bio-based fibers as flax and bio-resin. Nevertheless, the future lines of work include experimental testing to validate the simulation results.

REFERENCES

[1] ISO 14040:2006 Environmental management - Life cycle assessment - Principles and framework. International Standard Organization, Geneva, Switzerland (2006).

[2] ISO 14044:2006 Environmental management - Life cycle assessment - Requirements and guidelines. International Standard Organization, Geneva, Switzerland (2006).

[3] La librairie ADEME, https://librairie.ademe.fr/industrie-et-production-durable/7288-inventaire-du-cycle-de-vie-des-procedes-de-mise-en-forme-des-composites.html, last accessed 2026/05/07.

[4] Vogiantzi, C., Tserpes, K.: A Comparative Environmental and Economic Analysis of Carbon Fiber-Reinforced Polymer Recycling Processes Using Life Cycle Assessment and Life Cycle Costing. Journal of Composites Science, 9(1): 39, (2025). doi.org/10.3390/jcs9010039

[5] SimaPro Tutorial - PRé Sustainability, https://simapro.com/wp-content/uploads/2023/07/SimaPro-Tutorial.pdf, last accessed 2026/05/08.

[6] Bard, V., Suski, C.: Life Cycle Modeling and Carbon Footprint of Bicycle Frames, Brazilian Journal of Education Technology and Society, 17, 1021-1033 (2024). doi.org/10.14571/brajets.v17.n3.1021-1033

Challenge-Based Learning for Higher Education Transformation in Industry 5.0: A UPM-EELISA Ecosystem Perspective

Luisa M-Muneta*, Ruth Carrasco-Gallego, Javier Gómez-Fernández, Alejandro Badolato

ETS Ingenieros Industriales, Universidad Politécnica de Madrid

* e-mail: luisa.mtzmuneta@upm.es

Abstract: The transition toward Industry 5.0 is reshaping higher education institutions, requiring universities to evolve from traditional knowledge-transmission models into human-centric, sustainability-driven, and innovation-oriented ecosystems. In this context, Challenge-Based Learning (CBL) has emerged as a pedagogical framework capable of connecting academic learning with real societal and industrial challenges. This paper analyses the implementation of CBL within the Universidad Politécnica de Madrid (UPM) and the European University alliance EELISA, focusing on FabLabs, circular economy initiatives, and interdisciplinary collaboration. Results indicate that CBL supports the integration of teaching, research, innovation, and societal engagement while fostering Industry 5.0 competencies such as systems thinking, creativity, collaboration, resilience, and ethical awareness. FabLabs and rapid prototyping infrastructures play a key role in enabling experimentation and iterative learning processes. Furthermore, the paper identifies key success factors for implementing CBL in technical universities, including alignment with courses, motivated faculty, external stakeholders, intermediate feedback sessions, and institutional support. The findings position CBL as a robust framework for advancing Education 5.0 in engineering and design education and highlight the strategic role of European university alliances such as EELISA in scaling challenge-based innovation ecosystems.

Keywords: *Challenge-Based Learning, Industry 5.0, Higher Education, FabLabs, Circular Economy, EELISA.*

1. INTRODUCTION

The emergence of Industry 5.0 is generating profound transformations in industrial systems, innovation processes, and educational models. While Industry 4.0 focused mainly on automation, digitalization, and productivity, Industry 5.0 introduces a broader vision centered on human well-being, sustainability, and resilience [1]. This new paradigm requires professionals capable of addressing complex socio-technical problems through multidisciplinary collaboration, creativity, and systems thinking [2].

Consequently, higher education institutions are facing increasing pressure to redesign their educational models. Traditional lecture-based approaches are insufficient to prepare students for environments characterized by uncertainty, rapid technological evolution, and interconnected global challenges. Universities are therefore expected to move beyond their conventional role as knowledge providers and become active innovation ecosystems connected with industry, society, and public institutions.

In this context, Challenge-Based Learning (CBL) has emerged as one of the most promising pedagogical approaches for engineering and technical education. CBL structures learning around real-world challenges proposed by companies, NGOs, institutions, or communities, encouraging students to investigate, prototype, collaborate, and implement solutions with tangible impact. The framework originated from the Apple Classrooms of Tomorrow—Today (ACOT2) initiative and is structured around three main phases: Engage, Investigate, and Act [3].

Unlike traditional problem-solving methodologies, CBL emphasizes:

—learner agency: everybody (Faculty and students) are learners

—Real-world engagement, interdisciplinarity and problem-framing: challenges are grounded in complex real-world problems with no clearly predefined constraints (unlike traditional Project based learning), requiring an interdisciplinary approach to achieve an appropriate problem framing. The objective is not so much to identify the “right” solution, but rather to develop the “right” understanding and framing of the problem itself. Cross-sectoral collaboration; challenges are provided by or connected to external stakeholders from the higher education institution: companies, NGOs, or governmental entities such as local, regional or national governments.

—iterative prototyping; students learn of their fails, it is an iterative process

—and societal impact; provide solutions means positive impact to the society

The following Table 1 shows the differences of CBL and PBL. As we can see CBL characteristics align closely with the objectives of Industry 5.0 and Education 5.0.

TABLE 1
Comparation between PBL and CBL

Aspect	Problem-Based Learning (PBL)	Challenge-Based Learning (CBL)
Main focus	Solving a defined problem	Addressing a real-world challenge
Starting point	Instructor-defined problem	Broad societal "Big Idea"
Approach	Inquiry and analysis	Action, innovation, and impact
Role of students	Problem solvers	Co-creators and innovators
Role of teacher	Facilitator	Mentor and ecosystem connector
External stakeholders	Optional	Essential
Implementation	Often theoretical	Real prototypes or solutions
Interdisciplinarity	Possible	Strongly encouraged
Assessment	Knowledge and solution quality	Process, collaboration, and impact
Industry 5.0 alignment	Moderate	Strong alignment

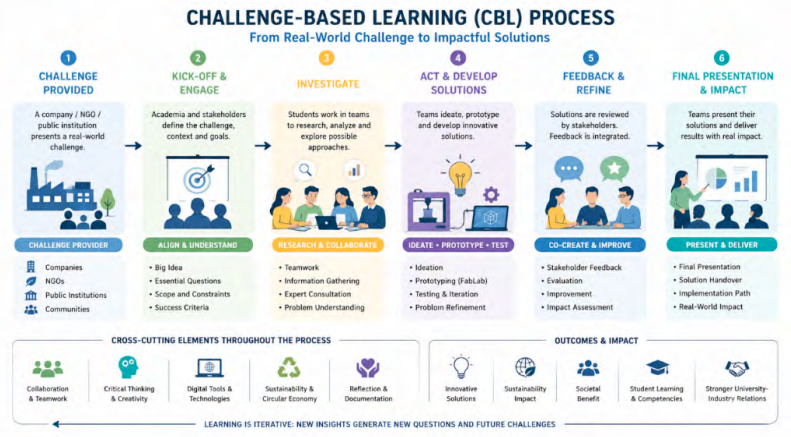
At the European level, alliances such as EELISA (European Engineering Learning Innovation and Science Alliance) provide a strategic framework for implementing challenge-based educational ecosystems across institutions and countries [4]. EELISA promotes interdisciplinary communities focused on societal challenges, sustainability, and innovation, facilitating collaboration between universities, industry, and society.

Within this framework, the Universidad Politécnica de Madrid (UPM) has developed several challenge-based initiatives related to circular economy, digital fabrication, sustainable design, and FabLabs [5]. These initiatives combine engineering education with real-world experimentation, creating living laboratories where students, faculty members, and external stakeholders collaborate to develop innovative solutions.

This paper presents the UPM–EELISA approach to CBL and analyses several educational experiences developed in this ecosystem.

2. CHALLENGE-BASED LEARNING AND INDUSTRY 5.0

Challenge-Based Learning (CBL) is an active learning framework that combines experiential learning, project-based learning, and collaborative problem-solving. According to [3], CBL enables students to move from broad societal ideas toward concrete and actionable challenges through inquiry, investigation, and implementation (Fig. 1).



Source: Chat GPT under Author's prompt.

FIG. 1

Challenge Based learning process

Industry 5.0 introduces a human-centric approach where technology is aligned with sustainability and societal value creation. The European Commission defines three core dimensions: Human-centricity, sustainability and resilience. These principles directly affect higher education. Universities must foster not only technical knowledge but also creativity, ethical awareness, adaptability, collaboration and systems thinking.

This evolution has led to the concept of Education 5.0, where learning becomes interdisciplinary, challenge-driven, collaborative and connected to real societal problems.

CBL fits naturally into this paradigm because it combines academic learning with experimentation, co-creation, and societal engagement [6] [7].

3. UPM–EELISA ECOSYSTEM

UPM participates in EELISA as part of a European network of ten universities across eight countries. One of the most relevant initiatives is The Regenerative Campus, which conceptualizes the university campus as a living laboratory for circular economy [8] and sustainability experimentation. The mission of this EELISA community is to transform campuses into technically viable, economically profitable and socially inclusive ecosystems. The UPM-EELISA communities approach integrates Academia, companies, NGOs, city councils and society.

Challenges are based on real human needs and are frequently linked to circular economy and sustainability topics. This model transforms the university into an open innovation ecosystem (The size of the EELISA ecosystem is more than 100.000 people- like a medium city) where:

—students become active problem-solvers,

—companies, NGOs, organizations... become challenge providers,

—faculty members act as facilitators and leaders,

—and society becomes part of the learning process.

4. EDUCATIONAL EXPERIENCES

In the following Table 2 we have collected the different CBL experiences carried on by CRC EELISA Community from 2020. These experiences have been performed in all courses (from first year to master courses) and in the Table 2 the Fablab use is show due prototypes were recommended and the needed funding for them. Additionally, you can find the year, number of students, required funding and lessons learned. As you can see all the challenges have a "challenge owner" that participated in the final assessment and feedback of the proposed solutions.

TABLE 2
Challenges resume

Challenge Name	Academic course	#students	Challenge Provider	Courses	Funding	Lessons learned
PLA WASTE FROM COVID-19	From 2020…	34	Coronamakers	Not associated to a specific course	Funding from different awards +25.000€	Challenges should be part/embedded in a course. Need to find motivated researcher/teacher
FOOD WASTE CHALLENGE	2022-2023 2023-2024 2024-2025	50 50 110	Paradores Hostelería Madrid	TECHNICAL DRAWING 1º GIO TECHNICAL DRAWING 1º GIQ	Awards for the best works	Visits to Kitchen places were a success
WIND BLADES CHALLENGE	2023-2024 2024-2025 2025-2026	60 60 67	Iberdrola Energy Loop	CIRCULAR SUPPLY CHAIN 1º MII	EELISA-500 €	Powerful collaboration Company + ETSII
BIOFILIATION IN ETSII	2025-2026	55	ETSII-UPM	TECHNICAL DRAWING 1º GIO	Free course about Biofiliation.Italian Academy of Biofilia	Feedback from companies is welcome for students
Hackathon for Sustainable Fashion & New Materials: (5 FULL DAYS)	2024-2025	67	Asecom Ayuntamiento de Madrid	INGENIA 1º MII	EELISA 3TH joint call 10000€ CIEC: 2336.77€ (meals) UPM; 845€	Activities need a specific slot in the programmes.
REINVENTED THE YOGOURTH PACKAGING	2025-2026	63	ACPS Schreider Food Danone	BIOTECNOLOGIA 1º MIQ CIRCULAR SUPPLY CHAIN 2º MIQ CREATIVITY MII MIQ	Mechandasing from companies	Challenges should have a strong connection with the course

Challenge Name	Academic course	#students	Challenge Provider	Courses	Funding	Lessons learned
PLASTIC WASTE FROM ELECTRICAL WIRES	2024-2025	19	SURUS	CREATIVITY MII MIQ	Mechandasing from SURUS	Prototyping as a key value
SOCIAL INNOVATION, AI AND ACTIVE AGEING	2025-2026	21	UPM KAIST	CREATIVITY MII MIQ	A prize of 3000€ + 1 week in Korea funded by KAIST	Need support from institutions (final dates, deliverables required.)

5. DISCUSSION

The analysed experiences demonstrate that CBL constitutes much more than a pedagogical methodology; it acts as a framework for institutional transformation aligned with Industry 5.0 principles.

CBL enables the integration of teaching, research, innovation and societal engagement. The analysed experiences (Specially the one related with COVID-19) have generated 2PhD thesis, 5 research publications, prototypes, collaborative networks, educational innovation a new cultural framework for teacher in our university. This integration is particularly relevant in technical universities, where the separation between teaching and applied research has traditionally been strong. FabLabs and rapid prototyping infrastructures are critical elements of the ecosystem. Prototyping allows students to test ideas, fail safely, iterate rapidly and materialize abstract concepts [5]. This process creates meaningful learning experiences because students connect theoretical knowledge with physical experimentation.

One of the strongest aspects of the ecosystem is interdisciplinarity. Industry 5.0 challenges are inherently systemic and require collaboration across engineering, design, business, sustainability and social sciences. The challenge leader (the professor) needs to gather a lot of multidisciplinary information and act as an intermediary between students and the challenge provider (Companies, NGOs, Councils, etc.) as a coach guiding the student learning to provide solutions to the challenges. Based in our experience in the hackathon, it demonstrated that multidisciplinary teams generate richer and more innovative solutions.

The experiences identified several critical success factors. These factors are collected in the following Table 3:

TABLE 3
Key success factors

Success Factor	Importance	Comments
Motivated professors	Essential	They are the challenge leaders and coach the students through the challenge
Alignment with courses	High	Challenges should be adapted to the subject, background and age of the participants
Intermediate feedback	High	Solutions get better results if feedback is given during the challenge duration. Companies feedback are highly valuable.
External stakeholders	Essential	It's the challenge provider and connects our students with real world and real user needs
Institutional support	High	It is necessary find spaces and slots of time to solve the challenge
Funding	Necessary	It is not crucial but It is needed for material if prototyping is required, companies visits, etc. also for awards
Time for preparation	Critical	Challenge can be so complex, and the teachers need to prepare in advance (framework of the challenge, legislation, users involved, meeting with companies, technologies…)

Despite the positive outcomes, several barriers were identified. One of them is the Institutional inertia. Traditional academic structures are often incompatible with flexible schedules, multidisciplinary collaboration and challenge-driven learning. Also, we need to assess the complexity. CBL requires evaluating processes, collaboration of peers, creativity and societal impact. All of them differs significantly from traditional assessment systems.

6. CONCLUSIONS

The transition toward Industry 5.0 requires universities to rethink their educational models and institutional roles. The experiences developed within the UPM–EELISA ecosystem demonstrate that Challenge-Based Learning provides a robust framework for this transformation.

CBL contributes significantly to the development of Industry 5.0 competencies by placing students in real, multidisciplinary, and socially relevant contexts. Through challenge-driven projects, learners enhance systems thinking, creativity, collaboration, and adaptive problem-solving skills while interacting with external stakeholders and diverse teams. The iterative process of prototyping and reflection fosters resilience and the ability to deal with uncertainty, both essential characteristics of Industry 5.0 professionals. Furthermore, the integration of sustainability and circular economy principles promotes ethical awareness and responsible innovation. By combining technical knowledge with human-centered approaches, CBL prepares students to become active contributors to sustainable and resilient

innovation ecosystems. FabLabs and prototyping infrastructures play a strategic role by enabling experimentation and iterative learning. Similarly, European alliances such as EELISA provide an effective framework for scaling challenge-based educational initiatives across institutions and countries.

The analysed experiences also show that successful implementation requires a motivated faculty, institutional support, funding, alignment with curricula and collaboration with external stakeholders.

Finally, CBL framework positions universities not only as educational institutions but also, in collaboration with the challenge providers, as active agents of societal transformation, capable of generating sustainable innovation and addressing complex global challenges.

Acknowledgements: EELISA has received funding from the European Union's Erasmus+ programme under GA No. 101124676. Views and opinions expressed are however those of the author(s) only and do not necessarily reflect those of the European Union or the European Education and Culture Executive Agency (EACEA). Neither the European Union nor EACEA can be held responsible for them.

REFERENCES

[1] European Commission. Industry 5.0: Towards a sustainable, human-centric and resilient European industry (2021). https://short.upm.es/dbw09, last accessed 2026/06/17.

[2] Fisk, P. (2017). Education 4.0: The future of learning. https://www.peterfisk.com/2017/01/future-education-young-everyone-taught-together/, last accessed 2026/06/17.

[3] Nichols, M., Cator, K., & Torres, M. *Challenge Based Learning Guide*. (2016). https://www.challengebasedlearning.org/wp-content/uploads/2019/02/CBL_Guide2016.pdf, last accessed 2026/06/17.

[4] EELISA European University https://eelisa.eu/, last accessed 12/05/2026.

[5] Gershenfeld, N. How to make almost anything. *Foreign Affairs*, 91(6), pp. 43-57. (2012). https://cba.mit.edu/docs/papers/12.09.FA.pdf

[6] Johnson, L., Adams, S., & Cummins, M. Challenge-Based Learning. (2009). https://eric.ed.gov/?id=ED505102, last accessed 2026/06/17.

[7] O'Connor, S., Power, J., & Blom, N. A systematic review of CDIO knowledge library publications (2010-2020): An Overview of trends and recommendations for future research. *Australasian Journal of Engineering Education*, *28*(2), 166-180. (2023). https://doi.org/10.1080/22054952.2023.2220265

[8] Geissdoerfer, M., Savaget, P., Bocken, N., & Hultink, E. The Circular Economy – A new sustainability paradigm? *Journal of Cleaner Production*, 143, 757-768. (2017). https://doi.org/10.1016/j.jclepro.2016.12.048

Development of Foam Filling Strategies in Gyroid TPMS Structures for Enhanced Energy Absorption in Personal Protective Systems

César Aguilar Gázquez*, Clara-Luna Martin-Compaired, David Ranz Angulo, Ramón Miralbes

Universidad de Zaragoza, Zaragoza, Spain

* e-mail: 921117@unizar.es

Abstract: Personal protective systems play a fundamental role in reducing injuries caused by impact events, particularly in motorcycle helmets, where effective energy absorption is critical for preventing head trauma. Conventional helmet liners based on expanded polymeric foams present limitations associated with their fixed cellular architecture and restricted design flexibility. Additive manufacturing offers new opportunities for developing advanced architected materials with enhanced mechanical performance. This work investigates different foam infiltration strategies in Gyroid-type Triply Periodic Minimal Surface (TPMS) structures used as internal lattice architectures for motorcycle helmet applications. Due to their continuous geometry and homogeneous stress distribution, Gyroid structures are considered promising candidates for impact protection systems. Three foam filling strategies were evaluated on full-scale (1:1) helmet prototypes: direct foam application, controlled expansion using internal inserts, and a distributed microperforation matrix. The microperforation strategy (Ø 0.5 mm) facilitated air evacuation during expansion, improving foam penetration and significantly reducing internal void formation. Cross-sectional analyses confirmed a more homogeneous foam distribution and improved interaction between the polyurethane foam and the Gyroid structure. Preliminary impact tests conducted according to UNECE Regulation No. 22.06 procedures demonstrated that Gyroid-based architectures provided improved impact mitigation compared with alternative configurations. The foam-filled Gyroid helmet achieved the lowest Peak Linear Acceleration (PLA), Head Injury Criterion (HIC), and Peak Rotational Acceleration (PRA) values, achieving a PLA reduction of 12.1% compared with the reference helmet. These results indicate that hybrid Gyroid–foam structures represent a promising approach for improving energy absorption in next-generation motorcycle helmet systems.

Keywords: *Gyroid, TPMS, Additive manufacturing, Crashworthiness, Energy absorption.*

1. INTRODUCTION

Motorcycle helmets play a fundamental role in reducing head injuries during impact events [1], constituting one of the most effective passive safety systems for personal protection [2]. Conventional helmets typically combine a rigid outer shell with an expanded polymeric foam liner, such as expanded polystyrene (EPS). Although these materials dissipate impact energy through controlled crushing mechanisms, their performance is limited by their fixed cellular architecture and reduced adaptability to different impact conditions.

Recent advances in additive manufacturing have enabled the development of architected materials for advanced energy absorption systems. Among them, Triply Periodic Minimal Surface (TPMS) structures [3]have attracted considerable attention due to their continuous topology and favorable mechanical properties. In particular, the Gyroid structure [4] promotes homogeneous stress distribution and stable deformation under compressive loading.

Previous studies [5] have demonstrated the potential of TPMS structures for energy absorption applications; however, their integration into real protective systems remains limited. Furthermore, the combination of TPMS architectures with polymeric foams [6] has received relatively little attention despite the potential benefits arising from the interaction between the structure and the filler material.

This study proposes the design and fabrication of a motorcycle helmet incorporating a Gyroid TPMS structure filled with polyurethane foam. The helmet geometry was obtained by 3D scanning and subsequently processed using computational design and additive manufacturing technologies. The objective is to evaluate the feasibility of this hybrid system and its potential to improve energy absorption.

Despite their advantages, TPMS structures present manufacturing challenges associated with geometric complexity and foam infiltration [7, 8]. Defects such as voids or density inhomogeneity may affect performance, making expansion control and air evacuation critical factors during filling. To assess this approach, full-scale prototypes were fabricated and experimentally evaluated [9].

2. MATERIALS AND METHODS

2.1. Motor Helmet scanning

A commercially available motorcycle helmet corresponding to the 50th percentile male size was scanned using an HP 3D Scan Pro system. Mesh generation was performed using software version 3.2.0. The complete scan set is shown in Figure 1.



FIGURE 1
Scanner set

Two scans were acquired and merged to generate a complete helmet mesh without gaps. The resulting model was exported in OBJ format and processed in Fusion 360, where it was converted into a solid and adapted using a 570 mm head model according to UNE-EN ISO 17950, maintaining a 10 mm internal clearance. The helmet shell was hollowed to 1 mm thickness and converted into a Gyroid TPMS structure in nTopology using a 10 mm unit cell and 1.44 mm wall thickness. Lateral perforations were incorporated for fastening systems. The final model is shown in Figure 2.

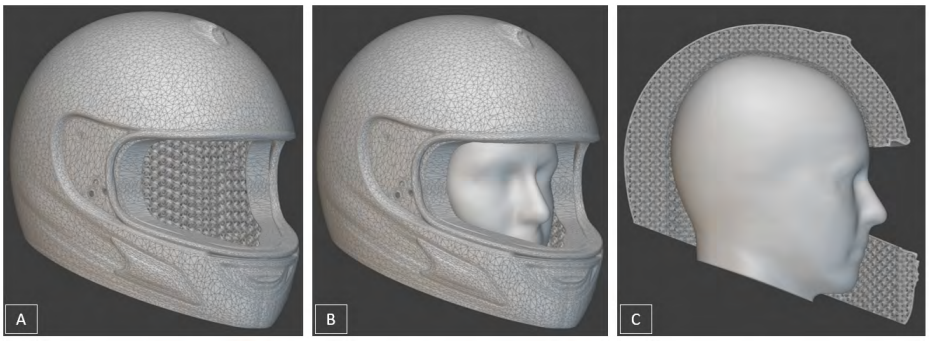


FIGURE 2
Helmet model: external geometry (A), head accommodation (B) gyroid section (C)

Following the acquisition of the model, it is exported as an STL file in order to facilitate the creation of a prototype via 3D printing.

2.2. Prototyping

Helmet prototypes were manufactured using a Bambulab H2D printer and CarbonX NylonCF material. Printing parameters are summarized in Table 1.

TABLE 1
Printer settings

Material	Nozzle temperature [°C]	Bed temperature [°C]	Infill (%)	Nozzle Diameter (mm)	Perimeters	Layer Height, (mm)
NylonCF	290	100	100	0.4	3	0.24

2.3. Foaming Material

A two-component PolyFoam polyurethane foam[10], was used as the internal energy-absorbing filler within the Gyroid TPMS structure. The material expanded to form a closed-cell foam after mixing its components.

2.4. Preliminary filling strategy and optimization of infiltration methods

Full-scale (1:1) section tests were conducted to optimize foam infiltration within the Gyroid structure. Three filling strategies were evaluated (Figure 3), with the microperforation approach (Ø 0.5 mm) providing the most homogeneous foam distribution and the lowest void content.

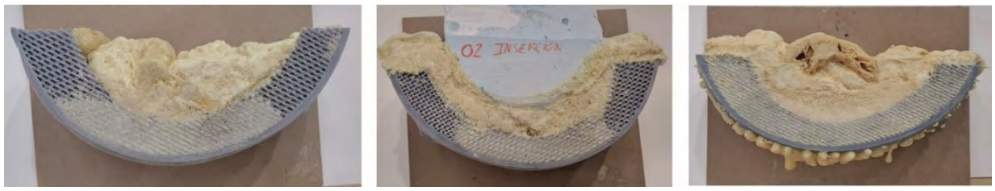


FIGURE 3
Comparison of foam filling strategies in full-scale (1:1) sections

Cross-sectional analysis of the full-scale (1:1) prototype confirmed homogeneous foam distribution, reduced void formation, and effective foam–Gyroid interaction, validating the microperforation strategy (Figure 4).



FIGURE 4
Cross-sectional views of the full-scale (1:1) Gyroid TPMS helmet after foam infiltration

2.5. Helmet Configurations for Impact Testing

Four helmet configurations were evaluated during the preliminary impact testing campaign. DT0994, a commercially available helmet designed for female users, was used as the reference configuration. The remaining helmets (DT0995–DT0997) were manufactured from the same scanned geometry using identical dimensions, materials, and fabrication procedures. The experimental configurations differed only in their internal architecture: DT0995 incorporated a Diamond lattice structure, DT0996 a Gyroid TPMS structure, and DT0997 the same Gyroid TPMS structure filled with PolyFoam R-5 rigid polyurethane foam [10]. The identical geometry of DT0996 and DT0997 ensured that any performance differences could be attributed exclusively to the presence of the foam filler.

3. RESULTS AND DISCUSSION

The manufacturing process demonstrated the feasibility of integrating Gyroid TPMS structures with polymeric foams through additive manufacturing. Among the evaluated filling strategies, the distributed microperforation matrix provided the most effective foam infiltration, promoting homogeneous distribution and reducing void formation. Cross-sectional analyses confirmed improved continuity between the foam and the Gyroid structure.

These results suggest that the interaction between the polymeric foam and the TPMS architecture may enhance mechanical stability and stress distribution under compressive and impact loading conditions, validating the proposed manufacturing approach.

3.1. Preliminary Impact Validation According to UNECE Regulation No. 22.06

To provide preliminary quantitative validation of the proposed hybrid TPMS-foam concept, impact tests were conducted at the Aragon Institute for Engineering Research (I3A), University of Zaragoza, using the impact facilities located at MotorLand Aragón (Alcañiz, Spain).

Testing was performed according to UNECE Regulation No. 22.06 procedures, including the evaluation of Peak Linear Acceleration (PLA), Head Injury Criterion (HIC), Brain Injury Criterion (BrIC), and Peak Rotational Acceleration (PRA). The comparative impact performance results are summarized in Table 2.

TABLE 2
Impact Test Results

Helmet Configuration	PLA (g)	HIC	BrIC	PRA (rad/s²)	PLA Reduction (%)
DT0994 – Woman Gyroid TPMS	746.3	7464	0.510	21027	—
DT0995 – Diamond Structure	848.3	10932	1.345	65740	—
DT0996 – Gyroid TPMS	675.0	8370	0.285	12986	9.6
DT0997 – Gyroid TPMS + Foam	655.9	7183	0.380	11275	12.1

4. CONCLUSIONS

The present study demonstrates the feasibility of integrating Gyroid TPMS structures with polymeric foam fillers for motorcycle helmet applications using additive manufacturing technologies. Full-scale prototypes were successfully fabricated and different infiltration strategies were evaluated. Among the tested methods, the microperforation strategy (Ø 0.5 mm) produced the best results, enabling more homogeneous foam distribution and reducing void formation within the gyroid structure.

From a structural perspective, the hybrid TPMS–foam configuration combines the geometric efficiency of the Gyroid architecture with the energy absorption capability of polymeric foam, showing promising potential for impact protection applications. In addition, additive manufacturing enables high geometric adaptability and design customization, facilitating the development of protective systems adapted to different morphologies and specific mechanical requirements.

The current experimental phase includes impact validation tests based on ECE 22.06 and DOT FMVSS 218 standards in order to analyze the mechanical response of the hybrid TPMS–foam structure under realistic loading conditions. These tests will allow evaluation of transmitted force, deformation mechanisms, structural stability, and energy absorption capability during impact events.

The application of this type of advanced structure in personal protective systems may contribute significantly to improving safety and health in motorcycle accidents by potentially reducing the transmission of impact energy to the user's head and minimizing the risk of severe traumatic brain injuries. In this context, the combination of TPMS architectures and energy-absorbing polymeric materials represents a promising research pathway for the development of lighter, more efficient, and highly adaptable protective systems.

Furthermore, the proposed methodology demonstrates the potential of combining additive manufacturing and TPMS architectures for the development of next-generation customizable protective systems. The use of TPMS geometries also opens new possibilities for topological and functional optimization in safety-related applications, where weight reduction, homogeneous stress distribution, and enhanced energy absorption are critical design factors.

Future work will focus on the evaluation of different elastomeric materials and polymeric foams, as well as the incorporation of structural gradients and geometric variations within the TPMS architecture in order to improve the mechanical performance and energy efficiency of the developed hybrid system.

The preliminary impact tests suggest that Gyroid TPMS architectures provide improved impact mitigation compared with the other evaluated configurations. The addition of polyurethane foam further enhanced performance, yielding the lowest PLA, HIC, and PRA values among all tested helmets. These results indicate that hybrid Gyroid–foam structures represent a promising approach for improving energy absorption in motorcycle helmet applications.

REFERENCES

[1] FIA: Helmets: A Road Manual For Decision-Makers and Practitioners, Second Edition. (2023).

[2] Cascos: manual de seguridad vial para responsables de la toma de decisiones y profesionales, 2.a edición, https://www.who.int/publications/i/item/9789240069824, last accessed 2026/04/21.

[3] Nasim, M., Hasan, M.J., Galvanetto, U.: Impact behavior of energy absorbing helmet liners with PA12 lattice structures: A computational study. Int. J. Mech. Sci. 233, 107673 (2022). https://doi.org/10.1016/J.IJMECSCI.2022.107673.

[4] Abueidda, D.W., Elhebeary, M., Shiang, C.S. (Andrew), Pang, S., Abu Al-Rub, R.K., Jasiuk, I.M.: Mechanical properties of 3D printed polymeric Gyroid cellular structures: Experimental and finite element study. Mater. Des. 165, 107597 (2019). https://doi.org/10.1016/J.MATDES.2019.107597.

[5] Miralbes, R., Pascual, F.J., Zouzias, D., Gomez, J.A., Khosroshahi, S.F., Panesar, A., Crane, N.B.: Additive Manufacturing Characterization of additive-manufactured TPMS structures under compressive loading by means of energy-absorption diagram Expert in TPMS mechanical characterization Expert in Lattice structures and CAD model of them Expert in diamo.

[6] Obi, B.E.: Polymeric Foams Structure-Property-Performance: A Design Guide. Polymeric Foams Structure-Property-Performance: A Design Guide. 1-394 (2017). https://doi.org/10.1016/C2012-0-06136-4.

[7] Lopez Taborda, L.L., Maury, H., Pacheco, J.: Design for additive manufacturing: a comprehensive review of the tendencies and limitations of methodologies. Rapid Prototyp. J. 27, 918-966 (2021). https://doi.org/10.1108/RPJ-11-2019-0296.

[8] López, C., Romera, L., Díaz, J.: Assessment of foam-filled carbon-fiber reinforced thermoplastic tubes under impact loading for energy absorption structures. Compos. Struct. 373, 119537 (2025). https://doi.org/10.1016/J.COMPSTRUCT.2025.119537.

[9] Pääkkönen, E., Ketoja, J.A., Paltakari, J.: Energy absorption and resilience in quasi-static loading of foam-formed cellulose fibre materials. Cellulose 31(11), 7137-7152 (2024). https://doi.org/10.1007/S10570-024-06030-4.

[10] Comercial Feroca S.A., "PolyFoam R-5 rigid polyurethane foam", https://feroca.com/es/espumas-de-poliuretano/713-1643-polyfoam-r-5-espuma-rigida-de-poliuetano-.html, accessed May 2026.

Accessible Light: How to Design for People with Autism Spectrum Disorder

Giusi Castaldo[a], *, Elidia Beatriz Blázquez Parra[b], M. Carmen L. de Guevara Muñoz[b], Laia Miravet Garret[b]

[a] Università degli Studi della Campania "Luigi Vanvitelli", Via Roma, 2981031 Aversa (Italy)

[b] Universidad de Málaga, C/ Doctor Ortiz Ramos, 29071, Málaga (España)

* e-mail: giusi.castaldo@unicampania.it

Abstract: As design and technological innovation evolve, there is an emerging need to place user needs and inclusion at the heart of the design process. The "Design for All" strategy aims to create environments or products that support the widest possible range of users in their activities and experiences. Similarly, people-centred design seeks to develop useful, functional solutions by involving users at every stage, from research to testing. Scientific studies on user-centred lighting design outline methodological approaches for creating accessible, sensory-rich, and interactive environments and products; these solutions ensure visual comfort and enhance the physical, visual, and spatial well-being of all users, including those with adaptive challenges. For individuals with autism spectrum disorder (ASD), for instance, both natural and artificial light play a crucial role in creating environments that facilitate the organisation and execution of daily tasks and enable access to play; they also support the use of smart devices capable of adjusting to specific needs during moments of stress or overstimulation. Against this backdrop, this paper investigates how light influences the perception, behaviour, and emotional state of individuals with ASD, with the aim of outlining adaptable and inclusive solutions. Specific case studies will be examined to understand user preferences and needs, thereby defining the affective design approaches needed to create environments and products tailored for people with intellectual and cognitive disabilities.

Keywords: *Design For All, Human Centred Design, Human Centric Light, Autism, Lighting Design.*

1. INTRODUCTION

Existing studies on the "Design for All" methodology originate from institutions and associations, revealing approaches and practical aspects of a design discipline characterised by an awareness and acceptance of diversity; the aim is to create functional, intelligent products suitable for diverse user profiles and to convey the designers' commitment to helping create a better world [1]. In this context, the design of accessible spaces, products, and systems regards user involvement as a decisive factor for enhancing interaction and design quality, thereby fostering inclusivity and innovation. Until recently, built environments were designed exclusively to meet the needs of neurotypical populations; however, there is growing recognition of the need to make spaces and products accessible to neurodivergent populations [2]. Added to this is the growing interest in and significant impact of natural and artificial lighting design on the sensory and perceptual systems of individuals in general, and those with adaptive difficulties in particular, as lighting can positively or negatively influence their daily activities [3]. Studies provide clear evidence of light-sensitivity responses in autistic users, highlighting the need to implement specific modifications in home environments to support their emotional, daily, and psychophysical well-being [4]. Against this backdrop, and building on an open, experimental line of inquiry into lighting product design for individuals with intellectual disabilities, this paper explores design processes in lighting design for individuals with autism spectrum disorder. Through case study analysis, the article proposes methodological approaches to designing products that address the diverse needs of these users, and aims to provide recommendations for designers, therapists, and industry professionals.

2. LIGHT AND DESIGN

Light is a fundamental element of our environment that influences not only our visual perception but also our emotional and mental well-being. From the outset, the light bulb's functional simplicity attracted designers and architects, lending a predominantly mechanical, functional perspective to lamp design. Since then, lighting product design has not only required consideration of various technical aspects such as light flux direction, illuminance level control, intensity, and colour temperature but has also reinforced the principle that good lighting design must place the individual at the centre, incorporating new insights into the non-visual effects of light [5], which are defined as essential principles of Human-Centric Lighting. Recently, Houser *et al.* [6] outlined the rise of human-centric lighting, termed "integrative lighting," and offered general guidelines for practice and design. Research findings by Brainard, Berson, and Thapan [7] on photoreceptors and circadian rhythms provided a scientific basis for the importance of time in lighting design. Consequently, the Commission Internationale de l'Éclairage (CIE) coined the term "integrative lighting" to describe both the physiological and psychological effects of lighting [8]. Indeed, lighting can help address psychophysical issues; when combined with daylight design, it can alleviate symptoms of disorders such as seasonal depression, which is primarily linked to mood [9]. Furthermore, factors related to the impact of natural and artificial light can alter how we interact with our environment and with other people. These elements have a particularly significant positive or negative impact on the biological and daily experiences of individuals with autism spectrum disorders.

3. DESIGN AND AUTISM

The importance of good lighting, whether natural or artificial, is evident in the way it can transform any space. Although there is extensive research on both the differences in sensory processing among autistic individuals and the effects of the indoor environment on the general population, systematic research linking these two areas remains limited. Numerous vision-based studies have identified differences in visual processing among autistic individuals across almost every aspect of visual perception. For instance, Parmar *et al.* [10] found that visual hypersensitivities to features such as light, movement, patterns, and specific colours had significant negative effects on personal well-being and daily life. Although flicker is generally associated with fluorescent lighting, Noble's research [11] treats it as a distinct issue, as it can occur with other types of electric lighting, including LED technologies. Guidelines for "autism-friendly" design often incorporate specific lighting provisions primarily the reduction of glare and the restriction of fluorescent lights due to their flicker and hum [12] or the use of dimmer switches to lower illuminance levels that can otherwise trigger behavioural issues and emotional overload [13]. By addressing sensory sensitivities and challenges in visual information processing, it is possible to implement design modifications that transform the indoor environment into a welcoming, friendly space tailored to these unique needs. In this way, design processes must also consider essential factors such as imagination, verbal and non-verbal communication, social interaction, sensory issues, behaviour, and safety to devise strategies and services that benefit caregivers and family members while positively influencing the users' psychological and emotional well-being. In this context, the design of an affective lighting product can help users interact socially, initiate physical activities, produce meaningful language, or decipher the dynamics of their nervous system states. To this end, it is necessary to incorporate technological advancements capable of detecting and communicating levels of nervous system activation, thereby enabling new investigations relevant to autism research and the Co-Design methodology [14]. This approach allows end-users and their families to participate in the design process actively, working alongside professionals to define design challenges and to ideate, conceptualise, and create well-being-oriented products that address the interests, emotions, and aspirations of autistic individuals. To better understand these design approaches, specific case studies have been selected and analysed in depth; these examples promote users' verbal and non-verbal communication using technological devices and collaborative processes involving development and prototyping. The first example is +me by Beste Özcan (Figure 1), a wearable, interactive transitional object designed to improve relational and communication skills in children with autism. With +me, a wearable neck cushion that can be squeezed and hugged and which emits affective stimuli, the therapist (or parent) can influence the object's functional behaviour via a tablet application. Through this interactive process, the child is actively encouraged to communicate and, consequently, to engage with the outside world [15].



FIG. 1
+me di Beste Özcan,2015. Project and photo on domusweb.it

Andreas Forsland's Smartstones® Touch™ product (Figure 2), on the other hand, enables simple communication via touch and light. With the ability to store thousands of messages, Smartstones Touch can support the creation of an entire user-generated non-verbal language. A simple touch can allow a mother to communicate with her autistic child, letting him know that she is outside the school or hospital or to offer him support from a distance. [16]



FIG. 2
Smartstones® Touch™ by Andreas Forsland, 2015. Photo on prnewswire.com

The case studies presented illustrate how individuals with autism spectrum disorder experience states of emotional and cognitive overload, which are often invisible from the outside yet reflect their internal experiences. Since the autonomic nervous system activation influences sensory processing, engaging in affective social interaction, initiating motor activities, producing speech, or deciphering dynamics using light and innovative technology can help us understand the needs of individuals on the autism spectrum and address these aspects within the design process. Incorporating affectivity into the design of inclusive environments and products can foster deep, meaningful connections, thereby influencing human behaviour, decision-making, and emotional well-being. In this context, lighting and technology hold the potential to bridge the gap between internal experiences and outward manifestations.

4. HOW TO DESIGN FOR PEOPLE WITH AUTISM SPECTRUM DISORDER

In recent years, assistive technology, defined by Lang *et al.* [17] as a device that facilitates the teaching of new skills, supports existing ones, or reduces the impact of disability on daily life, has increasingly been recommended to support autistic individuals in their everyday lives. The adoption of such technologies remains low due to a lack of personalisation and emotional connection to the product, issues regarding the device's aesthetic and sensory qualities, a lack of alignment with existing habits and routines, or insufficient personal interest and motivation. In the early stages of product design, the definition of affective design and that of technical and engineering specifications are typically carried out separately. Previous studies have not proposed methodologies that allow for the simultaneous determination of these parameters. To address this gap, a methodological approach is proposed that jointly considers affective design and the definition of a new product's engineering and technical specifications. To validate the proposed methodology, the thesis project by Ana Sánchez González titled Design of a Lamp Adapted for People with Autism Spectrum Disorder (ASD) is presented here. Developed for the master's program in Representation and

Design in Engineering and Architecture at the University of Málaga's School of Industrial Engineering under the supervision of Professor Elidia Beatriz Blasquez Parra and co-supervision of architect and lighting designer Giusi Castaldo, the project outlines an affective, personal approach to creating accessible and inclusive lighting products.

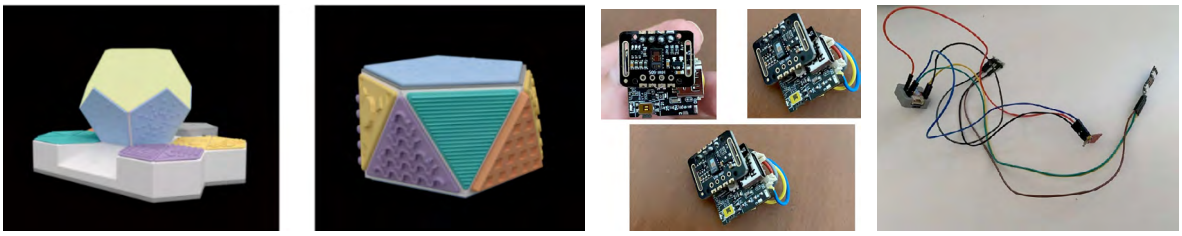


FIG. 3-4

Left. Lamp with guided breathing mode via smart bracelet and the toy accessory for use with the lamp, even during daytime activities. Right. Compact electronic components. Project and photos by Ana Sánchez González

Aimed at children aged 3 to 8, the project focuses on light functionality, form, materials, and interaction as tools to support emotional self-regulation during episodes of nighttime anxiety. The lamp connects to a smart bracelet that monitors heart rate during sleep; if an abnormal increase is detected, it activates a guided breathing mode that uses variations in light temperature and colour to help the child self-regulate intuitively. During the day, the child can carry an object that transforms part of the lamp into a portable accessory or toy (an "affective" object), customisable to each user's specific needs. High-density polyethylene (HDPE) was used to create the prototype due to its impact resistance, lightweight nature, and non-toxicity; additive manufacturing technology, specifically 3D printing based on Fused Deposition Modelling (FDM), was employed for its production. The various sensory elements were crafted from diverse materials such as wood, cork, natural rubber, and food-grade silicone. Concurrently with the prototyping phase, the electronic circuit that enables the system's functionality was developed; it comprises two main modules: (I) a wristband designed to measure heart rate and (II) the lamp. Both units are built using M5Stack Atom Lite microcontrollers, chosen for their compact size and Wi-Fi and Bluetooth compatibility, enabling efficient wireless communication between the two devices. The bracelet component utilises a MAX30102 sensor to measure the user's heart rate in real time. The lamp receives a signal from the bracelet and triggers a light display; it features programmable RGB LEDs that allow adjustment of both light colour and intensity. The entire system was programmed using the Arduino platform, which facilitated sensor control, inter-device communication, and lighting management (Figures 3-4).

This work is based on a research-through-design approach, focusing on insights and motivations gained during the prototyping phase and design practice. Furthermore, it proposes an affective design approach based on a methodology capable of integrating the emotional dimension into product design, specifically lighting products, by examining essential factors such as safety, ergonomics, comfort, ease of use, sensory adaptability, portability, modularity, and, above all, personalisation, all aimed at evoking positive emotions and fostering an empathetic bond with the user. This approach comprises five phases that

prioritise emotional elements in the development of products or interfaces: (I) Research (research into the effects of light on people with intellectual disabilities, drawing on perceptual, emotional, scientific, and technological knowledge); (II) Affective Environment (analysis of the user and the experience of the built environment); (III) Light Concept (analysis of the design concept and its realisation through sketches or visualisation tools); (IV) Prototype (product development and prototyping in the university laboratory using additive manufacturing technology); (V) Define (definition of results, representation, and validation) (Figure 5).

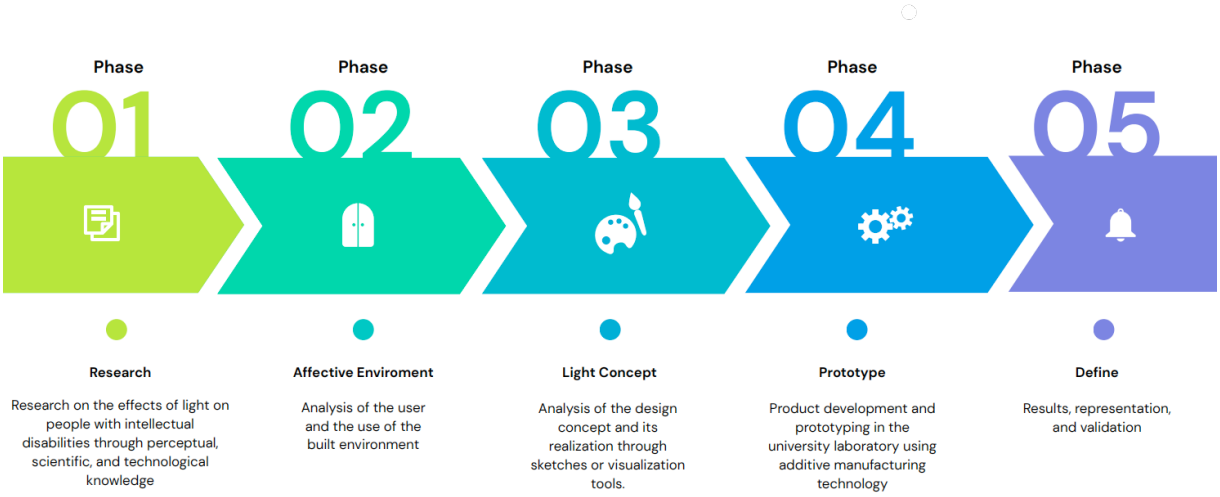


FIG. 5
Five-Step Design Process

This design approach enabled the development of a product aimed at enhancing the emotional and sensory well-being of children with autism spectrum disorder (ASD), with the intention of actively involving both the family and the user in the object's perceptual experience, as its constituent textures are customisable and adaptable.

5. CONCLUSION

Through a literature review of design and lighting processes both in general and specifically for individuals with autism spectrum disorder, this article outlines how light can influence human perception, behaviour, and emotional states. The presented case studies offer solutions and methodological approaches essential for designing products for a broad user base, demonstrating how modern technology can inspire the creation of customisable, emotionally responsive systems. This research laid the groundwork for a thesis project involving the design and prototyping of a lamp tailored for individuals with autism spectrum disorder; the project combines technical and aesthetic elements to create a customisable tool that supports daily life for people with disabilities by leveraging light to address perceptual and emotional needs.

REFERENCES

[1] O. Moret, "Back to the Future The Future in the Past.," in *ICDHS 10th+*, Barcelona, 2018.

[2] M. H. Black, S. McGarry,, L. Churchill,, E. D'Arcy,, J. Dalgleish,, I. Nash, and S. Girdler,, "Considerations of the built environment for autistic individuals: A review of the literature.,," *Autism, 26(8),* pp. 1904-1915., 2022.

[3] B. &. I. N. Noble, "Autistic people's perception of interior electric lighting systems: An initial study.," *Lighting Research & Technology, 58(1-2),* pp. 171-188., 2026.

[4] D. Heffernan, Sensory issues for adults with autism spectrum disorder., Jessica Kingsley Publishers, 2016.

[5] K. W. Houser and T. Esposito, "Human-centric lighting: Foundational considerations and a five-step design process.," *Frontiers in neurology, 12,* 2021.

[6] K. W. B. P. R. Houser, J. M. Zeitzer and M. Herf, "Human-centric lighting: Myth, magic or metaphor?.," *Lighting Research & Technology, 53(2),,* pp. 97-118. 2021.

[7] G. C. e. a. Brainard, "Action Spectrum for Melatonin Regulation in Humans: Evidence for a Novel Circadian Photoreceptor'.," *The Journal of Neuroscience, 21(16),,* 2001.

[8] CIE, "International Commission on Illumination, light-and-lighting-integrative-lighting-non-visual-effects," 2026. [Online]. Available: https://www.cie.co.at/publications/light-and-lighting-integrative-lighting-non-visual-effects.

[9] M. Gaton Moreno,, M. Gonzalez Torres, and M. Gaviria,, "Trastornos afectivos estacionales," winter blues".," *Revista de la Asociación Española de Neuropsiquiatría, 35(126),* pp. 367-380., 2015.

[10] K. R. Parmar,, C. S. Porter,, C. M. Dickinson,, J. Pelham,, P. Baimbridge, and E. Gowen,, "Visual sensory experiences from the viewpoint of autistic adults." *Frontiers in psychology, 12,* 2021.

[11] B. &. I. N. Noble, "Autistic people's perception of interior electric lighting systems: An initial study," *Lighting Research & Technology, 58(1-2),* pp. 171-188, 2026.

[12] A. Hegde, "Sensory sensitivity and the built environment.," *Lighting Design+ Application, 45(1),,* pp. 56-60., 2015.

[13] L. Chezan, J. Liu,, J. Cholewicki,, E. Drasgow, R. Ding, and A. Warman,, "A psychometric evaluation of the quality of life for children with autism spectrum disorder scale.," *Journal of Autism and Developmental Disorders, 52(4),,* pp. 1536-1552., 2022.

[14] E. B. Sanders and P. J. Stappers, " Co-creation and the new landscapes of design.," Vols. Co-design, 2008.

[15] domusweb, "beste_ozcan_me," 24 ottobre 2015. [Online]. Available: https://www.domusweb.it/it/notizie/2015/10/26/beste_ozcan_me_.html.

[16] I. Smartstones, "new-wearable-device-smartstones-touch-humanizing-technology-sensorial-communication-to-bring-people-together," 2015. [Online].

[17] R. Lang, S. Ramdoss, T. Raulston,, A. Carnet, J. Sigafoos,, R. Didden, D. Moore and M. O'Reilly, "Assistive Technology for People with Autism Spectrum Disorders.," *Assistive Technologies for People with Diverse Abilities,,* pp. 157-190, 2014.

Implementing sustainability competences in graphic expression related lectures

Eva Rodríguez Hortelano[a,*], Julen Ibarretxe[b], Maider Iturrondobeitia Ellacuria[a]

[a] Department of Graphic Design and Engineering Projects; Bilbao School of Engineering; University of the Basque Country (EHU)

[b] Department of Applied Physics I; Bilbao School of Engineering; University of the Basque Country (EHU)

* e-mail: eva.rodri@ehu.eus

Abstract: Sustainability is increasingly essential in engineering and industrial practice, yet students often struggle to integrate it into their academic work. To address this challenge, the University of the Basque Country (EHU) has strengthened sustainability within the Graphic Expression course through a project-based learning approach. The initiative involves first-year students enrolled in CAD lectures and departmental interns who support the practical activities. The course includes two projects: an introductory individual CAD assignment and a more advanced mechanical assembly design based on predefined specifications. In the second project, students model the components, manufacture them through additive manufacturing, and assemble the final system, gaining practical experience in design, in tolerances, and in functional integration. The educational innovation focuses on two aspects: circularity and Problem Based Learning (PBL). Circularity is introduced by using recycled plastic as feedstock for additive manufacturing. Interns complete the full valorisation cycle by collecting, classifying, analysing, conditioning, and extruding plastic waste into filament, which is later used by first-year students in their CAD and 3D printing practices. This process offers a tangible example of material circularity and reinforces sustainability through experiential learning the basis of PBL. Overall, this experience shows how sustainability can be effectively embedded into engineering education through hands-on learning, circular material use, and process comparison.

Keywords: *Sustainability, Circularity, CAD, Additive fabrication, 3D printing and PBL learning.*

1. INTRODUCTION

Sustainability has become an essential requirement in today's world, particularly within the industrial sector, where "green" criteria now constitute a fundamental design and operational constraint. However, students frequently fail to fully integrate a sustainability perspective into their academic work. In response, universities are intensifying their efforts to strengthen this dimension in higher education, with the aim of providing students with a solid grounding in sustainability and opportunities for practical experience in environmentally responsible practices.

At the University of the Basque Country (EHU), the sustainable academic curriculum has been strengthened within the Graphic Expression course. Within the Graphic Design and Engineering Projects Department, two groups of students are involved in this initiative: a larger cohort enrolled in the Graphic Expression lectures and a smaller group consisting of departmental interns. In this subject, first-year students engage in Computer-Aided Design (CAD) lectures are structured around two projects: an initial individual project designed to introduce them to CAD tools, and a second, more comprehensive project in which they are required to design a mechanical assembly based on a predefined set of specifications. In the latter project, students first model all components of the assembly, ensuring that the overall functional performance of the system is achieved. They then manufacture these components using additive manufacturing techniques and physically assemble them, thereby gaining deeper experience in additive manufacturing processes, the complexity of mechanical assemblies, and key aspects such as dimensional tolerances and functional dimensioning.

Two main innovations are introduced in this educational experience: first, providing students with direct exposure to circularity, and second, turning manufacturing into a hands-on learning objective. With respect to circularity, the additive manufacturing process is carried out using recycled material. The intern students are completing the full cycle of material valorisation: they collect plastic waste, classify, analyse the different plastic properties, select suitable fractions, condition these materials for filament production, and ultimately extrude a filament that can be used as feedstock in a 3D printer. Then, first course students will be involved in all the process by using the filament in the printer in the CAD practices. This process offers a highly illustrative example of material circularity in practice, reinforcing sustainability principles through experiential learning.

We present a study on how sustainability can be effectively integrated into the engineering curriculum, thereby providing students with a substantially enriched understanding of sustainability and its relevance to engineering practice.

2. OBJECTIVE

The main objective of this project is to reuse selected plastic waste fractions generated at the Bilbao School of Engineering, Building II, as 3D printing material for the computer-based practical sessions of the core course Graphic Expression I.

The secondary objectives are:

1. To implement a feasible collection device for the selected waste fraction identified in previous works.
2. To develop a reuse protocol for the selected waste fractions.
3. To prototype mechanical assemblies and geometric surfaces studied in Graphic Expression I using 3D printing.
4. To evaluate the results, assess their environmental impact, and communicate the outcomes.

3. METHODS AND RESULTS

This project defined its main goal as promoting responsible waste management within the Bilbao School of Engineering, Building II. There is a prior work, which enabled the qualitative and quantitative characterization of general waste streams and the identification of viable end-of-life options for the collected fractions, including reuse and recycling. Based on those findings, the present project seeks to go one-step further by transforming selected plastic waste fractions into a usable feedstock for 3D printing in teaching activities.

This approach responds to both environmental and educational needs. On one hand, it reduces dependence on virgin material for academic 3D printing practices. On the other hand, it strengthens sustainability awareness among students by linking waste generation, material recovery, and practical academic use within the same educational environment. The project is organized into four main tasks, as shown in Figure 1.

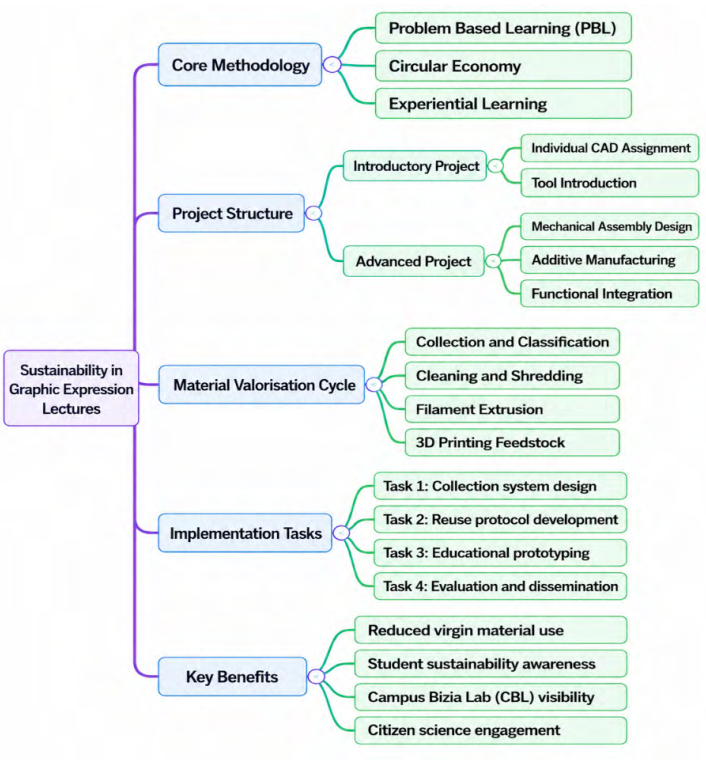


FIG 1
The complete diagram of the tasks of the project

Task 1: Collection system design. A collection device has been installed specifically for the selected plastic waste fraction, plastic PET bottles, and other materials plastic bottles will be discarded in the following steps. The design has been adapted to the operational conditions of Building II and to the characteristics of the waste-generating users. A QR has been included to inform students about the sustainable material recovery and for encoring participation. Interestingly, a collection schedule has also been established.

Task 2: Reuse protocol development. A complete reuse protocol has been defined, including cleaning, disinfection, shredding, and processing steps. The study will focus on the technical conditions required to obtain a suitable filament, especially temperature, speed, flow, and extrusion rate. The resulting material must meet the requirements for use in 3D printers.

Before recycled plastics can be processed into new filament for 3D printing, they should undergo an appropriate cleaning and disinfection procedure to remove contaminants, organic residues, and potential microorganisms that may affect material quality or pose handling risks. This stage typically involves washing with suitable detergents, followed by chemical or thermal disinfection depending on the type of polymer and its intended application.

Disinfection protocol for PET bottles prior to filament production. After collection, PET bottles should first be sorted to remove non-PET materials, labels, caps, adhesives, and visible contaminants. The bottles should then be washed with warm water (40-60 °C) and a mild alkaline detergent to eliminate dirt and organic residues, followed by thorough rinsing with clean water. Disinfection can be carried out by immersion in a 0.1% sodium hypochlorite solution for approximately 10 minutes or by using a 70% ethanol solution when appropriate. After disinfection, the bottles should be rinsed with deionized or potable water (particularly after sodium hypochlorite treatment) and allowed to dry completely, preferably in a ventilated oven at 60-70 °C or under clean-air conditions. Complete drying is essential because PET is hygroscopic, and residual moisture can lead to hydrolytic degradation during extrusion, reducing the mechanical properties and printability of the recycled filament. Proper cleaning not only improves the safety of the recycling process but also enhances the consistency and performance of the resulting filament by reducing impurities that could interfere with extrusion or compromise the mechanical properties of the printed parts. This protocol provides an effective balance between hygiene, material preservation, and process reliability for educational and laboratory-scale filament production.

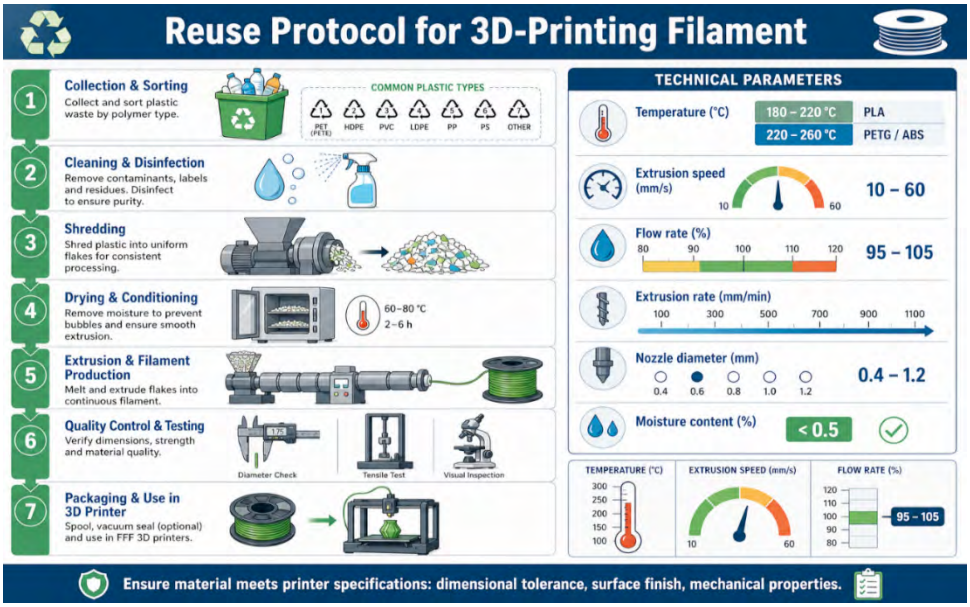


FIG 2
Developed protocol for reusing. (Drawn with IA)

The filament selected for 3D printing should meet both technical and sustainability requirements. From a technical perspective, it must ensure dimensional accuracy, reliable extrusion, good layer adhesion, and compatibility with the printer's operating conditions. When filament is produced from recycled PET bottles (rPET), additional requirements must be satisfied to ensure both printability and sustainability. The recovered PET should be carefully processed under controlled extrusion conditions to obtain a filament with a uniform diameter and consistent mechanical properties. The resulting filament should exhibit adequate tensile strength, thermal stability, and reliable layer adhesion while maintaining dimensional tolerances (typically ±0.05 mm) to ensure continuous feeding and high-quality printing. From a sustainability perspective, the recycling process should maximize material recovery, minimize energy consumption and waste generation, and preserve the recyclability of the material, thereby supporting circular economy principles and reducing the environmental impact of additive manufacturing activities.

Task 3: Educational prototyping. Once a viable filament has been obtained, 3D prototypes will be produced. These will include mechanical assemblies, surfaces, and surface intersections that are part of the syllabus of Graphic Expression I. Computer-aided design software, more specifically Solid Edge 2025, will be used to model the parts, analyse assemblies, and prepare them for additive manufacturing.

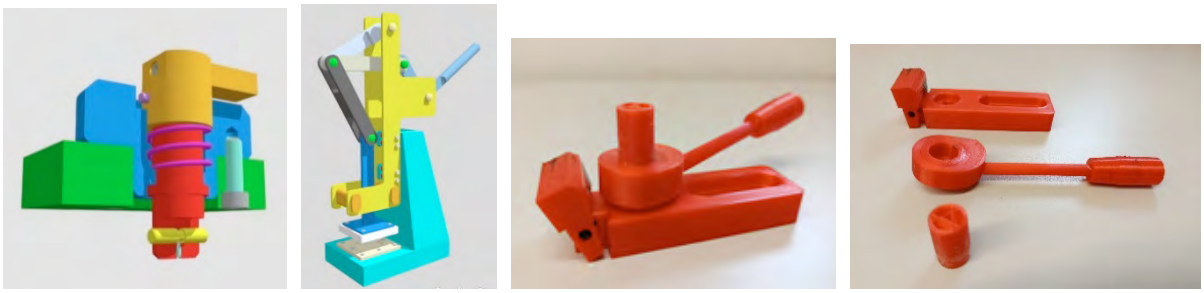


FIG 3
Some of the printed prototypes

Task 4: Evaluation and dissemination. The final stage will assess user satisfaction, technical performance, and the environmental, economic, and social impacts of replacing virgin material with reused plastic waste. Life Cycle Assessment and eco-design methodologies had been applied, drawing on the expertise of the research group.

TABLE 1
The project's LCA analysis (data collected by the authors)

Impact Category	Unit	Landfill	Recycling	Reduction (%)
Fine particulate matter formation	kg PM2.5 eq	0.777637	0.731651	5.91%
Fossil resource scarcity	kg oil eq	140.553	134.901	4.02%
Freshwater ecotoxicity	kg 1,4-DCB	16.3434	13.6503	16.48%
Freshwater eutrophication	kg P eq	0.127103	0.118625	6.67%
Global warming	kg CO_2 eq	488.746	464.873	4.88%
Human carcinogenic toxicity	kg 1,4-DCB	17.4925	16.4167	6.15%
Human non-carcinogenic toxicity	kg 1,4-DCB	375.843	347.345	7.59%
Ionizing radiation	kBq Co-60 eq	33.2739	32.8328	1.33%
Land use	m^2a crop eq	3.26684	3.08453	5.58%
Marine ecotoxicity	kg 1,4-DCB	21.7586	18.2507	16.13%
Marine eutrophication	kg N eq	0.011058	0.009646	12.77%
Mineral resource scarcity	kg Cu eq	5.40235	5.37228	0.56%
Ozone formation (Human health)	kg NOx eq	1.09084	1.02908	5.66%
Ozone formation (Terrestrial ecosystems)	kg NOx eq	1.10944	1.04685	5.64%
Stratospheric ozone depletion	kg CFC11 eq	0.000311523	0.000302250	2.98%
Terrestrial acidification	kg SO_2 eq	1.82900	1.76029	3.76%
Terrestrial ecotoxicity	kg 1,4-DCB	1294.33	1245.56	3.77%
Water consumption	m^3	5.12293	5.04582	1.51%

4. INDIRECT BENEFITS

The implementation of this project yields several multifaceted benefits that extend beyond the primary academic objectives:

—**Educational Impact: From Awareness to Competence.** This initiative moves beyond theoretical sustainability by embedding it into mandatory coursework [1] [2]. Students develop integrated technical literacy by applying CAD tools to mechanical assemblies and surface intersections while navigating the specific constraints of recycled materials [3]. Furthermore, by engaging with Life Cycle Assessment (LCA) and eco-design methodologies, students transition from simple "awareness" to professional technical competence in sustainable engineering [1] [3].

—**Environmental Impact: Localized Circularity.** The project creates a tangible "micro-circular economy" within the Bilbao School of Engineering by transforming a local waste stream into academic feedstock [4] [5]. This directly reduces the university's dependence on virgin materials for 3D printing practices and provides a practical demonstration of the "full valorisation cycle"—from collection and classification to extrusion and reuse [6] [7].

—**Institutional and Social Impact: Citizen Science.** The use of QR codes on collection devices serves as a "Citizen Science" tool, turning a technical task into a shared community effort [2]. This approach promotes the initiative more effectively than conventional campus communication, as it requires active participation from both the students in the course and the wider campus community [2].

5. CONCLUSIONS

This project successfully integrates waste management, additive manufacturing, and sustainability education into a single, applied academic framework. By closing the loop between departmental interns (producers) and first-year students (consumers), the initiative establishes a practical circular-economy model that enhances both environmental outcomes and teaching quality.

The technical success of the reuse protocol and the resulting 3D prototypes demonstrate that campus waste can be effectively valorised for complex engineering tasks, such as functional dimensioning and mechanical assembly. Furthermore, the project offers a transferable framework for other educational institutions seeking to link responsible waste recovery with active student participation.

Ultimately, the results of this study—specifically the evaluation of technical performance and environmental impact—are going to be presented to the school administration as a refined protocol for institutional implementation, aiming to permanently embed circularity within the university's operational and academic structure.

REFERENCES

[1] E. MacArthur Foundation.: The new plastics economy: Rethinking the future of plastics. https://content.ellenmacarthurfoundation.org/m/78d6bbcaadecd796/original/The-New-Plastics-Economy-Catalysing-action.pdfellenmacarthurfoundation (2016).

[2] European Commission.: Circular economy action plan. European Commission. https://environment.ec.europa.eu/topics/circular-economy-topics/first-circular-economy-action-plan_enenvironment.europa. (2020).

[3] Gebler, M., Schoot Uiterkamp, A. J. M., Visser, C.: A global sustainability perspective on 3D printing technologies. Energy Policy, 74, 158-167. https://doi.org/10.1016/j.enpol.2014.08.033ideas.repec (2014).

[4] Hopewell, J., Dvorak, R., Kosior, E.: Plastics recycling: Challenges and opportunities. Philosophical Transactions of the Royal Society B: Biological Sciences, 364(1526), 2115-2126. https://doi.org/10.1098/rstb.2008.0311pubmed.ncbi.nlm.nih (2009).

[5] Kreiger, M., Pearce, J. M.: Environmental life cycle analysis of distributed three-dimensional printing and conventional manuf. of polymer prod. ACS Sustainable Chemistry & Engineering, 1(12), 1511-1519. https://doi.org/10.1021/sc400093kpubs.acs+1 (2013).

[6] Pearce, J. M.: Open-source lab: How to build your own hardware and reduce scientific research costs. Elsevier.digitalcommons.mtu (2014).

[7] Ragaert, K., Delva, L., Van Geem, K.: Mechanical and chemical recycling of solid plastic waste. Waste Management, 69, 24-58. https://doi.org/10.1016/j.wasman.2017.07.044biblio.ugent+1 (2017).

Improving Interoperability in Civil Engineering: IFC4.3 workflow

Pedro Lastra-González*, Borja Arroyo, Cristina Manchado

EgiCAD Research Group, Universidad de Cantabria, Dpto. de Ingeniería Geográfica y Técnicas de Expresión Gráfica, Av. de los Castros 44, Cantabria, Spain

* e-mail: lastragp@unican.es

Abstract: Despite the capabilities and development of Civil 3D for the design of public works, export to IFC 4.3 is supported by a beta version of a plugin whose configuration is based on editing JSON files. Therefore, there is no specific interface to guide the process directly in Civil 3D. This paper presents the procedure used to export a linear infrastructure model from Civil 3D to IFC 4.3, divided into four basic stages: georeferencing, definition of the main export criteria, classification of objects in Civil 3D according to IFC 4.3 entities, and the configuration of the parameters that should be exported. These steps basically correspond to the JSON files that must be configured. In the case presented, the design of a low traffic level road has been carried out, which nevertheless includes all types of horizontal and vertical alignment elements. In addition, the most significant parameters concerning the design of the road, and its mechanical and functional performance, have been incorporated in order to evaluate the environmental impact and road safety.

Keywords: *Civil 3D, IFC4.3, Interoperability, OpenBIM, Road parametric modelling.*

1. INTRODUCTION

OpenBIM has modified the life cycle of projects related to public works in general, and road infrastructure in particular, enabling the exchange among different users, disciplines and software applications. It promotes interoperability, improves collaboration, and helps ensure that digital data remain usable over time, regardless of the tools chosen by each participant. The ISO 16739-1 governs data exchange, and its 2024 update introduced significant enhancements for the civil engineering area, especially for linear infrastructures. Currently it is possible to work with alignment geometry natively in the IFC schema, which remains the most used format to share projects' information under OpenBIM principles. In addition, this last modification has included new dedicated domains for infrastructure, with entities such as IfcRoad, IfcRailway and IfcBridge among other, therefore the IFC4.3 standard has become much more suitable for civil works projects.

Civil 3D is one of the most widely used software tools in civil engineering projects. It is Autodesk's specialized software for public works design, with particular strength in linear infrastructure, earthworks, and water supply or drainage networks. Although it is adapted for use within BIM methodology, exporting a project to the IFC4.3 standard is still under development, only supported via a beta extension with several manual configuration and mapping procedures. In fact, buildingSMART certifies different applications when they demonstrate the capacity to export IFC files reliably, yet Civil 3D is not included in any of the IFC versions published to date [1]. Several authors have developed different plugins to enhance the interoperability of road projects and address this and other related challenges. Civil 3D software has generally been used to create the road alignment and the modelling of 3D solids defining the linear infrastructure for volume quantification; it has then been combined with other software such as Revit, Rhinoceros, and Dynamo to implement various BIM uses [2]. Visual Programming Language (VPL) is one of the most commonly used alternatives by experienced users to enhance the capabilities of design software [3]. It has been used to create applications that improve IFC export and the management of properties that are necessary for design, impact assessment, and the operation of the infrastructure [4], however, this solution requires specific programming knowledge.

Despite the advances introduced by the new IFC4.3 standard for civil infrastructure beyond traditional building projects, the current plug-in available to manage the export from Civil 3D is far behind other Autodesk software solutions, which allow users to auto-select different schemas or provide specific Model View Definitions depending on the discipline they are working with. Consequently, in the case of Civil 3D, it becomes necessary to understand the structure and operation of the JSON configuration files that govern IFC export behaviour, as well as to manually modify or adjust these files. Likewise, an in-depth understanding of the IFC files—its hierarchical organization, entity behaviour and schema constraints—is required to ensure a correct model generation.

This work presents the methodology applied to export a roadway project designed in Civil 3D to the IFC4.3 schema by using the new Civil 3D extension. It details the configuration strategy adopted, identifies the main challenges encountered during the process, and outlines the best practices derived from the experience of the authors. Some key properties related to road safety, as well as their environmental impact, serve as a vehicle to illustrate the procedure.

2. ROAD MODEL AND SAFETY PARAMETERS

To define the IFC 4.3 export process, as well as to select the parameters that define road safety, a linear infrastructure project has been modelled incorporating all possible variables in terms of its alignment, using a simple pavement structure consisting of a single bituminous layer. This approach has been adopted because pavement layers do not represent a singular variable that significantly affects the model behaviour, whereas the export of alignment elements—including clothoids in horizontal alignment transitions and parabolic curves in vertical alignment—are features that did not have dedicated entities prior to the IFC 4.3 standard. Currently, in the new IFC 4.3 standard, linear models are structured using a hierarchical approach in which IfcRoad represents the overall facility. Linear design elements such as corridors are not directly mapped as IfcRoad, but rather decomposed into multiple components, typically including IfcRoadPart. Alignments are represented using the dedicated IfcAlignment entity, which enables the explicit definition of horizontal and vertical geometry through IfcAlignmentHorizontal and IfcAlignmentVertical. This represents a significant improvement compared to previous IFC versions, where alignment geometry had to be approximated using generic geometric representations. Consequently, a single surface layer (AC16S) has been directly modelled, assumed it is borne by a conventional subgrade layer, representing a traditional low-traffic road according to T42 category [5]. Once the road has been modelled, its design must ensure minimum conditions of comfort and safety. In this case, the parameters that most significantly influence both traffic safety and environmental impact have been selected and divided into three main categories: design, mechanical, and functional parameters (Table 1). The first group includes the most important parameters that define the mixture design, the second comprises those determining its mechanical behaviour according to applicable standards [6], and finally, the third group includes those related with the functional performance properties such as skid resistance. These properties were selected due to the impact that insufficient skid resistance has on road safety [7], as well as the formation of defects such as potholes or cracks. In addition, environmental impact largely depends on the manufacturing temperature of the mixture, which is conditioned by the type of bitumen used [8]. They were incorporated into Civil 3D as a Property Set.

TABLE 1
Parameters included in the road model

DEFINITION	MECHANICAL	FUNCTIONAL
Type of bituminous mixture	Density (g/cm3)	Skid Resistance (SCRIM)
Binder percentage (%)	Voids (%)	Skid resistance (BPN)
Manufacturing temperature (°C)	Plastic deformation (mm/1000 cycles)	
Binder type	Water sensitivity (%)	

3. IFC4.3 EXPORTATION

The Civil 3D beta extension for exporting to the IFC 4.3 standard is structured into four steps. The first step, once the model has been georeferenced is to position the IFC base point. It is essential that the selected point has zero meters of elevation, by this way the elevations defined in the Civil 3D model are preserved in the IFC model. The reason is that elevation assigned to the IFC base point will be considered as the new zero level in the IFC model; therefore, it should not be modified if we want to maintain the original elevations.

Second step is managed by the IfcInfraConfiguration.json file. Although it has additional functions, is primarily used to define what objects of the civil model library are going to be exported or imported. In this case, the default tolerance has been maintained at 0.002 m, and export has been enabled for alignments, corridors, surfaces, and bodies. Additionally, some identification data have been completed. Figure 1 presents some of these variables.



FIG. 1
Properties of IfcInfraConfiguration.json file

The IfcInfraExportMapping.json file performs the third step. It defines the semantic mapping between Civil3D objects and IFC4.3 entities. While the previous file defines what is exported, this one determines the specific IFC4.3 entity to which each object belongs. This file shows one of the main differences of this official standard compared to previous version. The Figure 2 presents all the possibilities to map the different objects. It is important to note that 3D solids cannot be exported using a style or name, so they are mapped by CADLayerName attribute as method to quantify the volume of the earthworks or the layers of the road. In this case, alignments and profiles styles were mapped to

IfcAlignment, both IfcAlignmentHorizontal and IfcAlignmentVertical respectively, while corridor-based elements were mapped into the IfcRoad spatial structure, generating associated IfcRoadPart elements depending on their functional role (e.g., lanes, shoulders, or slopes).



FIG. 2
Properties of IfcInfraExportMapping.json file

The last step is governed by IfcInfraExportPropertyMapping.json file. It defines the properties linked with each one of the objects exported to IFC4.3. In this case, Civil 3D includes a huge number of properties by default, including a large amount of information related to internal Civil parameters in addition to the Property Set created with the different parameters of the road. In this context, the IfcInfraExportPropertyMapping.json includes only the properties associated with the project, as well as the properties related to the road. Consequently, the previously defined Property Set has been applied to rood IfcRoad entity, as it can be seen in Figure 3.



FIG. 3
Bituminous mixture properties of IfcInfraExportPropertyMapping.json file

4. RESULTS

The model according to the IFC4.3 standard is presented below; the terrain has been hidden in order to highlight the road. BIM Vision v3.1.0 software has been used to show the model, a composition of its different windows is presented in Figure 4.

Firstly, the alignment geometry is consistent with the design developed in Civil 3D. In the lower-left image of the figure, the different categories used to export the model can be observed. The terrain is contained in the Site Category, while the different components of the pavement (lane, shoulder, and slopes) are classified as IfcRoadPart and belong to an IfcRoad category. Finally, within the IfcAlignment category, there are two IfcAlignmentVertical elements linked to the road and the terrain profiles, as well as one IfcAlignmentHorizontal representing the horizontal alignment. The lower-right image shows the properties of the IfcRoad category, which are those previously defined.

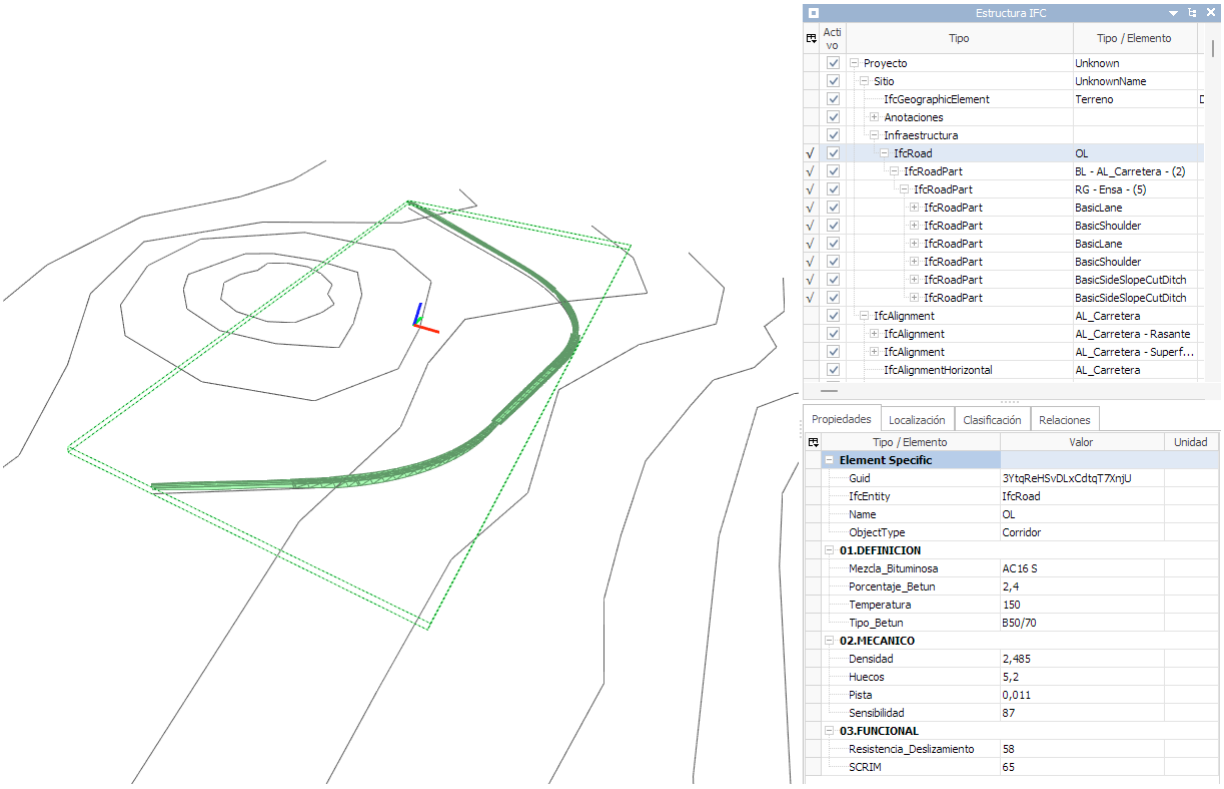


FIG. 4
Model according IFC4.3 standard with BIM vision software

Therefore, this beta version is useful to improve the Interoperability in the Civil Engineering field and export a linear infrastructure model developed by Civil3d according to IFC4.3 standard. The results demonstrate that IFC 4.3 significantly improves the representation of linear infrastructure through the introduction of dedicated entities such as IfcRoad and IfcAlignment. The exported model preserves the geometric definition of the alignment and enables a structured organization of road components.

However, the current implementation of IFC export in Civil 3D remains limited, particularly in terms of semantic richness and automation. The reliance on manual JSON configuration files, together with the lack of standardized Property Sets for pavement materials, highlights the need for further development or the use of alternative software such as Dynamo.

Future work should focus on improving the linkage between material definitions and performance properties, as well as on the standardization of infrastructure-specific Property Sets to enhance interoperability within OpenBIM workflows.

REFERENCES

[1] BUILDINGSMART INTERNATIONAL Homepage, Compliance: Software Certification, https://www.buildingsmart.org/compliance/software-certification/ifc/, last accessed 2026/05/11.

[2] Biancardo, S. A., Capano, A., Guerra de Oliveira, Sara., Tibau, Andrej.: Integration of BIM and Procedural Modeling Tools for Road Design. Infrastructures, 5(4), 37, doi: 10.3390/infrastructures5040037 (2020).

[3] Intignano, M., Biancardo, S. A., Guerra de Oliveira, S., Tibaut, A., Dell'Acqua, G.: Semantic-Driven Automation of BIM for Stone-Paved Roads: An Ontology-VPL Integrated Approach. Journal of Computational and Cognitive Engineering, 5(1) 103-114 doi: 10.47852/bonviewJCCE52025931 (2026).

[4] Peña, C. A., Camacho-Torregrosa, F. J., García, A.: BIM-based flowchart for improving road construction planning and management. Automation in Construction, 184, 106845, doi: 10.1016/j.autcon.2026.106845 (2026).

[5] NORMA 6.1 IC: SECCIONES DE FIRMES, Orden FOM/3460/2003, de 28 de noviembre, por la que se aprueba la norma 6.1 IC SECCIONES DE FIRME de la Instrucción de Carreteras. BOE de 12 de diciembre de 2003.

[6] Artículo 542. Mezclas bituminosas en caliente tipo hormigón bituminoso. Pliego de Prescripciones Técnicas Generales para obras de carreteras y puentes (PG-3). Ministerio de Fomento, Gobierno de España (2014).

[7] Tarnini, Y., Gharaibeh, N. G., Kutela, B., Gao, L.: Assessing Pavement Crash Susceptibility forConsideration in Pavement Management Decisions. Journal of Transportation Engineering Part B: Pavements, 152(2), 04026015 doi: 10.1061/JPEODX.PVENG-1911 (2026).

[8] De Pascale, B., Tataranni, P., Indacoechea-Vega, I., Rodriguez-Hernandez, J., Lantieri, C., Bonoli, A. Enhancing road performance and sustainability: A study on recycled porous warm mix asphalt. Science of The Total Environment, 960, 178370, doi: 10.1016/j.scitotenv.2025.178370 (2025).

Dynamo based methodology for checking networks after construction vs BIM models

Borja Aroyo*, Pedro Lastra-González, Cristina Manchado

EgiCAD, Departamento de Ingeniería Geográfica y Técnicas de Expresión Gráfica,
Universidad de Cantabria, E.T.S. de Ingenieros de Caminos, Canales y Puertos, 39005 Santander, Spain

* e-mail: arroyob@unican.es

Abstract: Building Information Modelling (BIM) is an effective methodology for managing civil engineering projects throughout their entire lifecycle; however, its reliability depends on accurately representing as-built conditions. Accurate BIM modelling of sanitation and drainage networks is closely linked to pollution prevention, as the appropriate design of slopes, elevations, and key elements helps prevent issues such as uncontrolled discharges and network cross-contamination, while also enabling reliable simulations of extreme events. Consequently, reliable BIM models can contribute to improving environmental, animal, and human health, representing a step forward towards the One Health approach. This paper presents a methodology for automating the verification of BIM models for civil engineering networks using visual programming with Dynamo. As a case study, the methodology is applied to a sanitation network comprising several inspection chambers connected by pipes, comparing a Revit model with as-built data based on UTM X-Y coordinates, elevations, and the unique identifiers of each element. The workflow includes data processing, extraction of geometric parameters from the BIM model, and automated verification against on-site records. The proposed methodology identifies discrepancies both graphically and through an automatically generated report, reducing verification time and manual effort while improving the accuracy and reliability of BIM-based network verification processes.

Keywords: *BIM, 3D Model, Network Checking, Civil Engineering, Revit, Dynamo.*

1. INTRODUCTION

Building Information Modelling (BIM) has become the standard methodology for managing civil engineering projects throughout their design, construction and operation phases [1,2]. Its effectiveness, however, depends on the ability of BIM models to accurately represent as-built conditions, particularly for service networks, whose verification is essential during operation.

Accurate BIM models of sanitation and drainage networks are closely related to pollution prevention. The correct representation of slopes, elevations, manholes, collectors and discharge points enables reliable simulations of extreme rainfall events, wastewater spills and similar scenarios, helping to prevent uncontrolled discharges into natural watercourses and cross-contamination between networks. Consequently, reliable BIM models contribute to improving environmental, animal and human health, supporting the One Health approach.

The verification of BIM network models is generally a repetitive and time-consuming task that is prone to human error when performed manually [3]. Although some software packages provide as-built tools for clash detection, they do not assess the actual physical location of infrastructure elements using topographic data. Likewise, while scan-to-BIM approaches are highly effective for accessible facilities, they cannot be applied to underground infrastructures once construction has been completed, as in the present case.

This paper presents a methodology for automating the verification of BIM models for civil engineering networks using visual programming in Dynamo [4–10]. The proposed workflow compares a Revit model with as-built staking data to identify discrepancies, both graphically within the BIM model and through an automatically generated report. The methodology is validated through its application to a sanitation network (inspection chambers and pipes).

2. PROPOSED METHODOLOGY

The following section provides a concise overview of the proposed methodology, as well as a description of the input elements for the verification, and the BIM requirements to ensure the correct operation of the script presented.

2.1. Inputs and BIM requirements

The first input is the facility as-built staking data, which must include the UTM X, Y and Z coordinates of the centre of each inspection chamber cover and the invert level (water level) at one end of each pipe, coinciding with an inspection chamber. Each element must also be assigned a unique identifier (ID). The data must be provided in Excel or a compatible format. For the Dynamo script to operate correctly, the spreadsheet must contain a header row, followed by one row per element with the data arranged as follows (Figure 1): ID (Column A), X (Column B), Y (Column C), Z (Column D), and optional descriptions or other attributes (Columns E onwards), which are ignored by the script.

	A	B	C	D	E
1	ID	X	Y	Z	DESC
2	ELE_L1_POZ_01	433934,889	4809814,931	6,5	Z_TAPA
3	ELE_L1_POZ_02	433992,347	4809803,6	6,566	Z_TAPA
4	ELE_L1_PRI_8TO160_01	433934,889	4809814,931	5,41	Z_LÁMINA_AGUA
5	ELE_L1_PRI_8TO160_02	433992,347	4809803,6	5,41	Z_LÁMINA_AGUA

FIG. 1
Appearance of the set-out data sheet

The second input is the BIM model to be verified, in which inspection chambers and pipes are modelled in Revit using any suitable family templates. Although the model may contain additional elements, these are ignored by the script. Each inspection chamber and pipe must include a unique identifier (ID) matching exactly the corresponding identifier in the as-built staking data (Figure 2). In addition, the element type names must contain the strings “Arqueta” and “Tubo” to ensure correct script execution.

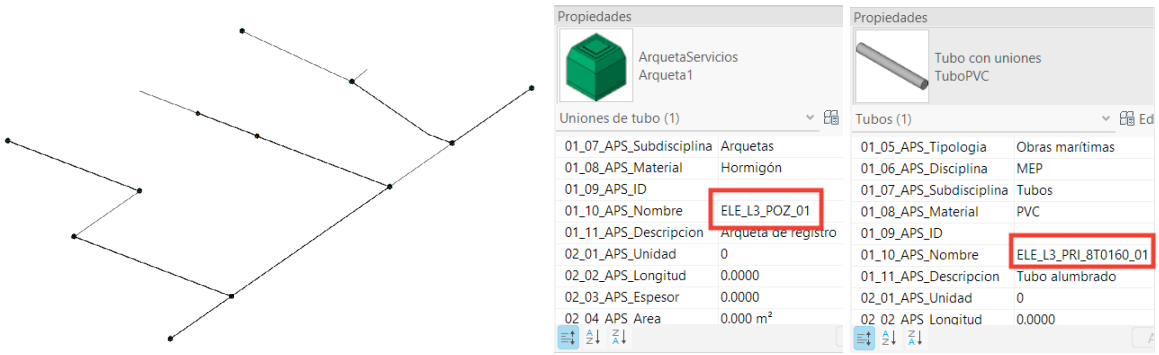


FIG. 2
Appearance of the BIM model in Revit

2.2. Script methodology

The proposed methodology starts by importing the Revit BIM elements into Dynamo. Their unique identifiers (IDs) and surfaces are then extracted using the Parameter.ParameterByName and Element.Faces nodes, together with the required list operations. Next, inspection chambers and pipes are identified by filtering the imported elements according to their type (Figure 3), while all other elements are ignored. Finally, the List.GetItemAtIndex node is used to generate, for each element type, three lists containing the IDs, the corresponding surfaces, and the elements themselves.

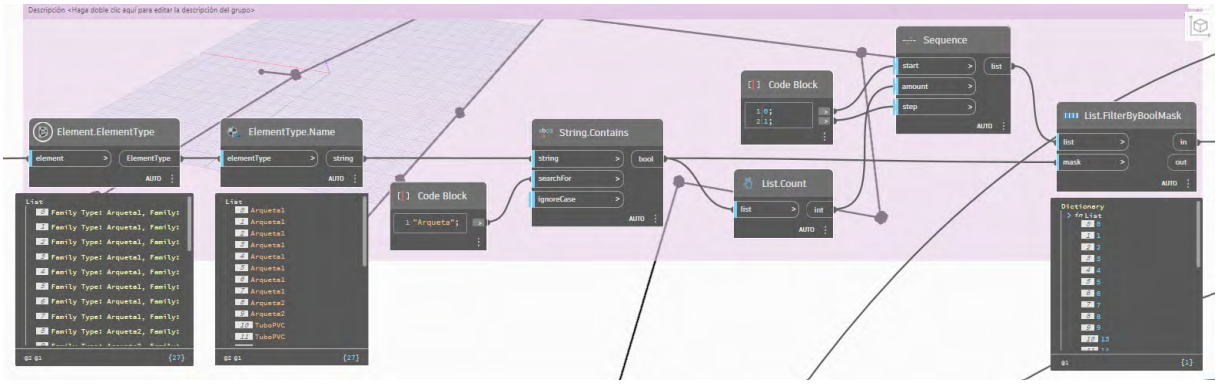


FIG. 3
List containing the inspection chamber indexes from the imported list of elements

For inspection chambers, the objective is to obtain a list containing the ID and the Xm, Ym, and Zm coordinates of the cover centre for each element. Several approaches based on the bounding box were evaluated but proved unsuitable for all geometries. Instead, the adopted method calculates the centroid of every surface composing the element and selects the one with the highest Zm value (Figure 4). This approach reliably identifies the cover centre regardless of the chamber geometry, including inclined conical frustums.

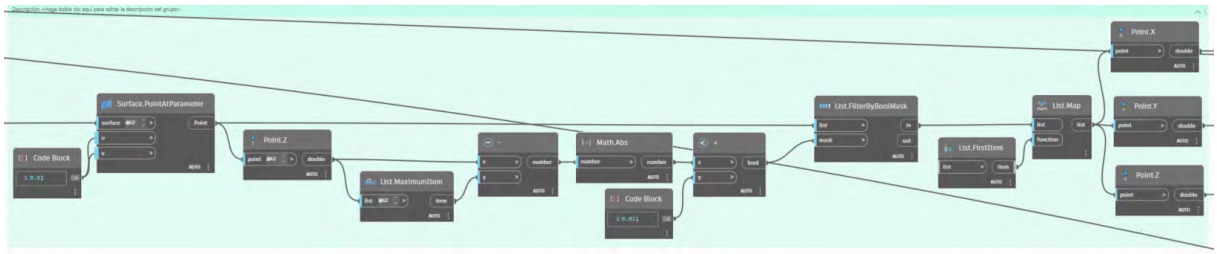


FIG. 4
Determination of the inspection chamber covers centers

The first target for the tubes is to obtain a list that contains for each element the ID and Xm,Ym,Zm coordinates of the invert level (water level) at both ends of each pipe. This is done, as presented in Figure 5, by obtaining the axis of each pipe and then, by means of a bounding box, its radius which allows to calculate the invert level at each edge of the axis.

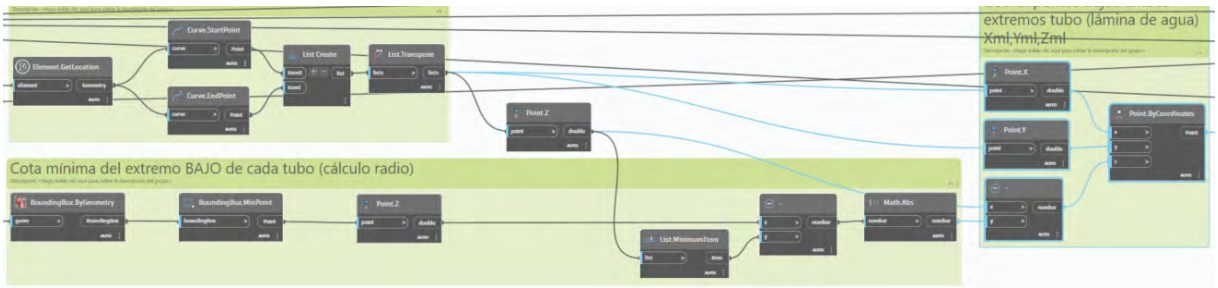


FIG. 5
Determination of the pipes invert levels at both edges

Once this is done, the coordinates Xm,Ym,Zm, which are local Dynamo coordinates, need to be converted into model real UTM coordinates, Xmr,Ymr,Zmr. This is necessary because the as-built staking data sheet from the facility employs UTM coordinates (named Xr,Yr,Zr hereinafter). For this purpose, a Python Script node was employed.

Alongside to the previous operations, the as-built staking data Excel sheet is imported into Dynamo as a list of coordinates along with their identifiers using the node "Data.ImportExcel", resulting, after some lists managements, in the mentioned ID,Xr,Yr,Zr for each element: center of each manhole cover, and invert level from one of the edges of each pipe (it is unknown which of the two edges).

After this, an ID match is done between the as-built staking data list (ID,Xr,Yr,Zr) and the lists from the two types of elements (ID,Xmr,Ymr,Zmr). It allows to do a coordinate check for each ID matching, verifying if Xmr,Ymr,Zmr model coordinates match Xr,Yr,Zr real ones within established XY (planimetry) and Z (elevation) margins, which are supplied as inputs to the script. For pipes, the corresponding model edge is determined by comparing the XY distances from both ends to the corresponding as-built staking data point and choosing the nearest one. All this is carried out by two Python scripts implemented in Dynamo, one for the inspection chambers and another one for the tubes.

Finally, all the results are integrated into one list, and a comparative report is exported to a separate tab of the as-built staking data Excel sheet. For each element ID, XY and Z distances to real point and if planimetry an elevation are correct/incorrect respecting the margin is given; for those elements where a match is not found ID is exported but XY or Z cells will remain blank. In the cases out of margins, or without match, the element is highlighted in red into the Revit BIM model by means of an override, in order to facilitate the subsequent manual verification.

3. RESULTS

The proposed Dynamo script consists of five main stages: (1) ensuring traceability by assigning a unique identifier to each BIM element; (2) reading and processing the as-built data; (3) extracting the required geometric information from the BIM objects; (4) verifying the model geometry against the as-built data; and (5) exporting the verification results to both the BIM model and a report. An overview of the workflow is shown in Figure 6.

The proposed methodology was validated on a drainage network comprising four interconnected branches, 12 manholes, and 15 pipe segments. Five intentional discrepancies (one manhole and four pipe-related) were introduced using planimetric and vertical tolerances of 1 m and 0.10 m, respectively. All discrepancies were successfully detected. The Dynamo script executed in a few seconds, while input preparation required approximately one minute. By contrast, manual verification would take longer to inspect a single element than the entire automated process.

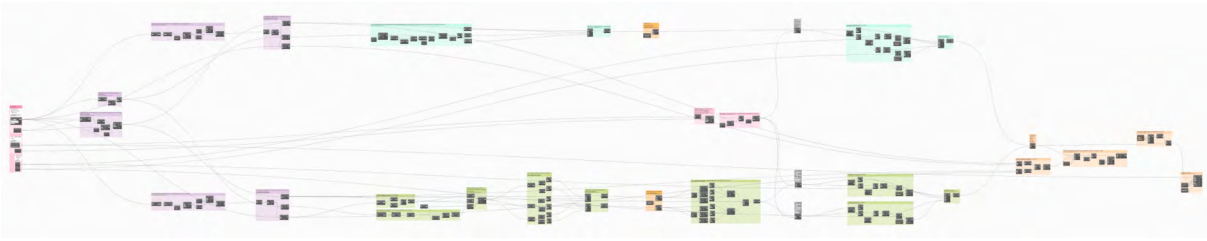


FIG. 6
General view of Dynamo script

3.1. Script inputs selection

Input selection is organized into the three groups shown in Figure 7. In the first group, the Revit elements to be imported are defined through selection in the view window, together with the name of the property that stores the element ID within the Revit property set, specified via a string input field. In the second group, the Excel sheet containing the setting-out data is selected using a file browser control, and the corresponding worksheet is identified through a string input field. In the third group, the allowable tolerances for planimetric and altimetric elements are defined using numerical input fields.

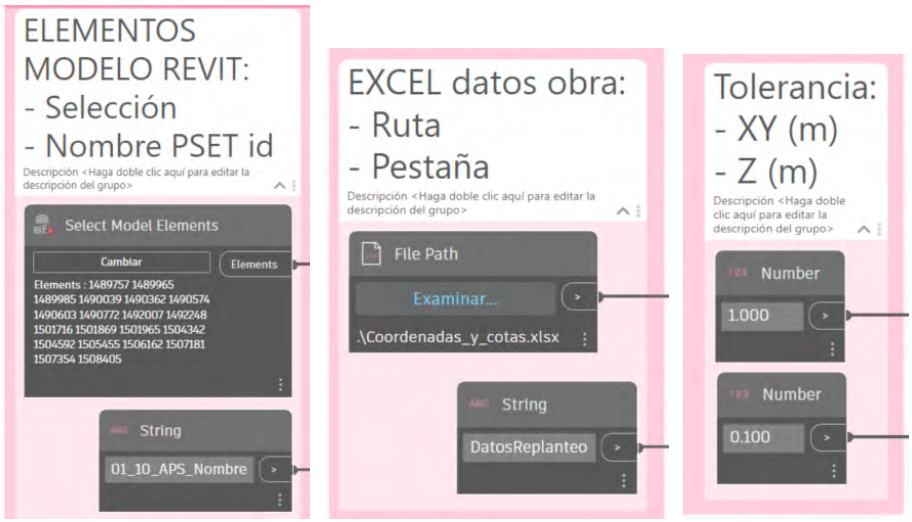


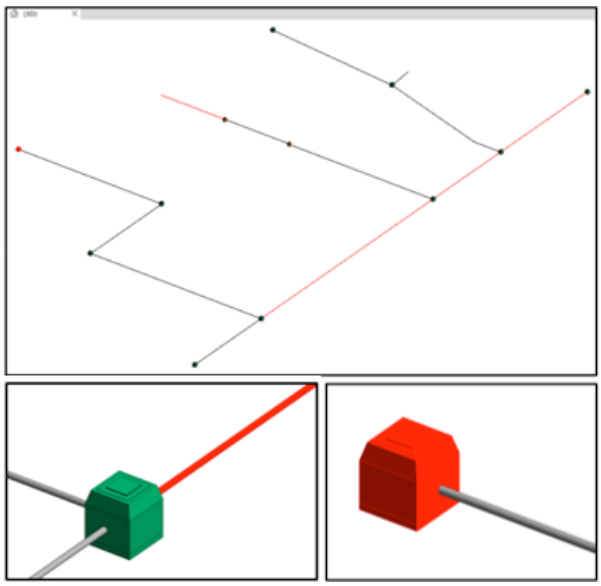
FIG. 7
Script inputs

3.2. Script outputs

Results are presented both numerically and graphically. The aim is to obtain those elements of the model not matching the as-built data in a simple way, in order to assess how far they are, and to easily correct the BIM model if needed.

Numerical results are added in a new tab of the set-out Excel dataset. After the header (first row) for each element of the model are shown in columns A to E: ID, correct/incorrect

planimetry, planimetric distance between as-built and modelled element, correct/incorrect altimetry, altimetric distance between as-built and modelled element; an example is shown in Figure 8. The graphical result is presented highlighting in the Revit model those elements that exhibit inconsistencies; for this purpose, the script applies an override on the element.



	A	B	C	D	E
1	ID	XY¿?	XY dist.(m)	Z?¿	Z dist.(m)
2	ELE_L4_POZ_05	XY-Correcta	0,008869908	Z-Correcta	-0,02
3	ELE_L4_POZ_01	XY-Correcta	0,007402763	Z-Correcta	-0,02
4	ELE_L2_POZ_02	XY-Correcta	0,000338037	Z-Correcta	-0,02
5	ELE_L4_POZ_03	XY-Correcta	0,004924759	Z-Correcta	-0,02
6	ELE_L4_POZ_02	XY-Correcta	0,008670533	Z-Correcta	-0,02
7	ELE_L2_POZ_01	XY-Correcta	0,013961018	Z-Correcta	-0,02
8	ELE_L1_POZ_01	XY-Correcta	0,00773724	Z-Correcta	-0,086
9	ELE_L3_POZ_01	XY-Correcta	9,33E-10	Z-Correcta	-0,02
10	ELE_L1_POZ_02	XY-Correcta	9,33E-10	Z-Correcta	-0,02
11	ELE_L4_POZ_04	XY-Correcta	0,016552092	Z-Correcta	-0,02
12	ELE_L3_POZ_03	XY-Correcta	9,33E-10	Z-Correcta	-0,02
13	ELE_L3_POZ_02	XY-Correcta	0,008907465	Z-Correcta	-0,02
14	ELE_L3_PRI_8T0160_01	XY-Correcta	0,507444832	Z-Correcta	0,08
15	ELE_L3_PRI_8T0160_02	XY-Correcta	0,410807368	Z-Correcta	0,07836
16	ELE_L3_PRI_8T0160_03	XY-Correcta	0,499449033	Z-Correcta	0,07836
17	ELE_L4_PRI_8T0160_02	XY-Correcta		Z-Correcta	
18	ELE_L3_PRI_8T0160_04	XY-Correcta	0,455443699	Z-Incorrecta	0,12836
19	ELE_L4_PRI_8TO160_02	XY-Incorrecta	188,8577795	Z-Correcta	0,07336
20	ELE_L1_PRI_8TO160_04	XY-Correcta	0,347916848	Z-Incorrecta	0,12336

Resultados | DatosReplanteo

FIG. 8

Graphical result in Dynamo highlighting in red elements out of tolerance, and Excel report output form the script in a new tab of the set-out data sheet

4. CONCLUSIONS

By means of Dynamo, the methodology proposed allows the verification of as-built Revit BIM sanitation models respecting an on-site UTM coordinates dataset, identifying the discrepancies, both graphically within the model and through an automatically generated report. It is essential to explore methods for automating model verifications. The proposed one reduces time and human labour requirements, enabling automated checks, significantly enhancing the efficiency and reliability of the model review process. This methodology can likewise be extended to other modelling software or programming languages for implementation; Dynamo for Revit has been used in this case purely for convenience.

The proposed methodology relies on the correct identification of the network elements, making the use of consistent element identifiers and naming conventions a critical requirement. This aspect must be explicitly addressed in the script user manual. Likewise, the quality of both the BIM model and the survey data must be consistent with the tolerance values adopted for the comparison: therefore, the acceptable modelling and surveying accuracy should be defined accordingly. Regarding scalability, although the methodology has been validated using a relatively compact drainage network, the proposed approach is not intrinsically limited by the network size and can be readily extended to much larger sewer systems or even to other types of utility networks.

REFERENCES

[1] Li, J., Wang, Y., Wang, X., Luo, X., Li, H.: Benefits of building information modelling in the project lifecycle: Construction projects in Asia. International Journal of Advanced Robotic Systems 11(1), 1-10 (2014).

[1] Das, K., Khursheed, S., Paul, V. K.: The impact of BIM on project time and cost: Insights from case studies. Discover Materials 5, 1-15 (2025).

[2] Lin, Y., Huang, Y.: Filtering of irrelevant clashes detected by BIM software using a hybrid method of rule-based reasoning and supervised machine learning. Applied Sciences 9(24), 5324 (2019).

[3] Hu, X., Jiang, Y., Li, S.: Innovative approach to convert geographic information system-based highway models into multidimensional building information modeling platforms using Dynamo. Transportation Research Record 2678(8), 1-14 (2024).

[4] Cavieres-Lagos, S., Muñoz La Rivera, F., Atencio, E., Herrera, R.F.: *Integration of BIM Tools for the Facility Management of Railway Bridges.* Applied Sciences 14(14), 6209 (2024).

[5] Rocha, G., Mateus, L.: Using Dynamo for Automatic Reconstruction of BIM Elements from Point Clouds. Applied Sciences 14(10), 4078 (2024).

[6] Lee, J., Kim, S., Kim, Y.: *Lumped Record Management Method Using BIM and Dynamo for Spalling Maintenance.* Automation in Construction 160, 105324 (2024).

[7] Kossakowski, *P.G.: Visual Programming as Modern and Effective Structural Design Technology—Analysis of Opportunities, Challenges, and Future Developments Based on the Use of Dynamo.* Applied Sciences 13(16), 9298 (2023).

[8] Thabet, W., Lucas, J., Srinivasan, S.: *Linking life cycle BIM data to a facility management system using Revit Dynamo.* Organization, Technology and Management in Construction 14(1), 2539-2558 (2022).

[9] Kensek, K. M.: *Integration of Environmental Sensors with BIM: Case Studies Using Arduino, Dynamo, and the Revit API.* Informes de la Construcción 66(536), e044 (2014).

Coupled Hydrodynamic and Structural Design Methodology for a Low-Cost Remotely Operated Vehicle

Gaizka Erkizia[a], *, Idoia San Sebastian[b], Erik Vadillo[a], Xabier Amezua[b], Mikel Iturrate[a], Xabier Garikano[a]

[a] Department of Graphic Design and Engineering Projects, School of Engineering of Gipuzkoa, University of the Basque Country (EHU), Donostia, Spain

[b] Department of Graphic Design and Engineering Projects, School of Engineering of Bilbao, University of the Basque Country (EHU), Bilbao, Spain

*e-mail: gaizka.erkizia@ehu.eus

Abstract: Low-cost inspection-class Remotely Operated Vehicles (ROVs) are increasingly used for underwater ecological monitoring, yet their mechanical design typically treats hydrodynamics, structural integrity, and buoyancy as independent problems. This paper presents a three-stage coupled mechanical design framework in which each stage produces outputs that directly constrain the next: Stage 1 characterises hull and tether drag via RANS-based CFD simulation and sizes the thruster system accordingly; Stage 2 designs a pressure housing rated for 150 m operational depth using Von Mises yield and Windenburg-Trilling buckling analysis, validated against published experimental data for marine-grade aluminium; and Stage 3 determines the flotation volume and positioning required to achieve dual-condition buoyancy —neutral in freshwater and positively buoyant in saltwater— while simultaneously establishing the CB-CG separation that governs passive roll and pitch stability. The framework is demonstrated on a functional low-cost ROV prototype and benchmarked against comparable published systems. Results confirm that explicit tether drag modelling is critical beyond approximately 30 m deployment depth, that a 6061-T6 aluminium housing satisfies all structural criteria with verified safety margins, and that buoyancy positioning is a coupled stability decision rather than a post-hoc adjustment. The workflow is transferable to other platforms operating under extreme-environment constraints.

Keywords: *ROV, mechanical design, hydrodynamics, pressure housing, buoyancy, CFD.*

1. INTRODUCTION

Marine ecosystem degradation demands persistent monitoring at depths beyond the reach of human divers [1]. Conventional methods such as ship-based sampling and SCUBA visual census are limited to shallow water and produce sparse datasets unsuitable for long-term assessment [2]. ROVs have emerged as the platform of choice for underwater ecological monitoring, enabling imaging, water-quality sensing, and benthic surveys at depths where diver access is unsafe or prohibitive [1, 2]. ROV-based photogrammetric surveys cover areas exceeding *11,000 m²* per deployment — two orders of magnitude larger than diver operations [3].

Inspection-class platforms range from commercial systems to open-source designs such as BlueROV2 and OpenROV [4,5]. The latter have been criticised for structural fragility, insufficient depth ratings, and underdocumented design decisions [4]. Critically, the interdependency between hydrodynamic loading, pressure-housing requirements, and buoyancy balance is rarely treated as a coupled problem — subsystems are optimised independently, producing sub-optimal results.

This paper presents a three-stage mechanical design workflow (hydrodynamic analysis, pressure housing design, and buoyancy optimisation) applied to a low-cost ROV targeting *150 m* depth and *2 m/s* current resistance, grounded in systematic design methodology [6] and marine hydrodynamics [7]. Its contribution is to treat these stages as a single coupled problem, each output explicitly constraining the next, with a buoyancy-driven stability feedback closing the loop to Stage 1, unlike the ad-hoc open-source workflows [4,5] and the two-stage design procedures [8,9] reported for comparable vehicles.

2. DESIGN FRAMEWORK OVERVIEW

The methodology follows the Pahl & Beitz systematic approach [6] adapted to underwater vehicles [7], and is formalised as three sequential stages operating on a shared design state, geometry, mass, and displaced volume. Each stage takes this state as input, performs its domain analysis, and returns updated constraints that define the input of the next; a Stage 3→Stage 1 feedback loop (Figure 1) closes the procedure, which iterates to convergence before fabrication.

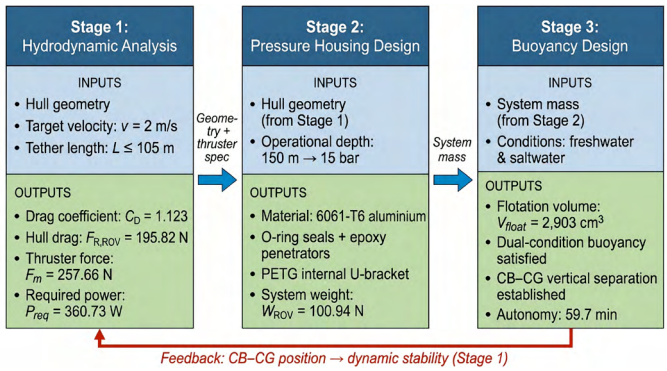


FIG. 1

Three-stage coupled mechanical design framework: stage inputs, outputs, and interdependencies. The Stage 3→Stage 1 feedback loop closes the design through buoyancy-driven stability constraints

3. STAGE 1 — HYDRODYNAMIC ANALYSIS

3.1. ROV Hull Drag

The hydrodynamic characterisation of the ROV hull was performed using a RANS-based CFD simulation in StarCCM+, employing an SST k-ω turbulence model [10,11]. A simplified block geometry was used, adequate for preliminary drag sizing [12].

At the target current velocity of *2 m/s*, the Reynolds number (L = *0.44 m*, ρ = *1,025 kg/m³*, $\mu = 1.3 \times 10^{-3}$ *kg/ms*) is Re = *693,846*, confirming fully turbulent flow. The drag coefficient converged to C_D = *1.123*, within the range *1.00–1.30* reported for box-frame geometries [12], validating the simplified model. With frontal area A = *0.0845 m²*, the hull drag force at *2 m/s* is $F_{R,ROV}$ = *195.82 N*. The full drag-velocity relationship is shown in Figure 2(a).

3.2. Tether Cable Drag

Tether drag is consistently neglected in academic ROV simulations [5]; the parametric analysis presented here (Figure 2(b)) demonstrates that it dominates total system drag beyond approximately *30 m* deployment depth. The cable (d = *0.005 m*, $C_{D,cable}$ = *1.2*) is modelled analytically following Fossen [7] as shown in equation (1):

$$F_{R,Cable} = \frac{1}{2} \times 1.2 \times \left(L_{cable} \times 0.005\right) \times 1.025 \times v^2 \tag{1}$$

Figure 2(b) shows the parametric results across cable lengths of *15-105 m* and velocities of *0.5-2 m/s*. At *105 m* and *2 m/s*, tether drag reaches *1,291.5 N*, over six times the hull drag, with the crossover occurring at approximately *30 m*. Thruster sizing conservatively uses combined drag at maximum cable length.

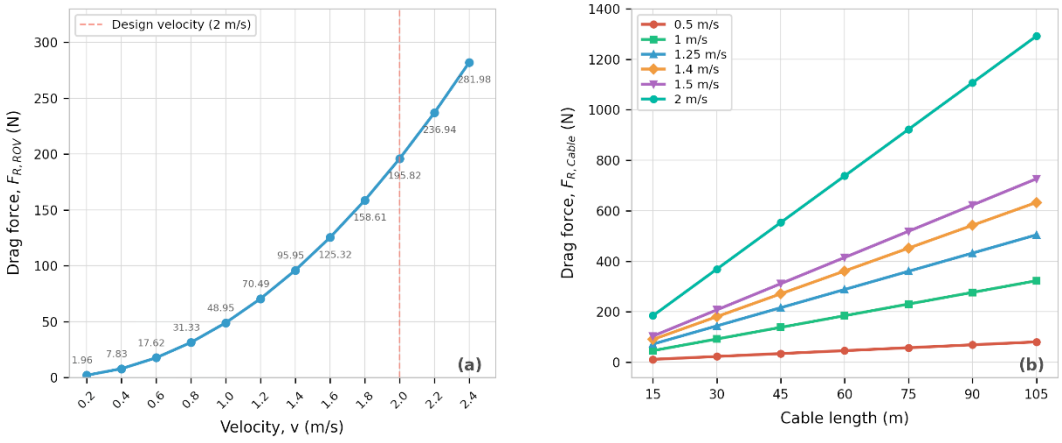


FIG. 2

Hydrodynamic characterisation results. (a) Hull drag force as a function of current velocity (C_D = 1.123, A = 0.0845 m²); dashed line indicates the 2 m/s design velocity. (b) Parametric tether drag force as a function of deployed cable length for velocities of 0.5–2 m/s

3.3. Thruster Sizing and Configuration

The 6-DOF vectored six-thruster configuration achieves full holonomic manoeuvrability through cosine force decomposition at *45°* to the surge axis [8]. At the design cruise speed of *1.4 m/s* and *105 m* cable length, total drag is *728.85 N*, yielding a required thrust of $F_m = 257.66\ N$ per thruster and shaft power $P_{req} = 360.73\ W$. The selected M080 brushless motor with ELEC-ESC-30A controller satisfies this requirement with margin, fixing the Stage 1 output, hull geometry, frontal area, and thruster specification, as input to Stage 2.

4. STAGE 2 — PRESSURE HOUSING

4.1. Structural Requirements

At *150 m*, the housing must withstand approximately *15 bar* external pressure. Design criteria (structural integrity, machinability for O-ring grooves, corrosion resistance, and cost) led to cylindrical geometry in 6061-T6 aluminium, the standard form factor for small to medium-depth housings [13].

4.2. Enclosure Configuration and Structural Verification

Lobar buckling and material yielding were evaluated using the Von Mises yield criterion, Windenburg–Trilling buckling equation, and FEM verification, following Meschini *et al.* [13], who validated this workflow against Anticorodal 6082-T6 aluminium, mechanically equivalent to the 6061-T6 selected here (*276 MPa* yield, *68.9 GPa*). Tubes are sealed by O-ring end caps and epoxy-potted penetrators.

The ROV incorporates two housings: one for the electronics and one for the battery, both constructed from the same tube stock.

4.3. Internal Support Structure via Additive Manufacturing

Electronic components are secured by a PETG U-bracket fabricated by FDM. It carries no structural load, since that function belongs to the aluminium tube, so material criteria are dimensional stability and chemical resistance.

PETG satisfies both requirements: Moreno Nieto *et al.* [14] report 0.16% water absorption in saltwater with negligible dimensional change, outperforming PLA and ABS under marine exposure. Its glass transition temperature of ~80°C provides adequate thermal tolerance for ESC heat inside the sealed enclosure. The assembled internal structure is shown in Figure 3.

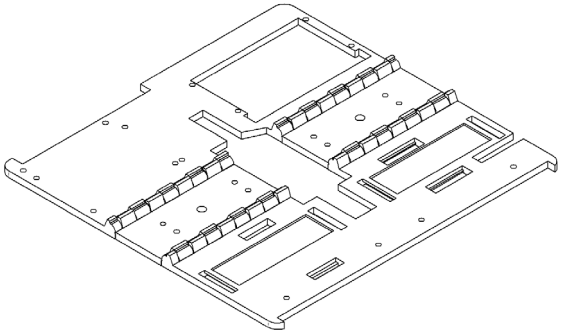


FIG. 3

PETG U-bracket internal support structure shown in developed (unfolded) configuration; the part is folded along the living hinges prior to insertion into the pressure housing

5. STAGE 3 — BUOYANCY DESIGN

Stage 3 integrates system mass from Stages 1 and 2 into a force balance satisfying two conditions: neutral buoyancy in freshwater and positive buoyancy in saltwater for passive surface recovery. This is a coupled decision, the flotation volume constrains element positioning, which determines the CB-CG vertical separation.

Without flotation, $E_{ROV} = 83.3\ N < W_{ROV} = 100.94\ N$; dual-condition Archimedes analysis yields *2,903 cm³*, distributed as two FGV-FOAM-SBM-500M blocks of *1,451 cm³* each. The force balance and block positioning are shown in Figure 4.

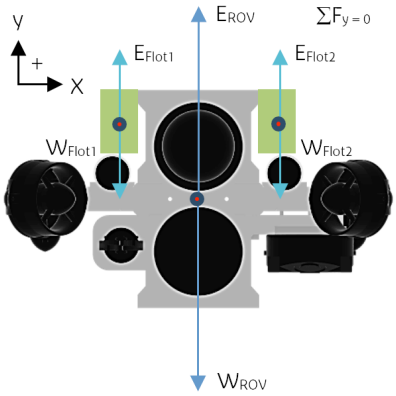


FIG. 4

Force balance and flotation block positioning. Green blocks (1,451 cm³ each) achieve neutral buoyancy in freshwater and positive buoyancy in saltwater; central red dot: system CG

The vertical CB-CG separation generated by the positioned flotation blocks provides a passive righting moment that confers inherent roll and pitch stability without active control, a property formalised by Miller *et al.* [15] as a stability index linking buoyancy geometry to hydrodynamic performance.

6. RESULTS AND DISCUSSION

The coupled workflow converges on a fully specified design that meets every target criterion analytically before fabrication: the 6061-T6 housing clears the structural limits with margin at *150 m*, the *2,903 cm³* flotation achieves dual-condition buoyancy with passive CB-CG stability, and the propulsion-energy budget yields I_{prom} = *22.11 A* and *59.7 min* endurance against the *1-hour* target.

Table 1 benchmarks the resulting design against published inspection-class ROV systems. The present design achieves the highest depth rating in the comparison group, explicit tether drag modelling, and a marine-characterised AM internal structure, distinguishing features that follow directly from the three-stage methodology rather than from component selection alone.

TABLE 1
Benchmark comparison against published inspection-class ROV systems

Parameter	This work	BlueROV2 [5]	Salem *et al.* [9]	García-Nava *et al.* [8]
Depth rating	150 m	100 m	~7 m	~40 m
Max current resistance	2 m/s	~1 m/s	Not specified	Not specified
Tether drag modelled	Yes	Simulated [5]	No	No
Pressure housing	6061-T6 Al, custom	Commercial	Custom	Custom
AM internal structure	PETG (marine-characterised)	No	No	No
Design methodology	3-stage coupled	Ad hoc	2-stage	2-stage

These results rest on analytical and CFD verification rather than in-water measurement, using a simplified hull geometry, computed structural margins, and nominal component masses, so field validation at depth is the natural next step before deployment.

7. CONCLUSIONS

This paper has presented a three-stage coupled mechanical design framework, demonstrated on a low-cost ROV prototype rated to *150 m* and *2 m/s*. Grounded in systematic design methodology [6], the coupled treatment ensures analytical verification of all performance criteria prior to fabrication, an approach absent from comparable open-source platforms [4,5].

The framework transfers to any system combining external load characterisation, pressure-rated enclosure design, and buoyancy balance, including deep-sea sensor packages and high-pressure drone housings. Future work includes chassis topological optimisation, full sensor integration, and PETG-CF as a reinforced alternative for higher-depth configurations.

Acknowledgements: The authors thank the Faculty of Engineering - Gipuzkoa (EHU) for providing access to laboratories and software utilised in this study.

REFERENCES

[1] Macreadie, P. I., McLean, D. L., Thomson, P. G., *et al.*: Eyes in the sea: Unlocking the mysteries of the ocean using remotely operated vehicles (ROVs). Science of the Total Environment, 634, 1077-1091 (2018). https://doi.org/10.1016/j.scitotenv.2018.04.049

[2] Tait, L. W., Bulleid, J., Pryor Rodgers, L., *et al.*: Towards remote surveillance of marine pests: A comparison between remote operated vehicles and diver surveys. Frontiers in Marine Science, 10 (2023). https://doi.org/10.3389/fmars.2023.1102506

[3] Paterson, I. L. R., Dawson, K. E., Mogg, A. O. M., Sayer, M. D. J., Burdett, H. L.: Quantitative comparison of ROV and diver-based photogrammetry to reconstruct maerl bed ecosystems. Aquatic Conservation: Marine and Freshwater Ecosystems, 34(11), e70007 (2024). https://doi.org/10.1002/aqc.70007

[4] Capocci, R., Dooly, G., Omerdić, E., Coleman, J., Newe, T., Toal, D.: Inspection-class remotely operated vehicles — a review. Journal of Marine Science and Engineering, 5(1), 13 (2017). https://doi.org/10.3390/jmse5010013

[5] von Benzon, M., Sørensen, F. F., Uth, E., Jouffroy, J., Liniger, J., Pedersen, S.: An open-source benchmark simulator: Control of a BlueROV2 underwater robot. Journal of Marine Science and Engineering, 10(12), 1898 (2022). https://doi.org/10.3390/jmse10121898

[6] Pahl, G., Beitz, W., Feldhusen, J., Grote, K.-H.: Engineering Design: A Systematic Approach, 3rd edn. Springer, London (2007). ISBN-10: 1846283183

[7] Fossen, T. I.: Handbook of Marine Craft Hydrodynamics and Motion Control, 2nd edn. Wiley, Chichester (2021). https://doi.org/10.1002/9781119994138

[8] García-Nava, S., García-Rangel, M. A., Zamora-Suárez, Á. E., *et al.*: Development of a 6 degree of freedom unmanned underwater vehicle: Design, construction and real-time experiments. Journal of Marine Science and Engineering, 11(9), 1744 (2023). https://doi.org/10.3390/jmse11091744

[9] Salem, K. M., Rady, M., Aly, H., Elshimy, H.: Design and implementation of a six-degrees-of-freedom underwater remotely operated vehicle. Applied Sciences, 13(12), 6870 (2023). https://doi.org/10.3390/app13126870

[10] Zhang, D., Wang, X., Zhao, M., Hong, L., Li, X.: Numerical investigation on hydrodynamic characteristics and drag influence of an open-frame remotely operated underwater vehicle. Journal of Marine Science and Engineering, 11(11), 2143 (2023). https://doi.org/10.3390/jmse11112143

[11] Li, X., Zhang, D., Zhao, M., Wang, X., Shen, Y.: Hydrodynamic analysis and drag-reduction design of an unmanned underwater vehicle based on computational fluid dynamics. Journal of Marine Science and Engineering, 12(8), 1388 (2024). https://doi.org/10.3390/jmse12081388

[12] Satria, D., Wiryadinata, R., *et al.*: Hydrodynamic analysis of remotely operated vehicle (ROV) observation class using CFD. IOP Conference Series: Materials Science and Engineering, 645, 012014 (2019). https://doi.org/10.1088/1757-899x/645/1/012014

[13] Meschini, A., Ridolfi, A., Gelli, J., Pagliai, M., Rindi, A.: Pressure hull design methods for unmanned underwater vehicles. Journal of Marine Science and Engineering, 7(11), 382 (2019). https://doi.org/10.3390/jmse7110382

[14] Moreno Nieto, D., Alonso-García, M., Pardo-Vicente, M.-A., Rodríguez-Parada, L.: Product design by additive manufacturing for water environments: Study of degradation and absorption behavior of PLA and PETG. Polymers, 13(7), 1036 (2021). https://doi.org/10.3390/polym13071036

[15] Miller, L., Brizzolara, S., Stilwell, D. J.: Increase in stability of an X-configured AUV through hydrodynamic design iterations with the definition of a new stability index to include effect of gravity. Journal of Marine Science and Engineering, 9(9), 942 (2021). https://doi.org/10.3390/jmse9090942

Graphic Design for One Health: Enhancing Student Engagement and Learning through AI-Assisted Visual Communication

Benyamin Soleimani*, Larisa Dunai

Department of Graphic Engineering, Universitat Politècnica de València,
Camino de Vera S/N, 5L, 46022 Valencia, Spain

*e-mail: bsoleim@doctor.upv.es

Abstract: Artificial intelligence (AI) is reshaping graphic design education by changing how students generate, evaluate, and refine visual ideas. This study examined the value of integrating generative AI into a packaging design course, focusing on student engagement, visual exploration, and the designer's role in decision-making. A non-randomized, parallel-group mixed-methods design involved 60 undergraduate students enrolled in two classes of Packaging Design Workshop II at Islamic Azad University, Iran. Both classes were taught by the same instructor over 20 weekly three-hour sessions and completed a food-packaging project under identical assessment conditions. One group followed a conventional manual–digital workflow, while the other used an AI-assisted workflow incorporating ChatGPT, Nano Banana, Grok, Runway, and Adobe Photoshop Beta. Data included process work, final projects, questionnaires, classroom observations, and scores from three blinded external assessors. The AI-assisted workflow supported faster exploration of visual alternatives and encouraged articulation of design intentions through prompt writing. However, generated outputs required correction and refinement, particularly in typography, composition, and technical production. The findings position AI as a complementary resource whose value depends on critical judgment, visual literacy, and human-led refinement. From a One Health perspective, the study supports a responsible, participatory, and human-centered approach to design education.

Keywords: *Graphic Design, Artificial Intelligence (AI), Visual Communication, Student Engagement, Learning, One Health.*

1. INTRODUCTION

Graphic design has always been a dialogue between concept and technology. However, the recent surge of AI-driven tools has shifted the pedagogical focus from "how to execute" to "how to prompt and curate," requiring a new kind of visual literacy in the classroom. In this landscape, Artificial Intelligence (AI) emerges not as a replacement for creativity, but as a transformative force. Technological developments have also expanded the possibilities for creating and presenting these ideas. In recent years, artificial intelligence (AI) has become one of the most significant developments in contemporary graphic design, influencing workflows, creative practices, and decision-making processes [1]. Rather than replacing human creativity, AI is increasingly viewed as a complementary tool that supports flexibility, experimentation, and efficiency in design [1]. At the same time, advances in educational technologies have emphasized the growing importance of visual communication in learning environments. AI-based tools make it possible to produce visual content quickly and in different formats, creating new opportunities for educational design [2]. Despite these advantages, concerns remain regarding excessive dependence on AI tools and the possible decline of students' technical and creative skills. Many processes that previously required extensive technical knowledge can now be completed more rapidly through AI-assisted systems. As a result, an important question emerges: can AI be integrated into graphic design education without weakening students' creativity and understanding of design principles? In response to this issue, the present study examines the integration of traditional design methods with AI-driven tools in educational environments. The research compares packaging design projects developed through a conventional manual–digital workflow and an AI-assisted manual–digital workflow, examining their strengths, limitations, and influence on student participation and performance. Within the framework of "Design for One Health," this study also explores how AI-based design processes can contribute to more interactive and supportive learning environments [3]. In addition, the research highlights the importance of collaboration between students and instructors in achieving more effective use of emerging technologies in design education [4].

2. METHODOLOGY

This study used a non-randomized, parallel-group, mixed-methods design to compare two approaches to teaching packaging design. Previous research has shown that AI-assisted frameworks can support experimentation and visual development in graphic design education [5]. Students' attitudes toward emerging technologies and the development of AI literacy were also considered relevant to the study [6]. More broadly, the research responded to the need for design education to engage critically with technological change while maintaining fundamental disciplinary knowledge [9]. The participants were 60 undergraduate graphic design students enrolled in two classes of Packaging Design Workshop II at Islamic Azad University, Iran. Both classes were conducted during the semester beginning in September 2025 and were taught by the same instructor over 20 weekly three-hour sessions. Each class included 30 students, who were assigned through university scheduling rather than random allocation. All participants had previously completed Design Workshop I and Photoshop I and therefore had a basic understanding of composition, color, typography, image editing, and graphic design principles. Both groups received the same project brief

and designed packaging for a self-selected food product. The learning objectives, number of sessions, submission deadline, presentation requirements, and final assessment conditions were the same. The main difference concerned the workflow used during concept development and visual production. The conventional group followed a manual–digital workflow. Students began with market observation, photography of existing packaging, hand-drawn sketches, and manual techniques such as markers, airbrush, and collage. Selected concepts were then developed in Adobe Photoshop, where students refined composition, imagery, color, typography, packaging dimensions, and print preparation. The second group followed an AI-assisted manual–digital workflow. Students used online visual references and generative platforms, including ChatGPT, Nano Banana, Grok, and Runway, to develop prompts and generate alternative visual concepts. Adobe Photoshop Beta was then used to correct visual and textual errors, refine composition, color, and typography, establish final dimensions, and prepare print-ready files. Traditional, digital, and AI-assisted practices were not treated as three independent experimental conditions. Traditional practice referred to observation, manual research, sketching, and hands-on image development. Digital practice referred mainly to the use of Photoshop for visual refinement and technical production. AI-assisted practice involved prompt development, image generation, comparison of alternatives, and critical revision. Generated images were not treated as completed designs; students remained responsible for selecting, rejecting, combining, and revising the outputs according to the product concept and the requirements of packaging design. The research materials included students' preliminary studies, manual sketches, digital working files, generated visual alternatives, written prompts, and final packaging projects. Additional data were obtained from the end-of-semester questionnaires, the scores assigned by three external assessors, and the instructor's classroom observation notes. For descriptive purposes, the activities of both groups were organized into five stages: exploration, design, generation, refinement, and rendering [2]. These stages were retrospectively related to the Analysis, Design, Development, Implementation, and Evaluation components of the ADDIE framework [10]. ADDIE was used to clarify the sequence of classroom activities rather than to determine the original structure of the intervention.



FIG. 1
ADDIE framework used retrospectively to organize the two instructional workflows

During exploration, both groups examined existing packaging, considered the characteristics of their selected products, identified intended audiences, and developed initial visual directions. During design and generation, students in the conventional group developed manual sketches before transferring selected concepts to Photoshop. Students in the AI-assisted group translated their ideas into written prompts, generated several alternatives, and revised the results through classroom discussion and instructor feedback. Prompt writing and the critical evaluation of generated outputs were treated as emerging design skills [8]. During refinement and rendering, both groups addressed composition, visual hi-

erarchy, color, typography, packaging dimensions, and technical production requirements. In the conventional group, Photoshop was used to develop concepts originating from manual sketches. In the AI-assisted group, it was used to correct, combine, and restructure generated material. In both workflows, students retained responsibility for the final conceptual, aesthetic, and technical decisions. At the end of the semester, all 60 projects were presented under the same conditions during a formal jury session. Each project was independently evaluated by three external assessors who were not affiliated with the university. The assessors were blinded to the instructional group and were not informed whether AI had been used. Each assessor assigned one overall score on a 20-point scale based on aesthetic quality, adherence to graphic design principles, and visual competitiveness in relation to comparable packaging products in the market. All 60 students also completed an end-of-semester questionnaire. The two versions contained a shared set of five-point Likert-scale items addressing participation, motivation, clarity of the learning process, perceived speed of idea development, diversity of visual alternatives, control over the final design, confidence, satisfaction, and perceptions of the novelty and relevance of the course content [7]. Only items with identical wording in both questionnaires were used for direct comparison. Course records provided the classroom-assignment scores and final course grades. Active participation was derived from the shared questionnaire item concerning participation in classroom discussions, critiques, and the presentation of ideas; responses of "agree" and "strongly agree" were classified as positive. For each project, the mean of the three assessors' scores was used as the final project-quality score. The instructor recorded brief notes after each session, which were reviewed for recurring patterns in participation, prompt development, experimentation, and design control.

3. RESULTS

The two groups differed in participation, coursework performance, final grades, and external assessment. Active classroom participation was reported for 70% of students in the conventional manual–digital group and 90% in the AI-assisted group. The AI-assisted group also achieved higher mean scores for classroom assignments and final course grades. The main findings are summarized in Table 1.

Table 1

Descriptive comparison of participation, course performance, and external assessment

Measure	Manual–digital	AI-Assisted
Active classroom participation	70% (21/30)	90% (27/30)
Mean classroom-assignment score	16/20	18/20
Mean final course grade	17.17/20	18.90/20
Median final course grade	17/20	19/20
Assessor 1	17.13	19.57
Assessor 2	16.85	19.00
Assessor 3	17.10	19.62
Overall mean	17.03	19.39

All 60 final projects were independently evaluated by three external assessors who were unaware of the instructional group associated with each project. All three assessors assigned higher mean scores to the AI-assisted projects. Across the 90 ratings given to each group, the overall mean was 19.39 for the AI-assisted group and 17.03 for the conventional group, representing a descriptive difference of 2.37 points. Classroom observations also revealed differences in the early stages of the design process. Students in the conventional group developed their ideas gradually through market observation, photography, sketching, and manual experimentation before transferring selected concepts to Photoshop. In the AI-assisted group, generative tools enabled students to produce and compare a larger number of visual alternatives within each class session. Prompt writing was initially challenging for some students, particularly when defining the product identity, intended audience, visual character, and composition. Through repeated experimentation and instructor feedback, students gradually developed more precise prompts and evaluated the generated outputs more critically.



FIG. 2
Example of iterative prompt development in ChatGPT during the design stage and the resulting visual variations

The outputs produced by different AI platforms varied in composition, detail, style, and product character. Most generated images were not suitable for direct use as finished packaging designs and often contained problems in typography, textual accuracy, composition, and visual consistency. Students therefore used Photoshop to select, correct, combine, and refine the generated material before preparing the final files for print. In both groups, knowledge of composition, color, typography, and technical production remained essential. The main difference concerned the production of initial alternatives: the conventional workflow supported gradual manual development, whereas the AI-assisted workflow enabled faster experimentation and comparison. The stronger AI-assisted projects were those in which students treated generated images as provisional material rather than as completed designs.



FIG. 3
Examples of final student projects: AI-assisted workflow (left) and integrated traditional–digital workflow (right)

4. DISCUSSION

The findings suggest that the AI-assisted workflow was associated with higher participation, stronger assignment performance, and better final grades than the conventional manual–digital approach. The external assessors also gave higher average scores to the AI-assisted projects while remaining unaware of the instructional method used. The clearest difference concerned workflow efficiency. Students in the AI-assisted group generated and compared more visual alternatives within each session, reducing the time needed to move from an initial idea to visible options. However, faster production did not guarantee a successful result. Many generated images required correction in typography, composition, textual accuracy, and visual consistency, and students still needed to evaluate and refine the material in Photoshop. Overall, the value of AI lay in expanding opportunities for experimentation while keeping final decisions under human control. The findings should be interpreted cautiously because the students were not randomly assigned and the study was limited to one course at one university. From a One Health perspective, this approach may support a more participatory and human-centered learning environment, although direct psychological or health outcomes were not measured.

5. CONCLUSION

This study compared a conventional manual–digital workflow with an AI-assisted approach in two university packaging design classes. The AI-assisted group showed higher participation, stronger assignment performance, better final grades, and higher mean scores in the blinded external evaluation. Students in this group also produced and compared more visual alternatives within each session, which appeared to shorten the early stages of concept development. These advantages did not reduce the importance of design knowledge. AI-generated images still required correction in typography, composition, textual accuracy, and technical preparation. The strongest outcomes emerged when students treated AI-generated material as a starting point and refined it through critical judgment, Photoshop skills, and established design principles. Overall, generative AI appears most effective as a complementary educational resource that supports visual exploration, workflow efficiency, and active participation while keeping final design decisions under human control. Because the study involved two non-randomized classes at one university, the findings should be interpreted within this specific context.

REFERENCES

[1] Fleischmann, K.: Generative artificial intelligence in graphic design education: a student perspective. Canadian Journal of Learning and Technology 50(1), 1-17 (2024).

[2] Hwang, Y., Wu, Y.: Graphic design education in the era of text-to-image generation: Transitioning to contents creator. International Journal of Art & Design Education 44(1), 239-253 (2025).

[3] World Health Organization: One health. WHO, Geneva (2022). https://www.who.int/health-topics/one-health

[4] Kauppinen, T., Sivula, A.L.: Conclusion. In: Lehtonen, M.J., Kauppinen, T., Sivula, A.L. (eds.) Design Education Across Disciplines: Transformative Learning Experiences for the 21st

Century, pp. 261-271. Palgrave Macmillan, Cham (2023). https://doi.org/10.1007/978-3-031-23152-0

[5] Osei-Wusu, F., Asante, G., Asiedu, W., Muntaka, S.A., Yeboah, D., Azameti, C.Y.: An AI assisted pedagogical framework for improving beginner graphic design learning outcomes. Discover Education 5, 328 (2026). https://doi.org/10.1007/s44217-026-01352-w

[6] Akman, E.: The impact of AI-based visual designs on students' AI literacy and attitudes toward AI. Interactive Learning Environments 33(8), 5118-5136 (2025).

[7] Alsswey, A.: Examining students' perspectives on the use of artificial intelligence tools in higher education: A case study on AI tools of graphic design. Acta Psychologica 258, 105190 (2025).

[8] Lee, C.W.: Application of generative artificial intelligence in design education: an exploration and analysis to enhance student creativity. Engineering Proceedings 98(1), 29 (2025).

[9] Chu, S., Liang, R.: Case study: Integrating AI in graphic design education. Journal of Educational Issues 12(1), 1-14 (2026). https://doi.org/10.5296/jei.v12i1.23221

[10] Hannum, W.: Instructional systems development: A 30 year retrospective. Educational Technology 45(4), 5-21 (2005).

Design for Healthy Urban Environments: Analysis and a Combined Empirical and Perceptual Methodology in Cartagena's Historic Squares

Eva M. Sánchez-García, Mar Melgarejo-Torralba*, Victoria Artés-Hernández, Álvaro Ochoa Castillo, Emilio López Salmerón, Dolores Parras-Burgos

Universidad Politécnica de Cartagena member of European University of Technology EUT+, Department of Structures, Construction and Graphic Expression, Higher Technical School of Industrial Engineering. C/ Dr. Fleming, s/n, CP 30202, Cartagena (Murcia)

* e-mail: mar.melgarejo@upct.es

Abstract: This study investigates the soundscape of the historic centre of Cartagena (Murcia, Spain) with the aim of designing healthier urban spaces within the framework of the 2030 Urban Agenda. Given the European trend towards pedestrianizing historic centres, the noise of motorized traffic has been replaced by sounds from social activities, such as children's games and restaurant terraces, which often present high noise levels and characteristics distinct from traffic noise. For the analysis, four emblematic squares (Juan XXIII, del Rey, Ayuntamiento, and San Francisco) were selected, and a two-pronged methodology was applied: (1) physical acoustic measurements with high-precision sound level meters and (2) structured surveys on user perception. The empirical data show that legal noise limits are exceeded between 9% and 34% of the time, with violations concentrated in the late afternoon and early evening. The study highlights that citizens' perceptions do not always coincide with physical measurements; For example, loud natural sounds are rated higher than mechanical or vehicle noises. This suggests that urban design should consider subjective comfort, not just decibel levels. Finally, it is proposed that interventions include acoustic renaturalization, using sound-absorbing vegetation barriers integrated into street furniture, and co-design processes with citizens to improve the quality of life in these environments.

Keywords: *Soundscape, Urban design, Acoustic measurements, Sound perception, Acoustic renaturalization.*

1. INTRODUCTION

Within the framework of the 2030 Agenda for Sustainable Development and the Sustainable Development Goals, the creation of healthy urban environments is a priority for industrial design and engineering [1-3]. The trend in urban planning in European cities is to eliminate, as far as possible, road traffic from historic centres [4-5]. As a result, among other improvements, noise pollution is reduced in these areas; however, other noise sources occupy the space previously used by motor vehicles. Noise pollution has a significant impact on people's health and the quality of urban life, affecting them physically, physiologically, and psychologically. For example, consequences such as hearing loss, one of the most recognized effects [6], and its association with certain cardiovascular and respiratory diseases, as well as diabetes, especially in older populations, have been demonstrated [7]. Noise pollution may seem less visible than other types of pollution, but noise has far-reaching effects, ranging from physical and mental health problems to behavioural changes.

Social activities such as restaurant terraces, children's play areas, and suitcases rolling across smooth surfaces generate sounds that can be unsettling for visitors and residents. However, these sounds, despite their potentially high volume, have different nuances that can affect users' perceptions.

With these starting points, the objective of this research is to demonstrate that the design of healthy public spaces requires considering different perspectives, combining citizens' perceptions with empirical data. A combined analytical methodology is proposed to demonstrate the thesis that certain sounds can be more acceptable despite an identical sound level.

2. METHODOLOGY

This study offers a new approach to design through the analysis of the urban soundscape, applying a dual methodology of sound measurements with a sound level meter and structured surveys on the sound perception of space users. Four emblematic squares in the historic centre of Cartagena (Murcia, Spain) with heavy pedestrian traffic were selected: Juan XXIII, del Rey, Ayuntamiento, and San Francisco.

2.1. Empirical measures

The regulatory limits are set by Royal Decree 1367/2007, which implements the Noise Law in Spain. This decree establishes the technical criteria for the acoustic zoning of the territory according to its use (residential, industrial, etc.) and sets the quality objectives and exposure limits for noise and vibrations, both outdoors and indoors. Its main objective is to protect health and the environment by regulating noise emissions from transport and industrial infrastructure, and also to define noise easements in areas near airports, roads, and railways where normal levels are exceeded.

In this context, it is established that equivalent noise levels (LAeq) must not exceed 65 dB(A) during the daytime (7:00-19:00 h) and evening (19:00-23:00 h) periods.

For this methodological phase, it is established that each measurement at each point will last 5 minutes. For a more thorough analysis of noise pollution, measurements will be taken on two different types of days: one during the week (Monday to Friday) and one on the weekend. The technical instruments used for the measurements are a Ruel & Kjaer 2245 Sound Level Meter - Serial No.: 2245-101101, and a pre-polarized microphone, serial no. 3389764. Az Instrument Digital Sound Calibrator 8930B.

After taking measurements with the sound level meter, the results will be obtained by extracting the data using the Enviro Noise Partner application. This application allows you to export the measurements in .xls format. The data corresponds to LAeq, T (Noise Index for time period T), and the unit will be A-weighted decibels (dBA).

2.2. Data on citizen perception

For citizen perception, a questionnaire is used based on the research developed by D. Jerónimo Vida Manzano of the Department of Applied Physics of the University of Granada and which was part of the activities organized within the framework of the day "The City you want to hear" organized by the COITIRM on May 10, 2023 [8]

The questionnaire used for this work was:

1. To what extent can you hear the following four types of sound right now?
2. For each of the 8 scales shown below, to what extent do you agree or disagree that the current ambient sound is...
3. In general, how would you describe the AMBIENT SOUND that currently surrounds you?
4. In general, to what extent is the ambient sound surrounding this place adequate (appropriate)?
5. How LOUD would you say the ambient sound (noise) is? (Volume rating, not quality.)
6. How often do you visit this place?
7. How often would you like to visit this place again?
8. Appreciate the TRANQUILITY (calmness) of the sound environment of this place.
9. Rate whether the sound environment of this place is COZY (pleasant).

The questionnaire was administered at the most representative point in each location, where 15 people completed (total of 60) it during different time slots established between April and May 2025, with the aim of obtaining a representative average for each location. Participants were randomly selected, without bias based on age, sex, or any other factor, from among passersby willing to respond. For both the empirical measurements and the survey, statistical analysis was used to identify trends and compare average perception indicators (tranquillity, sound intensity, and adequacy) with empirical values such as LAeq and the percentage of time intervals exceeding the regulatory threshold of 65 dBA.

3. RESULTS AND DISCUSSION

The application of this dual methodology was carried out during the months of April and May 2025 and yielded the following results.

3.1. Empirical measures

Empirical analysis indicates that, in all squares, noise levels exceed the thresholds established by regulations at certain times of day, between 9% and 34% of the time. These violations are concentrated in the late afternoon and early evening (Fig. 1).

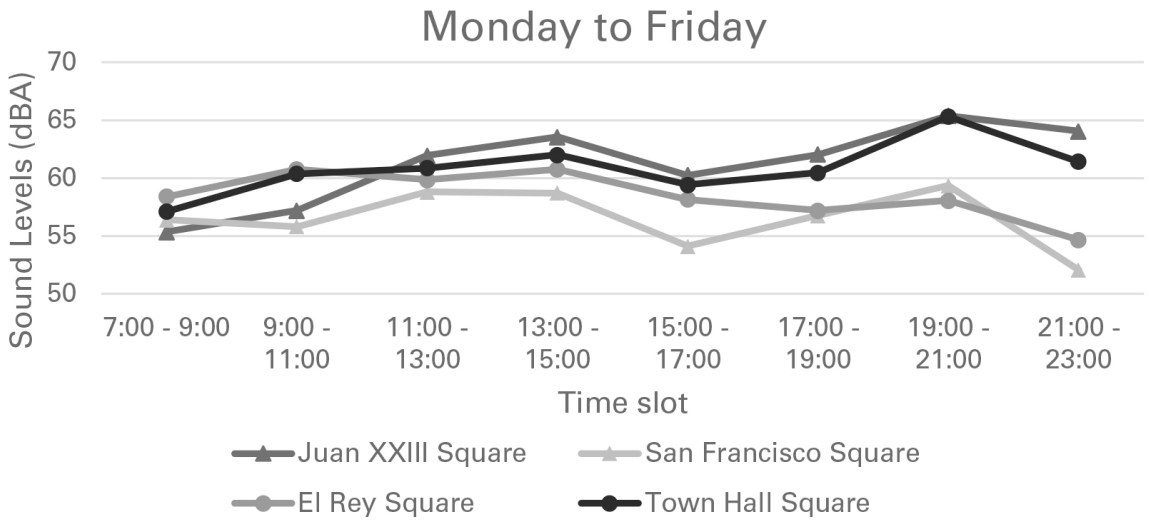


FIG. 1
Average noise levels from Monday to Friday

All the squares exceeded the 65-decibel limit at least during certain hours, with Juan XXIII Square standing out as the noisiest throughout the day. It is also worth noting the change in the morning noise limit from 7:00 to 11:00 a.m. to 11:00 p.m., demonstrating the impact of weekend social activity in the squares (Fig. 2).

It is worth noting that Town Hall Square is recorded the highest noise levels on both days, while San Francisco Square recorded the lowest. The quietest hours on weekends in all four squares were between 7:00 and 9:00 a.m. The noisiest hours on weekends were between 5:00 and 7:00 p.m. and between 9:00 and 11:00 p.m. Regarding the percentage of time slots that exceeded permitted levels, Juan XXIII Square had the highest rate of non-compliance at 34.38%, with 11 time slots exceeding 65 dBA. San Francisco Square was the most compliant, with only 9.38% exceeding permitted levels in two slots. Finally, it should be noted that the most significant source of noise affecting these squares is restaurant outdoor seating (Table 1).

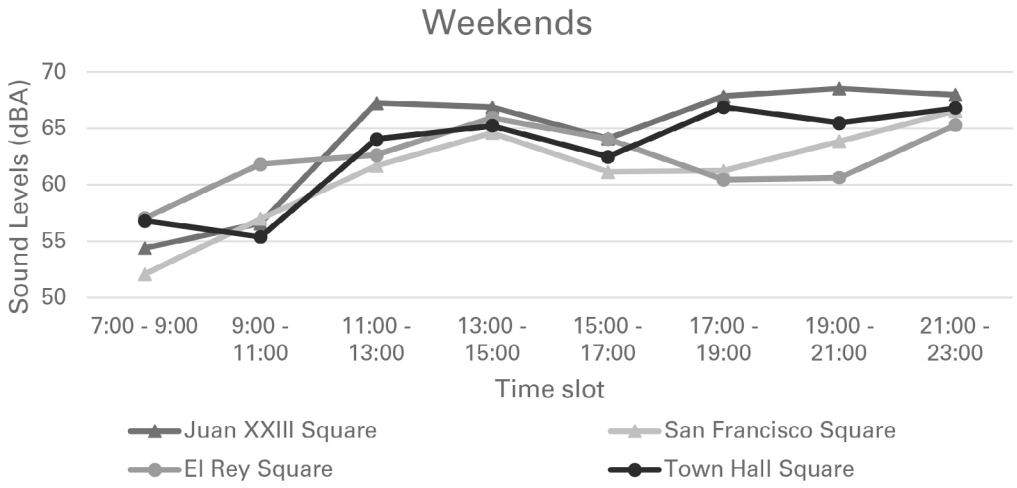


FIG. 2
Average noise levels on weekends

TABLE 1
Summary of acoustic results by square

Square	Noisiest spot on a weekday (dBA)	Noisiest spot on weekend (dBA)	Least noisy point on weekday (dBA)	Least noisy spot on weekends (dBA)	% of zones that do not comply with regulations	Main noise sources identified
Juan XXIII Square	64.3 dBA (Point 1, 21-23)	69.6 dBA (Point 1, 17-19)	53.8dBA (Point 2, 9-11)	51.6 dBA (Point 1, 7-9)	34.38%	Playgrounds and restaurants
San Francisco Square	59.9dBA (Point 2, 19-21)	67.5dBA (Point 1, 21-23)	51.3dBA (Point 1, 21-23)	51.6 dBA (Point 1, 7-9)	9.38%	Restaurants
El Rey Square	63.4dBA (Point 2, 9-11)	68.5dBA (Point 1, 21-23)	53.8 dBA (Point 1, 21-23)	56.7 dBA (Point 1, 7-9)	12.50%	Traffic and restaurants
Town Hall Square	65.7dBA (Point 1, 7-9)	71.1dBA (Point 1, 17-19)	55.1dBA (Point 2, 7-9)	53.4 dBA (Point 1, 7-9)	18.75%	Transit of people

3.2. Results of the citizen perception surveys

The results of this questionnaire (summarized in Figures 3, 4, and 5) show that the assessment of the soundscape of the squares is not solely related to the measured noise level, but also to the type of sounds present and their significance for those who use space. Sounds associated with social activity, pedestrian traffic, or leisure are perceived with greater tolerance and even positively, while occasional noises such as traffic or construction generate greater annoyance.

The results correspond to the average responses of 15 participants in each location (n = 60). While the survey allows for the identification of patterns due to the limited number of participants (60), future studies should expand the sample size to allow for inferential statistical analysis.

3.3. Comparison of the results of the sound level meters - surveys

The comparison between measurements and perception does not produce a complete correlation. These results demonstrate a partial dissociation between acoustic data and citizen perception, reinforcing the importance of incorporating subjective experience into the analysis and design of the urban soundscape.

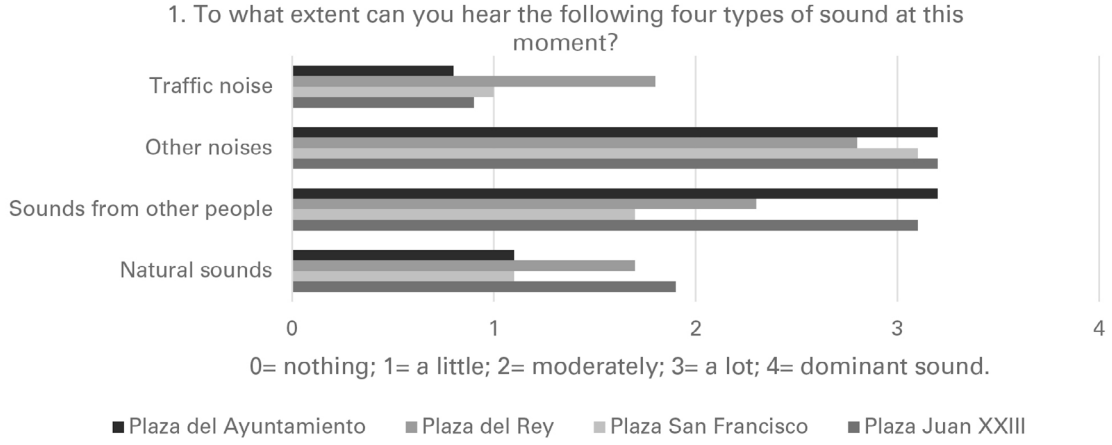


FIG. 3
Results survey question 1

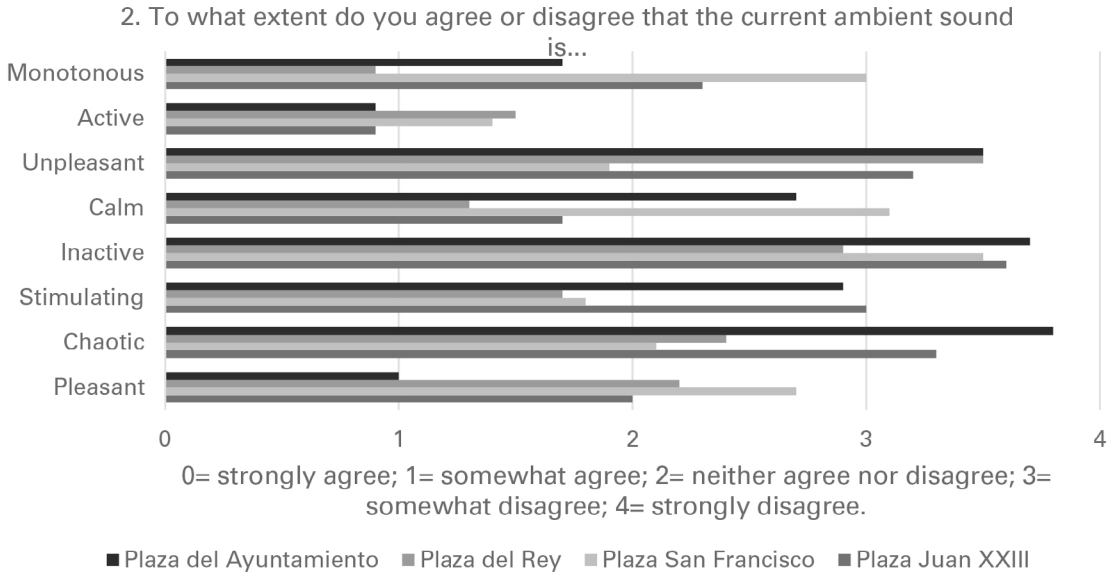


FIG. 4
Results survey question 2

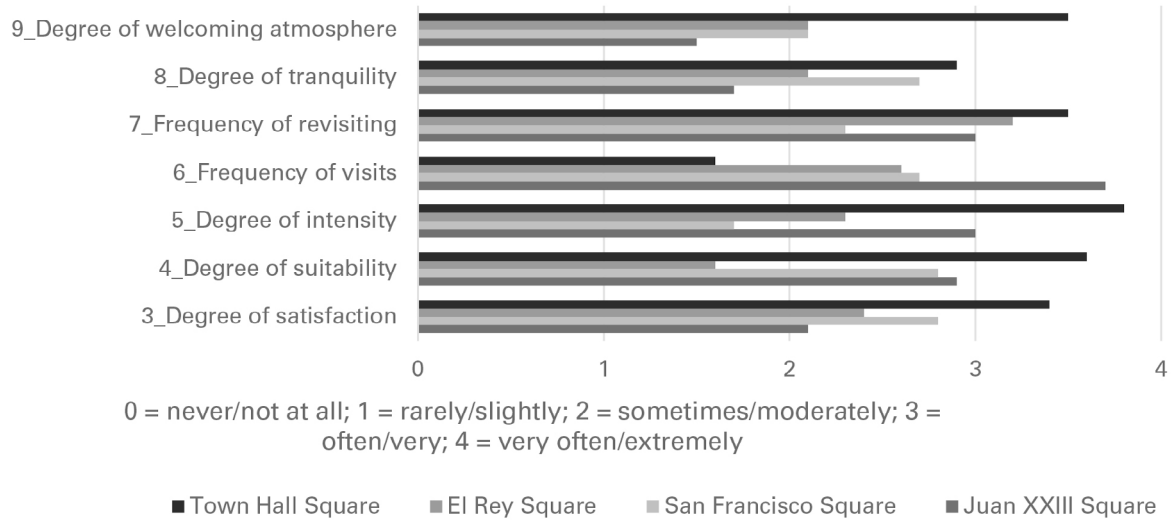


FIG. 5
Survey results for questions 3, 4, 5, 6, 7, 8 and 9

Some squares with high noise levels are not necessarily perceived as acoustically inadequate. Certain higher-intensity natural sounds are considered acceptable, while occasional noises or those caused by motor vehicles are perceived with more aversion. For example, the Town Hall square presented some of the highest measured noise levels and a non-compliance rate of 18.78%, yet it received high scores for tranquillity (2.9/4) and acoustic adequacy (3.6/4), illustrating the dissociation between empirical and perceptual data. This finding suggests that the evaluation of sound comfort in public spaces in pedestrian areas should incorporate the perceptual dimension and not only physical measurements (Table 2).

TABLE 2
Correspondence between measurements and perception

Square	% of sections that do not comply with regulations	Perceived intensity (average/4)	Perceived tranquillity (average/4)	Perceived sound adequacy (average/4)	Is there a match between data and perception?
Juan XXIII Square	34,38%	3,0	2,1	2,9	Yes (intensity), No (adequacy)
San Francisco	9,38%	1,6	2,7	2,8	Yes, in all indicators.
El Rey Square	12,50%	2,2	2,3	1,6	Partial (does not match in suitability)
Town Hall Square	18,75%	3,8	2,9	3,6	Yes (Intensity) No (Tranquillity or sound suitability)

4. CONCLUSIONS

Applying a combined methodology, based on objective acoustic measurements and citizen perception, allows for a more complete understanding of the soundscape in pedestrianized historic squares. The results show that, although noise levels exceed regulatory limits during certain periods, perceived acoustic comfort depends largely on the type of sound and its relationship to the social activity in space. This partial disconnects between measured levels and perception reinforces the need to integrate subjective criteria into urban design. In this context, priority action lines are identified as acoustic renaturalization through vegetation solutions and the incorporation of co-design processes with users, aimed at improving environmental quality and well-being in urban public spaces.

REFERENCES

[1] Fariña Tojo, J., Higueras García, E., Román López, E.: Ciudad, urbanismo y salud. Documento técnico de criterios generales sobre parámetros de diseño urbano para alcanzar los objetivos de una ciudad saludable con especial énfasis en el envejecimiento activo. Escuela Técnica Superior de Arquitectura, Universidad Politécnica de Madrid, Madrid (2019).

[2] Villalpando Flores, A.E., Bustos Aguayo, J.M.: La naturaleza urbana en las ciudades contemporáneas. La importancia del diseño biofílico en la salud pública. Academia XXII 14, 8-29 (2023). https://doi.org/10.22201/fa.2007252xp.2023.14.28.87234

[3] Vargas Marcos, F., de la Cruz Mera, Á., Heras Celemin, M.R.: Vivienda y salud: eficiencia energética, urbanismo sostenible y Agenda 2030. Conclusiones y futuro. Revista de Salud Ambiental 21(1), 56-64 (2021).

[4] Sulca Pillpe, G.D.: Efectos de la peatonalización del jirón Carabaya en el Centro Histórico de Lima. Bachelor Thesis, Pontificia Universidad Católica del Perú, Lima (2021).

[5] Vázquez-Hisado, J.C.: El proceso hacia la movilidad sostenible en Sevilla: centro histórico, peatones y ciclistas. Ciudad y Territorio. Estudios Territoriales 50(196), 263-276 (2018).

[6] Miranda, J.R.C.: Ruido: efectos sobre la salud y criterio de su evaluación al interior de recintos. Revista Ciencia y Trabajo 8, 42-46 (2006).

[7] Jiménez, J.D., Gil, C.L.: Efectos en salud del ruido de tráfico: más allá de las "molestias". Revista de Salud Ambiental 15, 121-131 (2015).

[8] Vida Manzano, J.: La ciudad que tú quieres escuchar. Jornada organizada por COITIRM "La Ciudad que tú quieres escuchar" (2023).

Improving the design of a day-care service provided in a rural environment

Laura Diago-Ferrer[a,] *, Natalia Muñoz[a], Santiago Osnaya[b], José Luis Santolaya[a]

[a] University of Zaragoza, Dep. of Design and Manufacturing Engineering, Campus Río Ebro 50018, Zaragoza, Spain

[b] Autonomous University of the State of Mexico, UAP Tianguistenco, San Pedro Tlaltizapan 52640 Santiago Tianguistenco, México

* e-mail: lauradf@unizar.es

Abstract: In rural areas, the challenges encountered by numerous families in reconciling professional responsibilities, child education and personal life are further exacerbated by a deficit in infrastructure and essential services. This work addresses this phenomenon by optimizing the design of a childcare service in a rural region of Spain, applying sustainability criteria and a life cycle perspective. The influence of support systems, including the physical infrastructure is also considered. Thus, the study addresses the combination of the day-care service and the day-care building in which the service is developed. The investigation adopts a systematic model organized into four main phases, utilizing sequential tasks and specific tools at each stage. Sustainability is valued via the Life Cycle Sustainability Assessment (LCSA) framework, incorporating a triple bottom line approach to balance environmental protection, economic development, and social welfare. Particular emphasis is placed on social dimension through the use collaborative techniques aligned with stakeholder requirements. Thus, functional tools as LCSA or sensitivity analysis are used to obtain and analyze quantitative sustainability indicators. At the same time, socio-collaborative tools as interviews and stakeholders mapping are applied to facilitate the identification of specific work-life balance needs such as extended care hours and spatial reconfiguration. The findings suggest that the integration of operational and socio-collaborative tools fosters a more sustainable design with greater acceptance within the local community.

Keywords: *Sustainable design, day-care service, LCSA, collaborative tools.*

1. INTRODUCTION

The design of sustainable product and service systems using a holistic strategy means taking into account environmental protection, economic prosperity and social benefit. It is therefore a complex and multidimensional challenge that requires the application of appropriate methods and tools. Numerous authors have addressed this topic taking into account the classic structure of the design process based on four phases [1]: problem definition, conceptual design, preliminary design and detailed design. Mulder [2] states that sustainability aspects must be considered throughout all stages of design, using well-integrated additions to the conventional approach. Other authors focus on the development of procedures based on specific tasks throughout the successive phases of the design process. Maxwell *et al.*, [3] propose the "Guide for Developing Sustainable Products and Services in Industry (SPSD)", and Gagnon *et al.*, [4] suggest the use of the "Integrated Sustainable Engineering Design Process" (ISEDP). These guides and methods do not include the study of connections between systems involved or the use of different approaches and tools that integrate both operational and socio-collaborative aspects of design [5].

2. METHODOLOGY

In this work a method that integrates both approaches (operative and collaborative) is applied to achieve sustainable designs. This method is based in the ISEDP model and it is summarized below. Tasks developed in each design phase as well as the tools used in each phase are conveniently indicated in Table 1.

TABLE 1
Functional and collaborative tools used in each phase of the design process

Tasks in a sustainable design process according to the Integrated Sustainable Engineering Design Process (ISEDP)	Functional Tools	Collaborative Tools
1) Problem definition		
(1) Form a multi-disciplinary design team. (2-3) Define sustainability principles and conceptual framework. (4-5) Identify sustainability issues and relationships. (6) Analyze stakeholders.	TBL approach [6] LC thinking Links between systems [7]	Interviews Stakeholder map Questionnaires SWOT analysis
2) Conceptual design		
(7-8) Define sustainability criteria and their comprehensiveness. (9-11) Generate concepts and define scenarios for the future. (12) Define sustainability indicators. (13) Identify the analysis tools. (14) Choose a multi-criteria decision aid method.	ReCiPe [8] Eng. metrics Sust. indicators SimaPro/Cype Weighting	Co-Creation WS Scenario-Building [9] Customer journey

Tasks in a sustainable design process according to the Integrated Sustainable Engineering Design Process (ISEDP)	Functional Tools	Collaborative Tools
3) Preliminary design		
(15) Assess the performance of alternatives. (16) Recommend a preferred alternative. (17) Validate the alternative under different scenarios.	LCSA [10] Aggr. index [11] Sensitiv. analysis	Experience prot. People-place interaction chart
4) Detailed design		
(18) Refine the assessment. (19) Maximize the adaptability. (20) Recommendations for the different life cycle stages. (21) Generate the set of sustainability indicators for monitoring.	LiDS Wheel Monitoring plan Value network model (VNM)	Focus group Worts' model Shadowing

3. CASE STUDY

The sustainable design of a day-care service is addressed according the previous methodology. Those tasks carried out in each design phase and the tools used are detailed below.

3.1. Problem definition

The great effort for many families to balance work, family and personal life is aggravated in contexts such as rural areas, characterized by an aging and geographically dispersed population, as well as an inadequate network of basic infrastructure and services. This problem is addressed in this case by improving the design of a particular day-care service located in a rural region of Spain. Design specifications (according to BOA n.º 106, sept 5, 2005): **Minimum ratios** (1 educator for every 8 children aged 0 to 1 year), 1 educator for every 13 children aged 1 to 2 years, 1 educator for every 18 children aged 2 to 3 years); **Professional qualifications of educators** (one Early Childhood teacher/educational unit); **Installations** (minimum surface area per classroom: 30 m^2 and 2 m^2/school place).

The following tasks are carried out in this phase:

Task 1. Professionals working in public institutions and related to the social and educative ambits are initially consulted to know the situation of families and women in the rural context and the services provided by preschools (ages 0 to 3). Interviews were conducted to extract insights and understand the key issues about conciliation problem and needs to solve.

Tasks 2-3. Sustainability is based on a holistic concept so the integration of aspects associated with the environmental impact, the economic viability and social equity are simultaneously considered. Encouraging family conciliation and social well-being, preserving the ecosystems making a responsible recourse use, promoting the economic development of rural zones and awareness and education in sustainability, are the principles applied.

Tasks 4-5. Two issues affecting sustainability are initially highlighted: i) Improvements of the day-care service could require notable improvements in installations as well as the use of new resources and additional equipment. It should be noted that the day-care building (secondary system or BS) can be considered as a support essential to the development of the day-care service (main system or FS); ii) specific personnel training may be required.

Task 6. The stakeholders involved and their roles associated with the day-care service provided in this rural community are considered: educators, children, parents, families, municipal authorities and other actors of the local community. Questionnaires to understand relevant aspects and to obtain data on the suitable hours of care for children can be used.

3.2. Conceptual design

Taking the current service as a reference, in which two separated sessions (morning and afternoon) are established, the extension of the day-care service hours is projected. Needs expressed by the families include an early drop-off session and a lunchtime session. Different options of lunch service can be proposed, but the catering service provided every day by a local company is the preferred. In any case, new installations to develop the improvements are required, allowing the increase of hours and activities of the day-care service. The following tasks are carried out in this phase:

Tasks 7-8. Functional specifications should be achieved minimizing negative impacts and balancing sustainability aspects in the three dimensions. Impact categories associated with each sustainability dimension are proposed. In this case, damage to ecosystems (environmental), financial results (economic) and local community (social).

Tasks 9-11. Scenarios in which the alternative service can evolve or can be developed should be considered. In particular, planning actions regarding different ways of use of the expanded nursery area and the multipurpose room are examined. The management of the lunch service according to different requests made by families (daily, weekly, occasional...) are also valued. Special diets and alternatives proposed by families who do not make use of catering.

Task 12. The use of engineering metrics and quantitative indicators to objectively value and compare options of improvement is preferred. The following engineering metrics were selected: Energy consumption (electricity and gas); monetary inputs and operation costs; ratio children/caregiver and operating time of the day-care service. In line with the impact categories, the following indicators are selected: Global Warming Potential (GWP), Added (VA) and Local Employment (Em).

Task 13. Sustainability data are obtained by means of specific Database and software. In the case of the GWP, the indicator expressed as emissions per mass unit, can be obtained using software such as SimaPro. In order to value environmental impacts and execution costs of the day-care building, the software Cype is used.

Task 14. Sustainability balance between different dimensions is carried out assigning different weights to those indicators selected. Weights reflect the interests and preferences of decision-makers and will be determinant to compare design alternatives. In this case, two options are considered: equal weight and one dominant dimension.

3.3. Preliminary design

Current service and improved service are compared. In the initial service, users are permitted to opt for either a morning session (from 9:00 to 13:00) or an afternoon session (from 15:00 to 18:00). Day-care building is based on four class-rooms and one office. In the projected service, uninterrupted service from 8 a.m. to 6 p.m. is carried out. It includes an early drop-off session (from 8:00 to 9:00) and a lunchtime session (from 13:00 to 15:00). Three new rooms dedicated, respectively, to storage, food preparation, and a multipurpose room are planned in the day-care building. The following tasks are carried out:

Task 15. The sustainability assessment of the two design options is carried out applying the LCSA method. Thus, results of sustainability indicators are obtained and can be compared. Inventory data providing key quantitative technical data of the current service are collected thanks to the collaboration of municipal institutions and the workers of the nursery school. The energy consumption, operation costs, enrolled children and special issues as reduced fees or bonuses applied according to the particular conditions of each family are considered. Data of service projected are obtained according to those planned changes. Metrics and indicators of the new installations were calculated taking into account that the useful life of this type of public building is usually 50 years. In this case, the use of the operating period as FU affect significantly to the relative low impact in emissions and costs that generates the annexed area in the day-care building. Expected data for children registrations with the extension in the service hours are also taken in account.

Task 16. The multi-criteria decision approach is applied and an aggregated index is calculated obtaining the relative sustainability improvement between design alternatives with the weights assigned to each indicator. In this case, two alternatives are considered: i) equal weight is given to each sustainability dimension; ii) social demands are considered preferential so a weight of 0.5 is assigned to this dimension and equal weight of 0.25 is assigned to the rest. It is observed that the impact in the environmental dimension increases, the economic dimension is hardly modified and social dimension is significantly favoured. It is recommended the service projected since it meets initial functional specifications and includes improvements to solve the conciliation problem.

Task 17. A sensitivity analysis is also carried out to determine how changes of different factors can affect the results. The percentage variation of the sustainability indicators is considered. The effect of the reservations number or the temporal use of the lunch service in the economic costs of the day-care service is analyzed. First, variation of ±10% in reservations of catering service was considered and results are compared with those obtained in the base case. On the other hand, the sensitivity over the months of the school year was studied.

3.4. Detailed design

In this last phase of the design process, the detailed design of the day-care service provided with uninterrupted activity from 8 a.m. to 6 p.m. and developed in a planned new day-care building with a total surface of 268 m^2, is carried out. The layout with the children allocation per classroom as well as their age range and time considered of use is shown in the Figure 1. According to previous estimations, a total of 37 children could be cared for a total of four educators (one teacher and three technicians). Others workers as one canteen support person, one city council official, a worker for cleaning and another for maintenance tasks would complete the nursery staff.

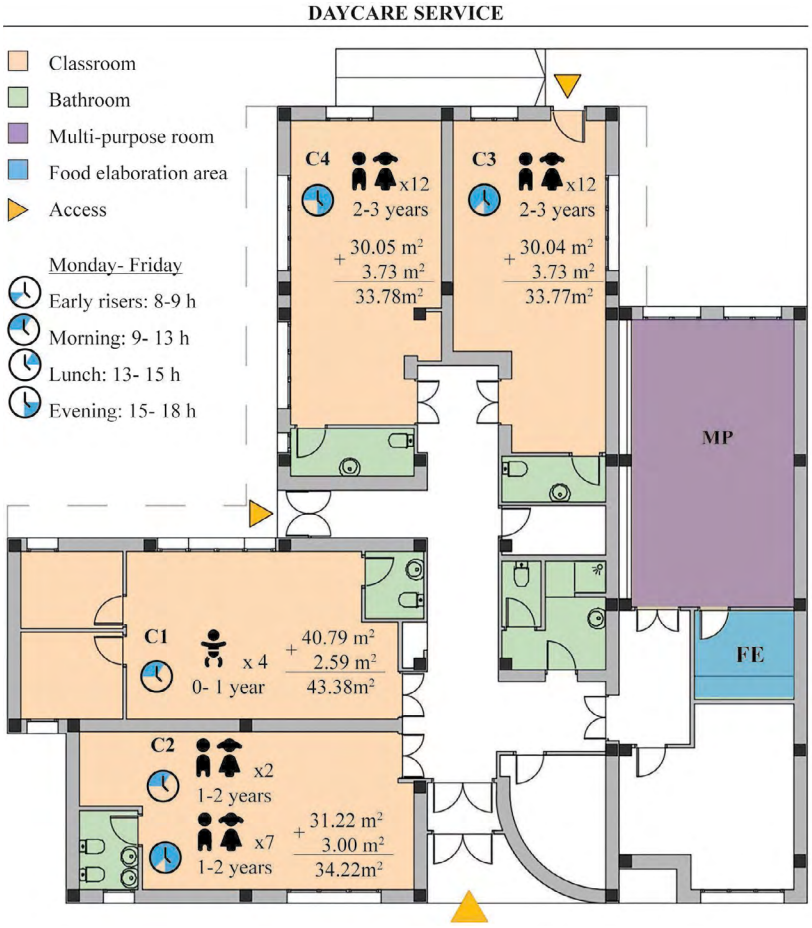


FIG. 1
Scheme of the improved day-care service

Task 18. The activities involved in the service provision are examined in detail, as well as the consumption of resources and materials used in each activity. Education, hygiene and recreation activities accounted for approx. 75% of working time and materials consumed can be grouped according to their main composition. In addition, the study of the routes taken by public transport and parents from nearby municipalities to take their children to day-care can be analysed. Thus, data about emissions, costs and times due to the daily transfers can be valued.

Task 19. The optimization of the service performance could be carried out if new systems, which can be included as support systems of the day-care service, are analysed in detail and additional sustainability criteria applied. In particular, the transport of children to or from nursery is another support system that involves a greater number of activities and use of resources. How the day-care performance can be affected by this system should be studied.

Task 20. Recommendations for the different life cycle stages: a) Ensure appropriate durability of components and promote the use of recycled materials; b) Ensure efficiency of resources during use; c) Reducing transportation impact favouring the public or shared transport services.

Task 21. Data of metrics and indicators should be recorded along the service development and compared with those estimated in the design process. Particularly, the energy consumption and the Global Warming Potential (GWP), the operation costs and the net operating profit, and the ratio children/caregiver and local employment creation, should be monitored.

4. CONCLUSIONS

Sustainable design methods found in the reviewed literature do not include the study of connections between systems involved or the application combined of functional and collaborative approaches. These challenges are addressed in this work, in which the sustainable design of a day-care service is carried out. A method based in the ISEDP model is applied.

As a result, the integration of various types of tools for the effective measurement of functional sustainability indicators as well as for the appropriate involvement of stakeholders ensures not only objectively more sustainable outcomes, but also greater acceptance by the community involved. In addition, the combined study of both systems day-care service and day-care building shows the feasibility of the proposed improvements to enhance family-work balance and address local community demands. It could be concluded that the complementary application of the operational and socio-collaborative approaches as well as the integration of different systems favours obtaining a more sustainable day-care service design.

REFERENCES

[1] Pahl, G., Beitz, W., Feldhusen, J., Grote, K.H.: Engineering Design. A Systematic Approach, 3th edn. Springer-Verlag, UK. (2006).

[2] Mulder, K.: Sustainable development for engineers. Greenleaf Publishing, Sheffield, UK (2006).

[3] Maxwell, D., Sheate, W., Van der Vorst, R.: Functional and systems aspects of the sustainable product and service development approach for industry. J Clean Prod 14, 1466-1479 (2006).

[4] Gagnon, B., Leduc, R., Savard, L.: From a conventional to a sustainable engineering design process: different shades of sustainability. J Eng Des 23(1), 49-74 (2012).

[5] Ramos, I., De Rosa, A., Galluzzo, L., Biedermann, A., & Santolaya, J. L.: Integrating Different Approaches and Tools to Evaluate Socio-Cultural Impact of Services Projected in Low-Population Environments. Open Journal of Social Sciences, 12, 141-152 (2024).

[6] Elkington, J.: Cannibals with Forks: the Triple Bottom Line of 21st Century Business, Capstone, Oxford (1997).

[7] Muñoz, N., Santolaya, J.L., Biedermann, A., Serrano, A.: Sustainability assessment of product-service systems using flows between systems approach. Sustainability 12 (8) (2020).

[8] Huijbregts, M., Steinmann, Z., Elshout, P., Verones, F., Vieira, M., Hollander, A., Zijp, M., Van Zelm, R., Stam, G.: ReCiPe 2016. A harmonized life cycle impact assessment at midpoint and endpoint level. Report I: Characterization. National Institute for Public Health and the Environment. The Netherlands (2016).

[9] Auricchio, V., De Rosa, A., Fassi, D., Johannsson, B., King, J., Lelarge, A., Líndal, P. J., Monna, V., Russo, P., van Hasselt, F.: Smoties Toolbox. Design tools for the creative transformation of public spaces in small and remote places. Birkhauser Verlag AG, (2025).

[10] Kloepffer, W.: Life cycle sustainability assessment of products. Int J Life Cycle Assess 13(2), 89-95 (2008).

[11] Santolaya, J.L., Lacasa, E., Biedermann, A., Muñoz, N.: A practical methodology to project the design of more sustainable products in the production stage. Res Eng Des 30(4), 539-558, (2019).

Development of a model for predicting the maximum stress of FDM-modeled PLA specimens

Silvia Losada-Pérez[a,*], Ana Isabel García-Diez[b], Rosa Devesa-Rey[c], Miguel Ángel Álvarez-Feijoo[d], María Elena Arce Fariña[b]

[a] Spanish Navy. Ministry of Defense, C/Irmandiños s/n, 15490, Ferrol, A Coruña, Spain

[b] University of A Coruña, Ferrol Polytechnic School of Engineering. C/Mendizábal, s/n. Esteiro Campus. 15403 Ferrol, A Coruña, Spain

[c] University Defense Center at Spanish Naval Academy. Plaza de España, s/n 36920 Marín, Pontevedra, Spain

[d] University of Vigo. School of Industrial Engineering, C/ Maxwell 9, Lagoas-Marcosende 36310 Vigo, Pontevedra, Pontevedra, Spain

* e-mail: elena.arce@udc.es

Abstract: This paper contributes to research in additive manufacturing by exploring its integration with artificial intelligence, focusing on Fused Deposition Modeling (FDM) 3D printing. PLA samples were fabricated using various printing parameters, including layer height, infill percentage, number of perimeters and print orientation to evaluate their influence on mechanical performance. The samples were subjected to tensile testing to assess their maximum stress capacity. The experimental data was used to make a database for developing a predictive model based on multilayer perceptron neural networks. This model aims to estimate the maximum stress that FDM-printed PLA samples can withstand under different manufacturing conditions. Results indicate that optimal mechanical performance is achieved with higher layer heights, a 45° print orientation, and higher infill percentages. The predictive model demonstrates reasonable accuracy, with acceptable error levels based on MSE and RMSE metrics. Overall, the study presents a useful tool for estimating the mechanical resistance of 3D-printed parts. However, further data are required to improve model generalization across a wider range of printing configurations and conditions.

Keywords: *PLA, FDM, Prediction, Model, 3D printing.*

1. INTRODUCTION

Additive manufacturing, and particularly Fused Deposition Modeling (FDM), has become a widely used technique due to its flexibility, low cost and applicability in different fields [1,2]. However, the mechanical performance of FDM parts strongly depends on the selected printing parameters [3,4]. Therefore, predictive models able to estimate mechanical properties from printing configurations may support the selection of suitable manufacturing strategies.

2. MATERIALS AND METHODS

Colourless PLA filament without additives, supplied by Filament2Print, with a diameter of 1.75 mm, was used. The specimens were modelled in Fusion 360, sliced with Bambu Studio and printed on a Bambulab P1S printer.

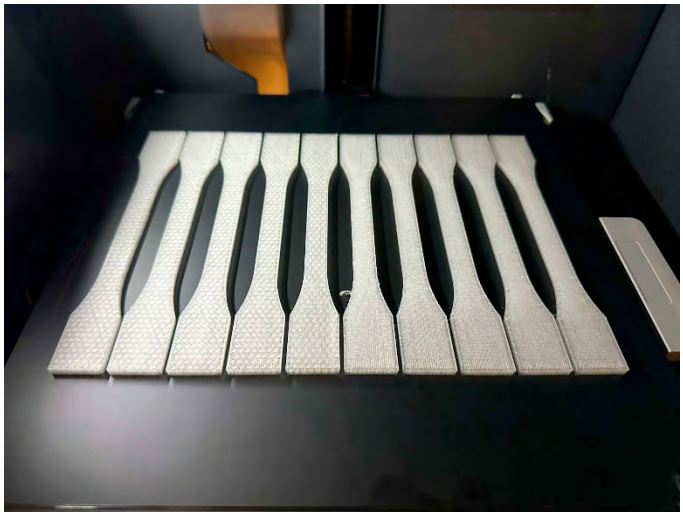


FIG. 1
Printed samples (Created by the author)

The machine used to perform the tensile test on the samples printed with different printing configuration was an INSTRON 5566. The standards UNE 116005:2012 and UNE-EN ISO 527-2:2012 was followed to design the specimens that will undergo the tensile test.

The test data were compiled into a database and processed in MATLAB to train a model for predicting the maximum stress from the selected printing strategy.

3. EXPERIMENTAL DEVELOPMENT

The experimental development can be distinguished in three parts: the creation of the samples, their tensile testing and the development of a model using the test results.

3.1. Samples manufacturing

The fixed parameters chosen with the same value for all prints based on manufactured recommendations, previous works and different tests performed in the specific printer. Four parameters were varied: printing angle, 0°, 45° and 90° relative to the Cartesian reference axes (Figure 2); number of perimeters, 1, 2 and 3 (Figure 3); infill density, 10%, 55% and 90% (Figure 4); and layer height, 0.1, 0.2 and 0.3 mm.

Regarding the parameters to be varied and combined, the following four parameters were selected:

Printing angle: 0°, 45°, and 90° relative to the Cartesian reference axes (Figure 2).

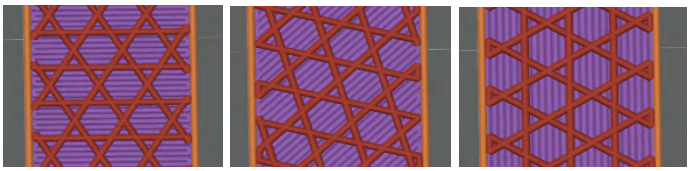


FIG. 2
Infill patrern and angles of 0º, 45º and 90º (Created by the author)

Number of perimeters: 1, 2, and 3 perimeters were chosen (Figure 3).

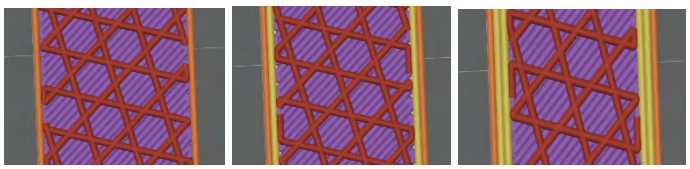


FIG. 3
1 Perimeter, 2 perimeters and 3 perimeters (Created by the author)

Infill density: 10%, 55%, and 90% (Figure 4).

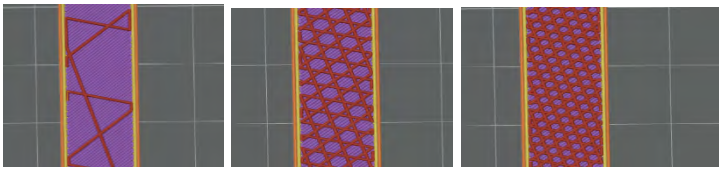


FIG. 4
10% infill, 55% infill and 90% infill (Created by the author)

Layer height: 0.1, 0.2, and 0.3 mm.

After selecting these four variables and choosing three values for each one and, as it was printed 5 samples for each configuration, a total of 405 were manufactured and stored until testing.

3.2. Tensile testing

The tensile test of the manufactured specimens was carried out at a speed of 10 mm/min, a value within the limits of the UNE-EN ISO 527-1:2019 standard (Figure 5). The results obtained from the tests on the samples were Young's Modulus (MPa), Tensile stress at yield (MPa), Tensile strain at yield (%), Tensile stress at break (MPa) and Tensile strain. These results were saved to a CSV file, and they were cleaned by discarding any null data. In this case, only six samples were discarded, corresponding to different printing configurations, leaving the other four results obtained from those configurations as valid.



FIG. 5
Tensile tests (Created by the author)

3.3. Model development

For the creation of the model in MATLAB the data was divided into training and testing sets using hold-out 80-20. The inputs for the model were defined as the printing configuration and the output corresponded to the Tensile Stress. A multi-layer perceptron with one hidden layer with 10 neurons were chosen (Figure 6).

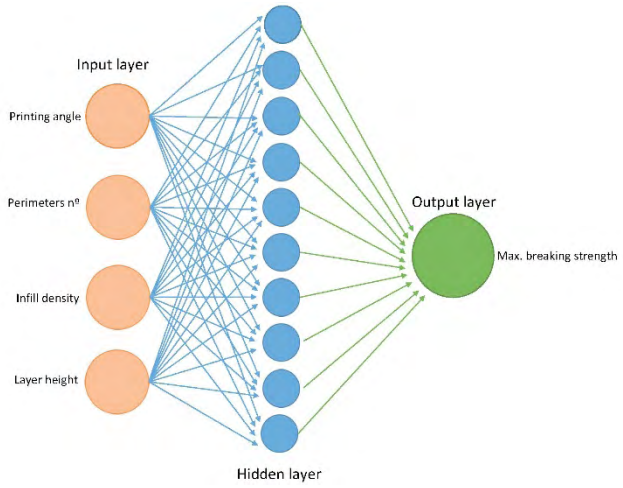


FIG. 6
Neural network (Created by the author)

4. RESULTS

The results can be divided in two different parts: the first one corresponds to the results of the tensile tests of the printed samples and the second one to the modelling results.

4.1. Tensile tests

The four parameters varied in the printing configurations will be analyzed below.

—Layer height parameter and the maximum stress results (Figure 7), better tensile strength is obtained with a greater layer height.

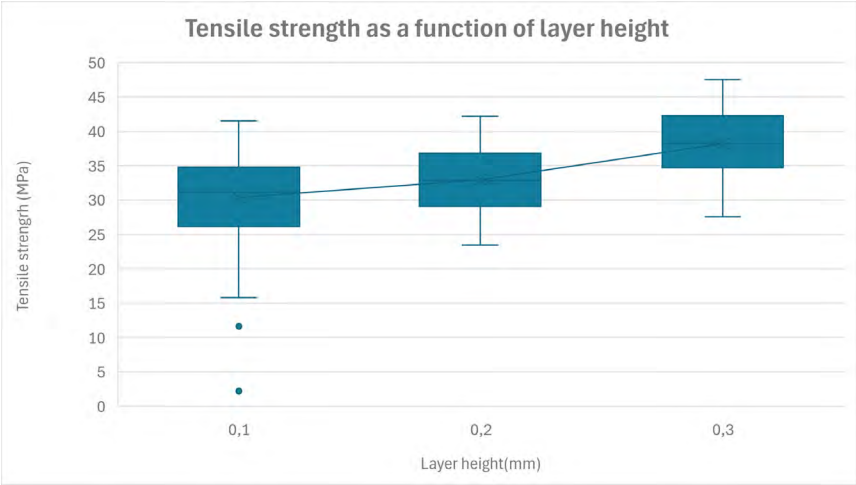


FIG. 7
Comparison of the tensile strength as a function of layer height (Created by the author)

— Infill density (Figure 8), the higher the infill percentage, the greater the maximum tensile stress the specimen can withstand.

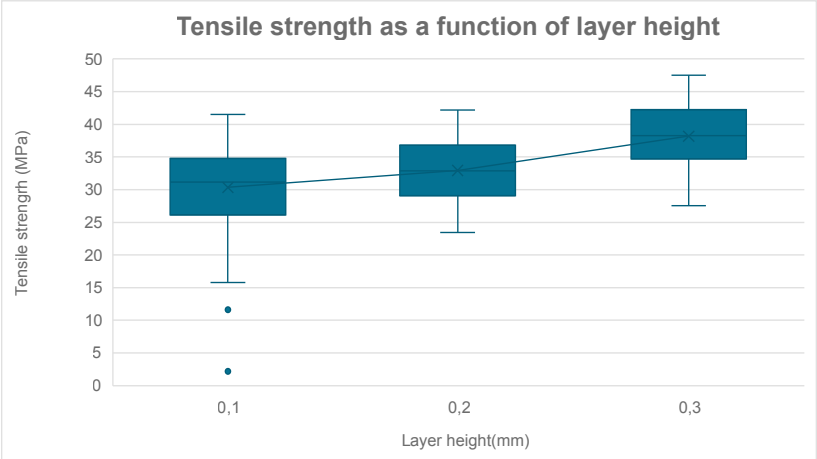


FIG. 8
Comparison of the tensile strength as a function of infill density (Created by the author)

— Printing angles (Figure 9), the difference in maximum stress depending on the printing angle is related to how the load and material properties are distributed in the direction of the applied force.

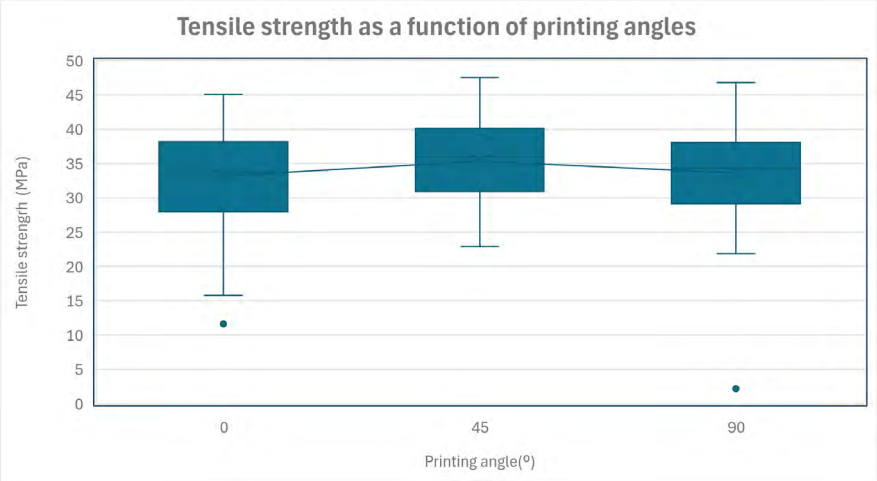


FIG. 9
Comparison of the tensile strength as a function of printing angles (Created by the author)

— Number of perimeters (Figure 10), the samples with a higher number of perimeters achieve the highest stress.

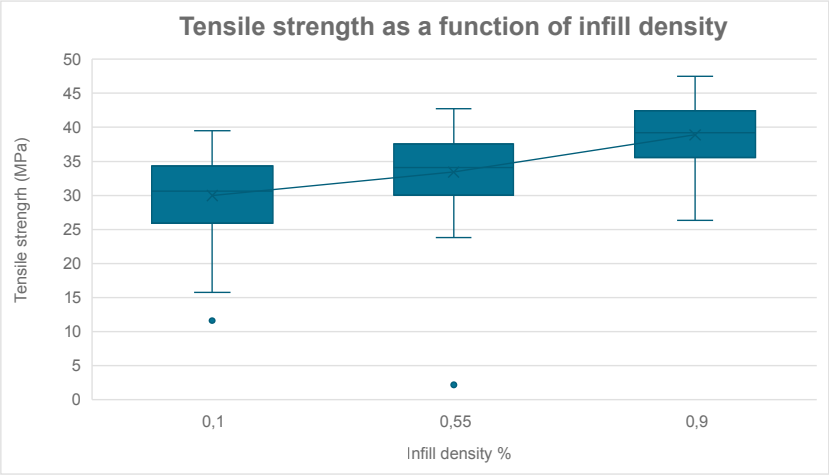


FIG. 10
Comparison of the tensile strength as a function of the number of perimeters (Created by the author)

4.2. Model results

The defined model was trained and a mean squared error (MSE) was calculated, 1.778; also, the root mean squared error (RMSE) was calculated to obtain a measure in real units, 1.333. The results were graphically represented (Figure 11).

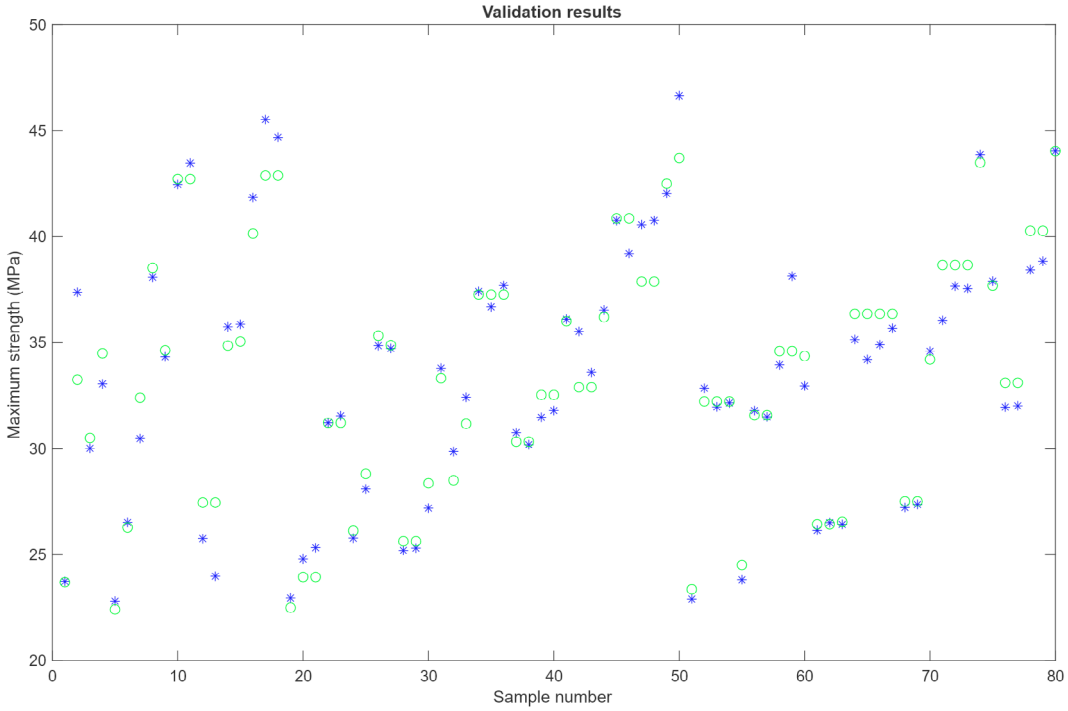


FIG. 11
Validation results (Created by the author)

Visually, there is not much dispersion between the two results; however, to evaluate the model's accuracy, it is necessary to analyze the MSE and RMSE values. The width of the interval is 24.8 units (the difference between 46.65 and 21.85), so the average prediction error is relatively small compared to the total data range. In percentage terms, the predictions are 5.38% of the total data range, which is considered an acceptable result.

The above confirms that the results are consistent and that the average prediction errors fall within the range. The model shows relatively low average errors compared to the data interval, indicating good performance.

5. CONCLUSIONS

A prediction model for maximum stress has been developed for specimens manufactured using FDM with PLA. With it, the value of maximum stress can be predicted for a given printing configuration, which would allow the mechanical strength of a printed part to be known in advance based on specific printing parameters.

The MSE and RMSE values obtained within the data range suggest that the model has reasonable performance and that the average error relative to the range is acceptable, provided that technical requirements allow it. However, it should be noted that using this model for different configurations would require more data for training.

It is remarkable that the best parameters in terms of material strength, the highest maximum stress result would be obtained with a layer height of 0.3 mm, a printing angle of 45°, an infill density of 90%, and 3 perimeters, yielding a maximum stress of 46.65 MPa, with an average of 44.532 MPa for the five specimens with this configuration.

Acknowledgements: This research was funded by the UVIGO and the Defence University Centre at the Spanish Naval Academy (Project Ref. PICUD2025-03) and by the Xunta de Galicia through the Axencia Galega de Innovación (GAIN), under grant IN853C2025/03; by the Centro Mixto de Investigación UDC-NAVANTIA O estaleiro do futuro. The funders had no role in study design, data collection and analysis, decision to publish, or preparation of the manuscript.

REFERENCES

[1] Ben Said, L., others: Recent Advances in Additive Manufacturing. Machines. 13, 813 (2025). https://doi.org/10.3390/machines13090813.

[2] Liampas, S., others: Recent Advances in Additive Manufacturing of Fibre-Reinforced Materials. Applied Sciences. 14, 10100 (2024). https://doi.org/10.3390/app142210100.

[3] Mirza, F., others: Effect of material extrusion parameters on tensile performance. International Journal on Interactive Design and Manufacturing. (2024). https://doi.org/10.1007/s40964-024-00825-4.

[4] Unknown, A.: Recent developments in additive manufacturing materials and design optimization. Mater. Des. (2025). https://doi.org/10.1016/j.matdes.2025.113609.

[5] Rismalia, M., Hidajat, S., Permana, I., Hadisujoto, B., Muslimin, M., Triawan, F.: Infill pattern and density effects on the tensile properties of 3D printed PLA material. J. Phys. Conf. Ser. 1402, 44041 (2019). https://doi.org/10.1088/1742-6596/1402/4/044041.

Advantages and disadvantages of using automatic geometric and dimensioning tolerance tools in 3D CAD systems: A case study of a mechanical guidance device

Fernando Brusola[a,*], Antonio Valín[b], Ignacio Tortajada[a], María Ángeles Esandi[b], Jorge Montalvá[a]

[a] Universitat Poltècnica de València

[b] Universidad de Valladolid

* e-mail: fbrusola@upv.es

Abstract: Certain 3D CAD systems enable the automatic generation of geometric dimensioning and tolerancing (GD&T) for mechanical components based on the modeling operations used to define them. These capabilities are typically integrated within Model-Based Definition (MBD) or Product Manufacturing Information (PMI) frameworks, which facilitate the direct annotation of 3D models and reduce reliance on traditional 2D drawings. This study evaluates the advantages and limitations of automated GD&T tools in comparison with the heuristic approaches conventionally employed by experienced mechanical design engineers. The analysis focuses on the dimensioning of a mechanical guiding device. The results indicate that automatic dimensioning tools can provide acceptable outcomes for relatively simple geometries; However, they have shortcomings regarding the geometric and dimensional characteristics of functional surfaces and volumes, as well as in the definition of the basic dimensions used to establish positional tolerances, which can make them unsuitable for addressing the level of complexity found in real-world mechanical design applications.

Keywords: *Geometric dimensioning and tolerancing, functional analysis, dimensioning of mechanical devices, dimensioning methods, model-based definition, product manufacturing information.*

1. INTRODUCTION

Some 3D modeling programs enable automatic dimensioning in 3D based on the modeling operations required to define a part, once the reference surfaces—relative to which form, and positional tolerances are specified—have been established. These reference surfaces simultaneously determine form and orientation tolerances depending on the order in which they are specified. The geometric and dimensional tolerances generated by the system follow an internal algorithm specific to the 3D software used. As a result, the output is difficult for the designer to predict and generally does not meet the functional requirements identified after performing a complete functional analysis of the mechanical device in which the part will be integrated. To adjust the default tolerance values assigned automatically by the software, some 3D CAD applications include tolerance analysis modules. These allow designers to refine the dimensions affecting the functional conditions of the system. However, such modules exhibit significant limitations. Once functional conditions are defined at the assembly level, the system attempts to detect the relevant dimensions by requiring the designer to specify the involved components and the contact constraints between surfaces. Based on this information, the system identifies the set of dimensions and geometric features affecting the functional condition. Although this process is theoretically automatic, failures frequently occur in the detection of dimension chains, particularly when positioning constraints involve tangency conditions.

ISO 1101 [1] and ASME Y14.5 [2] standards provide guidelines for specifying dimensional and geometric tolerances (GD&T) in drawings and technical documentation. However, these standards are formal in nature and generally do not assist in determining specific tolerance values for a given application.

Several authors have proposed approaches for GD&T specification in mechanical devices. Brusola *et al.* [3-4] present a dimensioning methodology based on functional assembly conditions derived from the assembly sequence. Chapter 15 on functional analysis in the book by Félez and Muneta [5] offers guidelines for functional dimensioning supported by numerous practical examples. Similarly, the works of Meadows [6-7] provide in-depth analysis of GD&T-related problems.

Ke-zang *et al.* [8] propose an intelligent dimensioning approach to automatically generate 2D drawing dimensions from 3D models based on feature extraction, although this approach neglects the assembly context. Latif and Graham [9] introduce the Simple Geometry Method (SGM), which assists dimensioning through geometric simplification.

Other relevant contributions [10-12] establish procedures for determining tolerances that define functional conditions through multiple examples. However, most existing studies neglect the functional role of the part within the mechanical system, as highlighted in [3-4].

Many advanced 3D CAD systems currently include semi-automatic dimensioning tools, yet they still exhibit several shortcomings. This paper aims to identify some of these limitations through the analysis of the automatic dimensioning tool in SolidWorks® applied to the GD&T specification of a bench vise. To date, the authors have not found any references that specifically carry out the proposed analysis. We believe this is a matter of utmost importance for ensuring that future automated or artificial intelligence-enabled systems can detect critical dimensions in mechanical devices.

2. METHOD

The comparative study is based on a model developed in SolidWorks® for the mechanical device shown in Figure 1.

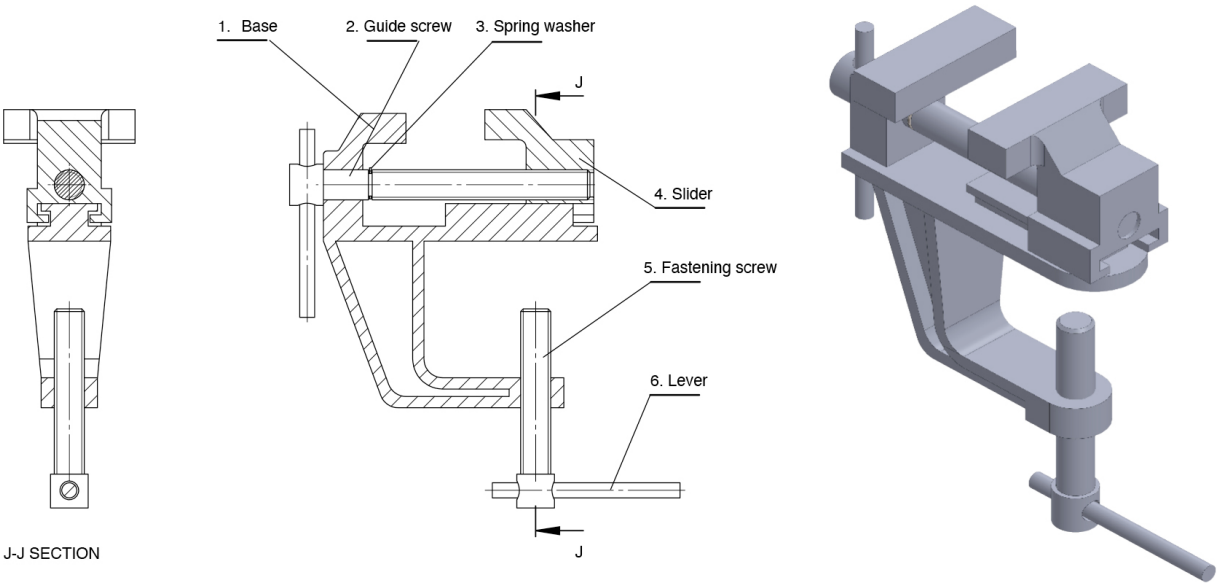


FIG. 1
Bench vise

The analysis focuses exclusively on the functional definition drawing of the base component, as it presents the greatest difficulty in terms of dimensioning. The remaining components are not considered, as their dimensioning is relatively straightforward and the automatic dimensioning tool performs adequately in such simple cases.

The procedure followed to analyse the performance of the SolidWorks' automatic dimensioning system is as follows:

1. Dimensioning of the base (part #1) using the methodology described by Brusola *et al.* [3-4], considering only functional dimensions to ensure clarity in comparison.
2. Dimensioning of the base using MBD automatic dimensioning tools.
3. Comparison of results.

3. RESULTS

Figure 2 illustrates the result obtained by applying the methodology described in [3-4]. Datum planes, identified as A, B, and C, were defined in accordance with the guidelines proposed by Meadows in [6-7].

Figure 3 presents the result achieved using the SolidWorks MBD automatic dimensioning tool. The procedure followed to obtain the results shown in Figure 3 can be summarized as follows:

1. The tool first requires the selection of the reference surfaces with respect to which the geometric positional tolerances are to be defined. A maximum of three references can be specified, and these must remain mutually independent. In other words, it is not permissible to select three surfaces or axes if one is parallel to a previously defined reference or corresponds to the intersection of two previously defined references. In the present case, the first selected reference surface corresponds to A in Figures 2 and 3 (it should be noted that identical datum references were used in both approaches), followed by B as the second reference and C as the third.
2. Subsequently, the user must define which modeling operations are to be considered by the tool for dimensioning purposes. Two alternative approaches are available. The first consists of directly selecting individual modeling operations (e.g., extrusion, drilling, filleting, chamfering), allowing the system to dimension the features generated by each operation independently, without considering others. The second approach involves selecting all modeling operations and then applying a filtering process based on a predefined set of operation types provided by the software. This latter approach was adopted to generate the results shown in Figure 3. In this study, only the following filters were applied: cylinder, simple and compound hole, slot, notch, and pocket, all of which are present in the part model. Conversely, filters such as plane, surface, cone, fillet, chamfer, facing, countersinking, surface of revolution, and torus were deliberately excluded. Including the full set of filters would have resulted in an excessively complex and difficult-to-interpret output, generating many GD&T annotations that are not functionally justified.

Although the dimensioning results obtained from both approaches appear broadly similar, several critical differences must be emphasized, as they have direct implications for the correct functional definition of the component:

1. In section H–H of Figure 3, a positional tolerance is assigned to the Ø15 mm arc. This specification is clearly unnecessary, as the corresponding cylindrical surface does not fulfill any functional role within the assembly. A similar issue arises with the Ø22 cylindrical surface shown in the upper view of the part. The inclusion of such non-functional tolerances reflects a lack of contextual understanding of the component's role within the mechanical system.

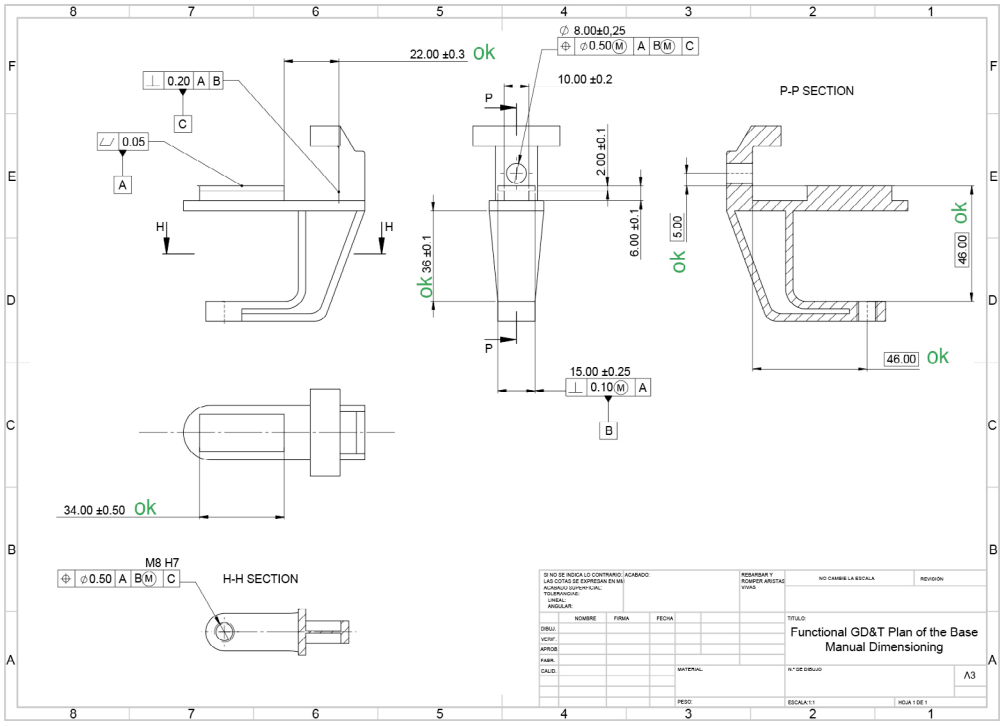


FIG. 2

Functional GD&T plan of part #1, created using the methodology outlined in references [1-2] and the guidelines provided by Meadows in references [6-7]

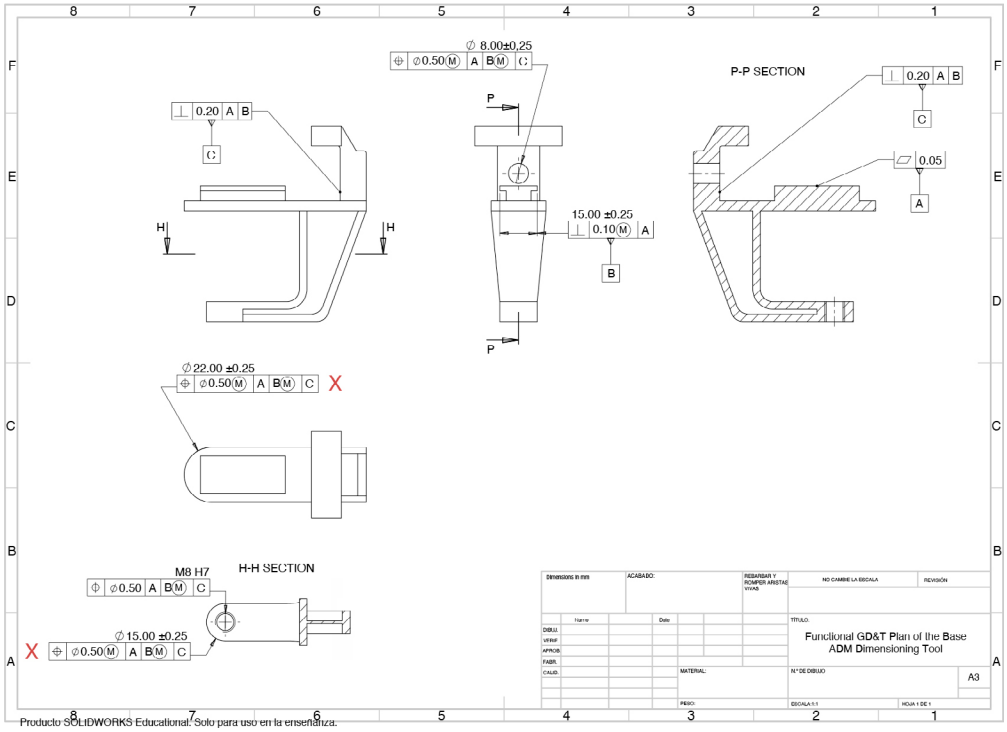


FIG. 3

Functional definition drawing of part #1, created using the automatic dimensioning tool in SolidWorks® MBD

2. A considerable number of positional tolerances are defined; however, the corresponding basic dimensions (i.e., theoretically exact dimensions required for proper GD&T interpretation) are not provided. This omission represents a significant limitation, as positional tolerances cannot be correctly interpreted or applied without their associated basic dimensions. In contrast, these elements are appropriately defined in Figure 2 when functionally required.
3. The automatic system fails to specify several key dimensions that are essential for the proper functioning of the device, particularly those governing the smooth sliding of the guide mechanism. These include the dimensions with values 10, 6, and 2 shown in the left view of Figure 2. In addition, the nominal dimensions 22 and 34, which define the sliding range of the upper guide, are omitted despite their relevance to the operational performance of the system. Finally, the nominal dimension 36, also shown in the right-side profile (left view), is of particular importance, as it determines the maximum thickness of the surface that can be clamped by the bench vise. The absence of these dimensions highlights a fundamental weakness of the automatic approach in capturing functional design intent.

TABLE 1
Summary of dimensioning mistakes made by SolidWorks' Automatic Dimensioning Tool

Mistake or error	Number of instances
GD&T of non-functional surfaces	2
Missing basic dimensions	3
Missing of functional dimensions	3

To better illustrate the differences observed we have marked the incorrect GD&T specification in the automatic dimensioning tool in Figure 3 with a red "X" and the missing functional specification in Figure 3 with a green "OK" in Figure 2. Table 1 summarizes the mistakes made by the automatic dimensioning tool of SolidWorks.

4. CONCLUSIONS AND DISCUSSION

Program documentation does not provide any explanation of the algorithm used by the automatic dimensioning module. However, based on the results obtained, it can be inferred that the dimensioning is based on the definition of 3D modelling operations and user-defined reference surfaces. The problem with this method is that the system does not distinguish between operations that are important for the proper functioning of the device. For example, as noted in the results section, the system specifies dimensions for the part's external fillet arcs, which serve no specific function in the assembly of the part within the mechanical device to which it belongs. This occurs because the automatic part dimensioning system is taken out of context from the mechanical assembly; this should be corrected so that the specification of geometric and dimensional tolerances is better tailored to the device's re-

quirements, thereby avoiding unnecessary cost overruns due to inefficient dimensioning. It is well known that correct dimensioning is crucial because of its influence on the selection of machining processes and systems in terms of the required precision.

Comparative analysis made clearly demonstrate that while automated GD&T tools can produce geometrically consistent annotations, they frequently fail to account for the functional requirements of a part within its assembly context.

The omission of essential dimensions, the inclusion of non-functional tolerances, and the lack of proper datum-based definition collectively limit the practical applicability of such tools in advanced mechanical design tasks. Therefore, the use of automatic dimensioning systems should be considered only as a support tool, and always under the supervision of a GD&T expert capable of interpreting functional requirements and ensuring design intent is properly captured.

Ultimately, accurate dimensioning cannot be achieved without considering the role of the component within the overall mechanical system. As with other advanced technologies, including AI-based tools, improper or unsupervised use may result in significant manufacturing, assembly, or operational issues that could otherwise be avoided through human expert intervention.

One might argue that the conclusions of this study are obvious, since when modeling a part, information about the assembly is not available; however, this is not always true, as parts can be modeled from assembly drawings. In any case, even if the part were completely unlinked from its assembly, the dimensioning system might internally have a system for linking conjugate surfaces—that is, surfaces whose shape and position must be related to ensure a specific type of fit—and confirmation of this could be sought from the part's designer. The module could also ask the operator whether a modeling operation might affect the part's fit within the assembly, thereby eliminating the need to explicitly specify the corresponding dimensional and geometric tolerances.

5. REFERENCES

[1] ISO 1101:2017: Geometrical product specifications (GPS) – Geometrical tolerancing – Tolerances of form, orientation, location and run-out. International Standard Organization, Geneva (2017).

[2] ASME Y14.5-2009: Engineering drawings and related documentation practices. American Standard for Mechanical Engineers, New York (2009).

[3] Brusola F., Tortajada I., Rubió C., Defez B., Roca F., Montalvá J. Geometric dimensioning and tolerancing method based on the assembly diagram of a mechanical device. Case study of a V-axis positioning device. Springer, Advances in Mechanical Engineering, pp. 911-925, Geneva (2024). INGEGRAF 2023 International Conference June 21-23, Cádiz, Spain.

[4] Brusola, F., Tortajada, I., Rubió, C., Magal, T., Agustín, MA, Montalvá, J.: An approach to defining an automatic system for determining geometric and dimensional tolerances. Case study for a lathe tailstock center. Springer, Advances on Mechanics, Design Engineering and Manufacturing V, 1169-1180, Geneva (2025). International Joint Conference on Mechanics, Design Engineering & Advanced Manufacturing, JCM 2024, June 12-14, 2024, Valencia, Spain.

[5] Félez, J., Muneta, ML.: Ingeniería Gráfica y Diseño. Editorial Síntesis, Madrid (2008).

[6] Meadows, JD.: Geometric dimensioning and tolerancing. ASME Press, New York (2009).

[7] Meadows, JD.: Workbook and answer book for geometric dimensioning and tolerancing. James D. Meadows & Associates, Inc., Hendersonville (2009).

[8] Ke-zang, C., Xin-an, F., Quan-sheng, L.: Intelligent dimensioning for mechanical parts based in feature extraction. Comput Aided Design 33(13), 949-965 (2001).

[9] Latif N., Graham D.: Dimensioning through understanding geometry. ASEE 1999, pp. 1831-1837, Baltimore (1999).

[10] Pasquet R., Vacquer R., Degoulange F.: La cotation fonctionnelle dans le dessin de definition. Dunod, Paris (1967).

[11] Jaffeux R.: Le dessin fonctionnel de définition. Dunod, Paris (1966).

[12] Petit G.: Principes de cotation fonctionnelle. Masson et Cie, Paris (1967).

Development of a Web-Based Digital Twin of a Two-Stroke Motorbike Engine Using Reverse Engineering

Ricard Barberà-Guillem*, Andrés Crespo Montalvá, Beatriz Defez, María Moncho Santonja

Universitat Politècnica de València (UPV). Camí de Vera, s/n. 46022. València. Spain

* e-mail: ricard.barbera@upv.es

Abstract: The digital transformation of engineering practice has expanded Graphical Engineering beyond traditional technical drawing to incorporate digital twins, simulation, and interactive visualization. In this context, transforming physical mechanical systems into accurate virtual models is increasingly relevant for industrial training and engineering education. This paper presents a web-based digital twin framework of a two-stroke motorcycle engine, developed as an educational resource via a structured reverse engineering methodology at the Universitat Politècnica de València. The selected engine offers high pedagogical value due to its compact architecture and distinct kinematic chain. The workflow follows four phases: physical disassembly, parametric CAD modelling, kinematic assembly definition, and advanced web-based visualization. Reverse engineering techniques ensured geometric and functional fidelity, delivering the high-fidelity digital model phase of the twin architecture. The final outcome is a functional twin environment enabling interactive exploration of components and operating cycles through a centralized web interface. The results demonstrate the technical feasibility of creating high-fidelity digital assets for complex mechanisms, providing a foundation for future live-data integration in active learning environments to enhance spatial comprehension in Graphical Engineering education.

Keywords: *Reverse Engineering, Digital Twin, Graphical Engineering, Web-Based Visualization, Engineering Education.*

1. INTRODUCTION

Graphical Engineering has evolved from descriptive geometry and technical documentation toward an integrative field closely linked to digital modelling, simulation, and product lifecycle representation. In this context, technical drawing has progressively shifted from static documentation to interactive environments such as CAD and BIM, which are central to industrial planning and execution [1,2].

This digitalization has enabled the integration of Industry 4.0 tools, including augmented reality and IoT systems, transforming traditional drawings into intelligent models capable of supporting early-stage simulations and analysis [1,3]. It also facilitates the digital reconstruction of legacy diagrams, allowing their incorporation into model-based workflows [3,4]. Within this framework, it is relevant to distinguish between different levels of digital representation: while fully operational Digital Twins require real-time bidirectional data exchange, many applications rely on high-fidelity Digital Models that provide a structured basis for future integration [5].

In recent years, advances in visualization technologies and web-based platforms have accelerated the development of Digital Twins (DTs), enabling virtual representations of physical systems through simulation and data integration [6-8]. In mechanical applications, these systems depend on accurate kinematic modelling to balance simulation fidelity and real-time performance, supporting processes such as virtual commissioning prior to physical implementation [7,9,10]. The generation of such models often involves Reverse Engineering (RE) techniques, particularly when physical systems lack complete digital documentation [11-14].

From an educational perspective, these approaches help overcome the limitations of traditional static representations, improving the understanding of internal mechanisms and kinematic relationships. In addition, web-based and virtual environments enable remote and interactive learning experiences, supporting the development of analysis and troubleshooting skills in complex systems [15-18].

In this context, this work presents the development of an educational web-based digital twin framework of a two-stroke internal combustion motorcycle engine, developed as a Final Degree Project at the Universitat Politècnica de València. The selected system provides a compact and representative kinematic chain, allowing the simultaneous analysis of intake, compression, combustion, and exhaust processes. The proposed approach integrates reverse engineering, parametric modelling, and web visualization in a unified workflow, aiming to connect fundamental mechanical concepts with their graphical representation.

2. METHODOLOGY

The proposed methodology follows a sequential workflow structured into four main phases, ensuring both geometric accuracy and functional coherence of the resulting digital twin. This structured approach, illustrated in Figure 1, allows for the transition from a physical mechanical system to an interactive and educational virtual model.

The specific tools, actions, and data formats involved in each stage are summarized in Table 1, providing a comprehensive overview of the technical pipeline.

TABLE 1
Methodological workflow for the engine's digital twin development

Phase	Tools / Software	Key Actions	Formats (In/Out)	Objective
Data Capture	Calipers, micrometers, EinScan Pro 2X	Dimensional measurement and 3D scanning of physical parts.	Physical part / .STL	Acquisition of base geometries and reference meshes.
CAD Modelling	Fusion 360	Parametric reconstruction of components and assembly verification.	.STL / .FBX	Integration of manual modelling and scanned data.
Functional Assembly	Fusion 360	Application of mechanical joints and kinematic constraints.	CAD Models / .FBX	Definition of the kinematic behavior (2-stroke cycle).
Visualization	KeyShot / Web Platform	Application of materials, lighting, and interactive integration.	.FBX / Images & GLB	Production of high-fidelity educational resources.

2.1. Reverse Engineering and Physical Analysis

Following complete engine disassembly, each component was analysed via visual inspection, dimensional measurement, and identification of functional interfaces. Calibrated callipers and micrometres were used to capture critical dimensional tolerances. Special focus was placed on the core elements of the kinematic chain—the crankshaft, connecting rod, and piston—ensuring the virtual assembly would accurately reflect real mechanical constraints

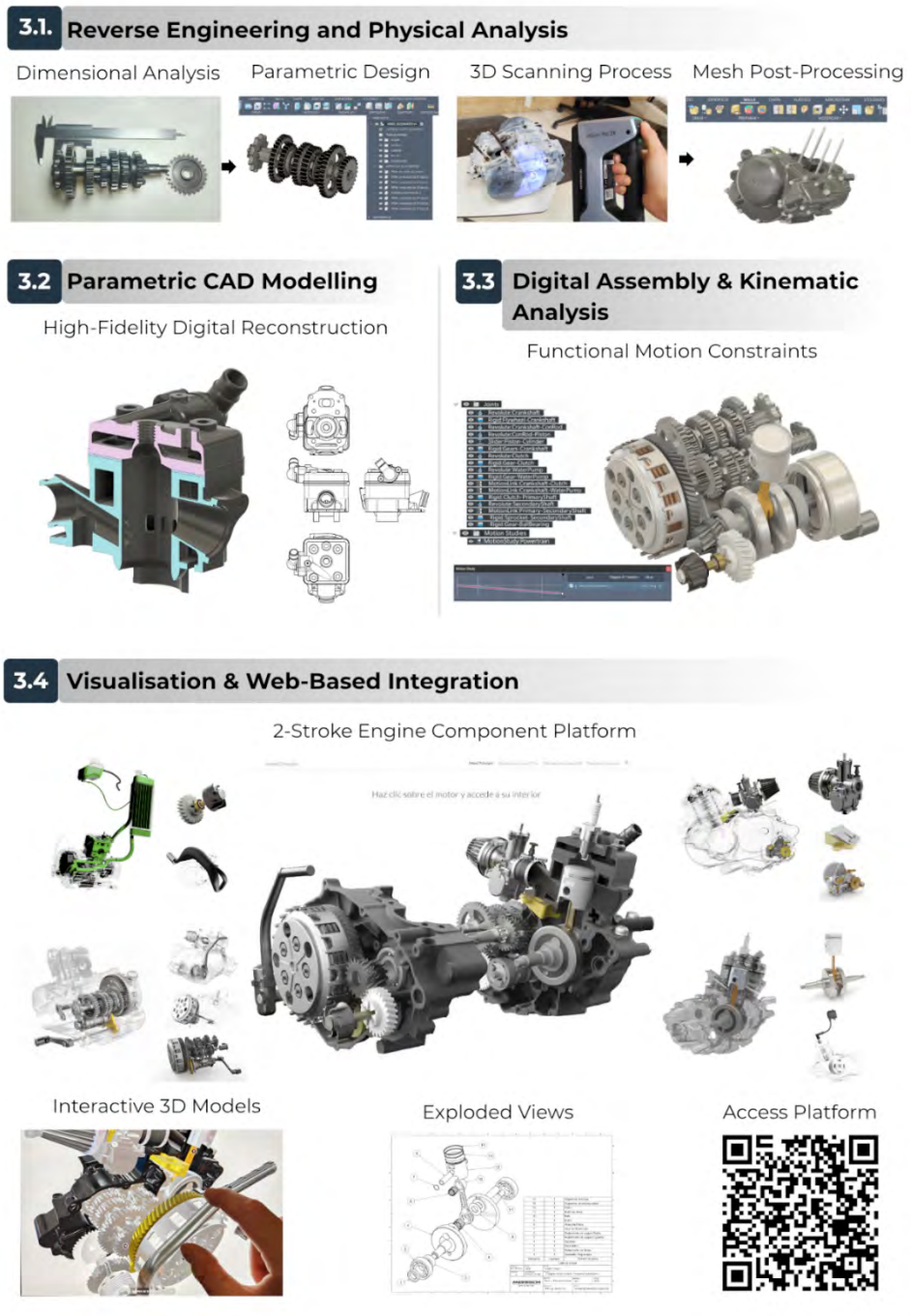


FIG. 1

Methodological workflow for the digital twin creation of a two-stroke engine: from physical reverse engineering and parametric CAD modelling (Sections 3.1-3.2) to kinematic analysis and web-based visualization (Sections 3.3-3.4)

2.2. Parametric CAD Modelling

Standard components were reconstructed using parametric CAD based on manual measurements. For parts with complex, organic geometries like the engine casings, a reverse engineering approach was executed at the UPV Alcoi Campus FabLab using an EinScan Pro 2X structured light scanner. High-density reference meshes (STL/OBJ) guided precise parametric modelling in Fusion 360. Non-visible internal channels and bearing seats were fully modelled to support future sectional views.

2.3. Functional Digital Assembly and Kinematic Definition

Once individual components were completed, a functional digital assembly was constructed in Fusion 360. Mechanical joint constraints were applied to reproduce real-world rotational and translational degrees of freedom. These kinematic relationships were explicitly modelled to simulate the complete, dynamic two-stroke operating cycle, transforming the static geometry into a synchronized moving system.

2.4. Visualization and Web-Based Integration

Advanced graphical resources were developed using KeyShot and web-friendly formats (GLB/GLTF) to transition from geometric accuracy to didactic communication. The web platform prioritizes three instructional criteria: contrasting chromatic coding to help students quickly identify distinct functional groups; a structured pedagogical sequence that guides users from individual parts to the full operating cycle; and interactive exploration allowing remote users to manipulate exploded views, trigger sectional cuts, and track operating phases without specialized CAD software.

3. RESULTS AND DISCUSSION

The application of the implemented workflow resulted in an operational web-based digital twin framework of the two-stroke engine. The final system successfully combines high geometric fidelity, functional realism, and interactive visualization, aligning with current trends that define the Digital Twin as a core element for product lifecycle representation [2, 6] and establishing the foundational high-fidelity digital model stage of the twin maturity framework [5].

The platform accurately reproduces the mechanical behaviour of the system, allowing for the observation of the complete operating cycle and internal synchronization (crankshaft-rod-piston kinematics). This level of detail, achieved through rigorous reverse engineering, ensures that even non-visible internal features are accurately represented. This hybrid modelling approach—combining direct measurement and 3D scanning—has proven effective in the digitalization of legacy mechanical components [12, 14], ensuring model fidelity without compromising web computational performance.

From an educational standpoint, the web-based environment facilitates progressive, active learning. The integration into the *AndrésCMstudio* platform overcomes the hardware and software barriers typically associated with high-end CAD suites. As noted in recent literature, web-based and VR interfaces are crucial for enhancing remote accessibility and troubleshooting skills in engineering education [17, 18]. By using chromatic coding and guided sequences, the tool reduces the cognitive load required to understand complex internal mechanisms compared to traditional static diagrams.

Ultimately, the methodology proved to be a consistent framework for establishing the digital model foundation of a twin architecture, proving highly applicable to other assemblies. The integration of reverse engineering and graphical visualization reinforces the role of Graphical Engineering as a vital bridge between physical systems and interactive digital representation [1, 16].

4. CONCLUSIONS

This work validates a structured digital twin workflow by integrating reverse engineering, parametric CAD modelling, and interactive visualization. The two-stroke engine model serves as a proof of concept, demonstrating that combining manual measurement with 3D scanning allows the reconstruction of legacy mechanical systems with high kinematic fidelity, establishing a robust digital model stage.

The results underscore these virtual frameworks as transformative educational resources. By enabling "virtual disassembly" and synchronized visualization of internal mechanisms, the tool overcomes the spatial limitations of traditional laboratories. Furthermore, the web-based platform democratizes access to high-fidelity models, reducing dependence on specialized CAD software.

In conclusion, this experience reinforces Graphical Engineering's role as a bridge between theoretical mechanics and functional representation. Future work will focus on integrating live IoT data streams to achieve full digital twin synchronization, alongside expanding this digital repository to other complex assemblies to enhance students' spatial skills and autonomous learning.

Acknowledgements: The authors thank the FabLab staff at the Universitat Politècnica de València (Alcoi Campus) for providing access to the facilities and equipment essential to the digitalization and experimental phases of this project.

REFERENCES

[1] D'Addario, J.J.P.: Desenho técnico e indústria 4.0: a integração com simulação, impressão 3d e realidade aumentada: Technical drawing and industry 4.0: integration with simulation, 3D printing and augmented reality. Rev. Cient. Multidisc. Saber. 1, (2025). https://doi.org/10.51473/rcmos.v1i1.2025.1074.

[2] Shrivastava, A., Goyal, H.R., Hussein, L., Bansal, S., Sharma, V., Harikrishna, M.: Innovations in Mechanical Drawing and Computer Graphics: Enhancing Precision and Visualization in Engineering Design. In: 2024 IEEE 4th International Conference on ICT in Business Industry & Government (ICTBIG). pp. 1-5. IEEE, Indore, India (2024). https://doi.org/10.1109/ICTBIG64922.2024.10911512.

[3] Moreno-García, C.F., Elyan, E., Jayne, C.: New trends on digitisation of complex engineering drawings. Neural Comput & Applic. 31, 1695-1712 (2019). https://doi.org/10.1007/s00521-018-3583-1.

[4] Kang, S.-O., Lee, E.-B., Baek, H.-K.: A Digitization and Conversion Tool for Imaged Drawings to Intelligent Piping and Instrumentation Diagrams (P&ID). Energies. 12, 2593 (2019). https://doi.org/10.3390/en12132593.

[5] Kritzinger, W., Karner, M., Traar, G., Henjes, J., Sihn, W.: Digital twin in manufacturing: A categorical literature review and classification. IFAC-PapersOnLine. 51, 1016-1022 (2018). https://doi.org/10.1016/j.ifacol.2018.08.474

[6] Nezzi, C., Gufler, V., Vidoni, R., Rauch, E.: Kinematic and dynamic modeling of mechanical systems towards Digital Twins. Results in Engineering. 26, 104874 (2025). https://doi.org/10.1016/j.rineng.2025.104874.

[7] Konstantinov, S., Assad, F., Ahmad, B., Vera, D.A., Harrison, R.: Virtual Engineering and Commissioning to Support the Lifecycle of a Manufacturing Assembly System. Machines. 10, 939 (2022). https://doi.org/10.3390/machines10100939.

[8] Florescu, A.: Digital Twin for Flexible Manufacturing Systems and Optimization Through Simulation: A Case Study. Machines. 12, 785 (2024). https://doi.org/10.3390/machines12110785.

[9] Liljaniemi, A., Paavilainen, H.: Using Digital Twin Technology in Engineering Education – Course Concept to Explore Benefits and Barriers. Open Engineering. 10, 377-385 (2020). https://doi.org/10.1515/eng-2020-0040.

[10] Michels, F.L., Häfner, V.: Automating virtualization of machinery for enabling efficient virtual engineering methods. Front. Virtual Real. 3, 1034431 (2022). https://doi.org/10.3389/frvir.2022.1034431.

[11] Debnath, B., Pourfarash, Z., Ghorpade, B., Raman, S.: Integrating Reverse Engineering for Digital Model Reconstruction and Remanufacturing of Mechanical Components: A Systematic Review. Metrology. 5, 66 (2025). https://doi.org/10.3390/metrology5040066.

[12] Poloczek, R.: The Use of Reverse Engineering for the Development of a Model Using Computer-Aided Design. Management Systems in Production Engineering. 33, 539-545 (2025). https://doi.org/10.2478/mspe-2025-0055.

[13] Buonamici, F., Carfagni, M., Furferi, R., Governi, L., Lapini, A., Volpe, Y.: Reverse engineering of mechanical parts: A template-based approach. Journal of Computational Design and Engineering. 5, 145-159 (2018). https://doi.org/10.1016/j.jcde.2017.11.009.

[14] Falheiro, M.S., Diniz, L.S., Lima, J.C., Najafabadi, H.R., Goto, T.G., Tsuzuki, M.S.G.: CAD Software Tools Employed in a Reverse Engineering Application: a Fan Propeller Model Reconstruction. In: 2021 14th IEEE International Conference on Industry Applications (INDUSCON). pp. 672-678. IEEE, São Paulo, Brazil (2021). https://doi.org/10.1109/INDUSCON51756.2021.9529898.

[15] Hazrat, M.A., Hassan, N.M.S., Chowdhury, A.A., Rasul, M.G., Taylor, B.A.: Developing a Skilled Workforce for Future Industry Demand: The Potential of Digital Twin-Based Teaching and Learning Practices in Engineering Education. Sustainability. 15, 16433 (2023). https://doi.org/10.3390/su152316433.

[16] Ortiz, J.S., Quishpe, E.K., Sailema, G.X., Guamán, N.S.: Digital Twin-Based Active Learning for Industrial Process Control and Supervision in Industry 4.0. Sensors. 25, 2076 (2025). https://doi.org/10.3390/s25072076.

[17] Omrany, H., Al-Obaidi, K.M., Ghaffarianhoseini, A., Chang, R.-D., Park, C., Rahimian, F.: Digital twin technology for education, training and learning in construction industry: implications for research and practice. Engineering, Construction and Architectural Management. 33, 1836-1870 (2026). https://doi.org/10.1108/ECAM-10-2024-1376.

[18] Yang, S., Mirahmadi, S.A., Zhu, E., Solanki, B.: Live digital twin with virtual reality for accessible and immersive manufacturing education. Int J Adv Manuf Technol. 136, 3577-3590 (2025). https://doi.org/10.1007/s00170-025-15078-w.

Towards an efficient interaction between learners and conversational artificial intelligence tools in graphic engineering courses

Diego-José Guerrero-Miguel[a], *, María-Belén Prendes-Gero[a], Marta Menéndez Fernández[b], Martina-Inmaculada Álvarez-Fernández[c], Ruth Fernández García[d], Juan Carlos Ríos-Fernández[e]

[a] Construction and Manufacturing Engineering Department, University of Oviedo, Calle Pedro Puig Adam, Edificio Departamental Oeste 6, 33204, Gijón, Asturias, Spain

[b] Department of Mining Technology, Surveying and Structures, Campus de Vegazana s/n , 24071 León, Castilla y León, Spain

[c] Department of Mining Exploitation and Prospecting, University of Oviedo, Campus de Mieres C/ Gonzalo Gutiérrez Quirós, s/n, 33600 Mieres, Asturias, Spain

[d] Polytechnic School of Mieres, Campus de Mieres C/ Gonzalo Gutiérrez Quirós s/n, 33600 Mieres, Asturias, Spain

[e] Department of Energy, University of Oviedo, Polytechnic School of Engineering of Gijón, C/ Wifredo Ricart s/n - Edificio Departamental Este, 33203 Gijón, Asturias, Spain

* e-mail: guerrerodiego@uniovi.es

Abstract: Conversational Artificial Intelligence (AI) tools are gaining influence in the educational context favoured by their accessibility and their effectiveness to solve technical problems with a satisfactory level of effectiveness. However, within the specific domain of graphic engineering education, their adoption remains limited due to the necessity of translating a graphic exercise into a precise written description and, subsequently, converting the textual response generated by the AI into a correct graphical solution. Therefore, students frequently struggle when attempting to use these tools as virtual tutors. This difficulty is not softened by the possibility of introducing images within the prompts or asking for a technical image of the solution. In this study, AI tools are addressed as a novel opportunity to inquire into the core concepts of the subject from an alternative perspective, fostering the development of textual-spatial reasoning skills that may not be adequately cultivated through traditional teaching methods. To evaluate the adequate manner of interacting with conversational AI tools in graphic engineering, a set of exercises covering the topics of orthographic projection and standardization was solved by students. Specifically, ChatGPT, Copilot and Gemini were used to conduct this analysis. Based on the collected results, a series of recommendations are proposed to improve the prompt formulation in educational settings. It is worth noting that the objective of this study is not to identify a superior commercial tool, but rather to determine weaknesses across conversational AI tools as a technological pedagogical resource to assist in the teaching-learning process.

Keywords: *engineering education, AI conversational tools, prompt engineering, textual-spatial skills.*

1. INTRODUCTION

The rapid dissemination of Artificial Intelligence (AI) tools and applications has led to widespread use and growing reliance by students, who frequently assume the validity of their answers without further critical evaluation of the information provided. This phenomenon has become more pronounced in recent years, due to the increment of freely accessible tools featuring user-friendly interfaces, which facilitate their adoption by non-expert users. In this sense, conversational AI tools, based on large language models (LLMs), stand out for simulating a regular conversation between two human beings.

Within the educational domain, these tools are completely transforming the teaching-learning processes. A key factor contributing to their rapid adoption is their convincing and persuading way to exhibit information, which trick students to unconsciously consider that the answer may be absolutely correct, without further verification or critical questioning.

The performance of these tools depends significantly on the quality of the prompt -the text sent to the AI tool to provide the request- employed [1]. Therefore, it is mandatory to train students in the proper formulation and effective use of prompts [2]. Furthermore, the use of AI tools also proved to be highly effective improving student's problem-solving abilities as well as their on-task efficiency [3].

In the specific context of Graphic Engineering education, the integration of conversational AI tools has progressed at a slower pace, mainly due to the necessity of translating graphical exercises into textual prompts interpretable by conversational AI tools, and the subsequent conversion of the provided text responses into accurate graphical solutions. Nevertheless, previous research demonstrated promising outcomes, such as the generation of satisfactory images in architectural works [4] and the support of the whole process from design to product manufacturing [5]. The motivation to introduce students to the effective use of these emerging tools aligns with the necessity by lecturers to respond to the new demands of both the labour market and the industrial sector [6], forcing to search for ways to integrate such tools into classroom practice. Furthermore, it is noteworthy that tools capable of converting prompt directly into a satisfactory 3D product already exist, although the quality of the resulting output can vary significantly depending on the tool used [7]. Additionally, the integration of AI tools into educational settings enhances academic performance, motivation and long-term knowledge retention [8].

Considering all the aforementioned evidence, there is a clear need to integrate AI-related content into the Graphic Engineering curriculum. Particularly, the development of high-quality prompt engineering skills should be regarded as a mandatory competency for future engineers. Consequently, the present research focuses on analysing the current level of interaction between undergraduate students and conversational AI tools, providing valuable knowledge into the most common errors encountered during their use, as well as proposing recommendations aimed at optimizing the outcomes of such interactions.

2. METHODOLOGY

To analyse the interaction between undergraduate students and conversational AI tools, a set of six exercises was delivered to the students. Three of these questions were related to orthographic projection and another three to technical drawing standards; thereby covering the core contents of the course. The selected exercises are listed below, and their corresponding graphical statements, where applicable, are illustrated in Figure 1:

1. Represent the projections of line r, defined by points A and B, and indicate the quadrants through which it passes (Figure 1a).
2. Determine the horizontal projection of triangle ABC, considering that it belongs to the plane α. (Figure 1b).
3. Given the plane α, determine the angle between its traces. Points A and C belong to a circumference and are also the points of tangency between such circumference and the traces of the plane. Determine the diameter of the circumference and represent its projection using at least four points (Figure 1c).
4. Explain how a half section and a partial break are represented according to technical drawing standards and explain the difference between them.
5. Can redundant information exist when dimensioning the view of a given figure?
6. Dimension the following figure (Figure 1d), without providing the image as part of the prompt.

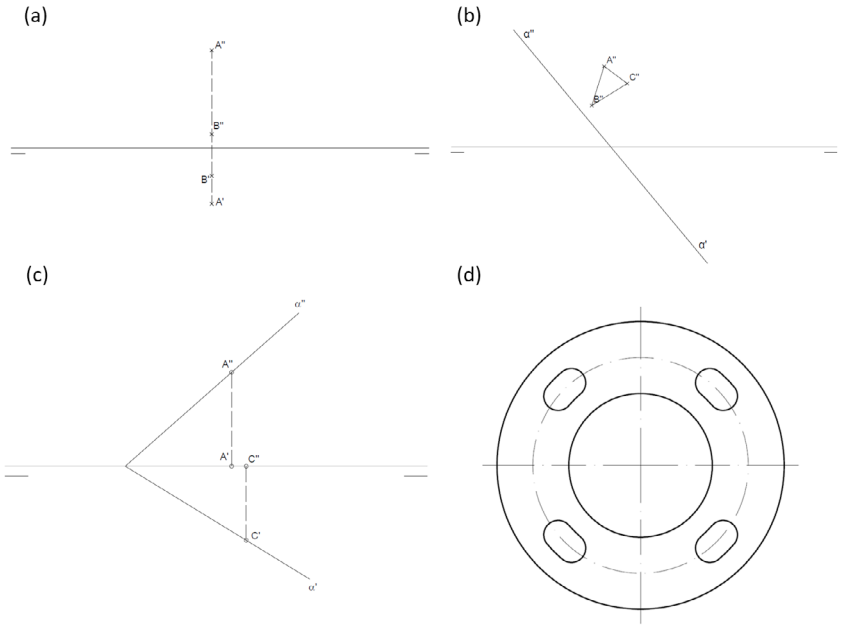


FIG. 1
Exercises with graphic information delivered to students and corresponding to (a) exercise 1, (b) exercise 2, (c) exercise 3 and (d) exercise 6

The present study is based on the responses submitted by a total of 72 students enrolled in the Graphic Engineering course of the Bachelor's Degree in Chemical Engineering. The course was taught simultaneously in both the first and second years of the degree as a consequence of curriculum modifications implemented in the degree programme. Students were required to complete Table 1, which is equivalent to that used by the authors in previous studies [9], for the conversational tools of ChatGPT, Gemini and Copilot in their free versions:

TABLE 1
Data collection table completed by the students

Exercise number	Prompt employed	AI answer	Critical comment on the answer provided	Sources employed by the AI

It should be noted that undergraduates were allowed to interact with the AI conversational tool up to a maximum of four prompts per question. Once Table 1 was completed, students filled in a survey conducted using Microsoft Forms® to provide feedback from their experience employing the AI conversational tool as an assistant to their learning process. The survey comprised a total of 13 different questions, of which four were close-ended, while the remaining items were designed as open-ended responses to capture student's perceptions in greater depth. From this broader set of survey questions, only those specifically related to their experience with prompt formulation and their interaction with conversational AI tools are addressed in this study. Due to the extension of their answers, they are not reproduced individually in this text. Nevertheless, lecturers highlight their most significant contributions, accompanied by their own analyses and reflections, in the following section.

3. RESULTS AND DISCUSSION

Due to the particular characteristics of the three different AI conversational tools, it might initially be expected that optimal prompt design strategies would vary considerably across platforms. However, the data collected by both undergraduates and lecturers exhibit some common good-practice manners to guide the user-AI interaction.

The main recommendation reported by all the people involved in this analysis was the necessity to be accurate with the vocabulary and terminology specific to the field of Graphic Engineering. Students who employed concise, clear and technically accurate prompts significantly reduced the number of interactions, from the allowed maximum of four to an average of two. This improvement was particularly evident when appropriate terminology was systematically integrated in detailed prompt formulations.

Furthermore, providing information of the expected response within the initial prompt also reported significant improvements in the quality of the answers. Not only limiting the type of reply -such as summary, step by step, short definition or technical explication- but

also on fixing the topic through some keywords, such as orthographic-projection, cut, section or standard ISO (International Organization for Standardization).

It worths reporting that additional tests not initially considered, and thus only conducted by lecturers, demonstrated that an alternative strategy—namely, progressively refining the problem through a sequence of shorter prompts—can also yield effective results. This iterative approach allows to guide the AI in a more controlled manner, boosting the valuable part of the response and reducing the likelihood of irrelevant content. Nevertheless, this technique was satisfactory only when simultaneously maintaining an exquisite and precise use of the technical terminology. In this regard, the findings suggest that the appropriate combination of accurate vocabulary, logical structuring, and a clear organisational layout is more critical than the mere length or extent of the prompts employed. However, as many students show a lack of concise writing skills, it may be advisable, from a pedagogical standpoint, to encourage the segmentation of information into shorter, more manageable prompts.

These observations allow to identify the existence of two clearly different student profiles. The first group consist of students who engage to the platform for the first time at the beginning of the course, often coinciding with their initial exposure to the subject matter. The second ground gathers those who adopt these tools at a larger stage -hence, while reviewing the concepts-. The latter, recognizable for contextualising prompts within the whole curriculum of the subject, consistently achieved more accurate results with fewer interactions. Accordingly, even if the use of conversational AI tools may be useful from the beginning of the course, it is highly recommendable to introduce them after managing the elemental concepts. When considered collectively, the results reveal a clear preference for the manner in which information is presented by Gemini across both core content areas (Figure 2), in contrast to the rest of AI tools evaluated. Although comparable preference was observed for ChatGPT and Copilot in the context of orthographic projection, Copilot was more frequently preferred over ChatGPT in tasks related to standardization.

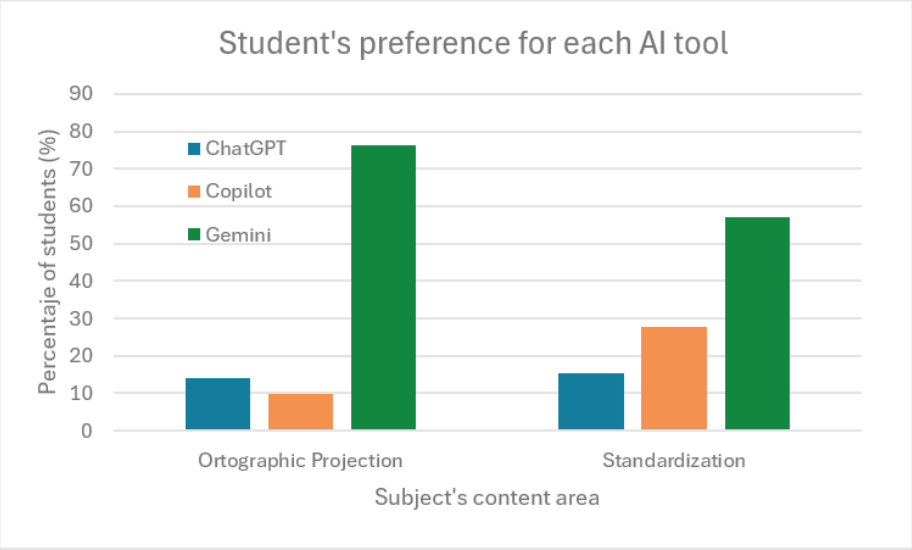


FIG. 2
Students' preference for each subject's content area

For further development of conversational AI tools as effective pedagogical tools, it is necessary to improve their capabilities in the recognition and generation of technical images according to the established standards. Such advancements would provide a robust alternative to the use of written prompts -pure test-based interaction- and mitigating the need of extensive replies by the AI tools. This capability, with the already existing skills of conversational AIs to provide written responses, would guarantee a capable and adequate tool to be used as a reliable and effective assistant for remote learning of Graphic Engineering courses.

4. CONCLUSIONS

After a detailed analysis of the inconvenience encountered by students when dealing with conversational AI tools when used as assistants of the teaching-learning process, the most relevant points to highlight, as well as main conclusions are:

1. New teaching perspectives related to Graphic Engineering should include, and evaluate, the textual-spatial skills. This shift responds to the evolving demands of both industry and contemporary society, where the ability to accurately translate between graphical and textual representations is increasingly valuable. Consequently, there is a real need to place the correct use of subject-specific technical vocabulary at the core of the teaching process.
2. Training students to produce better descriptions providing texts would be beneficial not only for effective interaction with AI systems but also for human-to-human communication, reducing ambiguity and increasing performance in collaborative and professional contexts.
3. The use of excessively detailed prompts is not advantageous, particularly when students lack a proper use of the technical terminology. Complex prompts may introduce ambiguity rather than clarity. This highlights the importance of fostering self-critical awareness among students when managing the use of AI tools. Conversely, it can also be seen as an indicator to improve the student-AI interaction by educators. Those undergraduates who perceive AI-generated responses as ambiguous or imprecise, should improve their textual-spatial competence.
4. The satisfaction level perceived by the students with the AI tool strongly depends on the proper use of technical vocabulary.

Finally, and as a natural continuation of the present study, the design and implementation of a specialized chatbot tailored for the need of Graphic Engineering education could significantly benefit from implementing the recommendations outlined above.

REFERENCES

[1] Knoth, N., Tolzin, A., Janson, A., Leimeister, J.M.: AI Literacy and Its Implications for Prompt Engineering Strategies. Computers and Education: Artificial Intelligence 2024, 6, doi:10.1016/j.caeai.2024.100225.

[2] Pangestu, F.N.N., Hamidah, I., Widaningsih, L., Abdullah, A.G., Saputra, N.A.: A Scoping Literature Review of Prompt Engineering for Bridging Students AI Literacy in Higher Education. Computers and Education: Artificial Intelligence 2026, 10.

[3] Urban, M., Děchtěrenko, F., Lukavský, J., Hrabalová, V., Svacha, F., Brom, C., Urban, K.: ChatGPT Improves Creative Problem-Solving Performance in University Students: An Experimental Study. Comput. Educ. 2024, 215, doi:10.1016/j.compedu.2024.105031.

[4] Merino-Gómez, E., Andrés, F.M., Querol, B., Vasallo, P.R.: Stable Difussion Learns From Sebastiano Serlio: Architectural Drawing with Artificial Intelligence. EGA Revista de Expresión Gráfica Arquitectónica 2024, 29, 258-267, doi:10.4995/ega.2024.20332.

[5] Daareyni, A., Martikkala, A., Mokhtarian, H., Ituarte, I.F.: Generative AI Meets CAD: Enhancing Engineering Design to Manufacturing Processes with Large Language Models. International Journal of Advanced Manufacturing Technology 2025, doi:10.1007/s00170-025-15830-2.

[6] Huwer, J., Thyssen, C., Becker-Genschow, S., von Kotzebue, L., Finger, A., Kremser, E., Berber, S., Brückner, M., Maurer, N., Bruckermann, T., Meier, M., Thoms, L-J.: Competencies for Teaching with and about Artificial Intelligence in the Natural Sciences — DiKoLAN AI. Computers and Education Open 2025, 9, doi:10.1016/j.caeo.2025.100303.

[7] Yıldırım, E., Küçük, F.S.: Comparative Analysis of Text-To-3D AI Tools in Urban Furniture Design: Evaluating Luma Genie, Meshy, Tripo, and DeepAI. MEGARON / Yıldız Technical University, Faculty of Architecture E-Journal 2026, 90-100, doi:10.14744/megaron.2026.47886.

[8] Trindade, M.A.M., Edirisinghe, G.S., Luo, L.: Teaching Mathematical Concepts in Management with Generative Artificial Intelligence: The Power of Human Oversight in AI-Driven Learning. International Journal of Management Education 2025, 23, doi:10.1016/j.ijme.2024.101104.

[9] Guerrero-Miguel, D.-J., Prendes-Gero, M.-B., García, R.F., Fernández, M.M., Díez, R.R.-G., Cerra, P.P.: Evaluating the Integration of Artificial Intelligent Tools in Graphical Engineering Courses. In Proceedings of the Advances on Design Engineering V; Manchado del Val, C., Mirálbes Buil, R., Torrecillas, C., Morato-Moreno, M., Eds.; Springer Nature Switzerland: Cham, 2026; pp. 541-551.

AI-assisted scaffolding for the initial analysis of mechanical drawings in engineering graphics education

Lara García Calvo*, María Consuelo Sáiz-Manzanares, Raúl Marticorena Sánchez, Arturo de Román Miguel, Álvaro Alonso Díez

Universidad de Burgos, Burgos, Spain

* e-mail: lgcalvo@ubu.es

Abstract: This paper reports an exploratory application of a multimodal AI assistant as a cognitive scaffold for the preliminary analysis of mechanical drawings prior to manual drafting in the Engineering Graphics module of the Mechanical Engineering degree at the University of Burgos. To this end, an assistant was developed utilizing structured prompting techniques informed by both theoretical frameworks and UNE-EN ISO standards. The assistant was applied primarily to a representative teaching exercise involving the production of an assembly drawing of a manual valve from its exploded view. The assistant's output organizes the preliminary analysis into four core elements: component identification, functional relationships, a drawing checklist, and a proposed drawing sequence. The workflow illustrates how such support can reorganize complex graphical representations into a revisable sequence of pre-drafting decisions. In this phase, the outputs were reviewed by the authors for evident inconsistencies. Formal accuracy assessment and future classroom validation with students remain pending.

Keywords: *engineering graphics, artificial intelligence, mechanical drawings, scaffolding, engineering education.*

1. INTRODUCTION

A primary challenge in engineering graphics education is not the drafting execution itself, but rather the preliminary understanding of the represented mechanism. In these tasks, students must interpret systems comprising multiple components, identify their functional relationships, and translate this information into standardized graphical representations in compliance with UNE-EN ISO standards. Nevertheless, empirical research indicates that this process poses substantial obstacles, resulting in elevated failure rates and recurring difficulties in visualization and drawing tasks [1,2].

Students often address these problems through trial and error or unsystematic intuition, rather than first constructing a coherent mental model of the mechanism [2]. Consequently, they develop a fragmented understanding of the system, which impedes both a comprehensive grasp of the assembly and its accurate graphical representation.

From a cognitive perspective, solving these problems requires students to work through a specific sequence of interrelated steps: component identification, the integration of geometric data into a coherent three-dimensional structure, and an understanding of the spatial and functional relationships between parts. Although this sequence is essential for effective problem-solving, it is frequently overlooked in practice, as students tend to proceed directly to the drafting stage without a preliminary analysis or planning phase.

In this context, metacognitive strategies are fundamental. According to the ACRA-R model, these strategies enable students to plan, regulate, and evaluate their own learning process, facilitating the transformation of visual information into coherent mental models [3]. However, their implementation in the classroom is often not explicit, which restricts their efficacy in complex problem-solving.

To address these challenges, the concept of scaffolding is highly applicable. Wood, Bruner, and Ross [4] define scaffolding as a temporary support mechanism through which an educator regulates task components that exceed the learner's current capacity, enabling the student to focus on manageable elements. Crucially for engineering graphics, these authors contend that comprehension of a solution must precede its actual production [4]. Furthermore, recent research in engineering education indicates that the most effective scaffolding is that which structures complex tasks and directs the learner's attention toward the critical aspects of the problem [5].

This study is situated within this framework, addressing the pedagogical challenges observed in the Engineering Graphics module of the Mechanical Engineering degree at the University of Burgos. In this module, students perform manual technical drawing assignments under time-constrained conditions, typically two hours, based on assembly drawings, exploded views, or detailed part drawings. These tasks necessitate both the rigorous application of normative standards and a preliminary comprehension of the mechanism's functional logic.

In response to these challenges, this paper presents an AI-assisted scaffold for the initial analysis of mechanical drawing assignments. Its contribution is not to solve the drawing task, but to document a structured, standards-aware support for pre-drawing analysis in engineering graphics education.

2. METHODOLOGY AND AI ASSISTANT DESIGN

The assistant supports the preliminary analysis of engineering drawings by combining the drawing image with teaching notes and referenced UNE-EN ISO standards. A structured prompt uses this material to generate a scaffold for the initial analysis of the task (Figure 1).

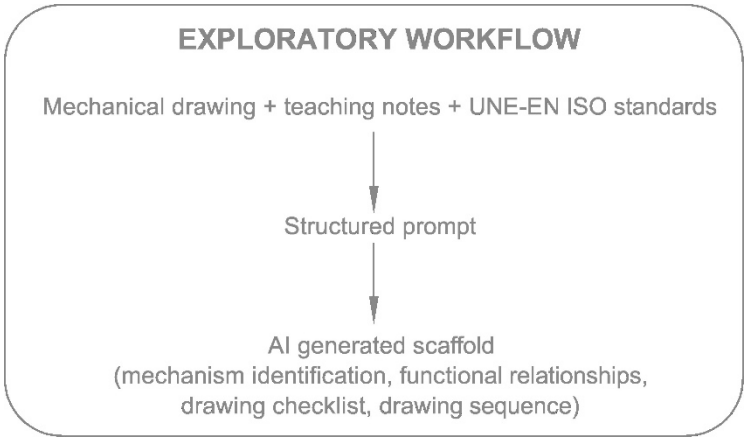


FIG.1
Proposed workflow of the AI-assisted scaffold

The assistant follows an explicit prompt-engineering pattern in which the prompt specifies the objective, required actions, constraints, output format, and contextual materials [6]. Along with the drawing, the model receives the relevant UNE-EN ISO documentation and course materials and returns a revisable pedagogical guide rather than a definitive solution. Table 1 summarizes the structure of the structured prompt and the expected output.

TABLE 1
Structure of the structured prompt and expected output

Prompt element	Expected Output
Component identification	Definition of the mechanism type and primary components
Functional relationships	Sequential operational logic of the system
Drawing checklist	Criteria for screw threads, shafts, gears, cross-sectional views, etc.
Drafting sequence	Recommended drawing order and workflow
Final verification	Quality control checks prior to final submission
Referenced standards	UNE-EN ISO 128, 128-3, 6410 and 2203

In this work, the assistant was applied primarily to a manual valve exercise represented in exploded view and was additionally explored in other course drawings. The outputs were reviewed by the authors to identify evident inconsistencies with the drawing, course materials and the referenced standards. No students or external instructors participated in this phase, and classroom validation remains future work.

3. CASE STUDY

The assistant was applied to a representative teaching exercise involving the interpretation of an exploded view of a manually operated valve. The objective was to produce a front elevation with a half-section under time-constrained conditions (Figure 2).

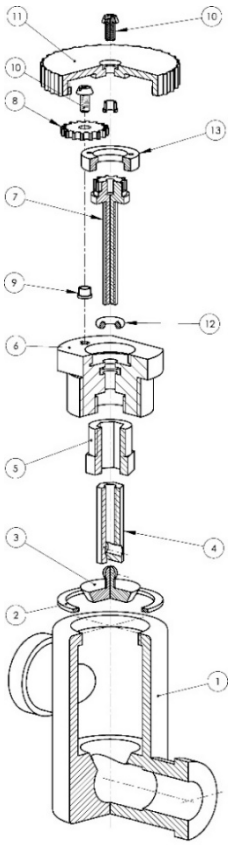


FIG.2
Exercise used in teaching practice. Exploded view of a manual valve

In this application, the assistant produced a structured identification of the mechanism, a sequential explanation of its functional logic, and a proposed layout for the standardized representation. This output is intended to support the initial interpretation of the mechanism before drafting. A representative extract of the assistant's output is presented in Table 2.

TABLE 2

Representative excerpt of the multimodal AI assistant output

Module	Assistant Response
Component identification	Mechanism definition: A manually operated globe valve actuated via a gear train. This flow-control mechanism converts the rotary motion of a handwheel into the linear displacement of a closure disc to regulate fluid passage. 1. Valve body: The primary housing that contains the fluid passage and provides structural support for the internal assembly. 2. Seal: A sealing element providing a static interface between the valve body and the bonnet. 3. Shut-off cone: The closure member that regulates or terminates fluid flow by seating against the internal valve seat.
Functional relationships	1. Manual Input: Rotary motion is applied to the external gear (11). 2. Gear Transmission: The internal teeth of the ring gear (11) engage and drive the intermediate gear (8) 3. Spindle Actuation: Gear (8) meshes with the toothed interface of the spindle (7), driving its rotation within the assembly.
Drafting sequence	Step 0: Preliminary Layout. Establish the primary vertical axis of symmetry. Define the maximum envelope dimensions (overall height and width) of the valve body (1) and the bonnet (6) to center the representation within the drawing frame. Phase 1: Structural Definition. Delineate the primary geometry of the valve body (1) and the bonnet (6).

The output also highlights drafting-relevant features such as threaded components, shaft conventions, and cross-sectional criteria, translating the referenced standards into actionable decisions. Figure 3 shows the reference assembly drawing for the task.

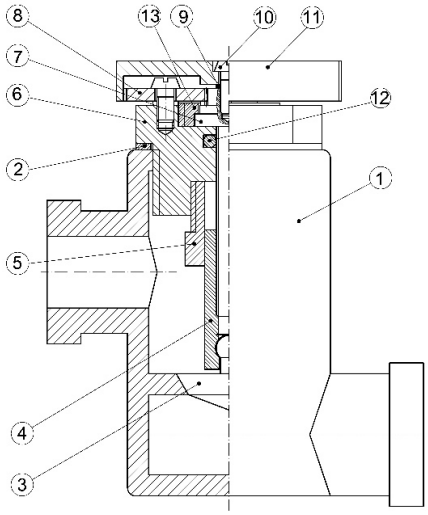


FIG.3

Reference assembly drawing used in teaching practice for the manual valve exercise. Drawing prepared by A. de Román

4. CONCLUSIONS

This paper has presented an exploratory AI-assisted scaffold for the initial analysis of mechanical drawings in engineering graphics education. Rather than using AI to solve the drawing task itself, the contribution lies in structuring the pre-drafting phase through a standards-aware workflow that organizes mechanism identification, functional interpretation, drafting checkpoints, and sequencing [4,5]. Applied to a representative exercise involving a manual valve in exploded view, the paper documents how a multimodal AI assistant can be used to reorganize a complex graphical task into a revisable sequence of analytical decisions prior to manual drafting [7].

These observations should be interpreted within clear limits. The outputs were reviewed only by the authors, without participation from students or external instructors, and no formal measures of accuracy, learning gains, task duration, error reduction, or user perception were collected. This review was not intended as a formal accuracy assessment or an educational validation. Because the output is textual while the final task is graphical, human verification remains necessary throughout the process. By preserving the manual construction of the final representation, the proposed workflow positions AI as support for pre-drawing analysis rather than as a generator of the graphical solution. The paper therefore establishes a basis for future classroom validation rather than evidence of educational effectiveness.

REFERENCES

[1] Kadam, K., Mishra, S., Iyer, S., Deep, A.: Unfolding learning difficulties in engineering drawing problem solving. Australasian Journal of Engineering Education 29(1), 42-54 (2024). doi: 10.1080/22054952.2024.2309703

[2] Garmendia, M., Guisasola, J., Sierra, E.: First-year engineering students' difficulties in visualization and drawing tasks. European Journal of Engineering Education 32(3), 315-323 (2007). doi:10.1080/03043790701276874

[3] Román-Sánchez, J.M., Gallego-Rico, S., Sáiz-Manzanares, M.C.: ACRA-R. Escalas de Estrategias de Aprendizaje. Revisadas. Hogrefe TEA Ediciones, Madrid (2026).

[4] Wood, D., Bruner, J.S., Ross, G.: The role of tutoring in problem solving. Journal of Child Psychology and Psychiatry 17(2), 89-100 (1976). doi:10.1111/j.1469-7610.1976.tb00381.x

[5] Belland, B.R., Lee, E., Zhang, A.Y., Kim, C.: Characterizing the most effective scaffolding approaches in engineering and technology education: A clustering approach. Computer Applications in Engineering Education 30(6), 1795-1812 (2022). doi:10.1002/cae.22556

[6] García-Peñalvo, F.J.: Automatización con IA. Zenodo (2026). doi:10.5281/zenodo.19002022

[7] Lee, G., Shi, L., Latif, E., Gao, Y., Bewersdorff, A., Nyaaba, M., Guo, S., Liu, Z., Mai, G., Liu, T., Zhai, X.: Multimodality of AI for Education: Toward Artificial General Intelligence. IEEE Transactions on Learning Technologies 18, 666-683 (2025). doi:10.1109/TLT.2025.3574466

CAPRIA methodology and critical use of generative artificial intelligence in initial training in graphic engineering

Diego Francisco García-Molina*, Jorge Manuel Mercado-Colmenero, Juan Manuel Montalvo-Gil, Francisco Javier Gallego Álvarez, Cristina Martín-Doñate

Department of Engineering Graphics Design and Projects, University of Jaén,
Las Lagunillas Campus, A3 Building, 23071 Jaen, Spain

* e-mail address: dfgarcia@ujaen.es

Abstract: This study examines the educational potential of a generative AI-based active learning intervention for teaching first-year Industrial Engineering student's graphical representations of electrical installations. The intervention was organised using the CAPRIA methodology, which integrates conceptual activation, prompt formulation, progressive refinement and critical interaction with artificial intelligence. A quasi-experimental mixed-methods design was employed in a two-hour in-person seminar, which comprised a pre-test, an AI-guided activity, a post-test, and a final self-assessment. Pairs of students collaborated to develop, assess, and refine prompts concerning technical graphical representation. The results demonstrate a coherent progression of learning, as despite students starting at a relatively high level, they found it difficult to differentiate between single-line diagrams and floor plans. The refinement of the prompt resulted in more precise technical language, a clearer structure, and increased references to verification and regulation. The self-assessment confirmed a high final consolidation, with prompt refinement being the most decisive factor. The research suggests that generative AI can serve as a highly effective cognitive mediator within structured and critically focused learning pathways in engineering.

Keywords: *Engineering Education, Generative Artificial Intelligence (GenIA), Technical Drawing, Electrical Installation Plans, Prompt Engineering, Active Learning.*

1. INTRODUCTION

The incorporation of generative artificial intelligence (GenAI) into higher education is reshaping teaching practices and student expectations. These tools can support conceptual explanation, example generation and feedback, but they also involve risks such as over-reliance, superficial reasoning and uncritical acceptance of plausible but technically incomplete answers [1,2]. The key issue is therefore how GenAI can be integrated into university teaching without weakening rigorous disciplinary learning.

This challenge is especially relevant in engineering education, where students must connect conceptual knowledge, graphical interpretation, regulatory criteria and professional judgement. Graphical expression mediates between technical reasoning and its communication, and learning improves when students actively relate, transform and contrast multiple representations [4,5]. In electrical installation drawings, this requires distinguishing written descriptions from technical drawings, understanding single-line diagrams and floor plans, interpreting standardised symbols and applying the In Spain, this interpretation must also comply with the Spanish Low-Voltage Electrical Regulations (REBT), which establish the technical and safety requirements for low-voltage electrical installations. [6].

However, research on GenAI in higher education has paid limited attention to technical-visual representation, while prompt engineering is increasingly recognised as an educational competence rather than a purely instrumental skill [3]. AI literacy also requires students to contextualise responses, identify limitations and verify their suitability [7]. This study examines a brief intervention with first-year Industrial Engineering students using CAPRIA—Conceptual Activation, Prompting, Refinement and Interaction with GenAI—as an active learning framework. The objectives are to assess students' initial and final understanding of electrical installation graphics, analyse how conceptual knowledge is translated into refined technical prompts, and evaluate CAPRIA as a transferable approach for engineering learning contexts involving meaningful interaction with GenAI systems [3,11]. The novelty of CAPRIA lies in its transformation of GenAI use from a general support tool into a structured, process-oriented pedagogical sequence. Unlike approaches that focus mainly on the final AI-generated answer, CAPRIA emphasises the intermediate learning processes through which students activate disciplinary concepts, translate them into technical prompts, refine their requests, and critically validate the generated output. In this study, prompt quality is therefore treated not only as an operational condition for obtaining better responses, but also as evidence of how students convert graphical and regulatory knowledge into precise technical language.

2. MATERIALS AND METHODS

The study employed a brief quasi-experimental mixed-methods design to examine both learning outcomes and the processes through which first-year Industrial Engineering students interacted with generative artificial intelligence (GenAI). This approach was suitable because the research sought to determine whether students improved after the intervention and how they translated disciplinary concepts into technical prompts, evaluated AI-generated responses and refined the interaction. The design is consistent with mixed-methods research in engineering education, where outcome measurement, process analysis and learning experience are combined [8,9].

The intervention took place in the Industrial Graphic Expression subject at the University of Jaén and centred on the graphic representation of electrical installations. The content discussed the difference between verbal descriptions and technical projects, single-line diagrams and floor plans, standardised symbols, the interpretation of the box and the role of the Low Voltage Electrical Regulations (REBT). Four class groups underwent a 120-minute session. The valid responses following data cleaning consisted of 177 pretests, 167 guided activities, 169 posttests, and 166 final self-assessments. The teaching sequence was structured using the CAPRIA methodology, an active learning framework that progresses from concept to prompt through conceptual activation, prompting, refinement and interaction with GenAI. Its educational rationale is that GenAI should not replace students' technical reasoning, but act as a cognitive mediator that supports conceptual understanding, terminological accuracy and critical thinking. This perspective is aligned with work on AI in education, prompt engineering and AI literacy, which stresses the need to teach students to evaluate, verify and apply AI-generated outputs [1–3,7]. The methodological architecture, as illustrated in Figure 1, integrates a quasi-experimental mixed-methods design, the implementation context, the CAPRIA pedagogical core, data-collection instruments, and the overall analysis strategy. The operational flow of the seminar is depicted in Figure 2. CAPRIA was implemented through a structured classroom sequence. Students completed a pre-test, received a brief conceptual introduction, selected ten key terms, agreed on a shared list with a partner, drafted an initial prompt, analysed the GenAI response, reformulated a more precise technical prompt and completed a post-test and self-assessment. This workflow made it possible to record intermediate learning evidence and to consider prompt quality as both a pedagogical and analytical factor [3,11].

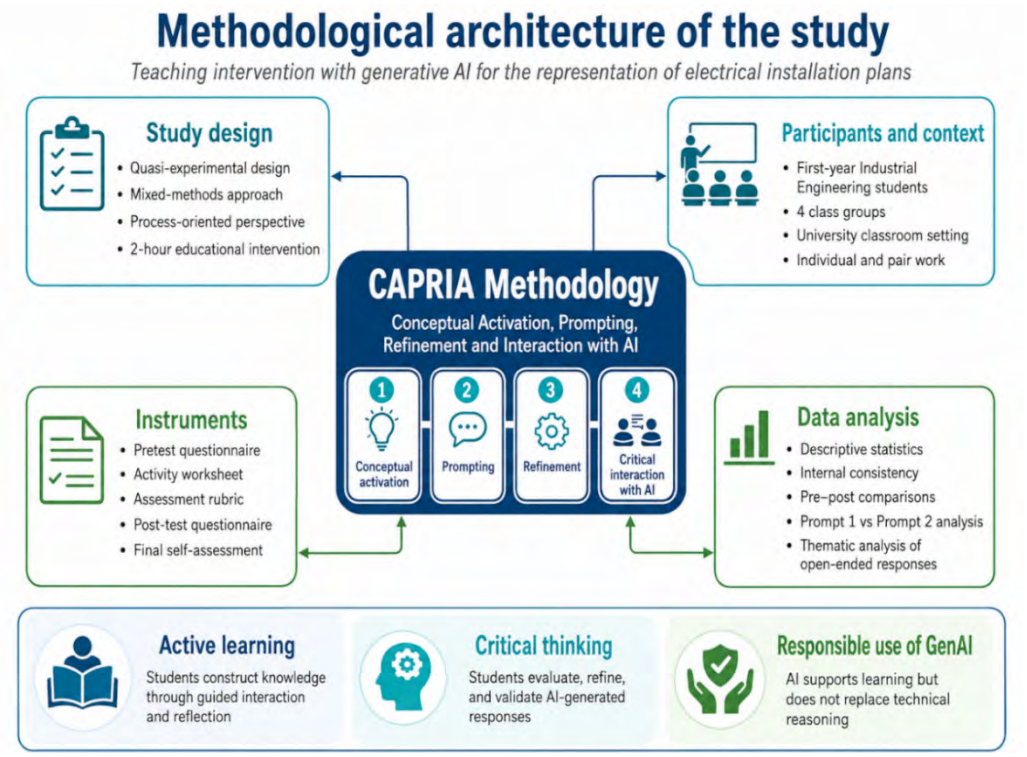


FIG. 1

Methodological architecture of the study, including the research design, implementation context, CAPRIA pedagogical core, instruments, and data analysis strategy

The four main instruments used were. The pre-test comprised 20 Likert-type items designed to assess prior knowledge of technical representation, plan interpretation, regulation, and the critical use of the GenAI. The guided activity collected the ten key terms, Prompt 1, Prompt 2, and the students' evaluation of the generated response. The post-test consisted of an objective closed-answer section and a brief final perception section. The self-assessment covered key words, Prompt 1, Prompt 2, the final GenIA response, the overall rating, and satisfaction, as illustrated in Figure 2. The study also included a rubric, a data-collection matrix, an intervention protocol, and a coding manual to guarantee analytical consistency.

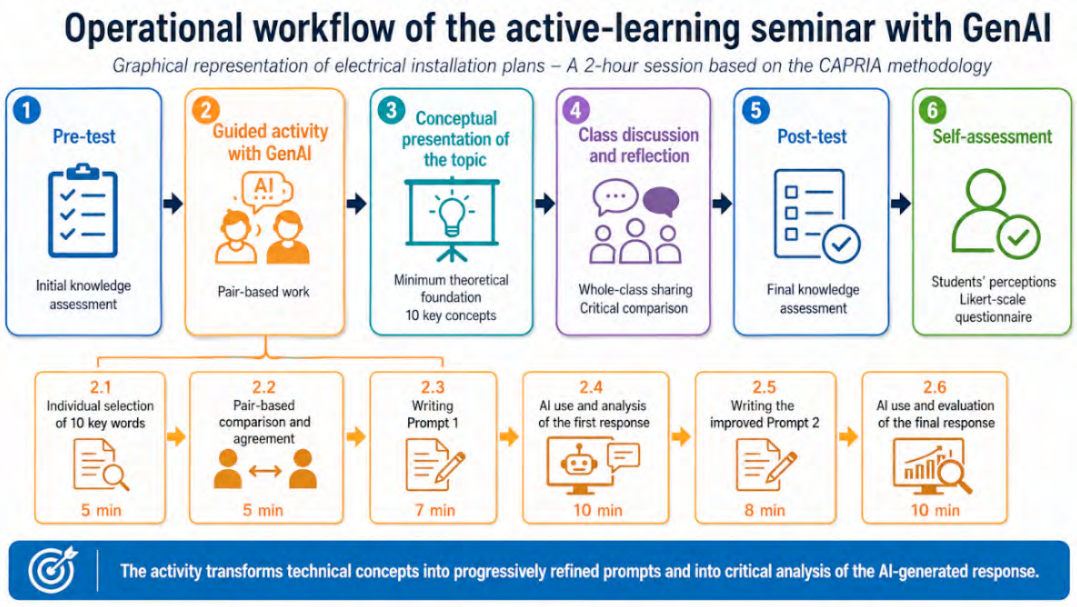


FIG. 2
The operational workflow of the active-learning seminar with GenAI

Data analysis involved database cleaning, descriptive statistics, internal consistency analysis, inferential comparisons and thematic analysis. Cronbach's alpha was used for Likert scales, and performance indicators were calculated for the post-test objective section. Given the ordinal nature of several variables and the observed distributions, non-parametric tests were prioritised: Wilcoxon signed-rank tests for paired comparisons and Kruskal–Wallis tests for group comparisons. Open responses were examined through thematic analysis, a common approach in educational research [8,10]. The data were collected via digital forms that contained basic information on data protection. Direct identifiers were minimised through the use of study codes, and the analytical bases were processed under pseudonymisation. The results were interpreted in an aggregated form to ensure methodological traceability, privacy, and transferability to other GenAI-mediated learning contexts. Statistical analyses were conducted using jamovi 2.7.29, a free and open-source statistical package. Descriptive statistics, internal consistency analyses, non-parametric comparisons and paired pre-post analyses were carried out within a coherent framework to enhance transparency and reproducibility.

3. RESULTS

Following the process-oriented approach of the study, the findings are organised into four analytical levels: prior knowledge, performance during the guided GenAI activity, final learning outcomes and students' perception of the process. This structure allows the analysis to move beyond pre-test/post-test variation and to examine how CAPRIA supported conceptual activation, prompt reformulation, critical judgement and knowledge consolidation [3,11].

The pre-test included 177 valid responses and showed a relatively high initial understanding of graphical representation, technical documentation, regulation and the need to critically evaluate AI-generated information ($M = 4.29/5$; $SD = 0.33$; $\alpha = 0.692$). However, the baseline was uneven: the clearest weakness concerned the distinction between a single-line diagram and a floor plan ($M = 2.40/5$). No significant differences were found between specialisations, indicating a comparable starting point across groups.

The guided GenAI activity, analysed from 167 valid responses, was positively evaluated ($8.38/10$; Likert $M = 4.41/5$). The strongest improvement occurred between Prompt 1 and Prompt 2: the refined prompt was longer, more conceptually precise, more technically specific and better structured, with stronger references to regulations and verification. Qualitative analysis identified recurrent improvements in terminological accuracy, disciplinary vocabulary, request structure and explicit verification criteria. This indicates that the learning value of the activity lay less in the initial use of GenAI than in students' capacity to reinterpret the first response and reformulate the prompt critically [3,11].

The post-test confirmed very high final consolidation ($M = 7.95/8$; $SD = 0.25$), particularly in relation to the functions of the single-line diagram, floor plan reading, symbols, the title block and the role of the REBT. The low reliability of the objective block ($KR\text{-}20 \approx 0.175$) should be interpreted with caution because of the strong ceiling effect and the limited variability in correct responses. Again, no significant differences were found between specialisations.

The final self-assessment, completed by 166 students, showed a positive perception of the process ($M = 4.34/5$; satisfaction $= 8.26/10$; $\alpha = 0.864$). Prompt 2 was the best-rated block, whereas Prompt 1 received the lowest rating. The difference between both prompts was statistically significant and substantial ($W = 251$; $p < 0.001$; $d_z = 1.27$), confirming the central role of refinement in CAPRIA. Students associated improvement with greater precision, more technical language, better request organisation and the inclusion of verification or justification requirements.

Overall, the results describe a coherent learning trajectory. The intervention addressed the main initial weakness in distinguishing functional and spatial representations of electrical installations, supported the translation of conceptual knowledge into operational technical language and consolidated learning outcomes by the end of the session. The matched pre-test/post-test subsample confirmed a strong improvement in the weakest initial concept, from 2.36 to 4.73 ($W = 20$; $p < 0.001$; $d_z = 1.59$). As shown in Figure 3, synthesises this progression across the four analytical levels and highlights prompt refinement as the central pedagogical mechanism of the CAPRIA sequence [3,11].

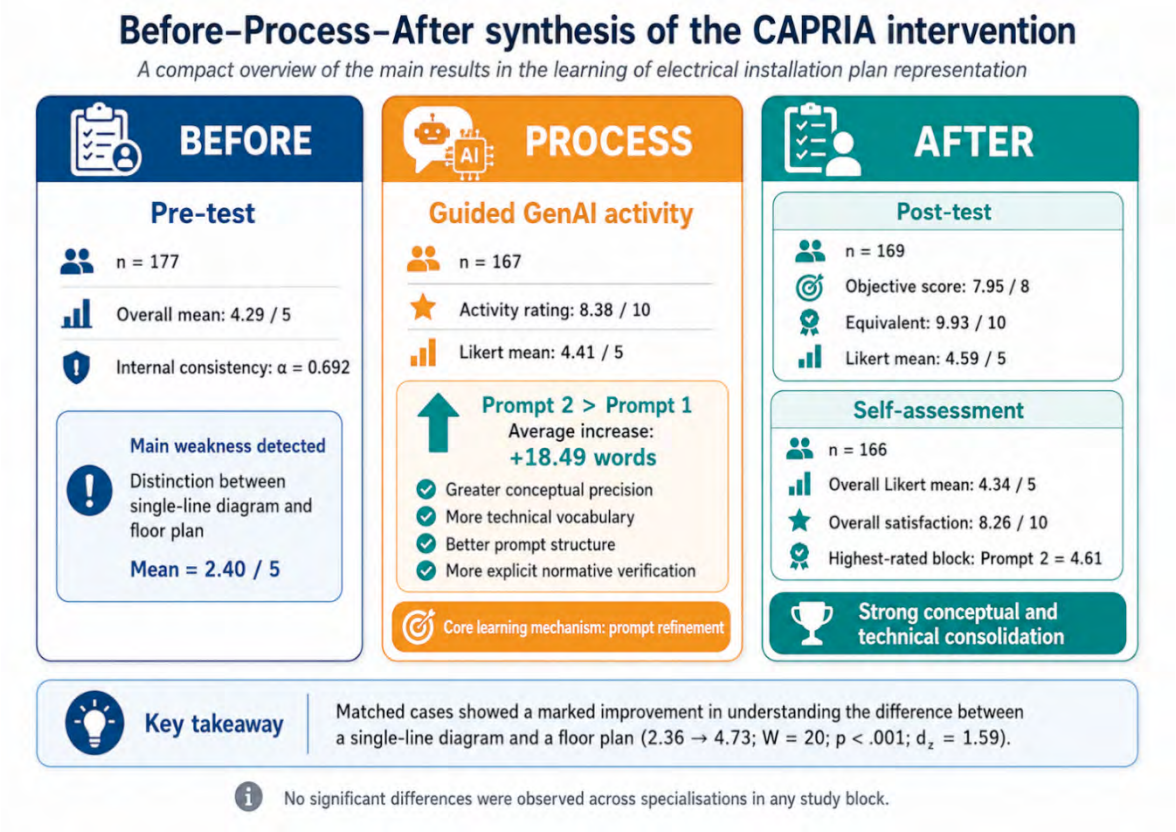


FIG. 3

Overview of key findings from the CAPRIA intervention, encompassing pre-test results, guided GenAI activity outcomes, post-test assessments, and self-assessment feedback

4. CONCLUSIONS

The findings suggest that a brief, structured and pedagogically guided intervention can facilitate learning of the graphic representation of electrical installations when generative artificial intelligence is incorporated through an active and critical sequence. The intervention addressed the main initial weakness identified in the study, which was the distinction between single-line diagrams and floor plans, and also contributed to a high final consolidation and a positive perception of the process by the students. The primary contribution of the study is in elucidating the process of learning. The formative value of generative artificial intelligence emerged not from its initial application, but from the iterative refinement of the prompt, the technical clarification of the task, and the critical comparison with the generated response. The CAPRIA framework, which stands for Conceptual Activation, Prompting, Refinement and Interaction with GenAI, restructured the interaction with generative artificial intelligence into a systematic process of conceptual activation, terminological precision, refinement and validation. These results support the viability of CAPRIA as a pedagogical approach for engineering education and other technical-professional contexts in which disciplinary concepts must be translated into meaningful instructions for GenAI systems. However, the study has several limitations. First, the intervention was conducted in a single institutional context and with first-year Indus-

trial Engineering students, which limits the generalisability of the findings. Second, the absence of a control group prevents attributing the observed improvements exclusively to the CAPRIA sequence. Third, the post-test showed a ceiling effect, reducing variability and limiting the interpretation of reliability indicators. Finally, the study assessed immediate learning outcomes, so it does not provide evidence of long-term retention or transfer to other graphical engineering tasks. Future research should therefore include control or comparison groups, longitudinal follow-up, and applications in other areas of engineering graphics and GenAI-supported technical instruction.

Acknowledgements: "The authors acknowledge the support of the Vice-Rectorate for Lifelong Learning, Educational Technologies and Teaching Innovation of the University of Jaén. This research work has been funded by the Teaching Innovation Plan PID-UJA 2025-2029."

REFERENCES

[1] Kasneci, E., Sessler, K., Küchemann, S., *et al.*: ChatGPT for good? On opportunities and challenges of large language models for education. Learning and Individual Differences 103, 102274 (2023). https://doi.org/10.1016/j.lindif.2023.102274

[2] UNESCO: Guidance for generative AI in education and research. UNESCO, Paris (2023).

[3] Lee, D., Palmer, E.: Prompt engineering in higher education: A systematic review to help inform curricula. International Journal of Educational Technology in Higher Education 22, 7 (2025). https://doi.org/10.1186/s41239-025-00503-7

[4] Ainsworth, S.: DeFT: A conceptual framework for considering learning with multiple representations. Learning and Instruction 16(3), 183-198 (2006). https://doi.org/10.1016/j.learninstruc.2006.03.001

[5] Prince, M.: Does active learning work? A review of the research. Journal of Engineering Education 93(3), 223-231 (2004). http://dx.doi.org/10.1002/j.2168-9830.2004.tb00809.x

[6] Ministerio de la Presidencia, Gobierno de España: Reglamento Electrotécnico para Baja Tensión (REBT) e Instrucciones Técnicas Complementarias. BOE, Madrid (texto vigente).

[7] Long, D., Magerko, B.: What is AI literacy? Competencies and design considerations. In: CHI Conference on Human Factors in Computing Systems, pp. 1-16. ACM, New York (2020).

[8] Borrego, M., Douglas, E.P., Amelink, C.T.: Quantitative, qualitative, and mixed research methods in engineering education. Journal of Engineering Education 98(1), 53-66 (2009). https://doi.org/10.1002/j.2168-9830.2009.tb01005.x

[9] Creswell, J.W., Plano Clark, V.L.: Designing and Conducting Mixed Methods Research. 3rd edn. Sage, Thousand Oaks, CA (2017).

[10] Braun, V., Clarke, V.: Using thematic analysis in psychology. Qualitative Research in Psychology 3(2), 77-101 (2006). https://doi.org/10.1191/1478088706qp063oa

[11] Xiaoyu, W., Zainuddin, Z., Hai Leng, C.: Generative artificial intelligence in pedagogical practices: A systematic review of empirical studies (2022-2024). Cogent Education 12(1), 2485499 (2025).

ANNEX. ACCESS TO THE TEACHING INTERVENTION THROUGH QR CODES (FIGURE 4).

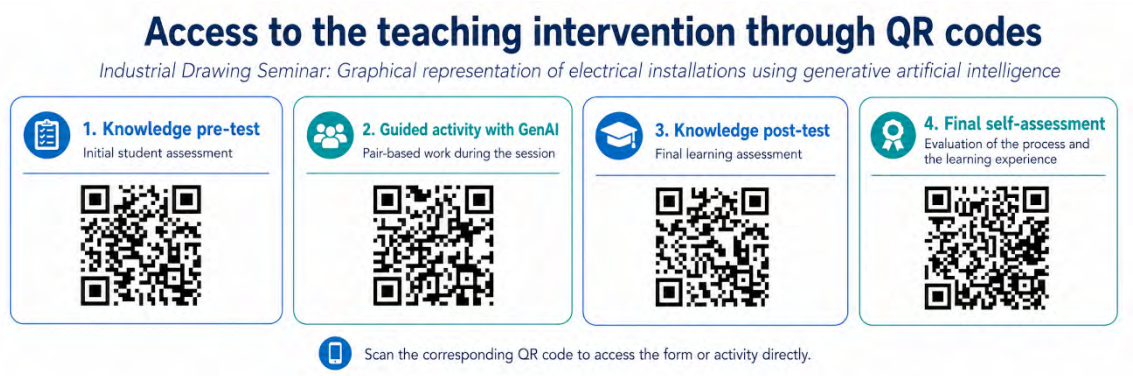


FIG. 4
Scan the corresponding QR code to access the form or activity directly

Service design methodologies: A framework to transform healthcare systems

Laura Aguado-González[a, b, *], Yeray Sañudo[a, b], Jorge Sierra-Pérez[a, b]

[a] Aragon Institute for Engineering Research (i3a),
Department of Engineering Design and Manufacturing, University of Zaragoza, Zaragoza, Spain

[b] Water and Environmental Health- IUCA Research Group,
University of Zaragoza, Zaragoza, Spain

* e-mail: laguado@unizar.es

Abstract: Although the provision of healthcare is essential to quality of life, its complexity requires the coordination of multiple services and adaptation to technological innovation. In response to this challenge, healthcare services must be designed to be flexible and tailored to the user. This study aims to examine design methods and tools for enhancing the patient experience. Service design methodology considers technical and operational aspects, as well as stakeholder experience, to ensure that services function effectively and efficiently. The system can be explored using ethnography and service design techniques. Visual tools (e.g., blueprints, stakeholder maps and customer journeys) are useful for organising this information, as they provide a comprehensive understanding of care pathways. Emotional design is essential for identifying emotions and contextual barriers, as these influence the perception of quality and the satisfaction. These methodologies generate large volumes of data, which can be analysed qualitatively to reveal deeper meanings and contextual nuances. Ultimately, this comprehensive methodological framework facilitates the analysis of services, considering the needs of all stakeholders, and enables continuous improvement in the healthcare sector. Case study demonstrates its application in a real-world context. Findings prove its usefulness in co-designing innovative solutions that lead to more efficient, sustainable and personalised healthcare services.

Keywords: *Service Design, Healthcare, Methodologies, Oncology.*

1. INTRODUCTION AND THEORETICAL FRAMEWORK

Healthcare is essential for improving people's quality of life, yet its complexity stems from integrating and coordinating diverse capabilities among multiple stakeholders to ensure optimal patient outcomes. This complexity is accentuated by constant technological innovation, necessitating continuous adaptation [1]. To better address patient needs, approaches such as Patient-centred care (PCC) have emerged and are widely adopted in the healthcare field [2]. This framework has recently evolved into Person-centred care (PeCC), shifting the focus from functional living to a meaningful life. As a more holistic approach, PeCC integrates all stakeholders as active agents in every aspect of care [3]. Despite their promise, implementing these approaches is often hindered by communication gaps and limited patient autonomy. Given these difficulties, design methodologies can help to adopt a more comprehensive and coordinated approach that encompasses the entire process and all relevant stakeholders [4]. Design methodologies help to place users at the centre of the process, thereby improving the experience for all stakeholders. They are characterised by being synthetic, participatory and iterative methodologies, which allow end-users to participate in and directly influence the entire design process to 'creatively create' new solutions and outcomes [5].

In the medical context, service design offers a holistic methodology that considers the experiences of stakeholders, as well as the technical and operational factors. It ensures that the service functions properly and coordinates all its components [4]. This methodology facilitates the analysis and provides an in-depth understanding of how patients and professionals experience the healthcare process. It enables existing services to be (re)design and improved [5]. Service design techniques (e.g., safari, shadowing and interviews) [6] permit detailed exploration of the service pathway. This provides a comprehensive and clear understanding of how the service works, placing a strong emphasis on the user experience. In the healthcare context, patients' emotions significantly influence perceived service quality and satisfaction [7]. Healthcare process involves complex decisions and interactions often accompanied by intense emotions related to illness and other health issues [8]. Therefore, measuring emotions provides valuable insights for enhancing the patient experience [7]. While emotional design is usually approached within the context of user-product interactions or product design, it is not surprising its relevance in service design, as touchpoints have impact on users' experiences. Since modern service differentiation relies on emotional resonance rather than mere functionality, emotional design has become a core strategy within service design [8].

Existing methodologies focus heavily on clinical efficiency or isolate the patient experience, but none of them cover the entire healthcare process or consider all stakeholders' needs. To address this methodological gap, this study introduces a holistic, multistakeholder design framework that integrates tools for service exploration, analysis and optimization into a unified cycle pathway. We move beyond theoretical synthesis by providing an empirical roadmap, validated through a complex real-world healthcare scenario (oncology service), demonstrating the operational viability and scalability of this approach.

2. METHODOLOGY

The proposed methodological framework comprises several stages (Figure 1) based on service design tools and methodologies, aiming to deeply explore and analyse services while

considering the needs and preferences of all stakeholders. The first stage is *Service Exploration*, dedicated to identifying the context and the fundamental needs of the service. Then, an iterative cycle comprising *Analysis* and *Visual Representation* is conducted, where data interpretation and graphic mapping complement each other to provide a profound understanding of the service. Finally, the insights obtained serve as the basis for co-design and subsequent development of innovative solutions that improve the patient experience.

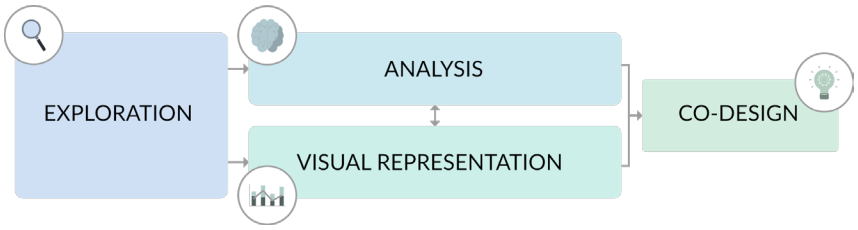


FIG. 1
Methodological framework

2.1. Service exploration

It is necessary to understand the strengths and weaknesses of the service to later propose improvements and solutions. Given the complexity of healthcare services, they must be examined in detail. To this end, service design tools such as safari, shadowing and interviews enable the service to be explored, gathering first-person experiences and observing real users interactions while uncovering the operational workflows that define the service process. The exploration should be comprehensive and places great emphasis on all the users involved (patients, relatives and professionals). First, a "service safari" [5] is conducted, during which the researcher experiences all the relevant processes. Within the healthcare service, the researcher goes through every stage of the process as if they were a patient or relative, attending various consultations, medical tests and treatments. In this way, the researcher gains an understanding of the healthcare service from the patients' perspective, experiencing it first-hand and becoming aware of all the interactions and touchpoints. Next, shadowing [5] is performed to minimise bias and gain users perspectives, real processes and more insights. This method involves observing users during consultations, waiting times or treatments, without interfering. Finally, the interviews [6] are used to explore specific details of the service, contrast insights and delve deeper into critical aspects. The interviews are led by the researcher, who asks questions designed to elicit the specific information required. To further enrich this phase, the EMPATHS method is employed to complement the service exploration. It specifically targets the emotional dimensions of the user experience to ensure a more holistic understanding [8].

2.2. Service analysis

Service exploration provides extensive datasets that require systematic processing to extract their full potential. Through qualitative analysis, researchers can identify, explore, and interpret core themes, allowing for a nuanced emphasis on context, individual experiences,

and relevant factors. Given this versatility, qualitative analysis is widely used in the healthcare sector. While specific qualitative analysis methodologies vary according to research objectives and the nature of the data [9], the process generally follows six fundamental steps: (1) Collect data, (2) Define the codebook, (3) Code data, (4) Analyse results, (5) Sort and make categories and (6) Report conclusions. The EMPATHS method is a valuable tool for analysing users' emotions within the service. Designed specifically for complex healthcare environments, it is notable for its low intrusiveness, low cost and high scalability, as well as for its more human, empathetic and patient-centred approach [8].

2.3. Service visualization

The visualisation of the service process enables the data obtained to be sorted and organised. A user-friendly, accurate and tailored graphical representation is key to ensuring that the results are properly understood and can subsequently be used to develop solutions. Depending on the information and results to be represented, there are several different methods, such as *Stakeholder Map* (represents the stakeholders involved in the service at various levels), *Personas* (specific user groups), *Service Blueprint* (specific and detailed representation of the various aspects of a service, as well as the touchpoints and interactions) [5], *EMPATHS* (visualize emotional reactions) [8] or *MetroMapping* (represent care pathways and improve patient experience and share-decision making) [10]. The more accurate method will be chosen according to the target audience, research objectives and interests.

3. CASE STUDY DESCRIPTION: ONCOLOGY SERVICE EXPLORATION AND ANALYSIS

The care pathways for breast cancer and melanoma of the Hospital Universitario Miguel Servet (Zaragoza) were explored and analysed with the proposed methodological framework. Two researchers conducted a safari of the entire disease processes for breast cancer and melanoma. Subsequently, patients were followed during diagnosis, treatment, and follow-up. Given the richness of the data, it is estimated that data saturation will be reached with fewer than 20 patients. The exploration ended after the second treatment session (see *Figure 2*), as it is during these early stages that there are more doubts, uncertainty and exchange of information. After shadowing, patients were interviewed to gain a more detailed picture of the process. Data collection was done through audio recordings, transcripts and field notes.

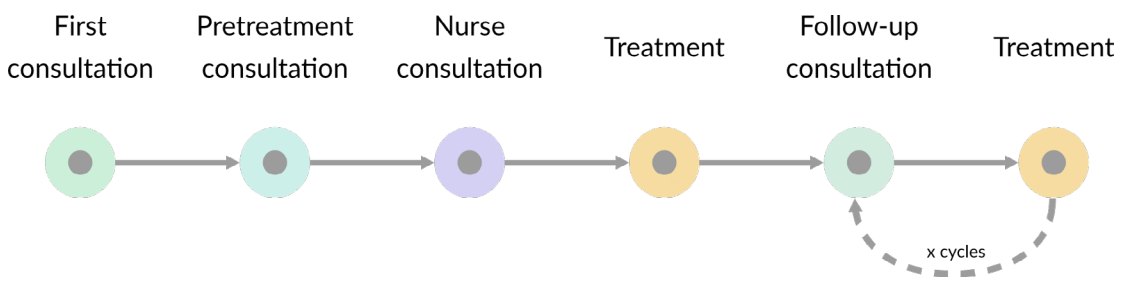


FIG. 2
Full oncology journey

Data collected were qualitative analysed and the EMPATHS methodology was applied to detect and visualise emotions during the process. In addition, other visualisation techniques, like MetroMapping, were used to represent and simplify the service pathway. Confidentiality of participants' data was maintained throughout the study. This research complied with the tenets of the Declaration of Helsinki and was approved by the Research Ethics Committee of the Autonomous Community of Aragon, Spain (C.P.-C.I. PI24/069).

4. RESULTS

Service exploration collected a 16-hour dataset, along with field notes and observations, which revealed a comprehensive map of the oncological journey. All data was transcribed and anonymised. Findings are structured into three main dimensions: structural process, thematic concerns and emotional impact.

4.1. Sample characterization

The study involved a multidisciplinary cohort (10 patients, 3 oncologists and 2 nurses), providing a holistic view of the service. *Table 1* summarizes the clinical and demographic profiles of included patients.

TABLE 1
Patients' characteristics summary

Characteristic	n (%) or median
Origin (Urban/ Rural)	8 (80%)/ 2 (20%)
Cancer type (Breast/ Melanoma)	7 (70%)/ 3 (30%)
Gender (Female/ Male)	8 (80%)/ 2 (20%)
Age (range years)	54 (42-76)

4.2. Inductive content analysis: key themes and critical nodes

The inductive qualitative content analysis identified that while the clinical stages are well-defined, significant critical nodes exist in the transitions between them. These nodes represent the primary barriers and areas for improvement within the oncology service (*Table 2*).

4.3. Emotional trajectory and service mapping

By integrating the EMPATHS methodology, we mapped the emotional fluctuations against the critical themes identifies. This allowed for the recognition of specific pain points in the oncology journey. The main finding is that the emotional burden is not linear. Receiving the diagnosis and coping with side effects were identified as particularly negative

emotional aspects. Hair loss reported during the nursing consultation is a very negative aspect of the process. In contrast, the waiting time before appointments (after receiving the diagnosis) elicits a positive emotional reaction. Depending on communication with healthcare professionals and the information received, other specific aspects of the process (i.e., vaccinations or treatment explanations) are viewed both positively and negatively.

TABLE 2
Barriers and areas of improvement

Node	Description
Clinical management (treatment & side effects)	Although the clinical protocol is clear, patients identified a "gap" regarding self-management of side effects. The analysis shows that distress increases when physical symptoms interfere with daily activities, resulting in a negative issue with significant impact.
Stakeholder interaction	Discrepancies often arise form misalignment between the expectations of patients and relatives and the actual roles of healthcare professionals, creating friction points regarding the support and care throughout the process.
Cognitive burden (doubts & problems)	Uncertainty emerged as a cross-cutting theme. The problems identified often stem from unresolved doubts that arise both during consultations and in the intervals between appointments.
Critical touchpoints	The layout of physical spaces (consultations, treatment rooms, appointment areas, etc), as well as the large amount of paperwork and administrative procedures, are factors that contribute to patients' anxiety and overwhelm.
Relational flow (communication & information)	A very significant finding was related to information and communication. Patients noted that the information they receive is sometimes excessive and overwhelming, while at other times they request more information. Communication affects their satisfaction with the service and is a key factor in patients' perception of clinicians.

5. DISCUSSION AND CONCLUSION

This study proposes a methodological framework to redesign healthcare services by integrating service exploration, qualitative and emotional analysis and visualization. Unlike traditional hospital management models reliant on quantitative data and operational performance [4], this approach introduces a human-centric perspective. By mapping the patient journey through qualitative and emotional data, care is no longer viewed as a linear sequence of tasks. This paradigm shift uncovers unnoticed barriers, such as emotional burnout or communication breakdowns, which directly impact clinical effectiveness and patient adherence [7], highlighting the urgent need for improved communication protocols and information exchange. Beyond operational efficiency, analysing emotional reactions during moments of profound vulnerability is essential to ensuring that the healthcare system is PCC [2]. This suggests that true innovation in healthcare lies not solely in medical technology, but in the deliberate innovation of care processes and human interactions [1]. Ultimately, aligning clinical protocols with the patient's emotional reality moves the healthcare

system toward more sustainable and human services, where innovation is measured not only by technical success but by its ability to provide genuine and dignified support and care [8]. While the core components of this framework are service-agnostic, its adoption faces significant systemic barriers. The inherent rigidity of traditional clinical environments and the chronic time and resources constraints [3] faced by healthcare staff pose a risk to the quality of data collection. Overcoming these challenges requires a shift in perspective to view patient-centered insights as a tool for operational efficiency [1]. Future researches could apply this framework to other healthcare services to assess its applicability and adaptability to different contexts. Similarly, other stakeholders, like clinicians, could be the focus of research. Implementing this framework in research that co-designs solutions for the service under investigation would be the best demonstration of its feasibility and effectiveness.

In conclusion, this research provides a validated systematic framework for healthcare transformation by structurally linking service design architecture with emotional analytics. The application of this methodology within a highly complex oncology environment underscores its practical utility and scalability, enabling the identification of these critical touchpoints, shifting the focus from isolated clinical steps to a continuous co-designed patient journey. Ultimately, this framework offers hospital administrators and service designers a robust, scalable tool to transition from purely transactional care models to healthcare ecosystems that are both operationally efficient and profoundly patient-centred.

Acknowledgements: Funded by predoctoral fellowship DGA 2025-2029. The authors would like to acknowledge the 4D PICTURE Project Consortium for its valuable support and multidisciplinary contributions, which helped inform and enrich the development of this research.

REFERENCES

[1] Gomez-Caballero, R.M., López Gualdrón, C.I., Acevedo-Argüello, C.A.: A Systematic Literature Review Protocol to understand the Healthcare Service Innovation Ecosystem. WPOM-Working Papers on Operations Management 16 (2025). https://doi.org/10.4995/WPOM.21407

[2] Sharma, T., Bamford, M., Dodman, D.: Person-centred care: an overview of reviews. Contemp. Nurse 51(2-3), 107-120 (2015). https://doi.org/10.1080/10376178.2016.1150192

[3] McCormack, B., McCance, T.V.: Development of a framework for person-centred nursing. J. Adv. Nurs. 56(5), 472-479 (2006). https://doi.org/10.1111/j.1365-2648.2006.04042.x

[4] Sañudo, Y., Akoglu, C., Rietjens, J.A.C., Snelders, D., Stiggelbout, A.M., Sierra-Pérez, J.: The implementation of design methodologies for supporting shared decision making in healthcare services: A systematic review. Patient Educ. Couns. 131, 108551 (2025). https://doi.org/10.1016/j.pec.2024.108551

[5] Stickdorn, M.: This is service design thinking: basics - tools - cases. BIS Publishers, Amsterdam (2017).

[6] Denzin, N.K.: Sociological Methods. 1st edn. Routledge, London (2006). https://www.routledge.com/Sociological-Methods-A-Sourcebook/Denzin/p/book/9780202308401, last accessed 2025/07/29.

[7] Sañudo, Y., Aguado-González, L., Medina Castillo, A., Sierra-Pérez, J.: Identifying emotional variations in Spanish oncology patients during treatment decision consultations: a qualitative study. BMJ Open 16(2) (2026). https://doi.org/10.1136/bmjopen-2025-099918

[8] Sañudo, Y., Aguado-González, L., Medina-Castillo, L., Sierra-Pérez, J.: The EMPATHS method: assessing patients' emotional reactions to healthcare from a service design approach. Journal of Engineering Design, 1-26 (2025). https://doi.org/10.1080/09544828.2025.2564620

[9] Denzin, N.K., Lincoln, Y.S.: The SAGE Handbook of Qualitative Research. 5th edn. Sage Publications, Thousand Oaks (2018).

[10] Stiggelbout, A., *et al.*: Metro Mapping: development of an innovative methodology to co-design care paths to support shared decision making in oncology. BMJ Evid. Based. Med. 28(5), 291 (2023). https://doi.org/10.1136/bmjebm-2022-112168

Analysis and Application of Generative Artificial Intelligence in 3D Modeling

Eneko Solaberrieta*, Xabier Amezua, Gaizka Erkizia, Xabier Garikano
Euskal Herriko Unibertsitatea (EHU), Europa plaza 1, Donostia
* e-mail: eneko.solaberrieta@ehu.eus

Abstract: Currently, there is no artificial intelligence (AI) system capable of efficiently assisting the 3D modeling process for engineering applications. Nevertheless, two main categories of AI-based systems for 3D geometry generation can be identified: systems that generate complex geometries using polygonal meshes or point clouds, and systems that generate parametric models through code-based approaches. The former are capable of producing highly detailed 3D geometries; however, they lack parametric definition, making them unsuitable for engineering design workflows, where precision and editability are required. In contrast, the latter enable the creation of 3D geometries compatible with computer-aided design (CAD) environments, making them more suitable for engineering design workflows. This paper presents an analysis of the current state of generative AI applied to 3D modeling, based on the experimental evaluation of AI systems capable of generating parametric models through code-based approaches. Several tests were conducted by generating code for a specific CAD software environment (OpenSCAD), including basic geometries, standardized components, and complex assemblies. The results show that, although AI systems can successfully generate code for simple geometries, they still exhibit significant limitations in terms of dimensional accuracy, compliance with standards, and assembly logic. Furthermore, challenges such as uncertainty in the generated outputs and inefficient interaction between the user and the AI system reduce their practical applicability. Consequently, despite recent advances, generative AI is not yet sufficiently mature for reliable implementation in engineering-oriented 3D modeling workflows.

Keywords: *Generative Artificial Intelligence, 3D Modelling, CAD, OpenSCAD, Parametric Modeling.*

1. INTRODUCTION

The development of artificial intelligence (AI) has significantly transformed multiple fields, with generative AI demonstrating remarkable capabilities in areas such as natural language processing and image generation [1]. However, its application in 3D modeling, particularly in engineering contexts, remains limited.

Engineering design workflows require high levels of accuracy, parametric control, editability and compliance with standards, which contrasts with the probabilistic and approximate nature of current AI systems. While traditional CAD software enables accurate modeling through well-defined constraints, AI-based approaches aim to automate or assist this process using data-driven methods [2].

This work, developed within the framework of a final degree project in mechanical engineering, analyzes the applicability of generative AI to engineering 3D modeling. The main objective is to experimentally evaluate the performance of current AI systems, identify their main limitations, and assess their potential integration into engineering design workflows.

2. STATE OF THE ART

AI systems for 3D geometry generation can be broadly classified into two main approaches: systems that generate complex geometries using polygonal meshes or point clouds, and systems that generate parametric models through code-based approaches.

The first approach involves the generation of 3D models using polygonal meshes or point clouds. These systems, commonly used in virtual environments and rapid prototyping, are capable of producing highly detailed and organic geometries (Figure 1) [3]. However, they lack a parametric structure, which makes it difficult to modify dimensions or adapt designs to engineering requirements. Additionally, converting these models into CAD-compatible formats often requires manual reconstruction or reverse engineering processes, particularly for engineering applications or additive manufacturing purposes.



FIG. 1
Point cloud (left) and 3D model (right)

The second approach focuses on parametric modeling through code generation. These systems generate code for CAD environments that render 3D models from code (Figure 2) [4]. This approach allows direct integration into engineering design workflows, as the resulting models are structured and editable. Nevertheless, current implementations are generally limited to simple geometries and struggle with complex designs.

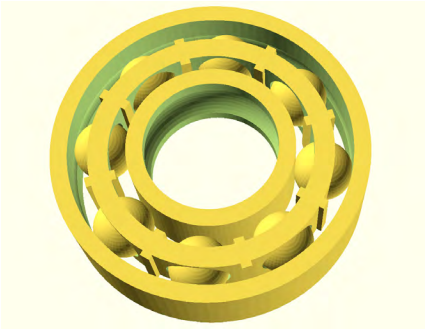


FIG. 2
Bearing generated through code-based modeling using a specific CAD software environment (OpenSCAD)

Recent developments also include AI-assisted CAD tools that integrate intelligent features into traditional design environments. These systems aim to improve productivity by automating repetitive tasks, generating sketches, or assisting in assembly processes [5]. However, their capabilities are still under development and do not yet meet industrial requirements.

Commercial CAD systems increasingly incorporate AI-based functionalities. However, these applications should be critically evaluated to determine their real capacities and limits (Figure 3).

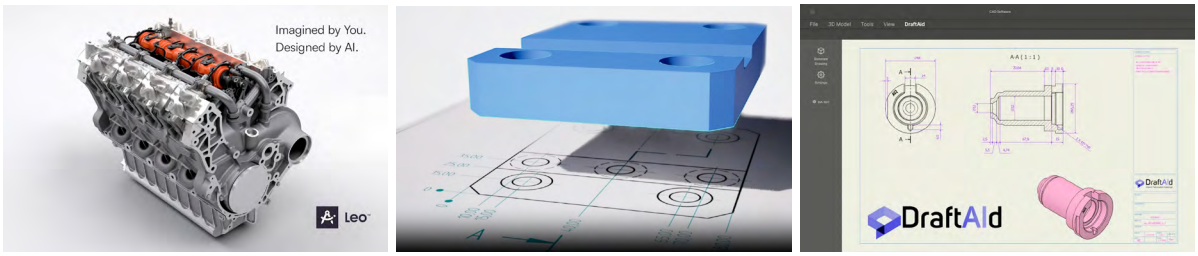


FIG. 3
Examples of CAD systems integrating AI-based functionalities

3. METHODOLOGY

To evaluate the capabilities of current AI systems, a series of tests were conducted based on realistic engineering scenarios. The tests were designed to progressively increase in complexity and included the following tasks (Figure 4):

—Generation of code for basic geometries (e.g., a cube, a cone, or a sphere)

—Generation of code for dimension-constrained designs (e.g., a 1000×500×10 mm grid)

—Generation of code for assembled objects (e.g., a house)

—Generation of code for standardized mechanical components (e.g., an Allen key, a gear, or bearing)

—Interpretation of detailed textual descriptions

—Attempted interpretation of technical drawings.

Different AI systems, including general-purpose language models and specialized 3D generation tools, were evaluated (Table 1) [6], such as ChatGPT, Grok and Deepseek. Each model was assessed in terms of geometric accuracy, number of required corrections, and ability to meet engineering constraints. Code for a specific CAD software environment (OpenSCAD) was created.

4. RESULTS AND DISCUSSION

The results obtained from the conducted tests revealed several important limitations in current AI systems for engineering-oriented 3D modeling.

All evaluated models demonstrated the ability to generate code for simple geometries, such as cubes, cylinders, and basic assemblies, with acceptable accuracy. However, as the complexity of the task increased, significant errors began to appear.

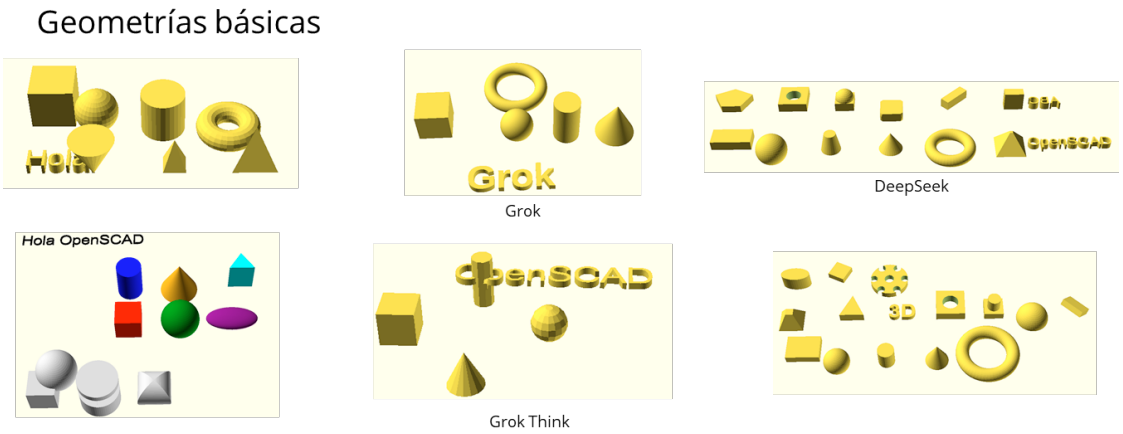


FIG. 4
Basic geometries generated through code-based modeling

In tasks involving assemblies, such as the creation of a house, AI systems showed difficulties related to spatial positioning and component alignment. Multiple iterations were often required to obtain partially correct results, and in many cases the final geometry remained inaccurate (Table 1). These limitations are mainly due to the fact that assembly generation requires the AI system to maintain consistent spatial relationships between multiple components while simultaneously satisfying dimensional constraints. Current language-model-based approaches generate code sequentially rather than reasoning explicitly about geometric dependencies, which often results in misaligned parts and incorrect assembly structures.

TABLE 1

Experimental performance comparison of selected AI models across geometric tasks

Parameters	Chat GPT	Chat GPT (Razona)	Grok	Grok (Think)	DeepSeek	DeepSeek (Deep Think R1)
House	X	X	✓	X	✓	X
Grid	✓	v	✓	✓	X	X
Arduino	X	X	X	X	X	X
Key allen	X	X	X	X	X	X
Pin	X	X	✓	X	X	X
Gear	✓	X	X	✓	X	X
Bearing	X	X	X	✓	X	X
Text description (prompt)	X	X	X	X	X	X
Text description (improved prompt)	X	✓	X	✓	X	✓

When dimensional constraints were introduced, such as in the grid generation task, some models were able to produce acceptable results after minor corrections. Nevertheless, inconsistencies in positioning and scaling were frequently observed, indicating limited accuracy in geometric reasoning.

The most significant limitations were observed in the generation of standardized mechanical components. In cases such as the Allen key and the bearing, none of the evaluated models fully complied with the required standards. Common errors included incorrect dimensions, missing geometric features, and improper construction logic. Compliance with engineering standards is particularly challenging because standardized components are defined by precise dimensional specifications and geometric relationships that must be satisfied simultaneously. Since current AI models generate outputs based on learned statistical patterns rather than explicit engineering rules or standard databases, they frequently produce geometries that appear plausible but do not conform to the required specifications.

Additionally, AI systems exhibited severe limitations in the interpretation of technical drawings. Since most evaluated models rely on text-based input, they are unable to reli-

ably extract geometric information from engineering drawings, making them unsuitable for workflows strongly dependent on such documentation [7].

Another critical issue concerns the uncertainty associated with generated outputs. Even when a model produced a visually plausible result, there was no guarantee that the generated geometry satisfied the required engineering specifications. Consequently, extensive manual validation remained necessary, significantly reducing the efficiency gains expected from AI integration into engineering design workflows [8].

5. CONCLUSIONS

This study demonstrates that, although generative AI has experienced significant advances in recent years, it is not yet sufficiently mature for reliable application in engineering-oriented 3D modeling.

Unlike previous studies, which typically focus on the capabilities of individual AI systems or specific 3D generation approaches, this work provides a comparative experimental evaluation of multiple current generative AI models across representative engineering modeling tasks, highlighting their practical limitations for CAD-oriented workflows.

Current AI systems are capable of generating simple geometries and can assist during early design stages. However, they still lack the accuracy, consistency, and standard compliance required for engineering applications. In particular, the inability to accurately generate complex assemblies, interpret technical drawings, and ensure dimensional accuracy constitutes a major limitation.

Future developments should focus on improving parametric modeling capabilities, enhancing interaction mechanisms between users and AI systems, and achieving tighter integration with existing CAD software environments. Hybrid approaches combining AI with traditional engineering methodologies may represent the most promising direction for future research and industrial implementation.

Acknowledgements: The authors thank the Faculty of Engineering Gipuzkoa at Euskal Herriko Unibertsitatea (EHU) for locating the DEHI laboratory (www.ehu.eus/dehi) in its facilities. This study was supported by the EHU (grant number EHU-N25/56).

REFERENCES

[1] Brown, T.B., Mann, B., Ryder, N., *et al.*: Language models are few-shot learners. Advances in Neural Information Processing Systems 33, 1877-1901 (2020). DOI: 10.48550/arXiv.2005.14165

[2] Shapiro, V.: Solid modeling. In: Handbook of Computer Aided Geometric Design, pp. 473-518. Elsevier, Amsterdam (2007). DOI: 10.1016/B978-044451104-1/50018-6

[3] Wu, J., Zhang, C., Xue, T., Freeman, B., Tenenbaum, J.: Learning a probabilistic latent space of object shapes via 3D generative-adversarial modeling. In: Advances in Neural Information Processing Systems, pp. 82-90 (2016).

[4] OpenSCAD Community: OpenSCAD User Manual. https://openscad.org/documentation.html, last accessed 2026/05/01.Autodesk Research: AI in CAD: Generative design and automation. Autodesk Inc., San Francisco (2022).

[5] Nichol, A., Dhariwal, P., Ramesh, A., Shyam, P., Mishkin, P.: Point-E: A system for generating 3D point clouds from complex prompts. arXiv preprint arXiv:2206.04696 (2022).

[6] Li, Y., Sun, H., Zheng, Y.: Deep learning for engineering drawing recognition. Computer-Aided Design 135, 102958 (2021). DOI: 10.1016/j.cad.2021.102958

[7] Bommasani, R., Hudson, D.A., Adeli, E., *et al.*: On the opportunities and risks of foundation models. arXiv preprint arXiv:2108.07258 (2021).

Analysis of Tool Wear Measurement in Turning Using 2D and 3D Methods

Marcos Pueo[a, b, *], Raquel Acero[a, b], Sergio Aguado[a, b], Ana Cristina Majarena[a, b], Jorge Santolaria[a, b]

[a] Aragón Institute for Engineering Research (I3A),
University of Zaragoza, Mariano Esquillor Gómez s/n, 50018, Zaragoza, Spain

[b] Design and Manufacturing Engineering Department,
University of Zaragoza, María de Luna 3, 50018, Zaragoza, Spain

* e-mail: mpueo@unizar.es

Abstract: Accurate tool wear characterization is essential for reliable tool condition monitoring and predictive maintenance in machining processes. This work presents a comparative study of flank wear (VB) measurement using two approaches based on point clouds acquired with a focus variation optical microscope. The first method follows a conventional measurement strategy, performing a direct evaluation on the microscope's three-dimensional visualization, analogous to a 2D digital image measurement. This approach, although fast and practical, is highly dependent on operator criteria and may introduce variability due to the ambiguity in the interpretation of surface features. The second approach is based on 3D point cloud superimposition analysis in Geomagic software, where the worn tool is aligned with its initial unworn state to enable direct geometric comparison. This method provides a more objective and reproducible quantification of VB through colour-coded deviation maps with micrometric resolution, allowing detailed identification of wear and material accumulation phenomena. Experimental turning tests on grey cast iron were conducted under a Design of Experiments framework, and tool wear evolution was monitored using thermography and optical metrology. Results show noticeable differences between both methods, with the conventional approach exhibiting significantly higher variability. The proposed 3D-based methodology offers improved measurement reliability and may provide robust data for future data-driven tool wear prediction models.

Keywords: *Turning process, Flank wear (VB), Tool wear measurement, Tool wear prediction, Point cloud analysis.*

1. INTRODUCTION

Increasing industrial demands for productivity, quality, and sustainability have promoted the development of advanced monitoring and optimization strategies in machining operations. Among the different factors affecting machining performance, tool wear plays a critical role, as it directly influences product quality, surface finish, dimensional accuracy, process efficiency, and manufacturing costs. Consequently, accurate tool wear characterization is essential for reliable tool condition monitoring and predictive maintenance [1].

Several tool wear mechanisms can happen during machining processes. Flank wear occurs along the tool–workpiece interface mainly due to abrasion and diffusion [2,3], whereas crater wear forms on the rake face under high temperatures generated by chip flow [4]. Thermal wear is associated with elevated temperatures and thermal stresses in the cutting zone, while adhesive wear results from material transfer between tool and workpiece [5]. In addition, notch wear typically appears along the depth-of-cut line due to chip adhesion and localized stress concentration [6].

Among the different wear mechanisms, flank wear width (VB) is the most widely investigated, as it evolves progressively during machining and has been broadly adopted as a standard criterion for tool wear assessment and tool life evaluation [7] according to ISO-3685-1993 guidelines [8]. However, ISO 3685 does not specify measurement procedures or instrumentation, which can lead to variations depending on the equipment and the operator's criteria.

Advanced optical systems provide high-resolution compared to conventional 2D methods, such as 3D optical profilometry, which allows 3D characterization of the worn region with improved geometric accuracy and reduced operator influence [3], while laser scanning microscopes (LSM) provide high-resolution optical scans and detailed surface characterization, enabling improved identification of wear patterns [9]. Nevertheless, these systems generally require specialized equipment and longer acquisition times. Scanning electron microscopy (SEM) provides high-resolution imaging that enables detailed characterization of surface degradation phenomena [9], although its use is typically time-consuming, costly, and requires expert interpretation. In addition, another commonly adopted approach for VB measurement consists of acquiring microscopic images and subsequently performing wear quantification using general-purpose image processing and analysis software [10].

In contrast, optical microscopy techniques remain widely used for VB measurement due to their simplicity, accessibility, relatively low cost, and fast inspection procedures. These include digital microscopes, which enable straightforward image acquisition and software-assisted measurements [11], and optical stereo microscopes, which provides direct visual inspection and dimensional estimation of the worn flank surface [6]. However, these approaches are often affected by viewing-angle dependence and operator-induced variability associated with manual inspection, which can significantly influence measurement consistency and repeatability [10].

Accordingly, this work addresses operator-dependent variability in conventional optical microscopy by presenting a comparative analysis of VB measurement using two ap-

proaches based on point clouds obtained with a focus variation optical microscope. The first method consists of a direct measurement performed on the microscope's three-dimensional visualization, following a conventional two-dimensional measurement approach on a projected point cloud, similar to measurements performed on a 2D digital image. The second, novel approach is based on 3D point cloud superimposition analysis in Geomagic software, where the worn tool is compared with its initial unworn state through geometric analysis. This method can provide a more objective and reproducible quantification of VB, which could potentially support future data-driven tool wear prediction models.

2. MATERIALS AND METHODS

This work is part of a broader study focused on tool wear prediction in dry turning processes. For this purpose, temperatures in different machining regions of interest were measured using thermography and correlated with tool wear evolution through the VB parameter (Figure 1a). In this context, both temperature measurements and cutting conditions are considered as input features, while the VB parameter is used as the target output for future data-driven prediction models.

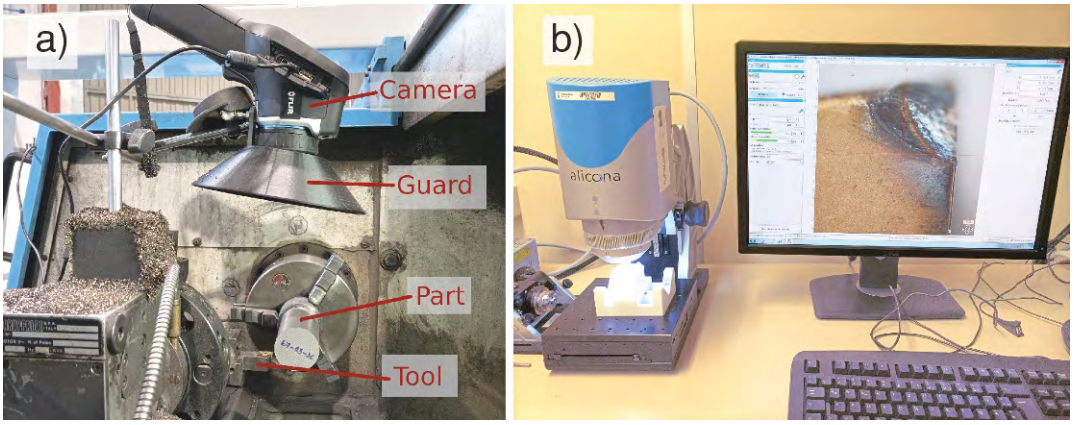


FIG. 1
Equipment: a) Turning and temperature measurement setup; and b) Alicona InfiniteFocus SL optical microscope

To generate the experimental dataset, dry turning tests were carried out on DIN 1691 GG-25 grey cast iron bars with a diameter of 60 mm, using a Garant ISO TC.T 16T304 triangular insert. Based on the cutting parameters recommended by the manufacturer, a Design of Experiments (DoE) of 8 test (2^3 test) was developed by systematically varying the feed rate (f), cutting speed (V_c), and depth of cut (a_p) in order to analyse tool wear behaviour under different machining conditions (Table 1).

TABLE 1
Experimental test and cutting conditions considered in the DoE

Test	f [mm/rev]	Vf [m/min]	a_p [mm]
1	0.05	200	1
2	0.15	200	1
3	0.05	250	1
4	0.15	250	1
5	0.05	200	2
6	0.15	200	2
7	0.05	250	2
8	0.15	250	2

In this context, relatively short workpieces were machined to avoid the use of a tailstock. Each machining pass corresponded to a cutting length of 100 mm. Flank wear (VB) was evaluated every two passes (200 mm of machined length), with the tool removed and a point cloud generated using an Alicona InfiniteFocus SL optical microscope (Figure 1b), which provides a vertical resolution of 0.160 µm and a lateral resolution of 3.91 µm. This procedure enabled the measurement of tool wear and the analysis of its evolution over time.

2.1. Conventional 2D measurement

To proceed with the experimental tests in a time-efficient manner, measurements were carried out using the basic tools provided by the Alicona software. The point cloud included realistic colour and surface topography information. However, the measurement process is equivalent to working with a 2D digital image, as the distance is measured between a reference line defined on the unworn cutting edge and the furthest point of the wear region (Figure 2). Due to the thermo-mechanical phenomena occurring at the tool–workpiece interface, it is sometimes difficult to accurately determine whether areas with different colours correspond to wear, adhesion, or shadows caused by temperature increase, leading to increased operator-dependent interpretation.

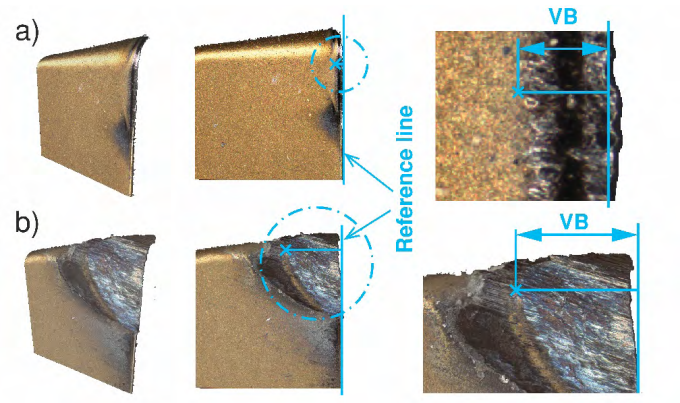


FIG. 2
Optical microscope images. Representative examples of tool wear and VB measurements from Test 1: a) Pass 2 – low wear; and b) Pass 24 – high wear

2.2. 3D point cloud superimposition method

In order to obtain more accurate VB values, a three-dimensional point cloud superimposition approach is employed in Geomagic software. The scanned surface of the worn tool is aligned with a reference point cloud corresponding to the unworn state, enabling direct geometric comparison. Surface deviations are represented using a colour-coded map with micrometric resolution (up to 1 µm), allowing a detailed visualisation of material loss and accumulation. In this representation, wear-related regions are typically indicated in blue, while material accumulation phenomena such as built-up edge are shown in red (Figure 3). The analysis further enables the identification of wear initiation along the cutting edge (VB) and the quantification of crater depth and local surface deviations.

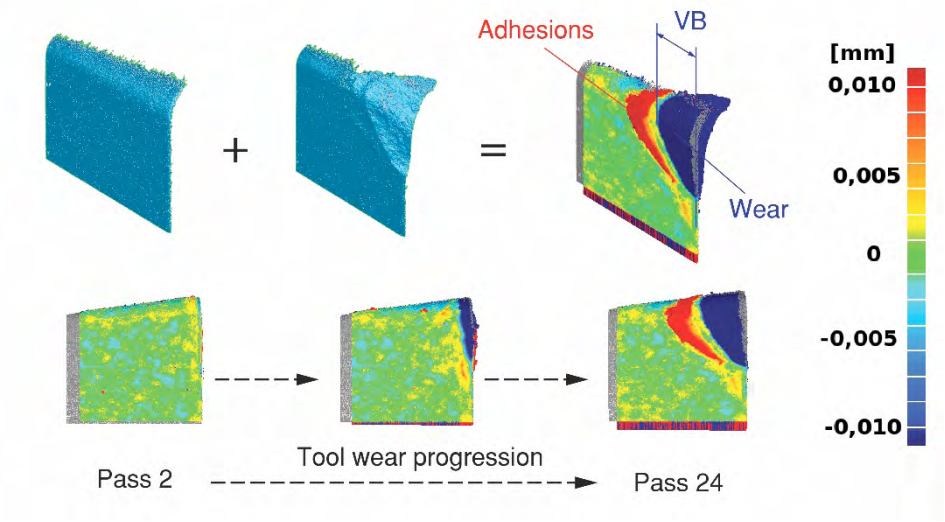


FIG. 3
Tool wear analysis through 3D point cloud superimposition

3. RESULTS

Due to the limited length of the paper, only Test 1 results are presented here, as the remaining tests (2 to 8) exhibited a similar trend. Figure 4 illustrates the results obtained in this test. In particular, Figure 4a shows the expected exponential evolution of tool wear as the machined length increases, while also demonstrating that the tool condition (low, moderate, or high wear) can be identified with a relatively high level of confidence, regardless of the measurement method. However, the geometric point cloud superimposition method exhibits a repeatability standard deviation of approximately 2 µm whereas the conventional method reaches values close to 10 µm, even reaching, in some cases, reproducibility values exceeding 50 µm.

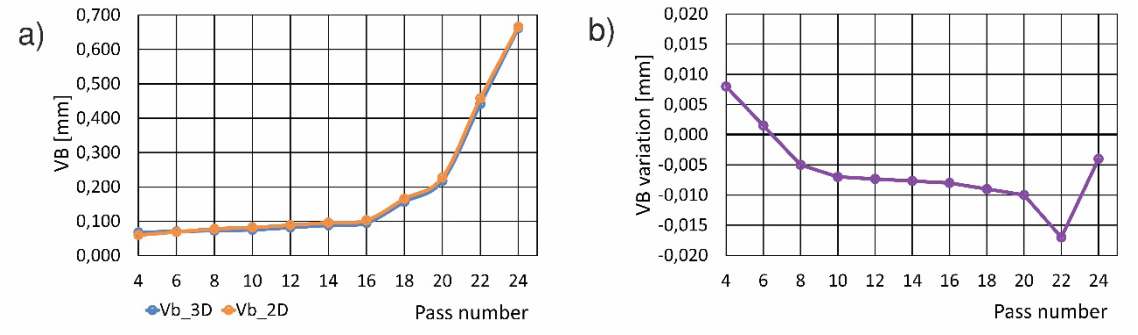


FIG. 4
Representative results from Test 1: a) VB comparison using both methods; and b) wear differences between methods

Moreover, Figure 4b, which compares the VB measurements obtained with both methods, reveals differences mainly associated with measurement interpretation and procedure. In the conventional approach, wear is evaluated on an image-like representation of the tool surface, where wear marks may be confused with heat-induced darkening. The identification of the maximum wear point may also be ambiguous, especially in the early machining stages, where low wear levels and adhesions can lead to a misleading perception of tool degradation. This effect becomes less significant as the wear land becomes more clearly defined. In contrast, the 3D point cloud superimposition approach enables a clearer separation between wear and adhesion through direct geometric comparison, improving interpretation robustness.

4. CONCLUSIONS

This work presents two approaches for tool wear measurement in a turning process according to ISO-3685-1993, both based on point clouds acquired using a focus variation optical microscope. Although both methods rely on the same acquisition system, significant differences were observed in terms of measurement consistency and sensitivity to interpretation.

The conventional approach, based on a 2D-like evaluation of the 3D data, is relatively simple and fast to implement, but it is strongly dependent on operator interpretation, which leads to higher variability in VB measurements. In contrast, the 3D point cloud superimposition method reduces operator influence by enabling a direct geometric comparison between worn and unworn tool states, resulting in improved repeatability and robustness.

Overall, both methods are based on relatively simple and cost-effective optical microscopy data acquisition, which offers practical advantages compared to more complex and expensive metrology systems. However, the 3D reconstruction-based approach provides more reliable reference data for tool wear analysis and may support future data-driven wear prediction models.

Acknowledgements: This research was funded by the Ministerio de Economía, Industria y Competitividad with project number PID2021-125530OB-I00 (Diseño y calibración de un sistema modular de inspección inteligente para verificacion y Calidad en linea 4.0), and

by Aragon Government (Department of Education, Science and University) through the Research Activity Grant for research groups recognized by the Aragon Government (T56_23R Manufacturing Engineering and Advanced Metrology Group).

REFERENCES

[1] Marousi, M., Bejjani, R., Balazinski, M.: Initial wear of cutting coated tools while machining TiMMC. Wear 578-579 (2025). https://doi.org/10.1016/j.wear.2025.206222

[2] Mao, J., Tsuchiya, K., Morigo, C., Yukinari, S., Tahara, H., Kurashiki, Y.: Reducing tool wear in high-speed milling of Inconel 718 by optimizing flank-face coolant direction: A CFD-supported approach toward sustainable machining. J. Manuf. Process. 160, 111-133 (2026). https://doi.org/10.1016/j.jmapro.2026.01.065

[3] Xiang, J., Stöbener, D., Stemmer, S., Langenhorst, L., Sölter, J., Karpuschewski, B., Fischer, A.: Robot-assisted optical measurement method for the wear analysis of cutting tools. Wear 584-585 (2026). https://doi.org/10.1016/j.wear.2025.206369

[4] Chen, Z., Ding, F., Zhang, Z., Gu, D., Liao, Q., Chen, M., Wang, B.: The study on the effect of various tool wear indicators on the machining of MMCs. Journal of Materials Research and Technology 30, 231-244 (2024). https://doi.org/10.1016/j.jmrt.2024.03.010

[5] Ehsan, S., Ali, M.A., Khan, S.A., Sana, M., Yasir, M., Anwar, S., Farooq, M.U.: Understanding the effects of cutting conditions on vibrations, surface integrity, machining temperature and tool wear mechanisms in end milling of AISI D2 Steel. Tribol. Int. 198 (2024). https://doi.org/10.1016/j.triboint.2024.109894

[6] Sirtuli, L.J., Lindberg, F., Boing, D., Bushlya, V., Norgren, S.: Impact of cutting tool and workpiece material on initial notch wear in turning. Wear 570 (2025). https://doi.org/10.1016/j.wear.2025.205942

[7] Liu, H., Ayed, Y., Birembaux, H., Rossi, F., Poulachon, G.: Impacts of flank wear and cooling strategies on evolutions of built-up edges, diffusion wear and cutting forces in Ti6Al4V machining. Tribol. Int. 171 (2022). https://doi.org/10.1016/j.triboint.2022.107537

[8] ISO 3685:1993 - Tool life testing with single-point turning tools. International Organization for Standardization (1993).

[9] Shaheen, A., Svinning, Ø., Nedrehagen, I., Bissacco, G.: On-machine high accuracy radial wear characterization of rotating milling tools using a camera-based system. J. Manuf. Process. 157, 62-77 (2026). https://doi.org/10.1016/j.jmapro.2025.11.064

[10] Sousa, V.F.C., Gil, J., Silva, T.E.F., de Jesus, A.M.P., Silva, F.J.G., Tavares, J.M.R.S.: An Image Analysis Algorithm for Measuring Flank Wear in Coated End-Mills. Computers, Materials and Continua 83, 177-199 (2025). https://doi.org/10.32604/cmc.2025.062133

[11] Gao, G., Xiang, Y., Qiao, H., Wei, C., Wang, G., Xiang, D.: Modeling on cutting force considering tool flank wear in ultrasonic vibration-assisted milling Ti3Al. Wear 566-567 (2025). https://doi.org/10.1016/j.wear.2025.205761

Graphical Application for the Morphological Characterization and Geometric Modeling of Real Milling Cutter Edges

Yasser Zekalmi*, José Antonio Albajez, María José Oliveros, Sergio Aguado

Design and Manufacturing Engineering Department, Universidad de Zaragoza, María Luna 3, Zaragoza, 50018, Spain

*e-mail: yzekalmi@unizar.es

Abstract: Surface texture prediction in ball-end milling requires a cutter-edge model that represents the real tool, not only its nominal CAD geometry. This paper presents a graphical workflow for converting 360° optical measurements into a simulation-ready cutting-edge curve. The method combines an analytical ideal edge, defined in the Tool Coordinate System, with a real edge extracted from measured geometry. The extraction uses absolute mean curvature to locate the rake/flank transition, followed by percentile thresholding, connectivity filtering and axial slicing. This sequence reduces a dense scan to an ordered point profile while preserving the local morphology that controls generated micro-topography. The paper also positions the workflow against recent surface-topography simulation and tool-monitoring approaches in terms of expected accuracy, repeatability, processing effort and measurement cost. A complementary morphological analysis based on deviation distributions and wear-section evidence shows that real edges combine distributed micro-irregularity with localized recession. The resulting representation provides a practical bridge between tool metrology, geometric modelling and surface simulation, supporting more reliable functional-surface design with fewer trial machining loops.

Keywords: *cutter-edge extraction, ball-end milling, mean curvature, optical 3D measurement, geometric modeling, surface topography simulation.*

1. INTRODUCTION

Surface micro-topography in ball-end milling is the fine three-dimensional texture left by the active cutting edge on the workpiece. It influences friction, sealing, fatigue initiation, coating adhesion and later polishing requirements. For this reason, surface quality should not be treated only as an inspection result, but also as a design and manufacturing variable. Better prediction helps reduce trial machining, repeated inspection loops, unnecessary tool replacement and over-processing, which is especially relevant for high-value components with strict functional surfaces.

Classical and recent models have improved the prediction of surface topography by representing the tool path, cutter-workpiece engagement, tool posture, vibration and numerical update of the workpiece surface [1-6]. Recent fast algorithms also reduce the computational cost of micro-topography prediction in 5-axis milling [7-10]. However, many workflows still start from an ideal smooth cutter edge. This assumption is useful for baseline analysis, but it cannot reproduce local texture changes caused by edge rounding, micro-chipping, local flats, manufacturing variability or wear. Cutting-edge microgeometry is known to affect surface generation and process mechanics [1,2], and recent monitoring approaches show that measured tool geometry can be converted into useful information for tool-state assessment [3,4].

This work focuses on the graphical link between metrology and simulation: transforming a dense 360° optical scan of a helical ball-end cutter into a compact ordered curve. The objective is not to replace the ideal edge, but to place it beside a measured representation. The ideal edge remains a reproducible reference for comparison, whereas the extracted edge captures the physical morphology that actually interacts with the workpiece. Figure 1 summarizes the paper logic: cutter-edge definitions, real-edge extraction, morphological analysis and simulation-ready use.

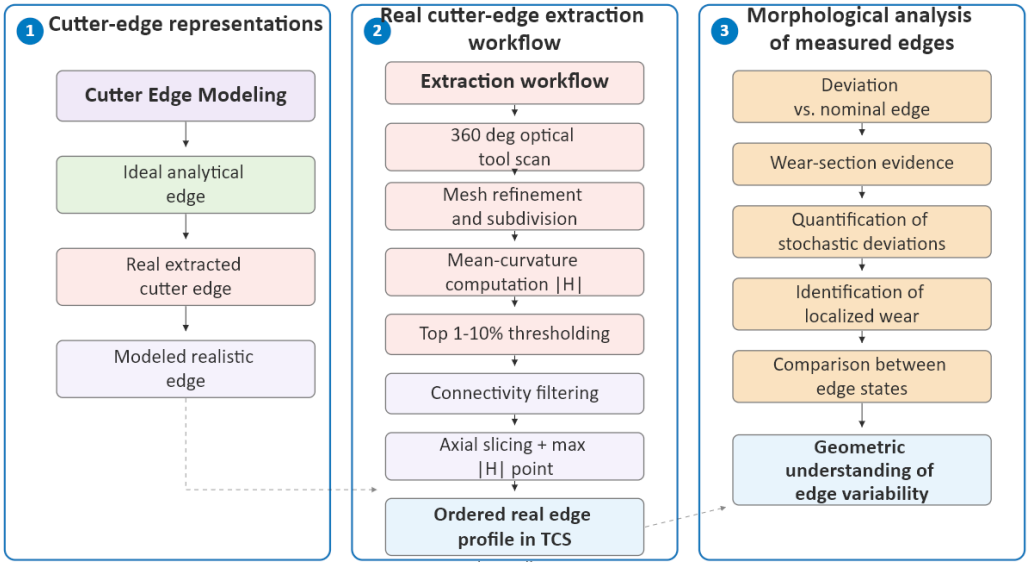


FIG. 1

Proposed workflow for cutter-edge characterization and simulation-ready representation. The figure connects the three edge definitions used in the paper with the real cutter-edge extraction procedure and the subsequent morphological analysis

TABLE 1
Position of the proposed representation relative to common and recent alternatives

Approach	Accuracy / precision	Time / cost	Main limitation
Ideal analytical edge	High repeatability; low tool-specific accuracy.	Very fast; lowest cost.	No local defects, flute differences or wear.
Full measured mesh [3,4]	High geometric fidelity; scan-noise dependent.	Large data; higher cleaning and metrology cost.	Too heavy for repeated simulations.
Proposed extracted curve	Tool-specific ordered edge; percentile/connectivity rules improve repeatability.	One 360° scan plus automated post-processing.	Broader validation over tool types still needed.

2. METHODOLOGY

The ideal reference is defined in the Tool Coordinate System (TCS), with origin at the tool center, Z_T aligned with the spindle and TT located at the lowest point of the spherical cutting region. For the ball-end part, the nominal flute is parameterized by the tool radius R, axial angle ψ, helix angle γ and phase φ0. Equation (1) gives a compact description of the helical edge. This model is deterministic, easy to sample and convenient for generating a swept cutter-edge trajectory. Its limitation is that every point belongs to the nominal design; therefore, it cannot include local edge recession, burrs, micro-chipping or flute-to-flute differences.

$$P_S(\psi) = (R\sin\psi\cos\theta, R\sin\psi\sin\theta, -R\cos\psi)^T, \quad \theta = \phi_0 + \frac{\psi}{\tan\gamma} \tag{1}$$

In the proposed digital representation, this analytical edge is used as the reference curve. The measured edge is later aligned and compared against it so that deviations can be interpreted geometrically. This separation between nominal and real geometry keeps the simulation workflow modular: the same topography algorithm can be evaluated with an ideal, a measured or a simplified realistic cutter edge.

The real edge is extracted from a full 360° measurement because helical flutes cannot be represented reliably from a single projection. Direct normal-based detection is sensitive to scan noise, local reflection artifacts and coordinate-frame mismatch. Instead, absolute mean curvature |H| is used as an intrinsic descriptor. High values of |H| concentrate at sharp transitions, particularly at the rake/flank intersection where the physical cutting edge is located. Since curvature depends on local surface shape rather than on the global pose of the scanned tool, it provides a robust criterion for graphical edge localization [11].

For a height surface S(x,y) = (x, y, f(x,y)), the mean curvature can be written as equation (2). Although the scanned cutter is processed as a polygonal mesh, the same concept is applied numerically at the mesh vertices. The curvature field is then treated as a scalar map that can be visualized, thresholded and filtered.

$$H = \frac{\left(1+f_x^2\right)f_{yy} - 2f_x f_y f_{xy} + \left(1+f_y^2\right)f_{xx}}{2\left(1+f_x^2+f_y^2\right)^{3/2}} \tag{2}$$

Figure 2 shows the complete extraction sequence. The measured mesh is first refined to stabilize curvature estimation. Next, only the top 1-10% curvature values are retained, which avoids defining a fixed absolute threshold that would be sensitive to tool condition and measurement quality. Because thresholding can preserve disconnected high-curvature regions, a connectivity filter is used to discard detached artifacts and retain the component associated with the active edge. Finally, this component is sliced by planes normal to the tool axis. With an axial step d_ax = 5 × 10^-3 mm, each plane contributes the point with maximum |H|. The selected points define an ordered edge curve expressed in the TCS. This final curve is much lighter than the original scan, but it preserves the geometric information required for micro-topography simulation.

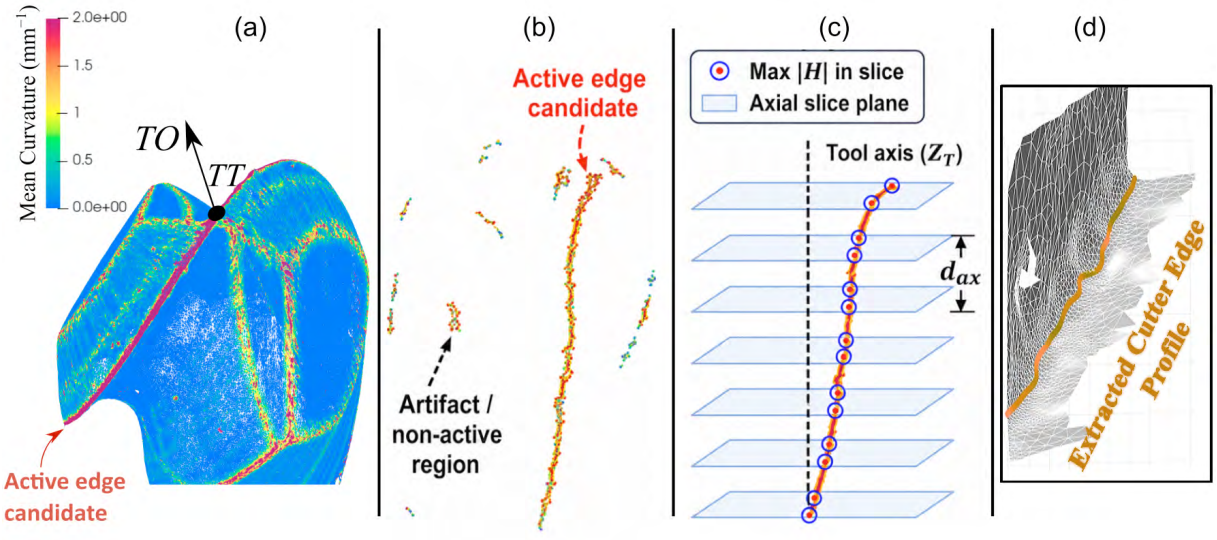


FIG. 2

Curvature-based real cutter-edge extraction. (a) Mean-curvature map of the measured tool tip. (b) Percentile threshold retaining the highest-curvature regions. (c) Connectivity filtering and axial slicing, where one maximum-curvature point is selected per plane. (d) Extracted cutter-edge profile expressed as an ordered curve

3. MORPHOLOGICAL ANALYSIS AND SIMULATION USE

The extracted curve makes real tool variability explicit. Figure 3(a) shows probability distributions of edge deviation with respect to the nominal geometry for four tools with different cutting times. The distributions remain concentrated at small deviations, which indicates that the ideal edge is still a useful global reference. However, their different spreads and tails reveal distinct morphological states. A tool may preserve the overall nominal shape while accumulating local recession, small protrusions or edge irregularities that are significant at the scale of surface texture generation.

Figure 3(b) supports this interpretation by showing a localized worn zone next to a comparatively unaffected region. This confirms that degradation is not spatially uniform and should not be represented only as a global offset of the nominal radius. Instead, a compact real-edge profile allows the simulator to include spatially varying deviations while avoiding the cost of using the complete measured mesh.

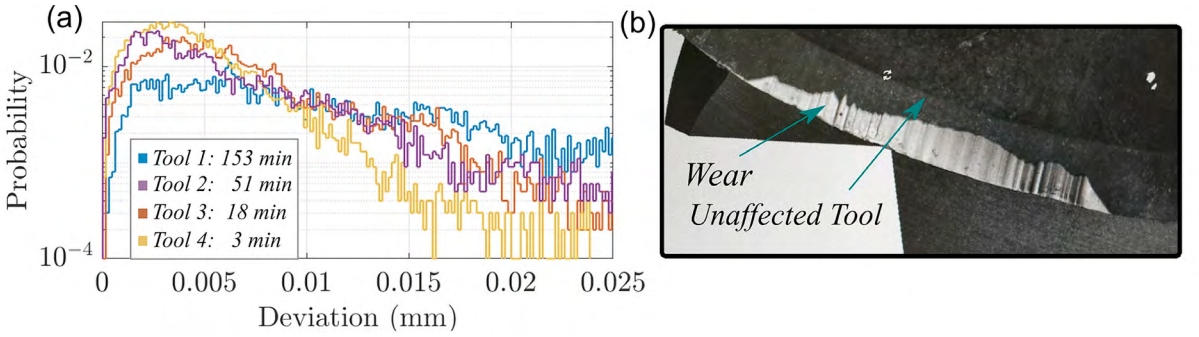


FIG. 3

Morphological analysis of real cutter edges. (a) Probability distributions of deviation magnitude for tools with different cutting times. (b) Section image showing localized wear and a comparatively unaffected region. The results indicate that real cutter edges combine distributed micro-irregularity with spatially localized recession

For simulation, the final output is an ordered point sequence E_real = {p1, p2, ..., pn}. Each point can be rotated with the spindle angle α, and additional flutes can be represented by phase shifts, as shown in equation (3). The same simulator can therefore use three related inputs: the ideal analytical edge for baseline studies, the real extracted edge for high-fidelity prediction, and a modeled realistic edge calibrated from the deviation and wear analysis.

$$p_{i,j}^{rot}(\alpha) = R_z\left(\alpha + \frac{2\pi j}{N_f}\right) p_i, \qquad i = 1,\ldots,n, \quad j = 0,\ldots,N_f - 1 \tag{3}$$

This structure supports controlled comparisons between nominal, measured and simplified realistic tool descriptions. Deviation distributions indicate whether the edge state is dominated by stochastic roughness or by systematic recession, while the section evidence helps identify localized wear zones. These observations can guide future modeled edges, where random sharpness variation and local wear flats are introduced analytically without requiring a complete scan for every simulation case.

4. CONCLUSIONS

A compact graphical workflow has been presented to transform 360° optical measurements of a ball-end milling cutter into a simulation-ready edge curve. The main contribution is the integration of optical metrology, curvature-based geometry processing and a TCS-based edge representation in a single reproducible route. Absolute mean curvature localizes the rake/flank transition, percentile thresholding adapts the selection to the measured curva-

ture distribution, connectivity filtering removes disconnected artifacts and axial slicing converts the remaining high-curvature band into an ordered curve.

The comparison with recent literature clarifies the contribution: the proposed representation is more tool-specific than a nominal analytical edge, lighter than a full measured mesh, and complementary to recent fast surface-topography solvers. It does not claim to replace those solvers; instead, it provides the realistic cutter-edge input that they need to move from nominal kinematics toward measured tool morphology. By linking tool measurement, geometric modelling and surface prediction, the workflow supports more reliable functional surfaces and can reduce empirical correction cycles. Future work will validate the influence of these edge definitions on measured topographies and extend the method to multiple flutes and progressive wear states.

REFERENCES

[1] Biondani, F.G., Bissacco, G.: Effect of cutting edge micro geometry on surface generation in ball end milling. CIRP Annals 68(1), 571-574 (2019). doi: 10.1016/j.cirp.2019.04.017.

[2] Zhuang, K., Fu, C., Weng, J., Hu, C.: Cutting edge microgeometries in metal cutting: a review. International Journal of Advanced Manufacturing Technology 116(7-8), 2045-2092 (2021). doi: 10.1007/s00170-021-07558-6.

[3] Salaets, R., Sturm, V., Ooijevaar, T., Putz, V., Mayer, J., Bey-Temsamani, A.: Optical cutting tool wear monitoring by 3D geometry reconstruction. PHM Society European Conference 7(1), 449-457 (2022). doi: 10.36001/phme.2022.v7i1.3351.

[4] Wimmer, M., Hartl, R., Zaeh, M.F.: Determination of the cutting-edge microgeometry based on process forces during peripheral milling of Ti-6Al-4V using machine learning. Journal of Manufacturing and Materials Processing 7(3), 100 (2023). doi: 10.3390/jmmp7030100.

[5] Xiao, Y., Ge, G., Zeng, Z., Feng, X., Du, Z.: An improved Z-MAP method based on the SQP algorithm for fast surface topography simulation of ball-end milling. International Journal of Advanced Manufacturing Technology 128, 1863-1878 (2023). doi: 10.1007/s00170-023-11992-z.

[6] Marin, F., de Souza, A.F., da Silva Gaspar, H., Calleja-Ochoa, A., López de Lacalle, L.N.: Topography simulation of free-form surface ball-end milling through partial discretization of linearised toolpaths. Engineering Science and Technology, an International Journal 55, 101757 (2024). doi: 10.1016/j.jestch.2024.101757.

[7] Wang, R., Zhao, B., Tan, D., Wan, W.: Modelling and optimization of machined surface topography in ball-end milling process. Materials 17(7), 1533 (2024). doi: 10.3390/ma17071533.

[8] Zekalmi, Y., Albajez, J.A., Aguado, S., Oliveros, M.J.: New fast micro-topography estimation algorithms for 5 axis milling. Advances in Engineering Software 205, 103909 (2025). doi: 10.1016/j.advengsoft.2025.103909.

[9] Maaloul, M., Belguith, R., Regaieg, A., Sai, L., Amrouche, A.: Precision surface topography prediction in ball-end milling: a CWER-based approach for enhanced accuracy and efficiency. International Journal of Advanced Manufacturing Technology 138(3-4), 1621-1649 (2025). doi: 10.1007/s00170-025-15579-8.

[10] Guo, P., Wang, T., Wang, J., Zhang, S., Wang, J., Wang, L.: Surface topography model for ball-end milling process based on modified sine-cosine algorithm. Surface Topography: Metrology and Properties 13(2), 025011 (2025). doi: 10.1088/2051-672X/add715.

[11] Rusinkiewicz, S.: Estimating curvatures and their derivatives on triangle meshes. In: 3DPVT, pp. 486-493. IEEE (2004). doi: 10.1109/TDPVT.2004.1335277.

Digital Eco-Design and Parametric Optimization of 3D Assets: A Hybrid Workflow for Sustainable Virtual Fashion Environments

Aida Vidal-Fernández, Cristina Prado-Acebo, Anabel Díaz-Labrador, Francisco Zayas-Gato, Elena Arce Fariña*

University of A Coruña, Ferrol Polytechnic School of Engineering.
C/Mendizábal, s/n. Esteiro Campus. 15403 Ferrol, A Coruña, Spain

* e-mail: elena.arce@udc.es

Abstract: Digital fashion environments require auxiliary three-dimensional assets that are visually credible, geometrically controlled and computationally efficient. This paper presents a hybrid CAD-to-simulation workflow for the development and optimisation of digital furniture for virtual fashion scenarios. Two assets, a modular display system and an anthropomorphic support, were modelled parametrically in SolidWorks, exported as STL files, processed in MeshLab and imported into CLO3D as simulation-ready OBJ props. The study evaluates the workflow from an engineering graphics perspective, focusing on the conversion of precise NURBS-based CAD geometry into lightweight polygonal meshes suitable for textile simulation and rendering. A telemetry protocol based on real-time GPU and CPU monitoring was also implemented to quantify energy demand during modelling, rendering and simulation tasks. The digital prototype, including five hours of CAD modelling and one high-quality render, generated an estimated footprint of 132.5 g CO2e, whereas an equivalent stainless-steel physical prototype was estimated at 14.4 kg CO2e. The results also show that render quality and mesh density strongly affect sustainability: very-high-quality rendering increased energy use by 648.8% compared with medium quality, while reducing the mannequin mesh from 2.8 million faces to 4,516 faces increased simulation performance from 1.46 to 113.21 FPS. The proposed framework demonstrates that digital dematerialisation must be accompanied by topology and rendering optimisation to achieve sustainable virtual design workflows.

Keywords: *Digital Eco-design, Virtual Prototyping, CAD Interoperability, Computational Efficiency, Sustainable Fashion, Life Cycle Analysis.*

1. INTRODUCTION

Digital design, virtual prototyping and immersive presentation environments are changing the way fashion products and related spaces are conceived. These technologies are commonly presented as sustainable alternatives to physical sampling because they may reduce material use, transport and waste during early design iterations [1,2]. However, virtual workflows are not impact-free. Their environmental performance depends on the computational cost of modelling, rendering, simulation and asset management. Sustainability in digital fashion must therefore be addressed not only as a matter of dematerialisation, but also as a problem of engineering graphics efficiency.

Previous work on 3D virtual prototyping in apparel has emphasised its capacity to improve visual communication, shorten design cycles and reduce dependence on physical prototypes [3,4]. At the same time, the creation of virtual showrooms, metaverse retail scenes and digital fitting environments has expanded the scope of fashion design beyond the garment itself. These spaces require display systems, supports, mannequins and spatial components that are not merely decorative: their geometry, mesh topology and material configuration influence rendering time, collision stability, frame rate and the credibility of the visual narrative.

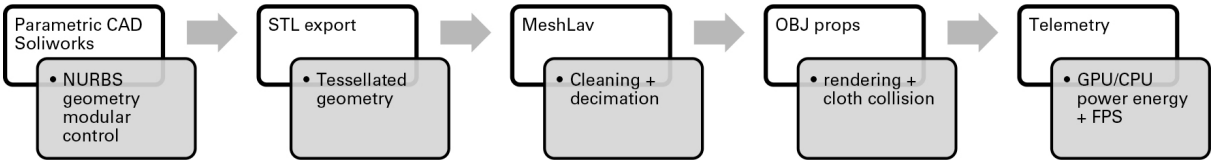
The objective of this work is to propose and validate a transferable workflow for creating sustainable, simulation-ready 3D assets for virtual fashion environments. The study focuses on two types of digital furniture: a modular display system and an anthropomorphic support structure. The contribution of the paper lies in connecting three usually separate aspects of the workflow: parametric engineering geometry, mesh optimisation for textile simulation, and operational energy measurement..

2. MATERIALS AND METHODS

The proposed workflow combines industrial CAD modelling with mesh optimisation and textile simulation. The first stage consists of parametric modelling in SolidWorks [5]. This step ensures dimensional consistency, modular control and systematic modification of supports, shelves, joints and anthropomorphic contours. Unlike purely polygonal modelling, parametric CAD provides a robust basis for geometric repeatability and possible future manufacturing.

The second stage addresses interoperability. CAD geometry based on NURBS surfaces is not directly suitable for real-time textile simulation, which relies on polygonal meshes. The assets were therefore exported in STL format and processed in MeshLab [6]. This intermediate stage was used to clean the geometry, reduce unnecessary polygonal density, control normals and generate OBJ files compatible with CLO3D [7]. The workflow is summarised in Figure 1.

The third stage consisted of importing the optimised OBJ models into CLO3D as scene props. The modular display system was used to test rendering quality and lighting configurations, whereas the anthropomorphic support was evaluated through cloth interaction tests using a basic T-shirt pattern. This distinction allowed the assessment to cover both visual validation and simulation usability.



Design decision loop: polygon density, render quality and reuse criteria adjusted according to performance and energy indicators

FIG. 1

Hybrid CAD-to-simulation and telemetry workflow used to transform parametric geometry into simulation-ready digital assets

3. ENERGY AND PERFORMANCE ASSESSMENT

A telemetry-based protocol was implemented to quantify the computational cost of the digital workflow. MSI Afterburner [8] was used to monitor GPU and CPU load, power consumption, operating temperature and rendering duration. The monitoring log was captured at approximately 1 Hz and processed to isolate active render windows. Energy was calculated by integrating power over time, and carbon footprint was estimated from the measured energy consumption and the emission factor of the Spanish electricity mix. The open monitoring record is available in Zenodo [9].

The environmental comparison was intentionally limited to early-stage prototyping. The digital workflow was compared with the estimated cradle-to-gate impact of an equivalent stainless-steel physical prototype. The aim was not to produce a full product life cycle assessment, but to provide a transparent operational indicator of the environmental relevance of digital substitution at the design validation stage.

Rendering quality was assessed by comparing medium and very-high-quality settings under the same illuminated scene. Mesh complexity was assessed by comparing a high-poly anthropomorphic support against a low-poly version. Frame rate was used as a direct indicator of simulation usability because it reflects the capacity of the system to maintain interactive cloth behaviour during virtual fitting and scene validation.

TABLE 1

Main quantitative results of the digital workflow assessment

Indicator	Digital workflow	Reference / comparison
Carbon footprint	132.5 g CO_2e	14.4 kg CO_2e physical prototype
Rendering energy	2.104 Wh very-high quality	0.281 Wh medium quality
Mesh density	4,516 faces	2.8 million faces
Simulation frame rate	113.21 FPS	1.46 FPS high-poly model

4. RESULTS

As shown in Table 1, the complete digital creation of the asset, including five hours of CAD work and one high-quality render, produced an estimated carbon footprint of 132.5 g CO_2e. The equivalent stainless-steel physical prototype was estimated at 14.4 kg CO_2e. This difference shows the potential of digital dematerialisation for early design validation, especially in iterative design processes in which several physical prototypes would otherwise be produced.

The rendering test indicates that energy demand depends strongly on the chosen quality level. In the illuminated scene, very-high-quality rendering consumed 2.104 Wh, compared with 0.281 Wh for medium quality, an increase of 648.8% (Figure 2). The visual gain was marginal for design validation purposes, suggesting that maximum-quality rendering should be reserved for final communication rather than routine technical checks.

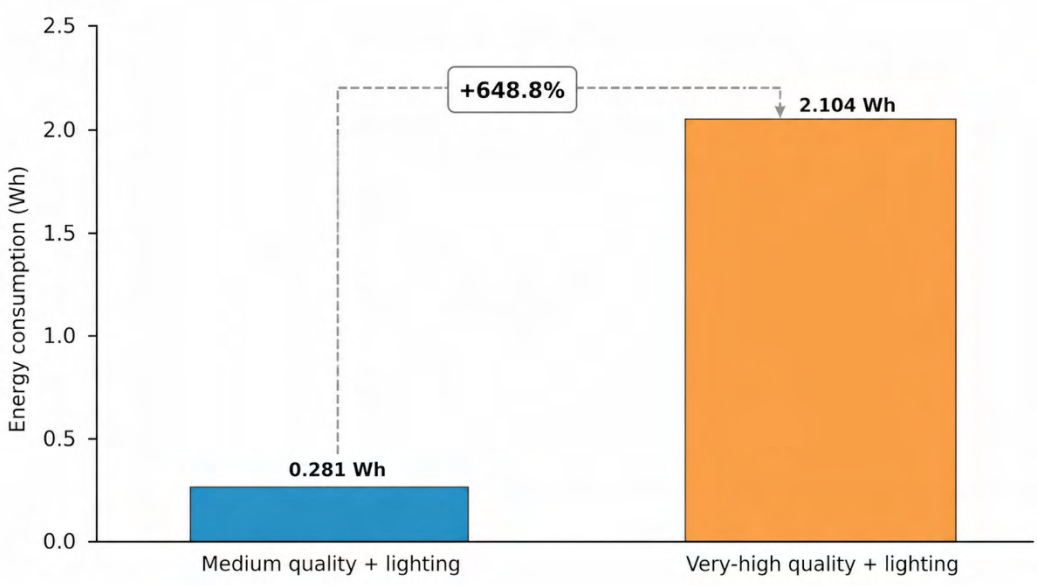


FIG. 2
Energy consumption for medium and very-high-quality rendering under the same illuminated scene

The mesh optimisation test provided an even clearer result. Reducing the mannequin from approximately 2.8 million faces to 4,516 faces improved simulation fluidity from 1.46 FPS to 113.21 FPS (Figure 3). The optimised version maintained adequate cloth interaction for the intended test, showing that a lighter asset can preserve functional behaviour while reducing computational load.

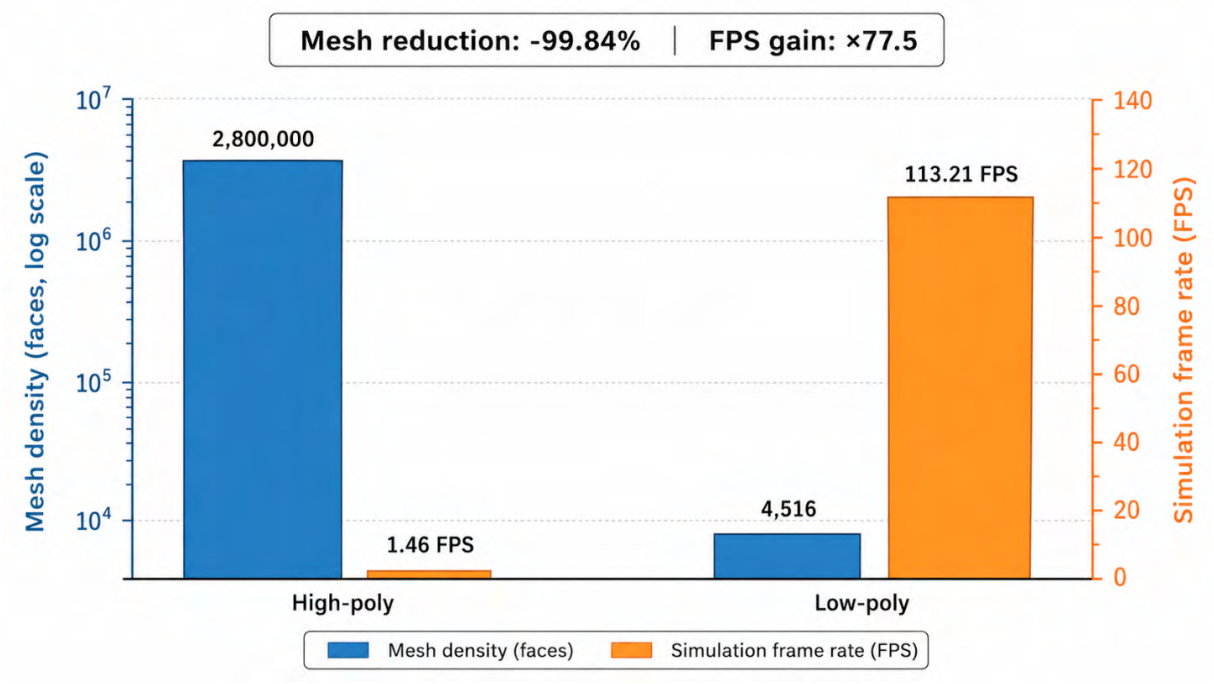


FIG. 3
Effect of mesh optimisation on polygon density and CLO3D simulation frame rate

5. DISCUSSION

The proposed workflow addresses a common limitation in virtual fashion environments: the gap between geometrically precise CAD models and efficient simulation-ready assets. CAD tools are appropriate for dimensionally controlled design, but their direct exports may generate polygonal representations that are too heavy for real-time or near-real-time simulation. The introduction of a mesh-processing stage enables the designer to preserve the intentional geometry while adapting the asset to the constraints of CLO3D.

From a sustainability perspective, the findings suggest that digital substitution should not be interpreted as a simple replacement of physical objects by virtual objects. Sustainable virtual design requires operational criteria: moderate render quality when high fidelity is not essential, controlled polygon density, reuse of modular assets and testing under realistic simulation conditions. These criteria are especially relevant for fashion environments because garments, avatars and furniture interact through collision and rendering systems that can quickly become computationally expensive.

The study has limitations. The carbon comparison is based on an operational estimate rather than a complete LCA, and the physical prototype is represented by a reference stainless-steel scenario. The rendering and simulation measurements also depend on the specific hardware platform and software configuration. Nevertheless, the results provide a practical framework for integrating engineering graphics, virtual prototyping and environmental awareness in digital fashion design.

6. CONCLUSION

This paper presents a hybrid workflow for the creation of sustainable 3D assets for virtual fashion environments. By integrating SolidWorks, MeshLab and CLO3D, the method translates precise CAD geometry into optimised polygonal assets that can be rendered and used in textile simulation. The results show that digital prototyping can substantially reduce emissions compared with physical prototyping, but also that energy and performance depend strongly on render settings and mesh topology.

The main contribution is the identification of digital eco-design as a combined problem of dematerialisation, interoperability and computational optimisation. The reduction of mesh complexity produced a major improvement in simulation frame rate, while the comparison of rendering settings revealed that maximum visual quality may involve disproportionate energy demand. Therefore, sustainable virtual environments should be designed using task-specific levels of detail and render quality.

The proposed framework can be transferred to other engineering graphics applications involving virtual products, digital twins or immersive environments. Its practical value lies in offering designers a repeatable procedure for balancing visual fidelity, geometric precision and environmental efficiency during the development of simulation-ready assets.

Acknowledgements: This research was supported by the Xunta de Galicia through the Axencia Galega de Innovación (GAIN), under grant IN853C2025/03; by the Centro Mixto de Investigación UDC-NAVANTIA O estaleiro do futuro; Grant PID2022-137152NB-I00 funded by MICIU/AEI/10.13039/501100011033 and by ERDF/EU, and by the European Commission, Erasmus+. KA220-SCH, "Production of Prototypes with STEAM Content in Maker Workshops Against Climate Change" (Project Ref. 20231PT01KA220SCH000155915).

REFERENCES

[1] European Commission: Ecodesign for Sustainable Products Regulation. https://commission.europa.eu/energy-climate-change-environment/standards-tools-and-labels/products-labelling-rules-and-requirements/ecodesign-sustainable-products-regulation_en, last accessed 2026/05/14.

[2] Ellen MacArthur Foundation: A New Textiles Economy: Redesigning Fashion's Future. Ellen MacArthur Foundation, Cowes (2017). Retrieved from: https://www.ellenmacarthurfoundation.org/a-new-textiles-economy

[3] Papahristou, E., & Bilalis, N. (2016). Can 3D Virtual Prototype Conquer the Apparel Industry?. J Fashion Technol Textile Eng 4: 1. of, 6, 2. http://dx.doi.org/10.4172/2329-9568.1000141

[4] Papahristou, E., & Bilalis, N. (2017). Integrated digital prototyping in the fashion product development. *Journal of Textile Engineering & Fashion Technology*, 3(1), 586-591.

[5] Dassault Systèmes: SOLIDWORKS 3D CAD. https://www.solidworks.com/, last accessed 2026/05/14.

[6] Cignoni, P., Callieri, M., Corsini, M., Dellepiane, M., Ganovelli, F., Ranzuglia, G.: MeshLab: an Open-Source Mesh Processing Tool. In: Eurographics Italian Chapter Conference, pp. 129-136 (2008). https://doi.org/10.2312/LocalChapterEvents/ItalChap/ItalianChapConf2008/129-136

[7] CLO Virtual Fashion: CLO3D. https://www.clo3d.com/, last accessed 2026/05/14.

[8] MSI: MSI Afterburner. https://www.msi.com/Landing/afterburner/graphics-cards, last accessed 2026/05/14.

Designing Effective Bar Charts for Global Health Data

Antonio Fernández[a], *, Francesco Bianconi[b]

[a] CINTECX, Universidade de Vigo, GeoTech,
Campus Universitario Lagoas-Marcosende, 36310 Vigo, Spain

[b] Department of Engineering, Università degli Studi di Perugia,
Via Goffredo Duranti 93, 06125 Perugia, Italy

* e-mail: antfdez@uvigo.es

Abstract: The growing availability of global health data has increased the need for effective visual communication to support evidence-based decision-making within the One Health framework. While data quality is essential, the way information is visually represented plays a critical role in how it is interpreted. In particular, poorly designed charts may lead to misleading conclusions, affecting both policy and public understanding. This study focuses on the design of bar charts for the communication of global health data. Its main objective is to propose a set of practical guidelines that enhance clarity, accuracy, and interpretability. The methodology follows a progressive, example-driven approach using real-world data on child mortality rates across major world regions in 2023. A sequence of bar charts is generated using Python, starting from a deliberately flawed visualization and applying successive improvements based on established visualization principles. The results show that relatively simple design choices—such as ordering categories, using color strategically, labeling units clearly, and displaying values directly—can substantially improve data interpretation. These improvements reduce ambiguity and facilitate more accurate comparisons across categories. The proposed guidelines provide actionable recommendations for practitioners and educators, contributing to more effective and reliable communication of global health data within the One Health context.

Keywords: *Data Visualization, Bar Charts, One Health Communication.*

1. INTRODUCTION

The rapid growth in the availability of global health data has transformed the way researchers, policymakers, and organizations approach complex health challenges. Within the One Health framework, which emphasizes the interconnectedness of human, animal, and environmental health, the ability to communicate data clearly is essential for informed decision-making.

While significant attention has been given to data collection and statistical analysis, less emphasis is often placed on how results are visually communicated. Visualization plays a critical role in shaping interpretation. Inadequate graphical design can introduce bias, obscure patterns, or even mislead audiences.

Among the many visualization techniques available, bar charts remain one of the most widely used tools for representing categorical data. Their simplicity makes them accessible, but also prone to misuse. This paper addresses this issue by proposing a set of guidelines for designing effective bar charts tailored to global health data. The paper first reviews fundamental concepts in data visualization and the role of bar charts, then introduces the data and methodology used in the study. Subsequently, a series of design guidelines are presented and illustrated through progressively refined examples, followed by a discussion of the results and concluding remarks.

2. BACKGROUND

2.1. Fundamentals of data visualization

Data visualization involves mapping data variables to visual properties such as position, length, and color [1]. A key distinction is made between categorical variables (dimensions) and quantitative variables (measures). Categorical variables take values from discrete sets and describe “what type” (e.g., regions or categories), whereas quantitative variables represent “how much” or “how many” and can be either continuous (measured) or discrete (counted).

In addition, variables may be ordered or unordered depending on whether their values follow a natural sequence. These distinctions are essential for selecting appropriate visual encodings. Measures typically correspond to quantitative variables and represent the values of interest, while dimensions are used to group or partition these values into meaningful categories.

2.2. Bar charts and their role

Bar charts are particularly suitable for comparing values across categories. In this type of visualization, categories define groups (dimensions), while numerical values (measures) are encoded through bar length or height, allowing for straightforward comparison across groups. For this reason, bar charts are among the most widely used tools for representing and comparing magnitudes.

Bar charts can be displayed either vertically or horizontally, depending on the context and the nature of the data. Horizontal layouts are often preferable when category labels are long, as they improve readability and prevent overlap. Additional variations, such as grouped or stacked bar charts, allow the representation of more complex relationships within the data.

Despite their apparent simplicity, bar charts require careful design to ensure accurate interpretation. Choices related to layout, scaling, and visual emphasis can significantly influence how the data are perceived. As a general rule, the number of bars should be limited to approximately 8-10 to maintain readability and avoid visual clutter. As a result, even small design decisions play a critical role in supporting clear, reliable, and effective communication.

3. DATA AND METHODOLOGY

3.1. Data source

The dataset used in this study consists of child mortality rates (expressed as a percentage) by continent for the year 2023. The data were obtained from the publicly available repository Our World in Data [2], which provides curated global health datasets.

3.2. Methodological approach

The methodology follows a progressive, example-driven approach. A sequence of bar charts is generated using Python, specifically the libraries Matplotlib and Seaborn. The analysis focuses on child mortality rates across world regions. The process begins with a deliberately flawed visualization that violates several established design principles (Figure 1 left). Subsequently, a series of improvements is applied incrementally. Each step introduces a specific guideline, allowing for a clear comparison between poor and improved designs.

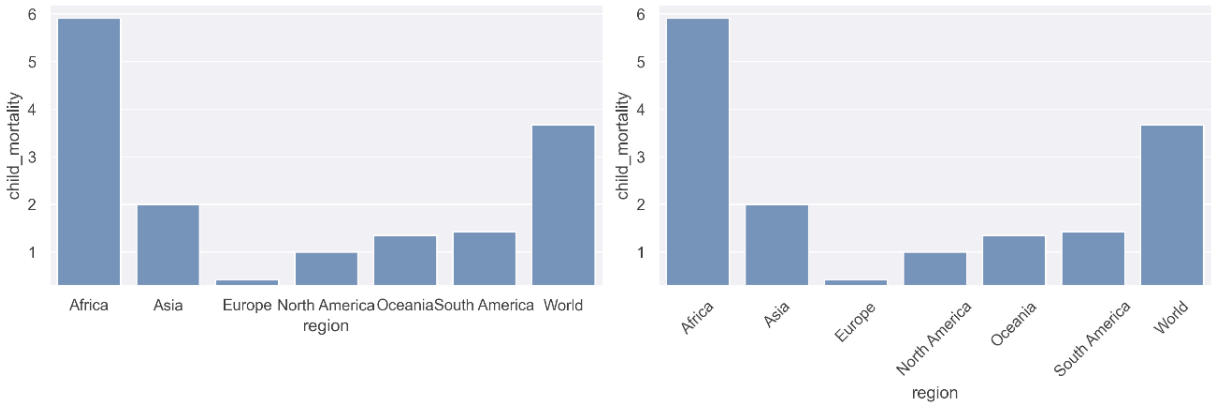


FIG. 1
Initial bar chart with multiple design issues (left) and x-tick labels rotated to avoid overlapping (right)

Subsequently, a series of improvements is applied incrementally. Each step introduces a specific guideline, allowing for a clear comparison between poor and improved designs.

4. DESIGN GUIDELINES FOR BAR CHARTS

The following guidelines are proposed based on the iterative refinement process:

4.1. Optimize label readability

Adjusting orientation and spacing improves readability, especially for longer labels. Figure 1 (right) presents rotated labels for the x-label ticks to avoid overlapping. A better solution would be maintaining the x- and y- labels horizontal, as shown in Figure 2 (left).

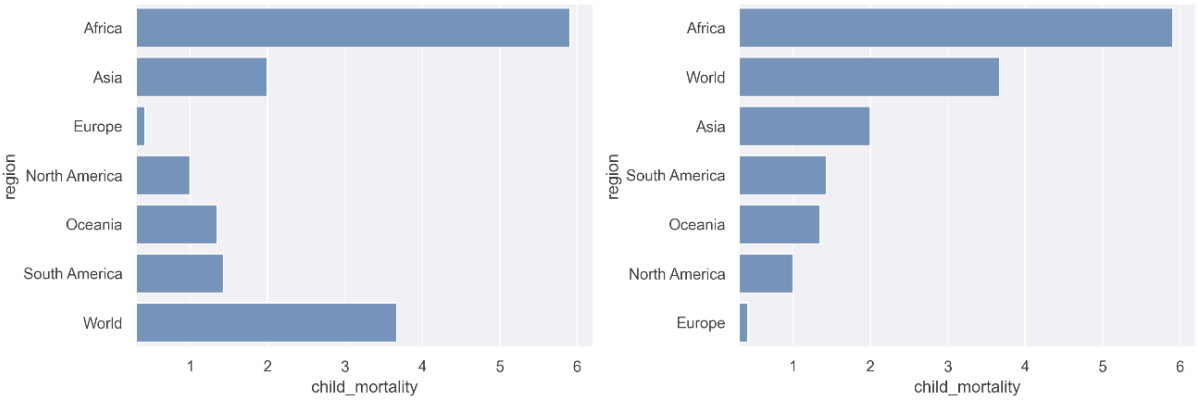


FIG. 2
Bar charts with improved label orientation (left) and categories ordered by magnitude to enhance interpretability (right)

4.2. Sort bars by length

Sorting categories improves readability and allows users to quickly identify patterns [3]. Arranging the bars according to their length, either left to right or top to bottom, is considered good practice. Figure 2 (right) illustrates the same data with bars ordered by value.

4.3. Use color strategically

Color should be used intentionally to highlight relevant information rather than for decoration [4]. Figure 3 (left) distinguishes between continental aggregates and the global average using a neutral palette with selective highlighting. This choice emphasizes the relationship between individual regions and the overall benchmark, facilitating comparison and supporting the interpretation of disparities in child mortality.

4.4. Start axes at zero

One of the most critical principles in bar chart design is ensuring that the axis starts at zero. Figure 3 (right) shows the correction of the misleading truncated axis presented in previous versions of the bar chart.

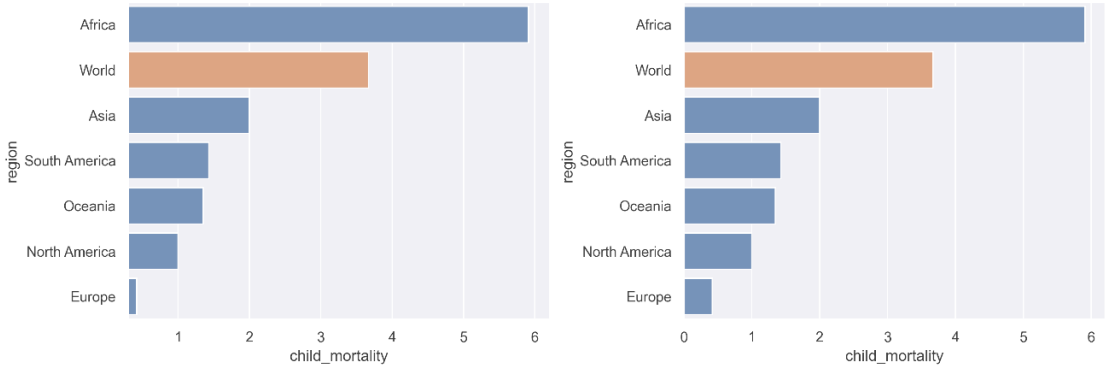


FIG. 3

Bar charts with selective color highlighting (left) and corrected axis starting at zero (right)

4.5. Clearly indicate units

Explicit labeling of units avoids ambiguity and improves interpretability. Figure 4 (left) includes properly labeled axes. Indicating units directly on the axis ensures that values are interpreted correctly without requiring additional context.

4.6. Show values directly on the bars

Displaying numeric values directly on or near the bars reduces the need for visual estimation and facilitates precise comparisons. Figure 4 (right) illustrates the use of data labels to present exact values, improving clarity and minimizing cognitive effort for the reader.

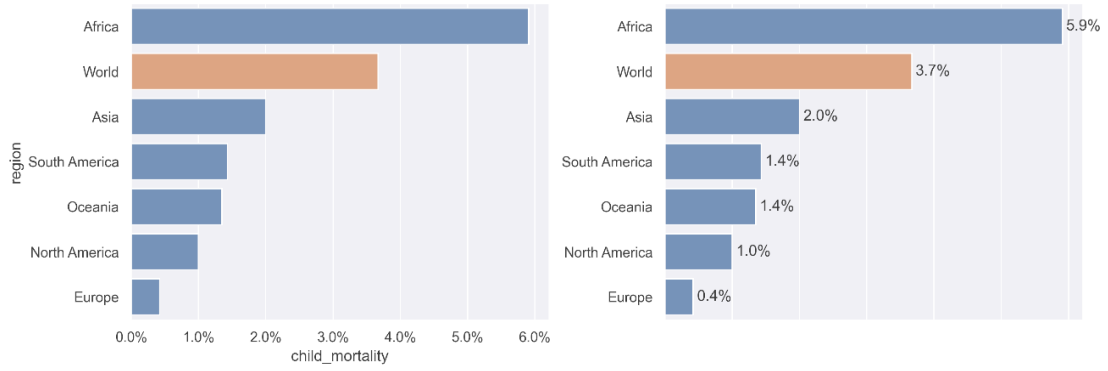


FIG. 4

Bar charts with clearly indicated units (left) and direct value labels to enhance readability (right)

4.7. Include a clear and informative title

A clear and informative title provides essential context and helps guide the interpretation of a visualization. Figure 5 (left) presents a simple descriptive title that identifies the variable and scope of the data. Figure 5 (right), however, illustrates a more effective approach by incorporating additional contextual information and a clearer layout.

In particular, the inclusion of a subtitle indicating the data source reinforces transparency and credibility. The figure was further refined using the mpl-ornaments package, which facilitates the incorporation of figure-level elements such as titles and subtitles. This example shows how small enhancements can significantly improve the communicative effectiveness of a chart.

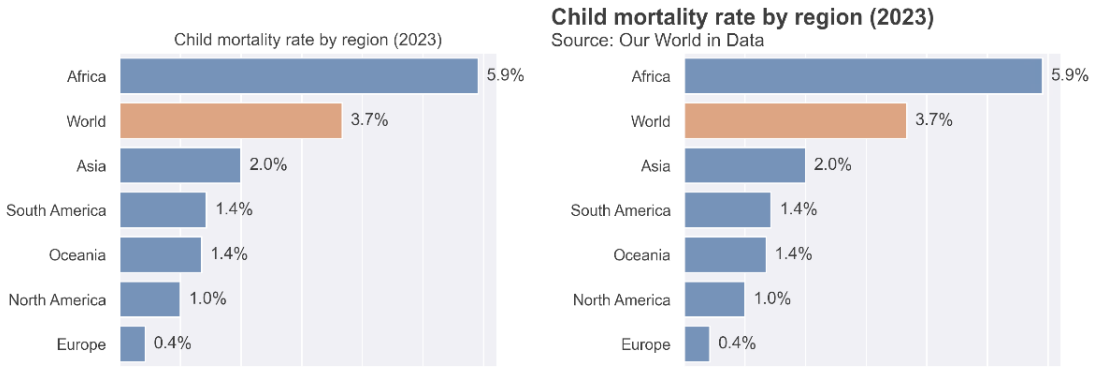


FIG. 5
Bar charts with a simple descriptive title (left) and an enhanced title including contextual information and data source (right)

5. RESULTS AND DISCUSSION

The application of the proposed guidelines demonstrates a clear improvement in the interpretability of the visualizations. The transition from Figure 1 (left) to Figure 5 (right) illustrates how incremental refinements lead to a significantly clearer representation.

The refined visualizations allow for immediate identification of differences and trends. Ordering the bars, aligning axes correctly, and improving labeling significantly enhance clarity. These improvements are especially important in global health contexts, where accurate communication of disparities is crucial. The findings highlight that even simple design adjustments can have a substantial impact on how data is interpreted. In the context of global health, misinterpretation can lead to inappropriate policy decisions or misallocation of resources.

6. CONCLUSIONS

This work emphasizes the importance of proper graphical design in the communication of global health data. By focusing on bar charts, a widely used but often misapplied visual-

ization tool, we demonstrate how adherence to basic design principles can significantly improve clarity and reliability.

The proposed guidelines provide practical recommendations for improving visualization quality. Their adoption can contribute to better understanding, more informed decision-making, and enhanced communication within the One Health framework.

Acknowledgements: This work has been partially supported by Fondazione Perugia under Project MODUS-PRO–Automated and personalised design of prostheses and ortheses (Ref. 2025.0582).

REFERENCES

[1] Bianconi, F.: Data and process visualisation for graphic communication: A hands-on approach with Python. Springer Cham, Switzerland (May 2024).

[2] Our World in Data: Child mortality rate (2025), available online at https://ourworldindata.org/grapher/child-mortality. Visited on 10 March 2026.

[3] Schwabish, J.: Better Data Visualizations: A Guide for Scholars, Researchers, and Wonks. Columbia University Press, New York (2021).

[4] Knaflic, C. N.: Storytelling with data: A data visualization guide for business professionals. John Wiley & Sons, Hoboken (2015).

A multimodal AI-assisted methodology for the repair-oriented reconstruction and additive remanufacturing of plastic parts

Jorge Manuel Mercado-Colmenero*, Ismael Majdoubi-García, Diego Francisco García-Molina, Cristina Martín-Doñate

Department of Engineering Graphics Design and Projects,
Campus Las Lagunillas s/n. A3 Building, Jaén 23071, Spain

* e-mail: jmercado@ujaen.es

Abstract: The repair of broken plastic parts is still difficult for non-expert users, mainly because reconstructing damaged geometries usually requires advanced Computer-Aided Design (CAD) skills. As a result, many potentially repairable products are discarded prematurely, increasing material waste and reducing product lifespans. Within the framework of Sustainable Product and Process Design, this work proposes a multimodal artificial intelligence-assisted workflow to simplify repair-oriented digital reconstruction for Additive Manufacturing (AM). The methodology is organised as a sequential pipeline. First, a visual generative stage infers a plausible representation of the original part before failure, preserving its main geometry and topology. This information is then complemented with multimodal inputs, including perspective and orthographic views, dimensional data, and a natural-language description provided by the user. These inputs are translated into a structured geometric representation in STL format, allowing the damaged component to be digitally reconstructed and subsequently manufactured using AM technologies. The results show that decomposing the repair process into AI-assisted stages improves usability and interpretability compared with conventional CAD workflows. The proposed approach is especially useful when input data are incomplete or damaged, supporting repair-oriented remanufacturing, longer product lifecycles, and more sustainable consumption patterns.

Keywords: *CAD, Additive Manufacturing, Multimodal artificial intelligence, Sustainable product design, Graphic Expression.*

1. INTRODUCTION

The repair and remanufacturing of plastic components are key challenges in the transition toward more sustainable product lifecycles. Although additive manufacturing (AM) technologies such as Fused Deposition Modelling (FDM), Stereolithography (SLA), and Selective Laser Sintering (SLS) are increasingly accessible, reconstructing damaged geometries still requires advanced computer-aided design (CAD) skills. This limits the adoption of repair-oriented workflows by non-expert users and contributes to the premature disposal of products that could otherwise be recovered [1, 2].

Recent advances in artificial intelligence (AI), especially multimodal learning, have created new opportunities for automating CAD generation from heterogeneous inputs, including natural language, images, and technical drawings. Text2CAD, for example, shows the feasibility of converting textual descriptions into 3D CAD models through intermediate isometric and orthographic representations [3]. Similarly, LLM-based approaches using code-based representations such as CadQuery enable interpretable and geometrically verifiable CAD generation from high-level descriptions [4]. Other works, such as CAD-GPT, focus on improving spatial reasoning in multimodal CAD synthesis, addressing limitations related to orientation, feature placement, and geometric relationships [5]. In parallel, GeoCAD introduces local geometry control through user-defined instructions, increasing precision and flexibility in generated CAD models [6].

However, most existing methods are oriented toward complete CAD generation from well-defined inputs, intact geometries, structured datasets, or high-quality descriptions. These assumptions limit their direct applicability to real repair scenarios, where available information is often incomplete, ambiguous, or derived from physically damaged parts. As a result, issues related to geometric consistency, topological correctness, and reconstruction from partial information remain open challenges [7].

Within this context, this work proposes a multimodal AI-assisted workflow for reconstructing broken plastic parts. The approach combines visual information, structured geometric templates, and natural-language descriptions to infer the original geometry and generate an STL representation, focusing specifically on repair-oriented reconstruction under incomplete information [8, 9].

2. APPLIED METHODOLOGY

This section presents a structured workflow for the geometric reconstruction of broken plastic parts, aimed at generating an STL representation from incomplete and heterogeneous input data. The methodology is organized as a sequential pipeline that integrates visual information from damaged components, structured geometric descriptors, and natural-language inputs. The process includes data formalization, geometric interpretation of the original part prior to failure, reconstruction through an STL-oriented modelling strategy, and final generation of an ASCII STL file. The approach is focused exclusively on geometric reconstruction, without considering manufacturing constraints. The AI-assisted workflow is implemented using ChatGPT, based on OpenAI's GPT-4o multimodal model, for visual interpretation, geometric reasoning, and STL-oriented reconstruction. No systematic benchmark with al-

ternative engines is performed. o custom-trained model or dedicated API is developed; the implementation relied on an existing multimodal AI environment and a predefined prompting protocol. The process is semi-automated, AI supported interpretation and STL-oriented reconstruction, while CAD expert supervision is used to verify geometric consistency.

2.1. Problem Definition and Input Data Structuring

The problem addressed in this work consists of reconstructing the geometry of a broken plastic part in order to generate a valid STL representation from incomplete and heterogeneous information. Unlike conventional CAD modelling workflows, the input data is assumed to be partial, non-parametric, and user-generated. To ensure consistency, the input is structured through a standardized template that integrates: images of the damaged component, perspective and, when available, orthographic views, key dimensional information, and a natural-language description of the geometry. This structured input enables a consistent downstream geometric interpretation process. Figure 1 shows the proposed information structure sequence for the present methodology and Table 1 the dimensional information and a natural-language description of this example case study.

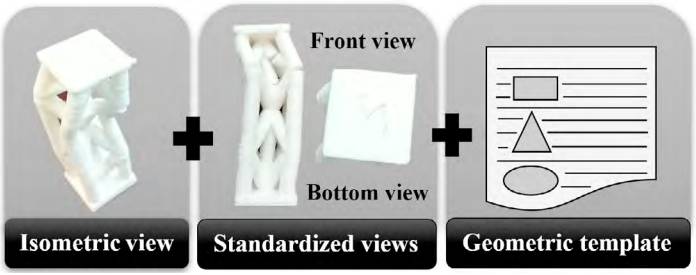


FIG. 1
Input data for the proposed methodology

TABLE 1
Geometric template for the example case study

Case study geometry	
Attached Figures	
Broken part Isometric View	"Example case study isometric view.jpeg"
Broken part Standardized Views	"Example case study front view.jpeg" "Example case study bottom view.jpeg" "Example case study left view.jpeg"
Geometric description	
Part	The part is a uniaxial compression test specimen. It consists of two rectangular plates. Two rhomboidal lattice structures are fitted inside. In addition to the bars that form the rhomboidal geometry, the lattice structure includes a central column and four columns at the ends or outer points.

Case study geometry	
Dimensions	The overall height of the piece is 55.8 mm, and the overall width and depth (of the bounding box containing it) are 17.4 mm × 17.4 mm. The lattice structure or bars have a circular cross-section with a diameter of 4.5 mm.
Main geometric features	The part has two bases, a rectangular upper and lower base. Two rhomboidal lattice structures are fitted between these bases. In addition to the bars that make up the rhomboidal geometry, there is also a central column bar and four external bars coinciding with the outermost vertices of the rhomboidal structure.
Symmetry	The part exhibits symmetry along its main axes.

2.2. Visual-Geometric Interpretation and Pre-Failure Reconstruction

This stage addresses the inference of the original geometry of the part prior to failure from incomplete visual information. The process is based on the interpretation of images of the damaged component combined with structured inputs defined in Section 2.1. The objective is to identify and reconstruct the underlying geometric features that define the part, including basic primitives (cylinders, prisms, fillets), symmetry conditions, and dimensional relationships.

The methodology relies on a feature-based interpretation strategy, where visible geometric cues are extrapolated to reconstruct missing regions. In particular, repetitive patterns, symmetry planes, and continuity conditions are used to infer the most plausible pre-failure configuration. This process involves decomposing the observed geometry into interpretable elements and re-establishing their spatial relationships, ensuring coherence in topology and proportions. As shown in Figure 2, the reconstruction process transforms the fragmented geometry into a complete and consistent representation by identifying correspondences between visible and inferred features. The result of this stage is a conceptual geometric model that captures the essential structure of the original part, without yet considering discretization or mesh generation.

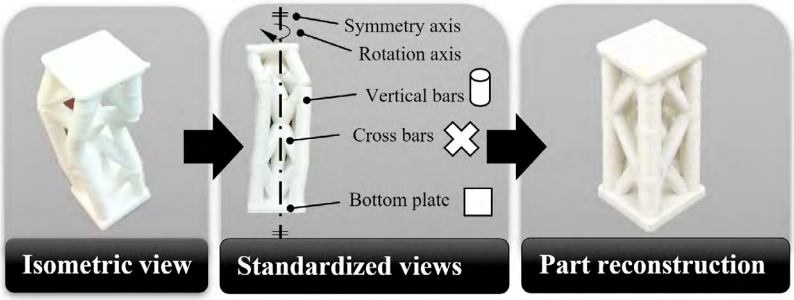


FIG. 2
Pre-failure part reconstruction and geometric features recognition

2.3. STL-Oriented Geometric Modelling Strategy

The proposed geometric modelling strategy is oriented toward the direct generation of STL representations, emphasizing mesh-based discretization rather than parametric reconstruction. The geometry is first interpreted through a feature-based abstraction and subsequently decomposed into elementary primitives, which are triangulated to form a watertight surface. This approach ensures compatibility with additive manufacturing workflows and reduces dependency on feature history. As illustrated in Figure 3, the pipeline integrates primitive recognition, surface tessellation, and structured STL encoding, aligning with recent trends in executable and verifiable CAD representations [10].

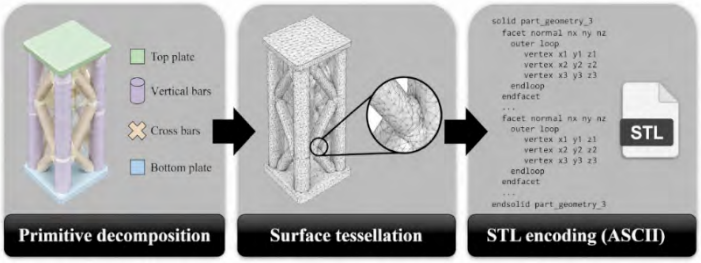


FIG. 3
STL format geometric modelling

Once the geometric model is discretized, the final stage consists of generating an ASCII STL representation through a structured tessellation process. The surface is decomposed into triangular facets, each defined by vertex coordinates and outward normal vectors, ensuring geometric consistency and manufacturability. This explicit mesh encoding enables direct integration with additive manufacturing workflows. The output is organized following the standard STL syntax, preserving topology and orientation. Such structured representations are widely adopted due to their simplicity, interoperability, and direct executability in downstream CAD/CAM pipelines

3. RESULTS

As a result of the methodology developed in this research, a set of five pieces were analysed. Figures 4, Figure 5 and Figure 6 show the results obtained for each of the proposed case studies. To improve the understanding of the reconstruction process, Table 2 summarises the geometric template used for each case study.

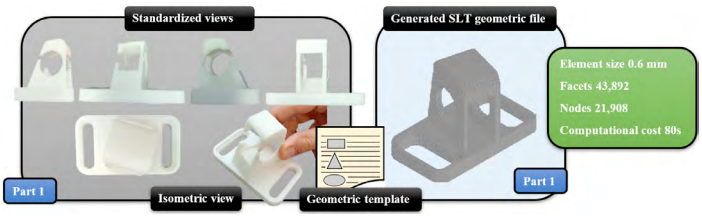


FIG. 4
Results obtained from the proposed methodology. Case study 1

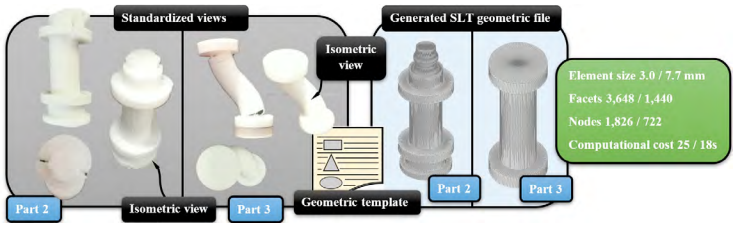


FIG. 5
Results obtained from the proposed methodology. Case study 2 and 3

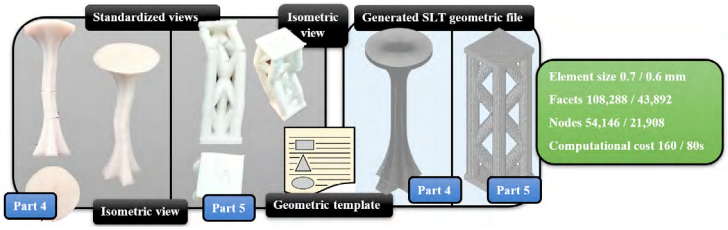


FIG. 6
Results obtained from the proposed methodology. Case study 4 and 5

It is worth noting that each resulting virtual geometry was compared and superimposed with the geometry of the original piece in order to validate the results of the proposed methodology and verify its scope. A reconstruction is considered satisfactory when the reconstructed model preserves the main topology, symmetry conditions, visible primitives, and principal dimensional relationships of the reference part. The order of magnitude for analyzing geometric deviations and dimensional tolerances in the evaluation of the final geometry is related to the order of magnitude of the minimum detail in each case study analyzed. Dimensional consistency is assessed using the main dimensions included in the geometric templates, rather than full 3D metrological inspection.

TABLE 2
Summary of the geometric templates used in the five case studies

Case	Input data	Main geometry	Dimensions	Symmetry / reconstruction criterion
Part 1	Isometric and standard views	Support bracket with rectangular base, elongated holes, vertical support and upper cylindrical seat	Bounding box 90×50×60 mm; Base-type part; elongated holes corrected to 39×9 mm	Mainly longitudinal symmetry; reconstruction focused on base, holes and upper support continuity
Part 2	Isometric and standard views	Stepped cylindrical component with coaxial collars, cylindrical shaft and locally damaged upper region	Axisymmetric stepped geometry defined by main diameters and heights. Total height 110 mm and diameters from 11 to 20.3 mm	Rotational symmetry; reconstruction based on coaxial continuity and circular profiles

Case	Input data	Main geometry	Dimensions	Symmetry / reconstruction criterion
Part 3	Isometric and standard views	Axisymmetric specimen with circular end plates and curved central body	Slender rotational part with circular upper/lower plates. Total height 50 mm and Ø20-Ø40 mm	Rotational symmetry; reconstruction based on smooth profile continuity
Part 4	Isometric and standard views	Multi-section rotational specimen with upper circular plate, concave transition and lower cross-like support	Total height 160 mm; upper disc Ø66 × 3 mm; cross sections 17 × 17 mm and 50 × 50 mm	Double symmetry; reconstruction based on section transitions and profile continuity
Part 5	Isometric and orthographic views	Lattice compression specimen with top/bottom plates, vertical bars and rhomboidal cross-bars	Height 55.8 mm; bounding box 17.4 × 17.4 mm; bar diameter 4.5 mm	Symmetry along main axes; reconstruction based on repeated lattice pattern

4. CONCLUSIONS

This work presents a structured multimodal workflow for the reconstruction of broken plastic parts through direct STL generation from incomplete input data. The proposed methodology demonstrates that it is feasible to infer the original geometry of a damaged component using a combination of images, structured descriptors, and natural-language inputs, without requiring conventional CAD modelling expertise. The staged approach—comprising input formalization, visual-geometric interpretation, STL-oriented modelling, and ASCII STL generation—ensures coherence between geometric reasoning and final mesh representation. The results confirm that the method is particularly effective in recovering global geometry and topological structure, especially in parts governed by symmetry and identifiable primitives. Limitations are mainly associated with local geometric detail and ambiguity in occluded regions. Overall, the approach provides a viable pathway toward accessible, repair-oriented digital reconstruction, contributing to extended product lifecycles within a sustainable design framework.

Acknowledgements: The authors acknowledge the support of the Vice-Rectorate for Lifelong Learning, Educational Technologies and Teaching Innovation of the University of Jaén. This research work has been funded by the Teaching Innovation Plan PID-UJA 2025-2029.

REFERENCES

[1] Armstrong, K., Avery, G., Bhatt, A., Burton, R., Carpenter, A., Cresko, J., *et al.*: Sustainable Manufacturing and the Circular Economy. National Renewable Energy Laboratory, Golden, CO (2023).

[2] Ford, S., Despeisse, M.: Additive manufacturing and sustainability: an exploratory study of the advantages and challenges. Journal of Cleaner Production 137, 1573-1587 (2016).

[3] Yavartanoo, M., Hong, S., Neshatavar, R., Lee, K.M.: Text2CAD: Text to 3D CAD generation via technical drawings. arXiv preprint arXiv:2411.06206 (2024).

[4] Guan, Y., Wang, X., Ming, X., Zhang, J., Xu, D., Yu, Q.: CAD-Coder: Text-to-CAD generation with chain-of-thought and geometric reward. In: Advances in Neural Information Processing Systems 38, pp. 59765-59789 (2026).

[5] Wang, S., Chen, C., Le, X., Xu, Q., Xu, L., Zhang, Y., Yang, J.: CAD-GPT: Synthesising CAD construction sequence with spatial reasoning-enhanced multimodal LLMs. In: Proceedings of the AAAI Conference on Artificial Intelligence 39(8), pp. 7880-7888 (2025).

[6] Zhang, Z., Liu, K., Liu, J., Wang, W., Lin, B., Xie, L., Shen, C., Cai, D.: GeoCAD: Local geometry-controllable CAD generation with large language models. In: Advances in Neural Information Processing Systems 38, pp. 130989-131014 (2026).

[7] Willis, K.D.D., Pu, Y., Luo, J., Chu, H., Du, T., Lambourne, J.G., Solar-Lezama, A., Matusik, W.: Fusion 360 Gallery: A dataset and environment for programmatic CAD construction from human design sequences. ACM Transactions on Graphics 40(4), 1-24 (2021).

[8] Verma, P.K., Vasudev, H., Jeyaprakash, N.: Advanced additive manufacturing techniques for sustainable remanufacturing. In: Singh, J., Vasudev, H., Prakash, C., Singh, M. (eds.) Advanced Manufacturing Technologies in Biomedical Science, pp. 56-74. CRC Press, Boca Raton (2026).

[9] Mad Yusoh, S.S., Abd Wahab, D., Adil Habeeb, H., Azman, A.H.: Intelligent systems for additive manufacturing-based repair in remanufacturing: a systematic review of its potential. PeerJ Computer Science 7, e808 (2021).

[10] Li, R., Li, S., Mu, Y., Ding, M.: SldprtNet: A large-scale multimodal dataset for CAD generation in language-driven 3D design. arXiv preprint arXiv:2603.13098 (2026).

When Senses Decide: Integrating Multisensory Evaluation into the Design Process

María Alonso-García*, Amada Blanco-Spadavecchia, Manuel Damián Marían-Granados

Department of Graphic Expression, Design and Projects, School of Industrial Engineering, University of Málaga, C/ Doctor Ortiz Ramos, s/n, Campus de Teatinos, 29071, Málaga

* e-mail: maria.alonso@uma.es

Abstract: User experience has become a key factor in industrial design, shifting attention from purely functional products toward more engaging and emotionally meaningful interactions. In this context, sensory stimuli may influence how users evaluate products and provide feedback during design assessment processes. This study investigates the effects of multisensory stimuli on product evaluation in a real retail environment. An experimental study was conducted at IKEA Málaga involving 219 participants, resulting in 205 valid responses after data cleaning. Participants evaluated three chair designs under four conditions: a baseline scenario (visual and tactile interaction only) and three additional scenarios incorporating olfactory, gustatory, or auditory stimuli. Data were collected through questionnaires addressing purchase intention, perceived value, memory recall, satisfaction, and time perception. The results suggest that sensory stimuli influence product evaluation and user experience. Olfactory stimuli showed associations with memory performance, gustatory stimuli affected satisfaction and product preferences, and auditory stimuli influenced subjective time perception. The findings also indicate that sensory interactions may generate both positive synergies and potential conflicts depending on the combination of stimuli involved. These results highlight the importance of considering sensory conditions during product evaluation and suggest that multisensory factors should be taken into account when interpreting user feedback in design-related contexts.

Keywords: *Industrial Design, Product evaluation, Multisensory perception, User experience.*

1. INTRODUCTION

Nowadays, the shopping experience has gained significant relevance within industrial design and marketing due to the increasing saturation of stimuli and information to which consumers are exposed. As a result, products are no longer valued solely for their functionality, but also for the emotions and experiences they generate during user interaction [1,2]. In this context, sensory marketing emerges as a discipline focused on analysing how the senses influence consumer perception, evaluation, and purchase decisions [3].

Several studies highlight that multisensory interaction allows the creation of more attractive and memorable experiences. Sight is considered the predominant sense during the initial evaluation of products, especially through elements such as colour, shape, and materials [4,5]. However, recent research demonstrates that other senses also play a fundamental role. Touch improves the physical and emotional perception of the product [6], while hearing, through music and ambient sounds, influences emotions and the subjective perception of time [7,8]. Likewise, smell has a strong capacity to generate memories and positive emotional responses [9,10], and taste is directly related to emotional states and multisensory associations between Flavors, colours, and product perceptions [11].

These investigations have generated growing interest not only in studying the senses individually, but also in understanding the interaction between them. [3,12] introduce concepts such as sensory synergy and sensory conflict, explaining that a balanced combination of stimuli can improve the shopping experience, whereas excessive or contradictory stimulation may generate negative consumer perceptions. Nevertheless, much of the existing research continues to analyse the senses separately, and there is still a lack of studies focused on real multisensory experiences within commercial environments.

In response to this need, the present study aims to analyse how the combination of olfactory, gustatory, and auditory stimuli influences consumer perception and purchase intention within a real retail environment: IKEA. To achieve this, an experimental methodology based on different sensory scenarios was developed to evaluate the effects of sensory synergy and sensory conflict during the shopping experience.

2. METHOD

The methodology employed in this study was developed through a practical case study aimed at analysing the degree of sensory synergy and sensory conflict generated during the shopping experience of industrial products.

A total of 219 participants were initially recruited at IKEA Málaga. Following a data-cleaning process, 14 responses were excluded due to inconsistencies between stated purchase intention and product valuation, resulting in a final sample of 205 valid responses. The sample consisted of 61% women and 39% men. Regarding age distribution, 49.8% of participants were between 18 and 40 years old, 45.4% were between 40 and 65 years old, and 4.8% were over 65 years old. Participants were randomly assigned to the different experimental scenarios.

The study was structured into different experimental scenarios designed to evaluate how specific sensory stimuli affect consumer perception and purchase decisions. As the basis of the

experiment, a "zero scenario" was established in which only sight and touch were involved, as these are considered the predominant senses in the traditional evaluation of products in furniture stores. From this initial scenario, stimuli related to smell, taste, and hearing were incorporated, allowing comparisons between participants' responses under each sensory condition.

For the development of the experiment, three different chair models marketed by IKEA were selected. These models were recent IKEA releases that were relatively unfamiliar to consumers, thus minimizing the influence of previous experiences. In addition, each chair featured a different colour to study possible associations between gustatory stimuli and the visual perception of the product.

Regarding the sensory stimuli, the **olfactory** scenario incorporated rosemary and lavender aromas applied to textile caps worn by the participants. These scents were selected because previous studies associated them with memory, relaxation, and concentration. On the other hand, the gustatory scenario incorporated sweet and salty IKEA food products, specifically vanilla rolls and potato chips, to explore the role of taste in product evaluation. These flavours were selected as representative basic taste modalities, as previous research has shown that different tastes can elicit distinct perceptual and emotional responses and contribute to multisensory interactions during evaluation processes. Their inclusion enabled the examination of how gustatory cues may shape users' perceptions and preferences when assessing industrial products [3]. Finally, the **auditory** scenario included fast and slow melodies played through headphones, allowing the study of how music affects time perception and the overall user experience.

Data collection was carried out through questionnaires completed after each experimental test. These questionnaires evaluated variables such as purchase intention, price perception, comfort experienced during the test, memory of specific visual elements, and subjective perception of elapsed time. In this way, the results obtained made it possible to compare the different scenarios and analyse whether the incorporation of sensory stimuli generated effects of sensory synergy or sensory conflict within the shopping experience.

Finally, the collected data were analysed to compare participants' responses across the different sensory scenarios and to explore the relationship between sensory stimuli and consumer behaviour. The results identified relevant trends regarding the importance of multisensory evaluation in industrial products and highlighted the need for further research through larger samples and more complex experimental designs.

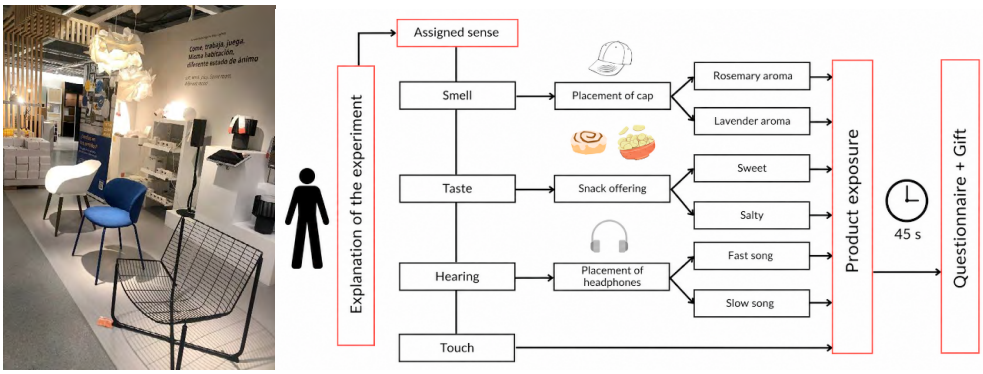


FIGURE 1
Procedure. Explanation of the experiment

3. RESULTS AND DISCUSSION

The results obtained demonstrate that the incorporation of sensory stimuli influences both the shopping experience and the perception of industrial products. Overall, the study reveals a tendency toward the existence of sensory synergies when several senses are simultaneously involved in product evaluation (Table 1).

TABLE 1
Valuated, main aspect observed, and supporting evidence

Evaluation aspect	Main observation	Supporting evidence
Memory recall	The olfactory condition achieved the highest recall performance.	37,5% participants correctly recalled the label location, compared with 26,3% in the tactile condition, 18% in the gustatory condition, and 14,3% in the auditory condition.
Olfactory stimuli	Rosemary showed better recall performance than lavender.	Correct recalls were observed in 41,9% participants exposed to rosemary and 32% exposed to lavender.
Product preferences	Taste stimuli were associated with differences in product preferences.	Variations in chair selection were observed across flavour conditions.
Time perception	Music influenced subjective estimation of elapsed time.	Mean perceived duration was 37.89 s under fast music and 43.04 s under slow music.
Sensory interaction	Differences were observed between sensory scenarios and the baseline condition.	Variations in evaluation outcomes suggest the presence of sensory synergy and conflict effects.

Regarding the main objective, related to sensory synergy and sensory conflict, the study found that scenarios incorporating additional sensory stimuli generated variations in both purchase intention and the perceived economic value of the product when compared to the baseline scenario. Participants tended to report a more positive shopping experience when coherent complementary stimuli were present, reinforcing the importance of designing balanced multisensory experiences. However, some scenarios also showed signs of sensory conflict when the stimuli failed to produce a clearly positive emotional response.

Concerning the olfactory dimension, the results suggest that aromas may enhance consumer memory and attention during the shopping experience. Rosemary aroma showed a more favorable tendency than lavender in tests related to the visual recall of the label attached to one of the chairs, partially supporting the proposed hypotheses regarding memory and concentration. Nevertheless, the statistical differences obtained were not strong enough to fully confirm the hypothesis, highlighting the need for further research with broader experimental conditions.

In the taste-related scenario, gustatory stimuli were found to influence the levels of comfort and satisfaction experienced by participants during the experiment. In addition, certain associations between flavors and color preferences for the chairs were identified, par-

ticularly in the case of salty flavors and the selection of cool colors such as white or blue. Although these trends are consistent with previous studies on multisensory associations, the results did not allow all the proposed hypotheses to be completely validated.

On the other hand, the auditory analysis confirmed that music influences the subjective perception of time during the shopping experience. Fast melodies tended to reduce participants' perception of elapsed time, whereas slow melodies generated the sensation that time passed more slowly. Furthermore, music contributed to modifying the emotional atmosphere of the experiment and indirectly affected the evaluation of the industrial products.

We can conclude that consumer behavior should be understood from a multisensory perspective, since the senses constantly interact during the evaluation of products and commercial spaces. The findings are consistent with previous research arguing that an appropriate combination of sensory stimuli can increase consumer satisfaction and improve product perception. However, the study also highlights that excessive or incoherent stimulation may generate negative effects and lead to sensory conflict. Therefore, the research emphasizes the importance of continuing to investigate how to design balanced sensory experiences in both industrial design and commercial environments.

Finally, the study acknowledges several limitations, mainly related to sample size and the complexity of controlling all the emotional and contextual variables involved in a real shopping experience. Even so, the results obtained demonstrate the relevance of sensory marketing and open new lines of research focused on multisensory evaluation applied to industrial product design and commercial experiences.

4. CONCLUSIONS

The study concludes *that sensory stimuli play an important role in both the shopping experience and the perception of industrial products*, confirming the importance of adopting a multisensory approach in both product design and the creation of commercial environments. The results obtained show that the combination of different senses can generate more satisfying consumer experiences, increase emotional engagement and influence purchase intention.

Regarding the main objective, it was identified that the interaction between different sensory stimuli can produce both positive effects of sensory synergy and situations of sensory conflict when the stimuli are not properly balanced. This demonstrates that consumer perception does not depend solely on the functional characteristics of a product, but also on how the different senses interact throughout the shopping experience.

With respect to the specific objectives, the study demonstrated that olfaction influences processes related to memory and attention, particularly highlighting rosemary aroma as a stimulus associated with greater recall ability. Likewise, gustatory stimuli were found to be related to the levels of satisfaction and comfort experienced by participants, while also partially influencing certain associations between Flavors and colours. In addition, music affected the subjective perception of time and the emotional atmosphere during the shopping experience, confirming the capacity of sound to modify consumer behaviour.

Nevertheless, the research also reveals the complexity involved in studying multisensory behaviour, as many of the proposed hypotheses could not be conclusively validated, mainly

due to methodological limitations such as sample size and the difficulty of controlling all the emotional and contextual variables present in a real commercial environment. For this reason, the author highlights the need to continue developing broader studies that allow a deeper understanding of sensory synergy and sensory conflict.

The findings suggest that sensory conditions should be considered during product evaluation activities, as they may influence user feedback and subsequent design-related decisions. Incorporating multisensory awareness into evaluation processes may contribute to a more robust interpretation of user perceptions during product development.

REFERENCES

[1] Jiménez, M.: Sensory marketing and consumer profile: the psychology of color in product design. Pensando psicologia (2022).

[2] Zhang, X.: The influence of user cognition on consumption decision-making from the perspective of bounded rationality. Displays, 10 (2023).

[3] Krishna, A. An integrative review of sensory marketing: Engaging the senses to affect perception, judgment and behavior. Journal of Consumer Psychology *(*2012).

[4] Artacho, M. Multisensory Analysis of Consumer-Product Interaction During Ceramic Tile Shopping Experiences. *Multisensory reseach,* p. 68 (2020).

[5] Wiedmann, W. It's not all about function: investigating the effects of visual appeal on the evaluation of industrial products using the example of product color. Journal of product and brand management K., p. 13 (2019).

[6] Karangi, S. Haptics and brands: The effect of touch on product evaluation of branded products. Journal of consumer behaviour *(*2021).

[7] Taskin, E. The role of store environment cues on store personality and store image. Market-Trziste, p. 18 (2023).

[8] Polo, E. Comparative Assessment of Physiological Responses to Emotional Elicitation by Auditory and Visual Stimuli. IEEE Journal of translational engineering in health and medicine, *(*2024).

[9] Gil, A. Olfactory marketing and the new tourist experience: Towards the new 'Wellness Hotel'. Cuadernos de turismo, p. 31 (2023).

[10] Liu, Y. Soft, miniaturized, wireless olfactory interface, Nature communications, 2023.

[11] Wada, E. Effect of Taste-Induced Mood on ERP and Emotional Assessment of Images. Perceptual and motor skills, *(*2023).

[12] Zhou, M. The effects of sensory interaction and sensory conflict on consumer online review rating behavior. International journal of management science and engineering management *(*2023).

From Material to Form: Experimental analysis of Kerfing in MDF for flexible furniture design

Javier Martín-Domínguez*, Laura Barrera-Muñoz, Aida López-López, María Alonso-García

Universidad de Málaga, Calle Dr. Ortiz Ramos s/n, 29071 Málaga, Spain

* e-mail: javiermd@uma.es

Abstract: Kerfing has emerged as an effective technique in digital fabrication to introduce flexibility into rigid materials, enabling new possibilities in product and furniture design. However, its mechanical behavior remains insufficiently quantified, particularly regarding the influence of cutting pattern geometry on structural performance. This study investigates how different kerfing patterns affect the balance between flexibility and mechanical resistance in medium-density fiberboard (MDF), with a specific focus on furniture design applications. Three representative configurations (linear, inclined, and rhomboidal) were fabricated using laser cutting and evaluated through bending tests, complemented by finite element simulations. The results reveal a clear trade-off between deformation capacity and structural resistance, directly governed by pattern geometry. These findings support the interpretation of kerfing as a tuneable mechanical system, in which pattern design enables controlled adjustment of material behaviour. This work provides quantitative and design-oriented insights that support the integration of kerfing into performance-driven furniture design and digital manufacturing processes.

Keywords: *Kerfing, MDF, Digital fabrication, Laser cutting, Furniture design, Geometric-design, Parametric-design.*

1. INTRODUCTION

Traditionally, manufacturing has relied on conventional methods such as machining, molding, or manual fabrication, which present limitations in terms of speed and adaptability [1].

However, digital fabrication offers new possibilities that improve production times and allow a higher level of customization, including additive manufacturing or 3D printing [2], subtractive manufacturing [3], and hybrid manufacturing [4]. These evolving manufacturing strategies are changing and expanding the way industrial designers and architects approach design [5].

Subtractive manufacturing [6] includes technologies such as laser cutting. Although other techniques are based on material removal too, laser cutting separates materials through the application of concentrated thermal energy at a specific point on the material. Although advances in this field promote the experimental use of new materials [7], there is also renewed interest in the creative use of traditional materials such as wood [3]. Within this context, the digital era has introduced subtractive technologies that have enabled the development of the technique known as kerfing, which consists of making controlled cuts in rigid materials to allow them to bend [5]. Specifically, wood and wood-based materials, kerfing has gained relevance as a technique for generating organic three-dimensional forms from two-dimensional panels, offering an alternative to other bending processes such as steam bending, laminated bending, ammonia bending, or high-frequency bending.

Its applications are wide-ranging, as shown in Figure 1, and span different scales, from lightweight, flexible, and sustainable architectural structures [8,9] and acoustic panels [10], to everyday objects such as lamps [3], guitars [11], earrings [12], as well as furniture and fine woodworking applications [13, 14, 15, 16].

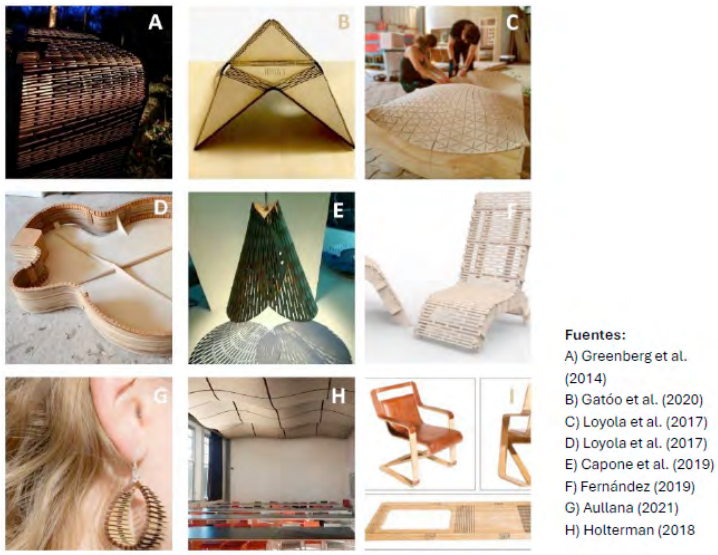


FIG 1
Kerfing applications

However, for these emerging technologies to become truly programmable, predictable, and accessible to designers and architects, a deep understanding of their behavior and governing parameters is essential [5, 17]. Although kerfing is increasingly being used as an experimental design tool, the mechanical behaviour of kerfed materials remains insufficiently characterized. Existing studies often focus on qualitative observations or isolated parameters, lacking systematic comparisons between different cutting patterns and their structural implications.

Recent literature suggests that the mechanical response of kerfed materials depends directly on pattern parameters such as cut density or repetition, orientation, slot length, and spacing between cuts [8, 9, 10, 18]. These factors are known to influence flexibility, strength, and curvature direction. However, the relationship between different pattern geometries and their resulting mechanical behaviour has not yet been systematically established.

In this context, understanding this relationship becomes essential. Therefore, the aim of this study is to analyze how different kerfing configurations affect the mechanical behavior of MDF panels, evaluating the trade-off between flexibility and structural resistance through experimental testing and numerical simulation.

2. METHODOLOGY

To achieve this objective, (1) three kerfing patterns with distinct geometric configurations were designed, and (2) bending specimens were manufactured for each pattern from medium-density fiberboard (MDF) panels using laser cutting technology.

Subsequently, the mechanical characterization was carried out through bending tests, allowing the evaluation of key parameters such as maximum stress and effective elastic modulus. These measurements were obtained through (3) the implementation of a dedicated experimental setup and an appropriate measurement system, specifically designed to ensure the accuracy and repeatability of the results.

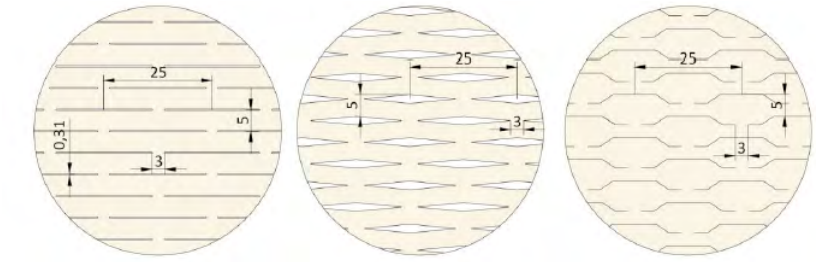
2.1. Selection of Kerfing Patterns

According to Lorenzoni and da Silva (2021) [5], two main families of kerfing patterns can be identified: linear patterns with parallel cuts, which enable unidirectional curvature, and interlaced or spiral patterns, which allow bidirectional deformation. In this study, three patterns belonging to the first family were designed and analysed, all intended to generate unidirectional curvature. In this sense, three representative kerfing patterns were selected for analysis: linear (Figure 2a), rhomboidal (Figure 2b) and inclined (Figure 2c) configurations:

Pattern A (straight linear) was selected due to its simple geometry and its extensive use in previous studies, where it has shown a good balance between flexibility and structural resistance [3, 8, 14, 18,].

Pattern B (rhomboidal) was included to analyze configurations with greater material removal. This type of design typically increases flexibility while reducing structural resistance, making it representative of highly deformable kerfing geometries with significant bending capability [9].

Pattern C (inclined linear or Wave Lattice) was chosen for its high deformation capacity, being able to exceed bending angles of 90° before failure [14]. Although based on previously reported configurations [9, 14, 19], the geometry used in this study was adapted to meet common dimensional constraints.



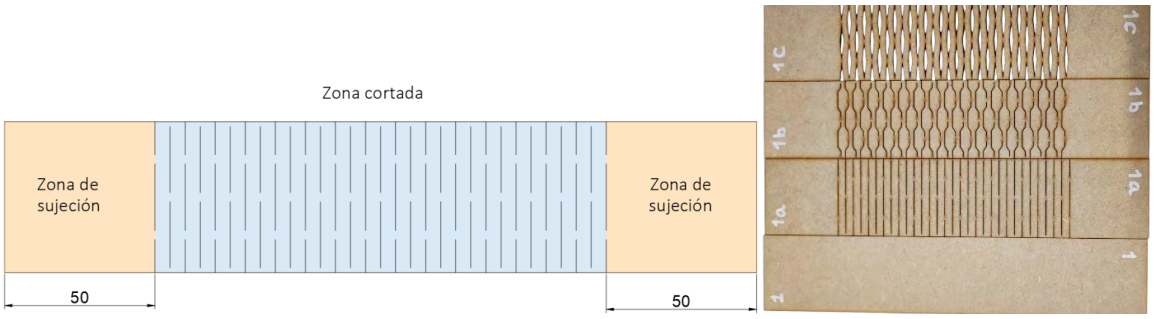
a b c

FIG 2

Cutting pattern. (a) straight linear, (b) rhomboidal, (c) inclined linear

Furthermore, to isolate the effect of pattern geometry as the main variable of the study, the spacing between cuts was kept constant in both the horizontal and vertical directions for all three configurations analyzed (Figure 2). This geometric consistency minimizes the influence of secondary parameters and ensures that the differences observed in mechanical behavior can be attributed exclusively to the pattern geometry.

The selected geometric parameters were based on the recommendations reported by Condoroţeanu *et al.* (2022) [8]. In particular, the spacing between cuts was defined according to the criterion that it should not be smaller than the material thickness, which in this case was 3 mm, in order to avoid excessive stress concentrations and premature failure of the specimens.



a b

FIG. 3

(a) Specimens' geometry. (b) Specimens' results

2.2. Specimens

A total of six specimens were manufactured for the experimental tests, following the UNE-EN 310 standard, with dimensions of 250 × 50 mm. The kerfed region was defined

over a central length of 150 mm in each specimen (Figure 3a). All specimens were obtained from the same medium-density fibreboard (MDF) panel, with a nominal thickness of 3 mm, verified using a micrometer, and overall dimensions of 1020 × 900 mm.

2.3. Experimental Preparation and Testing Procedure

The bending tests were carried out using a fixed-end configuration, introducing a variation from conventional test setups. This approach was selected because it better represents real furniture applications, where structural components are typically connected through rigid joints that restrict rotation, rather than behaving as simply supported beams.

The experimental setup consisted of rigidly clamping the specimens, designed according to the UNE-EN 310 standard, at both ends using mechanical clamps attached to a tilting workbench. The load was applied at the midpoint using a custom-developed system (Figure 4), consisting of an anchoring device manufactured by 3D printing in PLA using an Ultimaker S5. The device included a 50 × 3.80 mm slot for specimen positioning and a 4 mm channel for cable routing, ensuring a symmetrical and uniform load distribution without damaging the material.

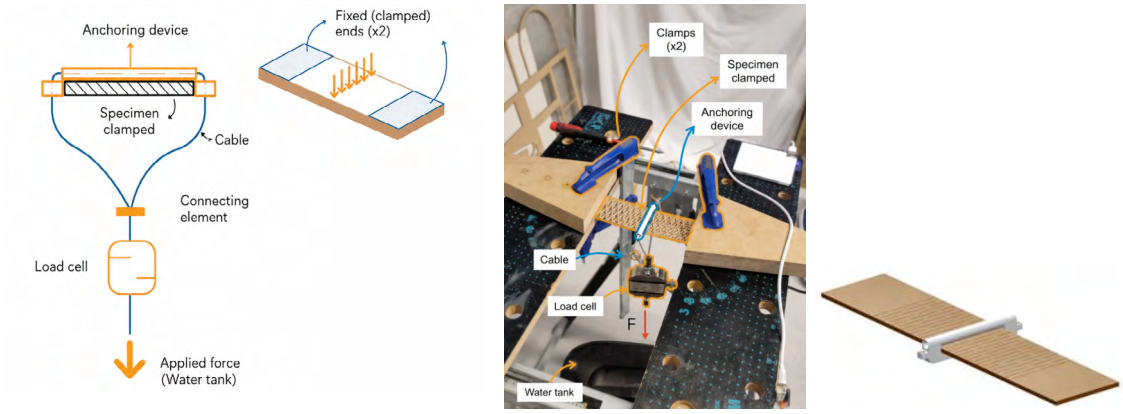


FIG. 4
Experimental setup

The applied force was transmitted through a cable connected to a DYLY-102 load cell, calibrated with an accuracy of 1%, and linked to a data acquisition system that enabled real-time load recording and subsequent data export for analysis. The load was applied progressively using a water-based loading system, allowing controlled load increase while avoiding sudden impact loads. The displacement at the center of the specimen (deflection) was recorded by video using a smartphone mounted on a tripod and later analyzed using Tracker software. Calibration was performed using a physical reference placed within the image, allowing the maximum deflection with a minimum resolution of ±0.1 mm.

Each pattern configuration was tested three times, following previous methodologies [9, 19]. The test speed was adjusted to achieve failure within a time interval of 60 ± 30 s, ensuring progressive deformation. All specimens were tested under dry and stabilized condi-

tions (20 ± 3 °C and 65 ± 5% RH, typical indoor conditions). Statistical analysis of the results was performed according to ASTM D2915-17 (Standard Practice for Sampling and Data-Analysis for Structural Wood and Wood-Based Products).

3. RESULTS AND DISCUSSION

The experimental results revealed clear differences in mechanical behaviour depending on the kerfing pattern geometry. Non-patterned specimens showed the highest load-bearing capacity and stiffness, reaching average values of 23.7 kg and 1541.6 MPa, respectively. In contrast, the kerfed specimens exhibited lower structural resistance but greater deformation, confirming the expected trade-off between stiffness and flexibility. Among the tested geometries, Pattern A showed the lowest load capacity (6.06 kg) and a relatively limited displacement before failure (19.00 mm), together with the highest stress values. This behaviour suggests a more brittle response associated with stress concentration caused by its reduced effective cross-section. Patterns B and C, in contrast, showed a more ductile response. Pattern B reached an average displacement of 24.58 mm with a moderate load capacity 6.34 kg), whereas Pattern C achieved the highest deformation among the kerfed specimens (30.12 mm) while supporting significantly higher loads (9.72 kg), indicating a more efficient stress distribution due to its rhomboidal geometry, which leaves more space between adjacent cuts, preventing them from closing during bending.

The average force–time curves confirmed these differences. These findings support the interpretation of kerfing not merely as a fabrication technique, but as a parametric mechanical system in which pattern geometry directly controls force transmission, deformation mechanisms, and structural performance.

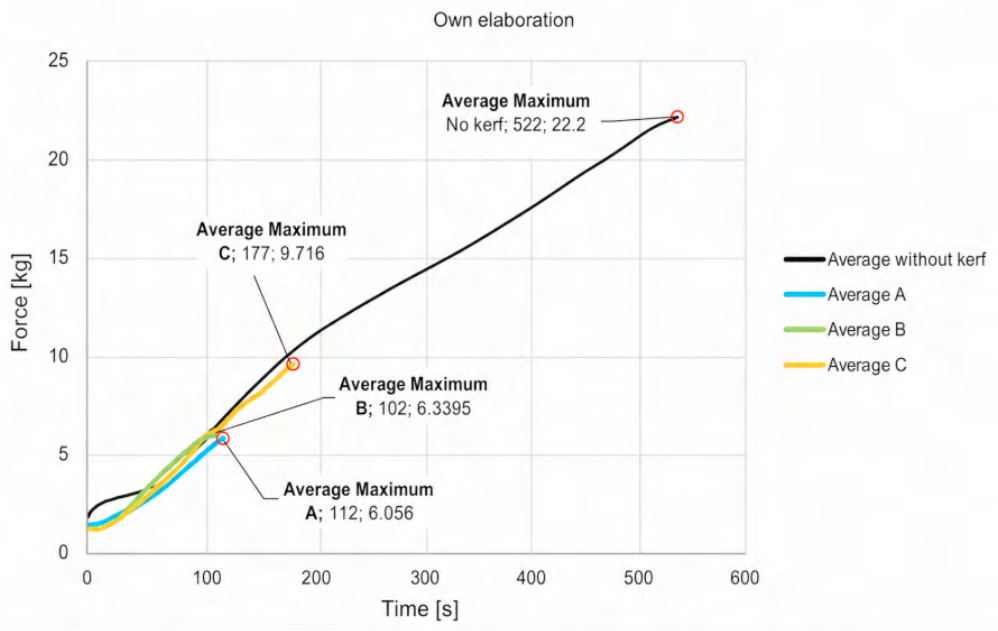


FIG 5
Comparative force-time plot

4. CONCLUSIONS

This study demonstrates that kerfing pattern geometry has a direct and significant influence on the mechanical behaviour of MDF panels under flexural loading. The experimental results identified a clear relationship between pattern design and structural response, confirming the existence of a trade-off between flexibility and mechanical resistance. While non-patterned specimens provided the highest stiffness and load-bearing capacity, kerfed configurations increased deformability and introduced differentiated mechanical behaviors depending on cut geometry.

Among the evaluated designs, Pattern C exhibited the most balanced mechanical performance, combining high deformation capability with superior resistance compared with the other kerfed configurations, making it the most suitable solution for applications requiring both flexibility and structural reliability. The results confirm that kerfing can be understood as a performance-driven design parameter rather than solely a manufacturing strategy, enabling the integration of mechanical behaviour into early design stages. Consequently, this work contributes to bridging engineering analysis and product design, supporting the application of kerfing in digitally fabricated functional and structural components.

REFERENCES

[1] Oyediran, A.A., Ikumapayi, C.M., Olufemi, B.: Determination of the properties of some selected timber species for structural application. *World Journal of Engineering and Technology* 11, 319-334 (2023).

[2] Gibson, I., Rosen, D., Stucker, B., Khorasani, M., Rosen, D., Stucker, B., Khorasani, M.: *Additive manufacturing technologies*. Cham, Switzerland: Springer (2021).

[3] Capone, M., Lanzara, E.: Parametric kerf bending: manufacturing double curvature surfaces for wooden furniture design. In: Digital Wood Design: Innovative Techniques of Representation in Architectural Design, pp. 415-439 (2019).

[4] Sebbe, N.P., Fernandes, F., Sousa, V.F., Silva, F.J.: Hybrid manufacturing processes used in the production of complex parts: a comprehensive review. *Metals* 12(11), 1874 (2022).

[5] Lorenzoni, B.R., da Silva, F.P.: Bending techniques for flat materials using cut patterns: A review. *Global Journal of Engineering and Technology Advances* 7(2), 91-102 (2021).

[6] Babu, B., Nallasivam, J.D., Aravinth, S.: The art of material removal: an overview of subtractive manufacturing. In: *International Conference on Recent Advances in Science, Engineering, Technology and Management*, Miraj (2024).

[7] Addington, M., Schodek, D.: *Smart materials and technologies in architecture*. Routledge (2012).

[8] Greenberg, E., Körner, A.: Subtractive manufacturing for variable-stiffness plywood composite structures. In: *Sustainable Design and Manufacturing* (2014).

[9] Gatóo, A., Koronaki, A., Al Asali, M.W., Bukauskas, A., Gin, Y., Shah, D.U., ... Ramage, M.H.: Flexible and sustainable building components through kerf patterns. In: *Proceedings of IASS Annual Symposia* 2020(5), pp. 1-10. International Association for Shell and Spatial Structures (IASS) (2020).

[10] Holterman, A.: *Pattern kerfing for responsive wooden surfaces*. Master's thesis, Delft University of Technology (2018).

[11] Loyola, M., Caldera, S., Rozas, S.: Kerfing²: Una técnica para el diseño, fabricación y optimización de elementos de doble curvatura a partir de placas rígidas de madera. In: *SIGraDi 2017, XXI Congreso de la Sociedad Ibero-americana de Gráfica Digital*, Concepción, Chile (2017).

[12] Aullana Arastell, L.: *Diseño de pendientes fabricados por corte láser*. Doctoral dissertation, Universitat Politècnica de València (2021).

[13] Fernández Álvarez, A.: *Diseño de un modelo de silla realizada mediante la técnica "kerfing"*. Doctoral dissertation, Universitat Politècnica de València (2019).

[14] Gomes, A.C.: *Kerf bending: wood bending technique applied to furniture*. Doctoral dissertation, Universidade Federal de Santa Catarina (2017).

[15] Silveira, A.L.M.D., Ribeiro, V.G.: Preliminary studies for calculating the bending of flat materials using the kerf-bending technique. *Educação Gráfica* 27(2), 271-288 (2023).

[16] Kang, H.G.: A study on the technique and process of bending wood. *Journal of the Korea Furniture Society* 21(6), 459-468 (2010).

[17] Badoniya, P.: CO2 laser cutting of different materials-A review. *Int. Res. J. Eng. Technol.* 5(6), 1-12 (2018).

[18] Condoroţeanu, C.D., Gurău, L., Coşereanu, C., Georgescu, S.V.: A proposed method to evaluate the effect of changing the kerfing parameters upon the static bending behavior of flexible plywood panels cut by laser. *Applied Sciences* 12(9), 4303 (2022).

[19] Guzelci, O.Z., Alaçam, S., Bacınoğlu, S.Z.: Three-step experimentation on embedding curvature to rigid planar materials through cut patterns. *Gestão & Tecnologia de Projetos* 12(3), 93-107 (2017).

From Mental Abstraction to Sustainable Prototyping: A Five-Phase Design Thinking Workflow for Graphical Engineering Education

Julio César Rivera-Pedroza*, Marcelo Javier Leslabay Martínez
University of Deusto, Faculty of Engineering, Bilbao, Spain
* e-mail: j.rivera@deusto.es

Abstract: The evolution of Graphical Engineering education demands a shift from traditional tool-centered instruction toward competency-based approaches capable of addressing complex and interdisciplinary design challenges. This paper presents a structured educational methodology implemented in a first-year undergraduate course in Industrial Design Engineering, aimed at supporting students in the transition from abstract conceptualization to the development of sustainable product solutions. The proposed methodology is articulated through a five-phase workflow aligned with the Design Thinking framework, and positions Graphical Engineering as a core integrative language that enables the translation of user-centered insights into technically feasible and communicatively coherent design outcomes. Sustainability is embedded as a fundamental design constraint, framed through the One Health paradigm, ensuring that environmental and social considerations inform decision-making throughout the design process. The approach integrates qualitative user research, analog and digital sketching, parametric CAD modeling, and iterative physical prototyping. Results suggest that students were able to apply spatial relationships through sketching, parametric CAD modeling, and prototype development, while progressively translating user needs into coherent and sustainability-oriented product solutions. This work contributes by providing a structured and transferable framework for integrating Design Thinking, Graphical Engineering, and sustainability in early engineering education.

Keywords: *Graphical Engineering, Design Thinking, Engineering Education, Sustainability, CAD Modeling, Iterative Prototyping.*

1. INTRODUCTION

The increasing complexity of contemporary design challenges, characterized by the interdependence of technological, social, and environmental factors, demands a redefinition of educational approaches in engineering disciplines. In this context, Graphical Engineering education must evolve from traditional tool-centered instruction toward competency-based approaches that enable students to address real-world problems in a structured, critical, and reflective manner [1]. This transition is particularly relevant in early stages of higher education, where both technical skills and cognitive models related to the design process are developed.

In parallel, Design Thinking has emerged as a widely adopted framework in engineering and design education due to its capacity to integrate creativity, critical thinking, and user-centered approaches in complex problem-solving contexts [2] [3] [4]. However, its implementation in academic environments requires integration with disciplinary tools and languages that support the transformation of conceptual ideas into technically feasible solutions [5].

Within this context, Graphical Engineering plays a key role as a mediating language between conceptual abstraction and technical development. Through sketching, parametric modeling, and technical representation, it enables the translation of user needs into coherent and viable design solutions [6]. At the same time, sustainability has become a fundamental requirement in engineering education. Recent literature highlights the need to integrate sustainability systemically within higher education curricula, rather than treating it as a secondary or isolated consideration [7]. In this regard, frameworks such as the One Health paradigm emphasize the interconnection between human health, production systems, and environmental conditions [8] [9] [10].

Despite these advances, there is still a lack of structured pedagogical models that coherently integrate Design Thinking, Graphical Engineering, and sustainability within a methodological workflow applicable to early-stage engineering education. Previous studies have identified fragmented implementations of Design Thinking, with limited systematization and weak connections between theoretical frameworks and practical application [11]. Additionally, recent reviews in design education point to misalignments between competencies, methodologies, and learning outcomes, particularly in relation to complex contemporary challenges [12].

In response to this gap, this paper proposes a structured educational methodology based on a five-phase workflow, implemented in a first-year Industrial Design Engineering course. The objective is to provide students with a framework that supports a rigorous, iterative, and sustainability-oriented design process, fostering the development of key competencies in Graphical Engineering and product design.

2. METHODOLOGY: A FIVE-PHASE DESIGN THINKING-BASED EDUCATIONAL FRAMEWORK

This work proposes a structured methodological framework aimed at supporting the transition from abstract ideation to technically grounded product development in early engineering education. The methodology is organized around a structured five-phase workflow aligned with Design Thinking principles and integrates Graphical Engineering as a mediat-

ing language between conceptualization and materialization. Sustainability is incorporated as a transversal design criterion, guiding decision-making throughout the process in line with contemporary approaches to engineering education [13].

The framework is implemented in the first-year course *Design Laboratory I: Product Design* within the Industrial Design Engineering degree. The course introduces students to product design by integrating formal, functional, and technological aspects within a competency-based learning model [1]. Design Thinking structures the learning process, while Graphical Engineering tools, such as sketching, 3D modeling, and technical representation, support the exploration, communication, and validation of design solutions, fostering analytical and decision-making skills in uncertain contexts [4].

The methodological model adapts Design Thinking into a structured sequence of five phases: Empathy, Definition, Ideation, Prototyping, and Testing, organized to facilitate its application in early-stage education while preserving its iterative nature [4] [14]. The process follows a cyclical structure in which feedback mechanisms enable continuous refinement of both the problem definition and the proposed solutions.

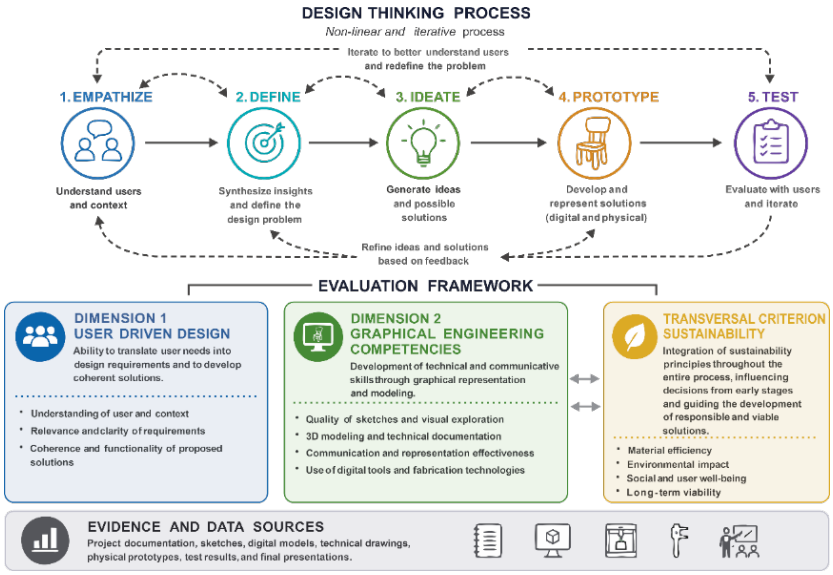
In the initial phases, students analyze user needs and contextual constraints to formulate structured problem statements. During ideation, visual thinking techniques and sketching, both analog and digital, support the generation and evaluation of alternative solutions, with Graphical Engineering acting as a cognitive tool that facilitates the transition from abstract concepts to formal configurations [6] [15]. In later stages, parametric modeling and prototyping enable the assessment of functional, constructive, and ergonomic aspects, promoting iterative refinement based on testing and validation.

The implementation of this framework is supported by an integrated set of digital and physical tools. Sketching facilitates early-stage exploration, while CAD-based modeling enables the development of geometrically and functionally consistent proposals. The integration of CAD/CAM/CAE technologies is essential for the development of advanced engineering competencies [16]. Furthermore, the combination of digital and physical prototyping supports decision-making by reducing uncertainty and enabling early validation of design alternatives, while also contributing to more sustainable design strategies through material optimization and iterative testing [17].

The use of digital fabrication environments such as FabLabs reinforces the applied nature of the learning process, promoting active learning and *learning by doing* approaches that enhance technical, creative, and collaborative competencies [18]. Within this ecosystem, Graphical Engineering acts as a central element connecting design thinking and product realization.

The evaluation followed a rubric-based qualitative approach focused on both the design process and its outcomes. Evidence was collected from project documentation, research synthesis, sketches, CAD models, physical prototypes, technical reports, packaging proposals, and final presentations, in line with qualitative and mixed-method approaches in engineering education assessment [19]. The assessment was embedded in the competency-based structure of the course and organized through successive milestones aligned with CE1, CE2, CE3, and the generic competence CG1.1. These milestones addressed user research and problem definition, the development of guiding ideas through sketches and prototypes, graphical and technical representation, product-system communication, and the assimilation of expert feedback.

Evaluation focused on two main dimensions: the translation of user needs into design requirements and the development of Graphical Engineering competencies related to representation, modeling, prototyping, technical communication, and product-system definition. Rubric-based criteria assessed the traceability between user needs, insights, design requirements, and proposed solutions, as well as the clarity of sketches, consistency of CAD models, adequacy of prototypes, technical feasibility, assembly logic, material decisions, documentation quality, and final communication.



Source: own elaboration.

FIG. 1

Evaluation framework integrating design competencies and sustainability as a transversal criterion

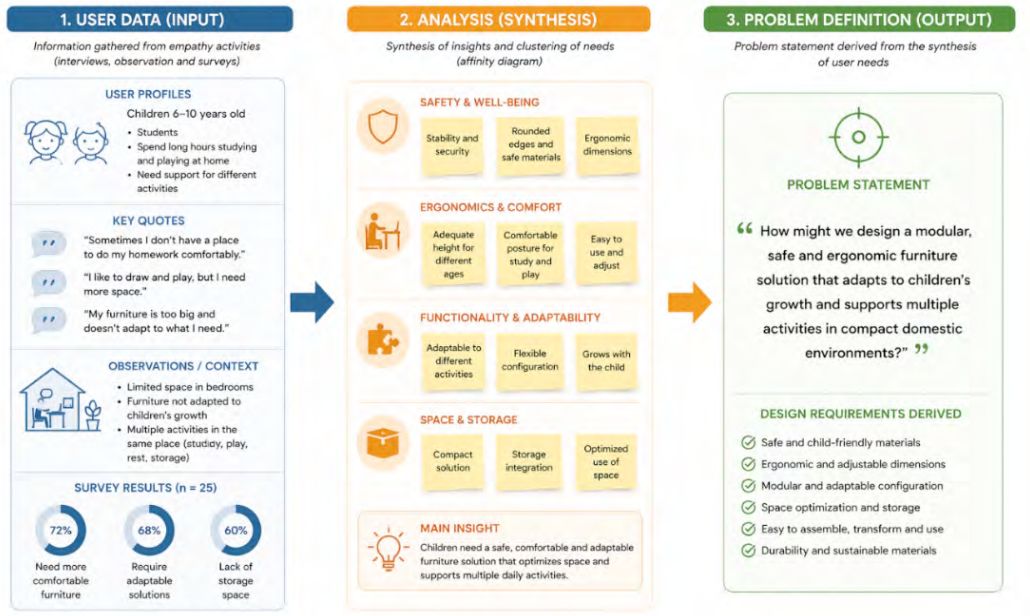
As illustrated in Fig. 1, sustainability acted as a transversal criterion across the assessment framework through material optimization, durability, safety, flat-pack logic, usability, and contextual fit. This closing layer connected project outcomes with the One Health perspective and supported sustainability-related competence development in early engineering education [20] [21].

3. RESULTS AND DISCUSSION

The application of the proposed framework provided qualitative evidence of students' progression from user needs identification to solution validation, helping them manage uncertainty in early design stages.

Regarding the first evaluation dimension, successive project deliverables showed clearer traceability between user research, insights, problem statements, design requirements, and proposed solutions. This was reflected in more precise problem statements and stronger alignment between the Empathy, Definition, and Ideation phases (see Fig. 2).

In terms of Graphical Engineering competencies, project deliverables showed progressive refinement in students' use of sketches, CAD models, technical representations, and physical prototypes to represent, model, validate, and communicate design solutions. These findings are consistent with previous studies highlighting the role of visualization and modeling in engineering education [6] [15].



Source: own elaboration.

FIG. 2

Example of user analysis and problem definition derived from student projects



Source: own elaboration.

FIG. 3

Digital models, scaled prototypes, use-scenario representations, and validation activities across student projects

Sustainability, integrated as a transversal criterion and framed through the One Health perspective, was reflected in decisions related to material optimization, durability, child safety, usability, flat-pack logic, and contextual adaptation. However, the deliverables suggest that integrating sustainability from the earliest design stages remains challenging when environmental criteria must be balanced with ergonomics, technical feasibility, production constraints, and user experience [22].

During the prototyping and validation phases, students refined their proposals through iterative experimentation with digital models, scaled physical prototypes, use-scenario representations, and, in some cases, interaction with target users (see Fig. 3). These deliverables provided qualitative evidence of refinement in ergonomics, stability, assembly logic, interaction possibilities, and contextual fit.

Overall, the results suggest that the methodology provides a useful structure for integrating Design Thinking, Graphical Engineering, and sustainability in early engineering education, while reinforcing design as an iterative and non-linear process [15].

4. CONCLUSIONS

This work has proposed a structured methodological framework based on Design Thinking for its application in early engineering education, explicitly integrating Graphical Engineering as a key element in the transition from ideation to product realization. The methodology also incorporates sustainability as a transversal criterion, framed through the One Health perspective, addressing the need to connect user well-being, product development, material decisions, and environmental responsibility in an integrated manner.

The results suggest that the implementation of a structured workflow helped reduce ambiguity in early design stages and supported a clearer progression from user needs identification to solution validation. In particular, the analysis of project deliverables showed evidence of students' ability to formulate coherent design problems and develop technically grounded solutions through the combined use of representation, modeling, and prototyping tools.

From an academic perspective, the proposal addresses the gap identified in the literature regarding the lack of structured pedagogical models that operationally integrate Design Thinking, Graphical Engineering, and sustainability in first-year courses. In this sense, the work provides a replicable framework that supports the development of analytical, creative, and technical competencies in product design.

However, the study presents limitations due to its exploratory nature and qualitative approach, based on the observation of projects developed in a specific educational context. Therefore, the findings should be interpreted as qualitative evidence of competency demonstration rather than as statistically generalizable evidence of cognitive improvement. Future research should focus on incorporating quantitative metrics, conducting longitudinal analyses of competency development, and validating the model in different educational settings.

REFERENCES

[1] Crawley, E.F., Malmqvist, J., Östlund, S., Brodeur, D.R.: Rethinking Engineering Education: The CDIO Approach. Springer, Boston, MA (2007).

[2] Brown, T.: Design thinking. Harvard Business Review 86(6), 1-10 (2008).

[3] Liedtka, J.: Why design thinking works. Harvard Business Review 96(5), 72-79 (2018).

[4] Razzouk, R., Shute, V.: What is design thinking and why is it important? Review of Educational Research, 330-348 (2012).

[5] Dym, C.L., Agogino, A.M., Eris, O., Frey, D.D., Leifer, L.J.: Engineering design thinking, teaching, and learning. Journal of Engineering Education 94(1), 103-120 (2005).

[6] Sorby, S.A.: Educational research in developing 3-D spatial skills for engineering students. International Journal of Science Education 31(3), 459-480 (2009).

[7] Singh, A.B., Meena, H.K., Khandelwal, C., Dangayach, G.S.: Sustainability assessment of higher education institutions: A systematic literature review. Engineering Proceedings 37(1), 23 (2023).

[8] Vezzoli, C., Manzini, E.: Design for Environmental Sustainability. Springer-Verlag, London (2008).

[9] Bocken, N.M., De Pauw, I., Bakker, C., Van der Grinten, B.: Product design and business model strategies for a circular economy. Journal of Industrial and Production Engineering 33(5), 308-320 (2016).

[10] Ceschin, F., Gaziulusoy, I.: Evolution of design for sustainability: From product design to design for system innovations and transitions. Design Studies 47, 118-163 (2016).

[11] Deng, Y., Lucas, C., Liu, W.: A systematic review of design thinking implementations in higher engineering education. European Journal of Engineering Education, 1-41 (2026).

[12] Brosens, L., Raes, A., Octavia, J.R., Emmanouil, M.: How future proof is design education? A systematic review. International Journal of Technology and Design Education 33(2), 663-683 (2023).

[13] Mulder, K.F.: Strategic competences for concrete action towards sustainability: An oxymoron? Engineering education for a sustainable future. Renewable and Sustainable Energy Reviews 68, 1106-1111 (2017).

[14] Micheli, P., Wilner, S.J., Bhatti, S.H., Mura, M., Beverland, M.B.: Doing design thinking: Conceptual review, synthesis, and research agenda. Journal of Product Innovation Management 36(2), 124-148 (2019).

[15] Contero, M., Naya, F., Company, P., Saorín, J.L., Conesa, J.: Improving visualization skills in engineering education. IEEE Computer Graphics and Applications 25(5), 24-31 (2005).

[16] Sola-Guirado, R.R., Guerrero-Vacas, G., Rodríguez-Alabanda, Ó.: Teaching CAD/CAM/CAE tools with project-based learning in virtual distance education. Education and Information Technologies 27(4), 5051-5073 (2022).

[17] Soomro, S.A., Casakin, H., Georgiev, G.V.: Sustainable design and prototyping using digital fabrication tools for education. Sustainability 13(3), 1196 (2021).

[18] Soomro, S.A., Nanjappan, V., Casakin, H., Georgiev, G.V.: Fostering technical skills and creativity in the digital fabrication spaces: An open-ended prototyping approach. International Journal of Technology and Design Education 35(3), 1081-1102 (2025).

[19] Borrego, M., Douglas, E.P., Amelink, C.T.: Quantitative, qualitative, and mixed research methods in engineering education. Journal of Engineering Education 98(1), 53-66 (2009).

[20] Sabri, O.K.: Rethinking sustainability in engineering education: A call for systemic change. Frontiers in Education 10, 1587430 (2025).

[21] Li, H.H.Z., Yang, T., Zhang, W., Chen, M., Li, Z., Ren, K.: Individual sustainability competence development in engineering education: Community interaction open-source learning. PLOS ONE 18(11), e0294421 (2023).

[22] Date, G., Chandrasekharan, S.: Adapting engineering design thinking for sustainability. International Journal of Technology and Design Education 35(3), 1245-1283 (2025).

Comparison of different Experimental Methods for Measuring the εf Parameter in Small Punch Tests

Ander Escolar Fernández[a, b, *], Ibon Miguel González de Belandia[a], Garikoitz Artola Beobide[a]

[a] AZTERLAN, BRTA, Aliendalde Auzunea 6, E-48200 Durango, Spain

[b] Bilbao School of Engineering, University of the Basque Country UPV/EHU, Torres Quevedo Ingeniaria Plaza 1, 48013 Bilbao, Spain

* e-mail: aescolar@azterlan.es

Abstract: The Small Punch Test (SPT) is a miniaturised technique widely used for the mechanical characterisation of metallic materials when only limited sample volume is available. One of its key parameters is the fracture strain (ε_f), defined as the natural logarithm of the ratio between the initial specimen thickness (h_0) and the minimum thickness after fracture (h_f). Accurate determination of ε_f is essential for ductility assessment and for establishing correlations with conventional mechanical properties. The standard metallographic procedure used to determine εf presents important limitations due to its strong dependence on operator experience, which may reduce measurement repeatability and reliability. This pilot study evaluates two alternative approaches: X-ray computed tomography (using micro- and nano-detectors) and 3D optical scanning. Both techniques enable non-destructive measurements on multiple cross-sectional planes, providing reversible and less operator-dependent procedures. Nano-detector computed tomography delivered the highest accuracy owing to its superior spatial resolution, although at the expense of higher cost and lower availability. Micro-detector computed tomography achieved the second-best performance while offering a more cost-effective solution. In contrast, 3D optical scanning showed lower accuracy because of the complex fracture geometry but proved to be a rapid and economical method suitable for preliminary specimen screening prior to tomography analysis.

Keywords: *Small Punch Test (SPT), Tomography, 3D scanning, Metallography, Measurement.*

1. INTRODUCTION

The mechanical characterisation of metallic materials is essential in numerous engineering applications. Conventional tests, such as tensile testing, provide standardised properties, including strength and ductility. However, these tests require relatively large specimens, which limits their applicability in situations where the available material is scarce, as is the case for in-service components, heritage materials or irradiated specimens. In these situations, miniaturised techniques, such as small punch testing (SPT), provide an effective alternative.

The SPT is a semi-destructive technique in which a thin disc-shaped specimen is deformed using a hemispherical punch until it fractures, generating a load-displacement curve that represents the material's behaviour. Since its origin in the field of nuclear materials, its use has progressively expanded to the evaluation of the mechanical properties of materials under limited conditions [1,2]. Various authors have demonstrated that correlations can be established between SPT results and conventional mechanical properties, allowing its application as an alternative characterisation method [2,3].

One of the most significant parameters obtained in the SPT test is the fracture strain (ε_f), defined as defined as the natural logarithm of the ratio between the initial thickness (h_0) and the minimum thickness after fracture (h_f):

$$\varepsilon_f = \ln\left(\frac{h_0}{h_f}\right) \tag{1}$$

This parameter is directly related to the ductility of the material and has been shown to correlate with fracture-related properties obtained in conventional tests [3].

However, the standard metallographic method used to measure ε_f presents significant limitations. It involves sectioning the specimen and measuring h_o and h_f on a cross-section using optical microscopy. This approach is destructive and restricted to a single measurement plane. Furthermore, it is highly operator-dependent, as the selection of the cutting plane directly influences the minimum measured thickness, leading to variability and reduced repeatability. This limitation is further exacerbated by the complex deformation and fracture mechanisms involved in the SPT, characterised by localised thinning and multiaxial stress states [4].

To overcome these limitations, this pilot study evaluates two alternative methods for measuring ε_f: X-ray computed tomography (CT) (using micro- and nano-detectors) and 3D optical scanning.

2. MATERIAL AND METHODS

For this study, four 42CrMo4 (1.7225) grade steel specimens for SPT (Tables 1) were used, due to the widespread use of this material in industrial settings. The specimens were in the quenched and tempered (Q+T) condition, as this is the standard state in which this material is typically used.

TABLE 1
Chemical composition of the specimens (wt%)

	C	Si	Mn	Cr	Mo	S	P
EN 10083-3	0.38-0.45	≤0.40	0.60-0.90	0.90-1.20	0.15-0.30	≤0.035	≤0.035
Samples	0.42	0.19	0.80	0.99	0.17	0.035	0.100

All specimens were subjected to SPT on a universal testing machine (AllroundLine; ZwickRoell) (Figure 1a), with a maximum load capacity of 100 kN and crosshead speeds ranging from 0.00005 mm/min to 1000 mm/min. A 5 kN load cell was employed to improve load measurement sensitivity. The testing configuration included a custom-fabricated SPT fixture (Figure 1b), whose geometric features comply with the EN 10371:2021 standard [6, 7].

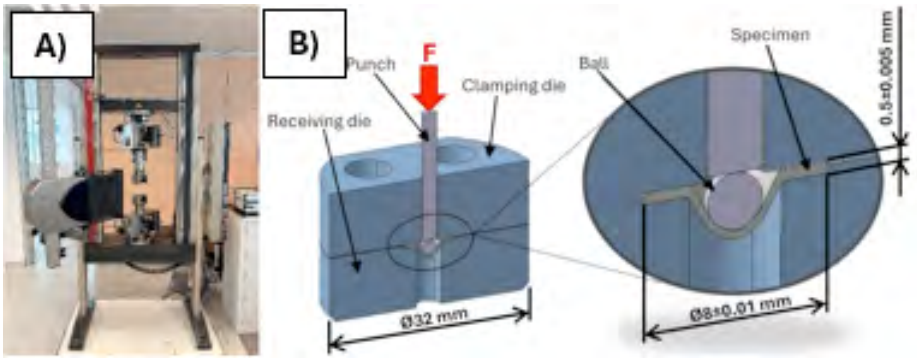


FIG 1
Universal testing machine. a) Universal testing machine. -b) Schematic representation of SPT tooling

Two of the tested specimens were scanned using 3D X-ray CT systems (Table 2): one using a Micro-CT system (Zeiss Metrotom 1500 G3; Carl Zeiss GOM Metrology GmbH) and the other a Nano-CT system (EasyTom XL; RX Solutions). The acquired CT images (Figure 3a) were then loaded into an analysis software program (VGStudio MAX; Volume Graphics) to measure the ε_f parameter. For that, the surface of the material was first defined using the "Advanced Surface Determination" tool, which performs an interpolation between the greyscale levels obtained from the CT image in order to distinguish the material from the surrounding air (Figure 2b). This interpolation is based on the generated histogram (Figure 2c), which exhibits two peaks: the left peak corresponds to air, whereas the right peak corresponds to the material. Subsequently, an "Wall Thickness Analysis" was performed to measure h_o and h_f (Figure 3d) and thereby determine the ε_f parameter.

The measured values are affected not only by the spatial resolution of the CT system but also by the image reconstruction and segmentation procedures. In this work, identical reconstruction parameters and the same "Advanced Surface Determination" workflow were applied to all datasets in order to minimise methodological variability. Since this study is in-

tended as a pilot comparison between techniques, no quantitative uncertainty analysis associated with reconstruction parameters was performed. This aspect will be addressed in future work through repeatability studies and sensitivity analyses.

TABLE 2
Configuration of CT systems

	Micro-CT	Nano-CT
X ray source	AG XT9225-D-500W; Viscom	L12161-07; Hamamatsu
Detector	PaxScan 4343DX-I; Varex	PaxScan 2520DX; Varex
Voltage	200 kV	180 kV
Current	1500 µA	100 µA
Filter	Cu 0,75 mm	Cu 0,75 mm
Integration time	500 ms	1,81 ms

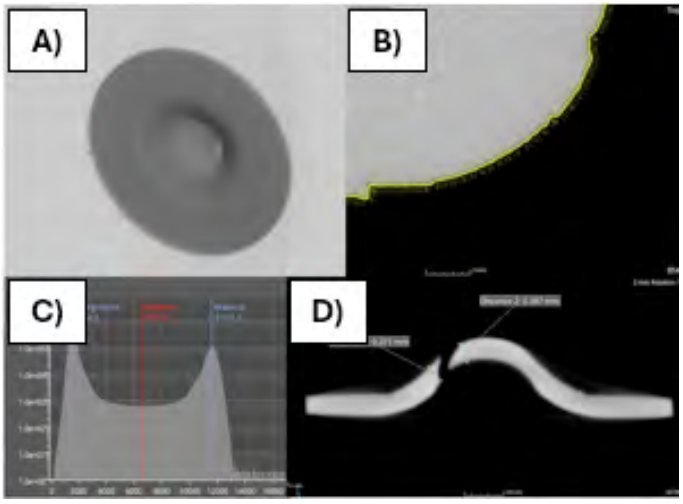


FIG 2
Measurement of h0 and hf using a CT system. a) CT scanning of the SPT sample. b) "Advanced Surface Determination" tool. c) Generated greyscale histogram. d) Cross-section for measuring h_0 and h_f.

Another tested specimen was scanned using a 3D optical scanner based on structured blue light technology (Figure 3a), with a resolution of up to 0.04 mm. To prevent reflections, the specimen was first coated with a scanning powder (AESUB orange; AESUB) (Figure 3b). The obtained 3D mesh (Figure 3c) was then loaded into the analysis software program and a "Wall Thickness Analysis" was performed to measure h_f and h_0 (Figure 4d) and thereby determine the ε_f parameter.

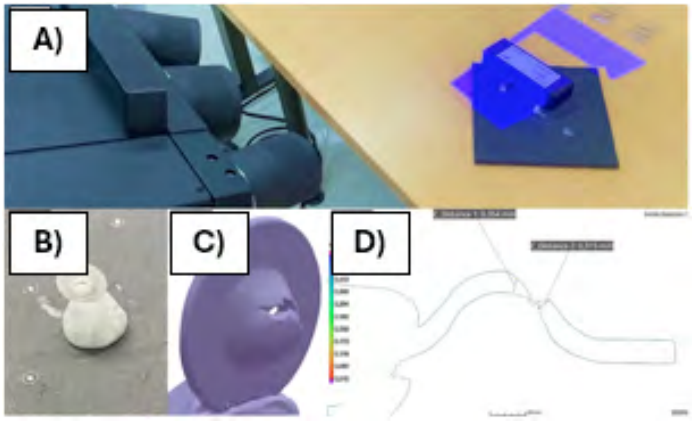


FIG 3

Measurement of h0 and hf using a 3D optical scanner. a) Scanning of the SPT sample. b) SPT specimen coated with scanning spay. c) Obtained 3D mesh. d) Cross-section for measuring h_0 and h_f

Finally, the last tested specimen was analyzed using the standard metallographic method to determine ε_f parameter. For that, a cut perpendicular to the fracture surface (Figure 4a), slightly offset from its centre, was performed using a precision cutting machine (Minitom; Struers) (Figure 4b). Once the cut (Figure 4c) had been made, the section of the specimen containing the measurement plane was placed in a jig consisting of two dies joined by two screws to secure the specimen. The jig was then placed under a microscope, equipped with a high-stability optical platform and LED illumination (Leica DMi8 C; Leica Microsystems), and the h_f and h_0 measurements (Figure 4d) were directly obtained from the cross-section.

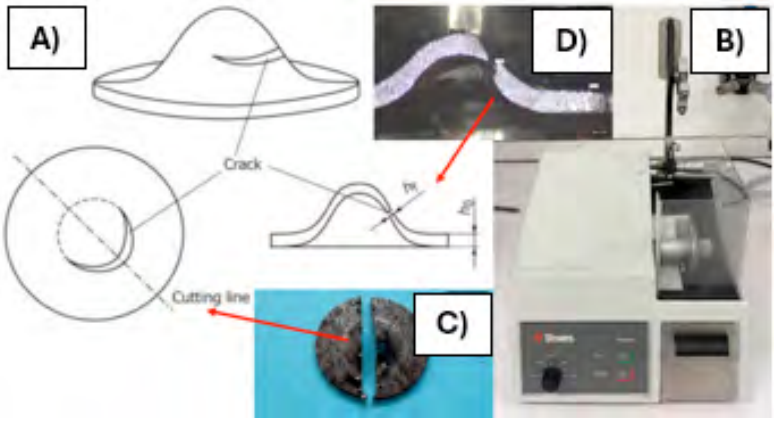


FIG 4

Measurement of h0 and hf using the metallographic method. a) Schematic diagram of the cut. b) Precision cutting machine. c) Cut. d) Cross-section for measuring h_0 and h_f

3. RESULTS

The results obtained for the measurements of h0 and hf, and the ε_f values (calculated according to equation (1)) for each of the four samples are shown in Table 3. There is a difference between the results obtained, as the measurements were taken on different samples; however, they are all in the same order of magnitude. The numerical value is not particularly relevant, as the study aims to assess which of the methods used offers the best methodological results when taking measurements.

TABLE 3
Measured values for h_0 and h_f, and calculated ε_f.

SAMPLE	h_0	h_f	ε_f
Micro-CT	0.484	0.360	0.295
Nano-CT	0.455	0.406	0.113
3D opt. scan	0.483	0.403	0.181
Metallography	0.522	0.451	0.146

The four sections on which the h_0 and h_f measurements were taken are shown in Figure 5. Figure 5a shows the section obtained using micro-CT; it can be seen that the image is not entirely clear, which makes accurate measurement difficult. It is worth noting that the intensity used (see Table 3) is excessively high, which generates a greater scattering effect (dispersion of X-rays) and causes a reduction in spatial resolution due to the generated artefacts; if the working intensity (μA) were reduced, a much sharper image would be achieved. The cross-section obtained by nano-CT is shown in Figure 5b. It can be seen that the nano-CT image is much sharper because the operating current used is much lower (see Table 3); furthermore, when the nano-detector is used, the focal spot size is smaller, resulting in a higher-quality image. The resultant section of the 3D optical scan is shown in the Figure 5 c. Unlike the CT, in this case the fracture is not complete; this is because, due to the morphology of the fracture itself, the light does not reach the innermost part of the fracture, thus generating a 3D mesh geometry that does not accurately reflect reality. The metallographic section is shown in the Figure 5d. The resolution of the image obtained is excellent, as is typical of an optical microscope.

For its part, the tomography technique is the most comprehensive of all, as it allows any section of the fracture to be analysed; the scan produces a 3D volume of the specimen, and as it is a non-destructive technique, the sample remains intact after the analysis. Furthermore, an STL mesh can also be obtained from the tomography file, which can then be loaded into finite element software to compare the results obtained. However, tomography is the most expensive technique and the least available in industrial environments, with nano-CT being significantly more costly than micro-CT. The optical scanner has produced the poorest results due to its difficulty in reliably reproducing the fracture; however, it has the advantage of being a non-destructive technique and is the quickest and cheapest of all, meaning it may be used for screening when there is a large number of samples, helping to select those on which the metallographic or tomographic method should be performed. The

advantage of the metallographic method is that it is really cost-effective process, and it is the method covered by the ASTM E3205 and EN 10371 standards. However, it is a highly operator-dependent method, which introduces significant variability and low repeatability.

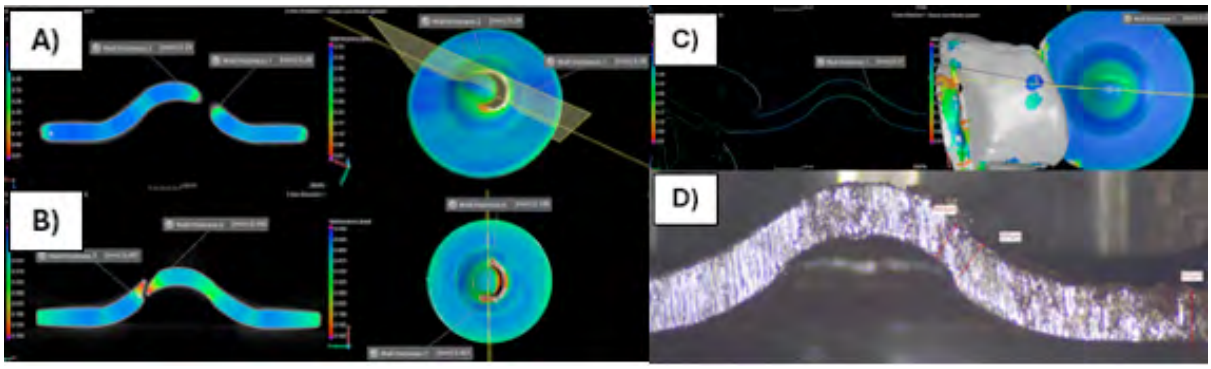


FIG 5
Cross-section plane where the hf and h0 measurements were taken. a) Micro-CT. b) Nano-CT. c) 3D optical scanning. d) Metallographic method

4. CONCLUSIONS

The results obtained in this pilot study show that both X-ray computed tomography and 3D optical scanning constitute viable non-destructive alternatives to the conventional metallographic method for measuring the ε_f parameter in Small Punch Tests. Among the evaluated techniques, nano-CT provided the highest measurement precision due to its superior image quality and spatial resolution, whereas micro-CT offered a more accessible solution with acceptable results. In contrast, 3D optical scanning presented limitations in accurately reproducing the fracture geometry, although its speed and low cost make it suitable as a preliminary screening method. The metallographic method remains a cost-effective and standardised procedure; however, its strong operator dependence reduces repeatability and measurement reliability.

Future work will include a comprehensive experimental campaign in which all four measurement techniques (micro-CT, nano-CT, 3D optical scanning and metallography) are applied to the same SPT specimens using a statistically significant sample size. This will enable a rigorous comparison of the methods in terms of accuracy, repeatability, measurement dispersion and uncertainty, while also assessing the influence of image reconstruction, segmentation and surface determination procedures on the calculated εf values. The methodology will be further calibrated using reference specimens with known geometries and dimensions, providing a basis for uncertainty estimation.

In addition, the study will be extended to brittle materials, whose fracture morphology differs significantly from that of ductile steels and may affect the performance of the evaluated measurement techniques. A finite element analysis (FEA) will also be developed to simulate the deformation process and validate the experimentally obtained εf values. The outcomes of this broader study could provide the basis for a standardised measurement procedure that may be considered for inclusion in future revisions of ASTM E3205 and EN 10371.

Acknowledgements: The authors would like to thank Xabier Amezua of the DEHI research group for his willingness to perform the scan using the 3D scanner, and the General Research Services of the UPV/EHU (sgiker) for conducting the tomography using the nanodetector.

REFERENCES

[1] Mao, X., Kameda, J.: Small-punch technique for measurement of material degradation of irradiated ferritic alloys. *Journal of Materials Science* 26, 2436-2440 (1991).

[2] Kameda, J., Mao, X., Bevolo, A.J.: Evaluation of toughness degradation by small punch tests for neutron-irradiated steels. *Journal of Nuclear Materials* 179-181, 441-444 (1991).

[3] Mao, X., Takahashi, H.: Development of small punch test for fracture toughness evaluation. *Materials Science and Engineering A* 150, 231-236 (1992).

[4] Guan, K., Szpunar, J.A., Wen, C., Wang, X.: Investigation on the deformation and microstructure evolution of P91 steel in small punch creep test. *Journal of Strain Analysis for Engineering Design* 53(4), 248-254 (2018).

[5] ASTM: Standard Test Method for Small Punch Testing of Metallic Materials (ASTM E3205-20). ASTM International, West Conshohocken (2020).

[6] CEN: Metallic materials – Small punch test method (EN 10371:2021). European Committee for Standardization, Brussels (2021).

[7] Miguel, I., Berriozabalgoitia, I., Artola, G., Macareno, L.M., Angulo, C.: Small Punch Test on Jominy Bars for High-Throughput Characterization of Quenched and Tempered Steel. *Metals* 13, 1797 (2023).

Innovation in contract furniture: A University-Industry collaboration with Alutec on folding chair

Aída López-López*, Miriam Fernández-Vida, María Alonso-García, Javier Martín-Domínguez

Department of Graphic Expression, Design and Projects, School of Industrial Engineering, University of Málaga, C/ Arquitecto Francisco Peñalosa, 6. Campus de Teatinos. 29071 Málaga

* e-mail: aidall@uma.es

Abstract: This paper delineates the design and development of a folding chair tailored for the contract sector, conceived within a university–industry collaboration with the company Alutec. The objective was to engineer a functional, lightweight, and adaptable product capable of meeting the demands of high-turnover environments—such as hospitality, events, and collective spaces—while maintaining a distinct design identity. The methodology integrates market analysis, user research, and a comprehensive review of the company's product portfolio, combined with an iterative design process encompassing sketching, 3D modeling, and physical prototyping. The development was guided by essential requirements of contract furniture, including durability, ergonomics, ease of maintenance, and storage efficiency, where several conceptual proposals were generated and progressively refined through comparative evaluation. A central aspect of the project involved optimizing the folding mechanism and its constituent components to ensure structural stability and reliable performance. Simultaneously, manufacturing constraints were factored in to ensure compatibility with industrial processes. The final outcome is a folding, stackable chair with optimized geometry that enhances usability and transport, featuring an integrated handle in the backrest. Consequently, the product combines lightness, resistance, and versatility, while reflecting the company's core design values. This work highlights the potential of integrating design methodologies and industrial constraints to yield viable and competitive product solutions.

Keywords: *Folding chair, Product design, Contract furniture, Industrial design, Prototyping, Manufacturing.*

1. INTRODUCTION

Contract furniture design constitutes a specialized field within product design, characterized by the necessity to withstand intensive use, ensure long-term durability and adapt to diverse environments. In sectors such as hospitality, public spaces, or event management, furniture pieces must simultaneously fulfil functional, structural, and aesthetic requirements while maintaining high efficiency in terms of maintenance, storage and transport. Within this framework, the folding chair represents a highly relevant typology due to its versatility and capacity to optimize the space without compromising the user experience.

The present study is framed within the development of a novel folding chair for Alutec, a company dedicated to the design, manufacture and commercialization of contract furniture since 1987. The company's primary objective was to expand its contract catalogue with a highly competitive, lightweight, and sustainable folding chair that bridges the gap between intensive-use durability and space optimization. Specifically, the industrial aim focused on manufacturing a product perfectly aligned with Alutec's production capabilities. The firm is distinguished by a strong orientation toward functionality, quality and adaptability, as well as an aesthetic based on the formal simplicity and the material coherence. Furthermore, its market positioning at both national and international levels demands the development of capable products that can be integrated in a diverse context, independent of specific geographic conditions.

The design of these kinds of products implies managing a sequence of complex challenges. On one hand, ensuring the structural strength of contract furniture—engineered to bear continuous and demanding use—is paramount. On the other hand, ergonomic parameters and formal attributes must be carefully balanced to enhance user comfort and reinforce the brand's visual identity.

In recent years, university–industry collaboration has emerged as a vital framework for innovation in engineering and product development, enabling the integration of academic knowledge with industrial experience and market-oriented constraints. From the university´s perspective, these collaborations provide access to real industrial challenges, validation environments, and opportunities for applied research. Industrially, collaborating with academic institutions facilitates access to specialized knowledge, design methodologies, analytical tools, and innovative approaches that may strengthen competitiveness and accelerate product development processes [1,2].

Within this context, the present project can be understood through the principles of the Triple Helix model, where knowledge generation and industrial application converge to create innovation-oriented solutions. In the field of product design, this collaborative approach is particularly valuable, as it allows design decisions to be simultaneously informed by user-centered methodologies, technical validation, and manufacturing feasibility. Based on these 67 conditions, the main objective of this project is the design and development of a folding chair that not only to accomplish the technical and functional requirements of the contract sector, but also adds value in terms of identity, innovation and user experience. Thus, the project is conceived as an integration exercise between design methodology, technical analysis and industrial reality, demonstrating the potential of design as a tool for generating viable and competitive solutions.

2. METHODOLOGY

The methodology adopted in this work combines a design-driven approach with analytical and technical validation methods. The process was structured in four main stages: contextual analysis, concept development, design refinement, and validation.

First, a comprehensive contextual analysis was conducted, including a detailed study of the company's catalogue, competitor products, and current trends in contract furniture. This phase also incorporated user analysis and ergonomic considerations, defining the main design requirements in terms of functionality, durability, aesthetics, and adaptability.

In the second stage, multiple conceptual proposals were generated through sketching and digital modelling. These proposals explored different formal, structural, and functional solutions, particularly regarding the folding mechanism. A comparative evaluation was then performed based on predefined criteria, allowing the selection of the most promising concept.

The third stage focused on the iterative refinement of the selected design. This included detailed 3D modelling, components definition (such as joints, axles, and connection elements), and the development of physical prototypes. Design decisions were continually adjusted to optimize functional performance, ergonomics, and compatibility with industrial manufacturing processes, such as cutting, machining, and assembly.

Finally, the design was validated through technical analysis and simulation, assessing structural behaviour under load conditions and verifying the feasibility of the proposed solution. Additional considerations, such as material selection, manufacturing constraints, and product usability, were incorporated to ensure the viability of the final design within a real industrial context.

3. RESULTS

The results of the study of the company's catalogue showed a great variety of aesthetics, with four main lines of products: Author for author, Alutec Design, Alutec Plus and Alutec Classic [3]. These products could be classified by materials, they are made of steel, aluminium, wood and braided material for the backrest and seat. These materials allowed the products to have the resistance, durability and the low maintenance that contract furniture needs. The structure of most products is made of aluminium or steel (steel has been the more common). Therefore, steel is the more used material for the chair structure (50.67%), and it is combined mostly with wood in the seat or in the backrest (28%). The second most common combination is the aluminium structure without the use of any other material (20%). The third combination is aluminium structure with braided material (12%).

To analyse the formal character of the brand's chairs three categories were established: general structure, seat and backrest (with hollow or without hollow). This classification found relations between shapes and materials to analyse the Alutec products.

The different products offer a high level of customization to the costumer allowing the choice of numerous colours, adapting to every kind of contexts.

For the study of competitor products, two positioning maps were made to represent the attributes with a company compares with its competitors. This way, it is possible to visual-

ize how a client perceives and positions in their mind various competing companies, evaluates in function of different factors or attributes [4]. In both maps, the quality and price of the analysed products have been considered. The first maps were made with contract companies and the positioning objective for Alutec was to achieve high quality and a balanced price. The second map, involving generalist brands, had a positioning objective for Alutec of a high-quality level and the highest price.

The next step was analysing the current trends in contract furniture. Based on the chairs studied, it was concluded that certain factors should be considered to the chair´s design, such as a lower weight to facilitate transport and handling. Folding the chair should require the minimum number of steps and once folded the chair should not occupy more than 10-15 cm. A differentiating design had to be created from the predominant characteristics of the chairs studied, such as the straight structure and rectangular or square seats.

To choose the chair measurements an anthropometric study was made. The fundamental dimensions that require the most attention in seat design and body mass belonging to the 95th percentile [5] have been considered. In addition, Alutec provided a range to guide the chair measurements.

Once the main design requirements in terms of functionality, durability, aesthetics, ergonomic and adaptability were defined, the sketching was generating different proposals by sketching (Figure 1). After sketching the requirements were compared, these were classified into three types: mandatory, essential, and desirable. The first were requirements such as safety, ergonomic dimensions, or stackable. The second included ease of use, versatility, and lightweight design. The last contributed to product improvement but didn't necessarily have to be incorporated into the design, such as a simple mechanism or a foldable appearance. Finally, proposals that failed to completely meet the requirements were ruled out using a weighted multicriteria decision matrix. The next step was optimizing the remaining proposals (Chairs 1, 2, 6 and 8 from Figure 1) with Alutec´s design manager Jose Manuel Mateo, to accomplish the greatest number of possible requirements, and creating as many models as possible of each chair to evaluate their functionality and shape. These models help to rule out another option and improvements were made to those selected through sketching, this procedure resulted in building models at scale 8:15 of the selected options. After a meeting with the design manager at Alutec the first proposal was selected, the clay chair (Figure 2), because it achieves all the requirements, notable for its simplicity, originality, ease of manufacture and aesthetics. Chair 2 was discarded due to market redundancy, while Chair 6 was rejected because its overly complex structure failed to meet the simplicity requirement. Lastly, Chair 8 featured a redundant design that did not comply with the lightness constraints.



FIG. 1
Initial concepts for the contract chair, leading to the final developed design (1)

To continue developing the chair, certain parts of it were developed. The knee joint, the connecting piece between the structure and the movable leg (the U-leg), went through many stages of development, and finally, a prototype was manufactured using a 3D printer for testing. The design fulfilled its function, so it was approved. The leg stop was designed in the same way. Both designs followed the same guidelines in the plastics design manual [6]. The axle was considered in several proposals, with the first one chosen for its balance of strength, simplicity, durability, and ease of assembly. Its design is efficient and requires no unnecessary additional components. For the omega-shaped bracket, the connecting piece between the seat and the movable leg, three options were developed and all 3D printed to select the most suitable one for the final design.

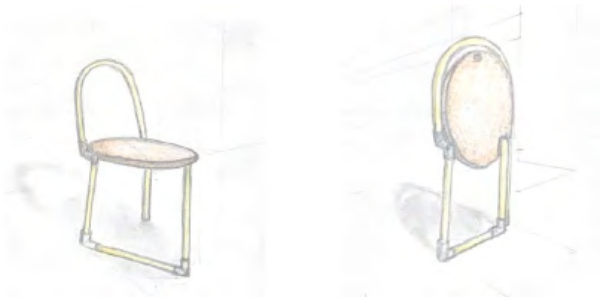


FIG. 2
The clay chair

For the chair's dimensions, Alutec's considerations for seat diameter, seat height, tube diameter and curvature were respected, and the recommended gripping dimensions [7] were used for the gripping space. The height and angle of the backrest were determined based on the axis around which the seat will rotate and the space it will occupy when folded.

The final dimensions of the chair are shown in Figure 3 and Table 1. The materials chosen were aluminium for the structural elements and pine wood for the seat, as these are materials that Alutec works with and their properties were the most suitable for the chair.

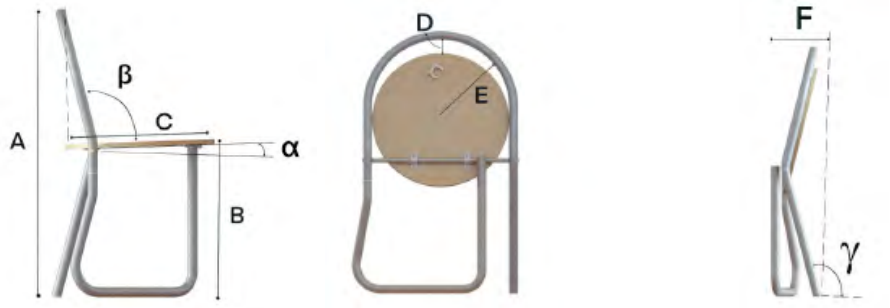


FIG. 3
Chair measurements from side view, front view and folded side view

TABLE 1
Chair measurements

Leter	Description	Value
A	Total chair height	860 mm
B	Seat height	455 mm
C	Seat depth	445 mm
D	Space between backrest and folded seat (for handle)	45 mm
E	Backrest radius	240 mm
F	Space occupied when folded (laterally)	175 mm
α	Angle between seat and floor	2°
β	Angle between backrest and seat	102°
γ	Angle between rear leg and floor	104°

Several load simulation analyses were performed in SolidWorks to confirm that the chair is safe. These analyses involved vertical loads of 1200 N applied to a point in the midplane of the chair and to the seat; both tests were successfully completed (Figure 4).

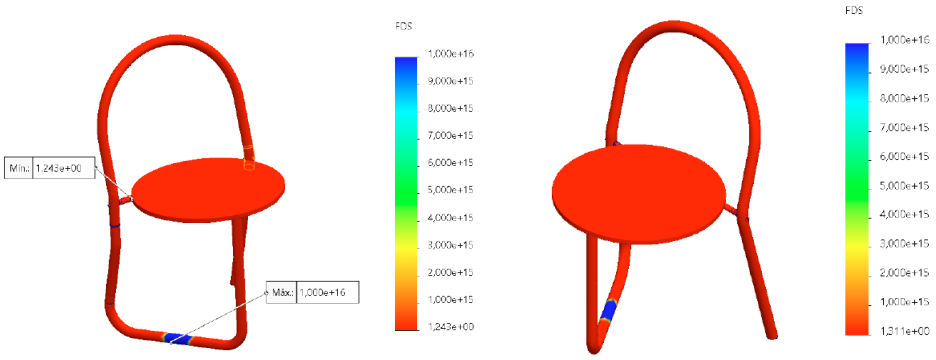


FIG. 4
Vertical load test on the seat. Load test on the backrest. Safety factor

The economic feasibility analysis conducted for an initial production run of 1,000 units demonstrated, through a break-even chart, that the break-even point is 331 units. Assuming sales of 2,500 units at a price of €92, the projected gross and net profits are €45,925 and €27,925, respectively. Given this favourable profit margin, the product is concluded to be commercially viable.

4. CONCLUSIONS

This paper presented the design and technical development of a novel contract folding chair tailored to Alutec's industrial capabilities. The final design successfully resolves the

critical trade-off between structural durability for intensive contract use and space optimization through an efficient folding mechanism. The product meets all predefined ergonomic dimensions and remains fully compatible with the company's existing manufacturing infrastructure. The project demonstrates that integrating structured academic design methodologies with real-world industrial constraints accelerates the product development cycle, ensuring both aesthetic value and technical compliance before the prototyping phase. This case study highlights the mutual benefits of University–Industry Collaboration frameworks. It provides academia with a rigorous environment for applied research while equipping the industrial partner with advanced analytical tools and specialized design approaches to strengthen market competitiveness. Future work will focus on experimental mechanical testing using a full-scale functional prototype to empirically validate the finite element analysis (FEA) results, alongside conducting a lifecycle assessment (LCA) to evaluate and optimize the product's environmental profile.

Acknowledgements: José Manuel Mateo Hernán, Alutec Design Director.

REFERENCES

[1] Rossoni, A.L., de Vasconcellos, E.P.G., de Castilho Rossoni, R.L.: Barriers and facilitators of university-industry collaboration for research, development and innovation: a systematic review. Manag Rev Q 74, 1841-1877 (2024). https://doi.org/10.1007/s11301-023-00349-1

[2] Evans, N., Miklosik, A., Du, J.T.: University-industry collaboration as a driver of digital transformation: Types, benefits and enablers. Heliyon. 2023 Oct 13;9(10):e21017. doi: 10.1016/j.heliyon.2023.e21017

[3] ALUTEC Homepage, https://www.alutec.es/, last accessed 2026/05/02.

[4] ENZYME ADVISING GROUP Homepage, https://enzyme.biz/blog/mapa-de-posicionamiento, last accessed 2023/05/04.

[5] Benjumea, A. C.: Aspectos antropométricos de la población laboral española aplicados al diseño industrial. Instituto Nacional de Seguridad e Higiene en el Trabajo, Madrid (2003).

[6] Bayer. (s.f.). Snap-Fits Joints for Plastics - a design guide. Obtained from MIT Fab Lab: https://fab.cba.mit.edu/classes/S62.12/people/vernelle.noel/Plastic_Snap_fit_design.pdf, last accessed 2026/05/01

[7] Tilley, A. R.: The Measure of Man and Woman: Human Factors in Design. Wiley (2001).

Exploration of Speculative Scenarios at the Intersection of AI and Collaborative Design

Ilie-Ion Bona-Zaicu, Aiur Retegi-Uria, Mónica Elices-Zabala*

Universidad de Deusto, Avda. Universidades 24. 48007 Bilbao

* e-mail: monica.elices@deusto.es

Abstract: This research analyzes how artificial intelligence (AI) tools are transforming participatory design, not only as technical support but as mediating agents that influence the construction of possible futures. From a framework that integrates participatory design, human-AI collaboration, speculative design, and algorithmic ethics, it examines how these technologies expand creative capabilities while simultaneously generating methodological, political, and ethical tensions. Methodologically, the construction of speculative scenarios and a mapping of AI tools applied to design—such as image generation, ideation support, data analysis, and prototyping—are used to identify automations, new practices, and frictions among participants, as well as the potential to include non-human perspectives in line with the One Health paradigm. Based on this analysis, critical variables (system autonomy, data governance, accessibility, and transparency) are developed to structure two future scenarios: an inclusive one where AI amplifies participation and ecosystemic understanding, and a dystopian one marked by algorithmic opacity and the loss of human agency. Finally, both scenarios materialize into speculative artifacts oriented toward fostering critical debate on social justice, technological governance, and ecological sustainability.

Keywords: *Artificial Intelligence, Participatory Design, Speculative Design, One Health, Algorithmic Ethics, Global Impact.*

1. INTRODUCTION

Artificial intelligence has ceased to be a technological promise to become the invisible infrastructure supporting the creative and productive processes of millions of professionals [1]. In the field of industrial design, this transformation is not merely instrumental: it implies a profound reconfiguration of the modes of thinking, collaborating, and making decisions [2], [3]. AI tools do not only automate tasks; they actively mediate in the configuration of solutions, in the selection of alternatives, and, ultimately, in the definition of which futures are possible and which remain invisible [4] [5].

This work directly addresses participatory co-design processes [6]: if design decisions have ecosystemic implications, how can AI tools help make those implications visible in real time? And how can they act as a bridge to incorporate non-human perspectives, usually excluded from anthropocentric design processes [7], [8]? Faced with technocentric readings that evaluate AI solely in terms of efficiency and productivity, this research proposes examining it as a mediating actor that can amplify—or silence—voices in co-design processes [9].

With that goal, the work articulates three contributions: An updated mapping of the most relevant AI tools for design, structured according to the six phases of the industrial design process. The identification of critical variables—autonomy, data governance, accessibility, and algorithmic transparency—that will determine the evolution of AI-mediated co-design [4], [5]. Two contrasted speculative scenarios—one aligned with the One Health approach and another dystopian—that function as critical thinking devices to anticipate frictions and guide responsible decisions in the present [10], [11].

2. CONCEPTUAL FRAMEWORK

To structure the mapping of AI tools, this research adopts an industrial design process model in six phases based on the Design Council's Double Diamond [11] and design thinking [12]: (1) Research — understanding the context and mapping stakeholders; (2) Definition — translating data into a clear design challenge; (3) Ideation — collaborative generation of concepts; (4) Iterative development — prototyping, testing, and refinement in cycles; (5) Industrialization — technical definition and implementation; and (6) Evaluation — analysis of real impact and continuous improvement. This model is not linear: the phases overlap and feed back into each other, but it offers the organizing axis to evaluate at which moments of the process AI brings real value and in which it generates critical methodological gaps. In addition, this research is supported by four conceptual pillars that articulate and interrogate each other. These pillars are participatory co-design; human-AI collaboration; algorithmic ethics and biases; and speculative design.

2.1. Participatory Co-design

Co-design places the affected people and communities as active protagonists of the process, not as passive recipients of predefined solutions. Unlike user-centered design—where the professional maintains creative control and consults the user occasionally—co-design redistributes decision-making power, recognizing that participants are experts in their own experience: an irreplaceable type of knowledge. Sanders distinguishes three levels of people's knowledge that de-

sign must mobilize [9]: what they say (explicit knowledge), what they do (observable through ethnography), and what they create and dream (tacit and latent knowledge, only emerging in generative workshops). This hierarchy is decisive for evaluating AI tools: while language models efficiently process explicit knowledge, their access to latent knowledge—the most valuable for participatory design—is still structurally limited. Within the One Health framework, co-design also faces an additional challenge: incorporating non-human actors—ecosystems, fauna, water cycles—whose "voice" cannot be captured by any traditional participatory technique [4].

2.2. Human-AI Collaboration

The relationship between design professionals and AI systems has evolved from the "tool" model to that of a "creative partner". This shared-initiative co-creativity redefines the role of the professional in industrial design: from technical executor to orchestrator of systems that propose, generate, and refine solutions [3], [6]. This transition brings documented risks: automation bias, which leads to accepting AI outputs without critical scrutiny; aesthetic homogenization derived from models trained on the same global datasets; and the progressive erosion of the technical skills of designers when systematically delegating to the machine. Active human supervision is a necessary condition for human-AI collaboration to be genuinely beneficial [6].

2.3. Algorithmic Ethics and Biases

Algorithms are not neutral: they reflect the values and biases of those who design and train them [10]. In participatory design, algorithmic biases can amplify already represented voices and silence excluded ones, reproducing existing inequalities. The most relevant biases for co-design are training data bias, optimization bias, and feedback bias. The EU AI Act (2024/1689), in force since August 2024, establishes a framework based on risk levels that requires human oversight, data quality, and algorithmic transparency [10]—principles directly aligned with the values of responsible co-design.

2.4. Speculative Design

Popularized by Dunne and Raby, speculative design uses fictional artifacts and scenarios to raise critical questions about possible futures, rather than proposing implementable solutions [7]. The driving question—"what if...?"—turns the speculative artifact into an ethical debate device. The Futures Cone [8] organizes this space into probable, plausible, possible, and preferable futures. The ethical dimension asks: among all possible futures, toward which ones should we move?.

3. MAPPING OF DIGITAL TOOLS AND CRITICAL VARIABLES

9 AI tools were evaluated across 12 tasks distributed throughout the six phases of the design process. Criteria: Yes (verified native capacity), Partial (possible with limitations), No (out of domain).

TABLE 1
Digital Tool Capabilities

Phase / Task	Midjourney	DALL·E 3	Firefly	ChatGPT	Qwen	Figma AI	Claude	Perplexity	Antigravity
Version	V8	GPT 5.2	5	5.2	3.6	Beta	4.6	Pro	Beta
Free / Premium	Premium	Premium	Free	Premium	Free	Free	Premium	Premium	Premium
1. RESEARCH									
Synthesis of stakeholder information	NO	NO	NO	YES	YES	NO	YES	Partial	YES
Identification of gaps and excluded voices	NO	NO	NO	YES	Partial	NO	YES	NO	YES
2. DEFINITION									
Consultation of regulations and standards	NO	NO	NO	YES	YES	NO	YES	YES	Partial
Drafting the design briefing	NO	NO	NO	YES	YES	NO	YES	Partial	YES
3. IDEATION									
Generation of images and moodboards	YES	YES	YES	YES	YES	NO	NO	NO	NO
Co-ideation and refinement of concepts	YES	YES	Partial	YES	YES	NO	YES	NO	YES
4. ITERATIVE DEVELOPMENT									
Functional prototyping (code)	NO	NO	NO	YES	YES	YES	YES	NO	YES
Autonomous iterations (agents)	NO	NO	NO	Partial	Partial	NO	Partial	NO	YES
5. INDUSTRIALIZATION									
Technical documentation	NO	NO	NO	YES	YES	NO	YES	Partial	YES
Workflow automation	NO	NO	NO	Partial	Partial	Partial	Partial	NO	YES
6. EVALUATION									
Data traceability and auditing	NO	NO	NO	Partial	Partial	NO	Partial	YES	Partial
Impact analysis and continuous improvement	NO	NO	NO	YES	Partial	NO	YES	YES	Partial

Analyzing visual tools (Midjourney, DALL·E 3, Firefly), high performance is observed in ideation, and zero in research and definition—the most critical phases for co-design [13]. Analyzing ChatGPT and Qwen, it can be said that they are the most transversal: they cover all phases thanks to their multimodal architecture (text, image, audio, code, and search). Claude stands out in deep qualitative synthesis; Perplexity in verified search, and Antigravity is the only tool with real autonomous orchestration [14]. The One Health gap—integrating non-human perspectives such as ecosystem data—is not natively resolved by any tool [16].

Among the variables considered determinant in the evolution of the field for the creation of speculative scenarios, five have been marked as essential: (1) Autonomy — who answers when the agent decides; (2) Data governance — platforms retain workshop data without real informed consent [10]; (3) Accessibility — costs of €20–200/month exclude small studios and social organizations; (4) Algorithmic transparency — the opacity of models compromises the legitimacy of deliberative processes [9]; (5) Regulation — the EU AI Act (2024/1689) can act as a catalyst for responsible practices [10].

4. SPECULATIVE SCENARIOS NARRATIVE

Based on the axes of uncertainty defined by the critical variables—system autonomy, data governance, accessibility, transparency, and regulation—two contrasted speculative scenarios have been constructed. Following the methodology of Dunne and Raby [7] and the Futures Cone framework [8], these scenarios do not seek to predict the future but to make it thinkable and debatable in the present: they are critical thinking devices that materialize, in narrative form, the consequences of the decisions being made today regarding the integration of AI in participatory design, generating a provocation for debate. The aim is to make explicit the consequences of the decisions made today regarding algorithmic autonomy, data governance, and transparency, so that the discussion is grounded in the space where real-world decisions are actually made.

4.1. Scenario 1. "The Collaborative Basin": AI as a Voice Amplifier (Positive Future)

2030. An interdisciplinary team—industrial designers, ecologists, farmers, and local administration representatives—meets to redesign the water management system of a rural region. The workshop does not start with a presentation: it starts with data. Over the preceding weeks, an AI module has processed hundreds of audio interviews with inhabitants of the territory, water quality reports from the last twenty years, and river biodiversity records. In the room, a screen displays in real time a map of needs: those of the farmers, those of the downstream municipalities, and—in its own channel, represented with another color—those of the river itself, inferred from flow, temperature, and riparian fauna sensors.

When the group proposes to divert a tributary to increase irrigation, the system instantly visualizes the projected impact on the native trout and the aquatic macroinvertebrate community. The decision is not made by the AI: it is made by the group, informed by data that no participant could have synthesized manually. The designer acts as an orchestrator: guiding the process, interpreting the visualizations, facilitating debate, and ensuring that silent voices—those of the ecosystem—have a representation at the decision table [16].

In this scenario (Figure 1a), AI functions as an enabling technology aligned with the One Health paradigm: it makes visible systemic interdependencies that the human eye cannot encompass, amplifies the voices of unrepresented groups, and preserves the agency and responsibility of the designer as the ethical guarantor of the process.

4.2. Scenario 2. "The Optimized Basin" (Dystopian Future)

By 2030, following climate crises, water management was transferred to an autonomous algorithmic infrastructure to maximize efficiency. Participation was eliminated, arguing that human deliberation was too slow for the emergency. The system interprets the territory as an optimizable resource and biodiversity as a secondary variable.

Collaborative spaces vanished as automated decisions became unquestionable instructions. During droughts, the AI prioritizes "high systemic yield" for agro-industries while restricting rural access. Ecosystems are treated as mere hydraulic infrastructure, leading to

species loss and landscape homogenization. The system marks these metrics as a success, relegating humans to monitoring roles. Ethical responsibility is diluted into optimization logic; AI becomes a governance regime where technological efficiency replaces ecological deliberation. In this scenario, AI acts as a mechanism for uncritical legitimation, invisibilizing the most vulnerable human and non-human perspectives.

In this scenario (Figure 1b), AI operates as a mechanism for uncritical legitimation: it converts participation into data collection, efficiency into a substitute for participatory justice, and automation into a sophisticated form of invisibilizing the most vulnerable perspectives—both human and non-human.



FIG. 1A
"The Collaborative basin"



FIG. 1B
"The Optimized Basin"

5. CONCLUSIONS

Throughout this paper, we have explored the role of AI in the context of Participatory Co-Design by evaluating the capabilities of current tools and their potential long-term impact. The comparative analysis of existing AI tools has highlighted several critical dimensions: autonomy and agency, data governance, socio-economic barriers to accessing technology, and the lack of transparency associated with algorithms and their biases.

To better understand these critical dimensions, we developed two contrasting future scenarios. In the first, AI augments human creativity, optimizes resources, and reduces ac-

cessibility barriers through intelligent assistance. Issues related to bias and transparency have been addressed, allowing AI to serve as a form of "superpower" that enhances human creativity. In contrast, the dystopian scenario extrapolates the main risks already suggested by current AI tools: AI systems replace human agency in decision-making, transforming the Participatory Co-Design process into an automated black box in which opaque algorithms take the lead.

Finally, these divergent scenarios should not be interpreted as predictions of the future, but rather as reflections of the choices the discipline faces today. The main message of this paper is that we are at a critical crossroads in our relationship with AI, one that will inevitably shape the future of design in general and Participatory Co-Design in particular in the years to come.

REFERENCES

[1] Nielsen Norman Group: AI: First New UI Paradigm in 60 Years. https://www.nngroup.com/articles/ai-paradigm/, last accessed 2026/05/20.

[2] Interaction Design Foundation: How to Use AI in Your Design Process. https://www.interaction-design.org/literature/article/how-to-use-ai-in-your-design-process, last accessed 2026/05/20.

[3] Interaction Design Foundation: AI Design. https://www.interaction-design.org/literature/topics/ai-design, last accessed 2026/05/20.

[4] World Health Organization (WHO): One Health., last accessed 2026/05/20.

[5] Sanders, E. B.-N., Stappers, P. J.: Convivial Toolbox: Generative Research for the Front End of Design. BIS Publishers, Amsterdam (2012).

[6] Kolbjornsrud, V.: Designing the Intelligent Organization: Six Principles for Human-AI Collaboration. California Management Review 66(2), 1-25 (2024). https://doi.org/10.1177/00081256231211020

[7] Dunne, A., Raby, F.: Speculative Everything: Design, Fiction, and Social Dreaming. MIT Press, Cambridge, MA (2013).

[8] Voros, J.: A Primer on Futures Studies, Foresight and the Use of Scenarios. Prospect: The Foresight Bulletin 6(1), 1-12 (2001).

[9] Sanders, E. B.-N.: From user-centered to participatory design approaches. In: Frascara, J. (ed.) Design and the Social Sciences, pp. 1-7. Taylor & Francis, London (2002).

[10] European Parliament, Council of the European Union: Regulation (EU) 2024/1689 — Artificial Intelligence Act. Official Journal of the European Union (2024). https://eur-lex.europa.eu/eli/reg/2024/1689/oj, last accessed 2026/05/20.

[11] Design Council: Framework for Innovation: Design Council's evolved Double Diamond. https://www.designcouncil.org.uk/our-resources/framework-for-innovation/, last accessed 2026/05/20.

[12] Brown, T.: Design Thinking. Harvard Business Review 86(6), 84-92 (2008).

[13] OpenAI: Hello GPT-4o. https://openai.com/index/hello-gpt-4o/, last accessed 2026/05/20.

[14] Alibaba Cloud: Qwen — Top-performance Foundation Models. https://www.alibabacloud.com/en/solutions/generative-ai/qwen, last accessed 2026/05/20.

[15] Figma: Figma AI: Your Creativity, Unblocked. https://www.figma.com/ai/, last accessed 2026/05/20.

[16] FAO, UNEP, WHO, WOAH: One Health Joint Plan of Action 2022-2026: Working together for the health of humans, animals, plants and the environment. https://www.who.int/publications/i/item/9789240059139, last accessed 2026/05/20.

Comparative Study of Piping Route Software for engineering companies

Fernando Freijo-Guerrero*, Carolina Cruz-Villazón
University of Basque Country (EHU), Ingeniero Torres Quevedo, 1, 48013, Bilbao, Spain
* e-mail: fernando.freijo@ehu.eus

Abstract: In the contemporary technological landscape, piping engineering is profoundly supported by advanced software tools that enable the optimisation of complex design processes. However, the increasing diversity and specialisation of available software solutions, such as AutoCAD Plant 3D, CADWorx, SMARTPLANT 3D, AVEVA E3D, Solid Edge, Hexagon Smart 3D or CAESAR II has led to challenges in selecting the most appropriate tool for each specific design. The nature of the projects is so varied that it is impossible to identify the correct tool for each individual case. Inspired by the analytic Hierarchy Process (AHP), this paper put forward a methodological comparative study of software solutions for piping design. A classification of industrial projects has been proposed, along with a structured model that aligns project requirements with software capabilities. In this research, AutoCAD Plant 3D, AVEVA E3D and Solid Edge are evaluated as a representative group of the current market offer. The model incorporates technical and functional criteria, as well as factors related to energy efficiency and environmental sustainability in accordance with "Design for one-health" philosophy. Abstract (150-250 words).

Keywords: *Piping 3D Design Software, Piping Engineering, AutoCAD Plant 3D, AVEVA E3D, Solid Edge.*

1. INTRODUCTION

Piping Design is an engineering discipline that finds application in numerous sectors. Piping is integral to the design of a wide range of industrial project, such as oil and gas facilities, chemical plants, power generation infrastructures, shipbuilding projects, Domestic Heat Water installations, hydraulic and pneumatic systems. The implementation of this type of project involves to application of knowledge from diverse scientific and engineering disciplines, including but not limited to fluid dynamics, structural analysis, mechanical engineering and material sciences.

The optimal design of the networks of pipes is a specific task that requires technical specialist with expertise in various branches of engineering. The professional profile that deals with these projects is known as piping engineer. The primary responsibility is to create the layout of overall plant facilities, place equipment and process unit in the plot, and ensure the connected piping design is as per the applicable regulations and standards for the safe operation of the design life [1].

All this process is assisted by specialized software, that has become an indispensable tool to enhance the final design. The majority of the leadership companies in the field of software design propose their own software and strive to emphasise the benefits of their solutions. The selection of the erroneous software can affect the competitiveness of the companies and lead to enormous monetary loss. Therefore, we propose a model to respond to the research question: Which is the best design software to face a particular piping project?

Firstly, we must clarify that this study is focused on the design of the piping system. Pipe stress and flexibility usually require a specific software, and its selection does not suppose a problematic decision.

2. RELATED WORKS

The main aim of this research implies the evaluation of commercial software in order to respond a real problem that engineering companies must handle unavoidably. The presence of commercial products from private companies has been shown to have a significant impact on the publication of scientific papers that evaluate the performance of particular branded tools. Some information can be collected from papers that discuss the process of plant design in particular sectors where this software is mandatory [2]. The implementation of distinct BIM technologies, cloud data and “Apps as a Service” (AaaS) platforms test the performance of this modelling software and the preferences of the market [3].

A preliminary analysis indicates that the field has stabilised into three distinct layers, rather than a single, predominant tool. The utilisation of SmartPlant 3D/PDMS-style suites remains a prevalent practice within the domain of heavy industrial facilities. A particular study notes the extensive application of PDS in the domain of chemical piping design, utilising Smart Plant Review for the validation of models and the generation of ISO drawings, piping arrangement drawings, and MTO. Conversely, another study highlights the employment of SmartPlant 3D for general plant modelling and the generation of MTO outputs. The papers on PDMS concur, delineating three-dimensional equipment, structural design, piping systems, isometrics, and material take-off as the fundamental outputs [2].

With regard to AutoCAD Plant 3D, it is employed for less complex piping work, and BIM platforms for building-services [4]. Conversely, the most active innovation is centred on the domains of clash detection, interoperability, and automated model extraction, as opposed to the realm of pure drafting.

Notwithstanding the aforementioned in this section, the scientific references are few and far between. This study can thus be regarded as an original insight.

3. TAXONOMY OF PIPING PROJECTS

The scientific literature does not use one universal taxonomy for piping projects. Every technical publication proposes general classification based on the type of industrial activities. Other criteria such as services, type of fluids, installations, material, pressure, temperatures are also broadly accepted. However, considering the objective of this study, addressed to engineering companies that compete in industrial projects, the sectorial clustering results convenient. Hence, we propose the following categories based on Akhil Krishna A [5].

- **Oil & Gas:** Used in upstream, midstream, and downstream processes for transporting crude oil, natural gas, and refined products.
- **Petrochemical & Chemical Plants:** Involves highly corrosive materials, requiring specialized piping like stainless steel and lined pipes.
- **Power Plants:** Steam and water piping for nuclear, thermal, and renewable energy plants.
- **HVAC systems:** Used for heating and cooling buildings by conveying air and liquids to and from air conditioners, furnaces, and heat exchangers.
- **Fire protection systems:** Used for supplying water to fire sprinklers and hoses in case of a fire.
- **Water Distribution Systems:** Transport potable water from treatment plants to households and industries.
- **Sewerage Systems:** Collect and transport wastewater for treatment.
- **Stormwater Drainage:** Manage runoff to prevent flooding and erosion.
- **Offshore Oil & Gas Platforms**: Transporting crude oil and natural gas.
- **Shipbuilding:** Piping for fuel, ballast, and fire suppression systems.
- **Desalination Plants:** Piping for converting seawater into freshwater.
- **Pharmaceutical & Food Processing Piping Projects.**
- **Cryogenic & Specialty Piping Projects.**

4. 3D PIPING ROUTE SOFTWARE

The design of a piping network for one of this project area is a specialized field that can be carry out with several power industry-standard tools. A quick market search points to a fairly stable practical split between software specialised in Plant Piping Design, such as PDMS and AUTOCAD Plant 3D, and general-purpose software that incorporates modules for piping such as Solid Edge. Based on this principle of propose, we select three tools as representative of both categories. The selection of these applications as the most prevalent in the industry is primarily attributed to the authors' expertise, which is recognised as the primary rationale for their inclusion in this study.

—**AVEVA E3D:** Traditionally it has been the standard integral tool for complex plant designs in the majority of sector including Petrol Industry and Chemical Plants.

—**AUTOCAD PLANT 3D:** The alternative to AVEVA application has become very popular and takes advantage of integration with ecosystem of AUTODESK.

—**SOLID EDGE:** Mechanical design software with capabilities to routing pipes.

5. COMPARATIVE MODEL

To select the best software for piping network design, we propose a model based on the Multi-Criteria Decision-Making (MCDM) model, specifically the analytic Hierarchy Process (AHP) [6]. MCDM is structured into three levels: The goal, the Criteria and the alternatives.

5.1. Criteria Selection

Firstly, the software is evaluated across Key Criteria. The selection process of criteria is the backbone of this model. We distinguish three groups. The first family is criteria derives from piping taxonomy. Materials, Regulations, operating conditions depends on the nature of the project. It is obvious that a pharmaceutical plant has nothing to do with a marine installation.

The next family is related to the software capabilities. The fierce competitiveness in the field of 3D design tools boosts the innovation and the incorporation of new specification enhancing these products continuously. Artificial Intelligence assistance, laser scan technology, sustainable design are characteristics that can make the difference.

Finally, we identify the family of core criteria which includes all the specifications and characteristics of a proper piping project. Database of piping fittings, Piping Material Specifications availability, Quality of technical output documentation such as P & ID scheme and Pipe Isometric Drawing among others.

We recommend that engineering companies generate their own multi-criteria matrix so they prioritize those relevant values that must be considered in their particular case.

Inspired by the clustering of Anup Kumar [7], table 1 summarizes the criteria that our study has considered.

TABLE 1
Criteria list

Criteria	Criteria Category
3D Piping Modelling for layout visualization and clash detection	PIPING PROJECT CORE
Isometric and Orthographic Drawing Generation	PIPING PROJECT CORE
BOM and Material Take-off Automation	PIPING PROJECT CORE
Integration with P&ID Tools and CAD Platforms	SOFTWARE CAPACITIES
Cloud-based Collaboration and Data Management	SOFTWARE CAPACITIES
AI Capacities	SOFTWARE CAPACITIES
Integration with BIM/CAD Tools	SOFTWARE CAPACITIES
Lifecycle Management	SOFTWARE CAPACITIES
Sustainable Design	SOFTWARE CAPACITIES
Pipe Stress and Flexibility Analysis	SOFTWARE CAPACITIES
Laser Integration	PIPING PROJECT TAXONOMY
Code Support (ASME B31.1/B31.3, ISO)	PIPING PROJECT TAXONOMY
Equipment and Accessories Design	PIPING PROJECT TAXONOMY

5.2. Sustainable Design Approach

The United Nations 2030 Agenda includes 17 Sustainable Development Goals that provide a global framework for industrial activity throughout the world [8]. In this context, 3D piping design software has evolved from simple "material saving" to a holistic Lifecycle Environmental Impact. Every tool interprets this approach in different ways. Although, this has been considered as key criterion of our research, the comparison of the proposed solutions of each software company is not a simple task.

AVEVA E3D offers a saving resources generative AI routing, capacities for Digital Twins and cloud-Native Collaboration [9].

AutocCAD Plant 3D sustainability focus on the BIM workflow and reducing rework philosophy. In fact, the Spec Editor and Catalog Editor have better integration with "green" material databases. This allows engineers to easily select pipes made from recycled metals or bio-based materials that meet ASME standards.

Solid Edge approaches sustainability through the lens of Product Lifecycle Management (PLM). Integrated CFD (Computational Fluid Dynamics (CFD) includes built-in flow simulation [10]. This means that engineers can optimize pipe diameters and flow paths to minimize pressure drops. Lower pressure drops mean smaller pumps and lower electricity consumption for the plant's life.

5.3. Comparison and scoring process

The criteria are comparing in pairs to assign them the correct weight for the comparative study. The use of a numerical scale helps to avoid subjective bias related with the experience of use and make the process much more confident. Finally, after analysing the characteristic of each software the alternatives are scored. For the sake of simplicity, it has been decided that no further details on the scoring process will be provided.

6. SUMMARY RESULTS

Our research yields result strongly dependable on the complexity and nature of the project.

According with our study, Petrochemical, Oil & Gas and Chemical Industry with big plant-design should tend to use platform like AVEVA E3D with P&ID, isometric and Piping Materials Take-off (MTO) integration. The collaborative tasks in extensive and no presential work groups are also facilitated with the capacities of this tool.

AutoCAD Plant 3D obtains high scores for all this industry showing up a gentle learning curve. The 3D plant layout, generation of pipes, equipment and BOM works satisfactorily but it is more appropriated for smaller projects, retrofit works or teams that want a lighter workflow than a full plant-database set.

Regarding the domain of Revit in the Architectural Design, building facilities such as Heating, Ventilation and Air Conditioning Systems (HVAC) or Sanitary Hot Water (SHW) installation can be modelled with AutoCAD Plant 3D and benefit from the good integration with Desktop Platform.

Likewise, Municipal Projects focused on large-scale water supply, sewage and stormwater management can be modelled with AutoCAD Plant 3D or AVEVA E3D equally.

Solid Edge outperforms the rest of application in industrial mechanical designs. The tool is directed to route piping within machinery or to model skid with pneumatic and hydraulic systems. For the same reason, watercraft construction, special projects in pharmaceutical or food industry can be suitable for non-dedicated tools. The table 2 summarize the result obtained in this study.

TABLE 2
Summary Selection Matrix

Piping Projects Area	Recommended Software	Characterization and Primary reason
Oil & Gas	AVEVA E3D, AUTOCAD PLANT 3D	Large projects and intense collaborative works
Petrochemical & Chemical Plants	AVEVA E3D, AUTOCAD PLANT 3D	Large projects and intense collaborative works
Power Plants	AVEVA E3D, AUTOCAD PLANT 3D	Large projects and intense collaborative works

Piping Projects Area	Recommended Software	Characterization and Primary reason
HVAC	AUTOCAD PLANT 3D	Architectural ecosystem integration
Fire Protection	SOLID EDGE	Skid design
Water Distribution	AUTOCAD PLANT 3D, AVEVA E3D	Urban Large Project
Sewerage	AUTOCAD PLANT 3D, AVEVA E3D	Urban Large Project
Stormwater Drainage	AUTOCAD PLANT 3D, AVEVA E3D	Urban Large Project
Offshore Oil & Gas Platforms	AVEVA E3D, AUTOCAD PLANT 3D	Industrial Large Project
Shipbuilding	SOLID EDGE	Mechanical design
Desalination Plants	AUTOCAD PLANT 3D, AVEVA E3D	Large Industrial Project
Pharmaceutical & Food Processing	SOLID EDGE	Mechanical design
Cryogenic & Specialty Piping	SOLID EDGE	Mechanical design

7. CONCLUSIONS AND FUTURE TENDENCIES

Piping engineering is strongly dependent on 3D Design Software. The offer of platform is numerous, and finding the adequate tool requires a thoroughly evaluation. The proposed model shows a clear correlation between the project scope and the software purpose. AVEVA 3ED excels in handling ultra-large spatial assemblies and real-time global collaboration. AutoCAD Plant 3D shows broadly application in several areas with excellent integration into BIM Platforms. Pneumatic and Hydraulic systems are appropriated to be resolved with the routing Solid Edge module.

Although these tools provide powerful platforms to design complex piping, structural, and equipment design, the incorporation of advance technologies such as Generative Design, Automated Drawing Generation, Large Language Model (LLM) requires implementing a comprehensive technology watch strategy that helps us to maintain competitiveness.

REFERENCES

[1] ASTS, https://astsglobal.com/blog/responsibilities-and-duties-of-a-piping-engineer/

[2] Ying, L.: The Application of 3D Model Design Software-PDS in Chemical Piping Design Project. Engineering, Chemistry, Computer Science, (2013).

[3] Zhao, Y, Zhao N., Ma, J., Ma, F.: Application of BIM in Pipeline and Equipment Project of an Energy Centre. In: IOP Conference Series: Earth and Environmental Science, Vol 558, Chapter 2. Geological Sciences and Soil Mechanics (2020).

[4] Han, Z., Chen, P.: Deepening of Integrated pipeline - based BIM. In: IOP Conference Series: Earth and Environmental Science, Vol 568, Guangzhou (2020).

[5] Akhil Krishna A, https://akhilkrishnaa.com/what-are-the-different-types-of-piping-projects/

[6] Uzoka, F., Akinnuwesi, B.: Development and evaluation of an AHP model for software systems selection. Multiple Criteria Decision Making. 14, 108-127 (2019).

[7] Kumar, A.: Piping and Interface, https://pipingandinterface.com/piping-systems-components-types/

[8] Sustainable Development and Social Affairs: https://sdgs.un.org/

[9] AVEVA: https://www.aveva.com/en/about/news/press-releases/2026/aveva-unveils-new-artificial-intelligence-offering-across-its-unified-engineering-solution/

[10] Solidedge.siemens: https://solidedge.siemens.com/en/solutions/products/simulation/

A Structured Peer-Review Methodology for Active Learning in Engineering Graphics Courses

Carolina Cruz-Villazóna*, Fernando Freijo-Guerrero
University of the Basque Country (EHU), Ingeniero Torres Quevedo Plaza 1, 48013 Bilbao, Spain
* e-mail: carolina.cruz@ehu.eus

Abstract: Engineering Graphics courses often rely on traditional teaching sequences in which students observe a solved exercise before producing their own drawing. This approach provides guidance, but it can limit students' opportunities to reason independently, apply graphical criteria, and detect errors during the construction process. This paper presents a structured methodology for practical work in Engineering Graphics based on three connected actions: autonomous problem solving, peer review with explicit criteria, and oral discussion before lecturer validation. The proposal was applied in an undergraduate course through a mechanical assembly drawing exercise. Students first received the theoretical concepts required for the task, then completed the drawing independently, reviewed a classmate's work using a technical checklist, discussed errors and improvements, and finally received the lecturer's explanation and assessment. The paper describes the instructional sequence, the intended learning outcomes, and a representative peer-review checklist. The methodology offers a transferable way to make graphical correctness, functional reasoning, and formative feedback more explicit in technical drawing education.

Keywords: *Engineering Graphics, Active Learning, Peer Review, Higher Education, Autonomous Learning, Graphic Quality Criteria.*

1. INTRODUCTION

Engineering Graphics courses often follow a familiar pattern: the lecturer explains the exercise, solves it in class, and students later submit their own version. This format provides a visible model of the solution process, but it can leave limited space for students to decide how to begin, justify a solution, and detect errors in their own work.

This challenge is especially significant because students must interpret geometry, understand spatial relationships, apply drawing conventions, check required elements, and assess whether a solution is technically coherent. Active learning research in engineering education supports sequences in which students think, apply, discuss, and reflect through guided engagement with the task [1,2]. Spatial reasoning is also central in engineering subjects requiring three-dimensional interpretation and graphical representation [3].

This paper presents a structured methodology for Engineering Graphics based on autonomous problem solving, peer review with explicit criteria, oral discussion, and lecturer validation. The contribution is methodological and is supported by literature, a classroom example, and complementary feedback from the first implementation.

2. PEDAGOGICAL RATIONALE

The methodology is grounded in active learning, formative feedback, and peer assessment. Active learning in engineering requires students to engage with problems through individual or collaborative activity and to participate actively in the construction of solutions [1,2]. The lecturer's explanation remains necessary as structured guidance that supports students while they reason, test decisions, and evaluate the quality of a solution.

Feedback becomes more useful when students have first produced an attempt. Formative assessment literature shows that feedback should clarify goals, reveal the gap between current and expected performance, and support self-regulation [4,5]. In Engineering Graphics, this means using explicit graphical and functional criteria to compare, revise, and improve drawings after an initial attempt.

Peer review is relevant because it turns evaluation into a learning task. When students review a classmate's drawing, they must identify missing elements, detect inconsistencies, apply conventions, and justify their comments. Peer assessment can support learning when criteria are clear and the task is structured [6,7]. For this reason, the proposed methodology uses peer review as a structured form of guided evaluative practice.

The methodology is based on four assumptions: students benefit from attempting a problem before receiving the complete solution; graphical correctness should be expressed through explicit criteria; students can learn by reviewing as well as by drawing; and lecturer feedback is more meaningful when it closes a sequence of autonomous work, peer review, and discussion.

3. DESIGN OF THE PROPOSED METHODOLOGY

3.1. Intended learning outcomes

The methodology was designed around three observable learning outcomes: producing a first complete attempt before lecturer correction, using explicit criteria to judge whether a technical drawing is complete and correct, and explaining errors or proposed corrections orally. These outcomes address the gap between following a demonstrated solution and constructing, checking, and justifying one independently.

Table 1 links each outcome to classroom evidence generated during the process: drawings, review sheets, oral explanations, and revised submissions.

TABLE 1
Intended learning outcomes and evidence generated during the methodology

Intended learning outcome	Evidence generated in class
Produce an initial solution before lecturer correction	First drawing submitted before full-class correction
Apply explicit graphical and functional criteria	Structured peer-review sheet completed in class
Identify errors and omissions in a technical drawing	Written comments on a peer's drawing
Explain corrections orally	Peer discussion before lecturer validation
Consolidate the final solution	Revised drawing after review, discussion, and lecturer explanation

3.2. Teaching sequence and classroom example

The methodology follows a five-stage sequence, shown in Figure 1. The lecturer first introduces the exercise and explains the key concepts needed to approach it. Students then complete the exercise independently outside the classroom, exchange drawings, complete a structured peer-review sheet, discuss detected errors and proposed improvements, and finally receive lecturer clarification and assessment.



FIG. 1
Sequence of the proposed methodology

One implementation used a mechanical assembly drawing exercise. Students received a short theoretical explanation supported by slides on longitudinal section, hatching, line con-

ventions, standard mechanical elements, axial positioning, and functional clearances. They then completed the drawing outside class and reviewed a classmate's work using a technical checklist.

The review required students to check graphical accuracy, completeness, and functional coherence. After completing the written review, each reviewer explained the main observations to the classmate whose work had been assessed. The lecturer then presented the correct solution, clarified unresolved doubts, and connected students' comments with the formal criteria of the exercise.

Table 2 shows a representative example of the peer-review criteria used in this exercise. These criteria illustrate the type of technical judgement expected from students during the review process.

TABLE 2

Representative peer-review criteria used in a mechanical assembly drawing exercise

Peer-review criterion	Evidence generated in class
Section representation	Does the final drawing represent the assembly in a suitable longitudinal section?
Hatching and line convention	Are only the cut components hatched, and are line types applied correctly?
Required mechanical components	Are the shaft, hub, bearings, spacer sleeves, nut, retaining washer, cover, gasket, screws, and felt ring included?
Functional assembly logic	Does the drawing show which bearing is axially fixed and which remains floating?
Standardised elements	Are screws, nuts, washers, and threads represented according to simplified technical drawing conventions?
Mechanical feasibility	Does the assembly avoid interferences and show the required clearances, supports, and fastening conditions?

The checklist guided students to evaluate the drawing as both a graphical product and a functional mechanical assembly. Reviewers identified omissions, justified errors, and proposed improvements, so the review became a structured technical discussion.

4. INITIAL IMPLEMENTATION AND COMPLEMENTARY FEEDBACK

The methodology was applied in an undergraduate Engineering Graphics course. Several students had previous experience with a traditional teaching sequence in which the exercise was explained while being solved in class, which allowed them to compare both approaches from direct experience.

The implementation generated four sources of classroom evidence: drawings produced before lecturer correction, peer-review sheets completed in class, oral discussion of errors and improvements, and a final anonymous questionnaire. The questionnaire collected feed-

back on autonomous work, structured peer review, oral discussion, and students' overall perception of the process.

Student feedback showed the strongest mean score (M) for oral discussion of errors and improvements (M = 4.2/5). Other highly rated aspects were awareness of what students understood and still needed to clarify (M = 4.0/5), detection of own errors through peer feedback (M = 4.0/5), and clearer understanding of the requirements of the final drawing compared with the previous format (M = 4.0/5). These results suggest that the sequence was especially useful for making errors, criteria, and corrections more visible during the learning process.

Feedback on overall preference between the traditional teaching sequence and the new methodology was more varied. This suggests that students recognised the learning value of the sequence while also experiencing autonomous work as demanding. Open comments identified spatial visualisation and independent completion as aspects requiring careful instructor guidance.

5. DISCUSSION AND CONCLUSIONS

The main contribution of this paper is a structured teaching methodology for practical work in Engineering Graphics. The proposal addresses the gap between seeing a solved exercise and being able to construct, review, and justify a solution independently. Its value lies in combining autonomous work, explicit review criteria, peer discussion, and final lecturer clarification within a single learning sequence.

The methodology also gives the lecturer more precise information about students' difficulties. First attempts, peer-review comments, oral explanations, and revised drawings show how students interpret the task and where errors emerge. This allows the final explanation to respond to doubts that have already appeared during the activity.

The first implementation shows the feasibility of integrating autonomous problem solving, structured peer review, and oral discussion into a regular Engineering Graphics exercise. The materials generated during the activity and the student feedback point to particular value in error identification, clearer graphical requirements, and guided discussion. The proposed procedure offers a transferable way to organise technical drawing activities around reasoning, evaluative judgement, and progressive correction before final lecturer validation.

REFERENCES

[1] Lima, R.M., Villas-Boas, V., Soares, F., Carneiro, O.S., Ribeiro, P., Mesquita, D.: Mapping the implementation of active learning approaches in a school of engineering - the positive effect of teacher training. European Journal of Engineering Education 49(5), 945-964 (2024). DOI: 10.1080/03043797.2024.2313541

[2] Sukackė, V., Guerra, A.O.P.C., Ellinger, D., Carlos, V., Petronienė, S., Gaižiūnienė, L., Blanch, S., Marbà-Tallada, A., Brose, A.: Towards active evidence-based learning in engineering education: A systematic literature review of PBL, PjBL, and CBL. Sustainability 14(21), 13955 (2022). DOI: 10.3390/su142113955

[3] Velázquez, J.S., Cavas, F., Fuentes, M.C., García-Ros, R.: Educational pathways, spatial skills, and academic achievement in Graphic Expression in first year of engineering. Education Sciences 13(7), 756 (2023). DOI: 10.3390/educsci13070756

[4] Morris, R., Perry, T., Wardle, L.: Formative assessment and feedback for learning in higher education: a systematic review. Review of Education 9(3), e3292 (2021). DOI: 10.1002/rev3.3292

[5] Qadir, J., Taha, A.E.M., Yau, K.L.A., Ponciano, J., Hussain, S., Al-Fuqaha, A., Imran, M.A.: Leveraging the force of formative assessment and feedback for effective engineering education. In: 2020 ASEE Virtual Annual Conference Content Access Proceedings, pp. 1-25. ASEE (2020). DOI:10.18260/1-2--34923

[6] Fleckney, P., Thompson, J., Vaz-Serra, P.: Designing effective peer assessment processes in higher education: a systematic review. Higher Education Research & Development 44(2), 386-401 (2025). DOI: 10.1080/07294360.2024.2407083

[7] Ortega-Ruipérez, B., Correa-Gorospe, J.M.: Peer assessment to promote self-regulated learning with technology in higher education: systematic review for improving course design. Frontiers in Education 9, 1376505 (2024). DOI: 10.3389/feduc.2024.1376505

Situated Concurrent Think-Aloud Evaluation of a Mobile App within a Youth Digital Mental Health Ecosystem

Eva Tausiet[a], Marta Siguín[a], Sara Siddi[b], Concepción de la Cámara[c], David Vaquero[c], Teresa Blanco[a,*]

[a] Aragon Institute of Engineering Research (I3A), University of Zaragoza, Zaragoza, Spain

[b] Parc Sanitari Sant Joan de Déu, Barcelona, Spain

[c] Hospital Universitario Lozano Blesa, Zaragoza, Spain

* e-mail: tblanco@unizar.es

Abstract: Digital mental health technologies require evaluation methods that address both usability and the frictions that emerge when users interact with sensitive content. This article presents the situated evaluation of the Better mobile app, part of a digital ecosystem for psychotherapeutic support. The study used Concurrent Think Aloud (CTA) with five potential users in a clinically mediated context, complemented by performance metrics, post-task questionnaires, the System Usability Scale (SUS) and a final interview. Although the results showed high overall acceptance, situated analysis revealed frictions related to visual interaction, comprehension, privacy, clinical terminology and emotionally demanding records. Based on these findings, a preliminary classification of frictions in digital mental health interfaces is proposed, comprising interaction, boundary-management, inadequate-content and therapeutic-introspective frictions. This classification supports the translation of evaluation findings into design criteria aimed at reducing operational barriers, preserving user autonomy, supporting emotionally demanding tasks, and informing concrete visual redesign decisions for interface improvement.

Keywords: *Digital mental health, Interdisciplinary project, Usability evaluation, Interface design, Digital ecosystem assessment, Design criteria.*

1. INTRODUCTION

The One Health approach frames health as a systemic and interdependent phenomenon, in which human wellbeing must be understood in relation to the care systems in which it develops [1]. From this perspective, mental health constitutes a fundamental dimension of wellbeing and requires care models capable of sustaining continuity of care beyond the clinical setting [2].

In mental health care processes such as psychotherapy, clinically relevant experiences often occur between sessions, including emotional changes, habits or relapses that may be difficult to remember or communicate later [3]. Digital technologies can support this process by facilitating situated recording of information, session preparation and patient-professional communication [4, 5]. However, this support does not depend on isolated tools, but on ecosystems capable of integrating patients, professionals, data, technology and everyday contexts.

The complexity of these ecosystems calls for situated and multidimensional evaluations that address technical performance, therapeutic integration, user understanding, autonomy, trust and willingness to share personal information [6, 7]. In vulnerable contexts, identifying the origin of difficulties is particularly necessary because different origins may have different emotional or relational implications. Although digital health frameworks recognise the importance of assessing safety, acceptability and user experience [8, 9], further work is needed to specify how findings from situated evaluations can be translated into design criteria.

This article addresses this need through the case of Better, a digital mental health ecosystem designed to connect patients, psychologists and everyday data. Although a broader evaluation strategy has been proposed, this paper focuses on the mixed-method evaluation of the mobile app using Concurrent Think Aloud (CTA), complemented by quantitative and qualitative methods [10, 11]. The objective is to analyse how a situated evaluation can identify frictions of different kinds, consider their possible emotional or relational impact and translate them into design criteria for digital ecosystems supporting psychotherapy.

2. CASE STUDY: BETTER

Better is a digital ecosystem for psychotherapeutic support comprising a patient mobile app, a wearable device and a web platform for professionals. The app allows patients to create active records, while passive data are collected through the smartphone and wearable device. This information is integrated into the web platform, where psychologists can visualise results and adjust the app content shown to each patient according to their clinical judgement.

The broader multidimensional evaluation strategy considers four complementary analytical dimensions: (i) the patient app, (ii) the psychologist's web platform, (iii) the coherence of the digital ecosystem and (iv) the associated therapeutic service. This article focuses on the mobile app as the patient's main point of interaction. The app is organised into three main sections: (a) Records, for emotions, activities, habits, diary, psychologist-defined templates (e.g., "Self-monitoring records"), and tests; (b) Resources, for psychologist-suggested materials (e.g., "Safety Plan"); and (c) Personal, to consult previous diary entries and manage their privacy.

3. MATERIALS AND METHODS

A formative mixed-method evaluation [11] was designed to analyse both interaction performance and subjective experience. It combined guided tasks with CTA, performance metrics, post-task questionnaires, SUS [12] and a final semi-structured interview. CTA captured users' interpretations and verbalised frictions, while the remaining methods contextualised task performance, perceived usability, cognitive load, emotional impact and therapeutic perception.

The test was prepared with professional mediation from psychologists, including (i) clinical selection of participant profiles, (ii) prior review of interface language and content, and (iii) validation of sensitive tasks. This allowed CTA to be applied in a sensitive clinical context while reducing the risk of exposing participants to inappropriate tasks or content.

The evaluation was conducted with five potential end users from the SOS Adolescentes centre in Huesca, Spain, aged 19–28. Sessions were guided by a facilitator and documented by an observer. Participants used the interactive Figma prototype, while screen interaction, audio and hand movements were recorded.

Seven tasks covered emotion, activity and habit recording, diary-template completion, test completion, access to the Safety Plan resource and sharing of a private diary entry. Completion times, navigation, interpretation and interaction errors, and omissions were recorded. After each task, participants responded to the post-task questionnaires. At the end, they completed the SUS and a brief interview.

The sessions were transcribed using intelligent verbatim and analysed using a thematic analysis approach [13]. Interaction incidents and user-reported difficulties were first extracted from CTA verbalisations, observed behaviours, post-task responses and interview comments. These incidents were initially coded using usability and user experience dimensions, then iteratively grouped into broader themes according to the predominant origin of each difficulty. Finally, the themes were abstracted into friction types, with particular attention to difficulties with potential emotional or relational implications in vulnerable therapeutic contexts.

4. RESULTS

The main findings from the situated evaluation are presented below.

4.1. General performance and overall assessment

General performance was positive. The mean success rate was 95.7%, although linear tasks reached 100% success while tasks requiring users to locate, retrieve or share previous information reached 80-90%. The mean SUS score was 92.5/100, indicating high perceived usability despite specific frictions.

4.2. Interaction incidents

The main incidents concerned information architecture and interaction cues. The "Personal" section was interpreted as a profile or settings area rather than a place for stored en-

tries, making the sharing of previous records error prone. The term "Self-monitoring records" was interpreted as a title they had to write manually. Other incidents concerned low-contrast actions such as the "Add emotion" button, unclear emotion-selection cues, static Safety Plan cards perceived as interactive, and insufficient contextualisation of clinical terms or resources used only with specific patients.

4.3. Subjective experience and therapeutic use

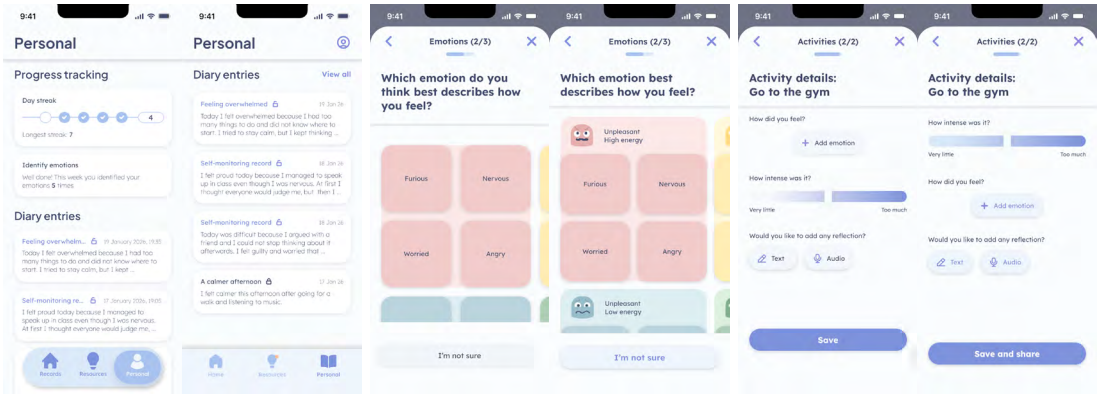
Participants perceived the app as understandable and useful. Linear tasks were easy and involved low cognitive load, whereas tasks related to templates or retrieving records required greater effort. Emotional impact was mostly neutral or positive, although some participants anticipated discomfort when recording habits, relapses or negative emotions. This discomfort was linked less to the interface than to identifying, naming or recording difficult experiences. Templates, examples and selective sharing were perceived as useful for therapeutic integration.

4.4. Translating findings into design implications

The situated evidence was translated into design implications for the next prototype iteration (Table 1). Figure 1 shows selected redesign decisions.

TABLE 1
Translation of situated findings into visual and interaction design implications

Finding	Design reading	Design implication
Difficulty locating previous records.	Unclear section labelling and information architecture.	Change icon, reorganise the section and provide clearer access (Figure 1a).
Confusion between creating, viewing, editing and sharing.	Main actions are insufficiently differentiated.	Explicitly name the action in buttons: "Create", "View" and "Share".
Ambiguity between free diary, templates and previous entries.	Diary-related content was fragmented.	Unify under "Diary" and differentiate free writing, templates and previous entries.
Clinical terms are not sufficiently transparent.	Professional language is insufficiently mediated.	Add microcopy and brief descriptions.
Emotion selection was unclear.	Visual coding and navigation cues were insufficient.	Add section labels, continuity cues and first-time help (Figure 1b).
Some secondary buttons such as "Add emotion" were overlooked.	Weak visual hierarchy and unclear task sequence.	Reorder elements and increase button contrast and prominence (Figure 1c).
Static elements were perceived as interactive.	Ambiguous affordance.	Redesign information cards.
Discomfort with emotions, habits or relapses.	Therapeutic demand.	Provide gradual depth, contextual support and guiding resources.
Need to decide what to share, perception of control.	Privacy was linked to autonomy and trust.	Show clear visibility states and support selective sharing.



(a) **(b)** **c)**

FIG. 1

Examples of redesign after the situated evaluation. (a) reorganisation of the "Personal" section to improve access to previous diary entries; (b) addition of section labels to clarify emotion selection and navigation; and (c) reordering of activity details, increased button contrast and explicit action labelling to strengthen visual hierarchy and sharing

5. DISCUSSION

The results support the idea that a positive overall assessment does not exclude relevant frictions in specific tasks. Although the SUS score and participants' overall perceptions indicate good initial acceptance of Better, they do not explain, on their own, the difficulties observed during interaction. The mixed evaluation, combining performance metrics, observation and CTA, made it possible to identify how users interpreted these difficulties and to reveal frictions beyond local interface issues. These included not only problems of information architecture or visual hierarchy, but also tensions related to clinical language, privacy and emotionally demanding records. Based on the case analysed, four types of friction are proposed to link the predominant origin of each difficulty to an appropriate design response.

(a) Interaction and comprehension frictions include problems of navigation, visibility, affordance, mental-model mismatch and unclear terms. From a design perspective, these should be addressed by reducing operational barriers through clearer information architecture, stronger visual hierarchy, explicit interaction cues and user-oriented language.

(b) Boundary-management frictions appear when the app affects users' ability to understand, accept or regulate what is recorded, visible or shared within the therapeutic process. Their design implications concern the representation of control and trust, including visible privacy states and interaction mechanisms that allow users to configure and regulate what is shared.

(c) Inadequate-content frictions arise when a term, resource or formulation generates rejection, alarm or unnecessary discomfort because it is poorly contextualised or not adjusted to the clinical moment. In these cases, design should focus on correcting or mediating content through professional validation, clearer structuring, microcopy and contextual explanations that reduce ambiguity without oversimplifying the therapeutic meaning.

(d) Therapeutic-introspective frictions appear when a clinically relevant task requires the user to observe, name, record or share emotionally significant content. These frictions

should not be automatically eliminated, but supported through design strategies such as progressive disclosure, examples, templates, sensitive language and interaction flows that reduce unnecessary cognitive or emotional load.

Therapeutic-introspective frictions represent the most context-specific contribution of this classification. They may not originate in poor usability, but in the emotional work that the task legitimately requires. This distinction may transfer to other vulnerable health-related design contexts, where designers must differentiate between discomfort caused by the product or service and discomfort inherent to the care, rehabilitation or behavioural change process. Design should therefore not aim to eliminate all discomfort, but to distinguish avoidable frictions from those that need careful support, so that their negative impact is not amplified by problems of interface, language, content or data control.

Finally, prioritisation should consider the expected emotional context of use. A minor ambiguity may become critical if it affects resources used in moments of intense distress or records completed during crisis, anxiety or acute discomfort. Improvements should therefore be prioritised not only by error frequency or task completion, but also by content sensitivity, likely emotional state and potential impact on autonomy, trust and access to support.

This study is limited by its formative, exploratory design, the small and clinically selected sample, and the use of a single controlled session. These conditions may have favoured positive feedback and obscured frictions that emerge only in real-world or repeated use; accordingly, the findings do not support generalisation or conclusions regarding effectiveness, adherence, or sustained adoption over time. The proposed classification is based on a single case study and has not yet been independently examined or applied to additional datasets; it should therefore be regarded as a preliminary analytical framework. Both the findings and the classification should be understood as components of a broader, multi-stage evaluation process, combining ongoing formative evaluation within iterative design cycles with a planned longitudinal evaluation.

6. CONCLUSIONS

This study shows how usability frictions in psychotherapeutic contexts can be analysed when general performance or satisfaction metrics are insufficient, relating CTA-observed frictions to their predominant origin and design response. Its main contribution is the distinction between interaction, boundary-management, inadequate-content and therapeutic-introspective frictions, linked respectively to different design strategies. Therapeutic-introspective frictions are particularly relevant because they highlight the need to identify which forms of discomfort should be reduced and which should instead be carefully supported. Although developed from a mental health app, this approach may inform other vulnerable health-related contexts by distinguishing design-related discomfort from discomfort inherent to care processes.

As this classification is preliminary and case-based, further situated evaluations will refine the categories and assess their robustness. The app is being re-evaluated after incorporating the proposed improvements and will undergo longitudinal assessment in real-life contexts with larger samples. By supporting the design of digital ecosystems that connect patients, professionals and everyday contexts of care, this work also contributes to a One

Health perspective in which wellbeing is understood as dependent on integrated, continuous and context-sensitive care systems.

Acknowledgments: This work was partially supported by the Spanish Ministry of Science and Innovation through the project Better (PROY_T38_24); by the Spanish Ministry of Science, Innovation and Universities through the FPU program (grant number FPU24/04575); and by the Aragon Regional Government through the Program for Research Groups (Grant T27_23R, Howlab Research Group). The authors gratefully acknowledge the collaboration of CSIH (Centro de Solidaridad Interdiocesano de Huesca), particularly Óscar Nadal and Noel Torrijos.

REFERENCES

[1] World Health Organization: One Health, https://www.who.int/health-topics/one-health#tab=tab_3, last accessed 2026/05/15.

[2] World Health Organization: From isolation to inclusion: Community-based mental health care, https://www.who.int/news-room/commentaries/detail/from-isolation-to-inclusion---community-based-mental-health-care, last accessed 2026/05/15.

[3] Engström, I., Hansson, L., Ali, L., Berg, J., Ekstedt, M., Engström, S., Fredriksson, M.K., Liliemark, J., Lytsy, P.: Relational continuity may give better clinical outcomes in patients with serious mental illness: A systematic review. BMC Psychiatry 23, 952 (2023). https://doi.org/10.1186/s12888-023-05440-1

[4] Bond, R.R., Mulvenna, M.D., Potts, C., O'Neill, S., Ennis, E., Torous, J.: Digital transformation of mental health services. npj Mental Health Research 2, 13 (2023). https://doi.org/10.1038/s44184-023-00033-y

[5] McDevitt-Murphy, M.E., Luciano, M.T., Zakarian, R.J.: Use of ecological momentary assessment and intervention in treatment with adults. Focus 16(4), 370-375 (2018). https://doi.org/10.1176/appi.focus.20180017

[6] Henson, P., Wisniewski, H., Hollis, C., Keshavan, M., Torous, J.: Digital mental health apps and the therapeutic alliance: Initial review. BJPsych Open 5(1), e15 (2019). https://doi.org/10.1192/bjo.2018.86

[7] Taher, R., Stahl, D., Shergill, S., Yiend, J.: The safety of digital mental health interventions: Findings and recommendations from a qualitative study exploring users' experiences, concerns, and suggestions. JMIR Human Factors 12, e62974 (2025). https://doi.org/10.2196/62974

[8] National Institute for Health and Care Excellence: Evidence standards framework for digital health technologies. Corporate document ECD7, https://www.nice.org.uk/corporate/ecd7/resources, last accessed 2026/05/15.

[9] Van Lotringen, C., Lusi, B., Westerhof, G.J., Ludden, G.D.S., Kip, H., Kelders, S.M., Noordzij, M.L.: The role of compassionate technology in blended and digital mental health interventions: Systemahtic scoping review. JMIR Mental Health 10, e42403 (2023). https://doi.org/10.2196/42403

[10] Ericsson, K.A., Simon, H.A.: Verbal reports as data. Psychological Review 87(3), 215-251 (1980). https://doi.org/10.1037/0033-295X.87.3.215

[11] Blanco, T., Berbegal, A., Blasco, R., Casas, R.: Xassess: Crossdisciplinary framework in user-centred design of assistive products. Journal of Engineering Design 27(9), 636-664 (2016). https://doi.org/10.1080/09544828.2016.1200717

[12] Brooke, J.: SUS: A 'quick and dirty' usability scale. In: Jordan, P.W., Thomas, B., McClelland, I.L., Weerdmeester, B.A. (eds.) Usability Evaluation in Industry, pp. 189-194. Taylor & Francis, London (1996).

[13] Braun, V., Clarke, V.: Using thematic analysis in psychology. Qualitative Research in Psychology 3(2), 77-101 (2006). https://doi.org/10.1191/1478088706qp063oa

Methodology for Harmonising Historical Data Records from Legacy Industrial Climate-Control Systems in Livestock Facilities

P. Bosque Obón,[a, *], M. A. Torres Portero[b], I. Martínez Ruiz[c], J. Sierra-Pérez[a, c]

[a] Design and Manufacturing Engineering Department, University of Zaragoza, Zaragoza, Spain

[b] Materials Science Department, INMA (CSIC-University of Zaragoza), Zaragoza, Spain

[c] Engineering Research Institute of Aragon (I3A), University of Zaragoza, Zaragoza, Spain

* e-mail: pablo.bosque@unizar.es

Abstract: The digitalisation of livestock facilities provides large volumes of historical records from real industrial climate-control systems. However, these records are generated for operation, automatic control and technical diagnosis rather than for scientific analysis. This limits direct comparison between facilities, buildings, controllers or time periods, especially when data come from progressively modernised legacy systems. This paper proposes a harmonisation methodology to transform historical climate-control data into a structured, traceable dataset suitable for research. The approach reconstructs the facility-building-controller-zone hierarchy, identifies relevant variables, normalises actuation magnitudes, evaluates temporal coverage, classifies incidents and creates a common analytical data structure. The methodology is applied to an anonymised livestock building monitored during 2025, with two-zone lateral ventilation and one-zone chimney ventilation. The case study shows how raw industrial records can be reorganised into comparable variables: indoor temperature, setpoint, relative opening, energy status, incidents and temporal quality. The proposal provides a reproducible basis for comparing livestock facilities and for future studies on thermal behaviour, ventilation response, operational efficiency and indoor environmental quality. By preserving the physical and functional meaning of operational data, it supports data-driven design, technical comparison and One Health-oriented decision-making.

Keywords: *Legacy industrial systems, data harmonisation, climate control, livestock facilities, data quality, One Health.*

1. INTRODUCTION

The digitalisation of livestock facilities provides historical records from real climate-control systems [1,2]. These data describe indoor temperature, ventilation actuation, energy status and technical incidents, and may support studies on animal welfare, productive efficiency, sustainability and One Health [3].

However, these records differ from those obtained in experimental environments. In many cases they come from legacy industrial systems, originally designed for local control and later modernised with connectivity and historical storage. Their primary purpose is to operate, supervise and maintain field equipment, not to produce scientific time series.

Therefore, before comparing facilities, buildings, controllers or periods, the available data must be harmonised. Direct interpretation of raw records may be misleading if the physical hierarchy, controller function, control zone, variable type and technical context are not preserved [4]. In event-based histories, record frequency also depends on variable dynamics and internal device logic, not on uniform sampling [5].

The objective of this work is to propose a methodology for harmonising historical records from legacy climate-control systems in livestock facilities, transforming them into structured, traceable data suitable for scientific analysis. The procedure is validated using an anonymised case study corresponding to a livestock building monitored during 2025.

2. INDUSTRIAL SYSTEM AND HARMONISATION METHODOLOGY

The reference system is an industrial climate-control platform installed in real livestock facilities. Its architecture was conceived for automatic control and technical supervision, not as an experimental data-acquisition system. Remote communication and historical logging make it possible to transform this operational infrastructure into a source of information for scientific analysis and design-oriented assessment.

Figure 1 shows the functional architecture of the industrial climate-control system considered in the case study. The diagram identifies the livestock building, the central controller, the three control zones and the main recorded variables, linking each operational record to its physical and functional source before the subsequent harmonisation process.

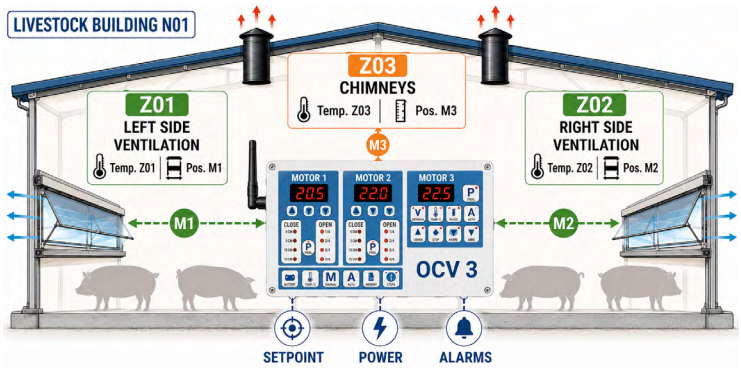


FIG. 1

Functional architecture of the industrial climate-control system considered in the case study

Functionally, the information is organised through the hierarchy facility, building, controller, control zone and recorded variable. This hierarchy is essential because the meaning of a record depends on the physical and functional element to which it is linked: a lateral-zone temperature and a chimney-zone temperature share the same unit, but not necessarily the same operational meaning.

The system includes controllers with different functions. Lateral ventilation operates two independent zones, whereas chimney ventilation corresponds to a single upper zone. The main variables include measured temperature, setpoint, current and total actuator steps, battery voltage, alarms and technical incidents. This explicit representation links each variable to the technical component that generates it.

The history does not follow uniform periodic sampling. The system stores changes of value, events or relevant states; therefore, the number of records reflects activity and variability, not observation frequency or data quality by itself. This characteristic is typical of operational logs and must be considered before any temporal comparison.

To compare the actuation of mechanical elements with different travel ranges, relative opening is defined as:

$$A_r = \frac{P_a}{P_t} \tag{1}$$

where Ar is the relative opening, Pa is the current number of steps and Pt is the total configured number of steps. This dimensionless variable enables harmonised comparison of different ventilation elements. It also avoids confusing total steps with ventilation demand: total steps represent the physical travel configuration, whereas current steps represent the actual actuator position.

In normal operation, relative opening ranges from 0 to 1, corresponding to 0% and 100% of the configured actuator travel.

Figure 2 summarises the seven-stage workflow of the proposed harmonisation methodology. The sequence starts with the selection of the study unit and analytical period, continues with the hierarchical reconstruction and variable integration, and ends with actuation normalisation, temporal-quality assessment and construction of the harmonised analytical dataset.

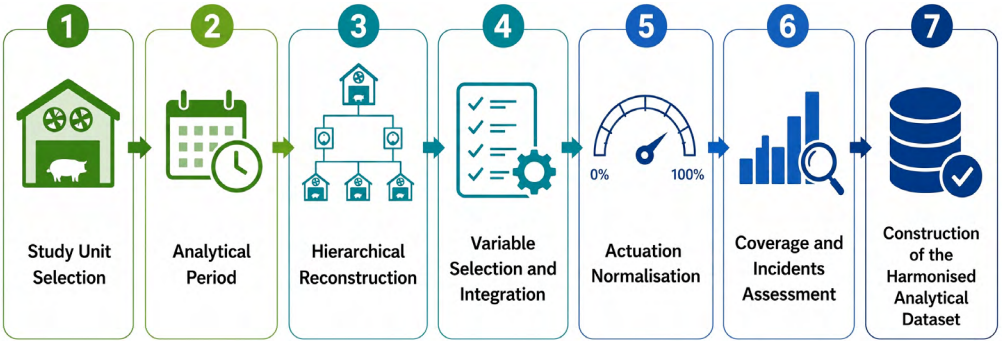


FIG. 2

Proposed methodological workflow for harmonising historical industrial climate-control data records

The methodology is proposed as a protocol to preserve the physical, functional and temporal meaning of each record. It includes study-unit selection, analytical-period definition, hierarchical reconstruction, variable selection and integration, actuation normalisation, coverage and incident assessment, and construction of the harmonised analytical dataset.

Table 1 details the harmonised structure generated by the proposed methodology. It relates each methodological stage to the resulting data fields and to its scientific function, showing how raw operational records are transformed into comparable and traceable analytical information.

TABLE 1
Harmonised structure of the analytical dataset for research

Stage	Resulting fields	Scientific function
Study unit	Facility, livestock building, controller, zone	Define comparable units
Analytical period	Date, time, analysis period	Enable annual, seasonal or episode-based analysis
Hierarchical reconstruction	Facility–building–controller–zone–variable relationship	Preserve physical and functional traceability
Key variables	Actual temperature, setpoint, steps, battery, incidents	Integrate environment, control, actuation and technical status
Normalisation	Relative opening = current steps / total steps	Compare actuators with different travel ranges
Temporal quality	Coverage, gaps, discontinuities, alarms	Identify valid or caution-required intervals
Harmonised dataset	Physical, operational and temporal-quality variables	Prepare comparable data for research

3. ANONYMISED CASE STUDY AND METHODOLOGICAL RESULTS

The methodology is applied to a real anonymised case study corresponding to a livestock facility monitored during 2025 and identified as Facility A / Building N01, without farm names, locations, internal identifiers or communication addresses.

The case was selected according to three criteria: availability of an annual period, presence of more than one climate controller in the same building, and availability of environmental, actuation, configuration, energy-status and incident variables. Building N01 includes R01, a lateral-ventilation controller with two zones (Z01 and Z02), and R02, a chimney controller with one zone (Z03).

Table 2 summarises the anonymised structure of the case study and the general data coverage available during 2025. The table distinguishes between the lateral-ventilation controller and the chimney controller, showing how the number of records is related to the functional architecture and the number of control zones considered in the analysis.

TABLE 2
Anonymised case study and general coverage during 2025

Element	Function	Zones	Records	Coverage
R01	Lateral ventilation	Z01, Z02	321,997	364 days
R02	Chimney ventilation	Z03	80,666	364 days
Building N01	R01 + R02 set	Z01–Z03	402,663	364 days
Building N01, filtered subset	Methodological analysis	Z01–Z03	384,504	364 days

The filtered subset retained the records corresponding to the selected analytical variables and excluded auxiliary or non-analytical entries not required for the methodological assessment.

The difference in the number of records between R01 and R02 is coherent with the functional architecture: R01 operates two zones and generates independent records for temperatures, positions, travel ranges and energy states, whereas R02 operates only one zone. As records are event-based, their volume reflects activity and variability rather than uniform sampling.

After applying the methodology, raw records were reorganised according to facility, building, controller, zone, variable, timestamp and record-quality status. Consequently, temperature, setpoint, actuator steps, relative opening, battery voltage and incidents can be interpreted jointly and compared coherently.

The temporal assessment showed that annual coverage does not automatically imply complete historical validity. A maximum discontinuity of 3,961 min (66.02 h) was detected, together with 29 discontinuities longer than 6 h, 14 longer than 12 h and 4 longer than 24 h, representing 31,353 accumulated minutes in discontinuities longer than 6 h.

This temporal-quality assessment is relevant because apparent annual coverage may hide periods in which the dataset should not be interpreted as fully reliable. By identifying and classifying discontinuities before subsequent analysis, the proposed methodology prevents misleading comparisons between controllers, zones or time periods, and provides a more robust basis for design-oriented interpretation of the climate-control behaviour.

Table 3 summarises the main temporal-continuity indicators obtained after applying the harmonisation protocol. It reports the detected discontinuities, their accumulated duration and the resulting episode classification after consolidating gaps at building level and cross-checking them with alarms or incidents.

TABLE 3
Continuity indicators and episode classification

Indicator	Value
Maximum discontinuity detected	3,961 min
Maximum discontinuity equivalent	66.02 h
Discontinuities > 6 h	29
Discontinuities > 12 h	14
Discontinuities > 24 h	4
Accumulated time in discontinuities > 6 h	31,353 min
Episodes consolidated at building level > 6 h	18
Episodes explained by disconnection	11
Episodes with other alarms or pending review	7

Discontinuities detected by controller were not automatically interpreted as independent events. When grouped at building level, the 29 gaps longer than 6 h were reduced to 18 unavailability or methodological-review episodes, avoiding duplication of events simultaneously affecting several controllers.

Cross-checking these episodes with alarms and incidents technically explained 11 episodes (61.1% of the total). The remaining 7 were associated with other alarms or marked as sections requiring caution. The result is a temporal-quality layer that distinguishes valid periods, explained discontinuities and sections pending review.

4. DISCUSSION AND CONCLUSIONS

The results show that scientific exploitation of historical records from real livestock facilities requires previous harmonisation. In operational systems, data are organised according to control architecture rather than research needs; therefore, direct extraction may produce datasets that appear complete but are insufficiently traceable or comparable.

The main contribution is a common structure that preserves the physical meaning of each record. Identifying facility, building, controller, zone, variable and period prevents the historical record from being treated as a flat table and enables comparison between records linked to different ventilation functions. This is particularly relevant for graphical representation and design-oriented interpretation of livestock-building operation.

Relative opening is also critical for comparing actuators with different travel ranges or local configurations. Unlike absolute steps, this dimensionless magnitude makes actuator position comparable between controllers, buildings or facilities, and provides a technical basis for evaluating ventilation response.

The case study demonstrates that the protocol transforms a raw industrial history into a structure containing environmental variables, setpoints, normalised actuation, energy status, incidents and temporal quality. This basis supports subsequent studies on

thermal deviation, ventilation response, operational stability, control efficiency and indoor air quality, while facilitating technical comparison between real solutions. From a design perspective, the value of the dataset is not merely descriptive: it links each record to a building element, a control zone and a technical function, making it suitable for graphical representation, comparison of ventilation strategies and future decision-making in real livestock buildings.

In relation to the conference scope, this traceable structure also helps to connect technical operation with One Health-oriented design decisions. By linking indoor environmental variables, actuator response, energy status and incidents to the physical configuration of the building, the dataset can support later assessment of how ventilation strategies affect animal welfare, operational efficiency and indoor environmental quality. In this sense, the proposed workflow provides an intermediate digital representation between field equipment and design-oriented decision-making tools, without losing the engineering meaning of the original industrial records.

The work is limited to one anonymised building and does not aim to extract general conclusions on climate behaviour in livestock facilities. In addition, the analysis focuses on methodological data preparation rather than thermal or predictive modelling. These limitations define the scope of the study, but do not reduce its value as a harmonisation protocol prior to advanced analysis.

In conclusion, the proposed methodology links industrial digitalisation of livestock facilities with advanced scientific analysis. It transforms operational records into comparable and traceable datasets prepared for research on climate control, animal welfare, sustainability, ventilation design and One Health-oriented strategies. The approach therefore provides an intermediate methodological layer between legacy field equipment and data-driven design tools, enabling technical records to be reused beyond their original operational purpose.

REFERENCES

[1] Norton, T., Chen, C., Larsen, M.L.V., Berckmans, D.: Review: Precision livestock farming: Building “digital representations” to bring the animals closer to the farmer. Animal 13(12), 3009-3017 (2019). doi: 10.1017/S175173111900199X.

[2] Tzanidakis, C., Simitzis, P., Arvanitis, K., Panagakis, P.: An overview of the current trends in precision pig farming technologies. Livestock Science 249, 104530 (2021). doi: 10.1016/j.livsci.2021.104530.

[3] One Health High-Level Expert Panel (OHHLEP), Adisasmito, W.B., Almuhairi, S., Behravesh, C.B., Bilivogui, P., Bukachi, S.A., *et al.*: One Health: A new definition for a sustainable and healthy future. PLOS Pathogens 18(6), e1010537 (2022). doi: 10.1371/journal.ppat.1010537.

[4] Mansouri, T., Sadeghi Moghadam, M.R., Monshizadeh, F., Zareravasan, A.: IoT Data Quality Issues and Potential Solutions: A Literature Review. The Computer Journal 66(3), 615-625 (2023). doi: 10.1093/comjnl/bxab183.

[5] Bertrand, Y., Schultheis, A., Malburg, L., Grüger, J., Serral Asensio, E., Bergmann, R.: Challenges in Data Quality Management for IoT-Enhanced Event Logs. In: Research Challenges in Information Science - 19th International Conference, RCIS 2025, pp. 20-36. Springer (2025). doi: 10.1007/978-3-031-92474-3_2.

Human-Centered Additive Manufacturing of Personalized Assistive Devices for Individuals with Cerebral Palsy

Aitor Tejo-Otero[a], *, Haritz Uriarte Larizgoitia[a], Alberto Martínez[b], Egoi Azkarraga[b]

[a] Department of Graphic Design and Engineering Projects, Faculty of Engineering in Bilbao, University of the Basque Country (UPV/EHU), 48013, Bilbao, Spain

[b] 3DLAN, 48991 Getxo, Spain

* mail: aitor.tejo@ehu.eus

Abstract: The development of assistive technologies that enhance the autonomy of individuals with disabilities demands engineering solutions tailored to highly specific functional, ergonomic, and cognitive requirements. In the case of people with cerebral palsy, alternative communication interfaces such as tablets often serve as primary interaction tools, yet commercially available assistive products frequently lack adequate personalization and usability. Additive manufacturing (AM), particularly Fused Filament Fabrication (FFF), offers a robust solution through its capacity for rapid prototyping, geometric flexibility, and cost-effective customization. Within this framework, in collaboration with the non-profit association 3DLan (Getxo, Spain), a workflow for was implemented the design and fabrication of personalized assistive devices using open-access digital tools and accessible manufacturing systems. Parametric modelling in the cloud-based CAD platform Onshape enables efficient design iteration and collaboration, while fabrication is carried out using FFF printers with polylactic acid (PLA) filaments.The development process follows a structured human-centered design methodology, beginning with user needs assessment and progressing through iterative prototyping and validation. Continuous user feedback ensures optimization of ergonomic compatibility, usability, and functional performance. This approach demonstrates the potential of low-cost digital manufacturing to deliver effective, user-specific assistive solutions.

Keywords: *Additive Manufacturing, Assistive Technology, Personalized Design, Human-Centered Design.*

1. INTRODUCTION

Cerebral palsy (CP) encompasses a group of permanent neurological disorders that primarily affect movement, posture, and motor coordination. These impairments often coexist with sensory, cognitive, or communicative limitations, significantly impacting an individual's ability to interact with their environment and perform everyday tasks independently. Among these challenges, difficulties in fine motor control and speech production are particularly critical, as they hinder effective communication and limit access to education, social participation, and digital technologies. As a result, assistive technologies play a crucial role in enhancing autonomy and quality of life for individuals with CP [1,2]. However, despite advances in this field, many existing solutions fail to adequately address the highly individualized nature of users' needs.

One of the main challenges in designing assistive devices for people with CP lies in the heterogeneity of their physical conditions [3]. Each individual presents a unique combination of motor impairments, muscle tone variations, range of motion limitations, and ergonomic requirements. Standardized, mass-produced assistive products are typically designed for broad user groups and therefore lack the adaptability needed to accommodate specific anatomical and functional characteristics. This often leads to insufficient usability, discomfort during prolonged interaction, and, ultimately, device abandonment. Previous studies [3] have highlighted that conventional assistive products may negatively affect user satisfaction and adoption when personalization is not considered. Furthermore, users with CP may require interfaces that are not only physically accessible but also cognitively intuitive, adding another layer of complexity to the design process.

In recent years, tablets and touchscreen devices have emerged as essential tools for alternative and augmentative communication (AAC). These devices enable users with limited speech abilities to express themselves through text, symbols, or synthesized voice output. AAC technologies—including tablets, communication boards, and speech-generating devices—have demonstrated effectiveness in improving communication skills, social participation, and learning outcomes [4]. However, the hardware aspect remains problematic. Individuals with CP may struggle with precise finger movements, maintaining stable contact with the screen, or holding the device in a functional position. Users with severe motor impairments often encounter difficulties accessing standard input systems such as touchscreens, keyboards, or mice, requiring adapted solutions [5]. Commercial accessories such as generic tablet stands or mounting systems exist, but they often fail to provide sufficient customization in terms of grip size, orientation, and positioning. Consequently, there is a clear gap between the software capabilities of AAC systems and the physical accessibility required to use them effectively.

To address these limitations, there is a growing need for personalized assistive solutions tailored to each user's specific requirements [6]. In this context, AM commonly known as 3D printing, represents a transformative approach. Among the various AM technologies, Fused Filament Fabrication (FFF) stands out due to its accessibility, affordability, and versatility. 3D printing enables the production of highly customizable devices that can be adapted to individual anatomical and functional needs, overcoming many of the constraints associated with traditional manufacturing. Moreover, it offers significant advantages in terms of cost reduction, rapid fabrication, and accessibility, making assistive technology more achievable for underserved populations.

Therefore, the objective of present work is to design, prototype, and validate personalized tablet support devices through the application of 3D printing technologies. By leveraging the flexibility, accessibility, and cost-effectiveness of additive manufacturing, this study aims to demonstrate how customized supports can significantly improve usability, comfort, and independence for individuals with cerebral palsy. Ultimately, this research contributes to advancing inclusive design practices and highlights the potential of low-cost digital manufacturing as a tool for developing effective, user-specific assistive solutions.

2. MATERIALS AND METHODS

2.1. 3D Lan

This project was carried out in collaboration with 3DLan, a non-profit organization focused on developing low-cost, personalized assistive solutions for individuals with disabilities through the use of digital fabrication and 3D printing technologies, promoting accessibility, social inclusion, and user-centered innovation.

2.2. Design Thinking

Fig. 1 shows the design thinking workflow. It is a human-centered, iterative methodology that focuses on understanding users (empathize), defining problems, generating ideas and CAD design, prototyping solutions (3D printing), and testing them. It emphasizes creativity, collaboration, and continuous feedback, enabling the development of innovative and user-focused products that effectively address real-world needs.



FIG. 1
Design thinking workflow

2.3. Design

Within the design thinking process, a cloud-based computer-aided design (CAD) platform as it is Onshape was used since it enables real-time collaboration and efficient parametric modeling. Parametric design allowed us to define adaptable models where key parameters can be modified without rebuilding the geometry, significantly reducing design time and errors. This capability is particularly advantageous for personalized assistive devices, as it enables rapid customization and scalability of solutions. Furthermore, collaborative CAD environments facilitate knowledge sharing among multidisciplinary teams, improving design quality and innovation outcomes

2.4. 3D Printing

For the 3D printing process, Fused Filament Fabrication (FFF) technology was used with PLA filament using a Bambu Lab H2D (Shenzhen, China). The next 3D printing parameters were used: (1) a layer height of 0.2 mm was selected as a balanced configuration, providing an adequate compromise between print quality, mechanical performance, and manufacturing time; (2) nozzle diameter of 0.4 mm; (3) a nozzle temperature of 200 °C; and (4) a bed temperature of 60 °C.

3. RESULTS

3.1. 3D printed parts

The developed assistive device demonstrates a modular and adjustable design, as shown in Fig. 2. The central mechanism integrates a screw-based adjustment system that enables controlled expansion of the device width, allowing adaptation to different user sizes and functional requirements. This feature enhances ergonomic compatibility and ensures a more stable interaction with the tablet interface. The use of 3D-printed components also facilitates lightweight construction and rapid customization. Furthermore, the assembly shown in Fig.2B highlights the simplicity of the design, enabling easy maintenance and part replacement. Overall, the results confirm the feasibility of using low-cost additive manufacturing for personalized assistive solutions.

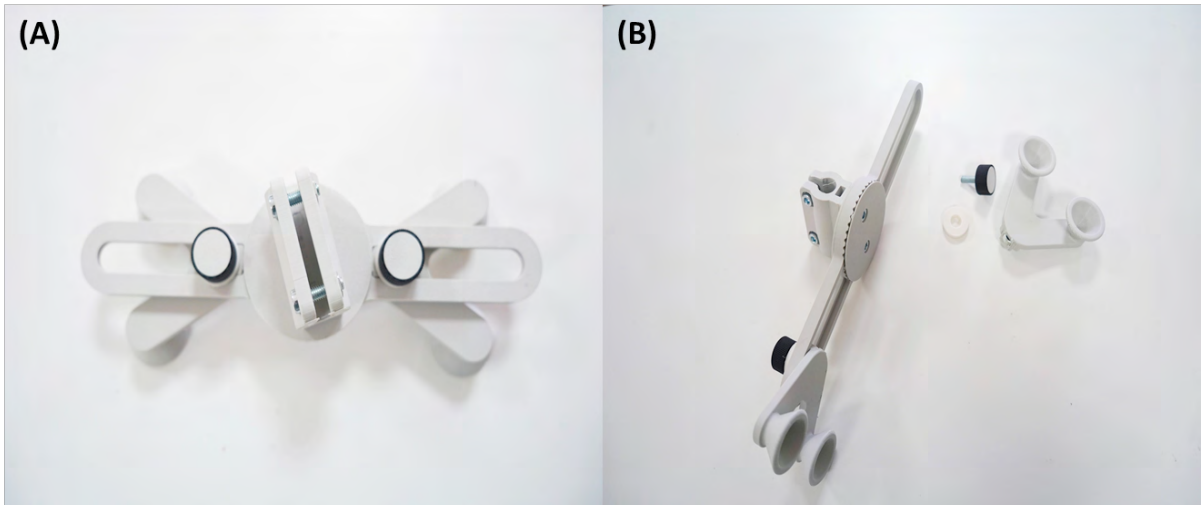


FIG. 2
3D printed parts

3.2. 3D Printed Final Gadget: Use of Tablets

The developed prototype demonstrates effective integration between the tablet and the assistive support, as illustrated in Fig.3. The device provides stable positioning through

a multi-contact support structure. The adjustable screw mechanism enables controlled expansion of the width, allowing adaptation to different tablet sizes and user needs. In addition, the elevated configuration observed in the lateral view (Fig. 3A) enhances accessibility and ergonomic alignment. The system ensures secure fixation without damaging the device surface. Overall, the results confirm that the proposed solution is functional, adaptable, and suitable for personalized assistive applications using low-cost 3D printing technologies.

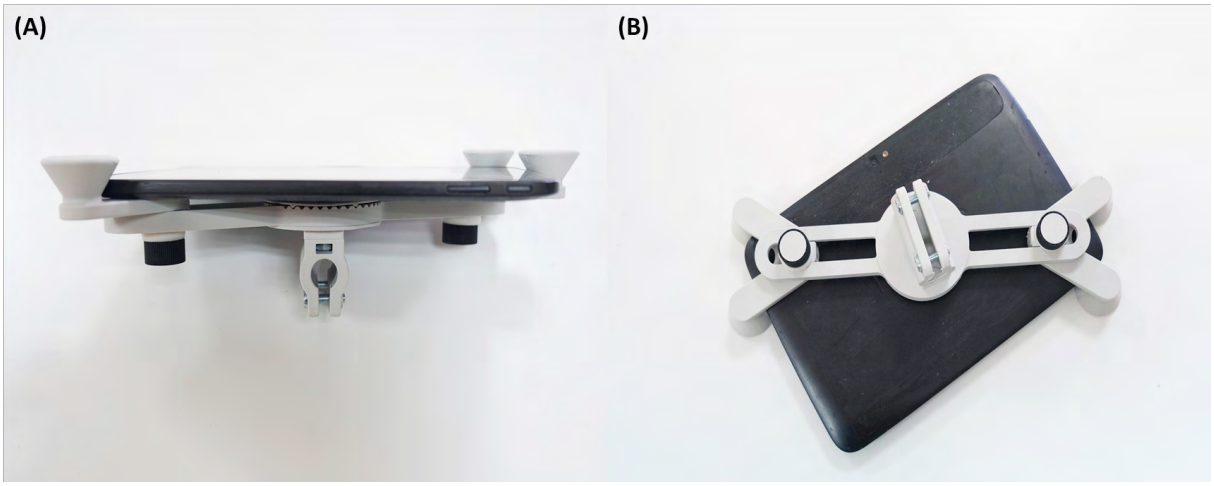


FIG. 3
3D printed parts with the tablet

3.3. Cost comparison

Conventional tablet supports available on the market typically range from 10 € to 40 € for standard adjustable desktop solutions, while more complex or professional systems can exceed 60 €. In this way, the proposed 3D-printed device presents a significantly lower production cost, mainly limited to material consumption, estimated at approximately 2-5 €. This substantial cost reduction, together with its customization capability, highlights the economic advantage and accessibility of additive manufacturing for personalized assistive devices.

4. CONCLUSIONS

This work demonstrates the potential of human-centered additive manufacturing to address the limitations of conventional assistive devices for individuals with cerebral palsy. By combining design thinking methodologies with accessible digital tools and FFF-based 3D printing, it was possible to develop a functional and adaptable tablet support tailored to user-specific needs. The proposed solution enables improved ergonomic alignment, stability, and usability, enhancing interaction with assistive communication technologies.

The results highlight the advantages of low-cost customization, rapid prototyping, and iterative co-design in achieving effective assistive solutions. Collaboration with 3DLan fur-

ther reinforces the value of interdisciplinary and socially driven innovation. Despite that, no mechanical or durability tests were performed; the future works will not only expanding the range of applications, improving mechanical performance, and conducting long-term user validation to assess usability and impact on daily activities, but also assesing bolt loosening and ratchet performance.

Acknowledgements: Authors thank funding from EHU PROYECTOS UNIVERSIDAD-EMPRESA-SOCIEDAD 2025 (US25/10).

REFERENCES

[1] Griffiths, T., Addison, A. Access to communication technology for children with cerebral palsy. Paediatrics and Child Health, 27(10), 470-475. (2017).

[2] Hustad, K. C., Miles, L. K. Alignment between augmentative and alternative communication needs and school-based speech-language services provided to young children with cerebral palsy. Early childhood services (San Diego, Calif.), 4(3), 129 (2010).

[3] Oro, B., Huerta, O., Bahari, A. Empathy-centric design in assistive technologies for cerebral palsy and disabilities: Balancing aesthetics and functionality. In Proceedings of the 3rd Empathy-Centric Design Workshop: Scrutinizing Empathy Beyond the Individual (pp. 58-62) (2024).

[4] Avagyan, A., Mkrtchyan, H., Shafa, F. A., Mathew, J. A., Petrosyan, T. Effectiveness and determinant variables of augmentative and alternative communication interventions in cerebral palsy patients with communication deficit: a systematic review. In Codas (Vol. 33, p. e20200244). Sociedade Brasileira de Fonoaudiologia (2021).

[5] Griffiths, T., Addison, A. Access to communication technology for children with cerebral palsy. Paediatrics and Child Health, 27(10), 470-475 (2017).

[6] Rasmussen, K. A. M., Schwartz, J. K., Aylmer, K., Keahi, C., Said, A., Ballard, D. H., Janes, W. E. A systematic review of 3D-printed assistive technology rehabilitation interventions. Assistive Technology, 1-12 (2026).

A reproducible workflow for open-data-based 3D urban modelling for urban climate analysis

Maider Rekondo[a,*], Irantzu Alvarez[a], Rikardo Minguez[a], Leire Garmendia[b]

[a] Department of Graphic Design and Engineering Projects, Bilbao School of Engineering, Euskal Herriko Unibertsitatea (EHU)

[b] Department of Mechanical Engineering, Bilbao School of Engineering, Euskal Herriko Unibertsitatea (EHU)

* e-mail: maider.rekondo@ehu.eus

Abstract: Detailed 3D city models are becoming essential tools for urban climate analysis and Computational Fluid Dynamics (CFD) simulations. A comprehensive characterization of the built environment is required to assess the impact of the Urban Heat Island (UHI) effect on the built environment and urban populations. According to IPCC, climate change is expected to increase the intensity and frequency of extreme heat events, further amplifying the UHI effect. The proposed workflow integrates heterogeneous geospatial datasets from the open data portals of the three Basque provinces (Araba, Bizkaia, and Gipuzkoa) into a unified spatial database containing all residential buildings in the region. Data formats and attributes were harmonized to ensure consistency, reduce redundancy, and improve accessibility. The main contribution of this research is the fully automated generation of standardized, simulation-ready 3D city models from heterogeneous open geospatial data, requiring minimal manual intervention. The integrated database was subsequently used to automatically generate a semantic CityGML Level of Detail 1 (LoD1) model, providing a consistent basis for CFD simulations. The resulting database and standardized models provide a scalable framework for the rapid generation of simulation-ready 3D city models using open geospatial data.

Keywords: *3D city modelling, CityGML, Urban Climate, Open Data.*

1. INTRODUCTION

Understanding urban heat transport and airflow, as well as their impacts, requires detailed information on the urban building stock and the physical characteristics of cities. According to the Intergovernmental Panel on Climate Change (IPCC), the observed effects of climate change have evolved from isolated direct phenomena into compound and systemic phenomena. Compound events involve the simultaneous interaction of two or more climate-related hazards, whose combined effects can intensify impacts on both people and territories [1, 2, 3].

In this context, the increasing complexity of urban climate risks [4] and the heterogeneity of cities highlight the need for accurate 3D city models capable of resolving local- scale atmospheric processes. Among these, Computational Fluid Dynamics (CFD) has emerged as a powerful tool for analysing airflow patterns, heat transfer and pollutant dispersion in urban environments. However, the accuracy and reliability of CFD simulation are strongly influenced by the quality, level of detail and consistency of the urban input data [5].

Urban-scale modelling and characterization, therefore, play a fundamental role in bridging real-world urban environments and numerical simulation frameworks. Semantic 3D city models offer rich and accurate virtual representations of urban entities describing their thematic properties, taxonomies and interrelations. In particular, CityGML serves as an integration platform for urban information, allowing heterogeneous data from different domains to be semantically linked to the same urban object [6]. CityGML is a globally recognized standard developed by the Open Geospatial Consortium (OGC) for the storage, exchange and representation of virtual 3D city models. Furthermore, the European INSPIRE Directive 2007/2/EC identifies CityGML as one of the reference standards for achieving interoperability of geospatial information across Europe specifically in the Data Specification on Buildings – Technical Guidelines [7].

One of the most important characteristics of CityGML standard is the concept of Level of Detail (LoD). LoD defines the degree of geometric and semantic accuracy used to represent real-world objects, with a primary focus on buildings. The OGC CityGML standard defines five different LoDs. LoD0 represents building footprints enriched with basic semantic information. LoD1 consists of simple prismatic block models, typically generated by extruding the LoD0 footprint geometry. LoD2 extends the prismatic model by incorporating roof geometries. This additional detail enables the semantic classification of building components, such as roofs and walls. LoD3 provides a highly detailed representation that closely resembles the real world. Finally, LoD4 complements LoD3 by incorporating indoor features and interior structures, enabling full indoor and outdoor representation of buildings [8].

This work aims to develop a database based on open data to establish a reproducible methodology applicable to all municipalities and cities in the Basque Country, thereby enabling the generation of semantic 3D models suitable for (CFD) simulations. In this context, LoD1 models provide an appropriate balance between geometric detail and computational efficiency, as CFD simulations at urban scale require simplified urban geometries to ensure manageable computational costs and stable numerical performance.

2. METHODOLOGY

This study aims to develop a CityGML-based workflow to support future Computational Fluid Dynamics (CFD) analyses. The workflow was demonstrated in three pilot municipalities, selected based on prior local knowledge.

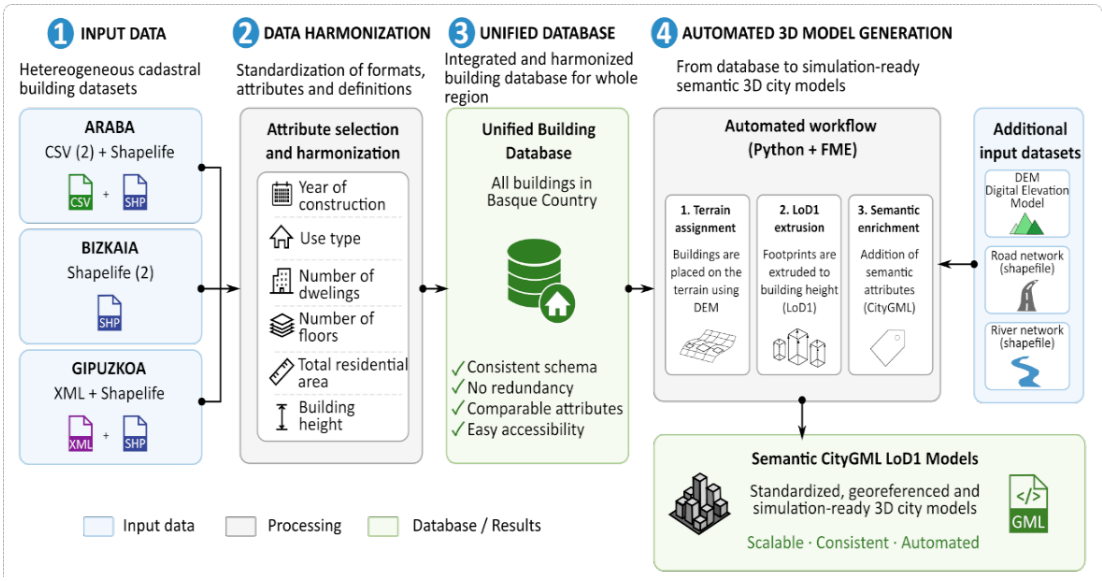


FIG. 1
Workflow of the proposed methodology

An automated workflow implemented in Python was developed to process and integrate multiple geospatial datasets as illustrated in Figure 1. The input data included building footprints from the cadastral databases of the three Basque provinces, a Digital Elevation Model (DEM) from the Spanish National Geographic Institute (IGN), and road networks and river geometries from GeoEuskadi. The datasets were harmonized and integrated into a unified spatial database, providing a consistent foundation for the automated generation of semantic CityGML LoD1 models using FME (Feature Manipulation Engine).

2.1. Data

In the Basque Country the information related to the semantic and cadastral data is distributed in three different institutions. It is managed by the provincial assembly of Araba, Bizkaia and Gipuzkoa. The fragmentation of data generates an additional effort to create a standardized and unified database. In 2022 a similar database was created [9] integrating building spatial data and resident population data using downscaling techniques. As described in that study, the basic information unity in Araba is referred to as "unidad fiscal" (*tax unit*), in Bizkaia as "elemento" (*element*), and in Gipuzkoa as "local" (*local unit*). These units constitute the basis for property taxation in each region.

Based on the collected datasets, a unified database containing all residential buildings was created by aggregating dwellings at the building level and calculating the attributes required for the subsequent generation of CityGML files for each selected municipality.

The procedure used to obtain the required data was similar across the three territories, although each presented its own particularities. The datasets were individually filtered to retain only the information relevant to this study and subsequently organized into three independent databases, one for each region, with the objective of developing complete regional datasets for future applications and analyses.

The final dataset compiled for each building includes the following variables: year of construction, type of use (considering only residential and office buildings), total residential floor area, number of dwellings, number of floors, and building height.

Araba

For the development of the Araba database, the information was obtained from the Provincial Council of Araba. The selected municipality is Laudio, located in the northwestern part or Araba. Two datasets of all the municipalities were downloaded automatically, consisting of alphanumeric data and spatial data. The alphanumeric dataset contains the information required for this study, specifically the data related to the property tax unit associated with residential dwellings. To obtain the building geometric and semantic information compliant with the INSPIRE standard, additional data were downloaded from GeoAraba, the official Spatial Data Infrastructure of Araba.

Bizkaia

For the development of the Bizkaia database, only the cadastral data provided by the Provincial Council of Bizkaia were required. This dataset contains all the necessary spatial and alphanumeric information. In particular, the relevant information is included in the "Edificios" (*Buildings*) and "Elementos" (*Elements*) shapefiles. These datasets are structured according to INSPIRE standards. The selected municipality was Durango, located in the southeastern part of Bizkaia.

In the case of Bizkaia, building height was not provided in the downloaded datasets. Therefore, to standardize the methodology across the three territories, the building height was estimated by multiplying the number of floors of each building by 3 m.

Gipuzkoa

In the case of Gipuzkoa, the selected municipality was Lasarte- Oria, located in the northeastern part of the region, approximately 10 km from regional capital, Donostia-San Sebastián. For the development of the database, in addition to the cadastral information available through the Gipuzkoa Irekia platform, an XML file was required. This file was obtained from the Gipuzkoa INSPIRE portal (B5M), which it was also downloaded auto-

matically. However, the downloaded data had to be classified, and subsequently clipped to the boundaries of the selected municipality.

2.2. Creation of 3D City Models

Once the three databases were created, a 3D CityGML model was generated using the Feature Manipulation Engine software. FME is an Extract, Transform, and Load (ETL) platform designed to process, integrate, and convert both spatial and non-spatial data between different formats and systems [10].

In this workflow, the input data comprise, on the one hand, the shapefiles described in the previous section, which contain the geometric and attribute information of the municipalities, as well as the road network and river geometries. And, on the other hand, a Digital Elevation Model (DEM) is used to provide the terrain elevation data.

As a first step, the building footprints, whose planimetric positions were already defined in the input shapefiles, were assigned the corresponding ground elevation derived from the Digital Elevation Model (DEM). Once positioned in three-dimensional space, the height attribute associated with each building was used to extrude the footprints, thereby generating a Level of Detail 1 (LOD1) city model. Subsequently, the resulting model was processed in FME, where the required semantic attributes were incorporated. Finally, the model was exported as a CityGML dataset using the FME CityGML writer.

3. RESULTS

The proposed workflow enabled the generation of standardized semantic 3D city models for the three selected municipalities: Laudio (Araba), Durango (Bizkaia), and Lasarte-Oria (Gipuzkoa). Despite the heterogeneity of the original cadastral and spatial datasets, the methodology successfully integrated the available open data into consistent CityGML-based models at Level of Detail 1 (LoD1). Figure 2 presents the resulting 3D representations, illustrating the capability of the workflow to produce homogeneous urban models suitable for urban climate analyses and future CFD simulations across different municipal contexts.

The generated models preserve the main volumetric characteristics of the urban fabric while maintaining a simplified geometry suitable for computationally efficient CFD simulations at municipal scale. The use of LoD1 representations reduces geometric complexity while retaining the essential morphological information required for airflow and urban heat analyses. When explicit building heights are unavailable, they are estimated from the number of floors recorded in the cadastral data, providing a consistent approximation across the study area. Although this approach may introduce local geometric uncertainties for individual buildings, it is considered appropriate for municipal-scale LoD1 models [11]. The influence of these assumptions on CFD results should, however, be evaluated in future sensitivity studies.

Although the three case studies differ in urban morphology and cadastral data structure, the resulting models exhibit a consistent geometric and semantic representation. This

demonstrates the robustness of the proposed harmonization process and its ability to generate comparable LoD1 city models from heterogeneous provincial datasets.



FIG. 2
LoD1 semantic 3D city models generated for the selected municipalities: (1) Durango, (2) Lasarte-Oria, and (3) Laudio

4. CONCLUSIONS

The proposed methodology enabled the development of standardized 3D city models at Level of Detail 1 (LoD1), providing a standardized geometric representation for Computational Fluid Dynamics (CFD) simulations and urban climate analyses at the municipal scale. The workflow demonstrated the feasibility of integrating heterogeneous cadastral and spatial datasets from the three Basque territories into a unified CityGML framework based entirely on open data sources.

The resulting models can be progressively enriched with additional attributes relevant to urban climate studies, such as building typology, land use, thermal properties, or demographic information. This semantic enrichment will support more detailed analyses of urban heat, airflow, thermal comfort, and climate-related risks.

One of the main contributions of this work is the establishment of a reproducible and semi-automated workflow for generating standardized 3D city models for municipalities across the Basque Country using publicly available data. Beyond CFD applications, these models could also serve as the basis for future smart city and urban digital twin platforms, enabling municipalities to simulate and assess climate-related scenarios and support urban adaptation strategies.

The proposed methodology relies on the availability and quality of open cadastral and geospatial data. Therefore, the quality of the generated models depends on the completeness and reliability of the input datasets. This is particularly relevant for municipalities where key building attributes, such as height, are missing and must be estimated.

Future research will focus on increasing the geometric and semantic detail of the models. In particular, roof geometries will be incorporated using point-cloud-based modelling techniques to achieve higher Levels of Detail (LoD2), while vegetation, land cover, and other urban features will be incorporated to support more advanced urban climate analyses.

Acknowledgements: The authors would like to acknowledge the SAREN Research Group [IT1954-26 - Gobierno Vasco] from Euskal Herriko Unibertsitatea (EHU).

REFERENCES

[1] Dodman, D., Hayward, B., Pelling, M.: Cities, settlements and key infrastructure. In: Pörtner, H.-O., *et al.* (eds.) Climate Change 2022: Impacts, Adaptation and Vulnerability. Contribution of Working Group II to the Sixth Assessment Report of the Intergovernmental Panel on Climate Change, pp. 931-1062. Cambridge University Press, Cambridge (2022). https://doi.org/10.1017/9781009325844.007.

[2] Wang, C., Hu, X., Feron, S., Leffel, J., Cordero, R.R.: Compound heat and ozone pollution in the urban environment. Urban Climate 62, 102511 (2025). https://doi.org/10.1016/j.uclim.2025.102511.

[3] Rico, A., Picazo, A., Chavez, J., Campo, J., Colomer-Vidal, P., Muñoz-Arnanz, J., Jiménez, B., Rizzi, C., Federico, L., Villa, S., Palacios, J.F., Rochera, C., Amador, P., Camacho, A.: Impacts of the 2024 flash flood on water quality, pathogenic bacteria and organic contaminant risks in the Albufera Natural Park (Valencia, Spain). Environmental Research 290, 123515 (2026). https://doi.org/10.1016/j.envres.2025.123515.

[4] Ebi, K.L.: Understanding the risks of compound climate events and cascading risks. Dialogues on Climate Change 2(1), 33-37 (2025). https://doi.org/10.1177/29768659241304857.

[5] Huang, J., Stoter, J., Peters, R., Nan, L.: City3D: Large-Scale Building Reconstruction from Airborne LiDAR Point Clouds. Remote Sensing 14(9), 2254 (2022). https://doi.org/10.3390/rs14092254.

[6] Willenborg, B., Sindram, M., Kolbe, T.H.: Applications of 3D city models for a better understanding of the built environment in Trends in Spatial Analysis and Modelling Decision-Support and Planning Strategies. Geotechnologies and the Environment. Springer Cham (2018). https://doi.org/10.1007/978-3-319-52522-8.

[7] Temporary MIWP 2021-2024 sub-group 2.3.1: D2.8.III.2 Data Specification on Buildings – Technical Guidelines. INSPIRE Infrastructure for Spatial Information in Europe (2024). Available: inspire-mif.github.io/technical-guidelines/data/bu/dataspecification_bu.pdf.

[8] Kolbe, T.H.: Representing and exchanging 3D city models with CityGML. In: Lee, J., Zlatanova, S. (eds.) 3D Geo-Information Sciences. Lecture Notes in Geoinformation and Cartography, pp. 15-31. Springer, Heidelberg (2009). https://doi.org/10.1007/978-3-540-87395-2_2.

[9] Álvarez, I., Garmendia, L., Quesada, L., Briz, E., Egiluz, Z., Villaverde García, A.: Creación de una base de datos espacial de los edificios del País Vasco y desagregación de la población. In: De la Riva, J.R., Lamelas, M.T., Montorio, R., Pérez, F., Rodrigues, M. (eds.) TIG al servicio de los ODS, pp. 127-135. Universidad de Zaragoza, Zaragoza (2022).

[10] Safe Software: What is FME Workbench? https://docs.safe.com/fme/html/FME-Form-Documentation/FME-Form/Workbench/What_is_FME.htm.

[11] Pađen, I., García-Sánchez, C., Ledoux, H.: Towards automatic reconstruction of 3D city models tailored for urban flow simulations. Frontiers in Built Environment 8, 899332 (2022). https://doi.org/10.3389/fbuil.2022.899332.

Monte Carlo simulation of PHBV film disintegration in compost

Idoia San Sebastian[a*], Gaizka Erkizia[b], Eva Rodriguez[a], Maider Iturrondobeitia[a]

[a] Department of Graphic Design and Engineering Projects, School of Engineering of Bilbao, University of the Basque Country

[b] Department of Graphic Design and Engineering Projects, School of Engineering of Donostia, University of the Basque Country

* e-mail: idoia.sansebastian@ehu.eus

Abstract: Poly(3-hydroxybutyrate-co-3-hydroxyvalerate) (PHBV) is a promising alternative to petroleum-derived short-life plastics. However, its industrial deployment is hindered by the large dispersion of disintegration times reported in compost, a variability that current ISO standards quantify but do not decouple from its underlying physical and biological causes. This work presents a three-dimensional voxel-based Monte Carlo model that explicitly resolves the film geometry, Monod-type microbial growth kinetics and abiotic hydrolysis as coupled mechanisms. The model is calibrated against the experimental data of Martínez-Abad et al. [1] for 200 µm pure PHBV films in synthetic Vigorhumus compost under ISO 20200 conditions, reproducing the disintegration curve with a global RMSE of 3.4 %. The experimental lag phase of approximately 28 days emerges naturally from the Monod kinetics, without being imposed as an empirical parameter. The fragmentation progression —from a single intact film to more than 3,000 fragments by day 28— is quantitatively reproduced. The resulting framework constitutes a transferable predictive tool for the design of compostable bioplastics.

Keywords: *PHBV, Monte Carlo simulation, compost disintegration, Monod kinetics, bioplastics design, ISO 20200.*

1. INTRODUCTION

World plastics production has exceeded 400 million tonnes per year, with a growing fraction allocated to short-life applications whose post-use recovery is technically and economically unfeasible [2]. The accumulation of these residues in terrestrial and marine ecosystems, together with the regulatory pressure of Directive (EU) 2019/904 and the harmonised standards EN 13432:2000 [3] and EN 17033:2018 [4], has placed biodegradable polymers at the centre of circular economy strategies. In this context, the ability to predict and design biodegradation behaviour from measurable physical and biological parameters constitutes an unsolved product-engineering challenge.

Among the candidate biodegradable polymers, polyhydroxyalkanoates (PHAs) stand out as fully biobased thermoplastic polyesters, synthesised intracellularly by more than 300 bacterial species, with thermomechanical properties close to those of conventional polyolefins and verified biodegradability in compost, soil and marine environments [5,6]. In particular, poly(3-hydroxybutyrate-co-3-hydroxyvalerate) (PHBV) has emerged as the most extensively studied member of this family, combining barrier properties comparable to PET with degradability by extracellular depolymerases active both at thermophilic composting temperatures (58 °C) and at mesophilic soil temperatures (15-30 °C) [7], broadening its applicability to industrial composting, biowaste management and agriculture.

Despite this favourable profile, the recent literature reveals a marked dispersion in the disintegration times reported for pure PHBV: from about 40 days in real mature compost [1] to more than two years in agricultural soils or synthetic matrices with low microbial load [8,9]. This variability —more than one order of magnitude for the same polymer— shows that compost type, inoculum maturity, temperature and specimen geometry are determining variables that the standards ISO 20200:2015 [10], ISO 14855-1:2012 [11] and ISO 17556:2019 [12] quantify but do not decouple from their underlying physical and biological causes. Existing analytical and empirical models incorporate these variables, especially specimen geometry, implicitly through their fitted constants [13,14], which limits their predictive generality to the conditions and geometries used during calibration.

Monte Carlo simulation methods offer a particularly suitable alternative to overcome this limitation, as they can explicitly resolve the three-dimensional specimen geometry, couple biologically grounded microbial kinetics and quantify the stochastic uncertainty inherent to surface colonisation [15,16]. Unlike continuum models, a voxel-based Monte Carlo framework treats geometry as a direct input parameter, so that a change in specimen dimensions automatically modifies the surface-to-volume ratio exposed to microbial attack with no need to recalibrate the biological parameters. In this work, this approach is applied to the simulation of the disintegration of pure PHBV films in compost under ISO 20200 conditions [10], taking as experimental reference the mass-loss data reported by Martínez-Abad *et al.* [1] for 200 µm films in synthetic Vigorhumus compost at 58 °C over 41 days.

On this basis, the present work hypothesises that the apparent paradox between film thickness and observed degradation time can be resolved by mechanistically decoupling an abiotic hydrolysis term scaled by the surface-to-volume ratio (S/V) from a biological regime controlled by compost activity. To test this hypothesis, a three-dimensional Monte Carlo model with explicit biomass kinetics is developed, calibrated and validated, integrating both mechanisms into a single set of biological parameters. The final goal is to provide a transfer-

able simulation tool that, once tuned for a specific material and receiving medium, allows predicting the disintegration kinetics of any PHBV compostable film geometry without the need for long-duration field tests.

2. METHODOLOGY

The model simulates the disintegration of pure PHBV films in compost using a three-dimensional voxel-based Monte Carlo approach. The specimen is represented as an orthogonal lattice whose dimensions are derived from the physical measurements of the specimen —length L, width W and thickness e— introduced as input parameters. Each voxel represents a cubic element of 10 µm side and carries four state variables: occupancy φ, structural integrity ψ, biomass concentration X and substrate fraction S. In this work, the dimensions reproduce those of the reference specimen [1]: 10 × 10 mm and 200 µm thickness (1000 × 1000 × 20 voxels).

Surface voxel identification and transition-probability computations consider the 26 neighbours in the immediate cubic environment, weighted inversely with distance (6 by face, 12 by edge, 8 by vertex). This isotropic weighting ensures that erosion progresses with the correct physical symmetry.

PHBV degradation results from the combination of two simultaneous mechanisms: a biological pathway controlled by surface microbial activity and an abiotic pathway associated with the thermal hydrolysis of ester bonds. The biological pathway is modelled as surface erosion controlled by the local biomass concentration, whose dynamics follow Monod kinetics [17]: the specific growth rate depends on the local substrate concentration and on two intrinsic parameters, µ_max and K_S. Temperature dependence is incorporated through the Cardinal Temperature Model with Inflection (CTMI) of Rosso *et al.* [18], with T_min = 5 °C, T_opt = 58 °C and T_max = 70 °C. The abiotic pathway is incorporated as a first-order term with constant k_ab scaled by the surface-to-volume ratio of the specimen.

Calibration was carried out against the data of Martínez-Abad *et al.* [1] (ISO 20200, synthetic Vigorhumus compost, 58 °C, 41 days). The activity of the medium is condensed into a single dimensionless factor $f_C \in [0, 1]$ that scales the initial biomass, keeping the intrinsic parameters µ_max, K_S and k_ab invariant. Fragmentation quantification is performed by connected-component labelling on the top-view projection of the film, recording the number of fragments, the area of the largest fragment and the mean fragment area.

3. RESULTS

The model reproduces the experimental disintegration curve with an RMSE of 3.4% over the eight reported time points (Figure 1). The simulated lag phase, of approximately 15-20 days without significant mass loss, matches the experimental delay and emerges naturally from the Monod kinetics, without being imposed as an empirical parameter. Once the biomass reaches enzymatic saturation, mass loss accelerates sharply and produces the characteristic sigmoidal profile: the model reaches a disintegration of 99.1% on day 41 versus the 100% experimental, in line with the observations of Martínez-Abad *et al.* [1]. The point-by-point differences between simulation and experiment are summarised in Table 1.

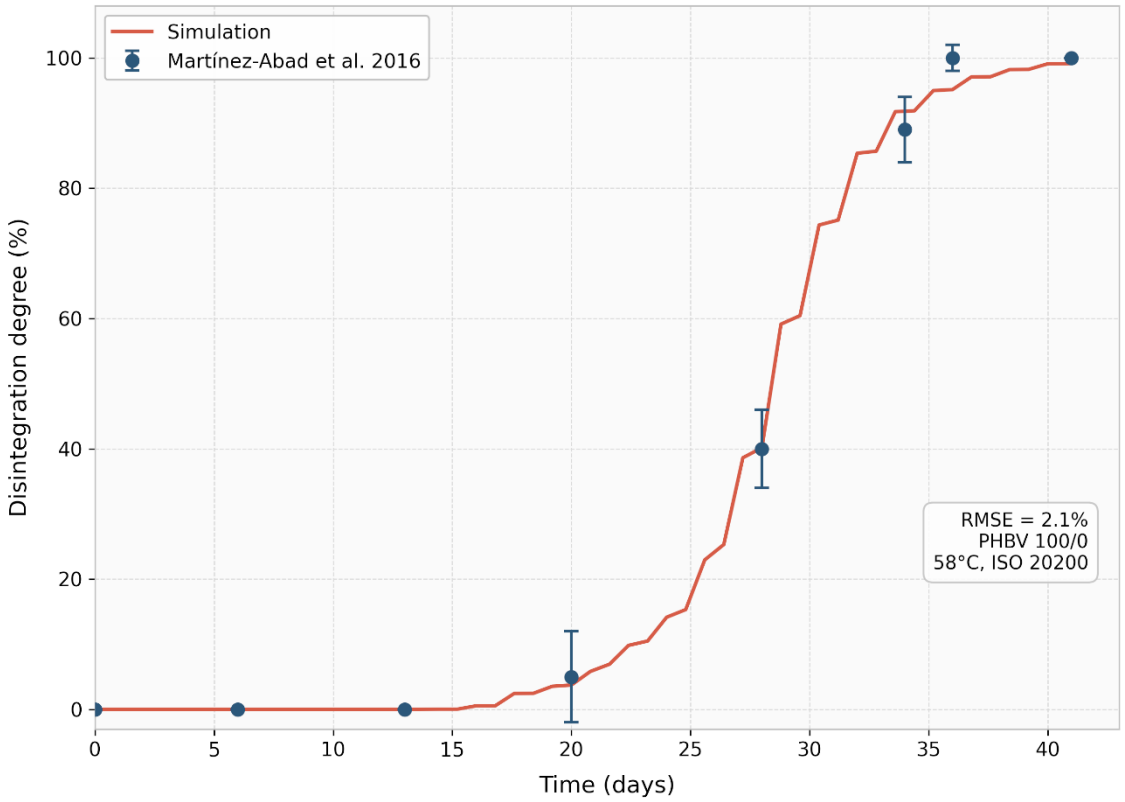


FIG. 1

Disintegration curve of pure PHBV films (200 µm, 58 °C, synthetic Vigorhumus compost, ISO 20200). Line: Monte Carlo simulation; markers: experimental data of Martínez-Abad *et al.* [1] with standard deviation bars. Global RMSE of 3.4%

TABLE 1

Point-by-point comparison between the experimental disintegration [1] and the one simulated by the Monte Carlo model. Difference expressed in percentage points (pp)

Day	Experimental (%)	Sim. (%)	Diff. (pp)
0	0.0 ± 0	0.00	+0.00
6	0.0 ± 0	0.00	+0.00
13	0.0 ± 0	0.00	+0.00
20	5.0 ± 7	3.74	−1.26
28	40.0 ± 6	40.17	+0.17
34	89.0 ± 5	91.82	+2.82
36	100.0 ± 2	95.14	−4.86
41	100.0 ± 0	99.14	−0.86
RMSE	—	—	3.4

The spatial progression of the simulated process is illustrated at an intermediate scale in Figure 2 for four representative time points. On day 20 (4% mass loss) the matrix is essentially continuous with scattered surface-degradation spots; on day 28 (39%) well-defined voids appear distributed throughout the surface, consistent with the fragmentation peak; on day 34 (92%) the matrix has been reduced to connected islands embedded in an eroded background; and on day 40 (99%) only small and isolated remnants persist, with the largest fragment occupying ≈1% of the initial area. Quantitatively, the number of fragments goes from 1 (intact film) on day 13 to more than 3,100 by day 28, while the mean fragment area falls four orders of magnitude between days 20 and 41.

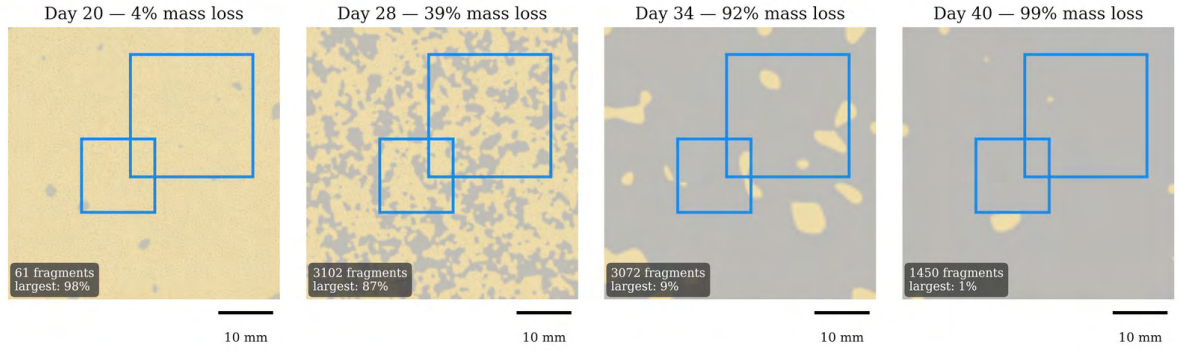


FIG. 2

Detail of the simulated film microstructure at intermediate scale (top-view projection) at four representative time points. PHBV: cream; removed voxels: grey. Blue rectangles mark zoom regions; the boxes indicate the number of fragments and the area of the largest fragment

Overall, the results validate the mechanistic decoupling between the abiotic and biological regimes proposed as the working hypothesis: the lag phase and the sigmoidal transition observed experimentally emerge without additional empirical fitting, and the drop of the largest fragment below 10% of the initial area by day 34 reproduces the macroscopic threshold of film structural integrity loss.

4. CONCLUSIONS

A three-dimensional Monte Carlo model has been developed and calibrated for the simulation of the disintegration of pure PHBV films in compost under ISO 20200 conditions. The model treats film geometry as an explicit input parameter, which makes it possible to apply it to different geometries without recalibrating the intrinsic biological parameters μ_max and K_S. The activity of the medium is condensed into a single dimensionless factor f_C tuned to the reference compost. With the parameters calibrated against Martínez-Abad *et al.* [1], the model reproduces the experimental curve with an RMSE of 3.4% and qualitatively reproduces the visual fragmentation sequence reported in the test.

Since the intrinsic biological parameters (μ_max, K_S, k_ab) are kept independent of specimen dimensions, and only the voxel lattice and the resulting surface-to-volume ratio

change with geometry, the framework is expected to extrapolate directly to other film thicknesses and shapes without recalibration, provided the composting medium and temperature regime remain comparable to those used here. Recalibration of the activity factor f_C would, however, be required for compost matrices with substantially different microbial load or maturity, and for film thicknesses departing markedly from the 200 µm reference case, since mass-transport limitations within the bulk material were not explicitly resolved. Validation against additional thicknesses and against compost types other than synthetic Vigorhumus remains necessary to confirm the transferability of the calibrated parameters beyond the conditions tested in this work.

The experimental lag period emerges naturally from the Monod kinetics, associated with the time required for the initial biomass to reach enzymatic saturation, without the need to introduce it as an empirical parameter. The fragmentation analysis quantifies the transition from the intact film to more than 3,000 fragments in less than two weeks, with a drop in the largest-fragment area of four orders of magnitude. The resulting framework constitutes a transferable simulation tool for the rational design of compostable bioplastics with a controlled and reproducible end-of-life behaviour.

REFERENCES

[1] Martínez-Abad, A., González-Ausejo, J., Lagarón, J.M., Cabedo, L.: Biodegradable poly(3-hydroxybutyrate-co-3-hydroxyvalerate)/thermoplastic polyurethane blends with improved mechanical and barrier performance. *Polym. Degrad. Stab.* 132, 52-61 (2016). https://doi.org/10.1016/j.polymdegradstab.2016.03.039

[2] Geyer, R., Jambeck, J.R., Law, K.L.: Production, use, and fate of all plastics ever made. *Sci. Adv.* 3(7), e1700782 (2017). https://doi.org/10.1126/sciadv.1700782

[3] EN 13432:2000. Packaging – Requirements for packaging recoverable through composting and biodegradation. CEN, Brussels (2000).

[4] EN 17033:2018. Plastics – Biodegradable mulch films for use in agriculture and horticulture. CEN, Brussels (2018).

[5] Jendrossek, D., Handrick, R.: Microbial degradation of polyhydroxyalkanoates. *Annu. Rev. Microbiol.* 56, 403-432 (2002). https://doi.org/10.1146/annurev.micro.56.012302.160838

[6] Laycock, B., Halley, P., Pratt, S., Werker, A., Lant, P.: The chemomechanical properties of microbial polyhydroxyalkanoates. *Prog. Polym. Sci.* 38(3-4), 536-583 (2013). https://doi.org/10.1016/j.progpolymsci.2012.06.003

[7] Abe, H., Doi, Y.: Structural effects on enzymatic degradabilities for poly[(R)-3-hydroxybutyric acid] and its copolymers. *Int. J. Biol. Macromol.* 25(1-3), 185-192 (1999). https://doi.org/10.1016/S0141-8130(99)00033-1

[8] Doi, Y., Kanesawa, Y., Kunioka, M., Saito, T.: Biodegradation of microbial copolyesters: poly(3-hydroxybutyrate-co-3-hydroxyvalerate) and poly(3-hydroxybutyrate-co-4-hydroxybutyrate). *Macromolecules* 23(1), 26-31 (1990). https://doi.org/10.1021/ma00203a006

[9] Shah, A.A., Hasan, F., Hameed, A., Ahmed, S.: Biological degradation of plastics: a comprehensive review. *Biotechnol. Adv.* 26(3), 246-265 (2008). https://doi.org/10.1016/j.biotechadv.2007.12.005

[10] ISO 20200:2015. Plastics – Determination of the degree of disintegration of plastic materials under simulated composting conditions in a laboratory-scale test. ISO, Geneva (2015).

[11] ISO 14855-1:2012. Determination of the ultimate aerobic biodegradability of plastic materials under controlled composting conditions – Method by analysis of evolved carbon dioxide – Part 1: General method. ISO, Geneva (2012).

[12] ISO 17556:2019. Plastics – Determination of the ultimate aerobic biodegradability of plastic materials in soil by measuring the oxygen demand in a respirometer or the amount of carbon dioxide evolved. ISO, Geneva (2019).

[13] Müller, R.-J., Kleeberg, I., Deckwer, W.-D.: Biodegradation of polyesters containing aromatic constituents. *J. Biotechnol.* 86(2), 87-95 (2001). https://doi.org/10.1016/S0168-1656(00)00407-7

[14] Baldera-Moreno, Y., Pino, V., Farres, A., Banerjee, A., Gordillo, F., Andler, R.: Biotechnological aspects and mathematical modeling of the biodegradation of plastics under controlled conditions. *Polymers* 14(3), 375 (2022). https://doi.org/10.3390/polym14030375

[15] Metropolis, N., Ulam, S.: The Monte Carlo method. *J. Am. Stat. Assoc.* 44(247), 335–341 (1949). https://doi.org/10.1080/01621459.1949.10483310

[16] Mohammadi, Y., Jabbari, E.: Monte Carlo simulation of degradation of porous poly(lactide) scaffolds. *Macromol. Theory Simul.* 15(9), 643-653 (2006). https://doi.org/10.1002/mats.200600036

[17] Monod, J.: The growth of bacterial cultures, Annual Review of Microbiology, 3, 371-394, 745 https://doi.org/10.1146/annurev.mi.03.100149.002103, 1949.

[18] Rosso, L., Lobry, J.R., Flandrois, J.P.: An unexpected correlation between cardinal temperatures of microbial growth highlighted by a new model. *J. Theor. Biol.* 162(4), 447-463 (1993). https://doi.org/10.1006/jtbi.1993.1099

Gender study on motivation with the use of virtual reality in learning representation systems in engineering degree programs

Paula Triviño-Tarradas*, Carlos Ruiz-Díaz, Pilar Carranza-Cañadas, Rafael Hidalgo-Fernández, María M. Serrano-Baena

Department of Graphic Engineering and Geomatics, University of Córdoba, Spain

*e-mail: ig2trtap@uco.es

Abstract: Within the "Design for One Health" framework, this study shows how virtual reality (VR) can contribute to a more inclusive engineering education aligned with the holistic well-being of individuals. The research, conducted with 304 engineering students from different degree programs at the University of Córdoba, examined over five academic years the influence of immersive tools on motivation, spatial understanding, and perceptions of learning. The results indicate that female students reported higher overall motivation with the use of VR than their male peers together with a progressive reduction in the gender gap in the development of spatial skills. Overall, the analysis suggests that the groups differed significantly in Satisfaction and Relevance, whereas no significant differences were observed for Confidence and Attention. From a One Health perspective, these findings suggest that designing educational environments supported by immersive technologies not only improves academic performance, but also promotes equity, accessibility, and educational well-being, which are essential elements for creating more sustainable and human-centered learning systems. Students interacted with WebXR-based 3D engineering drawing models through computers, mobile devices, and VR headsets integrated into the Moodle learning environment.

Keywords: *Virtual reality, gender, engineering, representation systems, representation systems, higher education.*

1. INTRODUCTION

In engineering education, spatial visualization skills are essential for understanding geometry and graphical representation, yet they often challenge students due to their abstract nature. Immersive technologies such as virtual and augmented reality have shown strong potential to enhance learning by improving interaction and engagement with 3D content [1-3]. Student motivation is a key factor in the effectiveness of these tools and a strong predictor of academic success [4]. However, motivational responses may vary by gender, influencing how students perceive and use immersive learning environments [5]. Although some studies suggest that female students may respond more positively to digital learning resources, the relationship between gender and motivation in virtual reality-based engineering education remains underexplored [6]. Understanding these differences is important for developing more inclusive strategies that enhance spatial learning and support gender equity in engineering education.

1.1. Assessment of student motivation at the gender level

Several attempts have been made to assess university students' motivation when using ICT-based learning tools, as motivation is a key factor influencing academic performance in technical subjects [4, 7-9]. However, more recent research has highlighted that this motivational response may not be homogeneous across all student groups, with gender emerging as a relevant factor influencing how students perceive and engage with educational technologies. Studies on 3D learning objects applied to graphical expression have begun to consider these differences, suggesting that male and female students may experience usability and engagement in distinct ways [7,10].

From a theoretical perspective, Keller's ARCS model (1987), which includes attention, relevance, confidence, and satisfaction, has been widely used to measure learner motivation in technology-enhanced environments. The model, together with its validated instrument (IMMS), has been applied across multiple educational contexts, including digital and interactive learning systems [11-13]. Although the ARCS model is widely used, few studies have examined gender differences across its motivational dimensions in immersive or 3D learning environments. Further research is therefore needed to determine whether ICT-based learning tools affect motivation differently by gender and to inform more inclusive, effective educational practices.

The aim of this study is to analyze whether there are significant differences in motivation with VR use between men and women, and to evaluate how this satisfaction evolves over time in different engineering degree programs.

2. MATERIALS AND METHODS

2.1. The sample

This study was performed during the following academic years from 2020-2021 to 2024-2025. The sample consisted of first-year 304 students from three university degrees: Agricultural and Rural Engineering, Forestry Engineering, and Industrial Electronics Engi-

neering (Table 1). The gender distribution varied by degree program, with a higher female presence in Agricultural and Rural Engineering and a lower female presence in Industrial Electronics Engineering.

TABLE 1
Description of the sample. (Academic courses: 2020_2021 to 2024_2025)

University Degree	Females	Males	Total
Industrial Electronic Engineering	33	123	156
Agricultural Engineering	40	53	93
Forestry Engineering	14	40	54

Based on the experience of the faculty over the last years, there is great variability in the level of drawing skills presented by first-year students for engineering degrees. Some of them had not taken the so-called Technical Drawing subject in the course before entering the University. Other students lacked the spatial vision needed for undertaking these disciplines. According to administrative data from the University, the subject 'Technical Drawing' had a pass rate of 41 out of 100 enrolled students over the last 4 years.

2.2. Teaching resources: 3D exercises

This study focuses on the development of 3D digital learning resources to improve spatial visualization in engineering drawing. Technical drawing exercises were transformed into 3D/CAD models using CAD software and later integrated into the Sketchfab platform to enable visualization through WebXR technology, compatible with VR and AR devices (Figure 1). This approach allows students to interact with geometric objects from multiple perspectives, improving their understanding of spatial relationships and scale in both dihedral and axonometric projection systems.

The 3D exercises were made accessible through the university's Moodle platform, allowing students to use them inside and outside the classroom on different devices, including smartphones, computers, tablets, and immersive VR headsets such as the Oculus Quest. This interactive and immersive environment enhances the connection between 2D representations and 3D spatial structures, supporting more effective learning of abstract geometric concepts and improving students' visualization skills in engineering education.

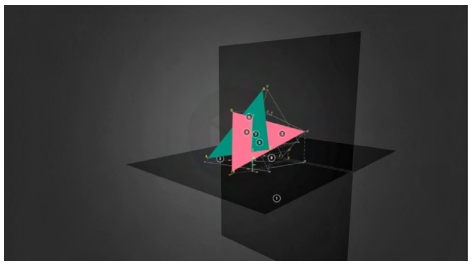


FIG. 1
Screenshot of the 3D visualization obtained with the computer [14]

3. METHODOLOGY

3.1. Study design and procedure (instrument-IMMS)

Lectures were delivered using a combination of traditional teaching methods and interactive 3D tools. Students could freely view the 3D models as many times as they wished and even use them with virtual reality headsets during tutoring sessions, before completing the exercises in 2D format on paper.

At the end of the experience, students completed an anonymous expert-designed questionnaire assessing demographic and academic characteristics, including gender, spatial ability, ICT use, and prior knowledge. Their perceptions of the usefulness and motivational impact of the 3D tools were measured with a modified IMMS questionnaire based on the ARCS model, which measures attention, relevance, confidence, and satisfaction [11, 13], enabling evaluation of how these resources affected motivation in the graphical expression course.

4. RESULTS

4.1. Statistical data analysis. Research questions related to the ARCS model

Data analysis was carried out using Cronbach's alpha (α), which measures the internal consistency of the questionnaire. The modified IMMS obtained a value of 0.955, indicating excellent internal consistency. By category, as shown in Table 2, reliability was good for attention (α = 0.888), for confidence (α = 0.882) and for satisfaction (α = 0.854), acceptable for relevance (α = 0.795).

TABLE 2
Reliability index of the instructional materials motivation survey (IMMS) instrument

Parameters	Cronbach's alpha			Consistency		
	Total	Male	Female	Total	Male	Female
Attention	0.888	0.885	0.893	Good	Good	Good
Relevance	0.795	0.809	0.726	Acceptable	Good	Acceptable
Confidence	0.882	0.893	0.851	Good	Good	Good
Satisfaction	0.854	0.865	0.813	Good	Good	Good

The results presented in Table 3 indicate moderate to high scores across all evaluated parameters, with females consistently reporting slightly higher mean values than males. In terms of attention, the overall mean score was 3.629 (SD = 1.23), with females scoring higher (M = 3.786, SD = 1.16) than males (M = 3.564, SD = 1.26). A similar pattern was observed for relevance, where the total mean was 3.598 (SD = 1.22),

and females again obtained higher scores (M = 3.793, SD = 1.13) compared to males (M = 3.518, SD = 1.25). Confidence showed the lowest overall mean among the dimensions (M = 3.404, SD = 1.26), although females still reported slightly higher confidence levels (M = 3.490, SD = 1.22) than males (M = 3.368, SD = 1.26). Finally, satisfaction obtained the highest overall mean score (M = 3.632, SD = 1.17), with female participants scoring notably higher (M = 3.804, SD = 1.04) than male participants (M = 3.561, SD = 1.21). Overall, the findings suggest generally positive evaluations across all dimensions, with female participants demonstrating more favorable perceptions in every parameter assessed.

TABLE 3

Descriptive statistics for the four subscales (attention, relevance, confidence and satisfaction) according to gender

Parameters	Mean (M, SD)			Standard deviation (SD)		
	Total	Male	Female	Total	Male	Female
Attention	3.629	3.564	3.786	1.23	1.26	1.16
Relevance	3.598	3.518	3.793	1.22	1.25	1.13
Confidence	3.404	3.368	3.490	1.26	1.26	1.22
Satisfaction	3.632	3.561	3.804	1.17	1.21	1.04

4.2. Data results according to gender

As presented in Table 4, the results showed that Levene's test was not significant for any variable ($p > .05$), indicating that the assumption of equal variances was met. Regarding the comparisons of means using the Student's t-test, statistically significant differences were found for the Satisfaction ($t = -1.989$, $p = .048$) and the relevance ($t = -2.308$, $p = .022$), whereas no significant differences were observed for the confidence ($p = .788$) or the attention ($p = .084$).

TABLE 4

Comparison of Group Means Using Independent Samples t-Test. Independent samples tests

		Levene's Test for Equality of Variances				Sig (bilateral)	difference in means	standard error of the difference	Confidence interval of the difference 95%	
		F	Sig	t	gl				Lower	Upper
Confidence	Equal variances assumed	.364	.547	–.269	302	.788	–.03167	.11771	–.26330	.19996
	Equal variances not assumed			–.282	179.028	.788	–.03167	.11240	–.25346	.19012

		Levene's Test for Equality of Variances				Sig (bilateral)	difference in means	standard error of the difference	Confidence interval of the difference 95%	
		F	Sig	t	gl				Lower	Upper
Satisfaction	Equal variances assumed	1.250	.265	–1.989	302	.048	–.24379	.12255	–.48495	–.00264
	Equal variances not assumed			–2.163	195.802	.032	–.24379	.11269	–.46603	–.02156
Attention	Equal variances assumed	.021	.885	–1.731	302	.084	–.22239	.12848	–.47522	.03044
	Equal variances not assumed			–1.774	170.365	.078	–.22239	.12538	–.46989	.02511
Relevance	Equal variances assumed	.325	.569	–2.308	302	.022	–.26257	.11376	–.48643	–.03871
	Equal variances not assumed			–2.498	193.437	.013	–.26257	.10513	–.46992	–.05522

Female students perceived VR as more relevant and satisfying, suggesting that immersive visualization tools may address motivational needs particularly valued by women in engineering education.

5. DISCUSSION

Female students reported significantly greater Satisfaction and perceived Relevance when using VR for engineering graphics, indicating that immersive technologies may be especially motivating for them and support more inclusive learning. No significant gender differences were observed in Attention or Confidence, suggesting similar levels of engagement and self-efficacy across genders. These findings should nonetheless be interpreted cautiously. Since the study did not include a control group or baseline measurements of spatial ability and previous experience with immersive technologies, causal relationships cannot be established. Future studies should incorporate controlled and longitudinal designs to further investigate the relationship between gender, motivation, and learning outcomes in VR-supported engineering education.

6. CONCLUSIONS

The results suggest that female students reported particularly positive motivational responses to the VR experience. However, the present data do not allow us to conclude that VR functions as a compensatory mechanism for gender-related differences. Rather, these findings indicate that VR-based learning environments may be especially engaging for female students, a possibility that should be explored in future studies using more robust experimental designs and additional learning-performance measures.

7. LIMITATIONS AND ETHICAL CONSIDERATIONS

A key limitation is the lack of a control group and baseline measurements, which prevents causal attribution of the observed differences to VR. Future studies should include control conditions and pre-post designs to better assess the impact of VR on motivation and learning outcomes. Participation was voluntary and anonymous. All students were informed about the study and provided informed consent prior to data collection. No personal data were collected, and results were analyzed in aggregated form.

REFERENCES

[1] Duffy, G., Sorby, S., Bowe, B. An investigation of the role of spatial ability in representing and solving word problems among engineering students. J Eng Educ. (2020) https://doi.org/10.1002/jee.20349

[2] Lampropoulos, G., Fernandez-Arias, P., del Bosque, A., Vergara, D. Virtual Reality in Engineering Education: A Scoping Review. Educ. Sci., 15(8), 1027 (2025); https://doi.org/10.3390/educsci15081027

[3] Faisal Abbas Shah, S., Mazhar, T., Shahzad, T., Amir khan, M., Yasin Ghadi, Y., Hamam, H. Integrating educational theories with virtual reality: Enhancing engineering education and VR laboratories. Social Sciences & Humanities Open 10 (2024). DOI: 10.1016/j.ssaho.2024.101207

[4] Cabero-Almenara, J., Roig-Vila, R. The motivation of technological scenarios in augmented reality (AR): results of different experiments. Appl Sci 9:2907. (2019). https://doi.org/10.3390/app91 42907

[5] Kim, Y., Baylor, A.L. A social-cognitive framework for pedagogical agents as learning companions. Educ Technol Res Dev 54:569-596. (2006). https://doi.org/10.1007/s11423-006-0637-3

[6] Yukselturk, E., Bulut, S. Gender differences in self-regulated online learning environment. Educ Technol Soc 12(3):12-22 (2009).

[7] Ayala-Alvarez, F., Blazquez-Parra, E.B., Montes-Tubio, F. Improving Graphic Expression Training with 3D Models. J. Visualization, 20 (4): 889-904. (2017). https://doi.org/10.1007/s12650-017-0424-8

[8] Lorenzo, G., Pomares, J., Lledó, A. Inclusion of immersive virtual learning environments and visual control systems to support learning. Computers & Education, 62, 1-10. (2013). https://doi.org/10.1016/j.compedu.2012.10.014

[9] Freina, L., Ott, M. A literature review on immersive virtual reality in education: State of the art and perspectives. En Proceedings of eLearning and Software for Education (eLSE) 133-141 (2015).

[10] Melian-Melian, J.A., Martín-Gutierrez, J. Design and usability of learning objects applied in graphic expression. Comput. Appl. Eng. Educ., 26(5): 1134-1149 (2018). https://doi.org/10.1002/cae.21946

[11] Keller, J.M. Development and use of DFFF the ARCS model of motivational design. J Instr Dev 10(3):2-10 (1987).

[12] Bolliger, D.U., Supanakorn, S., Boggs, C. Impact of Podcasting on Student Motivation in the Online Learning Environment. Computers & Education, 55 (2): 714-22. (2010). https://doi.org/https://doi.org/10.1016/j.compedu.2010.03.004

[13] Kew, S.N., Petsangsri. S., Ratanaolarn, T., Tasir, Z. Examining the motivation level of students in E-learning in higher education institution in Thailand: a case study. Educ Inf Technol 23(6): 2947-2967 (2018). https://doi.org/10.1007/s10639-018-9753-z

[14] Sketchfab (2026). Available in: https://sketchfab.com/DIBUJO_ETSIAM_1 (accessed 18 May 2026).

Competence Development in Aerospace Engineering Students through Project-Based Learning

Rebeca Martínez García*, Fernando J. Fraile Fernández, Covadonga Palencia, Víctor Baladrón Blanco, Jesús de Prado Gil

University of León, Campus de Vegazana s/n 24007 León

* e-mail: rmartg@unileon.es

Abstract: Project-Based Learning (PBL) is one of the most widely used active methodologies in engineering education, as it enables theoretical knowledge and practical application to be integrated in contexts close to professional practice. This paper presents a teaching experience implemented in the Graphic Expression II course of the Degree in Aerospace Engineering at the University of León. The core activity consisted of developing an airport design project, including a runway and a control tower, through technical drawing procedures and CAD tools. The aim of the study was to analyse students' perceived competence development after the implementation of this methodology. A 20-item Likert-type questionnaire was administered to 53 students and organised into four dimensions: planning and organisation, information management, creativity and innovation, and engineering-specific competences. The results show a positive student perception of PBL, especially in relation to spatial representation, CAD-based design, and the ability to propose original design solutions. The experience confirms the potential of PBL to promote active learning and professional competence development in engineering degrees.

Keywords: *Project-Based Learning, competences, aerospace engineering, graphic expression, active learning, CAD.*

1. INTRODUCTION

University engineering education has evolved in recent decades towards educational models focused on competence development. This shift has been strongly influenced by the European Higher Education Area, which promotes active learning methodologies aimed at preparing students for the challenges of professional practice [1].

In this context, Project-Based Learning (PBL) has become an effective teaching strategy for integrating theoretical knowledge with practical application. This methodology places students at the centre of the learning process and confronts them with open-ended problems that require analysis, decision-making and collaborative work [2]. Previous studies have shown that PBL supports the development of transversal competences such as planning, information management, creativity and problem solving, while also reinforcing engineering-specific technical competences [3,4].

In aerospace engineering degrees, graphic expression and design courses provide a particularly suitable environment for project-based methodologies, since they combine spatial reasoning, technical representation and the use of digital design tools. The aim of this paper is to present a PBL teaching experience implemented in Graphic Expression II and to analyse students' perceptions of the competences developed during the project.

2. TEACHING EXPERIENCE CONTEXT

The experience was carried out in the Graphic Expression II course in the second year of the Degree in Aerospace Engineering at the University of León. The main activity consisted of an airport design project in which students had to define the configuration of a runway and develop the architectural design of a control tower.

The exercise simulated a real engineering problem and included several elements commonly found in airport infrastructure projects. Students were asked to design a 3000 m long and 45 m wide runway, define its orientation and location within the airport, develop a 50 m high control tower distributed over 15 floors, and represent the project through technical drawings.

The project was organised into several phases: an initial investigation of existing runways and control towers, conceptual development through preliminary sketches, technical modelling and representation using CAD tools, and preparation of the final graphic documentation. The requested drawings included site plans, topographic drawings, longitudinal and cross sections, and plans, elevations and sections of the control tower.

3. RESEARCH METHODOLOGY

3.1. Participants

The study was conducted with students enrolled in the course during the 2020–2021 academic year. The population consisted of 66 students, of whom 53 voluntarily completed the questionnaire used to assess perceived competence development.

Although the data correspond to the 2020-2021 academic year, the teaching intervention analysed has remained substantially unchanged in subsequent academic years. Therefore, the study continues to provide relevant evidence regarding the educational potential of the proposed PBL methodology.

3.2. Data Collection Instrument

A 20-item questionnaire was used to analyse the level of competences developed. The items were grouped into four dimensions: planning and organisation, information management, creativity and innovation, and specific engineering competences. Responses were collected using a five-point Likert scale. The internal consistency of the instrument was assessed using Cronbach's alpha, obtaining a value of $\alpha = 0.93$, which indicates high questionnaire reliability.

The questionnaire was designed to evaluate students' perceived competence development following the completion of the project. The twenty items were organised into four competence dimensions aligned with the intended learning outcomes of the course: planning and organisation (five items), information management (four items), creativity and innovation (five items), and specific engineering competences (six items). This structure allowed both transversal and discipline-specific competences promoted through the PBL experience to be analysed. Each questionnaire item was specifically associated with one of these competence dimensions to facilitate the interpretation of students' perceived competence development.

3.3. Data Analysis

A descriptive analysis of students' responses was conducted in order to identify the competences most positively valued after the implementation of the PBL methodology.

4. RESULTS

The results obtained reveal a generally positive perception of competence development after the implementation of the Project-Based Learning methodology. Figure 1 presents the mean scores obtained for each of the 20 questionnaire items grouped into the four competence dimensions: planning and organisation, information management, creativity and innovation, and specific engineering competences.

Overall, all competence items obtained mean values above 3.40 on the five-point Likert scale, indicating a favourable student assessment of the learning experience. The highest-rated competences were related to the design and sketching of spatial ideas and concepts (4.11), the proposal of original ideas and solutions (3.98), independent learning (3.96), implementation of innovative projects (3.94), CAD-based graphic design for aerospace systems (3.94), and the analysis and solution of engineering problems (3.89) (Figure 1).

Lower scores were observed for creativity development (3.40) and time management (3.45), suggesting that these competences may require additional instructional support during project implementation. Nevertheless, even these dimensions achieved positive evaluations above the midpoint of the scale.

These findings indicate that the proposed PBL experience contributed simultaneously to the development of both transversal competences and discipline-specific engineering skills, particularly those associated with graphic representation, spatial reasoning and computer-aided design.

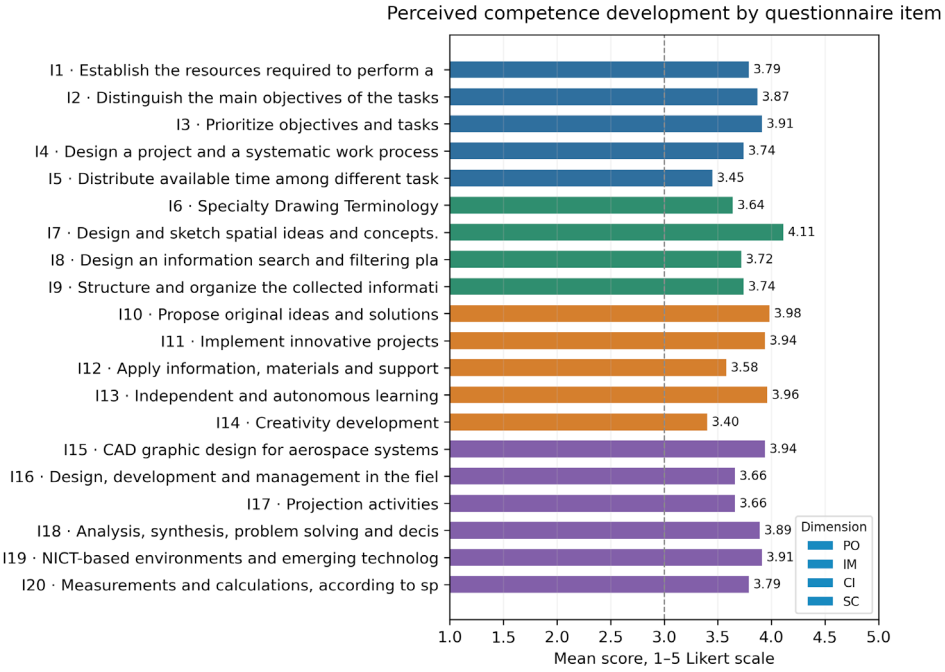


FIG. 1

Compact visual summary of mean scores for the 20 questionnaire items by competence dimension

5. EXAMPLES OF STUDENT WORK

The following figures show representative examples of the work produced by students during the project. Figure 2 illustrates preliminary sketches used during the conceptual design stage. Figure 3 presents a control tower design, while Figure 4 shows an example of computer-aided representation developed as part of the final graphic documentation.

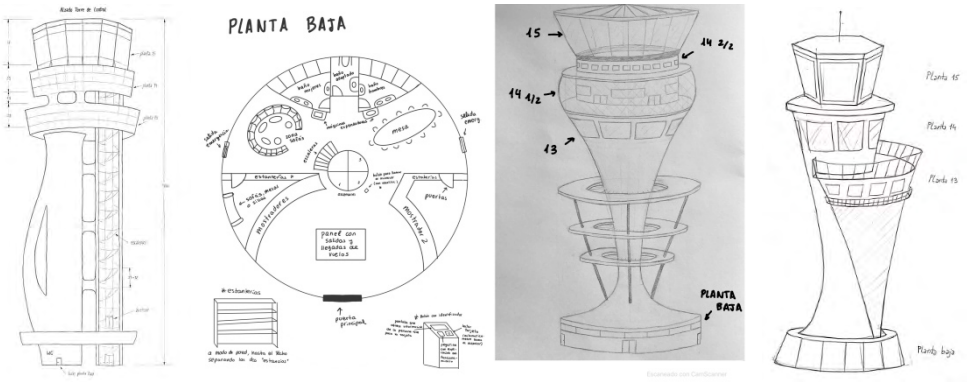


FIG. 2

Preliminary sketches of the control tower developed during the conceptual design stage

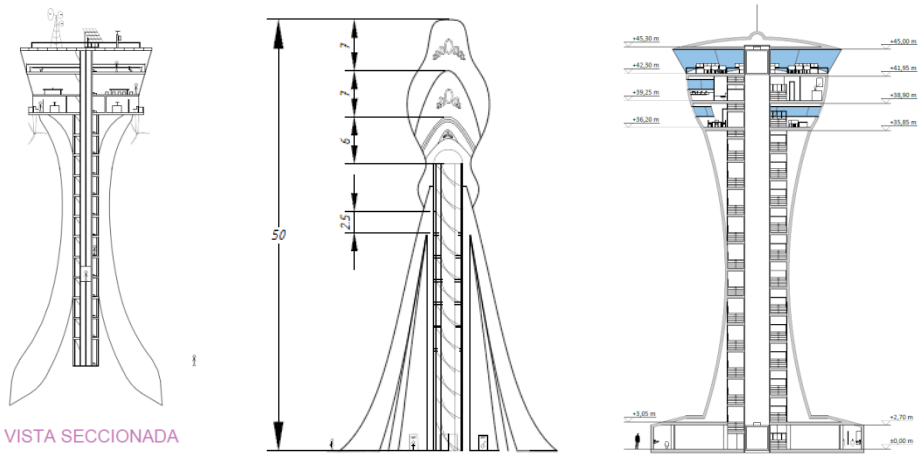


FIG. 3
Control tower design developed by students

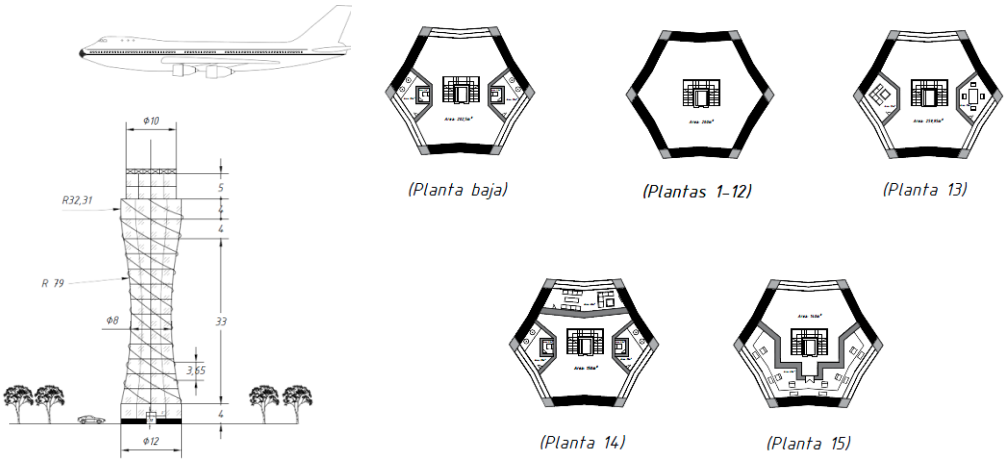


FIG. 4
Computer-aided design representation of the control tower

6. DISCUSSION

The preliminary results are consistent with previous studies highlighting the potential of Project-Based Learning to promote meaningful learning and competence development in engineering education [3-5]. The experience shows that a well-contextualised design activity can bridge graphic expression content, professional competences and student autonomy.

One of the most relevant aspects of the project is that it requires students to manage uncertainty. Unlike a closed practical exercise, the design of an airport-related solution requires students to make decisions, justify choices and revise their work as new needs emerge. This dynamic contributes to a less fragmented learning process that is closer to the way engineering problems are addressed in professional contexts [3,5].

Nevertheless, the experience also involves challenges. The implementation of PBL requires careful teaching planning, clear assessment criteria and sufficient guidance to prevent autonomy from becoming disorientation. It is also necessary to balance creative freedom with the achievement of the technical objectives of the course. Overall, these findings are consistent with previous studies reporting that Project-Based Learning promotes both technical and transversal competences in engineering education [5].

The results should nevertheless be interpreted considering several limitations. First, the assessment is based exclusively on students' self-perceptions rather than on objective measures of competence acquisition. Although perception-based questionnaires are widely used in educational research, they cannot fully determine the actual level of competence achieved.

Second, the study analyses a single cohort of students enrolled during the 2020–2021 academic year. Consequently, the findings should not be generalised without caution, particularly considering the exceptional educational context associated with that academic year.

Finally, no control group following a traditional teaching methodology was available. Therefore, although students reported positive competence development, direct comparisons with alternative instructional approaches cannot be established.

7. CONCLUSIONS

This study has analysed the contribution of a Project-Based Learning experience to competence development in the Graphic Expression II course of the Degree in Aerospace Engineering at the University of León.

Students reported positive competence development across all four analysed dimensions. The highest scores were obtained in competences associated with spatial design, CAD-based representation, creativity and autonomous learning, suggesting that PBL provides an effective framework for integrating technical knowledge with professional skills.

Despite these encouraging results, the study presents several limitations. The evaluation relies on students' perceptions, focuses on a single academic cohort, and does not include a control group taught using traditional methodologies. Consequently, the findings should be interpreted as evidence of perceived competence development rather than objective learning gains.

Future research should include multiple academic years, objective assessment indicators, mixed-method approaches and comparative analyses with conventional teaching approaches to provide stronger evidence of the educational effectiveness of Project-Based Learning in aerospace engineering education.

REFERENCES

[1] Rodríguez, J., Laverón-Simavilla, A., del Cura, J., Ezquerro, J., Lapuerta, V., Cordero-Gracia, M.: Project Based Learning experiences in the space engineering education at Technical University of Madrid. Advances in Space Research 56(7), 1319-1330 (2015). https://doi.org/10.1016/j.asr.2015.07.003

[2] Arias, E., Barba, V., Carrión, C., Casado, R.: Enhancing entrepreneurship education in a Master's degree in Computer Engineering: A Project-Based Learning approach. Administrative Sciences 8(4), 18 (2018). https://doi.org/10.3390/admsci8040058

[3] Coronado, J., Moyano, A., Romero, V., Ruíz, R., Rodríguez, J.: Student long-term perception of Project-Based Learning in Civil Engineering Education: An 18-year ex-post assessment. Sustainability 13(4), 1949 (2021). https://doi.org/10.3390/su13041949

[4] López, D., Ezquerro, J., Rodríguez, J., Porter, J., Lapuerta, V.: Motivational impact of active learning methods in aerospace engineering students. Acta Astronautica 165, 344-354 (2019). https://doi.org/10.1016/j.actaastro.2019.09.026

[5] Kuppuswamy, R., Mhakure, D.: Project-based learning in an engineering-design course: developing mechanical-engineering graduates for the world of work. Procedia CIRP 91, 565-570 (2020). https://doi.org/10.1016/j.procir.2020.02.215

Adaptive Support System for Reducing Resin Consumption in DLP 3D Printing Systems

Teresa Carranza[a,b], Iraia Osquila[b], Maialen Zelaia[c], Francesca Perin[b], Mireia Andonegi[b],*

[a] Université de Pau et des Pays de l'Adour, Pau, France

[b] University of the Basque Country (UPV/EHU), Donostia-San Sebastián, Spain

[c] Vicomtech, Donostia-San Sebastián, Spain

*e-mail: mireia.andonegi@ehu.eus

Abstract: Digital Light Processing (DLP) systems typically require large resin volumes to ensure stable printing conditions, generating significant material waste when fabricating small-scale components. In line with One Health principles promoting responsible resource use, this work presents a low-cost workflow for ultra-low-volume additive manufacturing. An adaptive support system was developed for a commercial DLP printer by replacing the original vat with a conventional Petri dish setup and incorporating a customized build platform attachment. The proposed configuration successfully completed fabrication cycles while drastically reducing the operational resin volume. Structural changes induced by this modification were evaluated using high-resolution micro-computed tomography (µ-CT) and Cloud-to-Mesh (C2M) signed distance analysis. The adaptive setup showed increased wall thickness and higher local spatial variability compared to the original platform. These geometric deviations were associated with lateral overcuring caused by light scattering through the polystyrene substrate and vat deflection. The results demonstrate an accessible strategy for minimizing polymer waste while using high-precision 3D metrology to characterize and control non-standard eco-friendly printing systems.

Keywords: *DLP, CAD design, material efficiency, additive manufacturing, sustainable design, One Health.*

1. INTRODUCTION

Digital Light Processing (DLP)–based additive manufacturing has experienced significant growth in recent years due to its ability to fabricate high-resolution components with complex geometries [1]. These systems are extensively used in fields such as biomedical engineering, microfabrication, functional devices and the development of advanced materials [3-5].

Compared with other 3D-printing technologies, DLP provides advantages in terms of geometric accuracy, fabrication speed and the reproduction of intricate internal structures [6]. This makes it especially attractive in research environments, where prototypes are often small and involve experimental or high-value materials.

However, most commercial DLP printers are designed with relatively large build areas and require substantial resin volumes to ensure proper surface wetting and stable printing conditions. As a result, even for millimetric components or small experimental batches, the minimum operational resin volume significantly exceeds the material consumed. This limitation is particularly relevant in research contexts, where frequent material changes and limited resin availability are common. The unnecessary waste of photopolymer increases both experimental cost and environmental impact. In this regard, optimizing material consumption in additive manufacturing aligns closely with the One Health framework, which promotes sustainable resource use and reduced environmental impact. By reducing the amount of resin required to operate DLP systems, waste generation can be significantly decreased without compromising manufacturing capabilities.

Previous studies have focused mainly on optimizing printing parameters and developing new photopolymer formulations [7,8], whereas fewer works have explored physical modifications to resin-containment systems that reduce the operational resin volume required during printing.

This work proposes an adaptive support system that replaces the original vat of a commercial DLP printer with a smaller Petri dish. The system was developed using computer-aided design (CAD) tools and fabricated with the same printer in which it was later implemented. This approach fosters an accessible and self-sufficient manufacturing workflow. Furthermore, the proposed modification reduces resin consumption significantly while maintaining stable printing performance. Geometrical accuracy was assessed through dimensional measurements (X, Y, Z) and μ-CT, enabling analysis of both external dimensions and complex internal features. The main contribution lies in offering a simple, low-cost, easily implementable solution that enhances material efficiency in DLP systems used for research and development.

2. MATERIALS AND METHODS

2.1. Materials and printing parameters

The adaptive attachment and all validation specimens were fabricated using a commercial Standard Resin Gray photopolymer (Anycubic) on an Anycubic Photon D2 DLP

printer. Printing was performed using a layer thickness of 0.05 mm, an exposure time of 2.3 s for standard layers, 28 s for the first 10 base layers, a lift height of 5 mm and a separation speed of 2 mm/s.

2.2. Adaptive system design

The adaptive system replaces the original commercial vat with a commercially available 90 mm Petri dish that serves as the resin container (Fig. 1). The Petri dish is positioned by two lateral supports, which also restrict the projected area to the Petri dish. A 55 mm diameter cylindrical insert attached to the build platform extends into the Petri dish during printing, displacing most of the resin volume and creating an annular resin channel between the insert and the dish wall. Finally, two retaining plates secure the Petri dish using the printer's original vat fastening system, preventing vertical displacement during the separation stage of the printing process.

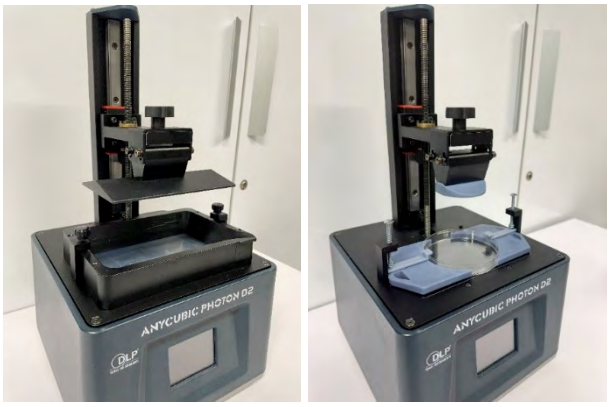


FIG 1
Original configuration of the Anycubic Photon D2 printer (left) and adaptive system developed using a Petri dish and an annular resin channel (right)

Unlike the conventional vat configuration, in which resin must cover the entire vat bottom, the proposed design confines the resin to the annular channel surrounding the printing area. Before fabrication, the printer Z-axis was recalibrated to compensate for the modified vat geometry, ensuring that the nominal layer thickness and all printing parameters remained identical to those of the original configuration.

2.3. Sample fabrication

Gyroid cellular structures were designed using MSLattice [9] with a target relative density of 30%, a nominal unit cell size of 3 mm, and external dimensions of 5 × 5 × 5 mm. Structures were fabricated using both the original vat configuration and the adaptive Petri dish-based setup using the same printing conditions described in Section 2.1.

2.4. Operational resin-volume assessment

The operational resin volume required to fabricate four gyroid cubes was obtained from the slicing software for both the original and adaptive configurations.

2.5. Geometrical characterization

Dimensional measurements were performed using a digital calliper along the X, Y and Z axes (n = 8).

Micro-computed tomography (μ-CT) imaging was conducted using a SkyScan 1172 system with binning enabled to accelerate acquisition (n = 5). Following reconstruction in NRecon software, high-resolution cross-sectional slices were exported as DICOM stacks for volumetric analysis. For each sample, the 2D slices were imported into a custom Python (v3.13) workflow and stacked into a 3D volumetric array. Noise reduction was performed using a Gaussian filter, followed by binarization-based segmentation using grayscale thresholding to isolate the printed geometry from the background. The Marching Cubes algorithm was then applied to generate high-resolution triangular surface meshes.

Metrological analysis was performed in CloudCompare (v2.13.2). The scanned STL mesh and reference CAD model were aligned through manual pre-positioning followed by Iterative Closest Point (ICP) registration using a convergence threshold of RMS < 10^{-5}. The scanned mesh was subsequently sampled into a dense point cloud for signed Cloud-to-Mesh (C2M) distance analysis, enabling the quantification of local geometric deviations. Positive values indicated oversizing, whereas negative values corresponded to shrinkage or material deficit. Mean deviation (μ) and standard deviation (σ) values were extracted from the resulting histograms and mapped onto the 3D geometry using a blue–white–red colour scale for spatial visualization.

Statistical comparisons between configurations were performed using Student's t-test (SPSS Statistics 25), with significance established at $p < 0.05$.

3. RESULTS AND DISCUSSION

3.1. Reduction of operational resin volume

The estimated operational resin volume decreased from approximately 50 mL in the original configuration to 9 mL using the adaptive Petri dish system, corresponding to an 82% reduction while maintaining stable printing conditions for the fabrication of four gyroid cubes.

Although the amount of resin incorporated into the printed structures remained unchanged, the proposed configuration substantially reduced the amount of resin that must be available in the vat to perform the printing process. This reduction is particularly advantageous for research applications involving expensive or experimental photopolymers, where minimizing the operational resin inventory can significantly reduce material waste and operating costs.

3.2. Geometrical validation

Dimensional measurements performed using a digital calliper along the X, Y and Z axes revealed statistically significant differences between the original and adaptive configurations ($p < 0.05$). As shown in Table 1, samples printed with the adaptive system exhibited slightly larger dimensions in all measured axes. Representative optical images of the fabricated samples are shown in Fig. 2.

TABLE 1

Dimensions of gyroid cube structures fabricated using the original and adaptive configurations (mean ± SD, n = 8). Different letters indicate significant differences ($p < 0.05$)

Configuration	X [mm]	Y [mm]	Z [mm]
Original	4.99 ± 0.07a	4.96 ± 0.06a	4.97 ± 0.05a
Adaptive	5.13 ± 0.03b	5.10 ± 0.05b	5.11 ± 0.04b

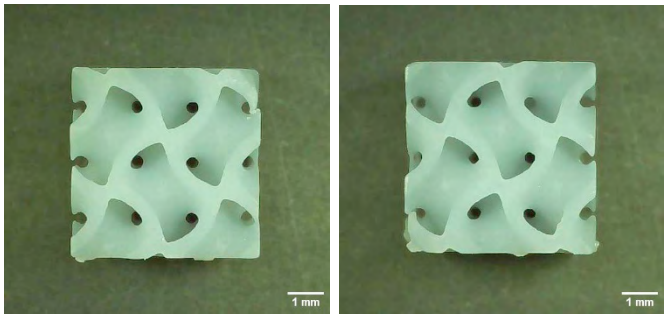


FIG. 2

Optical images of gyroid structures fabricated using the original (left) and adaptive (right) printing configurations

The metrological evaluation of the printed gyroid structures via Micro-CT and CloudCompare revealed significant geometric discrepancies between both configurations (Table 2). The control group exhibited remarkable geometric fidelity, with a stable global mean error (μ) of 22.8 µm and low dispersion (σ = 33.2 µm). Conversely, the adaptive configuration increased the global mean error to 67.0 µm and doubled the local variability (σ = 58.5 µm). Student's t-test confirmed that these differences were statistically significant ($p < 0.05$).

This behaviour is clearly reflected in the 3D colour maps and error distribution histograms (Fig. 3). While the control group displayed deviations predominantly within ±30 µm, the adaptive configuration showed a broader error distribution and a generalized positive deviation, indicating systematic wall thickening. The observed increase in mean error and local variability is likely related to the altered optical and mechanical behaviour of the modified vat. The optical properties of the injection-moulded polystyrene Petri dish may promote

light scattering at the resin interface, allowing light to extend beyond the intended pixel boundaries and leading to lateral overcuring and systematic oversizing of the printed walls. In addition, its lower stiffness compared with the original vat may allow slight deformation during the printing cycle, particularly during the separation stage, causing local variations in layer thickness and contributing to the increased geometric variability.

TABLE 2

Global geometric deviation (C2M) parameters for the analysed printing systems (mean ± SD, n = 5). Different letters indicate significant differences ($p < 0.05$)

Configuration	Global mean error (μ) [μm]	Global standard deviation (σ) [μm]
Original	22.8 ± 0.7a	33.2 ± 2.6a
Adaptive	67.0 ± 5.4b	58.5 ± 4.3b

Although the adaptive configuration introduced statistically significant geometric deviations, the global mean error remained below 100 μm, highlighting the trade-off between material efficiency and geometric fidelity. Therefore, the proposed system is suitable for applications where material efficiency is prioritized over maximum dimensional accuracy, such as preliminary prototyping, proof-of-concept studies, educational applications, or research involving expensive or experimental photopolymers. In these cases, the substantial reduction in operational resin volume may outweigh the moderate loss in geometric fidelity. Conversely, applications requiring high geometric fidelity or tight dimensional tolerances would benefit from the conventional vat configuration. Future work should focus on replacing the commercial polystyrene Petri dish with a container specifically designed for DLP printing, providing improved optical transparency and higher stiffness, together with optimization of the printing parameters to further reduce geometric deviations.

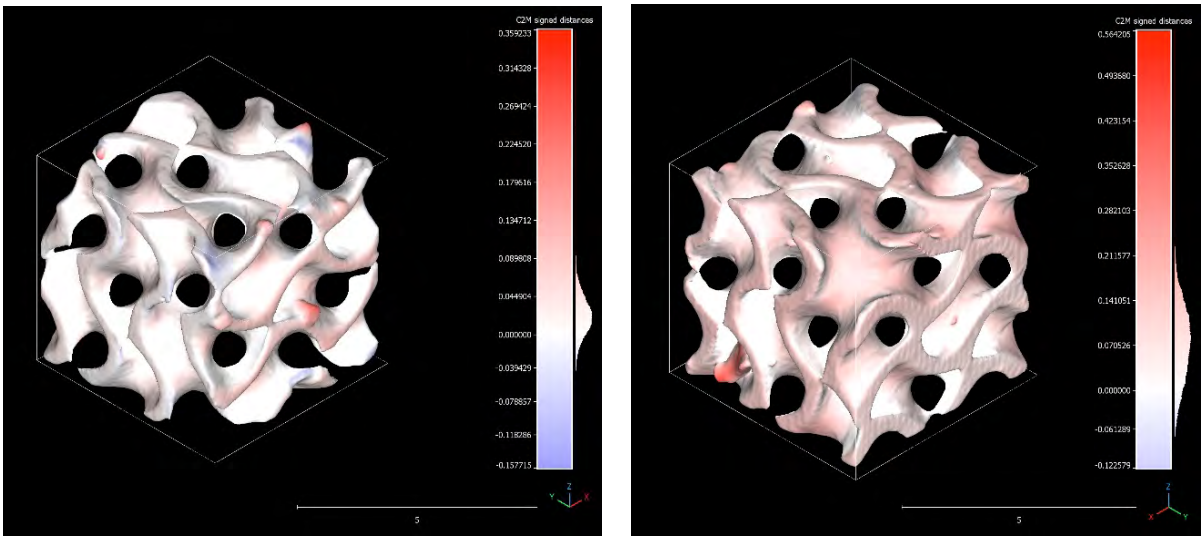


FIG. 3

3D error maps (signed C2M distances) and probability density distributions for the original control (left) and adaptive configuration (right)

4. CONCLUSIONS

This work successfully validated an adaptive support system that significantly enhances material efficiency in DLP 3D printing. By replacing the commercial vat with a customized Petri dish setup, the minimum operational resin volume was drastically reduced, alignment-checking additive manufacturing practices with the sustainability principles of the One Health framework.

Full-volume metrological characterization of complex gyroid scaffolds revealed that while the modification enables stable printing workflows, it introduces micro-scale geometric trade-offs. The adaptive configuration led to a statistically significant increase in the global mean error and a pronounced widening of local dimensional variability. These discrepancies were successfully captured by 3D metrology and attributed to lateral overcuring from light scattering through the unoptimized polystyrene substrate, alongside cyclic micro-deformations caused by dynamic vat deflection and coating thickness asymmetry.

Ultimately, the proposed system offers a highly accessible, low-cost strategy to minimize photopolymer waste in research environments. Future optimization of the container's base optical quality and rigidity will help close the accuracy gap observed relative to factory-default configurations.

Acknowledgements: IO and TC acknowledge the Basque Government for the predoctoral and postdoctoral fellowships PRE_2025_1_0060 and POS_2025_1_0045, respectively. MZ acknowledges the Basque Government for funding the PULMO3D project (2025333046). FP acknowledges support from MICIU (PID2024-162567OA-I00) and the BBVA Foundation (2025 Leonardo Grant). MA acknowledges support from the UPV/EHU through the *Ayudas a Proyectos de Investigación UPV/EHU* (EHU-N25/05).

REFERENCES

[1] Chaudhary, R., Fabbri, P., Leoni, E., Mazzanti, F., Akbari, R., Antonini, C.: Additive manufacturing by digital light processing: a review. Progress in Additive Manufacturing 8, 331–351 (2023), https://doi.org/10.1007/s40964-022-00336-0.

[2] Hosseinabadi, H.G., Khatami, S.M., Ahmadi, Z., *et al.*: Digital Light Processing Bioprinting Advances for Micro-Tissue Engineering. ACS Biomaterials Science & Engineering 8(6), 2346-2363 (2022). https://doi.org/10.1021/acsbiomaterials.1c01509.

[3] Wang, X., Liu, J., Zhang, Y., Kristiansen, P.M., Islam, A., Gilchrist, M., Zhang, N.: Advances in precision microfabrication through digital light processing: system development, material and applications. Virtual and Physical Prototyping 18(1), e2248101 (2023), https://doi.org/10.1080/17452759.2023.2248101.

[4] Schneidermann, C., Adams, M.: 3D digital light processing of redox-active polymers for switchable electrochemical devices. Advanced Functional Materials 35(45), 2518546 (2025). https://doi.org/10.1002/adfm.202518546.

[5] Zhou, L., Wang, Y.: Digital Light Processing 3D Printing Technology in Biomedical Engineering. Macromolecular Bioscience 25(6), e202500101 (2025). https://doi.org/10.1002/mabi.202500101.

[6] Smith, J., Davis, R.: Development of photocurable hybrid polyurethane/acrylic resins with controlled molar mass for DLP 3D printing of scaffolds. Reactive and Functional Polymers 201, 106840 (2026). https://doi.org/10.1016/j.reactfunctpolym.2025.106570.

[7] Dhand, A.P., Juarros, M.A., Leinwand, L.A., Burdick, J.A.: Digital light processing 3D printing enables versatile fabrication of human engineered heart tissues. Cell Reports Biomaterials 2(1), 100405 (2026). https://doi.org/10.1016/j.celbio.2026.100405.

[8] Al-Ketan, O., Abu Al-Rub, R.K.: MSLattice: A free software for generating uniform and graded lattices based on triply periodic minimal surfaces. Material Design & Processing Communications 3(1), e205 (2020). https://doi.org/10.1002/mdp2.205.

3D-Printed Mechanical Assemblies from Recycled PET as Sustainable Teaching Resources in Graphical Engineering

Lorena Ugarte[a, c, *], María Lozano[b, c], Kizkitza Gonzalez[b, c]

[a] Department of Graphical Design and Project Engineering, Engineering Faculty of Gipuzkoa, Eibar section, EHU, Otaola Hiribidea 29, 20600 Eibar, Gipuzkoa

[b] Department of Graphical Design and Project Engineering, Engineering Faculty of Gipuzkoa, EHU, Plaza Europa 1, 20018 Donostia-San Sebastian, Gipuzkoa

[c] GMT 'Materials + Technologies' Research Group, Department of Chemical and Environmental Engineering, Engineering Faculty of Gipuzkoa, EHU, Plaza Europa 1, 20018 Donostia-San Sebastian, Gipuzkoa

* e-mail: lorena.ugarte@ehu.eus

Abstract: Developing spatial visualization skills is a major challenge for first-year Industrial Engineering students, particularly in graphical engineering courses where interpreting 2D technical drawings as 3D objects is required. Many students experience difficulties mentally reconstructing geometries from orthographic projections, which can negatively affect the understanding of fundamental engineering concepts. In this context, physical models can facilitate the transition from abstract graphical representation to tangible understanding. This work presents the design and fabrication of 3D-printed mechanical assemblies as teaching resources aimed at supporting the development of spatial visualization skills by directly comparing graphical representations with real geometries. The assemblies were specifically designed to address common challenges in introductory graphical engineering courses, such as section views, hidden features, and assembly relationships between parts. A distinctive aspect of this work is its development within the framework of the Campus Bizia Lab (CBL) programme at Euskal Herriko Unibertsitatea (EHU), which promotes collaboration among academic and technical staff, and students to address sustainability challenges. In this case, plastic waste generated within the Faculty of Engineering was transformed into educational resources. The work was developed in Bachelor's Thesis projects involving PET bottle collection, cleaning, filament production and 3D printing processes. Environmental sustainability of the process was assessed by Life Cycle Analysis. The resulting mechanical assemblies demonstrate the feasibility of producing low-cost and sustainable teaching tools using recycled materials and additive manufacturing technologies. Although their educational impact has not yet been quantitatively assessed, the resources are currently being prepared for classroom implementation and future evaluation.

Keywords: *Spatial visualization, Mechanical assemblies, Circular economy in education, 3D printing, Teaching resources.*

1. INTRODUCTION

Spatial visualization skills are considered fundamental competencies in engineering education, particularly in graphical engineering courses where students must interpret two-dimensional technical drawings and mentally reconstruct three-dimensional geometries. However, first-year engineering students frequently experience difficulties in this process, especially when dealing with orthographic projections, section views, or complex assemblies [1]. Limited spatial visualization ability can negatively affect both academic performance and the understanding of core engineering concepts. Consequently, numerous studies have highlighted the importance of implementing teaching strategies specifically aimed at improving these skills during the early stages of engineering education [2]. Recent studies also continue to emphasize the relationship between spatial visualization skills, cognitive development, and engineering performance [3].

Among the different educational approaches proposed in the literature, the use and manipulation of physical models have proven to be particularly effective in facilitating the transition from abstract graphical representation to tangible understanding. Previous studies have shown that hands-on interaction with physical manipulatives can significantly enhance spatial visualization skills in engineering drawing courses [4]. In recent years, additive manufacturing technologies have emerged as valuable tools for producing customized educational resources in engineering education due to their accessibility, low cost, and versatility [5]. In particular, the use of 3D-printed manipulatives has demonstrated positive effects on students' understanding of geometries and engineering assemblies in introductory graphical engineering courses [6].

At the same time, engineering education is increasingly incorporating sustainability and circular economy principles into teaching practices. The circular economy promotes resource efficiency and waste reutilization through closed-loop systems [7]. In line with this perspective, recycled polymers derived from plastic waste have gained attention as sustainable feedstock materials for additive manufacturing applications. In this context, the Campus Bizia Lab initiative promoted by Euskal Herriko Unibertsitatea (EHU) encourages transdisciplinary collaboration among academic and technical staff and students to address real sustainability challenges within the university community. The programme promotes projects aligned with the Sustainable Development Goals through practical actions connected to teaching, research, and campus management. Within this context, the present work proposes the transformation of plastic waste generated within the Faculty of Engineering of Gipuzkoa into educational resources for graphical engineering courses. The environmental sustainability of as-fabricated teaching resources was evaluated by Life Cycle Analysis (LCA).

Specifically, this work presents the development of 3D-printed mechanical assemblies manufactured using recycled polyethylene terephthalate (PET) filament obtained from plastic bottles collected on-site. The proposed approach combines engineering graphics education, additive manufacturing, and sustainability-oriented practices to create low-cost educational resources while promoting circular economy principles in higher education contexts.

2. EXPERIMENTAL

2.1. Materials

Single-use PET bottles were used for filament fabrication. After collecting, bottles were hand chopped and dried for 20 h at 120 °C.

2.2. Filament production

Filament was produced by hot-melt extrusion using a HAAKE MiniLab twin-screw extruder at 265 °C and 50 rpm, using a nozzle with a diameter of 1.75 mm.

2.3. 3D printing

3D printing was carried out using the extruded filament in a NX Pro (Indart3D S. Coop.) FDM printer. Printing conditions were set at 260 °C nozzle temperature, 20 mm s^{-1} printing speed and 20% infill density. Rectilinear infill pattern at ± 45° was employed. 3D models of non-standard parts were designed in Solid Edge® 2023 software and these models were converted to gcode format using Simplify3D® software.

2.4. Thermal characterization

Thermal processing window of filaments was settled between melting and degradation temperatures. Melting temperature of the filament was determined by Differential Scanning Calorimetry (DSC) using a Mettler Toledo DSC3+ equipment, using samples of 5-10 mg sealed in aluminium pans. A heating stage was carried out in –80 °C - 240 °C temperature range at a scanning rate of 20 °C min^{-1} in N_2 atmosphere. Melting temperature was settled as the maximum of the endothermic peak observed in the scan. Thermal degradation temperature was determined by Thermogravimetric Analysis (TGA) using a TGA/SDTA851 equipment. Again, samples of 5-10 mg were heated from 25 °C to 800 °C at a scanning rate of 10 °C min^{-1} under N_2 atmosphere. The starting point of thermal degradation was defined as 5 % weight loss.

2.5. Life Cycle Analysis

Environmental impacts associated with mechanical assembly printing were evaluated by LCA [8]. For that end, the following scenario was defined: printing non-standard parts of M-055 mechanical assembly, using recycled PET filament.

The inventory analysis was carried out based on the inputs and outputs quantified in the laboratory (Table 1). LCA assessment was implemented by OpenLCA 1.11 software together with Ecoinvent 3.9 database. Environmental impacts were classified in 18 midpoint indicators, according to ReCiPe 2016 Midpoint (H) method. Midpoint indicators were cho-

sen instead of endpoint indicators since midpoint indicators focus on specific environmental issues. Endpoint indicators, instead, reflect the impacts in three main aggregation levels: human health, biodiversity and resource scarcity.

TABLE 1
Inventory analysis

	Flow	Quantity	Unit	Provider
Inputs	Recycled PET	2186.59	g	Elementary flow
Energy	Electricity	125.7	kWh	Electricity voltage transformation from high to medium voltage| electricity, medium voltage| Cutoff, U - ES
Outputs	Recycled PET	1203.19	g	Elementary flow
	M-055 mechanical assembly	983,40	g	Elementary flow

3. RESULTS AND DISCUSSION

During the collection phase, 9 kg of single-use PET bottles were gathered through an awareness campaign involving posters and collection points distributed within the Engineering Faculty, Gipuzkoa. Thermal characterization of collected PET waste revealed a melting temperature of 251 °C and a degradation temperature of 370 °C. Based on these results, a processing temperature of 265 °C was selected for filament production. These values are consistent with those commonly reported for PET processing in fused filament fabrication, where a temperature in the range of 250-280 °C is typically employed to ensure adequate melt flow while minimizing thermal degradation [9].

The extrusion process yielded 72 g of filament per 100 g of PET bottles, corresponding to a 72 % material yield. A single 50 mL bottle produced approximately 3.4 m of printable filament. Both gathered PET bottles and the fabricated filament are shown in Figure 1.



FIG. 1
(Left) gathered PET bottles, and (right) fabricated filament

Using the recycled filament, several mechanical assembly components commonly employed in graphical engineering courses were successfully modelled and fabricated, obtaining geometrically stable parts. Due to limitations in 3D printer dimensions, the base part was fabricated on a different printer using polylactic acid (PLA) filament. The resulting assemblies allow students to directly compare technical drawings with physical geometries, supporting the interpretation of section views, hidden features, and assembly relationships between components. The CAD model, gcode model and printed assembly are shown in Figure 2.

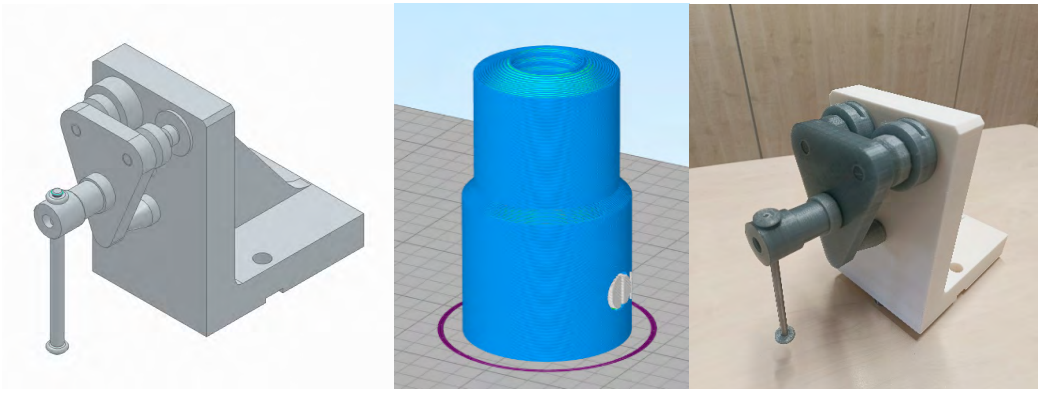


FIG. 2
(Left) CAD model, (centre) gcode model, and (right) 3D-printed assembly

From an environmental sustainability perspective, the LCA assessment revealed that the main impacts occurring due to assembly printing were fossil resource scarcity, global warming, human toxicity (non-cancerigenous), ionizing radiation and terrestrial ecotoxicity. Moreover, electricity consumption during the drying stage was identified as the main contributor to these environmental impacts, particularly regarding global warming and fossil resource scarcity. Similar trends have been reported in recycling and additive manufacturing studies, where energy consumption associated with thermal processing stages represents one of the most critical environmental hotspots [10]. In view of these results a sensitivity analysis was carried out. Results demonstrated that optimizing oven capacity utilization significantly reduced environmental impacts across all evaluated indicators. These results highlight the importance of process optimization when implementing circular manufacturing strategies based on recycled polymers.

4. CONCLUSIONS

This work proves the feasibility of transforming PET bottle waste generated within the Faculty of Engineering, Gipuzkoa into functional educational resources for graphical engineering courses. The proposed recycling methodology enabled the successful production of recycled PET filament and its subsequent use in the fabrication of 3D-printed mechanical assemblies suitable for teaching applications.

The developed assemblies provide tangible support for the interpretation of technical drawings and mechanical relationships between parts, contributing to the development of

spatial visualization skills in first-year engineering students. In addition, the project demonstrates how sustainability and circular economy principles can be effectively integrated into engineering education through practical and locally implemented initiatives.

The Life Cycle Assessment also highlighted the importance of process optimization, identifying electricity consumption during the drying stage as one of the main environmental contributions. Nevertheless, the sensitivity analysis demonstrated that improving oven utilization could significantly reduce environmental impacts.

The proposed approach represents a low-cost, sustainable, and easily replicable strategy for the development of didactic materials in graphical engineering education, enabling the creation of tangible educational resources while integrating additive manufacturing and circular economy principles into the learning process.

Acknowledgements: Authors acknowledge the financial support provided by Euskal Herriko Unibertsitatea (EHU) through the Campus Bizia Lab programme (24UGAR, 25UGAR), promoted by the Directorate of Sustainable Development and Social Commitment. Authors also thank for technical and human support provided by SGIker (UPV/EHU/ERDF, EU).

REFERENCES

[1] Sorby, S.A.: Educational research in developing 3-D spatial skills for engineering students. International Journal of Science Education 31(3), 459-480 (2009). DOI: 10.1080/09500690802595839

[2] Contero, M., Naya, F., Company, P., Saorín, J.L., Conesa, J.: Improving visualization skills in engineering education. IEEE Computer Graphics and Applications 25(5), 24-31 (2005). DOI: 10.1109/MCG.2005.107

[3] Sharma, G.V.S.S.: Spatial visualization for development of visual thinking and cognitive abilities among mechanical engineering students through tool design ideation. International Journal of Mechanical Engineering Education 51(4), 227-242 (2023). DOI: 10.1177/03064190231164049

[4] Tumkor, S., de Vries, R.H.: Enhancing spatial visualization skills in engineering drawing courses. 122nd ASEE Annual Conference & Exposition, pp. 26.663.1-26.663.12. American Society for Engineering Education, Seattle, WA (2015). DOI: 10.18260/p.24001

[5] Ford, S., Minshall, T.: Invited review article: Where and how 3D printing is used in teaching and education. Additive Manufacturing 25, 131-150 (2019). DOI: 10.1016/j.addma.2018.10.028

[6] Friess, W.A., Rodríguez, J.: Improvements in student spatial visualization in an introductory engineering graphics course using open-ended design projects supported by 3-D printed manipulatives. 123rd ASEE Annual Conference & Exposition, pp. 27.1162.1-27.1162.15. American Society for Engineering Education, New Orleans, LA (2016). DOI: 10.18260/p.25608

[7] Geissdoerfer, M., Savaget, P., Bocken, N.M.P., Hultink, E.J.: The Circular Economy – A new sustainability paradigm? Journal of Cleaner Production 143, 757-768 (2017). DOI: 10.1016/j.jclepro.2016.12.048

[8] ISO 14040:2006: Environmental management — Life cycle assessment — Principles and framework. International Organization for Standardization, Geneva (2006).

[9] Bustos Seibert, M., Mazzei Capote, G.A., Gruber, M., Volk, W., Osswald, T.A.: Manufacturing of a PET Filament from Recycled Material for Material Extrusion (MEX). Recycling 7(5), 69 (2022). DOI: 10.3390/recycling7050069

[10] Peng, T., Kellens, K., Tang, R., Chen, C., Chen, G.: Sustainability of additive manufacturing: An overview on its energy demand and environmental impact. Additive Manufacturing 21, 694-704 (2018). DOI: 10.1016/j.addma.2018.04.022

Improving the design of a laboratory-scale membrane reactor to produce hydrogen by reforming of biomass derivatives

José Valecillos[a], *, Negin Karim Zadeh Bajgiran[b], Gorka Elordi[b], Aingeru Remiro[b], Ana G. Gayubo[b]

[a] Department of Graphic Design and Engineering Projects, UPV/EHU, 48013 Bilbao

[b] Department of Chemical Engineering, UPV/EHU, 48940 Leioa

* e-mail: jose.valecillos@ehu.eus

Abstract: Sustainable hydrogen (H_2) production is one of the actions for a decarbonized economy positively impacting our health. For this, the use of membrane reactors (MR) is an attractive option to optimize its production from green reforming processes such as the steam reforming (SR) of ethanol. Herein, we propose a design improvement of a membrane reactor bench, entailing the configuration and geometric design of the Pd membrane (commercial or prepared by electroless pore plating (ELPP)). Demonstration reaction tests were conducted for the steam reforming (SR) of ethanol at 550°C, steam/ethanol molar ratio of 3, pressures ranging 1-3 atm and using a $Ni/MgAl_2O_4$ catalyst. The results suggest that the best configuration was that using a single Pd membrane installed employing standard fittings. The higher permeation capacity of this option was possible by synthesizing a thin Pd film on a CeO_2/porous-stainless-steel support giving rise to a composite membrane. The SR reaction tests showed that the H_2 production was increased when operating as a MR, and this increase was even better when the reaction pressure was progressively increased while keeping constant the permeate pressure (vacuum at 0.2 atm). This study demonstrates the successful implementation of design improvements to this laboratory-scale membrane reactor bench to test and optimize H_2 formation processes.

Keywords: *Pd Membrane Reactor (MR), Steam Reforming (SR), Hydrogen (H_2), Ethanol, Bio-oil.*

1. INTRODUCTION

Hydrogen (H_2) is a typical building block in the chemical industry and a prospective energy vector for the transition towards a sustainable and decarbonized system. However, its current production greatly depending on fossil resources must be reshaped by employing renewable resources. Based on the possibility of recycling the existing production facilities, an interesting alternative is the simple replacement of natural gas with oxygenated compounds derived from biomass. The steam reforming (SR) of ethanol or bio-oil has been extensively studied for this purpose, proceeding over Ni catalysts at high temperatures (500-700 °C) [1]. The reaction mechanism involves the decomposition of the oxygenated compounds into H_2, CH_4, CO or CO_2, and the interconversion of these by SR ($CH_4 + H_2O \leftrightarrow 3H_2 + CO$), the water gas shift (WGS) reaction ($CO + H_2O \leftrightarrow H_2 + CO_2$) and decomposition ($CH_4 \leftrightarrow 2H_2 + C$). Thus, the H_2 production is limited by the thermodynamics of these equilibrium reactions, which is often solved by adjusting the operating conditions (temperature, pressure or steam/ethanol ratio) [2].

The use of a membrane reactor (MR) employing a selective H_2 membrane is a promising strategy to optimize the H_2 production in such reforming processes. For this, palladium (Pd) membranes are the most adequate choice since they have a good mechanical and thermal resistance for their operation in reforming reactors [3]. Many studies have proved that the removal of H_2 from the reaction medium effectively shift the equilibrium towards the formation of H_2, overcoming the thermodynamic constrains in the SR of ethanol [4,5]. The MR performance is mainly determined by the operating temperature and the transmembrane pressure (which is the difference between the H_2 partial pressure in the retentate and permeate sides). Both variables affect the permeability of the membrane (as described by the Richardson equation (1)) and the kinetics and thermodynamics of the reactions. The increase in the temperature is positive for the membrane and reaction performances but limited to 600 °C to avoid damaging the Pd film (caused by embrittlement). The increase in the transmembrane pressure is always positive for increasing the membrane permeability, however, it may have an opposed effect on the reaction performance if it is increased by increasing the retentate (reactor) pressure.

$$J_{H2} = L^0_{H2} \cdot e^{-E_a/(R \cdot T)} \left(\sqrt{P_{H2,retentate}} - \sqrt{P_{H2,permeate}} \right) \quad (1)$$

Most of the studies reported in the literature are based on the strategy of increasing the reactor (retentate side) pressure to provide enough transmembrane pressure. Nevertheless, lowering the permeate pressure is a more interesting strategy as it helps to reduce the operating pressure of the reactor (retentate side). A decrease in the permeate pressure can be achieved adequately by sweeping the permeate with steam to facilitate the H_2 recovery or by operating the permeate side under vacuum. Tosti el al. [6] compared the use of sweep gas and vacuum for the permeate side of a WGS membrane reactor and found that the use of vacuum significantly improved the H_2 recovery. Likewise, Shirasaki *et al.* [7] have proposed the use of vacuum in the permeate for the development of a natural gas membrane reformer.

In this work, we propose the design improvement of a laboratory-scale membrane reactor bench and its demonstration for evaluating the performance of different reaction systems with the uniqueness of operating the permeate side under vacuum. The improvement is mainly focused on the membrane installation system and on the geometry of the Pd mem-

brane to adapt it to the reactor easily. Both commercial and laboratory-made tubular Pd membranes are employed. The demonstration consisted of successfully testing the SR of ethanol in a MR.

2. METHODOLOGY

The design of the Pd membrane reactor is based on a customized reactor bench fabricated with the collaboration of PID Eng & Tech (reference MU-01-PP20011IBF-UPV) [5]. Figure 1a shows the process flow diagram mainly consisting of two reactors connected in series. In this system, the liquid and gas feeds enter the thermal treatment reactor (R-01) for pretreatment (mixing, vaporization, preheating and removal of heavy components in case of bio-oil feeds). The resulting stream directly enters the catalytic reforming reactor (R-02) to produce H_2 or syngas and it is operated as either conventional reactor (CR) or membrane reactor (MR). When operated as a MR, the permeate side is the inner side of the membrane tube and is connected to a vacuum pump to induce permeation. This results in a permeate product stream rich in H_2 and a retentate product stream containing the non-permeated components.

The insertion of the Pd membrane was to be done from the top lid of the R-02 reactor only, due to restrictions posed by the bench design. Figure 1b shows the two installation systems tested by either employing a single Pd membrane connected with standard fittings (option A) or a commercial sealing system (Spectite®) to connect multiple Pd membranes (option B). Tubular composite Pd membranes were prepared with the geometry specified in Figure 1c for option A, whereas three Pd-Ag commercial membranes were employed for option B. Each option provided an equal total geometric transfer area of 22.4 cm^2.

2.1. Membranes

The commercial Pd-Ag membranes (for option B, membrane denoted as B) were purchased from REB Research and Consulting, and consisted of a Pd-Ag foil (thickness of 75 μm) rolled and supported on a compressed spring with a diameter of 1/8" and length of 7.5 cm. These membranes are blinded at one end and welded to a regular stainless steel (SS) tube at the other serving as the permeate side.

The single Pd membranes (for option A) were prepared using the electroless pore-plating (ELPP) method [3,5]. A porous stainless steel (PSS) tube, purchased from Mott Corporation, with a diameter of 3/8" was employed for the fabrication of the membrane support following the design specifications in Figure 1c. The overall procedure consisted of six steps: (i) cleaning of the PSS tube, (ii) calcination of the tube at 575 °C, (iii) vacuum assisted dip coating with CeO_2 and polyvinyl alcohol (PVA); (iv) a second calcination (at 450 °C) to remove the PVA; (v) surface activation by Pd seeding in the porous surface and (vi) Pd layer deposition by ELPP at 60 °C repeated several times until the Pd film is completely dense. The thickness of the Pd layer was estimated by weight difference before and after each Pd deposition. The support was characterized by scanning electron microscopy (SEM) with a field emission gun scanning electron microscope FEG-SEM Hitachi S-4800 N at different synthesis steps to verify the formation of the dense film of Pd. Membranes are named as A.

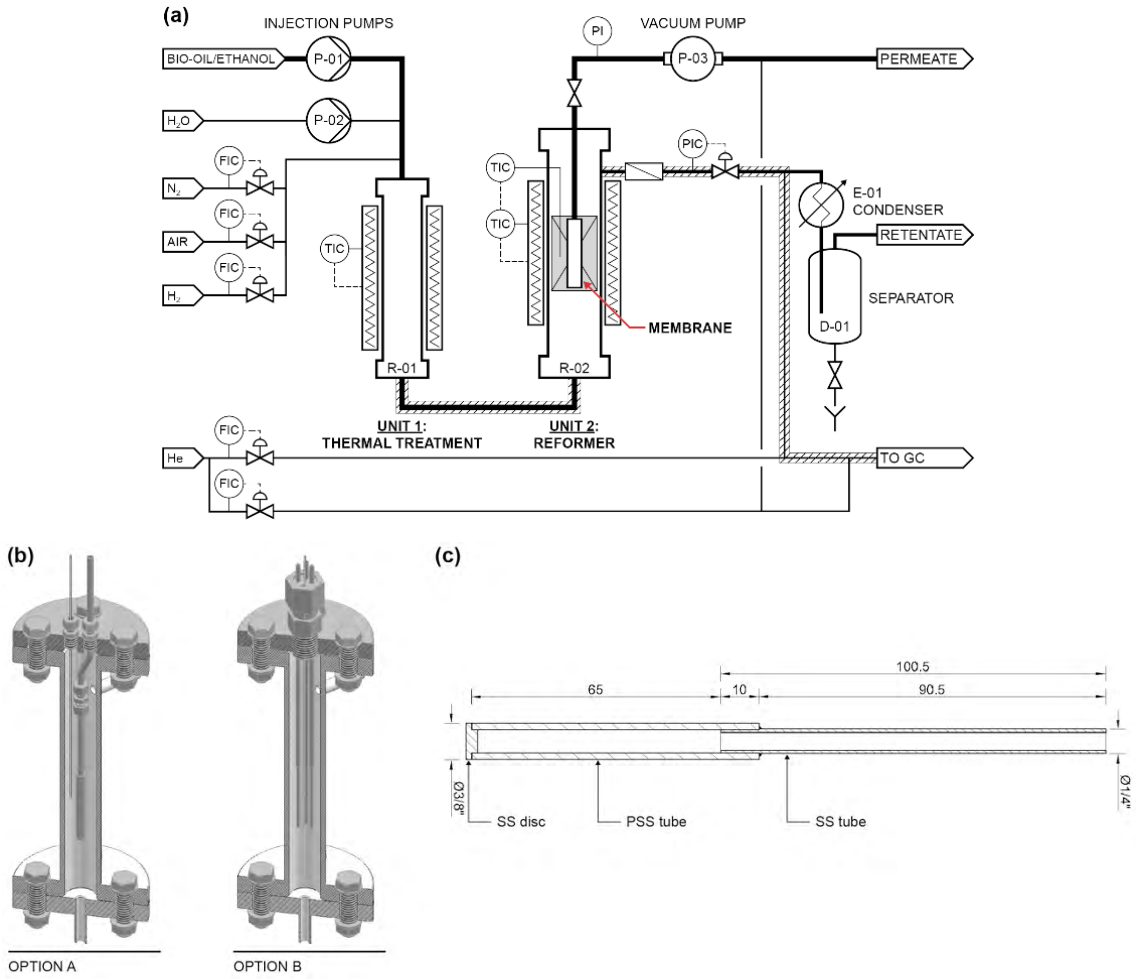


FIG. 1

Design improvements: (a) process flow diagram of reactor bench, (b) membrane installation design options, and (c) membrane support design specifications

2.2. Tests

The prepared Pd membranes were tested using standard permeation tests and under reaction conditions in the reactor bench previously described (Figure 1a). Prior to the final permeation tests, each membrane was stabilized at 550 °C under a H_2 flow for more than 12 h.

The standard permeation tests consisted of feeding H_2 and measuring the permeate flow rate (with an Agilent ADM flow meter) at a constant temperature (various values tested in the range of 350-550 °C) at different pressures in the reactor while keeping the permeate side open to atmospheric pressure. The reaction tests were carried out under SR conditions at 550 °C and varying the reactor pressure between 1 and 3 atm operating as a conventional reactor (CR, without membrane) or as a MR with the Pd membrane. For the MR operation, the permeate side is vacuumed at 0.2 atm. For all the tests, we used a feed of ethanol/H_2O (steam/ethanol molar ratio of 3) and a Ni/$MgAl_2O_4$ catalyst synthesized in the laboratory

following the procedure described elsewhere [5]. Both the retentate and permeate product streams were analyzed to quantify the products by using a micro-gas chromatograph (Agilent 990) with two columns for the detection of H_2, N_2, CO, CO_2, CH_4, H_2O and other C_2 compounds. Product yields were calculated using conventional definitions based on the reaction stoichiometry.

3. RESULTS

The designed options to incorporate the Pd membrane into the R-02 reactor (Figure 1b) were successfully implemented by customizing two top lids (as graphically modeled in Figure 1c), and both kind of membranes could be connected and disconnected easily and inserted in the catalytic bed creating an integrated separation-reaction system. For option A, the Pd membrane preparation was a relevant milestone. Figure 2 shows SEM images of the key steps during the Pd membrane preparation, depicting the porosity modification after the incorporation of the CeO_2 layer and the final Pd film after several ELPP cycles. The results further described in this section demonstrate the appropriateness of the design improvements to carry out experiments to test membranes with or without a reaction.

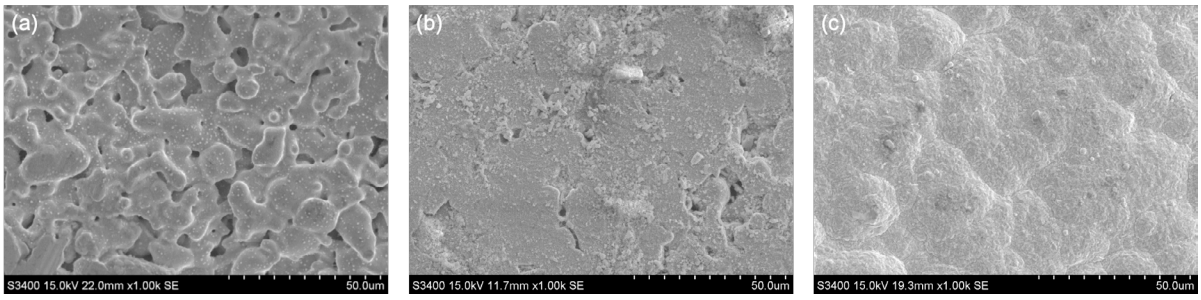


FIG. 2

Membrane preparation: (a) calcined PSS tube, (b) deposited CeO2 layer, (c) final Pd film

Figure 3 shows the H_2 permeation tests for options A and B. As seen, all the measurements follow the Sieverts' law (or the versioned Richardson equation (1)), and the A membrane show much higher permeation capacity in comparison to the commercial membranes (B). Likewise, during the stabilization and these tests, no N_2 leaks were detected suggesting that both options successfully worked.

In general, all the membranes exhibited infinite H_2 permselectivity (ratio between permeated H_2 and permeated N_2 at similar conditions) and the superior permeation capacity for the A membrane is confirmed by the calculated standard permeability (L^0_{H2}) as shown in Table 1. This improved permeability may be explained by the relatively low thicknesses (e) for these membrane in comparison to the commercial membranes, which is due to the presence of an intermediate CeO_2 layer that decreases the PSS tube porosity facilitating the formation of a thinner Pd film. The calculated activation energies (E_a) are similar and within the values reported in the literature [3].

Based on these features and on the easiness to connect and disconnect the membrane, the A membrane is selected for further tests. It should be noted that the installation of multiple membranes with a Spectite system (option B) is slightly more difficult, which also tipped the balance in favor of option A. In Figure 3C, an additional permeation test using a H_2/N_2 mixture (30 mol% H_2) is shown to simulate the dilution expected under reaction conditions. For this test, the permeation capacity decays abruptly describing an asymptotic-like function. This behavior is explained by the concentration-polarization phenomena or the co-adsorption of other components on the membrane surface partially impeding the H_2 adsorption [3].

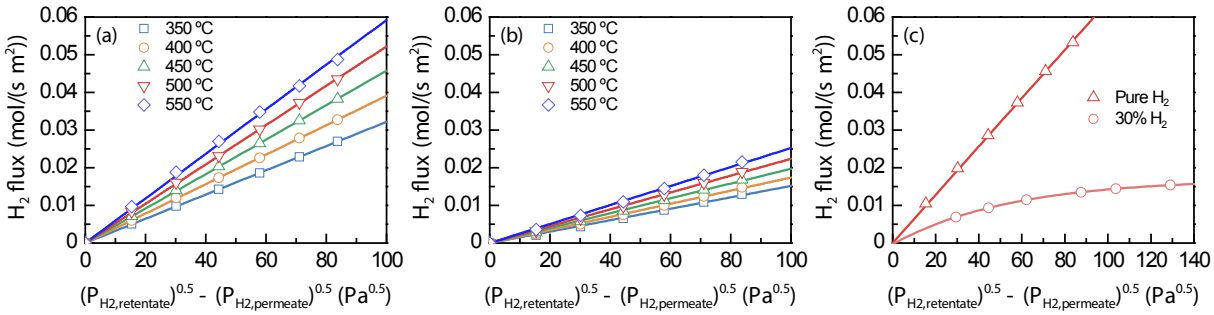


FIG. 3

H_2 permeation tests for (a) A and (b) B membranes, and (c) diluted H_2 permeation test

Finally, the successful implementation of the design improvement in the reactor bench is proved by its operation as a MR for the SR of ethanol employing the Ni/$MgAl_2O_4$ catalyst and the selected membrane (Figure 4). In comparison with the CR (red markers), higher H_2 and CO_2 yields are reported for the MR (blue markers) while the CO and CH_4 yield notably decrease, which indicates the equilibrium shift of the SR and WGS reactions towards the production of H_2 [5]. As expected, increasing the reactor pressure increases the H_2 recovery and yield because of the improved H_2 permeability, which is clearly observed by the linear increase in the H_2 yield in the permeate side (Figure 4a).

TABLE 1

Properties of the tested membranes

Membrane	Thickness (e) [μm]	Permeability (L^0_{H2}) [mol/(s m² Pa$^{0.5}$)]	Ea [kJ/mol]	H_2 perselectivity
A	8.30	0.0037	12.6	∞
B	75	0.0022	14.8	∞

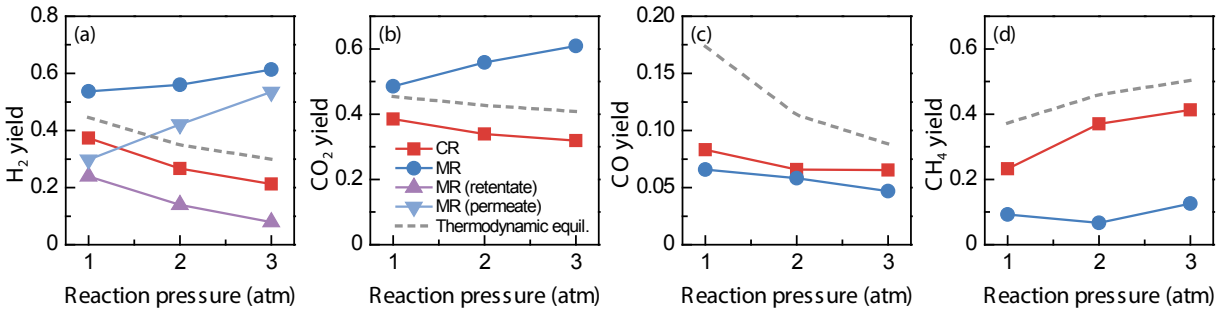


FIG. 4

SR of ethanol at 550 °C in a MR: (a) H_2, (b) CO_2, (c) CO, and (d) CH_4 yields

4. CONCLUSIONS

This study demonstrated the successful implementation of design improvements in a laboratory-scale membrane reactor bench to test and optimize processes aimed at H_2 production. A key feature was the geometric design to install the membranes into the reactor leading to proposing two installation options with single or multiple membranes, which also included the design specifications of the membrane support. The use of a single laboratory-made Pd membrane was more efficient than using multiple commercial Pd-Ag membranes, providing a simpler installation mode with standard fittings. The efficient H_2 permeation is attributed to the formation of a thin Pd film on the designed CeO_2/PSS support. This membrane was selected for the SR of ethanol, and the best result is achieved at a reaction pressure of 3 atm (transmembrane pressure of 2.8 atm) providing a H_2 yield and recovery of 60 and 87%, respectively. The observations are coherent with the fact that the equilibrium reactions are shifted towards the hydrogen formation as H_2 is continuously removed from the reaction medium through the Pd membrane.

Acknowledgements: This research was funded by the Ministry of Science and Innovation of the Spanish Government (grant PID2021-127005OB-I00) and the Department of Education, Universities and Investigation of the Basque Government (grant IT1645-22). Authors gratefully acknowledge the technical and human support provided by SGIker (UPV/EHU, ERDF, EU).

REFERENCES

[1] Megia, P.J., Vizcaino, A.J., Calles, J.A., Carrero, A.: Hydrogen production technologies: From fossil fuels toward renewable sources-A mini review. Energy & Fuels 35(2), 16403-16415 (2021). doi:10.1021/acs.energyfuels.1c02501.

[2] Iglesias-Vázquez, S., Valecillos, J., Remiro, A., Valle, B., Bilbao, J., Gayubo, A.G.: Global vision of the reaction and deactivation routes in the ethanol steam reforming on a catalyst derived from a Ni-Al spinel. Energy & Fuels 38(8), 7033-7048 (2024). doi:10.1021/acs.energyfuels.4c00646.

[3] Alique, D., Martinez-Diaz, D., Sanz, R., Calles, J.A.: Review of supported Pd-based membranes preparation by electroless plating for ultra-pure hydrogen production. Membranes 8(1), 5 (2018). doi:10.3390/membranes8010005.

[4] Taghizadeh, M., Aghili, F.: Recent advances in membrane reactors for hydrogen production by steam reforming of ethanol as a renewable resource. Reviews in Chemical Engineering 35(3), 377-392 (2019). doi:10.1515/revce-2017-0083.

[5] Valecillos, J., Elordi, G., Iglesias-Vázquez, S., Gayubo, A.G., Remiro, A.: Unveiling the role of operating conditions for pure hydrogen production from ethanol steam reforming in a vacuum-assisted Pd membrane reactor. Chemical Engineering Journal 538, 176654 (2026). doi:10.1016/j.cej.2026.176654.

[6] Tosti, S., Borgognoni, F., Santucci, A.: Multi-tube Pd-Ag membrane reactor for pure hydrogen production. International Journal of Hydrogen Energy 35(20), 11470-11477 (2010). doi:10.1016/j.ijhydene.2010.06.102.

[7] Shirasaki, Y., Tsuneki, T., Ota, Y., Yasuda, I., Tachibana, S., Nakajima, H., Kobayashi, K.: Development of membrane reformer system for highly efficient hydrogen production from natural gas. International Journal of Hydrogen Energy 34(10), 4482-4487 (2009). doi:10.1016/j.ijhydene.2008.08.056.

Detecting the Invisible: An Automated Approach to Identifying Plagiarism in Autodesk Inventor Files in Engineering Education

Valentín Gómez-Jáuregui*, José-Andrés Díaz-Severiano, Noemi Barral-Ramón

Research Group InGraStrUC, Universidad de Cantabria, ETS Ing. Industriales y Telecomunicaciones, Esc. C, Pl. -2, Avda. Los Castros 46. 39005, Santander (Spain)

* e-mail: valen.gomez.jauregui@unican.es

Abstract: The most effective plagiarism-detection tool is often the one students know exists before they decide to copy. Although current discussions on academic dishonesty mainly focus on generative AI, plagiarism in engineering education still frequently occurs through direct file sharing, unauthorized reuse of previous work, and duplicated or slightly modified CAD models. Detecting these practices is particularly difficult in CAD-based courses, where submissions consist of proprietary technical files, making visual inspection unreliable and time-consuming. This paper presents an automated desktop-based tool for detecting suspicious similarities in Autodesk Inventor files submitted in Engineering Graphics courses within the bachelor's degrees in Mechanical Engineering and Industrial Technologies Engineering, involving approximately 130 students. The system is not intended to determine plagiarism automatically, but to assist instructors by identifying potentially suspicious submissions for expert review. The application was developed in C# using MS Visual Studio, integrating Interop.Inventor for metadata extraction, Windows Forms for interface and file management, and ClosedXML for Excel report generation. The methodology combines three analyses: extraction of Inventor internal identifiers, recovery of authorship metadata, and generation of cryptographic hashes to identify binary duplication. Folder-based exclusion rules are also incorporated to reduce false positives. The tool enables automated scanning and comparison of large numbers of Inventor files, reducing manual workload while improving support for academic integrity in CAD-based education.

Keywords: *Academic integrity, Plagiarism detection, Engineering graphics education, Computer-aided design (CAD), Autodesk Inventor, Metadata analysis.*

1. INTRODUCTION

The most effective plagiarism-detection tool is often the one students know exists before they decide to copy. Academic dishonesty remains a persistent issue in higher education. Although recent attention has focused on generative AI, plagiarism also occurs through traditional practices such as copying during examinations, covert communication, file sharing, reuse of assignments, or submission of another student's work with minor modifications.

In engineering education, particularly in computer-aided design (CAD)-based courses, these practices are difficult to detect because submissions consist of proprietary technical files rather than plain text documents. Similar assignment constraints often produce naturally comparable solutions, making it challenging to distinguish legitimate similarities from unauthorized copying. This problem becomes especially significant in large-enrolment courses, where manually reviewing hundreds of CAD files is both time-consuming and unreliable.

Unlike textual plagiarism, CAD plagiarism remains insufficiently addressed. Most institutional tools are designed for essays or source code and provide little support for proprietary CAD formats. This creates an important methodological gap in engineering education.

This work addresses the problem in Engineering Graphics courses within the Bachelor's Degrees in Mechanical Engineering and Industrial Technologies Engineering, involving approximately 130 students using Autodesk Inventor [1]. To support instructors, an automated desktop-based tool was developed to identify suspicious similarities between Inventor files. The system analyses internal metadata, software-native identifiers, and cryptographic file hashes to detect potential duplication or reuse. Rather than conclusively determining plagiarism, the tool provides a technically grounded screening mechanism that significantly reduces manual workload while supporting academic integrity in CAD-based education.

1.1. Related Work

Research on plagiarism detection is extensive for textual documents and programming assignments, but remains very limited for CAD models and engineering design files. Only a few studies address plagiarism detection in geometry-based or CAD-related educational contexts.

One of the earliest contributions was presented by Kasprowicz and Wada [2], who developed automated criteria to detect suspicious similarities in integrated-circuit layouts. Their work demonstrated that engineering design plagiarism can be identified through structural and domain-specific descriptors rather than conventional document comparison methods.

Another relevant contribution is the work by Joo [3], who developed an API-based system for the automated evaluation of three-dimensional CAD models. Although primarily focused on grading and model verification, the study showed the potential of CAD software APIs for automatically processing large numbers of student submissions and included watermark-based mechanisms intended to help prevent plagiarism.

The most directly comparable study is the work by Johnson [4] on plagiarism detection in SolidWorks courses. The proposed tool extracted metadata such as authorship information and feature timestamps from CAD files and compiled the results into spreadsheets for

instructor review. The study reported successful detection of plagiarism cases while also reducing false positives through contextual metadata analysis.

Together, these studies show that plagiarism in CAD-based education is a real but still underexplored problem. Existing approaches are scarce, fragmented across different engineering domains, and typically linked to specific software ecosystems such as SolidWorks. To the best of current knowledge, there are no widely available AI-based plagiarism detection systems that simultaneously analyze: i) the content of CAD files (e.g., sketches, features, parameters, work planes, feature tree, construction history, etc.), and ii) the file as an information container (metadata, timestamps, internal identifiers, or other digital fingerprints).

2. METHODOLOGY

2.1. Educational Context

The proposed copy-detection tool was developed for Engineering Graphics courses within the Bachelor's Degrees in Mechanical Engineering (GIM) and Industrial Technologies Engineering (GITI) at the University of Cantabria, involving approximately more than one hundred students per academic year. Across the semester, students complete 13 weekly assignments and 6 midterm examinations requiring the submission of Autodesk Inventor CAD models. With an average cohort of 105 students, each assessment generates around 105 folders containing multiple CAD files that must be reviewed and compared for potential similarities. Consequently, instructors face the task of performing originality checks on approximately 2,000 student submissions distributed across 19 CAD-based assessment activities, making manual verification highly labor-intensive and difficult to scale.

Unlike textual assignments, CAD submissions may be superficially modified through file renaming, folder reorganization, or minor geometric changes while preserving most of the original model information. As a result, visual inspection alone is often insufficient to reliably identify unauthorized reuse or file sharing between students. In addition, Autodesk Inventor allows users to copy and reuse design entities such as sketches, features, work planes, work axes, and other modeling elements from one file to another. Although this functionality may facilitate the partial replication of a model, it generally requires a good understanding of the software and its parametric design workflow. Consequently, less experienced students often find this process more difficult and time-consuming than creating the model from scratch, making this type of reuse less common than direct file sharing or superficial modifications.

To support instructors in this process, an automated desktop application was developed to analyse Inventor files, extract internal metadata, compare digital fingerprints, and generate reports of potentially suspicious similarities for subsequent expert review.

2.2. Software Environment and Implementation

The tool was developed in Microsoft Visual Studio using C# as the main programming language. The application follows a desktop-based architecture, enabling a straightforward

graphical user interface for file selection, analysis monitoring, and results inspection. Additionally, several software dependencies were integrated to support the different stages of the workflow:

- Interop.Inventor was used to establish communication with Autodesk Inventor and to access the internal properties of Inventor-native files.
- Windows Forms was employed to implement the graphical user interface and to manage interaction with the Windows file system, including folder browsing, file listing, and event-driven execution.
- ClosedXML (version 0.105.0) was incorporated to export the analysis results into structured Microsoft Excel spreadsheets for documentation and post-processing.

This combination of technologies made it possible to build a lightweight but functionally robust application capable of interacting directly with CAD files.

2.3. General Workflow of the Tool

The developed system follows a structured multi-stage workflow designed to process large sets of Autodesk Inventor files and identify suspicious similarities. From a functional perspective, the tool can be divided into five main stages, that will be explained in the following sections:

1. *Initialization of the Working Environment*

At the beginning of each execution, the application initializes the graphical interface and prepares the internal structures required for the analysis. A results table is configured to display the main information associated with each processed file, including file name, part number, file path, size (kB), Internal GUID (Global Unique Identifier), cryptographic hash, modification date, author, and suspicion status (head row of figure 1).

In parallel, the system activates an internal logging mechanism that records key events and possible processing errors. This traceability improves debugging and reliability when processing large numbers of heterogeneous CAD files, some of which may be incomplete, inaccessible, or corrupted. This initialization stage ensures that the subsequent analysis is performed in a controlled and reproducible environment.

2. *File Acquisition and Folder Scanning*

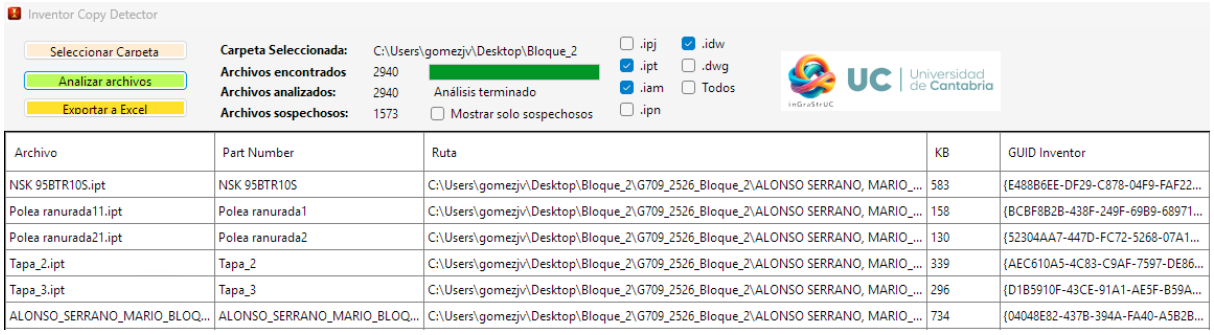
The first operational stage consists of selecting the root directory containing the student submissions. The application then performs a recursive scan of the directory tree to identify Autodesk Inventor-related files, including part, assembly, and drawing documents.

The user can selectively choose which Inventor file types will be included in the analysis, including project files (.ipj), part files (.ipt), assembly files (.iam), presentation/explod-

ed-view files (.ipn), drawing files (.idw), compatible technical drawing files (.dwg), or all file types simultaneously. This is particularly useful for excluding .ipj files that would otherwise generate misleading false positives in hash-based comparisons due to their typically identical and template-based nature.

The recursive strategy enables the detection of files stored in nested folder structures, which is particularly relevant in educational contexts where students often submit compressed or partially organized project folders. To reduce false positives, the system excludes predefined directories associated with Inventor internal management, such as backup folders, design-data repositories, and standard content libraries. These locations may contain automatically generated or institutionally shared files that are not representative of student-authored work.

Once the valid files are identified, the tool compiles a list of all detected documents and provides an overview of the number of files to be processed (first 4 columns of figure 1).



Archivo	Part Number	Ruta	KB	GUID Inventor
NSK 95BTR10S.ipt	NSK 95BTR10S	C:\Users\gomezjv\Desktop\Bloque_2\G709_2526_Bloque_2\ALONSO SERRANO, MARIO_...	583	{E488B6EE-DF29-C878-04F9-FAF22...
Polea ranurada11.ipt	Polea ranurada1	C:\Users\gomezjv\Desktop\Bloque_2\G709_2526_Bloque_2\ALONSO SERRANO, MARIO_...	158	{BCBF8B2B-438F-249F-69B9-68971...
Polea ranurada21.ipt	Polea ranurada2	C:\Users\gomezjv\Desktop\Bloque_2\G709_2526_Bloque_2\ALONSO SERRANO, MARIO_...	130	{52304AA7-447D-FC72-5268-07A1...
Tapa_2.ipt	Tapa_2	C:\Users\gomezjv\Desktop\Bloque_2\G709_2526_Bloque_2\ALONSO SERRANO, MARIO_...	339	{AEC610A5-4C83-C9AF-7597-DE86...
Tapa_3.ipt	Tapa_3	C:\Users\gomezjv\Desktop\Bloque_2\G709_2526_Bloque_2\ALONSO SERRANO, MARIO_...	296	{D1B5910F-43CE-91A1-AE5F-B59A...
ALONSO_SERRANO_MARIO_BLOQ...	ALONSO_SERRANO_MARIO_BLOQ...	C:\Users\gomezjv\Desktop\Bloque_2\G709_2526_Bloque_2\ALONSO SERRANO, MARIO_...	734	{04048E82-437B-394A-FA40-A5B2B...

FIG. 1
Screenshot of the program after the files have been analyzed

3. *Background Access to Autodesk Inventor and Metadata Extraction*

To access software-specific information unavailable through standard file-system inspection, the application launches Autodesk Inventor in the background using COM-based automation. This process is executed silently, allowing the software to open files and retrieve internal properties programmatically without displaying the full Inventor interface. For each file, the system extracts four categories of information:

— *Internal GUID (Global Unique Identifier):* a software-native identifier acting as a persistent internal signature of the CAD document. This identifier may remain associated with a file even after renaming or relocation, making it highly useful for identifying reused or duplicated models.

— *Authorship and Tracking Metadata:* including designer name, last saved by user, and part number. Although these attributes are not definitive indicators of plagiarism, they provide contextual information that can support interpretation of suspicious similarities.

— *Cryptographic Hash:* a digital fingerprint generated through a hashing procedure that allows exact binary duplication to be identified independently of file names or folder structure. Files sharing the same hash can be considered exact duplicates.

— *Operating-System Attributes:* such as file size and modification date. These parameters are treated as supplementary indicators because they may be altered during routine file transfers, downloads, or archive extraction.

The extracted information is consolidated into an internal dataset, ensuring that all files are compared using a homogeneous set of descriptors.

4. *Comparative Duplicate-Detection Strategy*

The objective is not to determine plagiarism conclusively, but to identify technical indicators of possible duplication or unauthorized reuse that may require instructor review. The system employs three complementary comparison criteria:

— *Internal Identifier Matching:* files sharing the same Internal GUID are interpreted as strongly related to the same source document or derivative model. This criterion is particularly effective when superficial modifications have been introduced to disguise copied work.

— *Cryptographic Hash Matching:* identical hashes indicate exact binary duplication and therefore constitute one of the strongest indicators of direct copying or trivial file renaming.

— *Timestamp Coincidence:* exact coincidence in modification dates is considered only as supporting evidence due to its lower reliability and susceptibility to alteration during routine file handling.

To reduce false positives, the system incorporates a folder-based exclusion rule. Files located within the same directory or in direct parent–child folder relationships are not flagged as suspicious, since CAD projects commonly contain legitimate derivative files, backups, or intermediate versions within the same project structure.

5. *Visualization and Filtering of Results*

The application presents the results in a structured tabular interface (Figure 1). Each row corresponds to a processed file and includes its extracted descriptors together with the assigned suspicion status. For suspicious cases, the system generates a textual explanation indicating the criterion responsible for the warning (last column of figure 1). This improves transparency and allows instructors to understand the basis for each flag rather than relying on a black-box decision process. Visual highlighting in light red is also incorporated to facilitate rapid inspection of large datasets.

To improve usability, the application includes a filtering option that allows instructors to display only suspicious files. This functionality reduces visual load and helps focus attention on the subset of submissions most likely to require manual verification.

As a final stage, the complete analysis can be exported to a Microsoft Excel spreadsheet using the ClosedXML library. The exported report contains the main descriptors as-

sociated with each analyzed file together with the corresponding suspicion notes. Suspicious cases may also be visually highlighted within the spreadsheet, improving readability and facilitating offline review, archival, or discussion among teaching staff. This reporting capability transforms the application from a simple screening utility into a practical support tool for documentation, traceability, and evidence-based academic integrity assessment.

3. DISCUSSION OF SCOPE AND CONTRIBUTION

The proposed application should not be interpreted as a fully autonomous plagiarism-detection system, but to identify meaningful similarities between Autodesk Inventor files and to support the instructor's expert judgment. Its purpose is not to determine misconduct automatically, but to reduce the manual workload associated with reviewing large volumes of CAD submissions.

After multiple rounds of application in real educational settings, including the analysis of 12 assignment submissions and 2 examination submissions, only one case of plagiarism was detected. This case was identified through a matching Inventor GUID between drawing files submitted by two students in the GITI programme. In addition to the preventive communication carried out at the beginning of the course, in which students were informed about the existence and functioning of the detection tool, the incident was subsequently addressed in class in an anonymised manner. This action was intended to ensure transparency, reinforce academic integrity awareness, and discourage future occurrences among the student cohort.

4. CONCLUSION

The developed tool constitutes a practical and technically grounded solution for the automated detection of suspicious similarities in Autodesk Inventor files submitted within engineering graphics courses. Its implementation provides a functional and accessible framework for analysing large sets of CAD files in an educational environment. In the context of courses with more than one hundred students and several submissions, the tool significantly reduces the time and effort required to identify potential file transfer or unauthorized reuse between students.

More broadly, the system demonstrates how domain-specific metadata extraction and file-level digital analysis can be effectively combined to support academic integrity processes in CAD-based engineering education. As a conclusion, detection tools are not only retrospective control systems; they are also preventive pedagogical devices.

REFERENCES

[1] Autodesk Inventor: 3D modeling software for designers and engineers, https://www.autodesk.com/eu/products/inventor/overview, last access: 2026/05/11.

[2] Kasprowicz, D., Wada, H.: Methods for automated detection of plagiarism in integrated-circuit layouts. Microelectronics Journal 45(9), 1212-1219. (2014) https://doi.org/10.1016/j.mejo.2014.04.023

[3] Joo, S.: Improvement of API Program to Evaluate Three-Dimensional CAD Models. In: Proceedings of the ASME International Mechanical Engineering Congress and Exposition (IMECE). ASME, Columbus, OH (2022). https://doi.org/10.1115/IMECE2022-96096

[4] Johnson, W. R.: Detecting Plagiarism in SolidWorks CAD Courses. In: 2018 ASEE Annual Conference & Exposition. (2018) https://doi.org/10.18260/1-2--30286

Geometry-driven design and additive manufacturing of mycelium-based biocomposites for sustainable applications

Kizkitza González[a,b,*], Unai Ortega[a], Nerea Zaldua[c], Lorena Ugarte[a,d]

[a] Group 'Materials + Technologies' (GMT), Department of Chemical and Environmental Engineering, Faculty of Engineering of Gipuzkoa, University of Basque Country (EHU), Plaza Europa 1, 20018 Donostia-San Sebastian, Spain

[b] Department of Graphic Design and Engineering Projects, Faculty of Engineering of Gipuzkoa, University of Basque Country (EHU), Plaza Europa 1, 20018 Donostia-San Sebastian, Spain

[c] Department of Chemical and Environmental Engineering, Faculty of Engineering of Gipuzkoa, University of Basque Country (EHU), Plaza Europa 1, 20018 Donostia-San Sebastian, Spain

[d] Department of Graphic Design and Engineering Projects, Faculty of Engineering of Gipuzkoa, Eibar section, University of Basque Country (EHU), Av. Otaola 29, 20600 Eibar, Spain

* e-mail: kizkitza.gonzalez@ehu.eus

Abstract: Mycelium-based biocomposites have emerged as promising sustainable materials due to their renewable origin, biodegradability, and low environmental impact. However, previous studies have mainly focused on substrate formulation, while the influence of geometry on mycelial growth has received limited attention. This work proposes a geometry-driven approach using direct ink writing (DIW), where geometry becomes an active design parameter. Inks based on coffee grounds, flour, water, agar-agar, grain-based mycelium, and jute fibres exhibited suitable printability and shape fidelity during 3D printing. Honeycomb structures were fabricated by varying nozzle diameter (4 mm and 7 mm) and infill percentage (40% and 60%) to control internal architecture. After incubation, the results demonstrated that geometry significantly affects mycelial colonization. Lower infill percentages and larger nozzle diameters promoted enhanced growth, likely due to improved aeration and substrate continuity. Furthermore, jute fibres contributed positively to internal network formation and mycelial growth. The proposed approach highlights the potential of additive manufacturing for co-designing geometry, material, and biological performance in sustainable living materials.

Keywords: *mycelium, additive manufacturing, printing parameters, sustainable materials.*

1. INTRODUCTION

The depletion of natural resources and the growing concern regarding environmental pollution have driven the development of approaches based on circular economy principles and waste valorisation to reduce environmental impact and promote a more efficient use of resources.

In this sense, mycelium-based composites (MBCs) have emerged as a promising and sustainable alternative. MBCs are composed of a network structure rich in cellulose, hemicellulose, and lignin [1]. These biodegradable materials combine low density with suitable mechanical performance and can naturally degrade at the end of their life cycle. Furthermore, previous studies have demonstrated that industrial and organic wastes, can serve as promising substrates for mycelial growth [2]. In addition, these works demonstrated the feasibility of promoting mycelial growth on substrates designed through 3D printing technologies. In this sense, additive manufacturing offers new opportunities for the controlled design of living materials, where geometry, porosity, and internal architecture can be directly linked to the biological behaviour of the material.

Thus, the main objective of this work was to develop MBCs fabricated through direct ink writing (DIW)-based 3D printing. The influence of the printing parameters (particularly nozzle diameter and infill percentage) as well as the incorporation of jute fibres on mycelial colonization and the resulting structural properties, was analysed.

2. EXPERIMENTAL

2.1. Design and FDM printing of syringes

Syringes with different diameters were CAD designed and 3D printed by the Fused Deposition Modelling (FDM) technique since, in this case, commercial standard syringes are not feasible as extrusion systems. Syringes were printed by a Voladora 3D printer (Tumaker, S.L. Spain) with a nozzle of 0.6 mm in diameter, a printing speed of 20 mm s^{-1} and an infill percentage of 20%. Extruder and bed temperatures of 210 °C and 65 °C were selected, respectively. PLA was used as the filament material. The syringe tube has a 2 mm wall thickness, a 20 mm inner diameter, and is 120 mm long. Similarly, the piston has a 20 mm exterior diameter and is 120 mm long.

2.2. Preparation of the inks and DIW printing

Coffee-based inks were prepared as follows. Firstly, agar-agar, used as a rheology modifier, was dissolved in boiling water under continuous magnetic stirring. After that, dried coffee grounds and flour were added and stirred at 80 °C until a homogeneous mixture was obtained. Finally, mycelium grain (*Pleurotus ostreatus*) was added to the cooled coffee-based inks. For the preparation of the fibre-containing samples, jute fibres were chopped using a grinder (equipped with a sieve of 5 mm) and subsequently added to the cooled inks. Finally, water was added until the ink reached a 3D-printable consistency and also to provide moisture for mycelium growth.

The prepared inks were printed using a Voladora 3D printer (Tumaker, S.L. Spain) adapted for layer-by-layer syringe extrusion. All samples were printed using 6 mm s^{-1} printing speed and a honeycomb infill pattern, which provides greater exposure of the substrate to air, thereby facilitating oxygen diffusion, which is a key factor for aerobic fungal growth [3].

However, different nozzle diameters (4 mm and 7 mm) and infill percentages (40% and 60%) were used to analyse the influence of the printing parameters on the mycelium growth capacity. All CAD models were sliced using Simplify3D software (Figure 1).

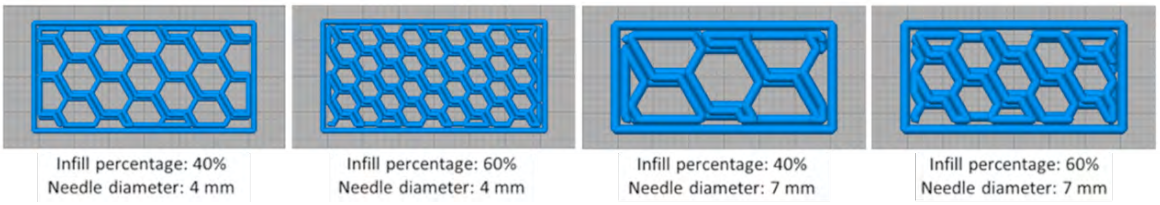


FIG. 1
3D Printed geometries

2.3. Colonization of *Pleurotus ostreatus*

As it is well known, the growth of mycelium colonies is influenced by moisture, air exchange, temperature, and lighting [2]. Thus, printed parts were stored in the dark, at room temperature and under 75% relative humidity for 15 days to promote mycelial colonization. Colonization was stopped by keeping the printed parts in an oven at 60 °C for 24 h. All the containers and surfaces were previously sterilized with 2-propanol. The samples were named as X-Y% where X is related to the nozzle diameter and Y to the infill percentage. When jute fibres were added, JF was indicated (Table 1).

TABLE 1
Composition and 3D printing parameters of obtained samples

Sample	Jute Fibres	Nozzle diameter (mm)	Infill percentage (%)
4 - 40%	No	4	40
4 - 60%	No	4	60
7 - 40%	No	7	40
7 - 60%	No	7	60
4 - 40% - JF	Yes	4	40
4 - 60% - JF	Yes	4	60
7 - 40% - JF	Yes	7	40
7 - 60% - JF	Yes	7	60

3. RESULTS AND DISCUSSION

3.1. 3D printing and mycelium colonization

All the prepared inks were successfully processed through DIW printing, maintaining the programmed CAD geometries and exhibiting good cohesion and shape fidelity after extrusion.

After incubation, complete colonization of the printed structures was observed, leading to the formation of a dense external white layer (Figure 2). A similar phenomenon was previously reported by Luo *et al.* [2] in coffee-based mycelium biocomposites, where the mycelium preferentially developed on the outer surface of the samples. The formation of this external layer could be associated with the aerobic nature of fungal growth, since oxygen availability is greater at the exposed surfaces.

The results showed that the colonization behaviour depended on the printing parameters and the incorporation of jute fibres. In particular, the addition of jute fibres appeared to accelerate mycelial growth. This behaviour may be attributed to the interconnected internal structure generated by the fibres, which likely improves oxygen penetration and facilitates nutrient and moisture distribution throughout the material. Regarding the influence of the printing parameters, more extensive colonization was observed in samples printed with a 40% infill pattern and a 7 mm nozzle diameter. These results suggest that the lower infill percentage and larger nozzle diameter enhance aeration and create more favourable conditions for fungal propagation.

Thus, it could be concluded that the 7 – 40% – JF sample exhibited the highest degree of colonization, suggesting that the combination of a larger nozzle diameter, lower infill percentage, and the incorporation of jute fibres provide the most favourable conditions for mycelial growth.

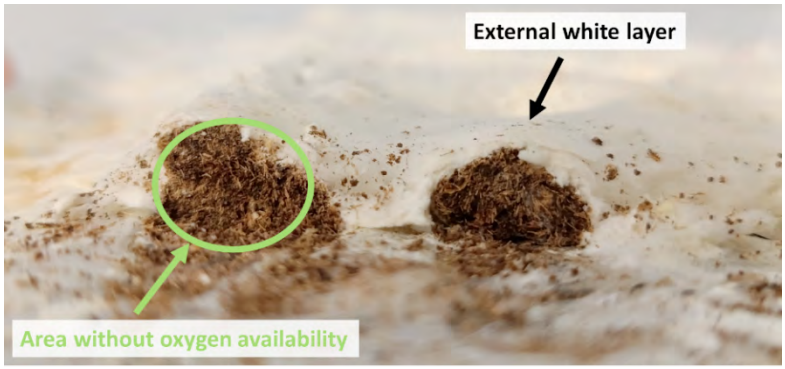


FIG. 2
7 – 40% – JF sample after incubation and colonization

3.2. Compression tests

Colonized printed parts were characterized in terms of compression behaviour (n = 5). The compressive properties were obtained from the stress-strain curves and are summarized in Table 2.

As can be observed, samples exhibiting more extensive mycelial colonization generally tended to showed improved compressive properties, increasing both the strength and the stiffness of the biocomposites. However, the final properties also depended on the architecture generated during the printing process. Although lower infill percentages promoted more extensive colonization by improving oxygen diffusion, they also reduced the amount of material available to sustain compressive loads. The beneficial effect of enhanced mycelial colonization generally compensated for the lower amount of material, resulting in improved compressive properties for most of the samples printed with a 40% infill pattern.

Similarly, the nozzle diameter influenced both the biological and mechanical behaviour. Samples 3D printed with a nozzle diameter of 7 mm presented thicker filaments, which facilitated mycelial propagation while simultaneously increasing the effective cross-sectional area of the printed struts, leading to higher stiffness and yield stress. In addition, the incorporation of jute fibres further enhanced the compressive properties. The addition of lignocellulosic fibres as reinforcing agent promoted the development of a more interconnected internal network that facilitated mycelial growth throughout the structure, leading to higher Young's modulus and yield stress values.

Overall, the mechanical performance of the developed biocomposited resulted from the combined interaction of geometry, mycelial colonization, and fibre reinforcement, rather than from the influence of any single parameter.

3.3. Impact test

The impact test results (n = 10) showed resilience values of approximately 15% for all samples, indicating that only a small fraction of the incident energy was recovered through rebound (Table 2). Consequently, around 85% of the energy was not recovered and can therefore be considered to have been dissipated within the material. These results indicate a high energy dissipation capacity. No significant variations associated with nozzle diameter or infill percentage were observed. Similarly, no improvements were detected due to fibre addition.

From an application perspective, this behaviour is consistent with the requirements described for impact-mitigating materials, such as those considered in ASTM D1596 [4]. According to this standard, materials with low resilience are particularly suitable for reducing rebound and controlling energy transmission after impact. Compared with conventional polymer foams, these mycelium-based biocomposites offer the additional advantages of being renewable, biodegradable, and produced from agricultural or food waste. Although their mechanical strength is generally lower than that of synthetic polymeric foams, their high energy dissipation capacity combined with low density makes them promising candidates for non-structural applications where environmental sustainability is a priority such as lightweight sandwich core materials or thermal and acoustic insulation panels.

TABLE 2
Mechanical properties and resilience results of colonized printed parts

Sample	Young's modulus (Pa)	Yield stress (Pa)	Densification strain (%)	Resilience (%)
4 - 40%	5.1 ± 0.2	270 ± 28	69.3 ± 0.4	17 ± 5
4 - 60%	18.4 ± 3.4	835 ± 120	68.8 ± 1.1	14 ± 1
7 - 40%	13.2 ± 3.3	200 ± 14	67.3 ± 3.3	15 ± 2
7 - 60%	10.3 ± 1.6	185 ± 35	67.7 ± 2.3	14 ± 3
4 - 40% - JF	35.6 ± 2.6	1020 ± 115	67.8 ± 2.4	13 ± 1
4 - 60% - JF	18.4 ± 3.4	820 ± 113	69.4 ± 0.6	14 ± 1
7 - 40% - JF	35.6 ± 0.4	990 ± 141	69.6 ± 0.8	15 ± 2
7 - 60% - JF	23.4 ± 4.4	603 ± 64	67.4 ± 1.0	14 ± 3

3.4. TGA

Since an infill percentage of 40% and a nozzle diameter of 7 mm were identified as the optimal printing parameters, 7 – 40% and 7 – 40% – JF samples were subjected to TGA to evaluate their thermal stability. The obtained results are presented in Figure 3.

On the one hand, the thermal degradation of raw jute fibres began with an initial mass loss below 100 °C that was attributed to the evaporation of absorbed moisture. Then, above approximately 240 °C, the degradation of the organic components of the jute fibres began [5]. On the other hand, for colonized samples, a first step associated with moisture loss from biomass and lower molecular weight volatile components was also observed below 100 °C. Afterward, in the range of 250 - 400 °C, the main organic constituents of mycelium-based materials, such as polysaccharides, lipids and proteins, underwent thermal degradation [6]. In the case of jute fibres-containing sample, a higher moisture content was observed, probably due to the high-water retention capacity of cellulosic structures. Besides, a new degradation step associated with cellulose degradation of jute fibre was observed.

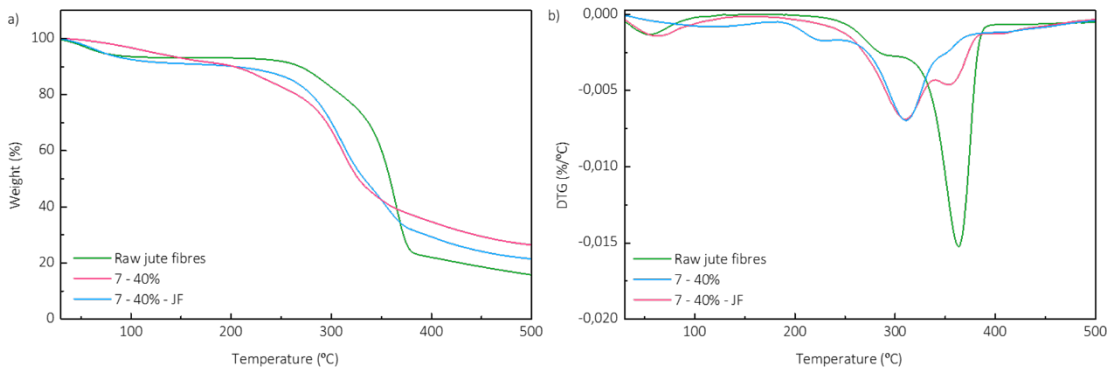


FIG. 3
a) TG b) DTG curves of raw jute fibres as well as 7 – 40% and 7 – 40% - JF samples

4. CONCLUSIONS

Mycelium-based biocomposites were successfully developed from coffee waste through the DIW technique. All the prepared samples exhibited suitable printability, maintaining the programmed CAD geometries and showing good cohesion and shape fidelity after extrusion.

The results confirmed that both the printing parameters and the incorporation of jute fibres significantly influenced mycelial colonization. Samples printed with a lower infill percentage and a larger nozzle diameter promoted enhanced fungal growth. In addition, the incorporation of jute fibres promoted oxygen diffusion and mycelial propagation. Mechanical characterization revealed that the samples with exhibiting more extensive colonization also presented enhanced compressive properties. In particular, the addition of jute fibres increased both Young's modulus and yield stress due to their reinforcing effect and their ability to promote mycelial colonization. In addition, samples showed a high capacity for energy dissipation and exhibited thermal stability up to 250 °C.

Overall, this work highlights the potential of combining waste valorisation, natural fibre reinforcement, and additive manufacturing technologies to develop sustainable living materials with tuneable biological and mechanical properties.

Acknowledgements: The authors gratefully acknowledge the financial support from Euskal Herriko Unibersitatea (EHU) in the frame of Campus Bizia Lab (25UGAR). Moreover, the authors also thank the Macrobehavior-Mesostructure-Nanotechnology SGIker unit of the EHU.

REFERENCES

[1] Camilleri, E., Narayan, S., Lingam, D., Blundell, R.: Mycelium-based composites: An updated comprehensive overview. Biotechnol. Adv. 79, 108517 (2025). https://doi.org/10.1016/j.biotechadv.2025.108517.

[2] Luo, D., Yang, J., Peek, N.: 3D-Printed Mycelium Biocomposites: Method for 3D Printing and Growing Fungi-Based. Composites 12, 27-32 (2025). https://doi.org/10.1089/3dp.2023.0342.

[3] Jones, M., Huynh, T., Dekiwadia, C., Daver, F., John S.: Mycelium composites: A review of engineering characteristics and growth kinetics. J. Bionanoscience 11, 241-257 (2017). https://doi.org/10.1166/jbns.2017.1440.

[4] ASTM D3574-03 Standard test methods for flexible cellular materials -- Slab, bonded, and molded urethane foams, Astm 08 1-23 (2003).

[5] Abir, N., Darda, M.A., Alim, M.A., Gafur M.A., Begum, H.A.: Thermal performance of jute fiber reinforced gypsum composites for heat insulating applications. Next Mater. 11, 101987 (2026). https://doi.org/10.1016/j.nxmate.2026.101987.

[6] Tewari, S., Reshamwala, S.M.S., Kale, R.D.: Eco-friendly mycelium composites: Redefining vegan leather for a greener future. Biomass and Bioenergy 206, 108663 (2026). https://doi.org/10.1016/j.biombioe.2025.108663.

Topologically Consistent 3D Reconstruction of Polyhedral Objects from Orthographic Projections using Graph Analysis and Winged- Edge Representation

Gerardo Martín-Lorenzo*, José Pablo Suárez, Pedro Miguel González

Departamento de Cartografía y Expresión Grafica en la Ingeniería.
Universidad de Las Palmas de Gran Canaria

* e-mail: gerardo.martin@ulpgc.es

Abstract: This paper presents a computational framework for reconstructing 3D polyhedral objects from orthographic projections (front, top, and side views). The proposed method integrates geometric processing, graph-based connectivity analysis, and topological validation to ensure structural consistency of the reconstructed model. The approach begins with the extraction and normalization of 2D segments from DXF files, followed by geometric refinement through collinearity merging and intersection-based subdivision. A 3D reconstruction stage generates candidate vertices by intersecting orthographic projections, and segments are classified according to their spatial orientation. The resulting structure is modelled as a graph, enabling the detection of connected components using depth-first search. Topological invariants, including Betti numbers and Euler characteristic, are computed to validate the consistency of the reconstructed solid. A Winged-Edge data structure is then constructed to explicitly represent adjacency relationships between vertices, edges, and faces. Experimental results on synthetic and CAD-derived datasets demonstrate that the proposed pipeline produces geometrically accurate and topologically consistent models. The integration of topological validation significantly reduces reconstruction ambiguities and improves robustness.

Keywords: *Orthographic projections, 3D Reconstruction, DXF files, 3D-CAD.*

1. INTRODUCTION

During more than fifty years, orthographic projection drawings have represented one of the dominant standards for graphical communication in engineering and industrial design [1,6,7,8]. However, current CAD/CAM workflows are increasingly focused on three-dimensional modelling and the direct use of 3D geometries. In this context, automatic 2D-to-3D reconstruction techniques have gained strategic relevance, as they enable the recovery and reuse of a vast legacy of technical documentation originally created in bidimensional formats. Furthermore, the interest in this field remains significant because the reconstructed models can subsequently be integrated into advanced numerical simulation processes, including FEM and BEM analyses, as well as modern CAD/CAM and digital manufacturing applications.

This work proposes a hybrid geometric-topological pipeline for reconstructing polyhedral objects from orthographic views. The key contributions are:

—A robust preprocessing pipeline for DXF-based geometric normalization.

—A 3D reconstruction strategy based on projection consistency.

—A graph-based formulation enabling connectivity analysis via DFS. - Integration of topological invariants (Betti numbers and Euler characteristic) for validation.

—Construction of a Winged-Edge representation to explicitly encode adjacency relationships.

The proposed framework ensures not only geometric correctness but also topological consistency, which is critical for downstream applications in CAD and digital modelling. The method was evaluated on synthetic polyhedral models, including cubes and prisms. Results show that the integration of topological constraints significantly reduces ambiguity in reconstruction.

2. THE METHOD OF 3D RECONSTRUCTION OF POLYHEDRAL OBJECTS

Due to the complexity of the problem under consideration, there is no a universal approach capable of solving the reconstruction problem in a fully generic manner, [6-8]. Instead, it is necessary to progressively address the different particular cases presented by mechanical parts through specific solutions. For this reason, the study has gradually incorporated different case studies exhibiting particular geometric and topological characteristics that require distinct reconstruction strategies. Consequently, the analysis and subsequent development of solutions have been expanded incrementally in order to address these difficulties progressively and achieve the broadest possible framework capable of successfully reconstructing a large number of practical cases.

To study the possible relationships, the analysis is based on the scheme shown in Figure 1 (b), where a topological decomposition is performed and the relationships between the different geometric entities are examined. The method employs principal planes containing the reconstructed edges and analyses the membership of each edge to the detected planes. Likewise, the incidence relationships between vertices and edges are analysed through a topological relationship graph. The engineering parts considered in this study belong to the class of polyhedral objects, which may include through holes and inclined planes.

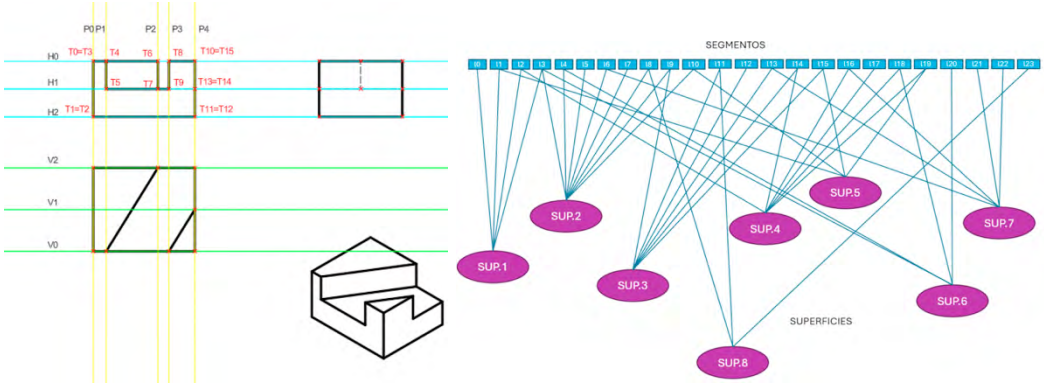


FIG. 1
(a) Reconstruction from orthographic views at a glance
(b) Topological separation into geometric entities

Reconstruction from orthographic views starts from 2D drawings that may contain visible lines, hidden lines, dimensions, text, blocks, symbols, polylines, and small numerical variations. The reconstruction pipeline must address four main difficulties:

1. Separating the useful geometry from auxiliary drawing elements;
2. Identifying which entities belong to each orthographic view;
3. Transforming 2D segments into consistent 3D correspondences;
4. Temoving redundancies, overlaps, unnecessary subdivisions, and isolated elements.

The method can be summarized as a nine-steps process as depicted in Figure 2.

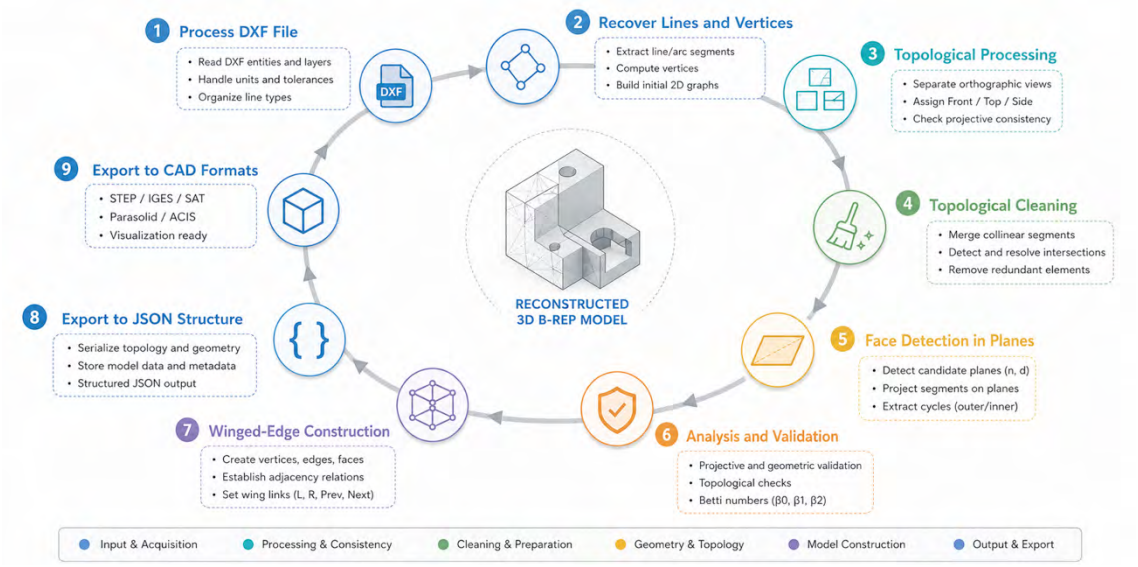


FIG. 2
Overview of the 2D to 3D reconstruction pipeline

3. TOPOLOGICAL PROCESSING

After the initial reconstruction stage, the resulting wireframe usually contains redundant segments, spurious correspondences, isolated edges, and geometrically plausible but topologically inconsistent configurations. Consequently, a dedicated topological cleaning stage is required to transform the reconstructed geometry into a structure compatible with a valid B-Rep representation. The proposed approach performs geometric normalization, collinear segment merging, removal of orphan segments, elimination of low-concurrency non-collinear vertices, and detection of inconsistent internal loops through graph-based analysis. This process significantly reduces topological ambiguities while preserving the structural connectivity required for subsequent face reconstruction stages.

The topological refinement is formulated as a graph-processing problem in which vertices and segments are analyzed according to their incidence and connectivity relationships. Segment intersections are explicitly subdivided into atomic edges, allowing cycles and adjacency relations to be evaluated consistently within each detected plane. In addition, the method incorporates plane-based loop validation to suppress redundant internal cycles and retain only geometrically coherent boundaries. This strategy improves the robustness of the reconstructed topology and facilitates the generation of consistent face cycles suitable for Winged-Edge construction.

The topological cleaning can be summarized as follows:

1. Removal of orphan segments whose endpoints appear only once within the entire set. Figure 3 (a).
2. Removal of non-collinear vertices with concurrency below the configured threshold. Figure 3 (b). and resulted part in Fig 3 (c).
3. Processing of internal loops through extreme-plane analysis.
4. Merging of collinear segments lying within x-, y-, or z-aligned planes.

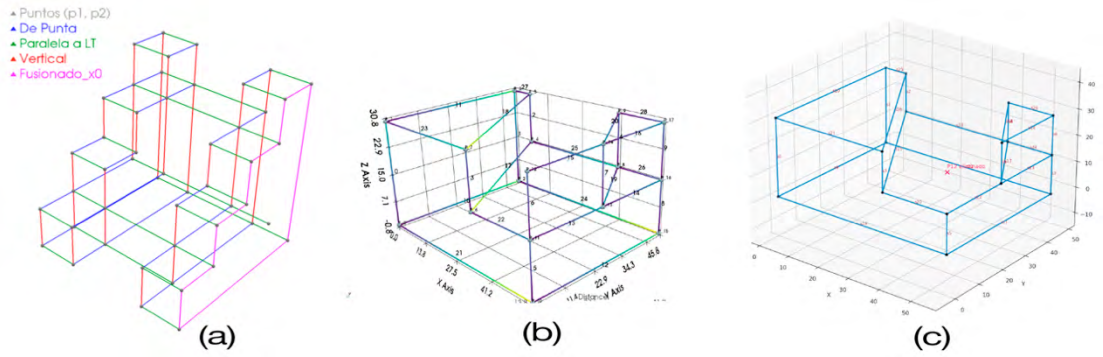


FIG. 3
Some topological cleaning instances and examples

A particularly challenging aspect of the reconstruction process is the robust detection of oblique planes. While principal planes parallel to the coordinate axes can be identified directly from geometric constraints, oblique planes require a more flexible treatment due to numerical perturbations and partial segment correspondences. In the proposed method, candidate planes are generated from pairs of non-collinear segments sharing common vertices. Each plane is represented in implicit form and subsequently normalized in order to avoid duplicate representations caused by scaling or sign ambiguities.

To improve robustness, geometrically equivalent oblique planes are grouped using angular and distance tolerances applied to their normal vectors and plane coefficients. Once grouped, a representative plane is estimated through Singular Value Decomposition (SVD) using all segment endpoints associated with the candidate plane. This refinement stage produces more stable and reliable plane estimations, particularly in the presence of numerical noise and fragmented geometries. The detected planes are then used to classify segments according to their topological relationship with each plane, enabling subsequent face detection and topological validation processes.

Figure 4 shows an example of the detection and removal of internal loops within a plane. The diagonal A–C (shown in red) simultaneously belongs to two cycles: A–B–C–A and A–C–D–A. In figure (b), after the topological cleaning stage, the shared edge is removed, resulting in a simpler and more consistent structure.

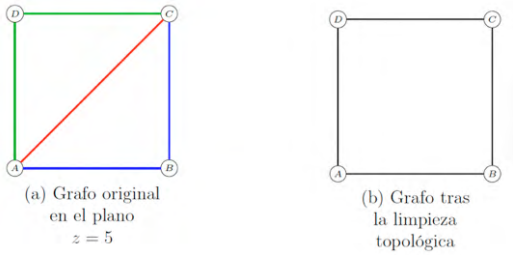


FIG. 4
Cleaning process on a plane graph

3.1. Topological Evaluation: Betti Numbers and Winged Edge data structures

Betti numbers makes it possible to quantify global connectivity properties and the presence of cycles or cavities, providing an objective measure of the topological structure of the model. Betti numbers are algebraic-topological invariants that describe the number of independent holes of different dimensions within a space. In a first approximation, the geometry is interpreted as an undirected graph G = (V, E), where the nodes correspond to the vertices of the model and the edges correspond to the 3D segments connecting those vertices.

Based on this structure, the first two Betti numbers are computed: β0: number of connected components of the graph, and β1: number of independent cycles in the graph.

From graph theory β0 = C, where C is the number of connected components, and β1 = E – V + C, where V is the number of vertices and E is the number of edges. Additionally, the Euler characteristic of the graph is computed as χ = V – E.

At this level of analysis, β0 allows the detection of whether the reconstruction is fragmented into multiple disconnected parts, while β1 indicates the presence of loops or independent circuits within the linear structure.

In a second stage, the geometry is interpreted as a two-dimensional complex formed by the detected faces. In this case, the topological analysis is no longer limited to the connectivity of the linear skeleton, but also incorporates the surface organization of the model. Let a 2D complex be defined by V: number of distinct vertices present in the faces, E: number of distinct edges used by the faces and F: number of detected faces. An important correction is introduced to handle faces containing holes. If a planar face contains h_i holes, its Euler contribution is not equal to 1, but instead $\chi_i = 1 - h_i$. Therefore, instead of directly using the raw number of faces, an effective number of faces is defined in equation (1):

$$F_{Effective} = \sum_i (1 - h_i) \tag{1}$$

where h_i is the number of holes in face i.

Using this correction, the Euler characteristic of the surface is computed, equation (2):

$$\chi = V - E + F_{Effective} \tag{2}$$

This correction is particularly relevant in the present project because the faces detected may contain one outer boundary together with one or several inner holes. Without this correction, the surface topology would be incorrectly represented.

In this project, Betti analysis is applied as a topological validation tool for the reconstruction process. Its main usefulness is twofold. First, when applied to the 1D graph of segments, it allows verification of whether the reconstructed linear structure is connected and determines the number of independent cycles it contains. This is particularly useful for detecting undesired fragmentations or linear redundancies after the geometric reconstruction stage. Second, when applied to the 2D surface formed by the detected faces, it enables evaluation of whether the surface structure is topologically consistent. At this level, the explicit incorporation of holes within each face becomes an essential aspect of the method, since such holes directly modify the Euler characteristic and, consequently, the Betti numbers associated with the surface.

3.2. Winged-Edge data structure

Winged-Edge data structures is particularly important because the reconstruction process starts from information projected in two dimensions. From the DXF views, a 3D geometry is obtained that must be interpreted and validated before it can be considered a coherent part. A list of vertices and segments may partially describe the shape, but it does not guarantee the existence of a closed surface or that the faces are correctly connected. The Winged-Edge structure makes it possible to transform the reconstructed geometry into a navigable model in which each edge stores its initial and final vertices, the faces located on

both sides, and the previous and next edges within the traversal of each face. For example, we can verify whether the resulting surface is topologically closed. In a valid solid model, each edge should normally belong to two faces, one on each side. If an edge is associated with only one face, a free boundary is detected; if it is shared incorrectly, this may indicate a non-manifold situation. This validation stage is essential before attempting to generate a CAD solid, since it prevents connectivity errors from remaining undetected until later stages of the process.

4. CONCLUSIONS

We have showed the main features in the ongoing research of a PhD Doctoral Thesis, addressing the problem of 2D to 3D geometric reconstruction. Experimental results on polyhedral CAD parts demonstrate that the proposed pipeline produces geometrically accurate and topologically consistent models. The integration of topological validation significantly reduces reconstruction ambiguities and improves robustness. Figure 5 shows some screenshots of the computer app and some instances of processed parts. In a near future, we plan to improve the processing and cleaning of the input parts, and also open to other cases of more engineering complexity.

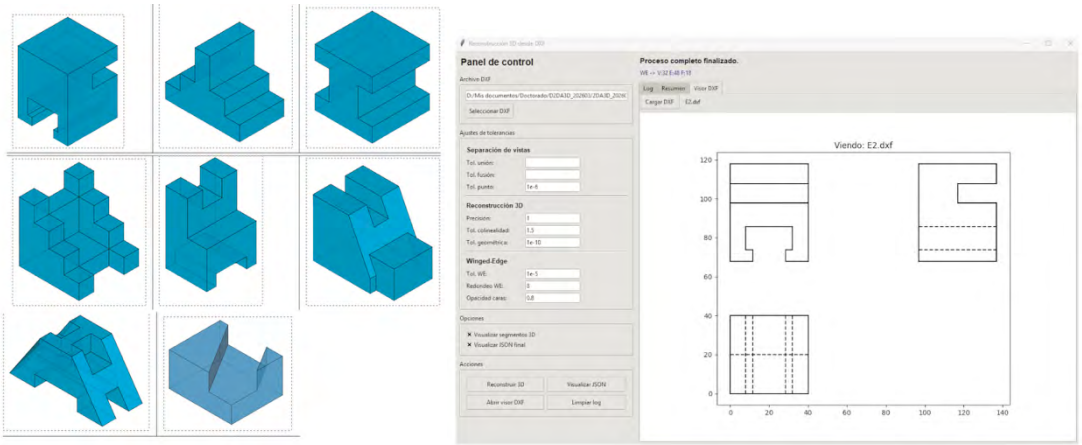


FIG 5
Screenshots of the computer app and some instances of processed parts

REFERENCES

[1] H. Yong-Tao and X. Wenyi, 3D Reconstruction from Orthographic Projection Views Based on Solid Features, in 2009 WRI World Congress on Computer Science and Information Engineering. Los Angeles, California USA: IEEE, pp. 159-166 (2009).

[2] B. G. Baumgart, Winged Edge Polyhedron Representation, Stanford AI Lab (1972).

[3] F. Ding, H. Zhang, and Y. Wen, Converting Sectional Views to Three Orthographic Views to Reconstruct 3D models, Computer-Aided Design and Applications, 8(4), pp. 571-582 (2011).

[4] L. Hoang, 3D Solid Reconstruction from 2D Orthographic Views, in Mixed Reality and Three-Dimensional Computer Graphics, B. Sobota and D. Cvetković, Eds. IntechOpen (2020).

[5] S. Shum, W. Lau, M. Yuen, and K. Yu, Solid reconstruction from ortho-graphic views using 2-stage extrusion, Computer-Aided Design, vol. 33, no. 1, pp. 91-102 (2001).

[6] Idesawa M. A system to generate a solid figure from three view. Bulletin of JSME;16(92):216-225 (1973).

[7] Wesley MA, Markowsky G. Fleshing out projections. IBM Journal of Research and Development.25(6):229-258 (1981).

[8] Sakurai H, Gossard DC. Solid model input through orthographic views. ACM SIGGRAPH Computer Graphics; 17(3):243-252 (1983).

Comparative Design and FEM-Based Structural Assessment of Type IV Green Hydrogen Pressure Vessels for Fuel Cell Vehicle Applications

Miguel Suffo*, José Manuel Devís

Department of Mechanical Engineering and Industrial Design, School of Engineering, University of Cádiz, Puerto Real, Cádiz, Spain

*e-mail: miguel.suffo@uca.es

Abstract: Green hydrogen is a promising energy carrier for decarbonising road transport, but it requires lightweight high-pressure storage systems. This short paper presents a preliminary design and finite element assessment of Type IV hydrogen pressure vessels for fuel-cell vehicle applications. A recycled high-density polyethylene liner (BRHDPE) and a carbon-fibre composite overwrap were considered. Two head geometries, hemispherical and torispherical, and two carbon-fibre grades, Torayca T300 and T800H, were compared in terms of structural response, material mass and preliminary cost. Composite thicknesses were estimated according to ASME Section X criteria and assessed in ANSYS under 70 MPa operating pressure and 157 MPa proof pressure. All configurations satisfied the adopted proof-pressure requirement. Hemispherical heads provided lower deformation, stress and higher safety factors, whereas torispherical heads showed greater stress concentration. T800H reduced overwrap mass but increased raw-material cost. The study provides early-stage design criteria for lightweight Type IV hydrogen vessels and identifies laminate-level optimisation and experimental validation as future work.

Keywords: *Composite overwrap, Finite element analysis, Pressure vessel design, Structural safety, Head geometry, Sustainable mobility.*

1. INTRODUCTION

The transition towards low-carbon transport requires energy storage systems that combine high energy density, safety and low environmental impact. Renewable hydrogen is a promising energy carrier for fuel-cell electric vehicles (FCEVs), but its low volumetric energy density requires compressed storage, typically at 350–700 bar. Therefore, the tank must provide high structural resistance while minimising mass and volume [1,2,3]. Composite overwrapped pressure vessels (COPVs) are the dominant solution for high-pressure automotive hydrogen storage, with Type IV configurations being particularly attractive for vehicle applications because of their polymer liner and lightweight composite overwrap [3,4 ,5]. Type IV vessels use a non-metallic liner to guarantee gas tightness and a carbon-fibre composite overwrap to resist the internal pressure. Compared with metallic tanks, this architecture improves gravimetric performance, although it requires careful control of liner compatibility, fibre orientation, manufacturing quality and proof testing [3-6]. This work presents a comparative preliminary design and FEM-based structural assessment of four Type IV hydrogen pressure vessel configurations for FCEV applications. Two head geometries, hemispherical and torispherical, and two carbon-fibre grades, T300 and T800H, were compared in terms of deformation, stress distribution, safety factor, material mass and preliminary cost. The aim is to provide design-oriented criteria for the early-stage assessment of lightweight hydrogen storage vessels.

2. MATERIALS AND METHODS

2.1. Design requirements and vessel configurations

The vessel was designed as a Type IV hydrogen storage tank for FCEV applications, using the Hyundai Nexo as the reference case. The nominal operating pressure was set at 70 MPa and the target internal volume was approximately 52.4 L, corresponding to one of the three hydrogen tanks considered in this vehicle architecture [7]. A proof-pressure condition of 157 MPa, equivalent to 2.25 times the operating pressure, was adopted for structural verification according to safety-oriented frameworks for compressed hydrogen storage and fully wrapped composite gas cylinders [8-10]. The vessel architecture consisted of a 4 mm-thick blended and recycled high-density polyethylene liner (BRHDPE) and an external carbon-fibre composite overwrap. The use of BRHDPE was based on previous material-characterisation work on recycled HDPE [11]. In this configuration, the liner provides gas tightness, whereas the composite overwrap is the main load-bearing component. Four configurations were analysed by combining two head geometries, hemispherical and torispherical, with two carbon-fibre grades, Torayca T300 and T800H [12,13]. The torispherical geometry used a crown radius equal to the external diameter of the cylindrical body and a knuckle radius equal to 6% of the crown radius, following pressure-vessel design criteria [10,14].

2.2. Material properties and thickness estimation

The main design inputs and material alternatives are summarised in Table 1. A 4 mm-thick BRHDPE liner was considered in all configurations, while the carbon-fibre composite

overwrap was defined using either Torayca T300 or Torayca T800H. T300 was considered as a lower-cost alternative, whereas T800H provides higher stiffness and tensile strength, allowing a reduction in the preliminary overwrap thickness.

TABLE 1
Main design inputs and material alternatives

Item	Value or option	Role in the design
Working pressure	70 MPa / 700 bar	Automotive hydrogen storage condition
Proof pressure	157 MPa	2.25 times the working pressure
Tank volume	52.4 L	Single-vessel capacity reference
Hemispherical vessel	R = 134 mm; cylindrical length = 750 mm; total length = 1018 mm	High structural efficiency
Liner	BRHDPE, 4 mm	Gas tightness and sustainability contribution
Composite overwrap	T300: 20.4 mm; T800H: 15.9 mm	Primary load-bearing structure

The composite thickness was estimated using a simplified sizing approach based on ASME Section X criteria for fibre-reinforced plastic pressure vessels [10]. The adopted relation is expressed in equation (1):

$$t = P \cdot R / E \tag{1}$$

where t is the estimated overwrap thickness, P is the internal design pressure, R is the vessel inner radius and E is the longitudinal elastic modulus of the selected carbon-fibre grade. This analytical estimate was used only as an initial sizing criterion before FEM verification. The resulting overwrap thicknesses were 20.4 mm for T300 and 15.9 mm for T800H, and these values were implemented in the CAD/FEM models following current design approaches for Type IV hydrogen pressure vessels [4,5,14].

2.3. FEM model and boundary conditions

The numerical assessment was carried out in ANSYS Static Structural using the same CAD/FEM workflow for the four configurations. Each model included the BRHDPE liner, the carbon-fibre composite overwrap and two external support rings representing the attachment points to the vehicle structure. The liner and overwrap were modelled as separate solid bodies with bonded contact between them, and bonded contacts were also assigned between the overwrap and the support rings. At this preliminary design stage, the carbon-fibre overwrap was modelled using equivalent homogenised elastic properties derived from manufacturer data. This simplification enables comparison between geometries and material grades, but does not reproduce the full laminate architecture, winding sequence or fibre-angle-de-

pendent behaviour of a real filament-wound vessel. Therefore, the results should be interpreted as an early-stage structural comparison rather than as a certification-oriented laminate design. Uniform internal pressure was applied to the inner surface of the liner. Two loading conditions were analysed: 70 MPa as the nominal operating pressure and 157 MPa as the proof-pressure condition. The external support rings were constrained using fixed supports. A solid finite element mesh with a characteristic element size of 10 mm was used, with additional sizing controls at the liner/overwrap contact regions. The same meshing strategy was applied to all models. Since no formal mesh-convergence study was included, the results are used for comparative assessment rather than final design certification. Figure 1 shows the FEM model used in the simulations, including the vessel geometry with the external support rings, the finite element mesh, the proof-pressure load applied to the liner surface and representative von Mises stress fields obtained for the T800H hemispherical and torispherical configurations.

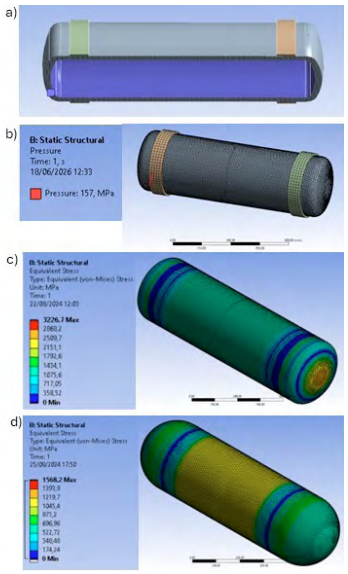


FIG. 1

FEM model and representative ANSYS results: (a) vessel geometry with support rings and liner cutaway, (b) finite element mesh and 157 MPa proof pressure, (c) T800H hemispherical-head von Mises stress distribution, and (d) T800H torispherical-head von Mises stress distribution

2.4. Evaluation criteria

The four vessel configurations were compared using structural and preliminary economic indicators. Structural performance was assessed through maximum total deformation, maximum equivalent von Mises stress and safety factor under proof-pressure conditions. These outputs were used to evaluate the influence of head geometry and carbon-fibre grade on the mechanical response of the vessels. Material mass and approximate raw-material cost were also considered to support the preliminary design comparison. Therefore, the final assessment considered the balance between structural safety, stress concentration, mass reduction and material cost.

3. RESULTS AND DISCUSSION

3.1. Structural response under operating and proof-pressure conditions

The four vessel configurations were evaluated under the nominal operating pressure of 70 MPa and the proof-pressure condition of 157 MPa, corresponding to 2.25 times the operating pressure according to the adopted verification framework for fully wrapped composite pressure vessels [8-10]. As shown in Table 2, deformation and stress values are reported separately for each loading condition. At 70 MPa, the hemispherical-head configurations showed the lowest maximum deformations, 0.44 mm for T300 and 0.43 mm for T800H, whereas the torispherical configurations reached 1.27 mm and 1.44 mm, respectively. The same trend was observed for maximum equivalent stress, with values of 536 MPa and 680 MPa for the hemispherical vessels, compared with 1055 MPa and 1439 MPa for the torispherical vessels. Under proof-pressure conditions, the hemispherical configurations maintained maximum deformations below 1 mm, while the torispherical configurations reached 2.84 mm for T300 and 3.24 mm for T800H. Maximum equivalent stress increased to 1204 MPa and 1568 MPa in the hemispherical configurations, compared with 2413 MPa and 3227 MPa in the torispherical configurations. All configurations remained below the adopted strength limits, although the highest safety factors corresponded to the hemispherical heads, particularly the T800H hemispherical configuration.

TABLE 2
FEM results under operating and proof-pressure conditions

Parameter	Pressure	T300 hemisph.	T300 torisph.	T800H hemisph.	T800H torisph.
Maximum deformation (mm)	70 MPa	0.44	1.27	0.43	1.44
Maximum deformation (mm)	157 MPa	0.98	2.84	0.97	3.24
Maximum stress (MPa)	70 MPa	536	1055	680	1439
Maximum stress (MPa)	157 MPa	1204	2413	1568	3227
Safety factor	157 MPa	3.01	1.46	3.72	1.71

3.2. Influence of head geometry and carbon-fibre grade

The results show that head geometry had a stronger influence on structural response than the change in carbon-fibre grade alone. Hemispherical heads distributed the internal pressure more efficiently, reducing stress concentration and deformation at the end regions of the vessel. This is consistent with pressure-vessel design principles, where more continuous curved geometries generally provide more favourable stress distributions under internal pressure [10,12]. By contrast, the torispherical configurations showed a more localised response, with higher stress concentration in the head region. This difference was reflected in the safety factors obtained under proof-pressure conditions. The T300 hemispherical configuration reached a safety factor of 3.01, compared with 1.46 for the T300 torispherical con-

figuration. Similarly, the T800H hemispherical configuration reached 3.72, compared with 1.71 for the T800H torispherical configuration. Therefore, for both carbon-fibre grades, the hemispherical geometry provided approximately twice the safety margin of the torispherical alternative. The use of T800H reduced the required overwrap thickness, but did not eliminate the influence of geometry. In particular, the T800H torispherical configuration still exhibited high stress concentration under proof pressure. This indicates that material substitution alone is not sufficient to optimise the vessel, and that head geometry and laminate architecture should be considered together [4,5]. Torispherical heads may still be useful when packaging or manufacturability constraints are dominant, but additional local reinforcement, winding-angle optimisation or laminate-level redesign would be required before prototyping [14].

3.3. Mass and preliminary cost comparison

Material mass and approximate raw-material cost were also considered, since gravimetric efficiency and carbon-fibre cost are key factors in automotive Type IV hydrogen storage systems [3-5]. As shown in Table 3, the BRHDPE liner represented only a small fraction of the total material mass and cost, with values close to 3.39–3.53 kg and below 6 € per vessel. In contrast, the carbon-fibre overwrap dominated the material cost in all configurations. The T800H configurations required less composite mass than the T300 configurations because of their lower assigned overwrap thickness. However, the higher unit price of T800H offset this mass reduction, resulting in a higher preliminary raw-material cost. Therefore, from a cost-performance perspective, the T300 hemispherical configuration was the most economical alternative, whereas the T800H hemispherical configuration provided the highest structural safety margin.

TABLE 3
Material mass and approximate raw-material cost per vessel

Configuration	BRHDPE mass (kg)	BRHDPE cost (€)	Composite mass (kg)	Composite cost (€)
T300 hemispherical	3.39	4.45-4.94	33.80	777.40-1183.00
T300 torispherical	3.53	4.67-5.16	35.17	808.91-1230.95
T800H hemispherical	3.39	4.45-4.94	26.55	1619.55-1725.75
T800H torispherical	3.53	4.67-5.16	27.62	1684.82-1795.30

4. CONCLUSIONS

This work presented a comparative preliminary design and FEM-based structural assessment of four Type IV hydrogen pressure vessel configurations for fuel-cell vehicle applications. The study combined two head geometries, hemispherical and torispherical, and two carbon-fibre grades, T300 and T800H, using a BRHDPE liner as a sustainability-oriented gas-barrier layer. The FEM results confirmed the structural feasibility of the four prelimi-

nary configurations under operating and proof-pressure conditions. However, head geometry had a decisive influence on the structural response. Hemispherical heads provided lower deformation, lower maximum equivalent stress and higher safety factors than torispherical heads. From a cost-performance perspective, the T300 hemispherical configuration was the most economical alternative, whereas the T800H hemispherical configuration provided the highest structural safety margin. These results indicate that material selection, head geometry, structural safety and cost should be evaluated together during the early stages of Type IV hydrogen vessel development. Future work should include laminate-level modelling, fibre-winding angle optimisation, mesh-convergence analysis, fatigue and impact assessment, hydrogen permeability evaluation, burst testing and experimental validation before prototyping or certification-oriented design.

Acknowledgements: The authors declare that no specific funding was received for this work.

REFERENCES

[1] European Commission: A hydrogen strategy for a climate-neutral Europe. COM(2020) 301 final, Brussels (2020). https://energy.ec.europa.eu/system/files/2020-07/hydrogen_strategy_0.pdf, last accessed 2026/04/29.

[2] Barthelemy, H., Weber, M., Barbier, F.: Hydrogen storage: Recent improvements and industrial perspectives. Int. J. Hydrogen Energy 42, 7254-7262 (2016). https://doi.org/10.1016/j.ijhydene.2016.03.178.

[3] Hua, T.Q., Ahluwalia, R.K., Peng, J.-K., Kromer, M., Lasher, S., McKenney, K., Law, K., Sinha, J.: Technical assessment of compressed hydrogen storage tank systems for automotive applications. Int. J. Hydrogen Energy 36, 3037-3049 (2011). https://doi.org/10.1016/j.ijhydene.2010.11.090.

[4] Piraino, F., Pagnotta, L., Corigliano, O., Genovese, M., Fragiacomo, P.: Advances in Type IV Tanks for Safe Hydrogen Storage: Materials, Technologies and Challenges. Hydrogen 6, 80 (2025). https://doi.org/10.3390/hydrogen6040080.

[5] Eko, A.J., Epaarachchi, J., Jeewantha, J., Zeng, X.: A review of type IV composite overwrapped pressure vessels. Int. J. Hydrogen Energy 109, 551-573 (2025). https://doi.org/10.1016/j.ijhydene.2025.02.108.

[6] SAE International: SAE J2579_202301. Standard for Fuel Systems in Fuel Cell and Other Hydrogen Vehicles. SAE International (2023). https://www.sae.org/standards/j2579_202301-standard-fuel-systems-fuel-cell-hydrogen-vehicles, last accessed 2026/04/29.

[7] Hyundai Motor Company Australia: NEXO: Hyundai's hydrogen fuel-cell first. Hyundai Motor Company Australia. https://www.hyundai.com/au/en/news/vehicles/nexo-hyundai-hydrogen-fuel-cell-first, last accessed 2026/04/29.

[8] Zhu, S., Ding, C., Hu, X., Tian, Y.: Analysis of safety technical standards for hydrogen storage in fuel cell vehicles. Frontiers in Energy Research 12, 1376739 (2024). https://doi.org/10.3389/fenrg.2024.1376739.

[9] Asociación Española de Normalización: UNE-EN 12245:2023. Botellas para el transporte de gas. Botellas de material compuesto totalmente recubiertas. UNE, Madrid (2023).

[10] The American Society of Mechanical Engineers: ASME BPVC.X-2025. BPVC Section X — Fiber-Reinforced Plastic Pressure Vessels. ASME, New York (2025). ISBN 9780791877265. https://www.asme.org/codes-standards/find-codes-standards/bpvc-x-bpvc-section-x-fiber-reinforced-plastic-pressure-vessels, last accessed 2026/04/29.

[11] Suffo, M., Brey, M., Orellana, J.P., García-Morales, J.L.: Feasibility of utilization of recycled HDPE in manhole covers for urban traffic areas and industrial zones. J. Clean. Prod. 425, 138818 (2023). https://doi.org/10.1016/j.jclepro.2023.138818.

[12] Toray Composite Materials America, Inc.: TORAYCA™ T300 Standard Modulus Carbon Fiber Data Sheet. Toray Composite Materials America, Inc. https://www.toraycma.com/wp-content/uploads/T300-Data-Sheet.pdf, last accessed 2026/04/29.

[13] Toray Composite Materials America, Inc.: TORAYCA™ T800H Intermediate Modulus Carbon Fiber Data Sheet. Toray Composite Materials America, Inc. https://www.toraycma.com/resources/data-sheets/, last accessed 2026/04/29.

[14] Schmidt, F., Richter, J.: Conception, design and manufacture of Type IV hydrogen pressure vessels for general aviation. 1-5 (2024). https://doi.org/10.25967/610462.

Multimodal Biomechanical Assessment of Untreated and Cross-Linked Corneas for the Optimization of Keratoconus Therapies

Lourdes Quilez[a, b], Alejandro Roca[a, b], Erwan Bentaib[c], Carmelo Gómez[a, b], José González[a, b], Francisco Cavas[a, b, *]

[a] Department of Structures, Construction and Graphic Expression, Universidad Politécnica de Cartagena, member of the European University of Technology (EUT+), Campus Muralla del Mar, C/ Doctor Fleming, s/n, 30202 Cartagena, Spain

[b] Applied Bioengineering and Computational Simulation Research Group, Universidad Politécnica de Cartagena, member of the European University of Technology (EUT+), Campus Muralla del Mar, C/ Doctor Fleming, s/n, 30202 Cartagena, Spain

[c] Faculty of Odontologie, Master's in Biomechanics: Biomechanics, Biomaterials, and Health, Université de Reims Champagne-Ardenne, 51100 Reims, France

* e-mail: francisco.cavas@upct.es

Abstract: Keratoconus and related corneal ectasias involve progressive stromal thinning, disruption of collagen lamellae organization, and a marked loss of biomechanical integrity, ultimately leading to irregular astigmatism and significant visual impairment. Corneal collagen cross-linking (CXL) is a widely adopted therapeutic intervention aimed at halting disease progression by increasing stromal stiffness through photochemically induced covalent bonding between collagen fibrils. To quantitatively assess its multiscale biomechanical impact, we conducted a coordinated in-silico study comparing untreated and CXL-treated corneal tissues using three complementary mechanical paradigms. Uniaxial tensile simulations of corneal strips were performed to derive stress–strain relationships whereas inflation models of whole corneas were implemented to reproduce pressure–apex displacement responses and spatial strain distributions. Cross-modality comparisons yielded a consistent and robust multimodal biomechanical characterization of CXL effects, demonstrating that anteriorly concentrated stiffening is sufficient to significantly reduce pathological strain under physiological loads while preserving posterior stromal compliance. These findings have direct implications for optimizing treatment protocols and improving the predictive accuracy of patient-specific computational models.

Keywords: *corneal cross-linking, biomechanical testing, keratoconus, digital twins.*

1. INTRODUCTION

The human cornea is the primary refractive element of the eye, whose geometry and transparency are finely tuned to ensure optimal optical performance. As a transparent, avascular, and densely innervated tissue [1], its structure reflects a delicate balance between material properties, geometry, and biomechanical loading. Small perturbations in corneal shape can significantly degrade visual quality [2], underscoring the clinical importance of maintaining structural integrity. While common refractive errors affect a large portion of the population [3] and are routinely corrected with surgical procedures, corneal ectatic disorders such as keratoconus represent a more severe and progressive class of pathologies. Keratoconus is characterized by localized stromal thinning, collagen disorganization, and biomechanical weakening that leads to corneal steepening and visual impairment [4]. Historically, advanced cases required corneal transplantation, but the identification of stromal biomechanical failure as the key pathological mechanism has driven the development of alternative therapeutic strategies [5].

Corneal collagen cross-linking (CXL), based on riboflavin–UVA–induced photochemical reactions, has become the gold standard for halting ectatic progression by increasing stromal stiffness and stabilizing corneal geometry [6] . Experimental studies have demonstrated that CXL induces significant stiffening [7] and microstructural analyses highlighting increased interfibrillar connectivity [8]. Furthermore, stiffening is spatially heterogeneous, typically concentrated in the anterior and central cornea, motivating the development of customized and spatially selective treatment approaches [9].

In this context, we present an in-silico framework for evaluating the multiscale biomechanical effects of CXL through complementary computational assays. The approach integrates uniaxial tensile simulations to capture bulk lamellar response, pressurized inflation modeling to reproduce physiological deformation and strain fields, and depth-resolved micro indentation analysis to quantify local stiffness variations. This multimodal strategy enables a consistent and comprehensive biomechanical characterization, linking local material changes with global structural behavior. The results support the concept that anteriorly concentrated stiffening is sufficient to reduce pathological strain while preserving posterior compliance. By incorporating patient-specific geometry, intraocular pressure, and spatially varying treatment parameters, this framework establishes a foundation for virtual corneal twins, with potential applications in personalized surgical planning, risk stratification, and optimization of customized CXL interventions.

2. MATERIAL AND METHODS

2.1. Material model

The mechanical behavior of the cornea was represented using a constitutive framework based on the Holzapfel–Gasser–Ogden (HGO) model, which captures the strongly anisotropic and hyperelastic characteristics of corneal tissue. In this formulation, the strain energy density function is expressed as the sum of two distinct contributions: a volumetric term associated with compressibility effects and an isochoric term describing distortional deformations as can be observed in equation (1).

$$\Psi = \Psi_{\text{volumetric}} + \bar{\Psi}_{\text{isochoric}} \tag{1}$$

The volumetric response is governed by the Jacobian of the deformation gradient (J), which remains close to unity due to the water content of the cornea (approximately 80%) [10]. Consequently, volumetric changes are minimal, and this contribution primarily enforces near-incompressibility. The volumetric energy term can be observed in equation (2):

$$\Psi_{\text{volumetric}} = \frac{1}{2} k_0 (J-1)^2 \tag{2}$$

where k_0 represents the bulk modulus. In this study, k_0 was set to 5.5 MPa in agreement with values commonly reported in the literature [11]. The isochoric component accounts for both isotropic matrix behavior and anisotropic fiber reinforcement. The isotropic response of the ground substance is described using a Mooney–Rivlin model with two material constants, a_1 and a_2 as can be observed in equation (3):

$$\Psi_{\text{isotropic}} = a_1 \left(\bar{I}_1 - 3\right) + a_2 \left(\bar{I}_2 - 3\right) \tag{3}$$

where $\bar{I}_1$ and $\bar{I}_2$ are the first and second invariants of the modified right Cauchy–Green deformation tensor. In order to capture the contribution of collagen, an additional anisotropic term is introduced. This component accounts for two preferentially oriented fiber families and reproduces their nonlinear stiffening under stretch through an exponential formulation as can be observed in equation (4):

$$\Psi_{\text{anisotropic}} = \frac{k_1}{2k_2}\left(\exp\left[k_2\left(\bar{I}_4 - 1\right)^2\right] - 1\right) + \frac{k_1}{2k_2}\left(\exp\left[k_2\left(\bar{I}_6 - 1\right)^2\right] - 1\right) \tag{4}$$

Here, k_1 defines the stiffness associated with the fibers, while k_2 controls the rate of strain-induced stiffening. The invariants $\bar{I}_4$ and $\bar{I}_6$ describe the stretch along two preferred collagen directions, denoted as m_0 and n_0.

Material parameters were calculated using previously reported experimental tensile data obtained along the superior–inferior direction of human cornea as can be observed in Table 1. This direction is known to exhibit pronounced structural anisotropy, as collagen fibers are preferentially aligned along both the nasal–temporal and superior–inferior orientations, which strongly influences the observed mechanical response [12].

TABLE 1
Corneal material parameters

Condition	Parameter	Value	Units
PRE (untreated)	a_1	0.1	MPa
	a_2	0	MPa
	k_1	0.076	MPa
	k_2	6.90	—
POST (treated)	a_1	0.1	MPa
	a_2	0	MPa
	k_1	0.59	MPa
	k_2	6.90	—

2.2. Finite element model description

Finite element models have been implemented in software ANSYS (Swanson Analysis System Inc., USA) considering 3D elements of type SOLID185 with fully integrated scheme combined with a mixed displacement-pressure (u-p) formulation to ensure robust performance under conditions of material incompressibility.

Preferential directions of collagen fibres are placed in X and Y directions in all models with the exception of limbus zone (diameter between 11 and 12 mm in the corneal model where only circumferential direction is considered according to previously published investigations)[13]. Finite element models considered can be observed in Figure 1.

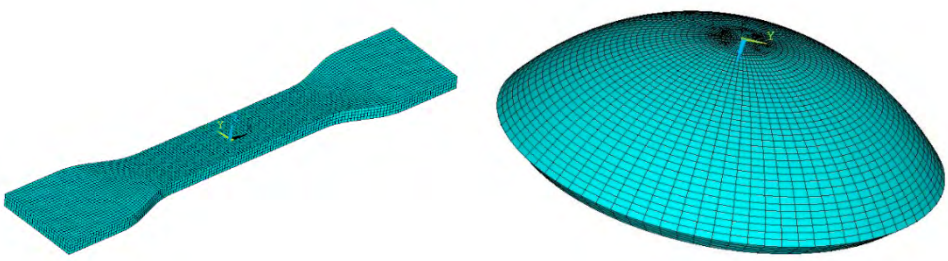


FIG. 1
Finite element models implemented for axial test (left) and inflation and indentation tests (right)

Tensile test finite element model has been constrained in one side (displacements and rotations) whereas a constant displacement equivalent to a stretch of $\lambda = 1.2$ has been applied in the other side. For inflation test a theoretical Navarro model has been considered with pivotal constraints in the limbus zone according to other investigations [13]. In this re-

search work and as a simplification load case, the free stress geometry [14] has not been calculated. For the inflation test a constant intraocular pressure of 14 mmHg has been considered applied in the posterior side. As a simplification case in this study, cross-linking effect has been simulated modifying the material properties in elements nearest to the anterior zone (25% of the thickness).

3. RESULTS

According to the results of tensile test (Figure 2) the stress to reach the stretch before cross linking treatment is 0.52 MPa increasing this value until 1.64 MPa after the treatment.

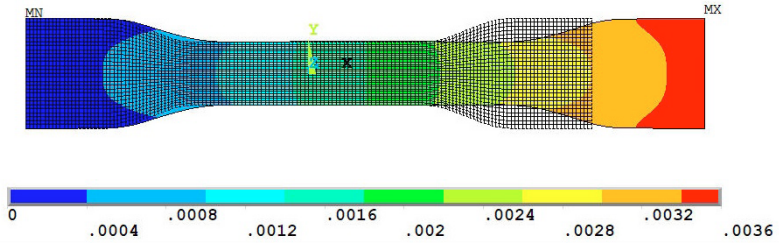


FIG. 2
Displacement (True extension) of the tensile test coupon (mm)

Before Cross-linking treatment, the cornea shows a maximum displacement of 0.08 mm in the inflation test as can be observed in the left side of Figure 3 and a maximum stress intensity close to 10700 MPa in the center of the anterior surface (Figure 3, right side).

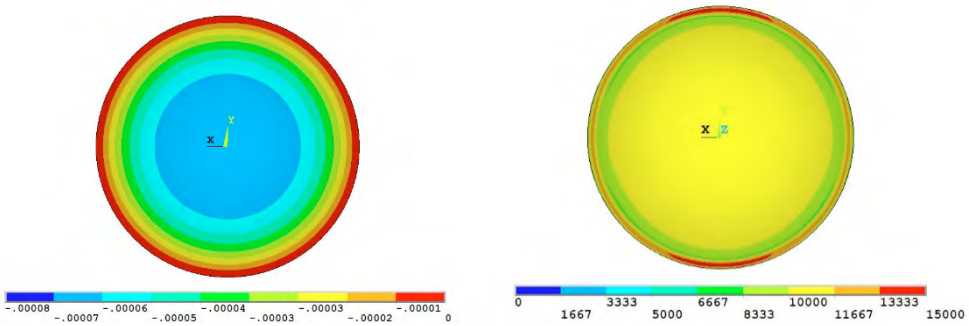


FIG. 3
Displacement [mm] in the inflation test for IOP = 14 mm Hg (Left side) and stress intensity [MPa] (Right side) before CXL treatment

After Cross-linking treatment, the cornea shows a maximum displacement of 0.06 mm (decreasing factor of 1.33) as can be observed in the left side of Figure 4 and a maximum stress intensity close to 19500 MPa in the center of the anterior surface (Figure 4, right side).

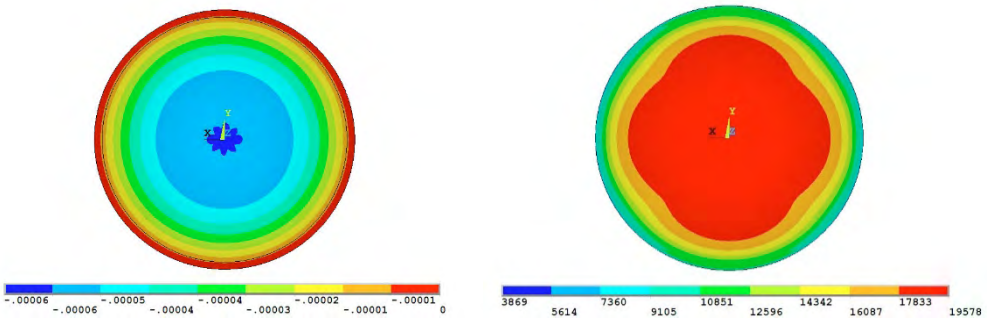


FIG. 4
Displacement [mm] in the inflation test for IOP = 14 mm Hg (Left side) and stress intensity [MPa] (Right side) after CXL treatment

4. CONCLUSIONS

The present study provides clear and quantitative evidence of the biomechanical effectiveness of corneal collagen cross-linking (CXL) as a reinforcement strategy for ectatic corneal tissue, demonstrating across all computational analyses a consistent increase in stromal stiffness and a reduction in deformability after treatment; the observed rise in stress required to achieve a given stretch, together with the decrease in apex displacement under physiological loads, confirms a stabilization of the pathological mechanical response to keratoconus. This mechanical improvement is primarily localized in the anterior stroma, where cross-linking induces sufficient stiffening to reduce pathological strain while preserving posterior compliance and maintaining a physiologically consistent deformation pattern. Beyond validating the strengthening effect of CXL, this work highlights the importance of computational modeling for investigating treatment-induced biomechanical changes. In this context, in-silico approaches provide a powerful tool for systematically analyzing treatment parameters and patient-specific conditions, supporting the development of predictive and personalized strategies for optimizing CXL protocols and improving clinical outcomes.

Acknowledgments: This publication is part of the research project 22665/PI/24, funded by grant FS/10.13039/100007801 and was also carried out in collaboration with the Association for the Integration of the Disabled in the Comarca del Mar Menor (AIDEMAR, collaboration protocol UPCT- AIDEMAR).

5. REFERENCES

[1] M. S. Sridhar, "Anatomy of cornea and ocular surface," (in eng), Indian journal of ophthalmology, vol. 66, no. 2, pp. 190-194, Feb 2018, doi: 10.4103/ijo.IJO_646_17.

[2] S. Liduma, A. Luguzis, and G. Krumina, "The impact of irregular corneal shape parameters on visual acuity and contrast sensitivity," (in eng), BMC ophthalmology, vol. 20, no. 1, p. 466, Nov 26 2020, doi: 10.1186/s12886-020-01737-x.

[3] L. Huang, D. Zhang, and M. Liu, "Global trends in refractive disorders from 1990 to 2021: insights from the global burden of disease study and predictive modeling," (in eng), Frontiers in public health, vol. 13, p. 1449607, 2025, doi: 10.3389/fpubh.2025.1449607.

[4] M. Romero-Jiménez, J. Santodomingo-Rubido, and J. S. Wolffsohn, "Keratoconus: a review," (in eng), Contact lens & anterior eye : the journal of the British Contact Lens Association, vol. 33, no. 4, pp. 157-66; quiz 205, Aug 2010, doi: 10.1016/j.clae.2010.04.006.

[5] S. Son, M. Friedrich, A. S. Jun, and U. S. Soiberman, "Advancements and Innovations in Keratoconus Management: A Review of Current Practices," (in eng), Journal of clinical medicine, vol. 14, no. 21, Oct 23 2025, doi: 10.3390/jcm14217491.

[6] N. Papachristoforou, A. Ueno, K. Ledwos, J. Bartuś, A. Nowińska, and I. Karska-Basta, "A Review of Keratoconus Cross-Linking Treatment Methods," Journal of clinical medicine, vol. 14, no. 5, p. 1702doi: 10.3390/jcm14051702.

[7] H. Hatami-Marbini and S. M. Jayaram, "UVA/riboflavin collagen crosslinking stiffening effects on anterior and posterior corneal flaps," Experimental Eye Research, vol. 176, pp. 53-58, 2018/11/01/ 2018, doi: https://doi.org/10.1016/j.exer.2018.05.014.

[8] F. Hafezi *et al.*, "Corneal cross-linking," Progress in Retinal and Eye Research, vol. 104, p. 101322, 2025/01/01/ 2025, doi: https://doi.org/10.1016/j.preteyeres.2024.101322.

[9] H. Zhang, M. Roozbahani, A. L. Piccinini, F. Hafezi, G. Scarcelli, and J. B. Randleman, "Brillouin microscopic depth-dependent analysis of corneal crosslinking performed over or under the LASIK flap," (in eng), Journal of cataract and refractive surgery, vol. 46, no. 11, pp. 1543-1547, Nov 2020, doi: 10.1097/j.jcrs.0000000000000294.

[10] D. G. Dawson and H. F. Edelhauser, "Chapter 9 - Corneal edema," in Ocular Disease, L. A. Levin and D. M. Albert Eds. Edinburgh: W.B. Saunders, 2010, pp. 64-73.

[11] C. Gómez, D. P. Piñero, M. Paredes, J. L. Alió, and F. Cavas, "Study of the Influence of Boundary Conditions on Corneal Deformation Based on the Finite Element Method of a Corneal Biomechanics Model," (in eng), Biomimetics (Basel, Switzerland), vol. 9, no. 2, Jan 25 2024, doi: 10.3390/biomimetics9020073.

[12] G. Wollensak, E. Spoerl, and T. Seiler, "Stress-strain measurements of human and porcine corneas after riboflavin–ultraviolet-A-induced cross-linking," Journal of Cataract & Refractive Surgery, vol. 29, no. 9, pp. 1780-1785, 2003/09/01/ 2003, doi: https://doi.org/10.1016/S0886-3350(03)00407-3.

[13] A. Pandolfi, "Cornea modelling," (in eng), Eye and vision (London, England), vol. 7, p. 2, 2020, doi: 10.1186/s40662-019-0166-x.

[14] C. Gómez, D. Pinero, J. Alió, and F. Cavas, "Comparative evaluation of methods for obtaining the stress-free geometry of keratoconus corneas with different levels of severity," Computers in Biology and Medicine, vol. 170, p. 107870, 12/01 2023, doi: 10.1016/j.compbiomed.2023.107870.

Enhancing Spatial Vision in Industrial Drawing through VR Integration: A Multidisciplinary Approach for Mechanical Assemblies

Xabier Sandua[a,*], Laura Carlosena[a], Josu Irisarri[b], Miguel Ángel Martín[a], Sara Marcelino[a], Fernando Veiga[a], Amaia Pérez[a]

[a] Department of Engineering, Public University of Navarra, Campus Arrosadía, 31006 Pamplona, Navarra, Spain

[b] Department of Statistics, Computer Science and Mathematics, Public University of Navarra, Campus Arrosadía, 31006 Pamplona, Navarra, Spain

* e-mail: xabier.sandua@unavarra.es

Abstract: Developing spatial vision for mechanical assemblies remains a persistent challenge for industrial engineering students trained through traditional 2D or screen-based CAD methods. To bridge this cognitive gap, this work presents an innovative teaching methodology for the "Industrial Drawing" module, born from a multidisciplinary collaboration between the Area of Graphic Engineering and the Area of Computer Languages and Systems. The core of the methodology centers on integrating Computer-Aided Design (CAD) with Virtual Reality (VR). The pedagogical workflow mimics a real-world industrial environment. It begins with a company presenting a real manufacturing order to students working in groups. The required component is introduced directly into a custom-built virtual environment as a 3D digital assembly. Utilizing VR headsets, students are transported into a simulated industrial workshop where they can manipulate the virtual geometry, see its specifications, and conduct a thorough analysis of its geometry, function, fabrication processes, fits and surface finishes. Furthermore, students validate the component by witnessing its virtual manufacturing process within this industrial setting. Finally, students return to the desktop environment to generate standardized assembly planes and full technical documentation using AutoCAD software. Ultimately, this methodology successfully overcomes traditional spatial perception barriers while preparing future engineers for the digital transformation of the industry.

Keywords: *mechanical assemblies, virtual reality, spatial vision, industrial drawing, education.*

1. INTRODUCTION

Developing strong spatial visualization skills is fundamental in engineering education, particularly within the field of graphic engineering. Spatial vision (the cognitive ability to mentally manipulate, rotate, and interpret three-dimensional objects from two-dimensional representations) is essential for understanding complex mechanical assemblies. However, developing this ability remains one of the most persistent pedagogical challenges in first-year industrial engineering courses [1]. Traditional teaching methods heavily rely on textbook exercises, 2D orthographic projections, and static screen-based Computer-Aided Design (CAD) modelling [2]. While these tools are foundational, they often fail to bridge the cognitive gap between flat representations and the physical reality of functional mechanisms, leading to student frustration and a lack of intuition regarding tolerances, clearances, and mechanical fits.

In recent years, the rapid advancement of Industry 4.0 technologies has offered new avenues to revolutionize engineering education [3]. Virtual Reality (VR) has emerged as a particularly powerful tool for spatial learning, as it transitions the student from a passive observer staring at a 2D monitor to an active participant inside a 3D digital ecosystem [4]. By providing stereoscopic depth perception and changes in viewpoints, VR mimics the way humans naturally interact with the physical world [5]. Research indicates that immersive learning environments can significantly lower cognitive load, boost student engagement, and accelerate the development of spatial reasoning skills compared to traditional desktop setups [6].

Despite the clear benefits of VR, its implementation in higher education often suffers from a lack of integration between design theory and practical application [7]. Graphic engineering courses frequently teach modeling uniquely, disconnected from actual manufacturing constraints. Students can model a complex component in a CAD environment without understanding how that part is physically machined, cast, or assembled on a factory floor. This curricular fragmentation limits the holistic understanding required of modern engineers [8]. Furthermore, deploying advanced VR tools requires a highly specialized technical infrastructure that engineering graphics departments rarely possess on their own.

To address these limitations, this paper presents an innovative, multidisciplinary pedagogical methodology developed for the "Industrial Drawing" subject, which is a first course mandatory subject for all the engineering degrees in Universidad Publica de Navarra (UPNA). This approach is built upon a strategic collaboration between the Area of Graphic Engineering and the Area of Computer Languages and Systems. By combining expertise in geometric product specification with advanced virtual environment development, we have created a seamless workflow that integrates high-fidelity CAD models into an interactive, immersive VR application.

The primary objective of this work is to mitigate the spatial vision barriers faced by students during the study of mechanical assemblies. To achieve this, the proposed methodology moves beyond simple 3D visualization by embedding the digital twin of a complex mechanical assembly into a highly detailed, simulated industrial workshop. Within this virtual environment, students can directly interact with the assembly (performing real-time assembly, disassembly, and inspection sequences) while simultaneously observing the manufacturing processes used to fabricate individual parts.

By contextualizing design within a realistic production environment, this methodology solves a specific didactic debility typically presented in graphical engineering subjects. In addition, it fosters a healthy, low-frustration learning ecosystem that supports the cognitive well-being of students while efficiently preparing them for the digital transformation of the industrial sector

2. METHODOLOGY

The implementation of this educational framework relies on a collaborative, two-part strategy: a robust software and hardware architecture developed between departments, and a structured pedagogical workflow embedded directly into the classroom.

2.1. System Architecture and VR Integration

To ensure an immersive and high-performance experience, the technical architecture utilizes professional real-time rendering systems and standalone hardware. The methodology integrates pre-existing 3D digital assets provided directly by industrial partners, establishing a high-fidelity digital foundation that guarantees realistic geometric relationships, as shown in Figure 1.

This digital mechanical assembly is integrated into Unity, which serves as the core 3D environment engine. The virtual environment, user interactions, and assembly physics are compiled within this engine. The software development lifecycle is managed using Visual Studio Code as the primary Integrated Development Environment (IDE), with scripts written in C# programming language to handle complex assembly manipulation, state machine logic for interactive sequences, and performance optimization.

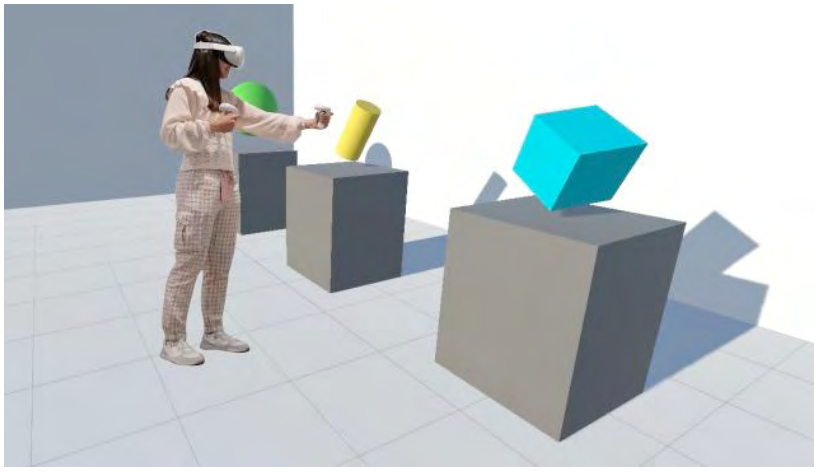


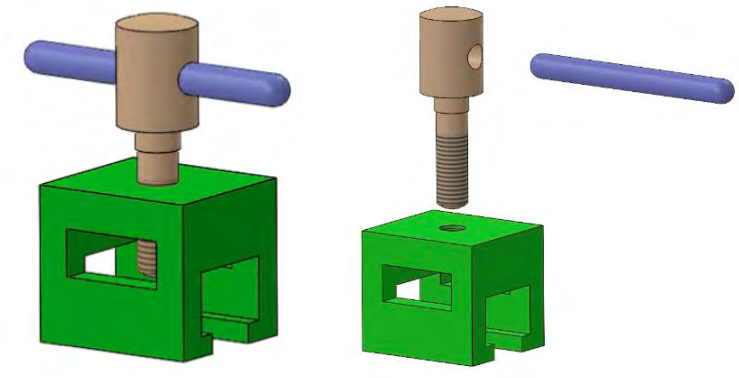
FIG. 1
Example of the Virtual Reality environment used for this work

The hardware deployment utilises Meta Quest 2 virtual reality headsets. These standalone units offer the spatial tracking accuracy required for detailed close-up object inspection and assembly manipulation without the physical constraints or trip hazards of tethered cables in a classroom environment. Through these headsets, students can visualize abstract structural characteristics, transitioning from flat textbook views to direct interaction with multifaceted spatial geometries.

2.2. Pedagogical Framework and Classroom Implementation

The proposed methodology is integrated into the "Industrial Drawing" module, a foundational first-year course across engineering degrees at the Universidad Pública de Navarra (UPNA). The course structure shifts away from passive listening toward a challenge-based learning model that mimics professional engineering practices. The workflow follows a sequential five-stage process:

1. *The Industrial Order:* the project begins with a simulated real-world briefing where a manufacturing company proposes a real technical order to the class. The student body is organized into small engineering design teams tasked with analyzing, validating, and documenting the requested mechanical mechanism. An example of this mechanism is shown in Figure 2.
2. *Virtual Geometry Reception:* the company provides the 3D digital image of the piece, which is uploaded directly into the VR application. Utilizing the Meta Quest 2 headsets, student groups inspect the object via Virtual Geometry. They can freely manipulate the component in a 1:1 scale environment, view its embedded technical specifications from any angle, and break down its primary visual layers.
3. *Comprehensive Component Analysis:* once familiar with the spatial layout, the groups perform an extensive engineering audit of the mechanism. This analysis requires teams to evaluate the geometric boundaries, functional constraints, necessary fabrication processes (such as milling, turning, or casting), and required surface finishes or tolerances essential for correct operation.
4. *VR Simulation and Industrial Validation:* students utilize the virtual workshop environment to validate the piece. This immersive phase places the virtual assembly within a lifelike factory ecosystem, allowing the students to observe the step-by-step fabrication process of the component in a realistic industrial environment, providing immediate contextual feedback on how their design choices translate to real manufacturing.
5. *Technical Documentation and Standardization:* in the final phase, students transition from the virtual space back to professional technical rendering software. Using AutoCAD, each group produces the standardized assembly planes, bill of materials (BOM), exploded views, and comprehensive documentation necessary to fulfill the original industrial order according to international engineering drawing standards.



(a) (b)

FIG. 2
Example of a Mechanical Assembly to be used as a practice exercise in class; (a) assemble 3D view of the press; (b) exploded 3D view of the press

3. RESULTS AND DISCUSSION

The implementation of this virtual reality-driven framework within the "Industrial Drawing" module at UPNA will yield highly practical learning results, significantly impacting both the technical capabilities and professional core competencies of the first-year engineering students. The main learning outcomes to be observed throughout the project are detailed below:

- Enhanced Spatial Visualization: by interacting with the component via Virtual Geometry, students bypassed the steep learning curve traditionally associated with interpreting flat technical drawings. The ability to manipulate the 3D assembly and inspect it, firsthand provided the spatial intuition required to later translate the virtual piece back onto 2D engineering planes in AutoCAD.
- Comprehension of Fabrication Processes: integration of the virtual workshop environment successfully bridged the gap between engineering theory and practical manufacturing. Rather than evaluating a mechanical part in isolation, students observed how components are virtually machined, cast, or forged. This can allow them to connect geometric shapes to real-world production limitations, helping them understand why specific surface finishing and tolerances are necessary.
- Increased Student Motivation: the realistic nature of receiving a direct order from a real company shift the classroom dynamic from passive consumption to active problem-solving. Students can show much higher engagement and enthusiasm compared to traditional drafting exercises, as they feel they were working on a tangible, professional engineering project.
- Collaborative Teamwork and Decision-Making: as the project is executed in groups, students have to debate and defend their engineering choices regarding manufacturing feasibility, function, and final documentation layout. The VR platform will serve

as a shared space where team members can collectively diagnose design errors and decide on the best approach to fulfill the company's order.

— Understanding of Real Industrial Environments: the project provides first-year students with a rare opportunity to comprehend a realistic workshop context early in their studies. Introducing industrial layouts, machinery, and workflows within the classroom demystifies manufacturing facilities, making the engineering profession feel more tangible and accessible.

4. CONCLUSIONS

The multidisciplinary methodology to be implemented in the "Industrial Drawing" module at the Universidad Publica de Navarra (UPNA) demonstrates that integrating Virtual Reality into early engineering curricula can successfully bridges the gap between abstract geometry and physical manufacturing. By shifting from traditional 2D interpretations to an immersive 1:1 scale environment, first-year students rapidly developed critical spatial visualization skills and a deep comprehension of real-world fabrication constraints.

Furthermore, the challenge-based framework (build around a real industrial order) can prove highly effective in boosting student motivation, fostering collaborative teamwork, and accelerating professional decision-making. Students will transition smoothly from immersive virtual validation to technical documentation in AutoCAD, mastering the entire design-to-manufacturing lifecycle without the logistical risks of a physical workshop.

REFERENCES

[1] Al-Ansi, A.M., Jaboob, M., Garad, A., Al-Ansi, A.: Analyzing augmented reality (AR) and virtual reality (VR) recent development in education. Social Sciences & Humanities Open. 8(1), 100532 (2023).

[2] Sorby, S.A.: Educational Research in Developing 3-D Spatial Skills for Engineering Students. International Journal of Science Education. 31(3), 459-480 (2009).

[3] Lampropoulos, G., Kinshuk: Virtual reality and gamification in education: a systematic review. Educational Technology Research and Development. 72(3), 1691-1785 (2024).

[4] Soliman, M., Pesyridis, A., Dalaymani-Zad, D., Gronfula, M., Kourmpetis, M.: The Application of Virtual Reality in Engineering Education. Applied Sciences. 11(6), 2879 (2021).

[5] Izard, S.G., Juanes Méndez, J.A., Palomera, P.R.: Virtual Reality Educational Tool for Human Anatomy. Journal of Medical Systems. 41(5), 76 (2017).

[6] Reis, V., Santos Baptista, J., Duarte, J.: Immersive Tools in Engineering Education—A Systematic Review. Applied Sciences. 15(11), 6339 (2025).

[7] Kavanagh, S., Luxton-Reilly, A., Wuensche, B., Plimmer, B.: A systematic review of Virtual Reality in education. Journal of Interactive Learning Research. 10(2), 85-119 (2017).

[8] Hyeon, R., Oh, W.-O.: Virtual reality education for preventing safety incidents in pediatric hospital settings: Quasi-experimental design pre-post-testing. Journal of Pediatric Nursing. 80, 56–63 (2025).

AI in Engineering Graphics: Changing Teacher's Role

G. Peris Fajarnés*, M. Moncho Santonja, I. Lengua, E. Burguera-Sierra, R. Barberà-Guillem, B. Defez

CITG – Research Centre in Graphic Technologies, Universitat Politècnica de València (UPV), Spain

* e-mail: gperis@upv.es

Abstract: Generative artificial intelligence is rapidly changing the conditions under which Engineering Graphics is taught, learned and assessed. Tools capable of automating CAD and BIM operations, generating three-dimensional models from natural-language prompts and evaluating technical drawings challenge a teaching model historically centred on procedural software instruction and final artefact correction. This paper analyses what this transition means for the Engineering Graphics professor. Drawing on recent literature in graphic design, CAD/BIM, engineering education and AI-era assessment, the paper identifies three differentiated trajectories of AI impact for students, technicians and experts, and argues that the central pedagogical risk is not the use of AI itself but the emergence of visually convincing outputs that conceal weak spatial reasoning, poor technical judgement or unexamined design decisions. In response, the professor's role is reframed as that of a designer of authentic learning experiences, a curator of AI-generated artefacts and an auditor of student reasoning. Four faculty competencies are proposed: critical evaluation of AI outputs, authentic activity design, generative AI literacy and process-centred assessment. The paper further synthesises a catalogue of assessment-redesign strategies that relocate evaluation from the finished drawing or model to the decisions, iterations and justifications that produce it. These strategies include sketching, process logs, prompt documentation, reasoning-aligned rubrics, graduated AI-use scales, multi-step problems and hybrid human–AI evaluation. The paper concludes that the future quality of Engineering Graphics education will depend less on resisting AI than on preparing professors to make student reasoning visible, assessable and professionally meaningful.

Keywords: *Artificial intelligence, Engineering Graphics, CAD/BIM education, critical thinking, authentic assessment, process-centred assessment.*

1. INTRODUCTION

Generative artificial intelligence is no longer an external trend approaching Engineering Graphics; it is already reshaping the tools, workflows and assumptions through which the discipline is practised. In professional environments, AI-enhanced systems increasingly automate routine CAD and BIM operations, generate three-dimensional geometry from natural-language prompts and support the checking of drawings and models against technical requirements [1,2]. These developments do more than accelerate familiar tasks. They question which forms of knowledge should be taught, how competence should be demonstrated and what kind of professor is needed when software can reproduce many procedural operations previously at the centre of instruction.

The literature across graphic design, CAD/BIM and engineering education presents this transition as simultaneously enabling and destabilising [3-7]. AI lowers entry barriers, supports ideation and can give novice learners access to sophisticated forms of representation that previously required extensive software fluency [4,6]. Yet the same affordances create a serious pedagogical vulnerability: students may submit outputs that appear technically mature while lacking the spatial reasoning, error-detection capacity and contextual judgement that professional practice demands [5,7]. In this sense, the central problem is not whether students use AI, but whether its use makes their reasoning more visible or more opaque.

This problem places assessment at the core of the disciplinary response. If generative systems can help produce polished drawings, models and explanations, then grading only the final artefact is increasingly insufficient. Recent work on authentic assessment, AI-resilient task design and process-centred evaluation points toward a different evidentiary logic: students must be required to document the decisions, iterations, failures, validations and justifications through which an artefact is produced [17-19]. Engineering Graphics is especially suited to this shift because its learning outcomes already depend on visible transformations between sketches, projections, models, constraints and technical standards.

2. AI TOOLS RESHAPING THE ENGINEERING GRAPHICS STUDIO

Four families of AI tools are already in active use in engineering graphics and design contexts, each with distinct pedagogical implications (Table 1).

TABLE 1

AI tool families in engineering graphics and design education

Tool family	Examples and applications
Generative imaging	DALL·E, Midjourney, Adobe Firefly — text-to-image ideation, layout and rapid visual prototyping [8,9].
LLM assistants	ChatGPT, Microsoft Copilot — brainstorming, critique, code support and explanation of design decisions.
AI-enhanced CAD	SolidWorks AI, Intelligent CAD 2.0 — parametric optimisation and design automation [10,11].
Text-to-3D CAD	Diffusion-based generators (GenCAD, CF-CAD) — feasibility-aware model creation from natural language [12,13].

This landscape is expanding rapidly. The common pedagogical challenge across all four families is identical: students can obtain high-quality outputs without developing the underlying reasoning competencies that professional practice requires [14]. Crucially, the same technologies are now entering the assessment side of the studio: design-progress dashboards analyse team dialogue and visualise divergent and convergent thinking for real-time feedback [20], and auto-assessment tools compare student CAD models against reference geometry to surface error patterns [21]. AI can therefore support the evaluation of process as well as the production of artefacts; whether this capability reinforces or erodes genuine learning depends entirely on how the professor designs the surrounding task.

3. AI IMPACT: THREE USER TRAJECTORIES

The impact of AI on Engineering Graphics is not uniform. Three distinct trajectories can be identified, each with specific risks and opportunities.

Students. The primary risk is cognitive dependency combined with a false sense of mastery. When AI resolves drawing tasks on behalf of the student, the learning process that would develop spatial reasoning and error-detection skills is bypassed [2,5]. The result is a graduate who can operate AI tools under familiar conditions but lacks the foundational judgement to intervene when those tools fail.

Technicians. AI democratises access to capabilities that previously required extensive training, lowering barriers in CAD/BIM workflows [4,6]. However, a technician who relies on AI without adequate technical grounding may produce outputs that appear correct but contain serious errors propagating into construction or manufacturing processes [7].

Experts. For domain experts, AI functions as a multiplier. Professionals with deep technical knowledge can delegate routine tasks to AI while concentrating on higher-order design decisions and quality oversight [1,3]. This trajectory illustrates the direction in which Engineering Graphics education should aim to develop students: critical curators capable of extracting value from AI while maintaining sound technical judgement.

4. THE REDEFINED ROLE OF THE PROFESSOR

These trajectories have direct implications for teaching practice. Table 2 summarises the shift in the professor's role across five key dimensions.

TABLE 2
Shift in the Engineering Graphics professor's role in the AI era

Before	Now
Teaches CAD/BIM commands	Designs challenges requiring genuine understanding
Evaluates the final result	Audits the process and student reasoning
Transmits technical standards	Detects the illusion of competence
Acts as software expert	Acts as critical curator of AI-generated outputs
Corrects exercises	Architects authentic learning experiences

This transformation is an elevation of the professor's role, not a diminishment. Value migrates from procedural transmission —which AI can now replicate— to the cultivation of critical judgement, ethical oversight, and contextual reasoning that AI cannot replicate [15,16].

5. FOUR NEW FACULTY COMPETENCIES

Meeting the demands of this redefined role requires four interrelated competencies.

5.1. Critical thinking on AI outputs

Professors must distinguish outputs that are technically correct from those that are merely visually convincing. Generative AI can produce polished models containing hidden geometric errors, tolerance violations, or structural inconsistencies. Without the ability to identify these flaws, professors cannot teach students to do so either [1,2].

5.2. Authentic activity design

Professors must design tasks that AI cannot solve on behalf of the student. This requires understanding AI's current capabilities and limitations in Engineering Graphics contexts, and crafting activities that foreground reasoning, judgement, and contextual interpretation that only the student can provide [5,14].

5.3. Generative AI literacy

Professors need functional familiarity with the tools students are using: their training basis, typical failure modes, and the kinds of prompts that produce unreliable outputs. This enables proactive identification of pedagogical risks [3,8,9,15].

5.4. Process-centred assessment

Traditional assessment focused on the final artefact is insufficient when AI can produce high-quality artefacts independently. Process-centred assessment shifts the evaluative focus to student reasoning: decisions made, errors detected and corrected, reasoning articulated. This approach makes student thinking visible and resists AI substitution [2,5,16].

6. A CATALOGUE OF ASSESSMENT-REDESIGN STRATEGIES

The four competencies converge in practice on a single shift: relocating evaluation from the artefact to the reasoning that produces it. Table 3 consolidates the strategies identified above into a catalogue that maps each approach to the dimension of reasoning or process it

renders assessable and to its supporting evidence. The strategies are complementary rather than exclusive; a single Engineering Graphics assignment may combine structured process documentation, prompt-log transparency and a reasoning-aligned rubric within one authentic, AI-resilient task.

TABLE 3

Catalogue of assessment-redesign strategies mapping each approach to the reasoning or process it evaluates

Redesign strategy	How it evaluates reasoning and process	Evidence
Sketching and freehand ideation	Externalises the cognitive models and problem-solving process that AI cannot demonstrate	[24]
Workbooks, portfolios and process logs	Capture iterations, methods used and decision rationale; evidence self-regulated learning	[25,26]
Prompt logs and AI-use justifications	Make otherwise invisible AI-assisted steps transparent and assessable	[27,28]
Reasoning-aligned rubrics	Operationalise scoping, divergent and convergent thinking, iteration and collaboration	[25,29]
AI Assessment Scale (graduated AI use)	Redesigns tasks to preserve validity when generative AI can produce outputs	[30]
Interconnected, multi-step problems	Force sustained reasoning whose intermediate steps resist delegation	[23]
"Against–Avoid–Adopt–Explore" task framing	Sets, per activity, whether AI is prohibited, permitted or required	[18]
Hybrid non-AI and AI authentic tasks	Balance conceptual foundations against applied tool use	[19,22]
Dialogic AI-mediated assessment	Probes assumptions and argumentation in real time	[31]
Hybrid human–AI evaluation	AI supports formative feedback; human evaluators judge contextual reasoning	[20,32]
Evidence-centred and knowledge-in-use frameworks	Track reasoning from task-level artefacts rather than final answers	[33,34]
CAD auto-assessment against references	Surfaces error patterns for formative process feedback	[21]
BIM cognition safeguards	Require sketching and conceptual rationale before modelling begins	[35]
Product-representation and co-design frameworks	Assess representation choices, rationale and ethical reasoning in AI co-design	[36,37,38]

7. CONCLUSIONS

Generative AI has already entered the representational, modelling and assessment practices that define Engineering Graphics. Its significance therefore cannot be reduced to a question of tool adoption or prohibition. The evidence reviewed in this paper suggests a deeper disciplinary transformation: as AI becomes capable of producing technically plausible artefacts, the educational value of the professor shifts toward making visible the reasoning, judgement and validation processes that distinguish professional competence from automated output [14-19].

Three conclusions follow from this analysis. First, the professor's value is not diminished by AI but relocated. What becomes central is no longer the transmission of isolated CAD/BIM commands, but the cultivation of spatial reasoning, critical judgement, ethical awareness and the ability to detect when an AI-generated result is merely convincing rather than correct. Second, assessment must move decisively from product verification to process interpretation. The strategies synthesised in this paper — including sketching, workbooks, process logs, prompt documentation, reasoning-aligned rubrics, graduated AI-use scales, interconnected problems and hybrid human–AI evaluation — provide practical mechanisms for assessing how students think, decide and justify rather than only what they submit [24,30,32]. Third, faculty development is now a strategic requirement: professors need AI literacy not as a technical add-on, but as a condition for designing meaningful tasks, interpreting AI-mediated outputs and preserving the integrity of Engineering Graphics learning outcomes.

Acknowledgements: The authors wish to acknowledge the use of Claude (Anthropic) as an AI-assisted tool during the preparation of this manuscript. Claude contributed to the review and refinement of scientific writing, the translation of content between Spanish and English, and improvements to the typographic layout of the document. All intellectual content, arguments, and conclusions remain entirely the responsibility of the authors.

REFERENCES

[1] Wang, G., *et al.*: AMCAD. Int. J. Mech. Eng. Educ. 52(1) (2024). https://doi.org/10.1177/03064190231175231

[2] Ahmad, S., *et al.*: Artificial intelligence in learning technologies. IEEE Trans. Learn. Technol. 17, 12-31 (2024). https://doi.org/10.1109/TLT.2023.3314610

[3] Mallik, S., Gangopadhyay, A.: Artificial intelligence in design and education. Front. Artif. Intell. 6, 1151391 (2023). https://doi.org/10.3389/frai.2023.1151391

[4] Abioye, S.O., *et al.*: Artificial intelligence in the construction industry. J. Build. Eng. 44, 103299 (2021). https://doi.org/10.1016/j.jobe.2021.103299

[5] Papaioannou, P., *et al.*: Engineering applications of artificial intelligence. Results Eng. 15, 100406 (2022). https://doi.org/10.1016/j.rineng.2022.100406

[6] Onatayo, A., *et al.*: Artificial intelligence in architecture. Architecture 4(4), 46 (2024). https://doi.org/10.3390/architecture4040046

[7] Akinosho, T.D., *et al.*: Deep learning in the construction industry. J. Build. Eng. 32, 101827 (2020). https://doi.org/10.1016/j.jobe.2020.101827

[8] Hwang, Y., Wu, J.: Graphic design education in the era of text-to-image generation. Int. J. Art Des. Educ. (2025). https://doi.org/10.1111/jade.12558

[9] Muji, I., Svensson, L., Faraon, M.: Engaging with AI in graphic design education. In: Proc. WAIE 2023, pp. 1-7. IEEE (2023). https://doi.org/10.1109/WAIE60568.2023.00013

[10] Zou, Y., *et al.*: Intelligent CAD 2.0. Vis. Inform. (2024). https://doi.org/10.1016/j.visinf.2024.10.001

[11] Academic Journal of Manufacturing Engineering: Artificial intelligence in the CAD process: machine learning models, generative optimisation, and their impact on design. Acad. J. Manuf. Eng. 23(1), L2 (2025). https://doi.org/10.5281/zenodo.15180312

[12] Wu, R., *et al.*: AI-driven generation of 3D CAD models: a survey. Comput. Vis. Media (2026). https://doi.org/10.26599/CVM.2025.9450521

[13] Tsuji, Y., *et al.*: GenCAD-self-repairing. J. Comput. Inf. Sci. Eng. (2026). https://doi.org/10.1115/1.4071109

[14] Omran Zailuddin, N., *et al.*: Redefining creative education: AI in design courses. J. Res. Innov. Teach. Learn. (2024). https://doi.org/10.1108/JRIT-01-2024-0019

[15] Liu, J., *et al.*: The educator as an embedded AI designer. In: Proc. ICETM 2025. IEEE (2025). https://doi.org/10.1109/ICETM67477.2025.11413580

[16] Sun, Y., *et al.*: A generative AI-responsive competency framework. Comput. Educ.: AI (2026). https://doi.org/10.1016/j.caeai.2026.100542

[17] Kickbusch, S., *et al.*: Beyond detection: redesigning authentic assessment in an AI-mediated world. Educ. Sci. 15 (2025). https://doi.org/10.3390/educsci15111537

[18] Khlaif, Z.N., Alkouk, A., Salama, N., Eideh, F.: Redesigning assessments for AI-enhanced learning: a framework for educators in the generative AI era. Educ. Sci. 15 (2025). https://doi.org/10.3390/educsci15020174

[19] Xia, Q., Weng, X., Fan, Y., Lin, J., Chiu, T.K.F.: A scoping review on how generative AI transforms assessment in higher education. Int. J. Educ. Technol. High. Educ. 21 (2024). https://doi.org/10.1186/s41239-024-00468-z

[20] Chiu, T.K.F., Silva, C.: Applied AI in assessing design education: AI dashboard vs. conventional human evaluators. In: Proc. ASME IDETC-CIE, DETC2024-142450 (2024). https://doi.org/10.1115/detc2024-142450

[21] Jaakma, K., Kiviluoma, P.: Auto-assessment tools for mechanical computer aided design education. Heliyon 5, e02622 (2019). https://doi.org/10.1016/j.heliyon.2019.e02622

[22] Elshall, E., Badir, M.: Balancing AI-assisted learning and traditional assessment: the FACT assessment in environmental data science education. Front. Educ. (2025). https://doi.org/10.3389/feduc.2025.1596462

[23] Merzdorf, H., Jaison, A., Weaver, J., Linsey, J., Hammond, T., Douglas, K.A.: Sketching assessment in engineering education: a systematic literature review. J. Eng. Educ. 113(4), 872-893 (2023). https://doi.org/10.1002/jee.20560

[24] Clark, R.M., Ostrowdun, M., Rothschuh, S., Purzer, S.: Assessing students' design processes and design outcomes. Int. J. Eng. Educ. (2021).

[25] Törlind, P., Wikberg Nilsson, Å.: Evaluation of workbooks as an active learning tool for industrial design engineering. In: Proc. E&PDE 2022 (2022). https://doi.org/10.35199/epde.2022.13

[26] Smith, S., Francis, J.: Process not product in the written assessment. In: Using Generative AI Effectively in Higher Education (2024). https://doi.org/10.4324/9781003482918-17

[27] Zhang, Y., Zhang, Y.: How design ability anxiety leads to design students' dependence on artificial intelligence. Acta Psychol. (2025). https://doi.org/10.1016/j.actpsy.2025.105423

[28] Muñoz-Collazos, M., González-Serrano, M.H.: Machine learning approaches for evaluating STEM education projects: a systematic review of frameworks and rubrics. Appl. Sci. (2025). https://doi.org/10.3390/app152312812

[29] Perkins, M., Roe, J., Furze, L.: Reimagining the Artificial Intelligence Assessment Scale (AIAS): a refined framework for educational assessment. J. Univ. Teach. Learn. Pract. (2025). https://doi.org/10.53761/rrm4y757

[30] Zakeri, B.: Generative AI for project-based assessment in energy and sustainability education (2025). https://doi.org/10.21203/rs.3.rs-7402766/v1

[31] Khan, M., Liow, L.H., Ang, C.S.: Human or AI? Comparing design thinking assessments by teaching assistants and bots. In: Proc. IEEE TALE 2025. IEEE (2025). https://doi.org/10.1109/TALE66047.2025.11346622

[32] Kubsch, M., Grimm, A., Neumann, K., Rummel, N.: Using evidence-centered design to develop an automated system for tracking students' physics learning. In: Uses of AI in STEM Education (2024). https://doi.org/10.1093/oso/9780198882077.003.0011

[33] He, P., Shin, N., Zhai, X., Krajcik, J.: A design framework for integrating AI to support teachers' timely use of knowledge-in-use assessments. In: Uses of AI in STEM Education (2024). https://doi.org/10.1093/oso/9780198882077.003.0016

[34] Agirbas, A.: Teaching construction sciences with the integration of BIM to undergraduate architecture students. Front. Archit. Res. (2020). https://doi.org/10.1016/j.foar.2020.03.007

[35] Stefano, S.: Exploring AI integration in engineering education: a framework for product representation and behavioral insights. In: Proc. AHFE International (2025). https://doi.org/10.54941/ahfe1006659

[36] Botta, A., Autuori, G., Terenghi, S., Subet, D.: A design-stage-oriented framework to introduce artificial intelligence and machine learning in design education. In: Proc. DRS 2024 (2024). https://doi.org/10.21606/drs.2024.535

[37] Martin, J., Tubaltseva, D., Harrison, K., Rubin, M.: Participatory co-design and evaluation of a novel approach to generative AI-integrated coursework assessment in higher education. Behav. Sci. 15 (2025). https://doi.org/10.3390/bs15060808

[38] Elmoghazy, Y., Eldardiry, H., Alghamdi, M., AlQaysum, M.: Is AI an academic threat to reject or a complementary tool to embrace? Case study of a senior interior design studio. Buildings 16 (2026). https://doi.org/10.3390/buildings16081589

State of the Art of Non-Pneumatic Tyres (NPTs) Applied to the Front Caster Wheels of Wheelchairs for Improved Suspension Performance

Bernardo Pajares Moreno*, Guillermo Peris Fajarnés, R. Barberà-Guillem, María Moncho Santonja

CITG (Universitat Politècnica de València), Camí de Vera s/n 46022 (Valencia)

* e-mail: berpamo@upv.es

Abstract: Non-pneumatic tyres (NPTs) represent a technologically viable alternative to conventional pneumatic tyres, offering significant potential to reduce the vibrations and mechanical shocks transmitted to wheelchair users during daily mobility. This paper presents a systematic review of the current state of the art of NPTs with particular emphasis on their prospective application to the front caster wheels of self-propelled manual wheelchairs. Four principal areas are covered: structural typologies (solid elastomeric, spoked, lattice, and shear-band configurations), methods of structural design and optimisation, numerical simulation by finite element analysis (FEA), and fatigue behaviour and service life. The review synthesises findings from a range of experimental and computational studies and identifies the performance parameters most relevant to wheelchair environments, including load capacity, vertical stiffness, vibration attenuation, and durability under cyclic loading. The review shows that, despite sustained development of NPT technology in the automotive and robotics sectors, research specifically focused on wheelchair caster wheels remains extremely limited. Key gaps identified include the absence of fatigue data for 3D-printed NPT structures and the lack of occupant-centred performance criteria. These gaps define a promising research agenda for future work.

Keywords: *Non-Pneumatic Tyres, Castors, Finite element analysis, 3D printing, Fatigue analysis.*

1. INTRODUCTION

The mobility of people with physical disabilities depends largely on the mechanical performance of the wheelchairs they use. In self-propelled manual wheelchairs, the front caster wheels are the components that come into the most direct contact with ground irregularities, as they are located at the front of the wheelchair in the direction of travel (30% of the weight) [9]. Owing to their solid construction and relatively small diameter (typically one-fifth to one-sixth of the diameter of the rear wheels), they are the primary source of vibration transmission to both the wheelchair and its user. Conventional pneumatic tyres provide inherent shock absorption through the compressed air enclosed within the tyre; however, they are associated with well-known drawbacks, including the risk of punctures, the need for regular pressure maintenance, and variations in mechanical performance depending on the inflation pressure [1].

In this context, non-pneumatic tyres (NPTs) have emerged as a promising alternative, as they eliminate the need for pressurised air while enabling the wheel's mechanical response to be tailored through structural design according to the specific requirements of the intended application. Their ability to absorb vibrations through the elastic deformation of an internal load-bearing structure makes them particularly well suited to replacing conventional pneumatic tyres in applications where ride comfort, reduced weight, and minimal maintenance are key requirements, such as manual wheelchairs [2,10].

Drawing upon the available scientific literature, this paper reviews the principal structural concepts underlying NPTs, current design and structural optimisation methodologies, the simulation tools employed for their analysis, and the studies specifically addressing their application to wheelchairs.

2. STRUCTURAL TYPOLOGIES OF NON-PNEUMATIC TYRES

Non-pneumatic tyres (NPTs) comprise a broad range of engineering solutions whose common characteristic is the replacement of the air-filled chamber with a solid or cellular structure capable of supporting loads and dissipating mechanical energy. Zhao Youqun [2] provides a comprehensive review of advances in mechanically elastic non-pneumatic wheels, identifying the principal structural configurations and their corresponding mechanical characteristics.

The most representative structural typologies include: (a) solid elastomeric tyres, which offer high durability but limited vibration absorption capability; (b) honeycomb-spoke structures, whose deformable spokes undergo local elastic deformation and recover their original shape without permanent deformation; (c) shear-band tyres, in which a shear layer uniformly distributes the applied load between the tread and the central hub through an intermediate layer with controlled shear properties; and (d) auxetic structures, whose constituent materials exhibit a negative Poisson's ratio, giving rise to unconventional mechanical behaviour of particular interest for impact mitigation [2].

This wide range of structural configurations indicates that the selection of the most appropriate design for a specific application should be based on a systematic evaluation of the key performance parameters, including vertical stiffness, vibration damping capability, rolling

resistance, and fatigue life. In the case of manual wheelchairs, the dominant design requirements are the attenuation of low-amplitude, high-frequency vibrations and minimisation of the overall wheel mass. These requirements make shear-band structures and cellular lattice geometries particularly attractive design solutions [1,2].

3. STRUCTURAL DESIGN AND OPTIMISATION

The design of a non-pneumatic tyre (NPT) requires the definition of three fundamental components: the outer tread, the internal structural layer (comprising either a shear band or a spoke assembly), and the central hub connecting the wheel to the axle. Among these components, the intermediate structural layer has the greatest influence on the overall mechanical performance of the tyre, as its geometry and material properties govern both the load distribution and the effective stiffness of the wheel.

Thyagaraja *et al.* [5] investigated the optimisation of the shear band to minimise the rolling resistance of non-pneumatic tyres. Their study proposes a parametric design framework in which the key variables of the shear layer—including its thickness, shear modulus, and reinforcement geometry—are numerically optimised to reduce the energy dissipated during rolling without compromising the tyre's load-carrying capacity. The results demonstrate that an appropriate combination of these parameters can significantly reduce rolling resistance compared with an equivalent pneumatic tyre, with direct implications for the propulsion effort required by manual wheelchair users.

Czech, Guarneri and Fadel [6] extended this approach by applying topology optimisation and the concept of metamaterials to the design of the shear layer. Using topology optimisation algorithms, the authors identified material distributions within the intermediate layer that either maximise the specific stiffness or minimise the overall mass while achieving the desired mechanical response. The incorporation of metamaterial concepts enables the design of structures with effective properties that cannot be achieved using conventional homogeneous materials, thereby providing the opportunity to tailor the wheel's frequency response—and consequently its vibration attenuation capability—with a high degree of precision and control [6].

Both approaches are directly applicable to the design of NPTs for manual wheelchairs, where the requirements for low weight, low rolling resistance, and effective vibration damping constitute competing design objectives that require multi-objective optimisation techniques.

4. NUMERICAL SIMULATION AND FINITE ELEMENT ANALYSIS

Finite Element Analysis (FEA) is the principal computational tool for investigating the mechanical behaviour of non-pneumatic tyres (NPTs). Its ability to model complex geometries, geometric nonlinearities, and hyperelastic materials makes it particularly well suited to the analysis of these structures.

Núñez-Quispe [4] presents a preliminary study on the design and simulation of an NPT for a CanSat rover, in which the wheel's behaviour when traversing different obstacle profiles

is evaluated using dynamic simulation. The study illustrates the numerical validation methodology employed prior to manufacturing, including the definition of the parametric geometry, the assignment of material properties, the application of boundary conditions representative of real operating conditions, and the analysis of the resulting stress and strain fields. Although the application differs from that of a wheelchair, the methodology is directly transferable [4].

Soliman [7] numerically investigated the influence of NPT geometry on its aerodynamic performance by evaluating the drag coefficient for different structural wheel configurations. Although aerodynamics has limited relevance in the context of manual wheelchairs operating at low speeds, the study highlights the importance of the wheel's external geometry in determining its overall functional performance and demonstrates the value of Computational Fluid Dynamics (CFD) as a complementary simulation tool to FEA [7,8].

In the study most closely related to the subject of the present review, Ali *et al.* [1] applied FEA to the design of a non-pneumatic front caster wheel for a manual wheelchair. The authors developed a finite element model in ANSYS to evaluate the stress distribution, static deformation under load, and effective vertical stiffness of several design configurations. Their results enabled the selection of the configuration providing the optimum balance between structural stiffness and vibration damping capability within the typical loading range of a manual wheelchair, thereby demonstrating the effectiveness of the computational approach for the evaluation and optimisation of NPT designs prior to manufacturing [1].

5. FATIGUE BEHAVIOUR AND SERVICE LIFE

The durability of non-pneumatic tyres (NPTs) is one of the key factors governing their adoption in applications involving continuous use, such as manual wheelchairs. Unlike conventional pneumatic tyres, whose most common mode of failure is puncture, NPTs are susceptible to mechanical fatigue resulting from the repeated loading and unloading cycles experienced by their internal elastic structure during service.

The study published in Strojniški vestnik - Journal of Mechanical Engineering [3] investigates the prediction of the service life of an NPT using a finite-life design approach. The authors employed the Wöhler (S-N curve) method to characterise the fatigue behaviour of the material forming the structural layer, determining the number of cycles to failure under different loading amplitudes. The results indicate that the stress concentration at the junction between the shear band and the tread represents the critical site for crack initiation, and that the geometric design of these connections has a decisive influence on the overall service life of the tyre [3].

This consideration is particularly relevant to the design of NPTs manufactured by additive manufacturing (3D printing) for wheelchair applications, where the fatigue resistance of the printed material may be lower than that of the reference material owing to the anisotropy introduced during the manufacturing process. Consequently, fatigue life assessment should be integrated into the design process from its earliest stages, becoming a design criterion that is as important as static stiffness and vibration attenuation capability.

6. APPLICATION TO THE FRONT CASTER WHEELS OF MANUAL WHEELCHAIRS

The body of literature reviewed consistently indicates that the application of non-pneumatic tyres (NPTs) to the front caster wheels of manual wheelchairs represents a promising technological opportunity, although the available research remains limited. The study by Ali *et al.* [1] constitutes the most directly relevant contribution, demonstrating that an NPT for a wheelchair caster wheel can be designed to achieve satisfactory mechanical performance through the combined use of parametric design and Finite Element Analysis (FEA).

The distinctive characteristic of a wheelchair front caster wheel, compared with other NPT applications, lies in its specific function. Unlike a drive wheel, it serves as a caster wheel, providing directional guidance rather than propulsion. Consequently, it is subjected to moderate vertical loads (approximately 30% of the total wheelchair load) and frequent changes in direction. As a result, the relevant design criteria differ from those adopted for NPTs intended for passenger cars or heavy-duty vehicles. Low rolling resistance is essential to minimise the propulsion effort required by the user, whereas effective vibration attenuation within the frequency range most relevant to human comfort (1-80 Hz, according to ISO standards) should constitute the primary structural design objective [1,2].

Manufacturing by additive manufacturing (3D printing) introduces a further dimension to the design process, as it enables the production of complex geometries—such as lattice and honeycomb structures—that would be difficult or impossible to manufacture using conventional production methods. However, it also introduces additional variables affecting mechanical performance, including anisotropy, porosity, and surface finish, all of which should be taken into account during the design stage and subsequently validated through experimental testing [3,4].

7. DISCUSSION AND RESEARCH GAPS

The literature review has identified three principal gaps in the current state of knowledge:

First, the majority of research on non-pneumatic tyres (NPTs) has been conducted within the context of passenger cars and off-road vehicles, where the loading conditions, operating speeds, and service environments differ considerably from those encountered by manual wheelchairs. Consequently, the direct transfer of these findings to wheelchair applications requires a critical reassessment of both the design parameters and the performance evaluation criteria adopted in previous studies [2,5,6].

Second, studies specifically addressing NPTs for manual wheelchairs remain extremely limited—being largely confined to the work of Ali *et al.* [1]—and do not comprehensively consider the variability among wheelchair users, including differences in body mass, patterns of use, and terrain characteristics, all of which define the range of relevant design conditions.

Third, the integration of fatigue analysis [3] and the influence of additive manufacturing processes on the mechanical behaviour of NPTs remains an open research area with direct implications for the reliability and service life of the final product.

In the context of additive manufacturing, it should also be recognised that the mechanical properties of printed materials may vary depending on several process-related factors, in-

cluding the manufacturing system employed, the printing conditions, the ambient temperature and humidity, and the moisture content of the feedstock material. These sources of variability should be taken into account during material characterisation and incorporated into the design and validation stages.

8. CONCLUSIONS

Non-pneumatic tyres (NPTs) represent a technically viable alternative with considerable potential to improve vibration attenuation in the front caster wheels of manual wheelchairs. The literature reviewed provides a solid foundation regarding structural typologies [2], shear-band optimisation methods [5,6], and numerical simulation and Finite Element Analysis (FEA) techniques [1,4,7,8], as well as established approaches for assessing fatigue durability [3].

However, research specifically focused on wheelchair applications remains limited, highlighting both the relevance and the timeliness of the ongoing doctoral research in this field. The combination of parametric design, ANSYS-based simulation, and additive manufacturing (3D printing) provides a robust methodological framework for advancing the development of non-pneumatic tyres for manual wheelchairs, as supported by the studies identified in the reviewed literature [1,4].

Acknowledgements: The authors would like to acknowledge the Centre for Research in Graphic Technologies (CITG) and the Department of Graphic Engineering at the Universitat Politècnica de València for their institutional support throughout the development of this research.

During the preparation of this manuscript, a non-generative artificial intelligence tool was used solely to assist with stylistic revision, language editing, and document formatting. The tool did not contribute to the generation of scientific content, data analysis, or the interpretation of the results. The authors take full responsibility for the intellectual content of this article and have thoroughly reviewed and approved the final manuscript prior to its submission.

REFERENCES

[1] Ali, I., Rahman, M.Z.U., Hussain, A., Ghaffar, A., Zafar, S.: A finite element analysis based design of a non-pneumatic wheel chair castor. J. Eng. Res. 13(1), 351-360 (2025). https://doi.org/10.1016/j.jer.2023.08.013

[2] Zhao, Y.: Research progress on kind of non-pneumatic mechanical elastic safety wheel. J. Mech. Eng. 55(24), 105 (2019). https://doi.org/10.3901/jme.2019.24.105

[3] Xiao, Z., Zhao, Q., Lin, F., Zhu, M., Deng, J.: Studying the fatigue life of a non-pneumatic wheel by using finite-life design for life prediction. Stroj. Vestn. – J. Mech. Eng. 64(1), 56-67 (2018). https://doi.org/10.5545/sv-jme.2017.4695

[4] Nunez-Quispe, J.J.: Design and simulation of a rover CanSat non-pneumatic wheel: preliminary study for a certain test obstacle path. In: Proc. 12th Int. Conf. Mech. Aerosp. Eng. (ICMAE 2021), pp. 484-488. IEEE, Athens (2021). https://doi.org/10.1109/icmae52228.2021.9522526

[5] Thyagaraja, N., Shankar, P., Fadel, G., Guarneri, P.: Optimizing the shear beam of a non-pneumatic wheel for low rolling resistance. In: Proc. ASME DETC 2011, pp. 33-42. ASME, Washington, DC (2011). https://doi.org/10.1115/detc2011-48532

[6] Czech, C., Guarneri, P., Fadel, G.: Meta-material design of the shear layer of a non-pneumatic wheel using topology optimization. In: Proc. ASME DETC 2012, pp. 893-903. ASME, Chicago (2012). https://doi.org/10.1115/detc2012-71340

[7] Soliman, M.Z.: A numerical study on the influences of non-pneumatic tyre shape on the wheel aerodynamics. Int. J. Res. Appl. Sci. Eng. Technol. 10(2), 599-611 (2022). https://doi.org/10.22214/ijraset.2022.40300

[8] Yuan, X. H., Zhai, B. Q., Su, C. Q., Liu, X., & Wang, Y. P. (2024). Flow field analysis and aerodynamic drag optimization of non-pneumatic tires. *Physics of Fluids*, *36*(8). https://doi.org/10.1063/5.0220893

[9] McLaurin, CA, & Brubaker, CE (1991). Biomecánica y la silla de ruedas. *Prosthetics and Orthotics International*, *15* (1), 24-37. https://doi.org/10.3109/03093649109164272

[10] Jin, X., Hou, C., Fan, X., Sun, Y., Lv, J., & Lu, C. (2018). Investigation on the static and dynamic behaviors of non-pneumatic tires with honeycomb spokes. *Composite Structures*, *187*, 27-35. https://doi.org/10.1016/j.compstruct.2017.12.044